| | |
|---|---|
| Title | A study of the presentation and biological effects of biofilm component poly-N-acetylglucosamine from Staphylococcus aureus and Acinetobacter baumannii using novel multidisciplinary platforms and methods |
| Author(s) | Flannery, Andrea |
| Publication Date | 2019-09-24 |
| Publisher | NUI Galway |
| Item record | http://hdl.handle.net/10379/15460 |

# A study of the presentation and biological effects of biofilm component poly-*N*-acetylglucosamine from *Staphylococcus aureus* and *Acinetobacter baumannii* using novel multidisciplinary platforms and methods

A thesis submitted to the National University of Ireland, Galway

for the degree of **Doctor of Philosophy** by


## Andrea Flannery, B.Sc.

Microbiology, School of Natural Sciences,

National University of Ireland Galway



September, 2019

**Thesis supervisor:** Dr. Michelle Kilcoyne

**Co-supervisor:** Prof. James P. O'Gara

**Head of Department:** Prof. Gerard Wall

# Table of Contents

## DECLARATION

The work described in this thesis was performed by myself, Andrea Flannery, between 2014 and 2018 at the Biomedical Sciences Building, National University or Ireland, Galway, under the supervision and mentorship of Dr. Michelle Kilcoyne.

I declare that the results presented in this thesis are from original experimental work which has been carried out by me for the purpose of this thesis. The work described within this thesis has not been submitted for degree, diploma or other qualification at any other university.

# Acknowledgements

Thank you to everyone who has helped me throughout my postgraduate years and supported me during the completion of my thesis. Michelle, thank you for being such an amazing and supportive supervisor. I remember the day I met you outside the BRB to tell you I was awarded the PhD Scholarship and you've never stopped helping me and guiding me since then. Thank you for your support and patience during the difficult times of research. It certainly was a roller coaster of emotions at times, but your advice, guidance and expertise helped me through it and left me with nothing but fond memories of my time as a Ph.D. student.

Another special thanks to Jim who believed in me and encouraged me to pursue a PhD in the final year of my B.Sc. You've always been there when I needed help or to troubleshoot any of my microbiology results. Your passion and enthusiasm for science lured me into the world of *Staphylococcus* and biofilms almost six years ago and here I am – writing a thesis about it and still hooked!

A massive thank you to everyone that is a part of the AGRC. Special thanks to Jared for helping me with laboratory techniques and methods, and for always listening to me and providing guidance when I needed some scientific expertise. Stephen, a big thank you for providing guidance, support and constructive feedback in the lab and during my annual GRC meetings. Thanks for the general good banter and for co-creating the infamous beaker. Last but not least – Marie. You have been such support in the lab and as a friend. The list would be too long for the amount of things that you have helped me with over the years - I don't think I can say thank you enough (perhaps I will pay you back with some saucisson?). You made my time in the lab so enjoyable! Morning coffee and scones and the BRB running club!! You're amazing-thank you! I must also thank Matthew Griffin and Joanna Cabral for your time and efforts planning and contributing to my flow cytometry experiment in chapter 4. Another thank you to Shirley for your technical support for my multiplex assay in chapter 4 and to Enda O'Connell for your technical support using the Operetta imaging system.

Thank you to the JOG lab for interesting discussions and all the fun times. Chris, thanks for being my coffee buddy, house mate and a great person for the scientific

chats in the evening. Big thank you to the microbiology department and everyone that was associated with MicroSoc. Ann, Mike and Maurice, thank you for your help and kindness throughout the years. Aoife, thank you for your help and support, on and off my GRC committee. Everyone in the microbiology department made my time as a postgraduate student so enjoyable, thank you.

Mathieu, Geraldine and Laura, you are like a second family to me. Thank you for your constant support and all your encouraging chats, help and love over the last few years. Mathieu and Geraldine I wish you all the best with your new life in Ireland. Special thanks to the Long family for their support and encouragement. Thank you for being such good fun and providing me with so many good times and experiences over the last few years. You truly are such a wonderful family!

None of this would be possible without my family. Mum, Dad and Ciara, thank you so much for everything. Thank you for your love, patience and understanding. You always have my best interests in mind and have sacrificed so much for me to get to where I am today – I am forever grateful. Thank you for always being there.

Finally, thank you Stephane. You've really been with me through the ups and the downs, from Galway to Dublin to London. You have been, and are incredible (did I tell you, you so great?). Thank you for your love, for always being there and being my number 1 supporter. I'm so grateful to have you in my life and happy you shared this important time in my life with me.

My work was funded by the Irish Research Council and the Tomas Crawford Hayes Trust Fund.

| Abbreviations | Name/meaning |
|---|---|
| %CV | Percentage coefficient of variation |
| Δ | delta |
| 4-AP | 4-aminophenyl-b-D-glucopyranoside |
| Aap | accumulation associated protein |
| AB-PNAG | PNAG from *A. baumannii* |
| AF555 | Alexa Fluor® 555 |
| AI-2 | Autoinducer 2 |
| AP-1 | Activating protein-1 |
| APD | Acetyl-phenylenediamine |
| APE | *p*-aminophenylethyl |
| ASF | Asialofetuin |
| Atl | Autolysin |
| Bap | Biofilm associated protein |
| BHI | Brain heart infusion |
| BHI glucose | Brain heart infusion supplemented with 1% glucose |
| BHI NaCl | Brain heart infusion supplemented with 4% NaCl |
| BPS | *Bordetella* polysaccharide |
| BSA | Bovine serum albumin |
| $Ca^{2+}$ | Calcium |
| CaCl2 | Calcium Chloride |
| CARD9 | Caspase recruitment domain-containing protein 9 |
| CDC | Centre for Disease Control and Prevention |
| CE | Capillary electrophoresis |
| CF | Cystic Fibrosis |
| CHO | Chinese hamster ovary |
| CL | Collectin |
| ClfB | Clumping Factor B |
| CO2 | Carbon dioxide |
| COPD | Chronic obstructive pulmonary disease |
| CPS | Capsular polysaccharide |
| CRD | Carbohydrate recognition domain |
| CsCl | Cesium chloride |
| DC | Dendritic cell |
| DD | Death domain |
| DMSO | Dimethyl sulfoxide |
| DNA | Deoxyribonucleic acid |
| ECL | enhance chemiluminescence |
| ECM | Extra-cellular matrix |
| eDNA | Extracellular DNA |
| EDTA | Ehylenediaminetetraacetic acid |
| Efb | Extracellular fibrinogen-binding protein |
| ELISA | Enzyme-linked immunosorbent assay |
| EPS | Extracellular polysaccharide |
| ERK | Extracellular signal-regulated kinase |
| *et al.* | et alia |

| | |
|---|---|
| FimH | Fimbriae component H |
| Fn | Fibronectin |
| FnBP | Fibronectin binding protein |
| FS | FluoSphere |
| FSL-1 | Synthetic diacetylated lipoprotein |
| Fuc | Fucose |
| FucNAc | *N*-Acetyl-Fucosamine |
| G418 | Geneticin |
| Gal | Galactose |
| GalNac | *N*-acetylgalactosamine |
| GAS | Group A *Streptococcus* |
| GBS | Group B *Streptococcus* |
| GL | endo-β-*N*-acetylglucosaminidase |
| GlcN | glucosamine |
| GlcNAc | *N*-acetylglucosamine |
| GndHCl | guanidine hydrochloride |
| GPI | glycosylphosphatidylinositol |
| $H_2O$ | Water |
| HAS | Human serum albumin |
| HCl | Hydrochloric acid |
| HIV | Human Immunodeficiency Viruses |
| HKLM | Heat killed Listeria monocytogenes |
| HPLC | High-performance liquid chromatography |
| HRP | Horse radish peroxidase |
| HTP | High throughput |
| HUVEC | Human umbilical cord vein endothelial cells |
| $IC_{50}$ | Half maximal inhibitory concentration |
| *ica* | Intercellular adhesin - *icaADBC* |
| ICAM | Intercellular adhesion molecule |
| IFN | Interferon |
| Ig | Immunoglobulin |
| IL | Interleukin |
| IRAK | IL-1R-associated kinase |
| ITC | β-D-glucopyranosyl isothiocyanate |
| ITIM | Immunoreceptor tyrosine-based inhibitory motif |
| JNK | Jun N-terminal kinase |
| LacNAc | *N*-acetyllactosamine |
| LAD | Leukocyte adhesion deficiency |
| LC | Liquid chromatography |
| Le | Lewis |
| LOS | Lipooligosaccharide |
| LPB | LPS binding protein |
| LPS | Lipopolysaccharide |
| LPXTG | Leu-Pro-X-Thr-Gly |
| LTA | Lipoteichoic acids |
| mAB | Monoclonal antibody |

| | |
|---|---|
| MAC | Membrane attack complex |
| Man | Mannose |
| ManLAM | Mannosylated lipoarabinomannan |
| ManNAc | N-Acetylmannosamine |
| MASP | MBL-associated serine protease |
| MBL | Mannose binding lectin |
| MES | 2-(N-morpholino)ethanesulfonic acid hydrate |
| $Mg^{2+}$ | Magnesium |
| MgCl | Magnesium Chloride |
| MGL | Macrophage galactose-type lectin |
| MRSA | Methicillin resistant Staphylococcus aureus |
| MS | mass spectrometry |
| MSSA | Methicillin sensitive Staphylococcus aureus |
| MurNAc | N-Acetylmuramic acid |
| MWCO | molecular weight cut off |
| NaCl | Sodium Chloride |
| NaOH | Sodium hydroxide |
| NF-κB | Nuclear factor- κB |
| NGC | Neoglycoconjugate |
| NIH | National Institute of Health |
| NK | Natural killer |
| nm | Nanometer |
| OH | Hydroxyl group |
| OmpA | Outer membrane protein A |
| Ov | Ovalbumin |
| Pam3CSK4 | Synthetic triacetylated lipoprotein |
| PAMPs | Pathogen associated molecular patterns |
| PAS | Periodic acid – Schiff's |
| PBMC | Peripheral blood mononuclear cell |
| PBS | Phosphate buffered saline |
| *pga* | Poly-glucosamine - *pgaABCD* |
| pH | potential of Hydrogen |
| PIA | Polysaccharide intercellular adhesion |
| PMN | Polymorphonuclear leukocytes |
| PMT | Photo-multiplier tubes |
| PNAG | Poly-*N*-acetylglucosamine |
| PNMN | Polymorphonuclear leukocytes |
| PS/A | Polysaccharide/adhesin |
| PSGL-1 | P-selectin glycoprotein ligand-1 |
| PSM | phenol soluble modulins |
| PVDF | Polyvinylidene difluoride |
| RANTES | Regulated on Activation, Normal T Cell Expressed and Secreted |
| RFU | Relative fluorescence intensity |
| RNase | Ribonuclease |
| rpm | Revolutions per minute |

| | |
|---|---|
| RTA | Ribotal teichoic acid |
| RT-PCR | Reverse transcription polymerase chain reaction |
| SAA | Slime-associated antigen |
| SA-LTA | *S. aureus* lipoteichoic acid |
| SA-PNAG | PNAG from *S. aureus* |
| SasC | *S. aureus* surface protein C |
| SasG | *S. aureus* surface protein G |
| SD | Standard deviation |
| SEAP | Secreted embryonic alkaline phosphatase |
| SEB | Staphylococcal exotoxin B |
| SEM | Scanning electron microscopy |
| SIB | Swiss Institute of Bioinformatics |
| sMAP | Small MBL-associated protein |
| SpA | Staphylococcal protein A |
| srt | Sortase |
| SSL5 | Staphylococcal superantigen–like 5 |
| sulfo-NHS | *N*-hydroxysulfosuccinimide sodium salt |
| sWGA | Succinylated wheat germ agglutinin |
| SYK | Spleen tyrosine kinase |
| TA | Teichoic acid |
| TBS | Tris-buffered saline |
| THP1 cells | THP1-XBlue™-CD14 cells |
| TLR | Toll-like receptor |
| TNF | Tumor necrosis factor |
| TRAF | TNF receptor-associated factors |
| TRAM | TRIF-related adaptor molecule |
| TRIFMA | Time-resolved immunofluorometric assay |
| Tris | Tris(hydroxymethyl)aminomethane |
| UPEC | Uropathogenic E. coli |
| v/v | volume / volume |
| w/v | weight / volume |
| WGA | Wheat germ agglutinin |
| WHO | World Health Organisation |
| WT | Wildtype |
| WTA | Wall teichoic acids |

Lectin abbreviations are listed in tables 2.2 and 3.1.

NGC and glycoprotein abbreviations are listed in table 2.3.

PRR abbreviations are listed in table 4.2.

# List of Figures

# List of Tables

# Abstract

Biofilm formation on medical devices is major cause of concern in today's society as implanted devices are associated with 60-70% of nosocomial infections. Poly-*N*-acetylglucosamine (PNAG) is a polysaccharide found on many Gram-positive and Gram-negative pathogenic bacteria and is associated with biofilm formation and bacterial virulence. PNAG production is regulated *via* the *icaADBC* (*ica*) operon in *Staphylococcus aureus* and the *pgaABCD* (*pga*) operon in *Acinetobacter baumannii*. We urgently need to understand how this polysaccharide interacts with the host's immune system. Methods of rapidly identifying novel PNAG host receptor targets are urgently needed to help to develop anti-bacterial and anti-biofilm compounds to prevent biofilm-associated infections.

We first employed lectin and neoglycoconjugate (NGC) microarrays to screen for lectin and carbohydrate interactions with wild type (PNAG-producing) and non-producing (*ica* or *pga* mutant, respectively) *S. aureus* and *A. baumannii* grown under various conditions. Depending on the environmental growth conditions, wild type *S. aureus* 8325-4 and Mn8m had increased binding to GlcNAc-specific lectins compared to their respective mutants, methicillin resistant *S. aureus* (MRSA) strain BH1CC wild type had increased binding to GlcNAc- and GalNAc- specific lectins and *A. baumannii* wild type had increased binding to Gal and GalNAc-specific lectins. However, as expected, PNAG isolated from *S. aureus* bound to only the GlcNAc-specific lectins, wheat germ agglutinin (WGA) and succinylated wheat germ agglutinin (sWGA). *S. aureus* wild type had increased binding to a range of carbohydrates including 3'- and 6'-sialyllactose and several Lewis structures including Lewis b and x. *S. aureus* BH1CC bound to the same and different structures compared to methicillin sensitive *S. aureus* (MSSA) strains, 8325-4 and Mn8m, but at much lower intensity and there was a general decrease in BH1CC Δ*ica* binding to NGCs compared to the wildtype, but no differences in binding patterns were observed. For *A. baumannii*, the mutant exhibited significantly reduced binding to GlcNAc-BSA, blood group A-BSA and ovomucoid. Overall, these results indicated that PNAG was recognised differently when on the surface of *A. baumannii* compared to *S. aureus* despite PNAG from either species being similarly recognised by itself. Furthermore, we provided a range of potential carbohydrate

ligands for *S. aureus*, *A. baumannii* and PNAG, indicating the presence of specific bacterial lectins.

In chapter 3, lectin microarrays were used to identify plant lectins that specifically recognised PNAG and used multivalent GlcNAc derivatives or glycoclusters to modulate these lectin interactions in a targeted manner. A PNAG preparation from *S. aureus* was fluorescently labelled and used to mimic secreted PNAG that would be released from a cell in to the biofilm matrix and PNAG was covalently bound to a 1.0 μm fluorescent carboxylate-modified microsphere to mimic the morphology of PNAG on a bacterial cell surface. Six bivalent glycoclusters with GlcNAc as the bioactive head group were used to target WGA binding to the GlcNAc-containing glycoprotein, ovalbumin, neoglycoconjugate, GlcNAc-BSA, PNAG and whole *S. aureus* bacteria. Glycocluster sos2211 had the lowest $IC_{50}$ value for inhibiting WGA binding to ovalbumin of 0.6554 μM and sos2210 produced to lowest $IC_{50}$ value for WGA binding inhibition to GlcNAc-BSA of 5.32 aM. Sos2211 at 1 mM significantly reduced WGA binding to PNAG (both directly labelled and covalently attached to a 1.0 μm carboxylate-modified microsphere) and *S. aureus* Mn8m. Glycoclusters were also used to inhibit biofilm formation and *S. aureus* attachment to mucin purified from a cystic fibrosis patient. Bivalent glycoclusters, sos2222 and sos2221 decreased *S. aureus* 8325-4 and Mn8m biofilm formation by 16% and 19%, respectively. The tri- and tetra- valent glycoclusters, sos2226 and sos2227, significantly reduced both MRSA and MSSA biofilm formation however both were found to precipitate by themselves in culture. Addition of 1 mM of sos2211 to PNAG decreased PNAG interactions with mucin purified from one cystic fibrosis patient, but increased *S. aureus* Mn8m interactions with the same mucin fraction. Overall, the work of chapter 3 demonstrated that the microarray platform is a suitable, sensitive and reproducible for calculating $IC_{50}$ values and glycoclusters may be a promising avenue for targeted therapeutic development.

Finally, in chapter 4 pathogen recognition receptors (PRRs) were screened for interactions with *S. aureus*, *A. baumannii* and PNAG on a PRR microarray. DC-SIGN, DC-SIGNR, LSECtin, MMR, ficolin-3 and CD14 bound to *S. aureus* and *A. baumannii*. PNAG increased CD14 binding to MSSA strains, the presence of the *ica* operon increased DC-SIGN, LSECtin and ficolin-3 binding to MRSA strain BH1CC though only LSECtin binding differences were significant, while PNAG on *A.*

*baumannii* resulted in increased adherence to siglec-1, DC-SIGN, dectin-1 and -2, LSECtin, TLR2/4, TLR2/6 and TLR2/CD14. Using a THP1-Blue-CD14 cell assay, PNAG purified from *S. aureus* or *A. baumannii* did not activate NF-κB/AP-1 signalling via TLRs or CD14. Instead, PNAG on the surface of *S. aureus* promoted activation of NF-κB/AP-1 signalling and increased concentrations of cytokines and chemokines including IL-8, RANTES and IL-1β. There was no difference in NF-κB/AP-1 signalling between wild type and *A. baumannii* Δ*pga*. A dot blot against lipoteichoic acid (LTA) for *S. aureus* wildtype and Δ*ica* mutant suggested that the Δ*ica* mutant had reduced expression of LTA. Furthermore, imaging flow cytometry demonstrated that PNAG from *S. aureus* and *A. baumannii* was internalised by monocytes. This chapter highlighted the different roles for PNAG on, and purified from, *S. aureus* and *A. baumannii* in PRR mediated interactions, monocyte penetration and innate immune system activation, and highlights the importance of the surface expression and presentation of pathogen associated molecular patterns (PAMPs) for eliciting signalling responses.

Overall, this work proves that the microarray platform was successful in screening for bacteria-receptor interactions and can also be used to screen for targeted modulatory compounds. This thesis also shows the different roles of PNAG in lectin-mediated interactions and innate immune system activation, and highlights the necessity of the surface expression and presentation of PAMPs for eliciting signalling responses.

# Chapter 1

# Introduction

# 1. Introduction

## 1.1. Nosocomial infections

According to a report from the World Health Organisation (WHO), 7.6% of patients in health care-associated environments acquired an infection in high-income countries from 1995 to 2010. In Europe, these infections resulted in 16 million extra days in hospital, costing €7 billion and resulted in 37,000 deaths. In the USA, 1.7 million patients acquired an infection in hospital between 1995 – 2010 and 99,000 died as a result of these infections (WHO, 2011). The ability of the pathogens that cause nosocomial infections to successfully reside in the host can be partially attributed to the multitude of mechanisms undertaken by the bacteria to resist antibiotics and manipulate or modulate host immune response. The so-called ESKAPE pathogens, *Enterococcus faecium*, *Staphylococcus aureus*, *Klebsiella pneumoniae*, *Acinetobacter baumannii*, *Pseudomonas aeruginosa* and *Enterobacter* spp., are the leading causes of nosocomial inflections globally and are known for their ability to 'escape' or resist treatment by antibiotics (Santajit & Indrawattana, 2016).

## 1.2. Biofilms and nosocomial infections

Biofilms are communities of microorganisms that encapsulate themselves within different substances, allowing them to attach to abiotic and biotic surfaces (Percival *et al.*, 2015). According to the U.S. Centre for Disease Control and Prevention (CDC) and the U.S. National Institute of Health (NIH), approximately up to 65% or 80% of nosocomial infections are associated with biofilms, respectively (Joo & Otto, 2012; Potera, 1999). Hospital-acquired infections usually originate from multiple sources, commonly a central line, catheter, surgical site or ventilator (WHO, 2011), and biofilms are frequently associated with infections. Implanted devices provide an entry route for bacteria, an abiotic surface for biofilm development and contribute to approximately 60-70% of nosocomial infections (Bryers, 2008). Bacteria encapsulated in this biofilm matrix are significantly less susceptible to antibiotic treatment and attack from the host immune system compared to planktonic cells (Bryers, 2008; Stewart, 2002), making medical device associated infections incredibly difficult to treat. This is primarily due to the fact bacteria within a biofilm matrix have a slower growth rate and adapt a more dormant lifestyle compared to

planktonic bacteria. These bacteria are often described as persister cells due to the fact that they are not replicating, causing antibiotics that target cell replication useless in killing these cells, and thus they persist within the biofilm and in the host (Lewis, 2007). Furthermore, the complex matrix of a biofilm renders antibiotics and immune cells less capable of penetration, allowing the bacteria to survive. As antibiotics prove to be insufficient for the treatment of biofilm associated infections, this results in chronic infections, and, if a medical device is involved, removal of the device and insertion of another is often required (Lebeaux *et al.*, 2014).

### 1.2.1. Biofilm formation

Biofilms are often described as communities of microorganisms, multi-species or single-species, commonly associated with medical device infections, that are attached to a surface (O'Toole *et al.*, 2000). Bacteria form a biofilm matrix by communicating with one another *via* quorum sensing to express proteins, polysaccharides and release DNA into the extracellular matrix (ECM). These macromolecules form a barrier around the bacterial community, preventing easy penetration of antimicrobial agents and immune cells reaching individual bacterial cells for destruction. Furthermore, bacteria within a biofilm matrix display altered growth rates, with cells in a more dormant state surviving antimicrobial challenges much better than cells growing at an optimal growth rate, allowing dormant cells to persist within the host contributing to chronic infections (Stewart, 2002).

### 1.2.2. Stages of biofilm formation

Biofilm formation occurs in different stages: attachment (reversible and irreversible attachment), colonisation, maturation and dispersion (Fig. 1.1), with the expression of proteins and/or polysaccharides and release of extracellular DNA playing important roles in different stages of development. Bacteria initially attach to a biotic or abiotic surface reversibly, then irreversibly to establish a matrix of microcolonies. Initial attachment of planktonic bacteria to a surface can be influenced by electrostatic interactions bacterial cell surface composition, shear forces and bacterial motility (Percival *et al.*, 2015). It has also been shown that a surface is not critical for biofilm development as described with cystic fibrosis, where *Pseudomonas aeruginosa* forms dense cell aggregates that are encapsulated in a matrix and located in the mucus (Römling & Balsalobre, 2012). For abiotic surfaces that are inserted

into the host, such as medical devices, these medical devices are usually coated with host ECM proteins that further aid attachment of bacteria to the abiotic surface. Following attachment, the biofilm undergoes maturation *via* cell aggregation (Fig. 1.2), matrix production and architecture remodelling with the help of bacteria-produced surfactants such as phenol soluble modulins (PSMs). As the biofilm matrix gets larger, intricate towers and channels are formed to allow for nutrient distribution throughout the biofilm (Arciola *et al.*, 2018). Finally, bacteria are dispersed from a biofilm matrix with the help of surfactants such as PSMs and rhamnolipids, nucleases and proteases. The production of surfactants is tightly controlled by quorum sensing, thus bacteria communicate with one another to disperse from a biofilm, helping them to infect other areas of the body (Kaplan, 2010; Solano *et al.*, 2014).

The WHO established carbapenen-resistant *A. baumannii* as a priority level 1 and methicillin-resistant and vancomycin intermediate resistant *S. aureus* as priority level 2 for the urgent need of research and development in to the development of antibiotics to tackle these bacteria (Tacconelli *et al.*, 2018). Furthermore, these two bacteria produce the same exopolysaccharide structure to promote biofilm formation, which further helps them to resist antibiotics. For these reasons, and taking into consideration that *S. aureus* is a Gram-positive and *A. baumannii* is a Gram-negative ESKAPE pathogen, this thesis will focus on these two species in detail.

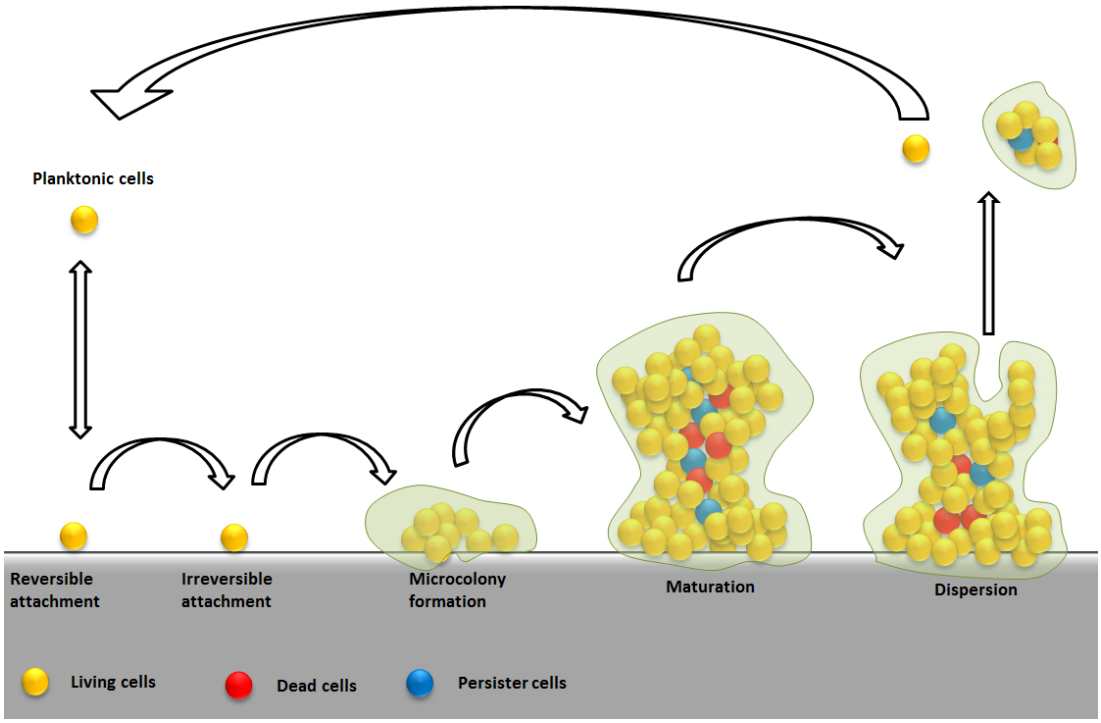


**Fig. 1.1. Stages of biofilm formation**. Diagram depicts the formation of biofilm that begin with planktonic bacteria reversibly attaching to an abiotic/biotic surface. Cells then irreversibly attach to the surface and form microcolonies. During attachment and microcolony formation, bacteria increase surface protein expression, produce extracellular polysaccharides and strategically lyse to release DNA into the biofilm matrix, promoting biofilm maturation. Bacteria also take on a persister phenotype and can be dormant within the biofilm matrix. With the help of surfactant and sheer force, biofilm microcolonies can detach to infect other areas of the body, or planktonic cells released can begin the formation of biofilm again.

### 1.2.3. Biofilm formation for *S. aureus* and *A. baumannii*

*Acinetobacter* species are part of the common skin microbiome, with the most frequent species colonising the skin being *A. lwoffii*, *A. johnsonii* and *A. junii*. In contrast, *A. baumannii* has been found on less than 1% - 4% of skin samples, yet is one of the most important and troubling pathogens in today's society (Berlau *et al.*, 1999; Chu *et al.*, 1999; Peleg *et al.*, 2008). *A. baumannii* is one of the most commonly detected bacteria isolated from biofilm-related catheter urinary tract, bloodstream infections and shunt-related meningitis (Rodríguez-Baño *et al.*, 2008), and is often associated with pulmonary infections in hospital settings. For example, *A. baumannii* pneumonia associated with ventilators correlates with a 75% mortality

rate (Fagon *et al.*, 1996). Furthermore, the ability of *A. baumannii* to withstand harsh antibiotic treatments has been correlated to its ability to form a biofilm (Babapour *et al.*, 2016; Krzyściak *et al.*, 2017). *S. aureus* colonises approximately 20% of the human population with the remainder being intermittently (approximately 60%) or never colonised (approximately 20%) (Kluytmans *et al.*, 1997). Following *S. epidermidis*, *S. aureus* is one of the most prevalent bacterial species in medical device infections (Arciola *et al.*, 2018). *S. aureus* is commonly isolated from catheter associated urinary tract infections, central-line associated septicaemia, ventilator-associated pneumonia and surgical-site infections (Percival *et al.*, 2015). Beyond medical device infections, *S. aureus* can cause biofilm related periodontitis and peri-implantitis, osteomyelitis, chronic wound infections, chronic rhinosinusitis, endocarditis, ocular infections and polymicrobial biofilm infections as part of complications of diseases such as cystic fibrosis (Archer *et al.*, 2011). Biofilm formation has been associated with increased resistance to antibiotics and shown to shield bacteria from the host's immune response (Donlan & Costerton, 2002; Hall & Mah, 2017; Otto, 2008).

With approximately 90% of the biofilm mass comprised of extracellular polysaccharides, proteins and DNA (Flemming & Wingender, 2010), a greater understanding of these extracellular components in terms of their regulation, host interactions and developing mechanisms of blocking these components is needed to tackle biofilm-related infections of *S. aureus* and *A. baumannii*.

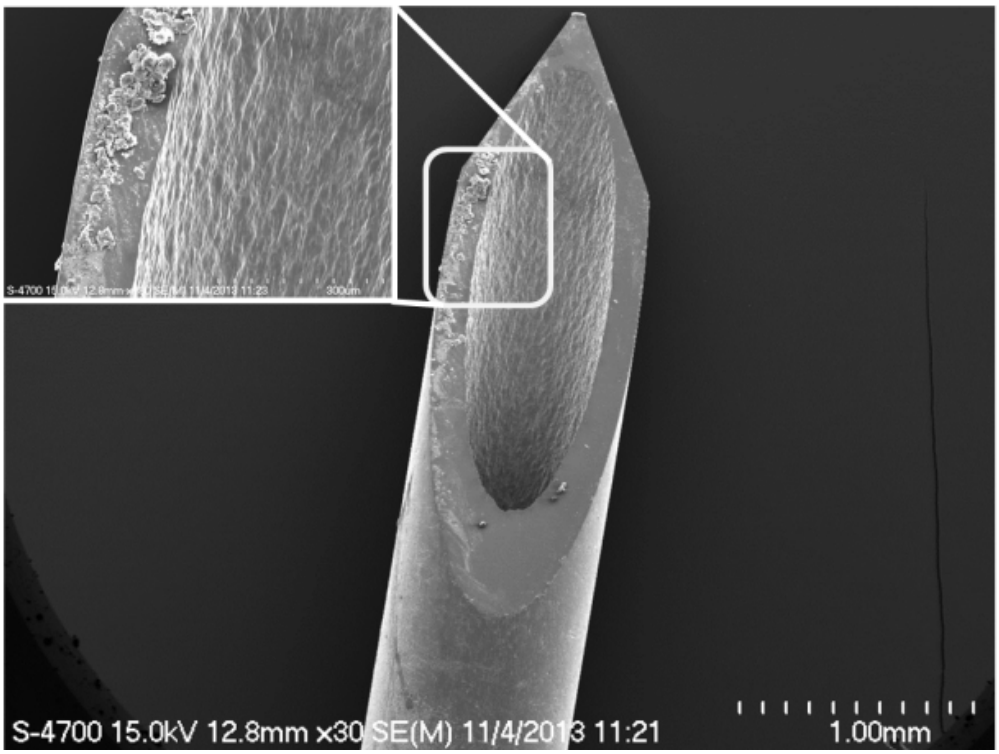


**Fig. 1.2. Staphylococcal biofilm on plastic and on a cannula. (**A) Scanning electron microscope (SEM) image scale at 1 μm (zoomed image at 300 μm) of *S. epidermidis* biofilm formation on cannula that would be used in the hospital setting.

### 1.2.4. Components promoting biofilm formation

A range of bacterial surface structures can contribute to initial attachment of bacteria to an abiotic surface. These are primarily physico-chemical interactions and are promoted by surface components such as lipoteichoic acids (LTA), wall teichoic acids (WTA), autolysins (Atl), pili and proteins (Berne *et al.*, 2015; Speziale *et al.*, 2014). Attachment to a medical device in the body often relies on these medical devices being coated with host ECM proteins such as fibronectin, fibrinogen and vitronectin for bacterial protein attachment (Zapotoczna *et al.*, 2016).

For *S. aureus*, there are many cell wall anchored proteins that are associated with biofilm formation, either in the attachment or accumulation stages. These include sortase-anchored surface proteins that contain a conserved C-terminal Leu-Pro-X-Thr-Gly (LPXTG) motif. Mutation of the sortase gene (*srtA*) results in reduced biofilm formation for *S. aureus*. These LPXTG-cell wall anchored proteins can include *S. aureus* surface protein G (SasG), fibronectin binding protein A and B (FnBPA and FnBPB), clumping factor B (ClfB) and *S. aureus* surface protein C

(SasC) (Abraham & Jefferson, 2012; Geoghegan *et al.*, 2010; O'Neill *et al.*, 2008; Schroeder *et al.*, 2009). Beyond the involvement of Atl in primary attachment, the endo-β-*N*-acetylglucosaminidase (GL) domain of this protein plays an important role in biofilm formation *via* mediated cell autolysis and release of DNA to become integrated into the biofilm matrix (Bose *et al.*, 2012).

On the other hand, *A. baumannii* relies heavily on Csu pili, the outer membrane protein OmpA and the biofilm-associated protein Bap (Gaddy *et al.*, 2009; Loehfelm *et al.*, 2008; Tomaras *et al.*, 2003). A Bap homologue is found in *S. aureus*, also termed as Bap, which has shown to be a crucial factor in biofilm formation associated with bovine mastitis and shown to build amyloid matrices. However, Bap has not been isolated from human *S. aureus* isolates (Taglialegna *et al.*, 2016).

Lectins are often involved in biofilm formation for bacteria. For example, the galactose specific lectin, LecA, and the fucose specific lectin, LecB, promotes biofilm formation for *P. aeruginosa* (Diggle *et al.*, 2006; Tielker *et al.*, 2005). The glucan-specific lectin of the *Streptococcus mutans* is also involved in biofilm formation for this dental pathogen (Lynch *et al.*, 2007). Furthermore, an outer membrane lectin associated with *Azospirillum brasilense* binds to EPS on the surface of the bacteria (Mora *et al.*, 2008). Although lectins have shown to be important in biofilm formation, it has not been determined whether lectins play a role in *S. aureus* or *A. baumannii* biofilm formation. Lectins have been identified on *S. aureus* and *A. baumannii*, for example, SraP on *S. aureus* binds to *N*-acetylneruaminic acid but this lectin has not been associated with biofilm formation (Yang *et al.*, 2014). *S. aureus* possesses a surface protein, SasG, that is involved in biofilm formation and is predicted to have a lectin domain *via* bioinformatic analysis, however this has yet to be confirmed *in vitro* (Sharif *et al.*, 2009; Speziale *et al.*, 2014). LysM on *A. baumannii* binds to peptidoglycan and hypothesised to play a role in cell attachment to abiotic surfaces (Cabral *et al.*, 2011). Beyond the above mentioned lectins, there has been very little research carried out to determine whether *S. aureus* and *A. baumannii* have lectins which bind to carbohydrates and whether these lectins play a role in biofilm formation for these pathogens.

### 1.2.5. Poly-*N*-acetylglucosamine and biofilm formation

Poly-*N*-acetylglucosamine (PNAG) is another common component involved in biofilm formation for both *S. aureus* and *A. baumannii*. The first reports of PNAG were described in *S. epidermidis* and the polysaccharide was referred to as polysaccharide/adhesion (PS/A), slime-associated antigen (SAA) and polysaccharide intercellular adhesion (PIA) (Baldassarri *et al.*, 1996; Mack *et al.*, 1996; McKenney *et al.*, 1998). Verification that these extracellular polysaccharides were the same was first carried out by McKenney *et al.* (1998), followed by reports that *S. aureus* produced the same polymeric substance at a later date. These reports showed that the extracellular polymeric substance was nearly identical in all cases (Jefferson *et al.*, 2003; McKenney *et al.*, 1999). PNAG is also referred to as polyglucosamine (PGA) in Gram-negative bacteria, poly-NAG, hms+ (*Y. pestis*) and *Bordetella* polysaccharide (BPS) in *Bordetella* species (Whitfield *et al.*, 2015).

Following structural identification of this polysaccharide, development of an antibody that targets PNAG and standardised methods to purify the polysaccharide, PNAG was identified as a polymer of β-(1,6)-linked *N*-acetylglucosamine with 5-50% of the amine groups deacetylated, depending on the organism, genus and species that produces the PNAG (Fig. 1.3). PNAG *O*-succinylation has been described in Gram-positive bacteria such as *S. epidermidis* and *S. aureus*, with between 6 – 10% of GlcNAc polymers being *O*-succinylated, respectively (Joyce *et al.*, 2003; Sadovskaya *et al.*, 2005). PNAG expression is associated with a wide range of bacteria including *Enterococcus faecium* and *Enterobacteria* species, and has been associated with biofilm formation by *Staphylococcus* species, *Klebsiella pneumoniae* and *A. baumannii* (Chen *et al*., 2014; Choi *et al*., 2009; Cywes-Bentley *et al*., 2013; Maira-Litrán *et al*., 2002). PNAG is also expressed on fungi and protozoan parasites as well as Gram-positive and Gram-negative bacteria. To date, PNAG has been shown to play important roles in biofilm formation and bacterial pathogenesis (Choi *et al.*, 2009; Ferreirinha *et al.*, 2016; Lin *et al.*, 2015; Maira-Litran *et al.*, 2004), but specific interactions between PNAG and the immune system and consequential immunomodulatory effects have not been thoroughly investigated, especially for PNAG associated with *S. aureus* and *A. baumannii*.

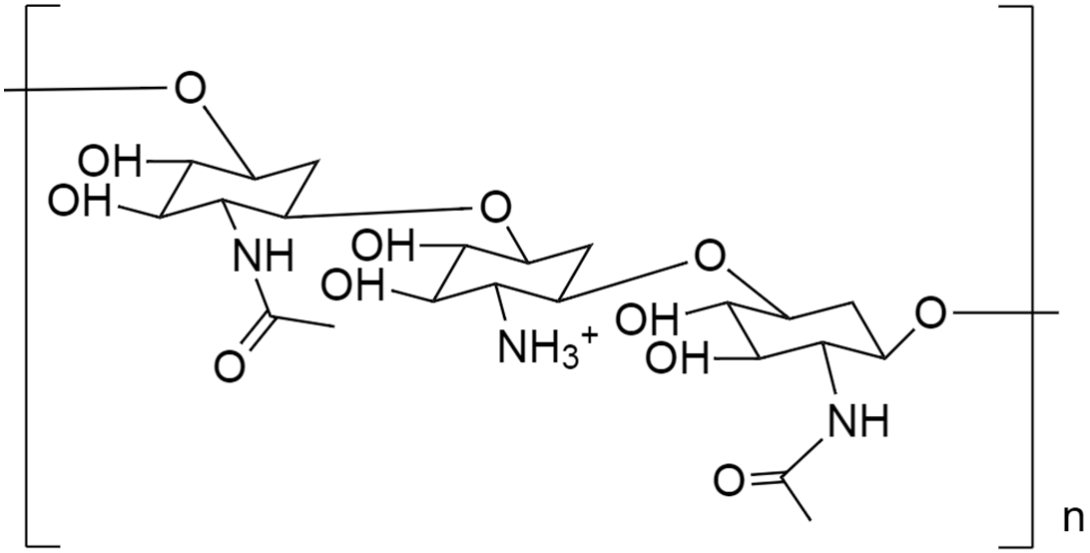


**Fig. 1.3. Structure of PNAG.** Image of PNAG consisting of β-(1,6)-linked *N*-acetylglucosamine. Deacetylation of PNAG can vary between 5-50%, depending on the genus and strain that produces the polysaccharide.

### 1.2.6. Proteins involved in PNAG production

PNAG production relies on the presence of a 4 gene locus, denoted *icaADBC* in Gram-positive bacteria, and *pgaABCD* in Gram-negative bacteria or the *hms* or *bps* operon in *Y. pestis* or *Bordetella* sp., respectively (Choi *et al*., 2009; Maira-Litrán *et al*., 2002; Wang *et al*., 2004). IcaAD and PgaCD produce GlcNAc oligomers of approximately 20 residues and export PNAG out of the cell (Gerke *et al.*, 1998). With the help of IcaC, long chains of PNAG are produced and it has also been suggested that IcaC is involved in translocation of PNAG out of the cell, while others hypothesise that IcaC adds *O*-succinate to the PNAG polymer of certain bacteria (Atkin *et al.*, 2014). IcaB is necessary for deacetylation of the PNAG polymer and attachment to the bacterial cell wall. PgaB deacetylates and hydrolyses deacetylated PNAG in Gram-negative bacteria and exports the polysaccharide out of the cell through the PgaA porin (Little *et al.*, 2018; O'Gara, 2007; Whitfield *et al.*, 2015). Although both IcaB and PgaB deacetylate PNAG, the architecture and localisation of the two proteins in Gram-positive and Gram-negative bacteria is drastically different. IcaB in Gram-positive bacteria is a single domain protein that resides on the surface of the bacteria, while PgaB is a two-domain lipoprotein located in the periplasm and has been predicted to have a carbohydrate binding

domain (Fig. 1.4) Using HHpred, this carbohydrate binding domain of PgaB had a match to the N-terminal domain of *Thermus thermophiles* β-galactosidase, and hypothesised that this domain binds to unmodified PNAG (Itoh *et al.*, 2008). Similarly, it has been suggested that the electropositive patch on IcaB and its location situated on the outside of the cell would be suitable for interacting with negatively charged phosphate groups such as LTA (Little *et al.*, 2014). Three different PNAG fractions were isolated from *S. aureus* Mn8m that had average masses of 460 kDa (PNAG I), 100 kDa (PNAG II) and 21 kDa (PNAG III). From PNAG III, a small fraction of PNAG was isolated with a molecular weight of approximately 780 kDa (Maira-Litrán *et al.*, 2002). To the best of our knowledge, the molecular weight and/or oligomer length of PNAG isolated from *A. baumannii* has not been investigated.

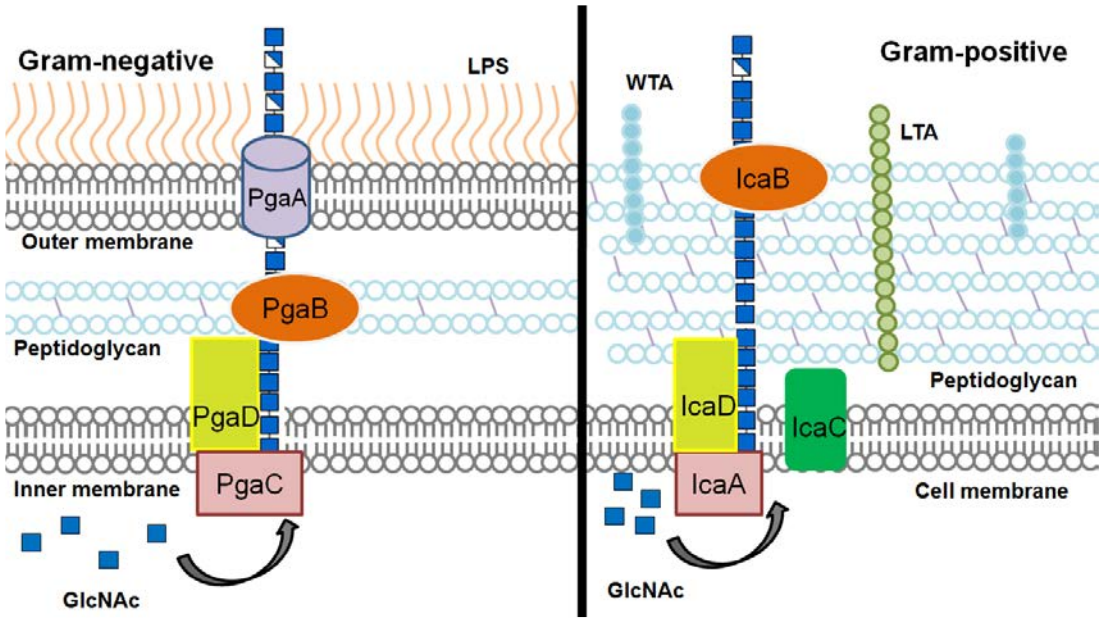


**Fig. 1.4. PNAG production in Gram-negative and Gram-positive bacteria.** PgaC/D and IcaA/D produce GlcNAc polymers. IcaC is hypothesised to help GlcNAc polymers out of the cell or to be involved in *O*-succinylation of the GlcNAc polymer. PgaB and IcaB deacetylate the GlcNAc polymer and for Gram-positive bacteria, IcaB promotes PNAG retention to the cell wall. PgaA in Gram-negative bacteria acts as a porin to release PNAG into the extracellular matrix.

### 1.2.7. PNAG and the immune system

Most of the research on PNAG and how it affects the immune system has been carried out with *S. epidermidis* wildtype (WT) and PNAG deficient mutants (Δ*ica*).

For *S. epidermidis*, the presence of the *ica* operon and PNAG on the cell surface, promoted protection against phagocytosis and killing by human polymorphonuclear leukocytes (PMNs) (Vuong *et al.*, 2004), while PNAG extracted from *S. epidermidis* biofilm prevented bacteria from antibody-mediated phagocytosis. Interestingly, in the same study, it was found that PNAG did not block antibody diffusion through the biofilm matrix (Cerca *et al*., 2006). Furthermore, it was shown that the presence of PNAG interferes with the activation of macrophages (Schommer *et al.*, 2011). WT *S. epidermidis* also induced the expression of more C3a compared to the Δ*ica* mutant, suggesting that PNAG may trigger an immune response. However, WT *S. epidermidis* were more resistant to human PMN killing, C3b and IgG deposition compared to the Δ*ica* mutant strain, indicating that PNAG and biofilm play a role in preventing the attachment of immune proteins to the bacterial cell surface, aiding survival within the host (Kristian *et al.*, 2008). Similarly, Aarag Fredheim *et al.* (2011) found that a PNAG producing *S. epidermidis* WT strain induced a higher degree of complement activation compared to the *ica* isogenic mutant in a human whole blood model (Aarag Fredheim *et al.*, 2011). *In vivo*, the presence of the *ica* operon and PNAG exacerbates host inflammation in a murine model of infection (Ferreirinha *et al.*, 2016). Therefore, from research carried out with PNAG from *S. epidermidis* to date would suggest that PNAG triggers an immune response but evades subsequent killing. However, there is debate as to whether PNAG is the actual causative agent in these instances as PNAG is difficult to purify. Furthermore researchers have suggested that interactions with pathogen recognition receptors (PRRs), such as TLR2 are due to contaminating lipoproteins in purified preparations (Nguyen *et al*., 2017). We hypothesise that *ica* mutants have drastically different cell surfaces compared to the WT, making it difficult to attribute changes seen in previous research to PNAG alone. Thus, there is a great need for research to be carried out to elucidate whether PNAG interacts with the host, and the corresponding consequences of these interactions.

Although there is much less data available for *Escherichia coli* and *S. aureus*, PNAG associated with *E. coli* O157:H7 was not required for binding to mammalian cells (Matthysse *et al.*, 2008). For *S. aureus*, PNAG was shown to be involved in binding to nasal epithelial cells and crucial for lung infection development in a mouse model (Lin *et al.*, 2015). Most research in to PNAG derived from *S. aureus* and the immune

system to date has focused on the capability to produce functional antibodies to target PNAG. Natural antibodies against PNAG were not functional and did not provide protection by mediating opsonisation *via* complement or bacterial killing. Natural antibodies against PNAG bound to the polymer *via* the acetyl groups, however, this resulted in the Fc regions of antibodies not in close proximity, which prevented binding to C1q and activation of the complement cascade (Skurnik *et al.*, 2016). Deacetylation of PNAG proved to be crucial in the deposition of C3 and consequent opsonisation. Therefore, a monoclonal antibody named F598 was produced which targeted deacetylated and acetylated PNAG and proved to be a successful antibody for opsonophagocytic activity in a *S. aureus*-infected mouse model (Kelly-Quintos *et al.*, 2006).

Despite investigations into how PNAG interacts with the adaptive immune response and the classical pathway of complement in *S. aureus*, there is a clear lack of data investigating the interactions and innate immune response to PNAG associated with *S. aureus*, and PNAG from other Gram-negative bacteria such as *A. baumannii*.

### 1.3. Bacterial cell surface carbohydrates beyond PNAG

Besides PNAG, other surface molecules on the surface of many Gram-positive and Gram-negative bacteria play important roles in cell homeostasis, biofilm formation, attachment, host recognition and immune evasion. The bacterial glycome represents all of the structural carbohydrates and carbohydrate-binding proteins, or lectins, expressed by a bacterium. These can include carbohydrates attached to proteins (glycoproteins) or lipids (glycolipids) and cell-surface polysaccharides. The structures and presentation of the cell surface polysaccharides can differ greatly depending on whether the bacteria is Gram-positive or Gram-negative, the species and strain of bacteria, and can be influenced by environmental factors including cell population density, pH, osmolarity, etc. (Götz, 2002; Laverty *et al.*, 2014). Cell surface carbohydrate-containing structures can include lipopolysaccharides (LPS), lipooligosaccharides (LOS), peptidoglycan, capsular polysaccharides (CPS), teichoic acid (TA) and extracellular polysaccharides such as PNAG (Kay *et al.*, 2010).

There are approximately ten monosaccharides common to mammals, including glucose, mannose, galactose, *N*-acetylglucosamine, *N*-acetylgalactosamine, glucuronic acid, galacturonic acid, fucose, and *N*-acetylneuraminic acid. On the other

hand, bacteria can contain many other residues that are not commonly found in humans such as *N*,*N*′-diacetylbacillosamine, *N*-acetylfucosamine, D-arabinofuranose, hexuronic acids, heptose and pseudaminic acid and do not follow the highly conserved template of mammalian glycosylation. Furthermore, bacteria have diverse methods of glycosylation including *N*-, *S*- and *O*-linked glycosylation (Hirabayashi *et al.*, 2013; Tan *et al.*, 2015). As carbohydrates associated with bacteria are frequently involved in pathogen-host interactions, methods to uncover the carbohydrate-containing components of bacteria are urgently needed to help develop drugs and therapeutics to target these interactions.

### 1.3.1. Carbohydrate-mediated microbial-host interactions

One of the first steps in pathogenesis is bacterial attachment to the host. The host often detects pathogens *via* recognition of carbohydrate structures on the bacterial cell surface. Attachment and host recognition of pathogens is usually mediated by carbohydrate-protein interactions. Indeed, microbes and their products can target particular cells or organs due to exclusively expressed carbohydrate structures (Sattin & Bernardi, 2016). For example, *Helicobacter pylori* binds to Lewis b ($Le^b$) and sialylated structures on epithelial cells, *Vibrio cholerae* toxin binds the ganglioside GM1, *E. coli* binds mannosylated structures on uroepithelial cells and Group A *Steptococcus* binds type 1 blood group H (Poole *et al.*, 2018).

Lectins of the host immune system, termed pathogen recognition receptors (PRRs), play an important role by recognising carbohydrates on microorganisms to subsequently clear infection. For example, Toll-Like Receptors (TLRs) recognise bacterial peptidoglycan and LPS, DC-SIGN recognises LPS of *E. coli*, dectin-1 recognises β-glucan on fungi and siglecs recognise sialic acids on LPS and glycoproteins (Brown *et al.*, 2003; Iwaki *et al.*, 2002; Klena *et al.*, 2005; MacAuley *et al.*, 2014; Oliveira-Nascimento *et al.*, 2012). However, microorganisms often exploit these interactions to subvert the immune system and persist in the host (Hajishengallis & Lambris, 2011). For instance, mycobacteria, *Candida albicans* and HIV-1 virus inhibits TLR-mediated immune responses *via* interactions with siglec-5 or -9, and phase variation of fucosylation on *Helicobacter pylori* LPS suppresses immune responses through DC-SIGN (Bergman *et al.*, 2004; Geijtenbeek *et al.*, 2003; Gringhuis *et al.*, 2007). Therefore, investigation of the mechanisms of

interfering with carbohydrate-mediated interactions have gained immense momentum in recent years, especially as proposed alternative routes to tackle microbes that are resistant to antibiotics, such as the ESKAPE pathogens.

### 1.3.2. Modulating carbohydrate-mediated microbial-host interactions

Glycoconjugates and glycomimetics have been explored in recent years as sugar antagonists and have proven successful as anti-adhesives and anti-infectives. In urinary tract infections, uropathogenic *E. coli* (UPEC) uses a lectin on fimbriae called FimH which binds α-mannopyranosyl structures on urothelial cells (Hung *et al.*, 2002). This finding has encouraged the development of different multivalent structures which targets FimH, including multimeric heptyl mannosides (Almant *et al.*, 2011; Gouin *et al.*, 2009), glycodendrimers (Imberty *et al.*, 2008), glycoclusters (Lindhorst *et al.*, 1998) and glycopolymers (Yan *et al.*, 2015). Interestingly, glyco-nanodiamonds have been used to prevent *E. coli* adhesion to bladder cells and have also proven to disrupt biofilm (Khanal *et al.*, 2015). Similarly, glycoclusters have been developed to inhibit lectin-mediated *P. aeruginosa*-host interactions to tackle infections associated with cystic fibrosis (Boukerb *et al.*, 2014). Multivalent glycoclusters reduced the bacterial load of *P. aeruginosa* in a lung infection mouse model and decreased lung permeability (Boukerb *et al.*, 2014). To our knowledge, there has been no other *in vivo* models to show the efficacy of glycoclusters preventing *P. aeruginosa* infections.

Glycoconjugates and glycomimetics have been developed to disrupt PRRs binding to carbohydrates on microorganisms that lead to persistent infections. An example of this is dendritic cell-specific ICAM-3 grabbing non-integrin (DC-SIGN) interactions with HIV. DC-SIGN usually recognises, internalises and degrades pathogens for dendritic cells. Degraded pathogen fragments are then presented on the cell surface for $CD4^+$ T cells. However, HIV has developed a way to avoid degradation, allowing the virus to be presented and transmitted via $CD4^+$ T cells (Sattin *et al.*, 2016). DC-SIGN plays a crucial role in HIV infection by providing the virus with a mechanism for entry and hijacking the immune system to spread within the host (Hajishengallis *et al.*, 2011). Many other viruses, such as Ebola and Dengue, have used DC-SIGN to evade the immune system (van Kooyk & Geijtenbeek, 2003). Therefore, anti-adhesives have been developed with the aim of blocking microorganisms

manipulating the host immune system, leaving them vulnerable for destruction. As DC-SIGN recognises mannosylated and fucosylated structures, mannose and fucose antagonists have been successfully developed to prevent DC-SIGN manipulation *in vitro* (Anderluh *et al.*, 2012). These include glycodendrimers (Garcia-Vallejo *et al.*, 2013; Lasala *et al.*, 2003; Tabarani *et al.*, 2006), manno-dendronanoparticles that resembled viruses (Ribeiro-Viana *et al.*, 2012) and glycopolymers (Q. Zhang *et al.*, 2013).

### 1.3.3. Detecting bacterial carbohydrates

Conventional methods of analysing carbohydrates include mass spectrometry (MS), liquid chromatography (LC), capillary electrophoresis (CE) and nuclear magnetic resonance (NMR) and chemical assays, while profiling carbohydrate compositions is frequently carried out with high-performance liquid chromatography (HPLC), if the mixture contains less than 50 different carbohydrates. Carbohydrate analysis via MS, LC, CE, NMR or HPLC requires the carbohydrates to be liberated from their source such as a protein or cell wall prior to analysis. Furthermore, carbohydrates lack UV absorption unlike proteins, and must be fluorescently labelled for separation and detection using HPLC. Fluorescent labelling carbohydrates is also often carried out with MS to improve ionisation efficiency. These methods can often require great expertise, are time consuming and laborious (Hirabayashi *et al.*, 2013; Hsu *et al.*, 2006).

Lectins have been used for many years as an alternative approach to help profile different carbohydrate containing structures. Lectin affinities towards different carbohydrates have been extensively elucidated for mammalian glycosylation, therefore, specific ligands for different lectins are known and exploited to isolate and detect different glycosylated molecules. Lectins are used with different methods including lectin-probed Western blot analysis, flow cytometry and histochemical staining, as well as carbohydrate-mediated fractionation using lectin-affinity chromatography. However, these methods are time-consuming and often require high concentrations of reagents, samples and lectins for analysis. One technology that provides a sensitive, high-throughput platform for lectin interactions is the lectin microarray platform (Hirabayashi *et al.*, 2013; Hu & Wong, 2009).

### 1.3.4. Microarray platforms

Microarrays consist of a functionalised glass slide with molecules conjugated to the glass slide through appropriate slide surface chemistry. Coated and functionalised slide surfaces include aldehyde, epoxide, nitrocellulose, polylysine, hydrogel and maleimide (Wang *et al.*, 2014). Often proteins, such as lectins, are immobilised to the glass surface and residual activated groups on the slide are blocked with a blocking agent containing agents such as amines (ethanolamine or Tris base) or periodate-treated albumin. Carbohydrates incubated on lectin microarrays are directly or indirectly labelled with a fluorescent dye/probe prior to incubation. Direct labelling of carbohydrates requires free functional groups for fluorescent probe conjugation, which can often be difficult. Alternatively, glycoproteins are fluorescently labelled or whole bacteria containing the carbohydrate(s) of interest are labelled with an intercalating nucleic acid stain, and subsequently incubated on the lectin microarray platform for profiling. Bound carbohydrates can also be detected using fluorescently labelled antibodies. In this instance, the target molecule must be known in advance to choose a specific antibody and good controls must be in place to eliminate the chance antibody glycosylation causing false positive interactions with lectins on the microarray (Hirabayashi *et al.*, 2013).

Besides lectins, microarray platforms have been used for a number of different applications including, but not limited to, DNA, glycans (including neoglycoconjugate and bacterial), mucins, antibodies, extracellular vesicles and lipids (Feng, 2005; Heller, 2002; Jørgensen *et al*., 2013; Kilcoyne *et al*., 2012; Stowell *et al*., 2014; L. Wang *et al*., 2014; Wingren & Borrebaeck, 2006). Regarding bacteria, microarray platforms have been used to profile bacterial surface glycosylation with the use of lectin microarray technology (Hsu *et al.*, 2006; Yasuda *et al.*, 2011). Bacterial interactions with mucins (Naughton *et al.*, 2013) and carbohydrates (Flannery *et al.*, 2015) have also been elucidated with microarray technology to elaborate bacterial adhesin specificity. Finally, whole bacteria and bacterial carbohydrates have been printed on microarray platforms for interactions with different lectins (Campanero-Rhodes *et al.*, 2015; Stowell *et al.*, 2014). Although there have been significant advances in the field of microarray technology and in applications to benefit host-pathogen interactions, there lacks a microarray platform to provide high throughput (HTP) analysis of bacteria and/or bacterial

carbohydrate interactions with the host's first line of defence against invading pathogens – the innate immune system.

### 1.4. The innate immune response against bacteria

When bacteria come in contact with a human, the first mechanism of defence they will encounter is the innate immune system. The innate immune system can eliminate many microbial challenges without the requirement of pre-existing encounters or previous memory of the bacteria. This is because the innate immune system comprises cells that are selective for specific markers on bacteria, but are not antigen-specific. Identification of a broad range of microbial components allows cells of the innate immune system to identify invading pathogens quickly and have a rapid response leading to elimination of the bacteria. Furthermore, the innate immune system plays an important role in the activation of the adaptive immune response. Cells that play a role in the innate immune system include mast cells, natural killer cells, monocytes, macrophages, dendritic cells, neutrophils, eosinophils and basophils. Each of these cell types have an array of common or cell-specific PRRs displayed on the cell surface. Initial recognition of invading pathogens by PRRs leads to the production of cytokines, chemokines, complement proteins and antimicrobial peptides, promoting the elimination of invading pathogens (Rivera *et al.*, 2016; Tosi, 2005).

The innate immune system detects antigens on bacteria, which are called PAMPs. PRRs detect PAMPs to activate the innate immune response and can be bound to the membrane of cells or soluble in the serum (Lu *et al.*, 2002; Takeuchi & Akira, 2010). When a PRR recognises a PAMP, this leads to activation of complement and/or signalling responses to regulate the production of cytokines and chemokines and cellular recruitment to the site of infection (Gasteiger *et al.*, 2017). Usually PRR-bacterial interactions are more complex than a one-to-one binding between a PRR and a bacterial ligand. Instead, an array of PRRs and receptors interact with an array of microbial surface molecules causing a highly orchestrated immune response *via* cross-talk between different PRR receptors (Fig. 1.5). The innate immune system succeeds to protect the human body from growing infections more times than not, however, bacteria have evolved to manipulate signalling and cross-talk associated with the innate immune system to evade killing. For example, bacteria such as

*Mycobacterium tuberculosis* and *H. pylori* promote cross-talk between TLRs and DC-SIGN leading to an increased production in the anti-inflammatory cytokine, IL-10, by dendritic cells (Hajishengallis *et al.*, 2011). Soluble PRRs found in the human serum are often associated with the complement cascade and membrane-bound PRRs, like some TLRs and DC-SIGN, are frequently associated with cell-mediated signalling responses (Mak & Saunders, 2006).

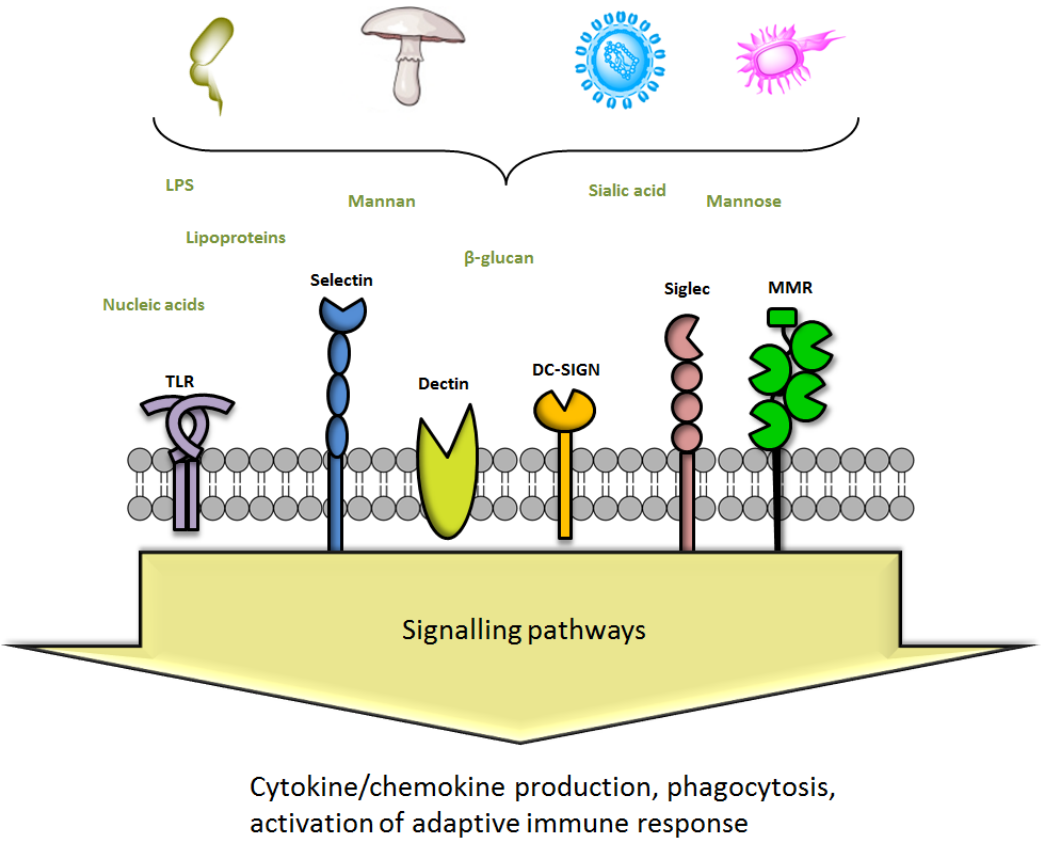


**Fig.1.5. PRR recognition of microorganisms.** PRRs such as TLRs, selectins, dectins, siglecs and MMR recognise specific carbohydrates associated with microorganisms to activate signalling pathways to promote cytokine, chemokine, phagocytosis and/or activation of the adaptive immune response.

The sections below will focus on the known interactions of PRRs with *S. aureus* and *A. baumannii*, focusing specifically on bacterial surface components responsible for these interactions.

### 1.4.1. Complement

The complement cascade plays an imperative role in the innate immune response and links the innate and adaptive immune response together. Complement proteins co-ordinate sequential enzymatic cascades to promote pathogen recognition, opsonisation and bacterial lysis. The complement cascade that leads to bacterial elimination requires protein fragments to become activated when they are non-covalently associated together in a sequential manner. These activated proteins form a convertase that cleaves proteins for the next complex in the enzymatic cascade. The dissociated complexes promote phagocytosis, cell lysis, antigen presentation, chemotaxis and opsonisation. There are three different pathways that converge on the formation of a C3 convertase: the classical pathway, the alternative pathway and the lectin pathway (Fig. 1.6). C3 convertase cleaves the protein C3, forming C3a and C3b. C3a acts as a chemoattractant for neutrophil recruitment while C3b covalently attaches to the microbial surface serving as an opsonin. C3b also binds to C3 convertases, forming a C5 convertase. This C5 convertase cleaves C5 generating C5a and C5b. C5a serves as a chemoattractant and anaphylatoxin. C5b initiates assembly of C6, C7 C8 and C9 to form the membrane attack complex (MAC) – a multiprotein structure that inserts into the bacterial membrane, forming a pore and eventually causing cell lysis (Fig. 1.6) (Nesargikar *et al.*, 2012; Song *et al.*, 2000).

As the lectin pathway primarily recognises carbohydrates, this pathway will be discussed in further detail with regard to mannose binding lectin (MBL), ficolin and collectin interactions with *S. aureus* and *A. baumannii*.

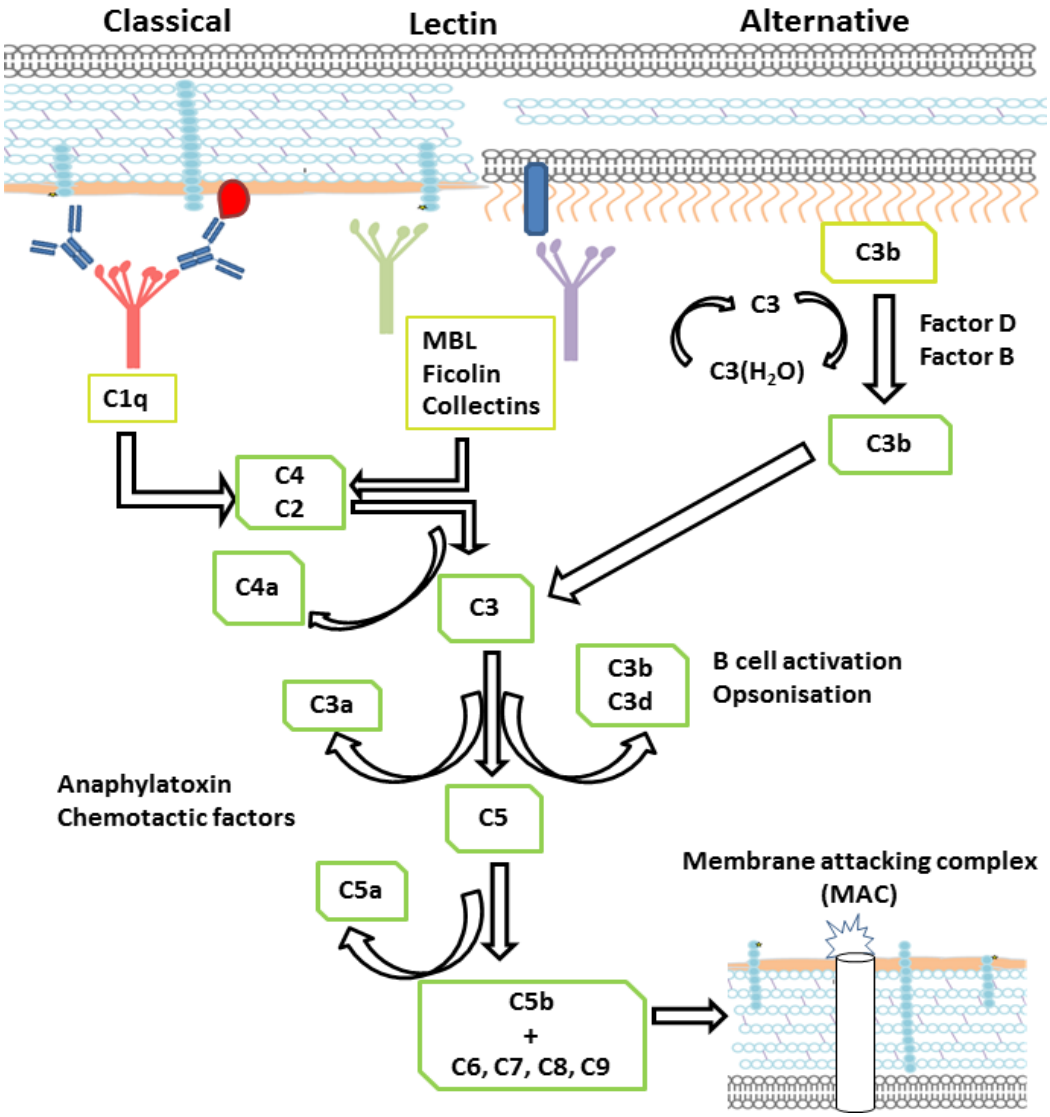


**Fig. 1.6. Overview of the complement cascade.** The complement cascade is initiated via three pathways: the classical, the lectin and the alternative pathway. The classical pathway involves C1q binding to antibodies on a microbial surface. The lectin pathway involves lectins (MBL, ficolins and collectins) binding to microbial carbohydrates. Finally the alternative pathway is constantly in a state of low activation, where C3 is continuously being hydrolysed to form C3b. C3b (or C3i) binds to Factor B, which is then cleaved by Factor D to form active C3b. When a microbe is present, C3b binds to the microorganism and heightens the alternative pathway response. All pathways converge to activate C3 and cleaves C3 in to C3a (anaphylatoxin) and C3b. C3b acts as an opsonin and remains bound to the microorganism to activate C5. C5 is then cleaved into C5a (chemoattractant for macrophages, neutrophils and activation of mast cells) and C5b. C5b remains attached to the microorganism and follows with the binding of C6, C7, C8 and eventually C9. This complex forms a pore in the microorganism called a membrane attack complex (MAC), promoting cell lysis.

The lectin pathway comprises of multimeric collectins that recognise carbohydrate moieties, such as PAMPs associated with microorganisms or carbohydrate structures on apoptotic, malignant, oxygen-deprived and necrotic cells (Fujita, 2002). Humans have MBL, CL-10 (collectin-1/CL-L1), CL-11 (collectin-11/CL-K1) and three ficolins: ficolin-1 (M-ficolin), ficolin-2 (L-ficolin) and ficolin-3 (H-ficolin), all of which are involved in the lectin pathway. Binding of MBL, ficolins, CL-10 or CL-11 to PAMPs triggers activation of the lectin pathway of the complement cascade by formation of a complex with the serine protease, MBL-associated serine protease (MASP). There are three MASPs – MASP-1, MASP-2 and MASP-3. Activated MASP cleaves C4 and C2 to form a C3 convertase from C2b and C4b, and converge with the classical and alternative pathways at this point (Fig. 1.6) (Garred *et al.*, 2016; Nesargikar *et al.*, 2012). Although the complement cascade is an efficient and often successful mechanisms of eradicating pathogens from the host, bacteria such as *S. aureus* have proteins like Eap that can block the lectin pathway at C3 activation (Woehl *et al.*, 2014). Therefore, understanding the interactions of bacterial cell surface molecules and PRRs associated with the complement cascade are crucial in understanding the pathogenesis of ESKAPE pathogens such as *S. aureus* and *A. baumannii*.

#### 1.4.1.1 Ficolins

Ficolins are multimeric lectins that closely resemble the well characterised MBL in that ficolins have a collagen-like domain. However, ficolins contain both a fibrinogen-like domain and a collagen-like domain (Kilpatrick & Chalmers, 2012). The ficolins contain an N–terminal domain, a collagen–like domain and, characteristic of ficolins, a fibrinogen–like domain. Ficolins are $Ca^{2+}$ dependent lectins and bind carbohydrates through their C-terminal fibrinogen-like domain (Fig. 1.7) (Ohashi & Erickson, 1998).

Ficolin-1 mRNA expression has been identified in lungs and leukocytes (Endo *et al.*, 1996; Harumiya *et al.*, 1996; Teh *et al.*, 2000), while expression of ficolin-1 protein has been found in secretion granules in neutrophil and monocyte cytoplasms, and also in type II alveolar lung epithelial cells (Liu *et al.*, 2005). Ficolin-1 recognises acetylated structures including *N*-acetylglucosamine (GlcNAc), *N*-

acetylgalactosamine (GalNAc), acetylated non-carbohydrates and sialic acid (Frederiksen *et al.*, 2005; Kjaer *et al.*, 2011; Y. Liu *et al.*, 2005; Teh *et al.*, 2000).

Ficolin-2 mRNA expression has been detected in myeloid and non-myeloid cell (such as the liver), and lymphoid cells and is subsequently found in serum (Kuraya *et al.*, 2003; Matsushita *et al.*, 1996). Ficolin-2 binds to acetylated carbohydrates, including GlcNAc, sialic acid, heparin, capsular polysaccharide and indeed to non-carbohydrate acetylated molecules (Aoyagi *et al.*, 2008; Gout *et al.*, 2010; Krarup *et al.*, 2004). Moreover, glycan microarray analysis has revealed that ficolin-2 does not bind to many acetylated mammalian oligosaccharides, but instead most likely requires multiple acetylated ligands in a particular conformation for recognition and binding (Krarup *et al.*, 2008). Ficolin-2 has also been shown to bind to (1→3)-β-D-glucan and DNA (Jensen *et al.*, 2007; Ma *et al.*, 2004).

Ficolin-3 mRNA is produced in the lung and the liver. Bile duct epithelial cells and hepatocytes produce ficolin and secrete the lectin into the bile duct, while Type II alveolar epithelial cells and ciliated bronchial epithelial cells secrete the lectin in to the bronchus and alveolus (Akaiwa *et al.*, 1999). Furthermore, ficolin-3 is produced in glioma cells suggesting that ficolin-3 may be expressed in the brain (Kuraya *et al.*, 2003). Ficolin-3 has shown affinities towards GlcNAc, GalNAc and D-fucose (Matsushita *et al*., 1996; Sugimoto *et al*., 1998).

Ficolins bind to carbohydrate antigens on the surface of bacteria to activate the lectin pathway. Here, ficolins form complexes with MASPs as well as the small MBL-associated protein (sMAP), which does not have a serine protease domain present (Fujita, 2002). This ficolin–MASP complex, binding to bacterial antigens causes MASP-2 to change from an inactive (a proenzyme consisting of a single polypeptide chain), to an activated structure (two polypeptide chains). Activated MASP-2 proteolytically cleaves C4 and C2, resulting in a C4bC2a complex, generating a C3 convertase, which in turn cleaves C3 into C3a and C3b (Fujita, 2002; Matsushita *et al.*, 2000; Matsushita, 2013). Ficolin-3 has shown the highest capacity to activate complement, compared to and ficolin-1 and -2 (Fig. 1.6) (Hummelshoj *et al.*, 2008).

*S. aureus* has many acetylated structures on its cell surface that would provide potential ligands for ficolins and in turn activate the complement pathway. These acetylated structures include WTAs (O–GlcNAc), CPSs (structures including

ManNAc, FucNAc and GalNAc), peptidoglycan (GlcNAc and MurNAc), LTA on some *S. aureus* strains (α-linked GlcNAc) and the polymeric substance involved in biofilm formation, PNAG (Maira-Litrán *et al*., 2002; Morath *et al*., 2001; Müller-Anstett *et al*., 2010; O'Riordan & Lee, 2004; Sharif *et al*., 2009; Winstel *et al*., 2015) while many other undiscovered surface carbohydrates may also serve as potential ligands for PRRs such as ficolins.

Liu *et al.* (2005) showed the binding of whole *S. aureus* cells to recombinant ficolin-1 *via* flow cytometry. This binding was inhibited by GlcNAc, suggesting that this *S. aureus* and ficolin-1 interaction was mediated via GlcNAc on the surface of *S. aureus* (Liu *et al.*, 2005). Contrary to this finding, a similar study was carried out to investigate *S. aureus*–ficolin-1 interactions and did not see any evidence of *S. aureus* binding to ficolin-1. This study did not use flow cytometry, but instead involved incubating whole bacteria with recombinant ficolin-1 for 2 hours, pelleting the bacteria cells and quantifying unbound ficolin-1 in the supernatant via a method based on a sandwich-type time-resolved immunofluorometric assay (TRIFMA). Here, no binding of capsulated or noncapsulated *S. aureus* was seen to ficolin-1. In fact, no binding of *S. aureus* to ficolin-1, -2 or -3 was observed in this study (Kjaer *et al.*, 2011).

The same group carried out similar binding studies with *S. aureus*, but focused on ficolin-2 and -3. Using the same bacterial binding assay, Krarup *et al.* (2005) found that several capsulated *S. aureus* strains were capable of binding to ficolin-2, whereas the noncapsulated control did not show binding to ficolin-2. This suggests that ficolin-2 may recognise specific structures associated with some capsulated serotypes, and not others. However, none of the capsulated *S. aureus* strains or noncapsulated strain, Wood, bound to ficolin-3 (Krarup *et al.*, 2005). Lynch *et al.* (2004) showed whole *S. aureus* cell binding to ficolin-2 via flow cytometry. This binding was attributed to LTA, as purified LTA from *S. aureus* bound ficolin-2 and caused C4 activation. Furthermore, ficolin-2 binding to *S. aureus* was inhibited by excess fluid–phase LTA from *S. aureus* (Lynch *et al.*, 2004). More recently, a microarray screening was carried out where 159 extracellular *S .aureus* proteins were screened against 75 human extracellular proteins, which included many proteins of the innate immune system (Scietti *et al.*, 2016). Here, staphylococcal protein A (SpA) was shown to directly bind to ficolin-2. However, this interaction was not

further investigated as their results may have been compromised due to residual GlcNAc-containing LPS in their purified SpA sample, and, putative hits were dismissed as detection methods rely on antibody detection which may have been hindered as SpA has the ability to bind immunoglobulins. Therefore, specific ficolin ligands for *S. aureus* have yet to be determined.

To our knowledge, *A. baumannii* interactions with any ficolins have not been elucidated to date.

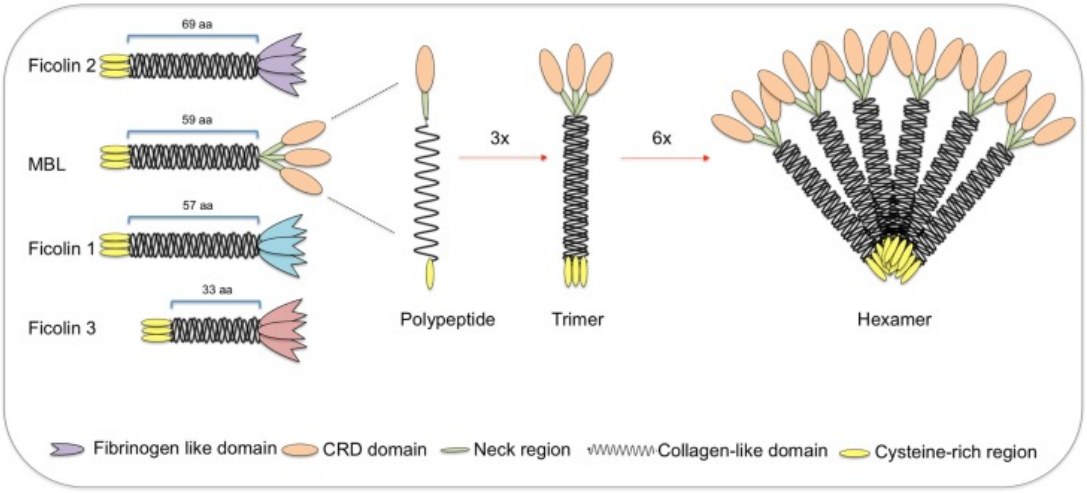


**Fig. 1.7. Structure of ficolins and MBL**. Ficolins and MBL consist of a cysteine region, a collagen-like domain , a neck region and ficolin-like domain for ficolin-1, -2 and -3, and a CRD domain for MBL. Ficolins and MBLs are arranged in trimers which can associate with other trimers to form hexamers. Image taken from Beltrame *et al.* (2015). Downloaded (01-Jun-2019), copyright permission allowed by publisher.

### 1.4.1.2 Collectins

Collectins, which are C-type lectins, comprise of a collagen-like domain that has a cysteine-rich N-terminus and a carbohydrate recognition domain (CRD) which is involved in microbial recognition (Hansen *et al.*, 2016). Nine collectins have been discovered to date, including MBL, CL-10, CL-11, CL-43, CL-46, collectin placenta 1 (CL-12), surfactant proteins A and D (SP-A and SP-D) and conglutinin (Van De Wetering *et al.*, 2004). Among the nine collectins that have been discovered so far, MBL, CL-10 and CL-11 have been shown to be involved in the lectin pathway of the complement cascade. CL-10 and CL-11 form complexes comprising of one CL-10

subunit and two CL-11 subunits *via* disulfide bridge formation (Henriksen *et al.*, 2013). These complexes circulate in serum and have been shown to complex with MASPs, specifically MASP-2, resulting in C4b deposition and complement activation (Henriksen *et al.*, 2013). It has been shown that CL-10 has specificity for mannose, GlcNAc, galactose and fucose, and CL-11 has specificity towards mannose, ManNAc and fucose (Hansen *et al.*, 2016). Interestingly, CL-12, which is a type II membrane protein with a coiled-coil region, collagen-like domain and CRD, has been shown to bind to bacteria such as *E. coli* and *S. aureus* and promote phagocytosis, but unlike, CL-10 and CL-11, CL-12 has been shown to activate the alternative pathway instead of the lectin pathway (Ma *et al.*, 2015; Ohtani *et al.*, 2001). CL-12 expression is associated with vascular endothelial cells, while CL-10 has been found in serum and plasma. CL-11 is expressed by the adrenal glands, liver and kidney and is also present in serum (Hansen *et al.*, 2016). The role of CL-10, CL-11 and CL-12 in detecting pathogens to activate the complement cascade has yet to be thoroughly investigated.

MBL also recognises various PAMPs, including those from bacteria, viruses, fungi and parasites, helping the host to prevent severe pathogenic microbial infections by activating the lectin pathway in the complement cascade. MBL consists of four main regions, a N–terminal cycteine rich domain, a collagenous domain, an α-helical coiled domain, and a CRD or lectin domains which form a globular head on the MBL molecule. A MBL triple helix is formed *via* three polypeptide chains, creating a trimeric structure which is the basic structural composition of MBL circulating in the body. Furthermore, oligomerisation of these trimeric structures can occur, leading to high binding affinity to particular carbohydrate ligands (Auriti *et al.*, 2017; Yokota *et al.*, 1995). MBL is primarily synthesized by hepatocytes in the liver (Wild *et al.*, 1983) although transcription in the small intestines and testis has also been reported (Seyfarth *et al.*, 2006). Following synthesis, MBL is released as a serum protein that circulates around the body. However, MBL can leave the blood circulation during infections and can be found in amniotic fluid, nasopharyngeal secretions, middle ear effusions and upper airway secretions (Garred *et al.*, 1993; Malhotra *et al.*, 1994).

MBL has a binding affinity towards terminal D-mannose, L-fucose (Fuc) and GlcNAc, but not to D-galactose (Gal) or sialic acid. It has been suggested that MBL

prefers binding to equatorial hydroxyl (OH) groups in the 3- or 4-position (Drickamer, 1992; Eddie Ip *et al.*, 2009; Weis *et al.*, 1992). Although Fuc contains an axial OH group on C-4, Weis *et al.* (1992) suggested the equatorial OH groups at C-2 and C-3 can be superimposed on the C-3 and C-4 OH groups on the pyranose ring. This results in the C-4 OH group occupying the same position as the C-2 OH group on mannose, and the C1 and C6 position on fucose being reversed compared to mannose. Binding of a single CRD to a monosaccharide is weak, therefore strong binding requires simultaneous binding from multiple CRDs such as a MBL triple helix to increase affinity (Eddie Ip *et al.*, 2009), and that carbohydrate ligands span a three dimensional 45 Å (Sheriff *et al.*, 1994).

MBL complement activation is very similar to that of ficolin activation of complement. When MBL binds to a PAMP, MBL and MASPs form a complex to initiate the lectin pathway of complement. This MBL–MASP complex is thought to occur *via* MBL collagen domains (Super *et al.*, 1992). Initiation of the lectin pathway occurs by MASP-2 autoactivation, which is subsequently initiated after MBL recognises and binds microbial carbohydrates. MASP–2 activation causes C4 and C2 proteolytical cleavage, resulting in a C3 convertase (Fig. 1.6) (Eddie Ip *et al.*, 2009).

For many years, it has been known that *S. aureus* (both MSSA and MRSA) can bind to MBL, activating the complement pathway (Ma *et al.*, 2004; Neth *et al.*, 2000, 2002; Shi *et al.*, 2004). It was shown that tetrameric MBL bound much greater to *S. aureus* compared to trimeric MBL, whereas dimeric MBL did not bind *S. aureus*, suggesting the importance of oligomerisation of MBL for the detection of *S. aureus* (Kjaer *et al.*, 2011). *S. aureus* peptidoglycan binding to MBL has been reported Ma *et al.*, 2004) along with *S. aureus* LTA binding to MBL (Eddie Ip *et al.*, 2008; Polotsky *et al.*, 1996), and more recently, specific binding of *S. aureus* WTA to MBL (Park *et al.*, 2010). *S. aureus* mutants used in this study included an α-GlcNAc glycosyltransferase mutant (Δ*tarM*), a β-GlcNAc glycosyltransferase mutant (Δ*tarS*), and a double mutant of the two genes (Δ*tarMS*). MBL bound to the mutants lacking either α-GlcNAc glycosylation of WTA or β-GlcNAc glycosylation of WTA, however, MBL was unable to bind the double mutant, Δ*tarMS*. This indicates that MBL requires GlcNAc modified WTA for binding, which may not necessarily depend on the anomeric linkage of the GlcNAc residue. However, higher levels of

anti–WTA β-GlcNAc IgG were present in human sera, as compared to anti–WTA α-GlcNAc IgG. Kurokawa *et al.*, (2013) hypothesized that β-GlcNAc residues on WTA may be more antigenic than α-GlcNAc residues, thus causing this heightened IgG immune response.

Similar to ficolins, no research has been published to identify whether MBL is involved in detecting *A. baumannii* or in the elimination of *A. baumannii* from the host.

### 1.4.2. Membrane-bound PRRs

Ficolins and collectins are usually found in the serum and plasma. Although collectins can be expressed on some cell surfaces, as well as found in the serum, other PRRs are predominately found on cell membrane. These membrane-bound PRRs include other C-type lectins such as DC-SIGN, selectins and dectins, TLRs and I-type lectins or siglecs. Typically these membrane bound PRRs have extracellular CRDs which detect PAMPs. They also have a transmembrane spanning region and a cytoplasmic tail required for signalling. These signalling events can often lead to elimination of the pathogen, or pathogens can manipulate these signalling events to persist within the host (Bradshaw & Dennis, 2010; Brubaker *et al.*, 2015).

#### 1.4.2.1 DC-SIGN

Dendritic Cell-Specific ICAM-3 Grabbing Non-Integrin receptor (DC-SIGN) is a type II membrane protein that was originally found to be a receptor for the gp120 glycoprotein from HIV envelope (Curtis *et al.*, 1992). Since then, DC-SIGN has been associated with a wide range of immunological functions ranging from intercellular migration, communication, pathogen recognition and presentation and cellular signalling (Geijtenbeek, Torensma, *et al.*, 2000; van Kooyk *et al.*, 2003).

DC-SIGN is expressed by immature dendritic cells (DCs) in the skin and mature DCs in lymphoid tissues, the placenta, macrophage populations and monocytes (Geijtenbeek, Krooshoop, *et al.*, 2000; Geijtenbeek, Torensma, *et al.*, 2000; Mummidi *et al.*, 2001). As a PRR, DC-SIGN binds to specific carbohydrate structures such as Fuc and Man in a calcium dependent manner. Therefore, DC-SIGN binding has been associated with the recognition of fucosylated (including

blood type Lewis antigens) and mannosylated (including mycobacterial mannosylated lipoarabinomannan (ManLAM)) structures. Due to DC-SIGNs broad range of specificity, it recognises pathogens such as HIV, Measles virus, Ebola virus, *H. pylori*, *Candida albicans* and indeed human derived glycoproteins such as ICAM-2, ICAM-3, immunoglobulins, butyrophilin, macrophage receptor 1 (Mac-1) (Alvarez *et al.*, 2002; Anthony *et al.*, 2008; Bergman *et al.*, 2004; Cambi *et al.*, 2003; De Witte *et al.*, 2006; Geijtenbeek, Torensma, *et al.*, 2000; Van Gisbergen *et al.*, 2005; van Liempt *et al.*, 2006). Interestingly, DC-SIGN can modulate TLR signalling *via* Raf-1 dependent acetylation of p65, increasing the production of different cytokines (Geijtenbeek *et al.*, 2003; Gringhuis *et al.*, 2009).

Some LPS structures found on the surface of pathogens, such as *H. pylori*, *K. pneumoniae* and *M. tuberculosis*, can interact with DC-SIGN via Lewis x, Man residues or ManLAM respectively (Appelmelk *et al.*, 2003; Bergman *et al.*, 2006; Tallieux *et al.*, 2003). These interactions cause distinct immunological responses; for example, ManLAM interaction with DC-SIGN causes an increase in the immunosuppressive cytokine IL-10 (Geijtenbeek *et al.*, 2003). Little research has been carried out to investigate whether *S. aureus* or *A. baumannii* binds to DC-SIGN or is involved in DC-SIGN signalling. Appelmelk *et al.* (2003) found no binding between a clinical *S. aureus* strain and DC-SIGN in a soluble DC-SIGN-Fc adhesion assay. However, this has to be investigated further as this study used only the extracellular portion of DC-SIGN and used only one strain of *S. aureus* (Appelmelk *et al.*, 2003). Similarly, a DC-SIGN homologue, SIGN-R1, was not capable of capturing *S. aureus* in a mouse model (Takahara *et al.*, 2004). For *A. baumannii*, there are no studies, that we are aware of, that show the direct interaction between *A. baumannii* and DC-SIGN. However, it has been shown that dendritic cells become activated in response to the *A. baumannii* surface porin protein, OmpA (Lee *et al.*, 2007). Purified OmpA increased the production of IL-12, promoted the polarisation of CD4+ T-cells towards a Th1 type, and activated MAPKs and NF-κB in dendritic cells. Thus, it was hypothesised that OmpA induces dendritic cell maturation and activates the adaptive immune response *via* polarisation of Th1 cells. Although it was shown that IL-12 mediated responses involved TLR2, no experiments were carried out to show the involvement of other PRRs, such as DC-SIGN, in dendritic cell activation of the adaptive immune response.

### 1.4.2.2 DC-SIGNR and LSECtin

Dendritic-cell specific ICAM3 grabbing non-integrin related (DC-SIGNR, also known as CD299, CD209L and L-SIGN) protein is a homologue to DC-SIGN. Although DC-SIGN and DC-SIGNR share 77% amino acid sequence, they are not found in the same locations in the body. DC-SIGN expression is often associated with dendritic cells and macrophages, while DC-SIGNR is found on endothelial placenta, liver and lymph node cells (Pöhlmann *et al.*, 2001; Soilleux *et al.*, 2000). Liver and lymph node sinusoidal endothelial cell C-type lectin (LSECtin or CLEC4G) shares a similar gene structure and location to DC-SIGN and DC-SIGNR but is detected on Kupffer cells, lymph nodes and sinusoidal endothelial cells (F. Zhang *et al.*, 2014). DC-SIGN, DC-SIGNR and LSECtin have intra-, trans- and extra-cellular domains. The intracellular domains of these lectins contain the N-terminal tails and causes binding-induced signalling, phagocytosis and ligand trafficking. Internalisation is permitted with di-leucine motifs, phagocytosis and endocytosis with triacidic motifs, and there is a tyrosine motif that is conserved in DC-SIGN and LSECtin, but not DC-SIGNR (Fig. 1.8). The trans-membrane domains consist of 18-23 amino acids that anchor the proteins to the membrane of the cytoplasm. Finally, the extracellular domains contain the C-type CRD, that interacts with self and non-self carbohydrates (Azad *et al.*, 2008; Koppel *et al.*, 2005). LSECtin recognises PAMPs on dendritic cells and activates spleen tyrosine kinase (SYK) and extracellular signal-regulated kinase (ERK) leading to cytokine production *via* the activation of caspase recruitment domain-containing protein 9 (CARD9) and Syk (Zhao *et al.*, 2016).

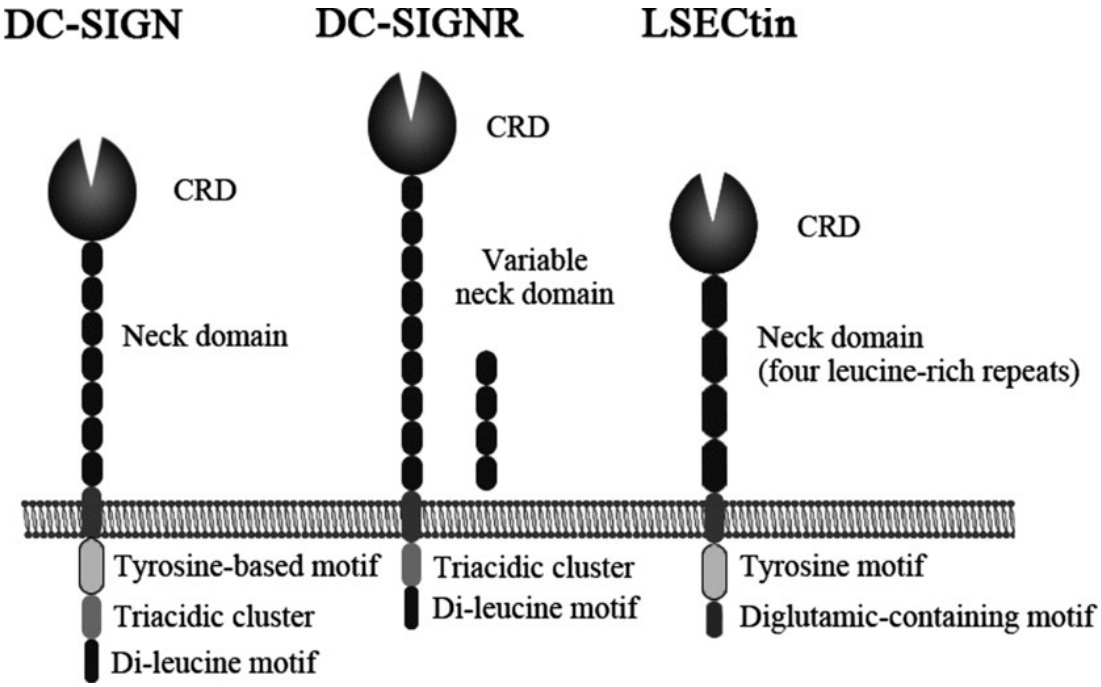


**Fig. 1.8. Diagram of DC-SIGN, DC-SIGNR and LSECtin.** DC-SIGN, DC-SIGNR and LSECtin have a CRD domain and a neck domain. DC-SIGN and LSECtin contain tyrosine motifs, which is absent from DC-SIGNR. DC-SIGN and DC-SIGNR contain a triacidic cluster and a di-leucine motif and LSECtin does not have a triacidic cluster and has a diglutamic-containing motif. Image taken from Zhang *et al.* (2014). Downloaded (01-Jun-2019), copyright permission allowed by publisher.

DC-SIGNR binds to high mannose type N-linked glycans (Feinberg *et al.*, 2001). Although both DC-SIGN and DC-SIGNR bind mannose structures, only DC-SIGN binds to blood group antigens. Furthermore, as PRRs, DC-SIGN binding to an antigen causes endocytosis, trafficking and ligand release at an endosomal pH, while DC-SIGNR does not release the ligand at endosomal pH and cause endocytosis. To date, it appears that DC-SIGNR has a more restricted function by acting only as an adhesion receptor (Guo *et al.*, 2004). LSECtin binds to Man, GlcNAc and Fuc in a calcium-dependant manner (Liu *et al.*, 2004)

Similar to LSECtin, DC-SIGNR has been primarily associated with viral infections. For example, DC-SIGNR binds to HIV and promotes viral infection of T cells (Pöhlmann, Baribaud, *et al.*, 2001). DC-SIGNR is also a receptor for many other viruses such as influenza A virus, Ebola, hepatitis C and alphavirus (Alvarez *et al.*, 2002; Gardner *et al.*, 2003; Gillespie *et al.*, 2016; Klimstra *et al.*, 2003; Pöhlmann *et al.*, 2001). Interestingly, DC-SIGNR binds to SARS coronavirus (SARS Co-V) viral

glycoprotein to help eliminate the virus, but also aids transmission of the virus, and LSECtin has been shown to bind to the spike protein of SARS-CoV further promoting infection. To date, the only indication that bacteria may interact with DC-SIGNR is *via* interactions with the lipoprotein LprG from *M. bovis* BCG (Carroll *et al.*, 2010) and there have been no associations made between LSECtin and bacteria to date.

#### 1.4.2.3 Neutrophil recruitment and selectins

In response to microbial infections, the body reacts by signalling for leukocytes, such as neutrophils and eosinophils, to migrate to extravascular sites of inflammation from the blood stream. This process also occurs in chronic and acute inflammatory processes, such as cancer metastasis, skin inflammation and atherosclerosis to name a few (Barthel *et al.*, 2007). During inflammation, selectins are expressed on the cell surface and bind to leukocytes while they roll along the blood vessel wall. Selectins adhere to carbohydrates, such as the glycoprotein P-selectin glycoprotein ligand-1 (PSGL-1), on leukocytes and this causes leukocytes to migrate from the blood vessel and to the site of infection and inflammation (Springer, 1994). Selectins play an instrumental role in leukocyte rolling, but other adhesion receptors are also involved in this orchestrated process of leukocyte transmigration through the epithelium. These receptors include Mac-1, $\beta_2$-integrins and LFA-1 which interact with the intercellular adhesion molecule-1 (ICAM-1) that is typically expressed on leukocytes and endothelial cells (Carlos & Harlan, 1994). Although selectins and these other receptors are often positively involved in directing leukocytes to the sites of inflammation, microorganisms also express surface proteins and carbohydrates that bind to these receptors, consequently inhibiting the recruitment of leukocytes to the site of infection (Kobayashi *et al.*, 2018).

#### 1.4.2.4 Selectins

Selectins consist of three transmembrane C-type lectins: Leukocytes selectin (L-selectin), endothelial cell lectin (E-selectin), and platelet and endothelial cell selectin (P–selectin) (Ley & Kansas, 2004). These prefixes were assigned based on the cell type of where the molecules were first identified. L–selectin is found to be expressed on most leukocytes, E-selectin is expressed on endothelium, while P–selectin can be expressed by endothelial cells and found in storage granules of platelets (Vestweber

& Blanks, 1999). All three selectins are multidomain type I transmemembrane proteins with C-type CRDs. As well as the CRDs, there is an epidermal growth factor–like domain, followed by numerous consensus repeats, a membrane spanning region and a carboxy-terminal domain located in the cytoplasm (Ley *et al.*, 2004; Somers *et al.*, 2000).

Homology analysis of all three lectins revealed the lectin domain is the most conserved region amongst the three selectins (Ley, 2003). Selectins require carbohydrate binding mediators, or glycoprotein scaffolds, which include the PSGL–1, which can bind all three selectins, and has been extensively studied (Somers *et al.*, 2000). PSGL-1 is a major contributer of P-selectin binding, is very important for L–selectin binding in inflammatory circumstances, but is not a major ligand for E–selectin. Selectins are crucial in neutrophil recruitment (Fig. 1.9), as is seen in patients that have leukocyte adhesion deficiency type (II) (LAD-II). These patients have a mutation in a fucose transporter gene which renders them unable to incorporate Fuc into selectin ligands. Consequently, selectins cannot bind leukocytes, contributing to skin and mucosal bacterial infections (Marquardt *et al.*, 1999).

Furthermore, selectins bind the sialyl Lewis (SLe) antigens, sialyl Lewis α ($sLe^{\alpha}$) and sialyl Lewis x ($sLe^{x}$), while fucosylated structures appear to help mediate leukocyte–endothelial adhesion in humans (Becker & Lowe, 2003). E–selectin expression has shown to be induced by lipopolysaccharide (LPS) and lipoteichoic acid (LTA) from Gram positive bacteria (Kawamura *et al.*, 1995).

#### 1.4.2.5 P-selectin

Bestebroer *et al.* (2007) used purified staphylococcal superantigen–like 5 (SSL5) to detect binding to leukocytes and PSGL-1. Specific binding of SSL5 to PSGL–1 was detected *via* CHO cells functionally expressing PSGL-1, and non-expressing PSGL-1 CHO cells as a control. This was further verified on a protein level *via* SPR analysis, and by using SSL5 to inhibit the binding of P–selectin to PSGL-1 expressing CHO cells. Not only did Bestebroer *et al.* (2007) show that SSL5 binds to PSGL-1, but also that SSL5 prevents the rolling of neutrophils on P–selectin under shear conditions, preventing the movement of neutrophils towards to site of *S. aureus* infection (Bestebroer *et al.*, 2007). In a similar manner, *S. aureus* SSL11 was

found to bind to sialyl lewis X and inhibited neutrophil attachment to P-selectin. Furthermore, SSL11 was able to attach to glycoproteins expressing sialyl structures allowing for internalisation by myeloid cells (Chung *et al.*, 2007).

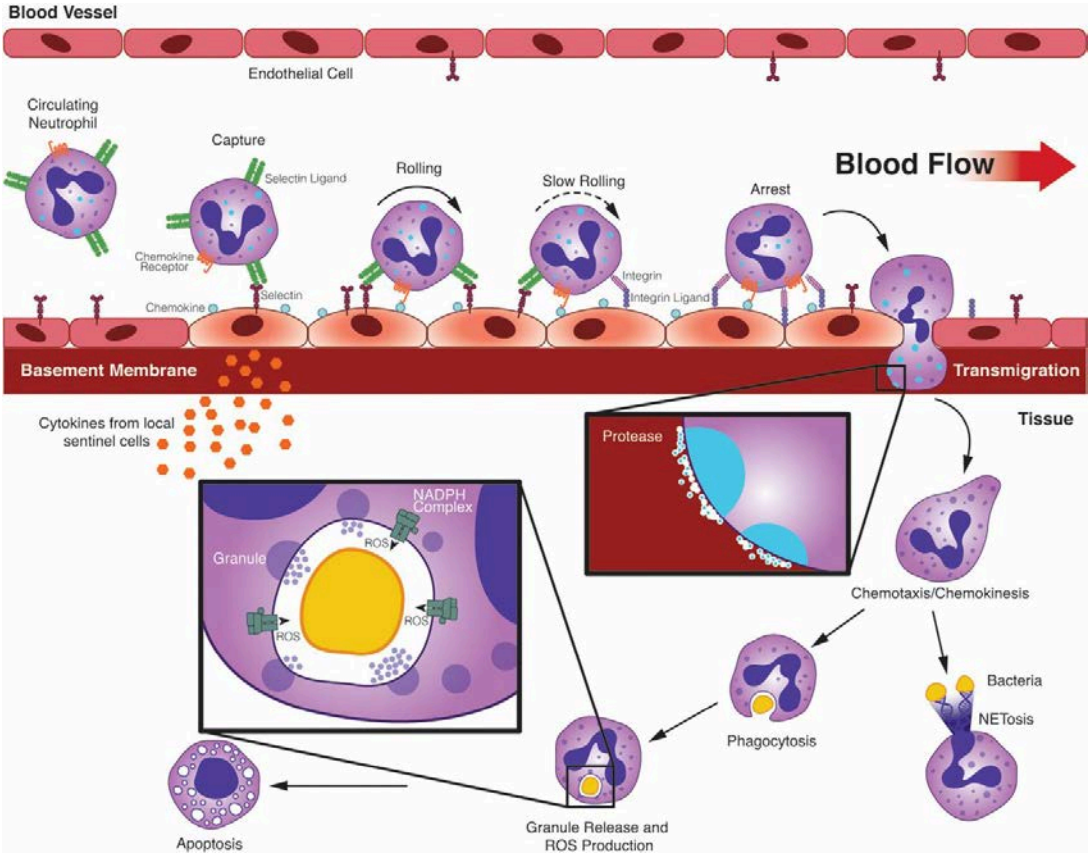


**Fig. 1.9. Siglecs and their role in neutrophil recruitment during infection.** Detection of PAMPs results in cytokine and chemokine release resulting in selectin expression on endothelial cells. Neutrophils are captured and released by selectins on endothelial cells resulting in neutrophil rolling. Neutrophils are forced to slowly roll and stop by integrins. Neutrophils transmigrate across the endothelial basement membrane. Proteases help neutrophils cross the basement membrane. Neutrophils are directed to pathogens via a chemoattractant pathway. Pathogens are phagocytosed and eliminated by the granules within phagosomes and by reactive oxygen species. Neutrophils are eliminated from the tissue *via* apoptosis. Image taken from Caster *et al.*, (2017). Copyright permission received from publisher (10-Jun-2019).

Similarly, Fevre *et al.* (2014) identified a *S. aureus* secretome protein, SEIX, that binds to glycosylated PSGL-1 and inhibits neutrophil binding to P-selectin, therefore preventing PSGL–1 mediated cell adhesion. This ability of the bacteria to produce

and excrete a protein that can mediate the innate immune system is crucial for *S. aureus* immune evasion (Fevre *et al.*, 2014).

*S. aureus* also evades the immune system *via* extracellular fibrinogen-binding protein (Efb). Efb is a surface protein that binds to platelets and fibrinogen. Furthermore, Efb has been known previously to exert immunosuppressive effects *via* complement pathway modulation and is required for effective virulence *in vivo* (Koch *et al.*, 2012). Here it was confirmed that Efb interacts with platelets, without the requirement for fibrinogen, and subsequently inhibits the formation of platelet–monocyte complexes helping *S. aureus* to escape host immune responses (Posner *et al.*, 2016). The *S. aureus* extracellular adherence protein Eap also inhibits neutrophil binding to endothelial cells, preventing leukocyte recruitment and inflammation at the site of infection (Chavakis *et al.*, 2002).

#### 1.4.2.6 E-selectin

*S. aureus* also affects E–selectin expression. In rat eyes injected with viable *S. aureus*, E–selectin expression was elevated for up for 24 hours, as compared to the control (saline solution). *In vitro* assays consisting of aortic endothelial cells and different components of *S. aureus* were also carried out to detect changes in E–selectin expression. E–selectin expression was induced following incubation with *S. aureus* purified ribotal teichoic acid (RTA) and peptidoglycan after 4 hours, however there was no change in E-selectin expression after incubation with *S. aureus* cell wall (CW) or heat treated *S. aureus* cells (Giese *et al.*, 2000). Similarly, out of a total of eighteen *S. aureus* clinical isolates, both methicillin sensitive *S. aureus* (MSSA) and methicillin resistant *S. aureus* (MRSA), except for one isolate, up-regulated the expression of E–selectin by human umbilical cord vein endothelial cells (HUVEC) (Strindhall *et al.*, 2002). This upregulation in E–selectin was seen only with viable *S. aureus* isolates, but not with the same isolates that had been UV–or heat-treated. Elevated E–selectin levels were correlated to patients suffering from *S. aureus* bacteraemia and endocarditis (Söderquist *et al.*, 1999). However, to date the mechanism of induction of E-selectin expression or any direct interaction between *S. aureus* or *S. aureus* molecules with E-selectin has not been demonstrated, and there is no research showing binding of E-selectin to *A. baumannii*.

#### 1.4.2.7 L-selectin

Similar to the other selectins, L-selectin has not been investigated for binding specifically to *S. aureus* or *A. baumannii*. However, recently it was shown that L-selectin played a crucial role in neutrophil recruitment to lymph nodes to phagocytose *S. aureus*, preventing dissemination in to the blood and organs (Bogoslowski *et al.*, 2018). Interestingly, in mice treated with fucoidin, which binds selectins, or mAb specific for L-selectin, inoculation with *S. aureus* resulted in decreased leukocyte recruitment, causing less severe septic arthritis, however, there was less effective clearance of *S. aureus* from the body as a result of modulating the binding sites of E– and L–selectin (Verdrengh *et al.*, 2000).

### 1.4.3. Siglecs

Sialic-acid binding immunoglobulin-like lectins (siglecs) are immunoglobulin-type (I-type) lectins that recognise a diverse range of carbohydrate structures and are thought to regulate self and non-self immune responses *via* intercellular signalling. Siglecs consist of type 1 membrane proteins and have an amino terminal V-set immunoglobulin domain that has been shown to have specificity for sialic acid, and often C2-set immunoglobulin domains. Based on sequence similarity and conservation in mammals through evolution, siglecs can be classified in to two groups. Siglec-1 (CD169/sialoadhesin), siglec-2 (CD22), siglec-4 (or myelin-associated glycoprotein (MAG)) and siglec-15 have orthologues in different mammals but share poor sequence similarity between species. However, the human CD33-related family, namely siglec-3 (CD33), -5 (CD170), -6 (CD327), -7 (CD328), -8, -9 (CD329), -10, -11, 14, 16 and a siglec-like molecule (Siglec-L1) show high sequence similarity to one another (Brinkman-Van der Linden *et al.*, 2003; Crocker *et al.*, 2007). Localisation of expression of different siglecs can vary in humans, with expression of certain siglecs exclusive to particular cell types (Table 1.1). Siglecs have different specificity for sialylated ligands, and depending on the siglec–terminal sialylated glycoconjugate interaction, can result in many different host immune responses, including pathogen internalisation, downregulation of inflammation, preventing cellular activation and attenuation of NK cell activation (Von Gunten &

Bochner, 2008). Therefore, bacterial binding to siglecs can often help the pathogen to evade the immune system by down-regulating host immune responses.

Siglec-2 and many siglecs from the CD33 family have at least one cytosolic immunoreceptor tyrosine-based inhibitory motif (ITIM). These ITIMs have inhibitory functions *via* the recruitment of tyrosine and inositol phosphatases, which suppress immune signalling cascades originating from receptors with immunoreceptor tyrosine-based activation motifs (ITAMs) (Crocker *et al.*, 2007). Therefore, siglecs have the ability to mediate cell-cell based interaction and mediate cell signalling cascades. Many bacteria are capable of binding siglecs (Table 1.1), most commonly binding to sialic acids on LPS, lipooligosaccharides (LOS) and most recently suggested to bind pseudaminic acid on *C. jejuni* flagella. Interestingly, *A. baumannii* contains pseudaminic acid on exopolysaccharides and these exopolysaccharides may be an interesting target to investigate interactions with siglecs in the future (Arbatsky *et al.*, 2016; Kasimova *et al.*, 2017). On one side, these interactions have been proposed to enhance binding of pathogens to siglecs to aid phagocytosis, yet on the other, have been suggested to attenuate immune responses, helping with asymptomatic colonisation of the bacteria in the mammalian host (Ali *et al.*, 2014; Avril *et al.*, 2006; Jones *et al.*, 2003; Khatua *et al.*, 2012; Klaas *et al.*, 2012; Stephenson *et al.*, 2014).

To date, there are few studies investigating *S. aureus*-siglec binding and no studies investigating siglec-*A. baumannii* interactions. Sialic acid has not been found on the surface of *S. aureus* to date, although various sialic acid-binding lectins have been shown to interact with *S. aureus.* These include SraP and SasA, which have a specificity for Neu5Ac-α-(2,3)-Gal-β-(1,4)-GlcNAc (Baker *et al.*, 2007; Bestebroer *et al.*, 2009; Fevre *et al.*, 2014; Kukita *et al.*, 2013; Yang *et al.*, 2014).

The impact of *S. aureus* and *S. aureus* cellular components on siglec-induced cell signalling has not been fully elucidated. *S. aureus* peptidoglycan was used to stimulate siglec-9 and siglec-5 expressing cell lines, RAW264 cells expressing siglec–9 and THP–1 cells transfected with a siglec-9 expression vector, which produced low levels of the proinflammatory cytokines, TNF–α and IL–6. Moreover, stimulation of cells with peptidoglycan caused siglec–9 to enhance the production of the anti-inflammatory cytokine IL–10, which was attributed to ITAMs. Siglec–5

expressed by RAW264 cells was also shown to be involved in IL–10 production following *S. aureus* peptidoglycan stimulation (Ando *et al.*, 2008). Thus *S. aureus* used cellular components to bind to siglecs, and consequently downregulated the production of proinflammatory cytokines such as IL–10, helping to prevent these pathogenic bacteria being destroyed by the immune system. A follow on study described the partial movement of siglec–9 into lipid rafts (cholesterol and glycosphingolipid concentrated plasma membrane microdomains) upon stimulation with *S. aureus* peptidoglycan (Ando *et al.*, 2014). Reasoning for this has not yet been fully elucidated, although it was hypothesized that it may be connected to a controlled regulation of IL–10 production. Some other cellular components on *S. aureus* have been shown to have no effect on the expression of other siglecs. For example, *S. aureus* LTA was shown to not induce siglec–1 expression in PBMCs (York *et al.*, 2007). Nonetheless, there are many more *S. aureus*-siglec interactions and corresponding cell signalling pathways that have yet to be investigated.

**Table 1.1. Summary of the siglec family.** Detailing where each siglec is found in humans, the specificity, bacterial interactions, regulatory effect and reference. GBS (Group B *Streptococcus*), GAS (Group A *Steptococcus*), COPD (chronic obstructive pulmonary disease), NK cells (natural killer cells), LOS (lipooligosaccharide).

| Siglec (synonyms) | Expression location | Binding specificity | Bacterial associations | Regulatory effect on immune system | Reference |
|---|---|---|---|---|---|
| Human sialoadhesin (siglec-1;CD169) | Macrophages and activated monocytes | α-(2,3)-linked sialic acid | GBS (bacterial killing), *C. jejuni* LOS, | Other | (Chang *et al.*, 2014; Heikema *et al.*, 2010; Klaas *et al.*, 2012; MacAuley *et al.*, 2014) |
| Human CD22 (Siglec-2) | B cells | α-(2,6)-linked sialic acid | No known association | Inhibitory | (MacAuley *et al.*, 2014) |
| Human CD33 (Siglec-3) | Myeloid pregenitors, monocytes, macrophages, monocytes, microglia and granulocytes | α-(2,6)-linked sialic acid | No known association | Inhibitory | (MacAuley *et al.*, 2014) |
| Human MAG (Siglec-4) | Oligodendrocytes and Schwann cells | α-(2,3)-linked sialic acid | No known association | Other | (MacAuley *et al.*, 2014) |
| Human Siglec-5 | Monocytes, neutrophils and B cells | α-(2,6)- and α-(2,3)-linked sialic acid | de-*O*-acetylated GBS capsule and GBS β-protein, *Neisseria meningitidis* (LOS) | Inhibitory | (Ali *et al.*, 2014; Carlin *et al.*, 2007; Jones *et al.*, 2003; MacAuley *et al.*, 2014) |
| Human Siglec-6 | Trophoblasts and B cells | Sialyl Tn structures | No known association | Inhibitory | (MacAuley *et al.*, 2014) |
| Human Siglec-7 | Monocytes, NK cells and mast cells | α-(2,8)- and α-(2,6)-linked sialic acid | de-*O*-acetylated GBS capsule, *C. jejuni* (LOS), binding to sialic acid acquired from *P. aeruginosa* | Inhibitory | (Avril *et al.*, 2006; Carlin *et al.*, 2007; Khatua *et al.*, 2010; MacAuley *et al.*, 2014) |
| Human Siglec-8 | Mast cells, eosinophils and | 6'-sulfated sialyl Lewis X | No known association | Inhibitory | (MacAuley *et al.*, 2014) |

| | | | | | |
|---|---|---|---|---|---|
| | basophils | | | | |
| Human Siglec-9 | Dendritic cells, neutrophils, monocytes and NK cells | α-(2,6)- and α-(2,3)-linked sialic acid | GAS and GBS (capsules) immune evasion, binding to sialic acid acquired from *P. aeruginosa* | Inhibitory | (Carlin *et al.*, 2007; Khatua *et al.*, 2010; MacAuley *et al.*, 2014) |
| Human Siglec-10 | Monocytes, B cells and eosinophils | α-(2,6)- and α-(2,3)-linked sialic acid | No known association | Inhibitory | (MacAuley *et al.*, 2014) |
| Human Siglec-11 | Macrophages and microglia | α-(2,8)-linked sialic acid | No known association | Inhibitory | (MacAuley *et al.*, 2014) |
| Human Siglec-14 | Neutrophils and monocytes | α-(2,8)- and α-(2,6)-linked sialic acid | GBS β-protein, *Haemophilus influenzae* and COPD | Activating | (Ali *et al.*, 2014; Angata *et al.*, 2013; MacAuley *et al.*, 2014) |
| Human Siglec-15 | Dendritic cells, osteoclasts and macrophages | α-(2,6)-linked sialic acid | No known association | Activating | (MacAuley *et al.*, 2014) |
| Human Siglec-16 | Macrophages and microglia | α-(2,8)-linked sialic acid | No known association | Activating | (MacAuley *et al.*, 2014) |

### 1.4.4. Toll-Like Receptors (TLR)

A Toll receptor was first discovered to have a role in innate immunity in *Drosophila melanogaster* (Lemaitre *et al.*, 1996). Since then, 10 homologues of Toll from *Drosophila* have been identified in humans, designated Toll-like receptors (TLR1 – TLR11). TLRs in humans also play a role in innate immunity *via* the detection of PAMPs, consequently causing immune responses to help clear pathogenic bacteria, fungi, protozoa and viruses from the body (Fournier & Philpott, 2005).

TLRs consist of type I transmembrane proteins with a leucine-rich repeating extracellular domain. The conserved cytoplasmic tail displays similarity to IL-1 family receptors and thus is called a Toll/IL-1 (TIR) domain. Localisation of TLR can differ based on the TLR, but generally TLR1, 2, 4, 5, 6 and 10 can be found in the plasma membrane, while TLR3, 7, 8 and 9 are expressed in endosomes and lysosomes where after pathogenic cell degradation, these TLR recognise the exposed DNA / RNA, helping to elicit an immune response. To date, it has been found that TLR1, 2, 4 and 6 recognise lipids associated with pathogenic microorganisms, while TLR3, 7, 8 and 9 detect nucleic acids. TLR5 has shown specificity for flagella, while no specific ligand has yet been discovered for TLR10 (Hayashi *et al.*, 2001; Parkunan *et al.*, 2014; Takeda & Akira, 2005). TLRs can also broaden binding specificities by forming heterodimers with one another, helping to shape TLR ligands to recognise microbial pathogens for destruction (Botos *et al*., 2011; Kang *et al*., 2009).

All TLRs use the MyD88–dependent pathway for signalling, except TLR3. Following TLR(s)-ligand binding, cell signalling cascades occur *via* myeloid differentiation primary-response protein 88-(My88-)dependent and My88-independent pathways (Takeda *et al.*, 2005). MyD88 has an amino terminal death domain (DD) and a carboxyl terminal TIR domain. My88 is an adaptor protein that connects TLR signalling cascades with other downstream molecules.

TLR–ligand binding results in the association of MyD88 to the TIR domain on TLRs. This association signals for the recruitment of IRAK1 and IRAK4, both of which have contain a DD domain and have kinase activity that is required for nuclear factor-κB (NF-κB) signalling. Activated IRAK4 leads to the association of TRAF6,

which acts as a signalling mediator, and can result in two different signalling pathways. In one of these pathways TRAF6 complexes with TAB2/TAB3/TAK1, resulting in TAK1 activation. Activated TAK1 couples to, and enhances, the activity of the IKK complex. This eventually leads to IκB phosphorylation and degradation, which is followed by nuclear localisation and activation of NF-κB, prompting the expression of inflammatory cytokines (IL–1, IL–12, TNF–α, etc.).

For MyD88-independent pathways, TLR4–ligand binding requires TRIF for signal transduction. TRIF along with TIRAP are TIR-domain containing adaptors. However, TIRAP is required for TLR2 and TLR4 signal transduction *via* the MyD88-dependent pathway, whereas this is not seen for TLR4-induced TRIF signalling. Upon TLR4–ligand interaction, TRIF associates with TRAF3 and TRAF 6, which adds the kinase RIP-1 and aids interactions with the TAK1 complex. This in turn activates NF-κB and MAPK, leading to the expression of inflammatory cytokines. TRAM, another adaptor containing a TIR domain also mediates TLR4 and TRIF–dependent cell signalling (Akira & Takeda, 2004; Kawasaki & Kawai, 2014; Takeda *et al.*, 2005). Thus, the plethora of cytokines expressed as a consequence of these TLR–induced signalling cascades, initiates a broad range of immune responses channelled at combating the infection (Fig. 1.10).

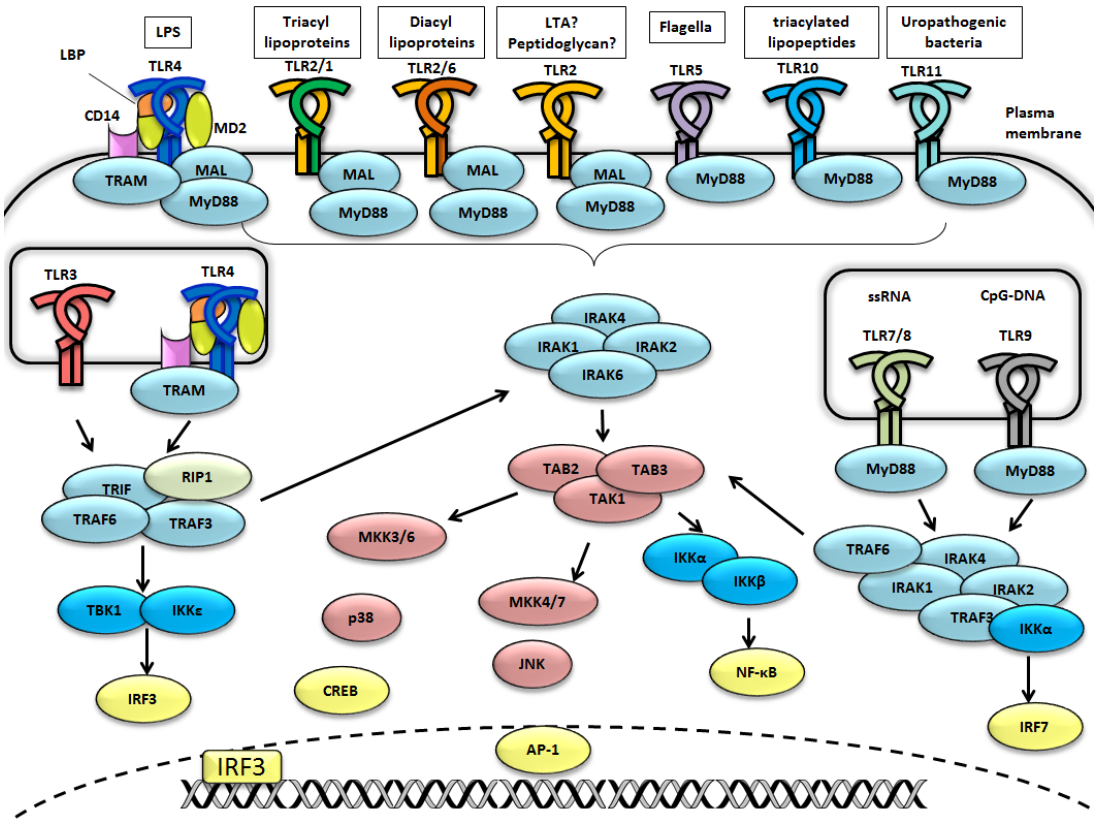


**Fig. 1.10. Overview of TLR signalling pathways.** TLRs become activated by surface components on microorganisms or nucleic acids. TLRs commonly form homodimers, but can also form heterodimers to distinguish between bacterial surface components such as diactyl and triacyl lipoproteins. In the case of LPS, CD14 and LPS binding protein (LBP) help detect LPS, promoting internalisation into endosomes and signalling via TLR4. Activation causes TLR dimerization and recruitment of adapter proteins (TRAM, MyD88). Downstream signals result in the associations between IL-1R-associated kinases (IRAKs) and adaptor molecules TNF receptor-associated factors (TRAFs). This then leads to the activation of mitogen-activated protein kinases (MAPKs), p38 and Jun N-terminal kinase (JNK), which eventually lead to the activation of transcription factors. These transcription factors include the proinflammatory transcription factors: cyclin AMP-responsive element-binding (CREB) protein, activator protein 1 (AP-1) and nuclear factor- κB (NF-κB), as well as the anti-inflammatory transcription factors such as interferons (IFN-α and IFN-β).

LPS–lipopolysaccharide, MD2-myeloid differentiation factor 2, LTA-lipoteichoic acid, dsRNA-double stranded RNA, ssRNA-single stranded RNA, CpG-DNA- CpG containing DNA, IKK-inhibitor of NF-κB kinase, TAB-TAK1-binding protein, MKK-MAP kinase kinase, TBK1-TANK-binding kinase, RIP1-receptor-interacting protein 1, TAK-TGKβ-activating kinase.

#### 1.4.4.1 TLR2

TLR2 is the main TLR previously shown to have involvement in binding to *S. aureus*. In particular, *S. aureus* LTA (Han *et al.*, 2003; Michelsen *et al.*, 2001), lipoprotein (such as SitC) (Müller *et al.*, 2010), peptidoglycan (Dziarski & Gupta, 2005; Iwaki *et al.*, 2002; Kielian *et al.*, 2005; Schwandner *et al.*, 1999), PSMs (Hanzelmann *et al.*, 2016; Peschel & Otto, 2013; Schreiner *et al.*, 2013), staphylococcal exotoxin B (SEB) (Mandron *et al.*, 2008), α-toxin (Niebuhr *et al.*, 2015), Panton-Valentine leukocidin (PVL) (Zivkovic *et al.*, 2011) and indeed, Staphylococcal superantigen-like protein 3 (SSL3) (Koymans *et al.*, 2015; Yokoyama *et al.*, 2012) have all been associated with TLR2 regulation or binding. However, some conflicting results have appeared with many studies, which may due to the possibility of other contaminating cell structures, or degradation of their tested potential TLR ligand after purification. For example, it has been suggested that peptidoglycan interactions with TLR2 may be due to contaminating LTA in the commercial *S. aureus* peptidoglycan preparations (Travassos *et al.*, 2004). Similarly, endotoxin has often been found in commercially purified LTA preparations, presumably from endotoxin from Gram-negative bacteria (Gao *et al.*, 2001; Morath, Geyer, *et al.*, 2002).

Nonetheless, it is clear that TLRs play an important role in combating *S. aureus* infections. This was seen with TLR-deficient mice, which were much more susceptible to *S. aureus* infections compared to the wildtype mice (Hoebe *et al.*, 2005; Takeuchi *et al.*, 2000). Although TLRs appear to be necessary for dealing with *S. aureus* infections, they can also have a negative effect on the body during a bacterial infection caused by *S. aureus*. As *S. aureus* infection results in an increase in TLR2 expression in the heart, this causes an increase in pro-inflammatory mediator expression, and is thought to contribute to cardiac dysfunction (Knuefermann *et al.*, 2004). TLR2 often associates with other co-receptors to broaden and assist *S. aureus* binding specificity. These include TLR1, TLR6, CD14 and CD36 (Fournier *et al.*, 2005). Although there is less research carried out in the area of *A. baumannii* and TLR activation, few studies have shown that LPS from *A. baumannii* is a potent stimulator of TLR2 and TLR4 activation (Erridge *et al.*, 2007; March *et al.*, 2010).

#### 1.4.4.2 CD14

TLRs often associate with other PRRs to recognise PAMPs. One of these PRRs is a glycosylphosphatidylinositol (GPI)-bound or soluble receptor named CD14. CD14 is a 55 kDa 'horseshoe' shaped glycoprotein that was originally used as a marker for monocytes before being recognised as a PRR associated with myeloid cells such as neutrophils, macrophages and monocytes and to a lesser degree endothelial cells, epithelial cells and fibroblasts (Anas *et al.*, 2010; Zanoni & Granucci, 2013). Initially, it was thought to be unlikely that CD14 was a recognition molecule due to the fact that it lacks a transmembrane domain. However, later researchers showed that CD14 recognises LPS on the surface of Gram-negative bacteria together with TLR4 and MD-2 (Zanoni *et al.*, 2013). CD14 has high specificity for LPS and can recognise the structure in picomolar concentrations (Miyake *et al.*, 2000; Triantafilou & Triantafilou, 2002). Furthermore, the presence of CD14 in mice was shown to be required for response to purified LPS or Gram-negative bacteria to elicit septic shock, highlighting the importance of CD14 in Gram-negative associated infections (Haziot *et al.*, 1996). Following further investigations, CD14 was shown to recognise LPS with the aid of TLR4 and MD-2, causing the proteins to associate together. Following translocation of the proteins, TLR4 activates NF-κB and AP-1 *via* the transmembrane domain. For LPS, it is thought that CD14 plays an important role in presenting LPS to TLR4 and helps CD14-TLR4-MD-2 translocate to the endosome for eventual NF- κB and AP-1 activation and cytokine/chemokine production (Zanoni *et al.*, 2013).

After CD14 was recognised as a vital protein in the recognition of LPS and activation of the innate immune response against Gram-negative bacteria, further research in to the protein revealed pivotal roles in the recognition of other microorganisms, including Gram-positive bacteria, viruses and fungi (Anas *et al.*, 2010; Bagasra *et al.*, 1992; Dziarski *et al.*, 1999; Figueiredo *et al.*, 2011). CD14 was found to bind to crude extracts of *S. aureus* (Kusunoki *et al.*, 1995) and it was later verified that CD14 binds to *S. aureus* LTA (Morath *et al.*, 2001; Morath, Stadelmaier, *et al.*, 2002), with the help of TLR2 and lipopolysaccharide-binding protein (LBP) (Schröder *et al.*, 2003). Moreover, peptidoglycan from *S. aureus* was shown to bind to CD14 and up-regulate the expression of CD14 and TLR2 in human monocytes (Dziarski *et al.*, 1998; Hadley *et al.*, 2005). However, contaminating LTA

in commercially available preparations of peptidoglycan was suggested to be the real source of this TLR2 mediated interaction (Travassos *et al.*, 2004).

CD14 also plays a role in the activation of the innate immune response against *A. baumannii.* As seen in a murine model for pneumonia, CD14 and TLR4 deficient mice had higher *A. baumannii* bacterial counts compared to the wildtype mice and it was deduced that CD14 and TLR4 target *A. baumannii via* the LPS moiety on the bacterial cell surface (Knapp *et al.*, 2006). In support, March *et al.*, 2010 showed that an increase of IL-8 production of *A. baumannii* infected epithelial cells was dependent on TLR2 and TLR4 activation as well as soluble CD14. It was hypothesised that LPS was responsible for this IL-8 production (March *et al.*, 2010).

#### 1.4.4.3 TLR2 cooperation with TLR1 and TLR6

TLR2 has been proposed to form a homodimer with itself and has been shown to form a heterodimer with TLR1 or TLR6 depending on the molecule that it is sensing. It is known that TLR2 is involved in binding to particular ligands such as bacterial peptidoglycan and LTA (Kielian *et al.*, 2005; Oliveira-Nascimento *et al.*, 2012; Travassos *et al.*, 2004). However, other reports have suggested that TLRs do not detect peptidoglycan but instead LTA, which is sensed by a TLR1/2 heterodimer (Travassos *et al.*, 2004). TLR2 heterodimer with TLR1 has specificity for triacyl lipoproteins and TLR2 heterodimer with TLR6 for diacyl lipoproteins. Crystal structures of these heterodimers showed an M-shape formation with the internal pockets binding to specific PAMPs, such as diacyl and triacyl lipoproteins. It is thought that TLR2 detects PAMPs by associating with different TLRs and PRRs to elegantly discriminate between different microbial PAMPs to fine tune the immune response (Takeuchi *et al.*, 2010).

It has been suggested that TLR2 and TLR6 recognised *S. aureus* peptidoglycan (Ozinsky *et al.*, 2000). However, it was also suggested that these interactions may be due to contaminating lipoproteins or LTA, as removal of these from Gram-positive bacteria rendered the bacteria undetectable *via* TLR2, TLR1/2 or TLR2/6 (Travassos *et al.*, 2004). Supporting other reports of lipoproteins binding to TLR2 heterodimers, it was found that lipoprotein from *S. aureus* is a predominant TLR2 ligand and mediates inflammation *in vivo* (Hashimoto *et al.*, 2006; Park *et al.*, 2010; Schmaler *et al.*, 2009). Notably, TLR2/1 was shown to bind to the synthetic bacterial

triacylated lipopeptide, Pam3CSk4, and TLR2/1 showed specificity towards the synthetic diacylated lipopeptide Pam2CSK4. Crystal structures of Pam3CSK4 and Pam2CSK4 with TLR2/1 and TLR2/6 respectively highlight the importance of these heterodimers for recognition of these lipoproteins but are also required for the signalling domains on TLRs to be in close proximity to initiate dimerization and consequential signalling (Jin *et al.*, 2007). Predominately, triacylated lipoproteins have been associated with *S. aureus*, however, it has been shown that certain environmental conditions such as acid pH and late log phage can promote the accumulation of diacylated lipoproteins instead (Kurokawa *et al.*, 2012). SitC, which is found in most environmental conditions in a triacylated form, requires TLR2 to elicit cytokine activation, and not TLR1 or TLR6 (Ozinsky *et al.*, 2000). This contradicts other reports that triacylated lipoproteins require TLR2/1 detection for cytokine production (Kurokawa *et al.*, 2009). Although heterodimer associations are often involved in the clearance of *S. aureus* infections, *S. aureus* can also attach to TLR2/TLR6 to negatively regulate immune responses by suppressing the immune system (Skabytska *et al.*, 2014). Cell wall structures associated with *A. baumannii* may bind TLR heterodimers, there has been no thorough investigation to date. Presently, TLR2 and TLR4 are the only known TLRs involved in *A. baumannii* infections, but no specific ligands have been elucidated to date (March *et al.*, 2010).

### 1.4.5. Current methods of identifying specific PRR interactions

To date, elucidation of PRR interactions with bacteria has been primarily carried out using flow cytometry or cell-based assays (Ando *et al.*, 2008; Bestebroer *et al.*, 2009; Liu *et al.*, 2005; Lynch *et al.*, 2004; Travassos *et al.*, 2004). For the initial identification of interactions, ELISA, cell-based assays with antibody blocking, SPR, immunofluorescence microscopy or flow cytometry can be used to screen for interactions with ligands. However, for each of these methods, individual PRRs must be chosen and assessed individually against each hypothesised target ligand. Similarly, when screening for PRRs that bind to a particular ligand, PRRs have to be assessed individually. Thus, screening to initially identify PRR-mediated interactions can be incredibly time consuming, labour intensive and costly. For ELISAs, immunofluorescence microscopy and flow cytometry, fluorophore-conjugated antibodies against specific targets are required for detection, which increases the cost of screening significantly. Furthermore, cell-based assays and flow cytometry

involves the identification of suitable PRR knock-out or over-expressing cell lines, as well as use of PRR-specific antibodies, which would increase the labour, cost and time spent screening for PRR-mediated interactions. SPR does not require fluorophore-conjugated antibodies, but would require high concentrations of purified PRR and hypothesised ligand, again increasing the cost of screening. Based on current screening approaching for identifying novel PRR-bacteria interactions, there is a need for a novel screening approach to rapidly identify PRR interactions for further investigation prior to cell-based studies.

### 1.4.6. PNAG and PRRs

To date, the interactions of PNAG and PRRs have only been assessed with *S. epidermidis* (Stevens *et al.*, 2009) and PNAG purified from *S. epidermidis* was found to induce IL-8 production in astrocytes. This IL-8 induction was not due to lipoproteins, LTA or nucleic acid and the interaction was carbohydrate-mediated, not lipid-mediated and dependent on high levels of carbohydrate acetylation in the purified preparation. Increased IL-8 production was attributed to TLR2, and not TLR4. Other TLRs or PRRs were not investigated for this increased IL-8 response. However, confirmation that PNAG was responsible for this IL-8 response was not carried out with a WT and isogenic *ica* mutant, which could be more confirmatory (Stevens *et al.*, 2009). Thus, further research is required to confirm whether PNAG interacts with TLR2 from a different PNAG preparation, with the use of WT and isogenic *ica* mutants and with different cells of the immune system.

In addition, *S. aureus* biofilm was shown to circumvent TLR2- and TLR9-mediated innate immune responses, however PNAG was not specifically investigated as the basis for this subversion (Thurlow *et al.*, 2011). Beyond these studies, there has been no research to identify PRR interactions with PNAG from Gram-positive or Gram-negative bacteria, and it is crucial to elucidate the recognition, or lack of recognition, of PNAG by the host innate immune system.

## 1.5. Hypothesis

Our knowledge of PNAG and how it interacts with the host is limited to date. We propose that PNAG interacts with a specific subset of receptors to contribute to or

modulate the immune response in favour of persistent colonisation or immune evasion for the PNAG-expressing bacteria.

### 1.6. Aims of this thesis

1. ***To use HTP microarray platforms to identify specific lectin interactions of* S. aureus and A. baumannii.** In chapter 2 we used lectin microarrays to screen for lectins that bind *S. aureus* and *A. baumannii*. We also screened PNAG-negative mutant *S. aureus* and *A. baumannii* to elucidate interactions associated with PNAG.
2. ***To use HTP microarray platforms to identify specific carbohydrate interactions of* S. aureus *and* A. baumannii.** In chapter 2 we used neoglycoconjugate microarrays to screen for carbohydrate ligands of *S. aureus* and *A. baumannii*. We also screened PNAG-negative mutant *S. aureus* and *A. baumannii* to elucidate interactions associated with PNAG.
3. ***To identify lectin interactions of PNAG and to modulate targeted lectin interactions.*** In chapter 3 we identified lectins for PNAG using wildtype and mutant bacteria as well as PNAG isolated from *S. aureus*. We used a panel of glycoclusters to modulate whole bacteria and PNAG-mediated targeted interactions using lectin microarrays.
4. ***To identify PRR interactions of* S. aureus, A. baumannii *and PNAG.*** In chapter 4 we used PRR microarrays to screen for PRR receptors of *S. aureus*, *A. baumannii* and PNAG.
5. ***To determine signalling responses due to a particular PNAG-PRR interaction.*** In chapter 4 we used a monocytic derived cell line, THP1-XBlue-CD14 cells, and cytokine ELISAs to determine the signalling response created by PNAG expressing/non-expressing *S. aureus* and *A. baumannii* and PNAG isolated from these two bacteria.

This work will expand our knowledge on PNAG-mediated interactions by identifying receptors and ligands associated with PNAG, which will pave way for the development of novel therapeutics to target these interactions. Furthermore, this work will provide an ample amount of potential PRR receptors for *S. aureus*, *A. baumannii* and PNAG for the scientific

community to provide the groundwork for future PRR-*S. aureus*, *A. baumannii* and/or PNAG studies.

## 1.7. References


**Aarag Fredheim, E. G., Granslo, H. N., Flægstad, T., Figenschau, Y., Rohde, H., Sadovskaya, I., Mollnes, T. E., & Klingenberg, C.** (2011). *Staphylococcus epidermidis* polysaccharide intercellular adhesin activates complement. *FEMS Immunology and Medical Microbiology*, *63*(2), 269–280.

**Abraham, N. M., & Jefferson, K. K.** (2012). *Staphylococcus aureus* clumping factor B mediates biofilm formation in the absence of calcium. *Microbiology (United Kingdom)*, *158*(6), 1504–1512.

**Akaiwa, M., Yae, Y., Sugimoto, R., Suzuki, S. O., Iwaki, T., Izuhara, K., & Hamasaki, N.** (1999). Hakata antigen, a new member of the ficolin/opsonin p35 family, is a novel human lectin secreted into bronchus/alveolus and bile. *Journal of Histochemistry and Cytochemistry*, *47*(6), 777–785.

**Akira, S., & Takeda, K.** (2004). Toll-like receptor signalling. *Nature Reviews Immunology*, *4*(7), 499–511.

**Ali, S. R., Fong, J. J., Carlin, A. F., Busch, T. D., Linden, R., Angata, T., Areschoug, T., Parast, M., Varki, N., Murray, J., Nizet, V., & Varki, A.** (2014). Siglec-5 and Siglec-14 are polymorphic paired receptors that modulate neutrophil and amnion signaling responses to group B Streptococcus. *Journal of Experimental Medicine*, *211*(6), 1231–1242.

**Almant, M., Moreau, V., Kovensky, J., Bouckaert, J., & Gouin, S. G.** (2011). Clustering of *Escherichia coli* type-1 fimbrial adhesins by using multimeric heptyl α- D -mannoside probes with a carbohydrate core. *Chemistry - A European Journal*, *17*(36), 10029–10038.

**Alvarez, C. P., Lasala, F., Carrillo, J., Muñiz, O., Corbí, A. L., & Delgado, R.** (2002). C-type lectins DC-SIGN and L-SIGN mediate cellular entry by Ebola Virus in cis and in trans. *Journal of Virology*, *76*(13), 6841–6844.

**Anas, A., Poll, T. V. D., & de Vos, A. F.** (2010). Role of CD14 in lung inflammation and infection. *Critical Care*, *14*(2).

**Anderluh, M., Jug, G., Švajger, U., & Obermajer, N.** (2012). DC-SIGN antagonists, a potential new class of anti-infectives. *Current Medicinal Chemistry*, *19*(7), 992–1007.

**Ando, M., Shoji, T., Tu, W., Higuchi, H., Nishijima, K.-I., & Iijima, S.** (2014). Lectin-dependent localization of cell surface sialic acid-binding lectin Siglec-9. *Cytotechnology*, *67*(4), 601–608.

**Ando, M., Tu, W., Nishijima, K. -i., & Iijima, S.** (2008). Siglec-9 enhances IL-10 production in macrophages via tyrosine-based motifs. *Biochemical and Biophysical Research Communications*, *369*(3), 878–883.

**Angata, T., Ishii, T., Motegi, T., Oka, R., Taylor, R. E., Soto, P. C., Chang, Y.-C., Secundino, I., Gao, C.-X., Ohtsubo, K., Kitazume, S., Nizet, V., Varki, A., Gemma, A., Kida, K., & Taniguchi, N.** (2013). Loss of Siglec-14 reduces the risk of chronic obstructive pulmonary disease exacerbation. *Cellular and*

*Molecular Life Sciences*, *70*(17), 3199–3210.

**Anthony, R. M., Wermeling, F., Karlsson, M. C. I., & Ravetch, J. V**. (2008). Identification of a receptor required for the anti-inflammatory activity of IVIG. *Proceedings of the National Academy of Sciences of the United States of America*, *105*(50), 19571–19578.

**Aoyagi, Y., Adderson, E. E., Rubens, C. E., Bohnsack, J. F., Min, J. G., Matsushita, M., Fujita, T., Okuwaki, Y., & Takahashi, S.** (2008). L-ficolin/mannose-binding lectin-associated serine protease complexes bind to group B streptococci primarily through *N*-acetylneuraminic acid of capsular polysaccharide and activate the complement pathway. *Infection and Immunity*, *76*(1), 179–188.

**Appelmelk, B. J., van Die, I., van Vliet, S. J., Vandenbroucke-Grauls, C. M. J. E., Geijtenbeek, T. B. H., & van Kooyk, Y.** (2003). Cutting Edge: Carbohydrate Profiling Identifies New Pathogens That Interact with Dendritic Cell-Specific ICAM-3-Grabbing Nonintegrin on Dendritic Cells. *The Journal of Immunology*, *170*(4), 1635 LP-1639.

**Arbatsky, N. P., Shneider, M. M., Shashkov, A. S., Popova, A. V, Miroshnikov, K. A., Volozhantsev, N. V, & Knirel, Y. A.** (2016). Structure of the *N*-acetylpseudaminic acid-containing capsular polysaccharide of *Acinetobacter baumannii* NIPH67. *Russian Chemical Bulletin*, *65*(2), 588–591.

**Archer, N. K., Mazaitis, M. J., Costerton, J. W., Leid, J. G., Powers, M. E., & Shirtliff, M. E.** (2011). *Staphylococcus aureus* biofilms: Properties, regulation and roles in human disease. *Virulence*, *2*(5), 445–459.

**Arciola, C. R., Campoccia, D., & Montanaro, L.** (2018). Implant infections: Adhesion, biofilm formation and immune evasion. *Nature Reviews Microbiology*, *16*(7), 397–409.

**Atkin, K. E., Macdonald, S. J., Brentnall, A. S., Potts, J. R., & Thomas, G. H.** (2014). A different path: Revealing the function of staphylococcal proteins in biofilm formation. *FEBS Letters*, *588*(10), 1869–1872.

**Auriti, C., Prencipe, G., Moriondo, M., Bersani, I., Bertaina, C., Mondì, V., & Inglese, R.** (2017). Mannose-Binding Lectin: Biologic Characteristics and Role in the Susceptibility to Infections and Ischemia-Reperfusion Related Injury in Critically Ill Neonates. *Journal of Immunology Research*, *2017*.

**Avril, T., Wagner, E. R., Willison, H. J., & Crocker, P. R.** (2006). Sialic acid-binding immunoglobulin-like lectin 7 mediates selective recognition of sialylated glycans expressed on *Campylobacter jejuni* lipooligosaccharides. *Infection and Immunity*, *74*(7), 4133–4141.

**Azad, A. K., Torrelles, J. B., & Schlesinger, L. S.** (2008). Mutation in the DC-SIGN cytoplasmic triacidic cluster motif markedly attenuates receptor activity for phagocytosis and endocytosis of mannose-containing ligands by human myeloid cells. *Journal of Leukocyte Biology*, *84*(6), 1594–1603.

**Babapour, E., Haddadi, A., Mirnejad, R., Angaji, S.-A., & Amirmozafari, N.**

(2016). Biofilm formation in clinical isolates of nosocomial *Acinetobacter baumannii* and its relationship with multidrug resistance. *Asian Pacific Journal of Tropical Biomedicine*, *6*(6), 528–533.

**Bagasra, O., Wright, S. D., Seshamma, T., Oakes, J. W., & Pomerantz, R. J.** (1992). CD14 is involved in control of human immunodeficiency virus type 1 expression in latently infected cells by lipopolysaccharide. *Proceedings of the National Academy of Sciences of the United States of America*, *89*(14), 6285–6289.

**Baker, H. M., Basu, I., Chung, M. C., Caradoc-Davies, T., Fraser, J. D., & Baker, E. N.** (2007). Crystal Structures of the Staphylococcal Toxin SSL5 in Complex with Sialyl Lewis X Reveal a Conserved Binding Site that Shares Common Features with Viral and Bacterial Sialic Acid Binding Proteins. *Journal of Molecular Biology*, *374*(5), 1298–1308.

**Baldassarri, L., Donnelli, G., Gelosia, A., Voglino, M. C., Simpson, A. W., & Christensen, G. D.** (1996). Purification and characterization of the staphylococcal slime-associated antigen and its occurrence among *Staphylococcus epidermis* clinical isolates. *Infection and Immunity*, *64*(8), 3410 LP-3415.

**Barthel, S. R., Gavino, J. D., Descheny, L., & Dimitroff, C. J.** (2007). Targeting selectins and selectin ligands in inflammation and cancer. *Expert Opinion on Therapeutic Targets*, *11*(11), 1473–1491.

**Becker, D. J., & Lowe, J. B.** (2003). Fucose: Biosynthesis and biological function in mammals. *Glycobiology*, *13*(7).

**Beltrame, M. H., Catarino, S. J., Goeldner, I., Boldt, A. B. W., & de Messias-Reason, I. J.** (2015). The lectin pathway of complement and rheumatic heart disease. *Frontiers in Pediatrics*, *2*, 148.

**Bergman, M., Del Prete, G., van Kooyk, Y., & Appelmelk, B.** (2006). *Helicobacter pylori* phase variation, immune modulation and gastric autoimmunity. *Nature Reviews Microbiology*, *4*(2), 151–159.

**Bergman, M. P., Engering, A., Smits, H. H., Van Vliet, S. J., Van Bodegraven, A. A., Wirth, H.-P., Kapsenberg, M. L., Vandenbroucke-Grauls, C. M. J. E., Van Kooyk, Y., & Appelmelk, B. J.** (2004). *Helicobacter pylori* modulates the T helper cell 1/T helper cell 2 balance through phase-variable interaction between lipopolysaccharide and DC-SIGN. *Journal of Experimental Medicine*, *200*(8), 979–990.

**Berlau, J., Aucken, H., Malnick, H., & Pitt, T.** (1999). Distribution of *Acinetobacter* species on skin of healthy humans. *European Journal of Clinical Microbiology and Infectious Diseases*, *18*(3), 179–183.

**Berne, C., Ducret, A., Hardy, G. G., & Brun, Y. V**. (2015). Adhesins involved in attachment to abiotic surfaces by gram-negative bacteria. *Microbiology Spectrum*, *3*(4).

**Bestebroer, J., Poppelier, M. J. J. G., Ulfman, L. H., Lenting, P. J., Denis, C. V.,**

**Van Kessel, K. P. M., Van Strijp, J. A. G., & De Haas, C. J. C.** (2007). Staphylococcal superantigen-like 5 binds PSGL-1 and inhibits P-selectin-mediated neutrophil rolling. *Blood*, *109*(7).

**Bestebroer, J., Van Kessel, K. P. M., Azouagh, H., Walenkamp, A. M., Boer, I. G. J., Romijn, R. A., Van Strijp, J. A. G., & De Haas, C. J. C.** (2009). Staphylococcal SSL5 inhibits leukocyte activation by chemokines and anaphylatoxins. *Blood*, *113*(2), 328–337.

**Bogoslowski, A., Butcher, E. C., & Kubes, P.** (2018). Neutrophils recruited through high endothelial venules of the lymph nodes via PNAd intercept disseminating *Staphylococcus aureus*. *Proceedings of the National Academy of Sciences of the United States of America*, *115*(10), 2449–2454.

**Bose, J. L., Lehman, M. K., Fey, P. D., & Bayles, K. W.** (2012). Contribution of the *Staphylococcus aureus* Atl AM and GL Murein hydrolase activities in cell division, autolysis, and biofilm formation. *PLoS ONE*, *7*(7).

**Botos, I., Segal, D. M., & Davies, D. R.** (2011). The structural biology of Toll-like receptors. *Structure*, *19*(4), 447–459.

**Boukerb, A. M., Rousset, A., Galanos, N., Méar, J.-B., Thépaut, M., Grandjean, T., Gillon, E., Cecioni, S., Abderrahmen, C., Faure, K., Redelberger, D., Kipnis, E., Dessein, R., Havet, S., Darblade, B., Matthews, S. E., De Bentzmann, S., Guéry, B., Cournoyer, B., Imberty, A., & Vidal, S.** (2014). Antiadhesive properties of glycoclusters against *Pseudomonas aeruginosa* lung infection. *Journal of Medicinal Chemistry*, *57*(24), 10275–10289.

**Bradshaw, R. A., & Dennis, E.** (2010). *Handbook of cell signaling*. *Handbook of Cell Signaling, 2/e* (Vol. 1–3).

**Brinkman-Van der Linden, E. C. M., Angata, T., Reynolds, S. A., Powell, L. D., Hedrick, S. M., & Varki, A.** (2003). CD33/Siglec-3 binding specificity, expression pattern, and consequences of gene deletion in mice. *Molecular and Cellular Biology*, *23*(12), 4199–4206.

**Brown, G. D., Herre, J., Williams, D. L., Willment, J. A., Marshall, A. S. J., & Gordon, S.** (2003). Dectin-1 mediates the biological effects of β-glucans. *Journal of Experimental Medicine*, *197*(9), 1119–1124.

**Brubaker, S. W., Bonham, K. S., Zanoni, I., & Kagan, J. C.** (2015). Innate immune pattern recognition: A cell biological perspective. *Annual Review of Immunology*.

**Bryers, J. D.** (2008). Medical biofilms. *Biotechnology and Bioengineering*, *100*(1), 1–18.

**Cabral, M. P., Soares, N. C., Aranda, J., Parreira, J. R., Rumbo, C., Poza, M., Valle, J., Calamia, V., Lasa, I., & Bou, G.** (2011). Proteomic and functional analyses reveal a unique lifestyle for *Acinetobacter baumannii* biofilms and a key role for histidine metabolism. *Journal of Proteome Research*, *10*(8), 3399–3417.

**Cambi, A., Gijzen, K., de Vries, I. J. M., Torensma, R., Joosten, B., Adema, G. J., Netea, M. G., Kullberg, B.-J., Romani, L., & Figdor, C. G.** (2003). The C-type lectin DC-SIGN (CD209) is an antigen-uptake receptor for Candida albicans on dendritic cells. *European Journal of Immunology*, *33*(2), 532–538.

**Campanero-Rhodes, M. A., Llobet, E., Bengoechea, J. A., & Solís, D.** (2015). Bacteria microarrays as sensitive tools for exploring pathogen surface epitopes and recognition by host receptors. *RSC Advances*, *5*(10), 7173–7181.

**Carlin, A. F., Lewis, A. L., Varki, A., & Nizet, V.** (2007). Group B streptococcal capsular sialic acids interact with siglecs (immunoglobulin-like lectins) on human leukocytes. *Journal of Bacteriology*, *189*(4), 1231–1237.

**Carlos, T. M., & Harlan, J. M.** (1994). Leukocyte-endothelial adhesion molecules. *Blood*, *84*(7), 2068–2101.

**Carroll, M. V, Sim, R. B., Bigi, F., Jäkel, A., Antrobus, R., & Mitchell, D. A.** (2010). Identification of four novel DC-SIGN ligands on Mycobacterium bovis BCG. *Protein and Cell*, *1*(9), 859–870.

**Caster, D. J., Powell, D. W., Miralda, I., Ward, R. A., & McLeish, K. R.** (2017). Re-Examining Neutrophil Participation in GN. *Journal of the American Society of Nephrology*, *28*(8), 2275 LP-2289.

**Cerca, N., Jefferson, K. K., Oliveira, R., Pier, G. B., & Azeredo, J.** (2006). Comparative antibody-mediated phagocytosis of *Staphylococcus epidermidis* cells grown in a biofilm or in the planktonic state. *Infection and Immunity*, *74*(8), 4849–4855.

**Chang, Y.-C., Olson, J., Louie, A., Crocker, P. R., Varki, A., & Nizet, V.** (2014). Role of macrophage sialoadhesin in host defense against the sialylated pathogen group B *Streptococcus*. *Journal of Molecular Medicine*, *92*(9), 951–959.

**Chavakis, T., Hussain, M., Kanse, S. M., Peters, G., Bretzel, R. G., Flock, J.-I., Herrmann, M., & Preissner, K. T.** (2002). *Staphylococcus aureus* extracellular adherence protein serves as anti-inflammatory factor by inhibiting the recruitment of host leukocytes. *Nature Medicine*, *8*(7), 687–693.

**Chen, K.-M., Chiang, M.-K., Wang, M., Ho, H.-C., Lu, M.-C., & Lai, Y.-C.** (2014). The role of pgaC in *Klebsiella pneumoniae* virulence and biofilm formation. *Microbial Pathogenesis*, *77*, 89–99.

**Choi, A. H. K., Slamti, L., Avci, F. Y., Pier, G. B., & Maira-Litrán, T.** (2009). The pgaABCD locus of *Acinetobacter baumannii* encodes the production of poly-β-1-6-*N*-acetylglucosamine, which is critical for biofilm formation. *Journal of Bacteriology*, *191*(19), 5953–5963.

**Chu, Y. W., Leung, C. M., Houang, E. T. S., Ng, K. C., Leung, C. B., Leung, H. Y., & Cheng, A. F. B.** (1999). Skin carriage of acinetobacters in Hong Kong. *Journal of Clinical Microbiology*, *37*(9), 2962–2967.

**Chung, M. C., Wines, B. D., Baker, H., Langley, R. J., Baker, E. N., & Fraser, J. D.** (2007). The crystal structure of staphylococcal superantigen-like protein 11

in complex with sialyl Lewis X reveals the mechanism for cell binding and immune inhibition. *Molecular Microbiology*, *66*(6), 1342–1355.

**Crocker, P. R., Paulson, J. C., & Varki, A.** (2007). Siglecs and their roles in the immune system. *Nature Reviews Immunology*, *7*(4), 255–266.

**Curtis, B. M., Scharnowske, S., & Watson, A. J.** (1992). Sequence and expression of a membrane-associated C-type lectin that exhibits CD4-independent binding of human immunodeficiency virus envelope glycoprotein gp120. *Proceedings of the National Academy of Sciences*, *89*(17), 8356 LP-8360.

**Cywes-Bentley, C., Skurnik, D., Zaidi, T., Roux, D., DeOliveira, R. B., Garrett, W. S., Lu, X., O'Malley, J., Kinzel, K., Zaidi, T., Rey, A., Perrin, C., Fichorova, R. N., Kayatani, A. K. K., Maira-Litràn, T., Gening, M. L., Tsvetkov, Y. E., Nifantiev, N. E., Bakaletz, L. O., Pelton, S. I., Golenbock, D. T., & Pier, G. B.** (2013). Antibody to a conserved antigenic target is protective against diverse prokaryotic and eukaryotic pathogens. *Proceedings of the National Academy of Sciences of the United States of America*, *110*(24), E2209–E2218.

**De Witte, L., Abt, M., Schneider-Schaulies, S., Van Kooyk, Y., & Geijtenbeek, T. B. H.** (2006). Measles virus targets DC-SIGN to enhance dendritic cell infection. *Journal of Virology*, *80*(7), 3477–3486.

**Diggle, S. P., Stacey, R. E., Dodd, C., Cámara, M., Williams, P., & Winzer, K.** (2006). The galactophilic lectin, LecA, contributes to biofilm development in *Pseudomonas aeruginosa*. *Environmental Microbiology*, *8*(6), 1095–1104.

**Donlan, R. M., & Costerton, J. W.** (2002). Biofilms: Survival mechanisms of clinically relevant microorganisms. *Clinical Microbiology Reviews*, *15*(2), 167–193.

**Drickamer, K.** (1992). Engineering galactose-binding activity into a C-type mannose-binding protein. *Nature*, *360*(6400), 183–186.

**Dziarski, R., & Gupta, D.** (2005). *Staphylococcus aureus* peptidoglycan is a toll-like receptor 2 activator: A reevaluation. *Infection and Immunity*, *73*(8), 5212–5216.

**Dziarski, R., Tapping, R. I., & Tobias, P. S.** (1998). Binding of bacterial peptidoglycan to CD14. *Journal of Biological Chemistry*, *273*(15), 8680–8690.

**Dziarski, R., Ulmer, A. J., & Gupta, D.** (1999). Interactions of CD14 with components of gram-positive bacteria. *Chemical Immunology*, *74*, 83–107.

**Eddie Ip, W. K., Takahashi, K., Alan Ezekowitz, R., & Stuart, L. M.** (2009). Mannose-binding lectin and innate immunity. *Immunological Reviews*, *230*(1), 9–21.

**Eddie Ip, W. K., Takahashi, K., Moore, K. J., Stuart, L. M., & Ezekowitz, R. A. B.** (2008). Mannose-binding lectin enhances Toll-like receptors 2 and 6 signaling from the phagosome. *Journal of Experimental Medicine*, *205*(1), 169–181.

**Endo, Y., Sato, Y., Matsushita, M., & Fujita, T.** (1996). Cloning and Characterization of the Human Lectin P35 Gene and Its Related Gene. *Genomics*, *36*(3), 515–521.

**Erridge, C., Moncayo-Nieto, O. L., Morgan, R., Young, M., & Poxton, I. R.** (2007). *Acinetobacter baumannii* lipopolysaccharides are potent stimulators of human monocyte activation via Toll-like receptor 4 signalling. *Journal of Medical Microbiology*, *56*(PART 2), 165–171.

**Fagon, J.-Y., Chastre, J., Domart, Y., Trouillet, J.-L., & Gibert, C.** (1996). Mortality due to ventilator-associated pneumonia or colonization with *Pseudomonas* or *Acinetobacter* species: Assessment by quantitative culture of samples obtained by a protected specimen brush. *Clinical Infectious Diseases*, *23*(3), 538–542.

**Feinberg, H., Mitchell, D. A., Drickamer, K., & Weis, W. I.** (2001). Structural basis for selective recognition of oligosaccharides by DC-SIGN and DC-SIGNR. *Science*, *294*(5549), 2163–2166.

**Feng, L.** (2005). Probing lipid-protein interactions using lipid microarrays. *Prostaglandins and Other Lipid Mediators*, *77*(1–4), 158–167.

**Ferreirinha, P., Pérez-Cabezas, B., Correia, A., Miyazawa, B., França, A., Carvalhais, V., Faustino, A., Cordeiro-da-Silva, A., Teixeira, L., Pier, G. B., Cerca, N., & Vilanova, M.** (2016). Poly-*N*-acetylglucosamine production by *Staphylococcus epidermidis* cells increases their in vivo proinflammatory effect. *Infection and Immunity*, *84*(10), 2933–2943.

**Fevre, C., Bestebroer, J., Mebius, M. M., de Haas, C. J. C., van Strijp, J. A. G., Fitzgerald, J. R., & Haas, P.-J. A.** (2014). *Staphylococcus aureus* proteins SSL6 and SElX interact with neutrophil receptors as identified using secretome phage display. *Cellular Microbiology*, *16*(11), 1646–1665.

**Figueiredo, R. T., Carneiro, L. A. M., & Bozza, M. T.** (2011). Fungal surface and innate immune recognition of filamentous fungi. *Frontiers in Microbiology*, *2*(DEC).

**Flannery, A., Gerlach, Q. J., Joshi, L., & Kilcoyne, M.** (2015). Assessing Bacterial Interactions Using Carbohydrate-Based Microarrays. *Microarrays* *4*(4), 690-713.

**Flemming, H.-C., & Wingender, J.** (2010). The biofilm matrix. *Nature Reviews Microbiology*, *8*(9), 623–633.

**Fournier, B., & Philpott, D. J.** (2005). Recognition of *Staphylococcus aureus* by the innate immune system. *Clinical Microbiology Reviews*, *18*(3), 521–540.

**Frederiksen, P. D., Thiel, S., Larsen, C. B., & Jensenius, J. C.** (2005). M-ficolin, an innate immune defence molecule, binds patterns of acetyl groups and activates complement. *Scandinavian Journal of Immunology*, *62*(5), 462–473.

**Fujita, T.** (2002). Evolution of the lectin-complement pathway and its role in innate immunity. *Nat Rev Immunol*, *2*(5), 346–353.

**Gaddy, J. A., Tomaras, A. P., & Actis, L. A.** (2009). The *Acinetobacter baumannii* 19606 OmpA protein plays a role in biofilm formation on abiotic surfaces and in the interaction of this pathogen with eukaryotic cells. *Infection and Immunity*, *77*(8), 3150–3160.

**Gao, J. J., Xue, Q., Zuvanich, E. G., Haghi, K. R., & Morrison, D. C.** (2001). Commercial preparations of lipoteichoic acid contain endotoxin that contributes to activation of mouse macrophages in vitro. *Infection and Immunity*, *69*(2), 751–757.

**Garcia-Vallejo, J. J., Koning, N., Ambrosini, M., Kalay, H., Vuist, I., Sarrami-Forooshani, R., Geijtenbeek, T. B. H., & van Kooyk, Y.** (2013). Glycodendrimers prevent HIV transmission via DC-SIGN on dendritic cells. *International Immunology*, *25*(4), 221–233.

**Gardner, J. P., Durso, R. J., Arrigale, R. R., Donovan, G. P., Maddon, P. J., Dragic, T., & Olson, W. C.** (2003). L-SIGN (CD 209L) is a liver-specific capture receptor for hepatitis C virus. *Proceedings of the National Academy of Sciences of the United States of America*, *100*(8), 4498–4503.

**Garred, P., Brygge, K., Sorensen, C. H., Madsen, H. O., Thiel, S., & Svejgaard, A.** (1993). Mannan-binding protein - Levels in plasma and upper-airways and frequency of genotypes in children with recurrence of otitis media. *Clinical and Experimental Immunology*, *94*(1), 99–104.

**Garred, P., Genster, N., Pilely, K., Bayarri-Olmos, R., Rosbjerg, A., Ma, Y. J., & Skjoedt, M.-O.** (2016). A journey through the lectin pathway of complement—MBL and beyond. *Immunological Reviews*, *274*(1), 74–97.

**Gasteiger, G., D'osualdo, A., Schubert, D. A., Weber, A., Bruscia, E. M., & Hartl, D.** (2017). Cellular Innate Immunity: An Old Game with New Players. *Journal of Innate Immunity*, *9*(2), 111–125.

**Geijtenbeek, T. B. H., Krooshoop, D. J. E. B., Bleijs, D. A., van Vliet, S. J., van Duijnhoven, G. C. F., Grabovsky, V., Alon, R., Figdor, C. G., & van Kooyk, Y.** (2000). DC-SIGN–ICAM-2 interaction mediates dendritic cell trafficking. *Nature Immunology*, *1*, 353.

**Geijtenbeek, T. B. H., Torensma, R., van Vliet, S. J., van Duijnhoven, G. C. F., Adema, G. J., van Kooyk, Y., & Figdor, C. G.** (2000). Identification of DC-SIGN, a Novel Dendritic Cell-Specific ICAM-3 Receptor that Supports Primary Immune Responses. *Cell*, *100*(5), 575–585.

**Geijtenbeek, T. B. H., van Vliet, S. J., Koppel, E. A., Sanchez-Hernandez, M., Vandenbroucke-Grauls, C. M. J. E., Appelmelk, B., & van Kooyk, Y.** (2003). Mycobacteria Target DC-SIGN to Suppress Dendritic Cell Function. *The Journal of Experimental Medicine*, *197*(1), 7–17.

**Geoghegan, J. A., Corrigan, R. M., Gruszka, D. T., Speziale, P., O'Gara, J. P., Potts, J. R., & Foster, T. J.** (2010). Role of surface protein SasG in biofilm formation by *Staphylococcus aureus*. *Journal of Bacteriology*, *192*(21), 5663–5673.

**Gerke, C., Kraft, A., Süßmuth, R., Schweitzer, O., & Götz, F.** (1998). Characterization of the *N*-Acetylglucosaminyltransferase activity involved in the biosynthesis of the *Staphylococcus epidermidis* polysaccharide intercellular adhesin. *Journal of Biological Chemistry*, *273*(29), 18586–18593.

**Giese, M. J., Shum, D. C., Rayner, S. A., Mondino, B. J., & Berliner, J. A.** (2000). Adhesion molecule expression in a rat model of *Staphylococcus aureus* endophthalmitis. *Investigative Ophthalmology and Visual Science*, *41*(1).

**Gillespie, L., Roosendahl, P., Ng, W. C., Brooks, A. G., Reading, P. C., & Londrigan, S. L.** (2016). Endocytic function is critical for influenza A virus infection via DC-SIGN and L-SIGN. *Scientific Reports*, *6*.

**Götz, F.** (2002). *Staphylococcus* and biofilms. *Molecular Microbiology*, *43*(6), 1367–1378.

**Gouin, S. G., Wellens, A., Bouckaert, J., & Kovensky, J.** (2009). Synthetic multimeric heptyl mannosides as potent antiadhesives of uropathogenic *Escherichia coli*. *ChemMedChem*, *4*(5), 749–755.

**Gout, E., Garlatti, V., Smith, D. F., Lacroix, M., Dumestre-Pérard, C., Lunardi, T., Martin, L., Cesbron, J.-Y., Arlaud, G. J., Gaboriaud, C., & Thielens, N. M.** (2010). Carbohydrate recognition properties of human ficolins: Glycan array screening reveals the sialic acid binding specificity of M-ficolin. *Journal of Biological Chemistry*, *285*(9), 6612–6622.

**Gringhuis, S. I., den Dunnen, J., Litjens, M., van der Vlist, M., & Geijtenbeek, T. B. H.** (2009). Carbohydrate-specific signaling through the DC-SIGN signalosome tailors immunity to *Mycobacterium tuberculosis*, HIV-1 and *Helicobacter pylori*. *Nature Immunology*, *10*(10), 1081–1088.

**Gringhuis, S. I., den Dunnen, J., Litjens, M., van het Hof, B., van Kooyk, Y., & Geijtenbeek, T. H.** (2007). C-Type Lectin DC-SIGN Modulates Toll-like Receptor Signaling via Raf-1 Kinase-Dependent Acetylation of Transcription Factor NF-κB. *Immunity*, *26*(5), 605–616.

**Guo, Y., Feinberg, H., Conroy, E., Mitchell, D. A., Alvarez, R., Blixt, O., Taylor, M. E., Weis, W. I., & Drickamer, K.** (2004). Structural basis for distinct ligand-binding and targeting properties of the receptors DC-SIGN and DC-SIGNR. *Nature Structural and Molecular Biology*, *11*(7), 591–598.

**Hadley, J. S., Wang, J. E., Foster, S. J., Thiemermann, C., & Hinds, C. J.** (2005). Peptidoglycan of *Staphylococcus aureus* upregulates monocyte expression of CD14, Toll-like receptor 2 (TLR2), and TLR4 in human blood: Possible implications for priming of lipopolysaccharide signaling. *Infection and Immunity*, *73*(11), 7613–7619.

**Hajishengallis, G., & Lambris, J. D.** (2011). Microbial manipulation of receptor crosstalk in innate immunity. *Nature Reviews Immunology*, *11*(3), 187–200.

**Hall, C. W., & Mah, T.-F.** (2017). Molecular mechanisms of biofilm-based antibiotic resistance and tolerance in pathogenic bacteria. *FEMS Microbiology Reviews*, *41*(3), 276–301.

**Han, S. H., Kim, J. H., Martin, M., Michalek, S. M., & Nahm, M. H.** (2003). Pneumococcal lipoteichoic acid (LTA) is not as potent as staphylococcal LTA in stimulating Toll-like receptor 2. *Infection and Immunity*, *71*(10), 5541–5548.

**Hansen, S. W. K., Ohtani, K., Roy, N., & Wakamiya, N.** (2016). The collectins CL-L1, CL-K1 and CL-P1, and their roles in complement and innate immunity. *Immunobiology*, *221*(10), 1058–1067.

**Hanzelmann, D., Joo, H.-S., Franz-Wachtel, M., Hertlein, T., Stevanovic, S., Macek, B., Wolz, C., Götz, F., Otto, M., Kretschmer, D., & Peschel, A.** (2016). Toll-like receptor 2 activation depends on lipopeptide shedding by bacterial surfactants. *Nature Communications*, *7*.

**Harumiya, S., Takeda, K., Sugiura, T., Fukumoto, Y., Tachikawa, H., Miyazono, K., Fujimoto, D., & Ichijo, H.** (1996). Characterization of ficolins as novel elastin-binding proteins and molecular cloning of human ficolin-1. *Journal of Biochemistry*, *120*(4), 745–751.

**Hashimoto, M., Tawaratsumida, K., Kariya, H., Aoyama, K., Tamura, T., & Suda, Y.** (2006). Lipoprotein is a predominant toll-like receptor 2 ligand in *Staphylococcus aureus* cell wall components. *International Immunology*, *18*(2), 355–362.

**Hayashi, F., Smith, K. D., Ozinsky, A., Hawn, T. R., Yi, E. C., Goodlett, D. R., Eng, J. K., Akira, S., Underhill, D. M., & Aderem, A.** (2001). The innate immune response to bacterial flagellin is mediated by Toll-like receptor 5. *Nature*, *410*(6832), 1099–1103.

**Haziot, A., Ferrero, E., Köntgen, F., Hijiya, N., Yamamoto, S., Silver, J., Stewart, C. L., & Goyert, S. M.** (1996). Resistance to endotoxin shock and reduced dissemination of gram-negative bacteria in CD14-deficient mice. *Immunity*, *4*(4), 407–414.

**Heikema, A. P., Bergman, M. P., Richards, H., Crocker, P. R., Gilbert, M., Samsom, J. N., Van Wamel, W. J. B., Endtz, H. P., & Van Belkum, A.** (2010). Characterization of the specific interaction between sialoadhesin and sialylated *Campylobacter jejuni* lipooligosaccharides. *Infection and Immunity*, *78*(7), 3237–3246.

**Heller, M. J.** (2002). DNA microarray technology: Devices, systems, and applications. *Annual Review of Biomedical Engineering 4*(1), 129-153.

**Henriksen, M. L., Brandt, J., Andrieu, J.-P., Nielsen, C., Jensen, P. H., Holmskov, U., Jorgensen, T. J. D., Palarasah, Y., Thielens, N. M., & Hansen, S.** (2013). Heteromeric Complexes of Native Collectin Kidney 1 and Collectin Liver 1 Are Found in the Circulation with MASPs and Activate the Complement System. *The Journal of Immunology*, *191*(12), 6117 LP-6127.

**Hirabayashi, J., Yamada, M., Kuno, A., & Tateno, H.** (2013). Lectin microarrays: Concept, principle and applications. *Chemical Society Reviews*, *42*(10), 4443–4458.

**Hoebe, K., Georgel, P., Rutschmann, S., Du, X., Mudd, S., Crozat, K., Sovath,**

**S., Shamel, L., Hartung, T., Zähringer, U., & Beutler, B.** (2005). CD36 is a sensor of diacylglycerides. *Nature*, *433*(7025), 523–527.

**Hsu, K.-L., Pilobello, K. T., & Mahal, L. K.** (2006). Analyzing the dynamic bacterial glycome with a lectin microarray approach. *Nature Chemical Biology*, *2*(3), 153–157.

**Hu, S., & Wong, D. T.** (2009). Lectin microarray. *Proteomics. Clinical Applications*, *3*(2), 148–154.

**Hummelshoj, T., Fog, L. M., Madsen, H. O., Sim, R. B., & Garred, P.** (2008). Comparative study of the human ficolins reveals unique features of Ficolin-3 (Hakata antigen). *Molecular Immunology*, *45*(6), 1623–1632.

**Hung, C.-S., Bouckaert, J., Hung, D., Pinkner, J., Widberg, C., DeFusco, A., Auguste, C. G., Strouse, R., Langermann, S., Waksman, G., & Hultgren, S. J.** (2002). Structural basis of tropism of *Escherichia coli* to the bladder during urinary tract infection. *Molecular Microbiology*, *44*(4), 903–915.

**Imberty, A., Chabre, Y. M., & Roy, R.** (2008). Glycomimetics and glycodendrimers as high affinity microbial anti-adhesins. *Chemistry - A European Journal*, *14*(25), 7490–7499.

**Itoh, Y., Rice, J. D., Goller, C., Pannuri, A., Taylor, J., Meisner, J., Beveridge, T. J., Preston III, J. F., & Romeo, T.** (2008). Roles of pgaABCD genes in synthesis, modification, and export of the *Escherichia coli* biofilm adhesin poly-β-1,6-*N*-acetyl-D-glucosamine. *Journal of Bacteriology*, *190*(10), 3670–3680.

**Iwaki, D., Mitsuzawa, H., Murakami, S., Sano, H., Konishi, M., Akino, T., & Kuroki, Y.** (2002). The extracellular toll-like receptor 2 domain directly binds peptidoglycan derived from *Staphylococcus aureus*. *Journal of Biological Chemistry*, *277*(27), 24315–24320.

**Jefferson, K. K., Cramton, S. E., Götz, F., & Pier, G. B.** (2003). Identification of a 5-nucleotide sequence that controls expression of the ica locus in *Staphylococcus aureus* and characterization of the DNA-binding properties of IcaR. *Molecular Microbiology*, *48*(4), 889–899.

**Jensen, M. L., Honoré, C., Hummelshøj, T., Hansen, B. E., Madsen, H. O., & Garred, P.** (2007). Ficolin-2 recognizes DNA and participates in the clearance of dying host cells. *Molecular Immunology*, *44*(5), 856–865.

**Jin, M. S., Kim, S. E., Heo, J. Y., Lee, M. E., Kim, H. M., Paik, S.-G., Lee, H., & Lee, J.-O.** (2007). Crystal Structure of the TLR1-TLR2 Heterodimer Induced by Binding of a Tri-Acylated Lipopeptide. *Cell*, *130*(6), 1071–1082.

**Jones, C., Virji, M., & Crocker, P. R.** (2003). Recognition of sialylated meningococcal lipopolysaccharide by siglecs expressed on myeloid cells leads to enhanced bacterial uptake. *Molecular Microbiology*, *49*(5), 1213–1225.

**Joo, H.-S., & Otto, M.** (2012). Molecular basis of in vivo biofilm formation by bacterial pathogens. *Chemistry and Biology*, *19*(12), 1503–1513.

**Jørgensen, M., Bæk, R., Pedersen, S., Søndergaard, E. K. L., Kristensen, S. R., & Varming, K.** (2013). Extracellular Vesicle (EV) array: Microarray capturing of exosomes and other extracellular vesicles for multiplexed phenotyping. *Journal of Extracellular Vesicles*, *2*(1).

**Joyce, J. G., Abeygunawardana, C., Xu, Q., Cook, J. C., Hepler, R., Przysiecki, C. T., Grimm, K. M., Roper, K., Yu Ip, C. C., Cope, L., Montgomery, D., Chang, M., Campie, S., Brown, M., McNeely, T. B., Zorman, J., Maira-Litrán, T., Pier, G. B., Keller, P. M., Jansen, K. U., & Mark III, G. E.** (2003). Isolation, structural characterization, and immunological evaluation of a high-molecular-weight exopolysaccharide from *Staphylococcus aureus*. *Carbohydrate Research*, *338*(9), 903–922.

**Kang, J. Y., Nan, X., Jin, M. S., Youn, S.-J., Ryu, Y. H., Mah, S., Han, S. H., Lee, H., Paik, S.-G., & Lee, J.-O.** (2009). Recognition of Lipopeptide Patterns by Toll-like Receptor 2-Toll-like Receptor 6 Heterodimer. *Immunity*, *31*(6), 873–884.

**Kaplan, J. B.** (2010). Biofilm Dispersal: Mechanisms, Clinical Implications, and Potential Therapeutic Uses. *Journal of Dental Research*, *89*(3), 205–218.

**Kasimova, A. A., Shneider, M. M., Arbatsky, N. P., Popova, A. V, Shashkov, A. S., Miroshnikov, K. A., Balaji, V., Biswas, I., & Knirel, Y. A.** (2017). Structure and gene cluster of the K93 capsular polysaccharide of *Acinetobacter baumannii* B11911 containing 5-N-Acetyl-7-N-[(R)-3-hydroxybutanoyl]pseudaminic acid. *Biochemistry (Moscow)*, *82*(4), 483–489.

**Kawamura, N., Imanishi, N., Koike, H., Nakahara, H., Phillips, L., & Morooka, S.** (1995). Lipoteichoic acid-induced neutrophil adhesion via E-selectin to human umbilical vein endothelial cells (HUVECs). *Biochemical and Biophysical Research Communications*, *217*(3), 1208–1215.

**Kawasaki, T., & Kawai, T.** (2014). Toll-like receptor signaling pathways. *Frontiers in Immunology*, *5*(SEP).

**Kay, E., Lesk, V. I., Tamaddoni-Nezhad, A., Hitchen, P. G., Dell, A., Sternberg, M. J., Muggleton, S., & Wren, B. W.** (2010). Systems analysis of bacterial glycomes. *Biochemical Society Transactions*, *38*(5), 1290–1293.

**Kelly-Quintos, C., Cavacini, L. A., Posner, M. R., Goldmann, D., & Pier, G. B.** (2006). Characterization of the opsonic and protective activity against *Staphylococcus aureus* of fully human monoclonal antibodies specific for the bacterial surface polysaccharide poly-*N*-acetylglucosamine. *Infection and Immunity*, *74*(5), 2742–2750.

**Khanal, M., Larsonneur, F., Raks, V., Barras, A., Baumann, J.-S., Martin, F. A., Boukherroub, R., Ghigo, J.-M., Ortiz Mellet, C., Zaitsev, V., Garcia Fernandez, J. M., Beloin, C., Siriwardena, A., & Szunerits, S.** (2015). Inhibition of type 1 fimbriae-mediated *Escherichia coli* adhesion and biofilm formation by trimeric cluster thiomannosides conjugated to diamond nanoparticles. *Nanoscale*, *7*(6), 2325–2335.

**Khatua, B., Bhattacharya, K., & Mandal, C.** (2012). Sialoglycoproteins adsorbed

by *Pseudomonas aeruginosa* facilitate their survival by impeding neutrophil extracellular trap through siglec-9. *Journal of Leukocyte Biology*, *91*(4), 641–655.

**Khatua, B., Ghoshal, A., Bhattacharya, K., Mandal, C., Saha, B., Crocker, P. R., & Mandal, C.** (2010). Sialic acids acquired by *Pseudomonas aeruginosa* are involved in reduced complement deposition and siglec mediated host-cell recognition. *FEBS Letters*, *584*(3), 555–561.

**Kielian, T., Esen, N., & Bearden, E. D.** (2005). Toll-like receptor 2 (TLR2) is pivotal for recognition of *S. aureus* peptidoglycan but not intact bacteria by microglia. *GLIA*, *49*(4), 567–576.

**Kilcoyne, M., Gerlach, J. Q., Gough, R., Gallagher, M. E., Kane, M., Carrington, S. D., & Joshi, L.** (2012). Construction of a natural mucin microarray and interrogation for biologically relevant glyco-epitopes. *Analytical Chemistry*, *84*(7), 3330–3338.

**Kilpatrick, D. C., & Chalmers, J. D.** (2012). Human L-ficolin (ficolin-2) and its clinical significance. *Journal of Biomedicine and Biotechnology*, *2012*, 1-10.

**Kjaer, T. R., Hansen, A. G., Sørensen, U. B. S., Nielsen, O., Thiel, S., & Jensenius, J. C.** (2011). Investigations on the pattern recognition molecule M-ficolin: Quantitative aspects of bacterial binding and leukocyte association. *Journal of Leukocyte Biology*, *90*(3), 425–437.

**Klaas, M., Oetke, C., Lewis, L. E., Erwig, L. P., Heikema, A. P., Easton, A., Willison, H. J., & Crocker, P. R.** (2012). Sialoadhesin promotes rapid proinflammatory and type I IFN responses to a sialylated pathogen, *Campylobacter jejuni*. *Journal of Immunology*, *189*(5), 2414–2422.

**Klena, J., Zhang, P., Schwartz, O., Hull, S., & Chen, T.** (2005). The core lipopolysaccharide of *Escherichia coli* is a ligand for the dendritic-cell-specific intercellular adhesion molecule nonintegrin CD209 receptor. *Journal of Bacteriology*, *187*(5), 1710–1715.

**Klimstra, W. B., Nangle, E. M., Smith, M. S., Yurochko, A. D., & Ryman, K. D.** (2003). DC-SIGN and L-SIGN Can Act as Attachment Receptors for Alphaviruses and Distinguish between Mosquito Cell- and Mammalian Cell-Derived Viruses. *Journal of Virology*, *77*(22), 12022–12032.

**Kluytmans, J., Van Belkum, A., & Verbrugh, H.** (1997). Nasal carriage of *Staphylococcus aureus*: Epidemiology, underlying mechanisms, and associated risks. *Clinical Microbiology Reviews*, *10*(3), 505–520.

**Knapp, S., Wieland, C. W., Florquin, S., Pantophlet, R., Dijkshoorn, L., Tshimbalanga, N., Akira, S., & Van Der Poll, T.** (2006). Differential roles of CD14 and Toll-like receptors 4 and 2 in murine *Acinetobacter pneumonia*. *American Journal of Respiratory and Critical Care Medicine*, *173*(1), 122–129.

**Knuefermann, P., Sakata, Y., Baker, J. S., Huang, C.-H., Sekiguchi, K., Hardarson, H. S., Takeuchi, O., Akira, S., & Vallejo, J. G.** (2004). Toll-like receptor 2 mediates *Staphylococcus aureus*-induced myocardial dysfunction

and cytokine production in the heart. *Circulation*, *110*(24), 3693–3698.

**Kobayashi, S. D., Malachowa, N., & DeLeo, F. R.** (2018). Neutrophils and Bacterial Immune Evasion. *Journal of Innate Immunity, 10,* 432-441.

**Koch, T. K., Reuter, M., Barthel, D., Böhm, S., van den Elsen, J., Kraiczy, P., Zipfel, P. F., & Skerka, C.** (2012). *Staphylococcus aureus* Proteins Sbi and Efb Recruit Human Plasmin to Degrade Complement C3 and C3b. *PLoS ONE*, *7*(10).

**Koppel, E. A., van Gisbergen, K. P. J. M., Geijtenbeek, T. B. H., & van Kooyk, Y.** (2005). Distinct functions of DC-SIGN and its homologues L-SIGN (DC-SIGNR) and mSIGNR1 in pathogen recognition and immune regulation. *Cellular Microbiology*, *7*(2), 157–165.

**Koymans, K. J., Feitsma, L. J., Brondijk, T. H., Aerts, P. C., Lukkien, E., Lössl, P., van Kessel, K. P., de Haas, C. J., van Strijp, J. A., & Huizinga, E. G.** (2015). Structural basis for inhibition of TLR2 by staphylococcal superantigen-like protein 3 (SSL3). *Proceedings of the National Academy of Sciences of the United States of America*, *112*(35), 11018–11023.

**Krarup, A., Mitchell, D. A., & Sim, R. B.** (2008). Recognition of acetylated oligosaccharides by human L-ficolin. *Immunology Letters*, *118*(2), 152–156.

**Krarup, A., Sørensen, U. B. S., Matsushita, M., Jensenius, J. C., & Thiel, S.** (2005). Effect of capsulation of opportunistic pathogenic bacteria on binding of the pattern recognition molecules Mannan-binding lectin, L-ficolin, and H-ficolin. *Infection and Immunity*, *73*(2), 1052–1060.

**Krarup, A., Thiel, S., Hansen, A., Fujita, T., & Jensenius, J. C.** (2004). L-ficolin is a pattern recognition molecule specific for acetyl groups. *Journal of Biological Chemistry*, *279*(46), 47513–47519.

**Kristian, S. A., Birkenstock, T. A., Sauder, U., Mack, D., Götz, F., & Landmann, R.** (2008). Biofilm formation induces C3a release and protects *Staphylococcus epidermidis* from IgG and complement deposition and from neutrophil-dependent killing. *Journal of Infectious Diseases*, *197*(7), 1028–1035.

**Krzyściak, P., Chmielarczyk, A., Pobiega, M., Romaniszyn, D., & Wójkowska-Mach, J.** (2017). *Acinetobacter baumannii* isolated from hospital-acquired infection: biofilm production and drug susceptibility. *APMIS*, *125*(11), 1017–1026.

**Kukita, K., Kawada-Matsuo, M., Oho, T., Nagatomo, M., Oogai, Y., Hashimoto, M., Suda, Y., Tanaka, T., & Komatsuzawa, H.** (2013). *Staphylococcus aureus* SasA is responsible for binding to the salivary agglutinin gp340, derived from human saliva. *Infection and Immunity*, *81*(6), 1870–1879.

**Kuraya, M., Matsushita, M., Endo, Y., Thiel, S., & Fujita, T.** (2003). Expression of H-ficolin/Hakata antigen, mannose-binding lectin-associated serine protease (MASP)-1 and MASP-3 by human glioma cell line T98G. *International Immunology*, *15*(1), 109–117.

K**urokawa, K., Jung, D.-J., An, J.-H., Fuchs, K., Jeon, Y.-J., Kim, N.-H., Li, X., Tateishi, K., Park, J. A., Xia, G., Matsushita, M., Takahashi, K., Park, H.-J., Peschel, A., & Lee, B. L.** (2013). Glycoepitopes of staphylococcal wall teichoic acid govern complement-mediated opsonophagocytosis via human serum antibody and mannose-binding lectin. Journal of Biological Chemistry, 288(43), 30956–30968.

**Kurokawa, K., Kim, M.-S., Ichikawa, R., Ryu, K.-H., Dohmae, N., Nakayama, H., & Lee, B. L.** (2012). Environment-mediated accumulation of diacyl lipoproteins over their triacyl counterparts in *Staphylococcus aureus*. *Journal of Bacteriology*, *194*(13), 3299–3306.

**Kurokawa, K., Lee, H., Roh, K.-B., Asanuma, M., Kim, Y. S., Nakayama, H., Shiratsuchi, A., Choi, Y., Takeuchi, O., Kang, H. J., Dohmae, N., Nakanishi, Y., Akira, S., Sekimizu, K., & Lee, B. L.** (2009). The triacylated ATP binding cluster transporter substrate-binding lipoprotein of *Staphylococcus aureus* functions as a native ligand for toll-like receptor 2. *Journal of Biological Chemistry*, *284*(13), 8406–8411.

**Kusunoki, T., Hailman, E., Juan, T. S.-C., Lichenstein, H. S., & Wright, S. D.** (1995). Molecules from *Staphylococcus aureus* that bind CD14 and stimulate innate immune responses. *Journal of Experimental Medicine*, *182*(6), 1673–1682.

**Lasala, F., Arce, E., Otero, J. R., Rojo, J., & Delgado, R.** (2003). Mannosyl Glycodendritic Structure Inhibits DC-SIGN-Mediated Ebola Virus Infection in cis and in trans. *Antimicrobial Agents and Chemotherapy*, *47*(12), 3970–3972.

**Laverty, G., Gorman, S. P., & Gilmore, B. F.** (2014). Biomolecular mechanisms of *Pseudomonas aeruginosa* and *Escherichia coli* biofilm formation. *Pathogens*, *3*(3), 596–632.

**Lebeaux, D., Ghigo, J.-M., & Beloin, C.** (2014). Biofilm-related infections: Bridging the gap between clinical management and fundamental aspects of recalcitrance toward antibiotics. *Microbiology and Molecular Biology Reviews*, *78*(3), 510–543.

**Lee, J. S., Lee, J. C., Lee, C.-M., Jung, I. D., Jeong, Y.-I., Seong, E.-Y., Chung, H.-Y., & Park, Y.-M.** (2007). Outer membrane protein A of *Acinetobacter baumannii* induces differentiation of CD4+T cells toward a Th1 polarizing phenotype through the activation of dendritic cells. *Biochemical Pharmacology*, *74*(1), 86–97.

**Lemaitre, B., Nicolas, E., Michaut, L., Reichhart, J.-M., & Hoffmann, J. A.** (1996). The dorsoventral regulatory gene cassette spatzle/Toll/Cactus controls the potent antifungal response in Drosophila adults. *Cell*, *86*(6), 973–983.

**Lewis, K.** (2007). Persister cells, dormancy and infectious disease. *Nature Reviews Microbiology*, *5*(1), 48–56.

**Ley, K.** (2003). The role of selectins in inflammation and disease. *Trends in Molecular Medicine*, *9*(6), 263–268.

**Ley, K., & Kansas, G. S.** (2004). Selectins in T-cell recruitment to non-lymphoid tissues and sites of inflammation. *Nature Reviews Immunology*, *4*(5), 325–335.

**Lin, M. H., Shu, J. C., Lin, L. P., Chong, K. Y., Cheng, Y. W., Du, J. F., & Liu, S.-T.** (2015). Elucidating the crucial role of poly *N*-acetylglucosamine from *Staphylococcus aureus* in cellular adhesion and pathogenesis. *PLoS ONE*, *10*(4).

**Lindhorst, T. K., Kieburg, C., & Krallmann-Wenzel, U.** (1998). Inhibition of the type 1 fimbriae-mediated adhesion of *Escherichia coli* to erythrocytes by multiantennary α-mannosyl clusters: The effect of multivalency. *Glycoconjugate Journal*, *15*(6), 605–613.

**Little, D. J., Bamford, N. C., Pokrovskaya, V., Robinson, H., Nitz, M., & Howell, P. L.** (2014). Structural basis for the De-*N*-acetylation of poly-β-1,6-*N*-acetyl-D-glucosamine in gram-positive bacteria. *Journal of Biological Chemistry*, *289*(52), 35907–35917.

**Little, D. J., Pfoh, R., Le Mauff, F., Bamford, N. C., Notte, C., Baker, P., Guragain, M., Robinson, H., Pier, G. B., Nitz, M., Deora, R., Sheppard, D. C., & Howell, P. L.** (2018). PgaB orthologues contain a glycoside hydrolase domain that cleaves deacetylated poly-β(1,6)-*N*-acetylglucosamine and can disrupt bacterial biofilms. *PLoS Pathogens*, *14*(4).

**Liu, W., Tang, L., Zhang, G., Wei, H., Cui, Y., Guo, L., Gou, Z., Chen, X., Jiang, D., Zhu, Y., Kang, G., & He, F.** (2004). Characterization of a novel C-type lectin-like gene, LSECtin: Demonstration of carbohydrate binding and expression in sinusoidal endothelial cells of liver and lymph node. *Journal of Biological Chemistry*, *279*(18), 18748–18758.

**Liu, Y., Endo, Y., Iwaki, D., Nakata, M., Matsushita, M., Wada, I., Inoue, K., Munakata, M., & Fujita, T.** (2005). Human M-ficolin is a secretory protein that activates the lectin complement pathway. *Journal of Immunology*, *175*(5), 3150–3156.

**Loehfelm, T. W., Luke, N. R., & Campagnari, A. A.** (2008). Identification and characterization of an *Acinetobacter baumannii* biofilm-associated protein. *Journal of Bacteriology*, *190*(3), 1036–1044.

**Lu, J., Teh, C., Kishore, U., & Reid, K. B. .** (2002). Collectins and ficolins: sugar pattern recognition molecules of the mammalian innate immune system. *Biochimica et Biophysica Acta (BBA) - General Subjects*, *1572*(2), 387–400.

**Lynch, D. J., Fountain, T. L., Mazurkiewicz, J. E., & Banas, J. A.** (2007). Glucan-binding proteins are essential for shaping *Streptococcus mutans* biofilm architecture. *FEMS Microbiology Letters*, *268*(2), 158–165.

**Lynch, N. J., Roscher, S., Hartung, T., Morath, S., Matsushita, M., Maennel, D. N., Kuraya, M., Fujita, T., & Schwaeble, W. J.** (2004). L-Ficolin Specifically Binds to Lipoteichoic Acid, a Cell Wall Constituent of Gram-Positive Bacteria, and Activates the Lectin Pathway of Complement. *Journal of Immunology*, *172*(2), 1198–1202.

**Ma, Y. G., Cho, M. Y., Zhao, M., Park, J. W., Matsushita, M., Fujita, T., & Lee, B. L.** (2004). Human mannose-binding lectin and L-ficolin function as specific pattern recognition proteins in the lectin activation pathway of complement. *Journal of Biological Chemistry*, *279*(24), 25307–25312.

**Ma, Y. J., Hein, E., Munthe-Fog, L., Skjoedt, M.-O., Bayarri-Olmos, R., Romani, L., & Garred, P.** (2015). Soluble collectin-12 (CL-12) is a pattern recognition molecule initiating complement activation via the alternative pathway. *Journal of Immunology*, *195*(7), 3365–3373.

**MacAuley, M. S., Crocker, P. R., & Paulson, J. C.** (2014). Siglec-mediated regulation of immune cell function in disease. *Nature Reviews Immunology*, *14*(10), 653–666.

**Mack, D., Fischer, W., Krokotsch, A., Leopold, K., Hartmann, R., Egge, H., & Laufs, R.** (1996). The intercellular adhesin involved in biofilm accumulation of *Staphylococcus epidermidis* is a linear β-1,6-linked glucosaminoglycan: Purification and structural analysis. *Journal of Bacteriology*, *178*(1), 175–183.

**Maira-Litrán, T., Kropec, A., Abeygunawardana, C., Joyce, J., Mark III, G., Goldmann, D. A., & Pier, G. B.** (2002). Immunochemical properties of the Staphylococcal poly-*N*-acetylglucosamine surface polysaccharide. *Infection and Immunity*, *70*(8), 4433–4440.

**Maira-Litran, T., Kropec, A., Goldmann, D., & Pier, G. B.** (2004). Biologic properties and vaccine potential of the staphylococcal poly-*N*-acetyl glucosamine surface polysaccharide. *Vaccine*, *22*(7), 872–879.

**Mak, T., & Saunders, M.** (2006). *The Immune Response*. *The Immune Response*, 85-86.

**Malhotra, R., Willis, A. C., Lopez Bernal, A., Thiel, S., & Sim, R. B.** (1994). Mannan-binding protein levels in human amniotic fluid during gestation and its interaction with collectin receptor from amnion cells. *Immunology*, *82*(3), 439–444.

**Mandron, M., Ariès, M.-F., Boralevi, F., Martin, H., Charveron, M., Taieb, A., & Davrinche, C.** (2008). Age-related differences in sensitivity of peripheral blood monocytes to lipopolysaccharide and *Staphylococcus aureus* toxin B in atopic dermatitis. *Journal of Investigative Dermatology*, *128*(4), 882–889.

**March, C., Regueiro, V., Llobet, E., Moranta, D., Morey, P., Garmendia, J., & Bengoechea, J. A.** (2010). Dissection of host cell signal transduction during *Acinetobacter baumannii* - triggered inflammatory response. *PLoS ONE*, *5*(4).

**Marquardt, T., Lühn, K., Srikrishna, G., Freeze, H. H., Harms, E., & Vestweber, D.** (1999). Correction of leukocyte adhesion deficiency type II with oral fucose. *Blood*, *94*(12), 3976–3985.

**Matsushita, M.** (2013). Ficolins in complement activation. *Molecular Immunology*, *55*(1), 22–26.

**Matsushita, M., Endo, Y., & Fujita, T.** (2000). Cutting edge: Complement-

activating complex of ficolin and mannose- binding lectin-associated serine protease. *Journal of Immunology*, *164*(5), 2281–2284.

**Matsushita, M., Endo, Y., Taira, S., Sato, Y., Fujita, T., Ichikawa, N., Nakata, M., & Mizuochi, T.** (1996). A novel human serum lectin with collagen- and fibrinogen-like domains that functions as an opsonin. *Journal of Biological Chemistry*, *271*(5), 2448–2454.

**Matthysse, A. G., Deora, R., Mishra, M., & Torres, A. G.** (2008). Polysaccharides cellulose, poly-β-1,6-*N*-acetyl-D-glucosamine, and colanic acid are required for optimal binding of *Escherichia coli* O157:H7 strains to alfalfa sprouts and K-12 strains to plastic but not for binding to epithelial cells. *Applied and Environmental Microbiology*, *74*(8), 2384–2390.

**McKenney, D., Hübner, J., Muller, E., Wang, Y., Goldmann, D. A., & Pier, G. B.** (1998). The ica locus of *Staphylococcus epidermidis* encodes production of the capsular polysaccharide/adhesin. *Infection and Immunity*, *66*(10), 4711–4720.

**McKenney, D., Pouliot, K. L., Wang, Y., Murthy, V., Ulrich, M., Döring, G., Lee, J. C., Goldmann, D. A., & Pier, G. B.** (1999). Broadly protective vaccine for *Staphylococcus aureus* based on an in vivo-expressed antigen. *Science*, *284*(5419), 1523–1527.

**Michelsen, K. S., Aicher, A., Mohaupt, M., Hartung, T., Dimmeler, S., Kirschning, C. J., & Schumann, R. R.** (2001). The role of toll-like receptors (TLRs) in bacteria-induced maturation of murine dendritic cells (DCs): Peptidoglycan and lipoteichoic acid are inducers of DC maturation and require TLR2. *Journal of Biological Chemistry*, *276*(28), 25680–25686.

**Miyake, K., Ogata, H., Nagai, Y., Akashi, S., & Kimoto, M.** (2000). Innate recognition of lipopolysaccharide by Toll-like receptor 4/MD-2 and RP105/MD-1. *Journal of Endotoxin Research*, *6*(5), 389–391.

**Mora, P., Rosconi, F., Franco Fraguas, L., & Castro-Sowinski, S.** (2008). Azospirillum brasilense Sp7 produces an outer-membrane lectin that specifically binds to surface-exposed extracellular polysaccharide produced by the bacterium. *Archives of Microbiology*, *189*(5), 519–524.

**Morath, S., Geyer, A., & Hartung, T.** (2001). Structure-function relationship of cytokine induction by lipoteichoic acid from *Staphylococcus aureus*. *Journal of Experimental Medicine*, *193*(3), 393–397.

**Morath, S., Geyer, A., Spreitzer, I., Hermann, C., & Hartung, T.** (2002). Structural decomposition and heterogeneity of commercial lipoteichoic acid preparations. *Infection and Immunity*, *70*(2), 938–944.

**Morath, S., Stadelmaier, A., Geyer, A., Schmidt, R. R., & Hartung, T.** (2002). Synthetic lipoteichoic acid from *Staphylococcus aureus* is a potent stimulus of cytokine release. *Journal of Experimental Medicine*, *195*(12), 1635–1640.

**Müller-Anstett, M. A., Müller, P., Albrecht, T., Nega, M., Wagener, J., Gao, Q., Kaesler, S., Schaller, M., Biedermann, T., & Götz, F.** (2010). Staphylococcal

Peptidoglycan Co-Localizes with Nod2 and TLR2 and Activates Innate Immune Response via Both Receptors in Primary Murine Keratinocytes. *PLOS ONE*, *5*(10), e13153-.

**Müller, P., Müller-Anstett, M., Wagener, J., Gao, Q., Kaesler, S., Schaller, M., Biedermann, T., & Götz, F.** (2010). The *Staphylococcus aureus* lipoprotein SitC colocalizes with toll-like receptor 2 (TLR2) in murine keratinocytes and elicits intracellular TLR2 accumulation. *Infection and Immunity*, *78*(10), 4243–4250.

**Mummidi, S., Catano, G., Lam, L., Hoefle, A., Telles, V., Begum, K., Jimenez, F., Ahuja, S. S., & Ahuja, S. K.** (2001). Extensive repertoire of membrane-bound and soluble dendritic cell-specific ICAM-3-grabbing nonintegrin 1 (DC-SIGN1) and DC-SIGN2 isoforms: Inter-individual variation in expression of DC-sign transcripts. *Journal of Biological Chemistry*, *276*(35), 33196–33212.

**Naughton, J. A., Mariño, K., Dolan, B., Reid, C., Gough, R., Gallagher, M. E., Kilcoyne, M., Gerlach, J. Q., Joshi, L., Rudd, P., Carrington, S., Bourke, B., & Clyne, M.** (2013). Divergent mechanisms of interaction of *Helicobacter pylori* and *Campylobacter jejuni* with mucus and mucins. *Infection and Immunity*, *81*(8), 2838–2850.

**Nesargikar, P. N., Spiller, B., & Chavez, R.** (2012). The complement system: history, pathways, cascade and inhibitors. *European Journal of Microbiology & Immunology*, *2*(2), 103–111.

**Neth, O., Jack, D. L., Dodds, A. W., Holzel, H., Klein, N. J., & Turner, M. W.** (2000). Mannose-binding lectin binds to a range of clinically relevant microorganisms and promotes complement deposition. *Infection and Immunity*, *68*(2), 688–693.

**Neth, O., Jack, D. L., Johnson, M., Klein, N. J., & Turner, M. W.** (2002). Enhancement of complement activation and opsonophagocytosis by complexes of mannose-binding lectin with mannose-binding lectin-associated serine protease after binding to *Staphylococcus aureus*. *Journal of Immunology*, *169*(8), 4430–4436.

**Nguyen, T. H., Park, M. D., & Otto, M.** (2017). Host response to *Staphylococcus epidermidis* colonization and infections. *Frontiers in Cellular and Infection Microbiology*, *7*, 90.

**Niebuhr, M., Schorling, K., Heratizadeh, A., & Werfel, T.** (2015). Staphylococcal α-toxin induces a functional upregulation of TLR-2 on human peripheral blood monocytes. *Experimental Dermatology*, *24*(5), 381–383.

**O'Gara, J. P.** (2007). ica and beyond: Biofilm mechanisms and regulation in *Staphylococcus epidermidis* and *Staphylococcus aureus*. *FEMS Microbiology Letters*, *270*(2), 179–188.

**O'Neill, E., Pozzi, C., Houston, P., Humphreys, H., Robinson, D. A., Loughman, A., Foster, T. J., & O'Gara, J. P.** (2008). A novel *Staphylococcus aureus* biofilm phenotype mediated by the fibronectin-binding proteins, FnBPA and FnBPB. *Journal of Bacteriology*, *190*(11), 3835–3850.

**O'Riordan, K., & Lee, J. C.** (2004). *Staphylococcus aureus* Capsular Polysaccharides. *Clinical Microbiology Reviews*, *17*(1), 218–234.

**O'Toole, G., Kaplan, H. B., & Kolter, R.** (2000). Biofilm formation as microbial development. *Annual Review of Microbiology*.

**Ohashi, T., & Erickson, H. P.** (1998). Oligomeric structure and tissue distribution of ficolins from mouse, pig and human. *Archives of Biochemistry and Biophysics*, *360*(2), 223–232.

**Ohtani, K., Suzuki, Y., Eda, S., Kawai, T., Kase, T., Keshi, H., Sakai, Y., Fukuoh, A., Sakamoto, T., Itabe, H., Suzutani, T., Ogasawara, M., Yoshida, I., & Wakamiya, N.** (2001). The Membrane-type Collectin CL-P1 Is a Scavenger Receptor on Vascular Endothelial Cells. *Journal of Biological Chemistry*, *276*(47), 44222–44228.

**Oliveira-Nascimento, L., Massari, P., & Wetzler, L. M.** (2012). The role of TLR2 ininfection and immunity. *Frontiers in Immunology*, *3*(APR).

**Otto, M.** (2008). Staphylococcal biofilms. *Current Topics in Microbiology and Immunology*.

**Ozinsky, A., Underhill, D. M., Fontenot, J. D., Hajjar, A. M., Smith, K. D., Wilson, C. B., Schroeder, L., & Aderem, A.** (2000). The repertoire for pattern recognition of pathogens by the innate immune system is defined by cooperation between Toll-like receptors. *Proceedings of the National Academy of Sciences of the United States of America*, *97*(25), 13766–13771.

**Park, K.-H., Kurokawa, K., Zheng, L., Jung, D.-J., Tateishi, K., Jin, J.-O., Ha, N.-C., Kang, H. J., Matsushita, M., Kwak, J.-Y., Takahashi, K., & Lee, B. L.** (2010). Human serum mannose-binding lectin senses wall teichoic acid glycopolymer of *Staphylococcus aureus*, which is restricted in infancy. *Journal of Biological Chemistry*, *285*(35), 27167–27175.

**Parkunan, S. M., Astley, R., & Callegan, M. C.** (2014). Role of TLR5 and flagella in *Bacillus* intraocular infection. *PLoS ONE*, *9*(6).

**Peleg, A. Y., Seifert, H., & Paterson, D. L.** (2008). *Acinetobacter baumannii*: Emergence of a successful pathogen. *Clinical Microbiology Reviews*, *21*(3), 538–582.

**Percival, S. L., Suleman, L., Vuotto, C., & Donelli, G.** (2015). Healthcare-Associated infections, medical devices and biofilms: Risk, tolerance and control. *Journal of Medical Microbiology*, *64*(4), 323–334.

**Peschel, A., & Otto, M.** (2013). Phenol-soluble modulins and staphylococcal infection. *Nature Reviews Microbiology*, *11*(10), 667–673.

**Pöhlmann, S., Baribaud, F., & Doms, R. W.** (2001). DC-SIGN and DC-SIGNR: Helping hands for HIV. *Trends in Immunology*, *22*(12), 643–646.

**Pöhlmann, S., Soilleux, E. J., Baribaud, F., Leslie, G. J., Morris, L. S., Trowsdale, J., Lee, B., Coleman, N., & Doms, R. W.** (2001). DC-SIGNR, a DC-SIGN homologue expressed in endothelial cells, binds to human and simian

immunodeficiency viruses and activates infection in trans. *Proceedings of the National Academy of Sciences of the United States of America*, *98*(5), 2670–2675.

**Polotsky, V. Y., Fischer, W., Ezekowitz, R. A. B., & Joiner, K. A.** (1996). Interactions of human mannose-binding protein with lipoteichoic acids. *Infection and Immunity*, *64*(1), 380–383.

**Poole, J., Day, C. J., Von Itzstein, M., Paton, J. C., & Jennings, M. P.** (2018). Glycointeractions in bacterial pathogenesis. *Nature Reviews Microbiology*, *16*(7), 440–452.

**Posner, M. G., Upadhyay, A., Abubaker, A. A., Fortunato, T. M., Vara, D., Canobbio, I., Bagby, S., & Pula, G.** (2016). Extracellular fibrinogen-binding protein (Efb) from *Staphylococcus aureus* inhibits the formation of platelet-leukocyte complexes. *Journal of Biological Chemistry*, *291*(6).

**Potera, C.** (1999). Forging a link between biofilms and disease. *Science*, *283*(5409), 1837–1839.

**Ribeiro-Viana, R., Sánchez-Navarro, M., Luczkowiak, J., Koeppe, J. R., Delgado, R., Rojo, J., & Davis, B. G.** (2012). Virus-like glycodendrinanoparticles displaying quasi-equivalent nested polyvalency upon glycoprotein platforms potently block viral infection. *Nature Communications*, *3*.

**Rivera, A., Siracusa, M. C., Yap, G. S., & Gause, W. C.** (2016). Innate cell communication kick-starts pathogen-specific immunity. *Nature Immunology*, *17*(4), 356–363.

**Rodríguez-Baño, J., Martí, S., Soto, S., Fernández-Cuenca, F., Cisneros, J. M., Pachón, J., Pascual, A., Martínez-Martínez, L., Mcqueary, C., Actis, L. A., & Vila, J.** (2008). Biofilm formation in *Acinetobacter baumannii*: Associated features and clinical implications. *Clinical Microbiology and Infection*, *14*(3), 276–278.

**Römling, U., & Balsalobre, C.** (2012). Biofilm infections, their resilience to therapy and innovative treatment strategies. *Journal of Internal Medicine*, *272*(6), 541–561.

**Sadovskaya, I., Vinogradov, E., Flahaut, S., Kogan, G., & Jabbouri, S.** (2005). Extracellular Carbohydrate-Containing Polymers of a Model Biofilm-Producing Strain, *Staphylococcus epidermidis* RP62A. *Infection and Immunity*, *73*(5), 3007 LP-3017.

**Santajit, S., & Indrawattana, N.** (2016). Mechanisms of Antimicrobial Resistance in ESKAPE Pathogens. *BioMed Research International*, *2016*.

**Sattin, S., & Bernardi, A.** (2016). Glycoconjugates and Glycomimetics as Microbial Anti-Adhesives. *Trends in Biotechnology*, *34*(6), 483–495.

**Schmaler, M., Jann, N. J., Ferracin, F., Landolt, L. Z., Biswas, L., Götz, F., & Landmann, R.** (2009). Lipoproteins in *Staphylococcus aureus* Mediate

Inflammation by TLR2 and Iron-Dependent Growth in Vivo. *Journal of Immunology*, *182*(11), 7110–7118.

**Schommer, N. N., Christner, M., Hentschke, M., Ruckdeschel, K., Aepfelbacher, M., & Rohde, H.** (2011). *Staphylococcus epidermidis* uses distinct mechanisms of biofilm formation to interfere with phagocytosis and activation of mouse macrophage-like cells 774A.1. *Infection and Immunity*, *79*(6), 2267–2276.

**Schreiner, J., Kretschmer, D., Klenk, J., Otto, M., Bühring, H.-J., Stevanovic, S., Wang, J. M., Beer-Hammer, S., Peschel, A., & Autenrieth, S. E.** (2013). *Staphylococcus aureus* phenol-soluble modulin peptides modulate dendritic cell functions and increase in vitro priming of regulatory T cells. *Journal of Immunology*, *190*(7), 3417–3426.

**Schröder, N. W. J., Morath, S., Alexander, C., Hamann, L., Hartung, T., Zähringer, U., Göbel, U. B., Weber, J. R., & Schumann, R. R.** (2003). Lipoteichoic acid (LTA) of *Streptococcus pneumoniae* and *Staphylococcus aureus* activates immune cells via Toll-like receptor (TLR)-2, lipopolysaccharide-binding protein (LBP), and CD14, whereas TLR-4 and MD-2 are not involved. *Journal of Biological Chemistry*, *278*(18), 15587–15594.

**Schroeder, K., Jularic, M., Horsburgh, S. M., Hirschhausen, N., Neumann, C., Bertling, A., Schulte, A., Foster, S., Kehrel, B. E., Peters, G., & Heilmann, C.** (2009). Molecular characterization of a novel *Staphylococcus aureus* surface protein (SasC) involved in cell aggregation and biofilm accumulation. *PLoS ONE*, *4*(10).

**Schwandner, R., Dziarski, R., Wesche, H., Rothe, M., & Kirschning, C. J.** (1999). Peptidoglycan- and lipoteichoic acid-induced cell activation is mediated by Toll-like receptor 2. *Journal of Biological Chemistry*, *274*(25), 17406–17409.

**Scietti, L., Sampieri, K., Pinzuti, I., Bartolini, E., Benucci, B., Liguori, A., Haag, A. F., Lo Surdo, P., Pansegrau, W., Nardi-Dei, V., Santini, L., Arora, S., Leber, X., Rindi, S., Savino, S., Costantino, P., Maione, D., Merola, M., Speziale, P., Bottomley, M. J., Bagnoli, F., Masignani, V., Pizza, M., Scharenberg, M., Schlaeppi, J.-M., Nissum, M., & Liberatori, S.** (2016). Exploring host-pathogen interactions through genome wide protein microarray analysis. *Scientific Reports*, *6*.

**Seyfarth, J., Garred, P., & Madsen, H. O.** (2006). Extra-hepatic transcription of the human mannose-binding lectin gene (mbl2) and the MBL-associated serine protease 1-3 genes. *Molecular Immunology*, *43*(7), 962–971.

**Sharif, S., Singh, M., Kim, S. J., & Schaefer, J.** (2009). *Staphylococcus aureus* peptidoglycan tertiary structure from carbon-13 spin diffusion. *Journal of the American Chemical Society*, *131*(20), 7023–7030.

**Sheriff, S., Chang, C. Y., & Ezekowitz, R. A. B.** (1994). Human mannose-binding protein carbohydrate recognition domain trimerizes through a triple α-helical coiled-coil. *Nature Structural Biology*, *1*(11), 789–794.

**Shi, L., Takahashi, K., Dundee, J., Shahroor-Karni, S., Thiel, S., Jensenius, C., Gad, F., Hamblin, M. R., Sastry, K. N., & Ezekowitz, R. A. B.** (2004). Mannose-binding lectin-deficient mice are susceptible to infection with *Staphylococcus aureus*. *Journal of Experimental Medicine*, *199*(10), 1379–1390.

**Skabytska, Y., Wölbing, F., Günther, C., Köberle, M., Kaesler, S., Chen, K.-M., Guenova, E., Demircioglu, D., Kempf, W. E., Volz, T., Rammensee, H.-G., Schaller, M., Röcken, M., Götz, F., & Biedermann, T.** (2014). Cutaneous innate immune sensing of toll-like receptor 2-6 ligands suppresses T cell immunity by inducing myeloid-derived suppressor cells. *Immunity*, *41*(5), 762–775.

**Skurnik, D., Cywes-Bentley, C., & Pier, G. B.** (2016). The exceptionally broad-based potential of active and passive vaccination targeting the conserved microbial surface polysaccharide PNAG. *Expert Review of Vaccines*, *15*(8), 1041–1053.

**Söderquist, B., Sundqvist, K.-G., & Vikerfors, T.** (1999). Adhesion molecules (E-selectin, intercellular adhesion molecule-1 (ICAM- 1) and vascular cell adhesion molecule-1 (VCAM-1)) in sera from patients with *Staphylococcus aureus* bacteraemia with or without endocarditis. *Clinical and Experimental Immunology*, *118*(3).

**Soilleux, E. J., Barten, R., & Trowsdale, J.** (2000). Cutting edge: DC-SIGN; a related gene, DC-SIGNR; and CD23 form a cluster on 19p13. *Journal of Immunology*, *165*(6), 2937–2942.

**Solano, C., Echeverz, M., & Lasa, I.** (2014). Biofilm dispersion and quorum sensing. *Current Opinion in Microbiology*, *18*(1), 96–104.

**Somers, W. S., Tang, J., Shaw, G. D., & Camphausen, R. T.** (2000). Insights into the Molecular Basis of Leukocyte Tethering and Rolling Revealed by Structures of P- and E-Selectin Bound to SLeX and PSGL-1. *Cell*, *103*(3), 467–479.

**Song, W.-C., Rosa Sarrias, M., & Lambris, J. D.** (2000). Complement and innate immunity. *Immunopharmacology*, *49*(1–2), 187–198.

**Speziale, P., Pietrocola, G., Foster, T. J., & Geoghegan, J. A.** (2014). Protein-based biofilm matrices in staphylococci. *Frontiers in Cellular and Infection Microbiology*, *4*(NOV).

**Springer, T. A.** (1994). Traffic signals for lymphocyte recirculation and leukocyte emigration: The multistep paradigm. *Cell*, *76*(2), 301–314.

**Stephenson, H. N., Mills, D. C., Jones, H., Milioris, E., Copland, A., Dorrell, N., Wren, B. W., Crocker, P. R., Escors, D., & Bajaj-Elliott, M.** (2014). Pseudaminic acid on *Campylobacter jejuni* flagella modulates dendritic cell IL-10 expression via Siglec-10 receptor: A novel flagellin-host interaction. *Journal of Infectious Diseases*, *210*(9), 1487–1498.

**Stevens, N. T., Sadovskaya, I., Jabbouri, S., Sattar, T., O'gara, J. P., Humphreys, H., & Greene, C. M.** (2009). *Staphylococcus epidermidis*

polysaccharide intercellular adhesin induces IL-8 expression in human astrocytes via a mechanism involving TLR2. *Cellular Microbiology*, *11*(3), 421–432.

**Stewart, P. S.** (2002). Mechanisms of antibiotic resistance in bacterial biofilms. *International Journal of Medical Microbiology*, *292*(2), 107–113.

**Stowell, S. R., Arthur, C. M., Mcbride, R., Berger, O., Razi, N., Heimburg-Molinaro, J., Rodrigues, L. C., Gourdine, J.-P., Noll, A. J., Von Gunten, S., Smith, D. F., Knirel, Y. A., Paulson, J. C., & Cummings, R. D.** (2014). Microbial glycan microarrays define key features of host-microbial interactions. *Nature Chemical Biology*, *10*(6), 470–476.

**Strindhall, J., Lindgren, P.-E., Löfgren, S., & Kihlström, E.** (2002). Variations among clinical isolates of *Staphylococcus aureus* to induce expression of E-selectin and ICAM-1 in human endothelial cells. *FEMS Immunology and Medical Microbiology*, *32*(3), 227–235.

**Sugimoto, R., Yae, Y., Akaiwa, M., Kitajima, S., Shibata, Y., Sato, H., Hirata, J., Okochi, K., Izuhara, K., & Hamasaki, N.** (1998). Cloning and characterization of the Hakata antigen, a member of the ficolin/opsonin p35 lectin family. *Journal of Biological Chemistry*, *273*(33), 20721–20727.

**Super, M., Gillies, S. D., Foley, S., Sastry, K., Schweinle, J.-E., Silverman, V. J., & Ezekowitz, R. A. B.** (1992). Distinct and overlapping functions of allelic forms of human mannose binding protein. *Nature Genetics*, *2*(1), 50–55.

**Tabarani, G., Reina, J. J., Ebel, C., Vivès, C., Lortat-Jacob, H., Rojo, J., & Fieschi, F.** (2006). Mannose hyperbranched dendritic polymers interact with clustered organization of DC-SIGN and inhibit gp120 binding. *FEBS Letters*, *580*(10), 2402–2408.

**Tacconelli, E., Carrara, E., Savoldi, A., Harbarth, S., Mendelson, M., Monnet, D. L., Pulcini, C., Kahlmeter, G., Kluytmans, J., Carmeli, Y., Ouellette, M., Outterson, K., Patel, J., Cavaleri, M., Cox, E. M., Houchens, C. R., Grayson, M. L., Hansen, P., Singh, N., Theuretzbacher, U., Magrini, N., Aboderin, A. O., Al-Abri, S. S., Awang Jalil, N., Benzonana, N., Bhattacharya, S., Brink, A. J., Burkert, F. R., Cars, O., Cornaglia, G., Dyar, O. J., Friedrich, A. W., Gales, A. C., Gandra, S., Giske, C. G., Goff, D. A., Goossens, H., Gottlieb, T., Guzman Blanco, M., Hryniewicz, W., Kattula, D., Jinks, T., Kanj, S. S., Kerr, L., Kieny, M.-P., Kim, Y. S., Kozlov, R. S., Labarca, J., Laxminarayan, R., Leder, K., Leibovici, L., Levy-Hara, G., Littman, J., Malhotra-Kumar, S., Manchanda, V., Moja, L., Ndoye, B., Pan, A., Paterson, D. L., Paul, M., Qiu, H., Ramon-Pardo, P., Rodríguez-Baño, J., Sanguinetti, M., Sengupta, S., Sharland, M., Si-Mehand, M., Silver, L. L., Song, W., Steinbakk, M., Thomsen, J., Thwaites, G. E., van der Meer, J. W., Van Kinh, N., Vega, S., Villegas, M. V, Wechsler-Fördös, A., Wertheim, H. F. L., Wesangula, E., Woodford, N., Yilmaz, F. O., & Zorzet, A.** (2018). Discovery, research, and development of new antibiotics: the WHO priority list of antibiotic-resistant bacteria and tuberculosis. *The Lancet Infectious Diseases*, *18*(3), 318–327.

**Taglialegna, A., Navarro, S., Ventura, S., Garnett, J. A., Matthews, S., Penades, J. R., Lasa, I., & Valle, J.** (2016). Staphylococcal Bap Proteins Build Amyloid Scaffold Biofilm Matrices in Response to Environmental Signals. *PLoS Pathogens*, *12*(6).

**Takahara, K., Yashima, Y., Omatsu, Y., Yoshida, H., Kimura, Y., Kang, Y., Steinman, R. M., Park, C. G., & Inaba, K.** (2004). Functional comparison of the mouse DC-SIGN, SIGNR1, SIGNR3 and Langerin, C-type lectins. *International Immunology*, *16*(6), 819–829.

**Takeda, K., & Akira, S.** (2005). Toll-like receptors in innate immunity. *International Immunology*, *17*(1), 1–14.

**Takeuchi, O., & Akira, S.** (2010). Pattern Recognition Receptors and Inflammation. *Cell*, *140*(6), 805–820.

**Takeuchi, O., Hoshino, K., & Akira, S.** (2000). Cutting edge: TLR2-deficient and MyD88-deficient mice are highly susceptible to *Staphylococcus aureus* infection. *Journal of Immunology*, *165*(10), 5392–5396.

**Tallieux, L., Schwartz, O., Herrmann, J.-L., Pivert, E., Jackson, M., Amara, A., Legres, L., Dreher, D., Nicod, L. P., Gluckman, J. C., Lagrange, P. H., Gicquel, B., & Neyrolles, O.** (2003). DC-SIGN is the major *Mycobacterium tuberculosis* receptor on human dendritic cells. *Journal of Experimental Medicine*, *197*(1), 121–127.

**Tan, F. Y. Y., Tang, C. M., & Exley, R. M.** (2015). Sugar coating: Bacterial protein glycosylation and host-microbe interactions. *Trends in Biochemical Sciences*, *40*(7), 342–350.

**Teh, C., Le, Y., Lee, S. H., & Lu, J.** (2000). M-ficolin is expressed on monocytes and is a lectin binding to *N*-acetyl-D-glucosamine and mediates monocyte adhesion and phagocytosis of *Escherichia coli*. *Immunology*, *101*(2), 225–232.

**Thurlow, L. R., Hanke, M. L., Fritz, T., Angle, A., Aldrich, A., Williams, S. H., Engebretsen, I. L., Bayles, K. W., Horswill, A. R., & Kielian, T.** (2011). *Staphylococcus aureus* biofilms prevent macrophage phagocytosis and attenuate inflammation in vivo. *Journal of Immunology*, *186*(11), 6585–6596.

**Tielker, D., Hacker, S., Loris, R., Strathmann, M., Wingender, J., Wilhelm, S., Rosenau, F., & Jaeger, K.-E.** (2005). *Pseudomonas aeruginosa* lectin LecB is located in the outer membrane and is involved in biofilm formation. *Microbiology*, *151*(5), 1313–1323.

**Tomaras, A. P., Dorsey, C. W., Edelmann, R. E., & Actis, L. A.** (2003). Attachment to and biofilm formation on abiotic surfaces by *Acinetobacter baumannii*: Involvement of a novel chaperone-usher pili assembly system. *Microbiology*, *149*(12), 3473–3484.

**Tosi, M. F.** (2005). Innate immune responses to infection. *Journal of Allergy and Clinical Immunology*, *116*(2), 241–249.

**Travassos, L. H., Girardin, S. E., Philpott, D. J., Blanot, D., Nahori, M.-A.,**

**Werts, C., & Boneca, I. G.** (2004). Toll-like receptor 2-dependent bacterial sensing does not occur via peptidoglycan recognition. *EMBO Reports*, *5*(10), 1000–1006.

**Triantafilou, M., & Triantafilou, K.** (2002). Lipopolysaccharide recognition: CD14, TLRs and the LPS-activation cluster. *Trends in Immunology*, *23*(6), 301–304.

**Van De Wetering, J. K., Van Golde, L. M. G., & Batenburg, J. J.** (2004). Collectins: Players of the innate immune system. *European Journal of Biochemistry*, *271*(7), 1229–1249.

**Van Gisbergen, K. P. J. M., Sanchez-Hernandez, M., Geijtenbeek, T. B. H., & Van Kooyk, Y.** (2005). Neutrophils mediate immune modulation of dendritic cells through glycosylation-dependent interactions between Mac-1 and DC-SIGN. *Journal of Experimental Medicine*, *201*(8), 1281–1292.

**van Kooyk, Y., & Geijtenbeek, T. B. H.** (2003). DC-SIGN: escape mechanism for pathogens. *Nature Reviews Immunology*, *3*, 697.

**van Liempt, E., Bank, C. M. C., Mehta, P., García-Vallejo, J. J., Kawar, Z. S., Geyer, R., Alvarez, R. A., Cummings, R. D., Kooyk, Y. v., & van Die, I.** (2006). Specificity of DC-SIGN for mannose- and fucose-containing glycans. *FEBS Letters*, *580*(26), 6123–6131.

**Verdrengh, M., Erlandsson-Harris, H., & Tarkowski, A.** (2000). Role of selectins in experimental *Staphylococcus aureus*-induced arthritis. *European Journal of Immunology*, *30*(6).

**Vestweber, D., & Blanks, J. E.** (1999). Mechanisms that regulate the function of the selectins and their ligands. *Physiological Reviews*, *79*(1), 181–213.

**Von Gunten, S., & Bochner, B. S.** (2008). Basic and clinical immunology of Siglecs. *Annals of the New York Academy of Sciences*.

**Vuong, C., Voyich, J. M., Fischer, E. R., Braughton, K. R., Whitney, A. R., DeLeo, F. R., & Otto, M.** (2004). Polysaccharide intercellular adhesin (PIA) protects *Staphylococcus epidermidis* against major components of the human innate immune system. *Cellular Microbiology*, *6*(3), 269–275.

**Wang, L., Cummings, R. D., Smith, D. F., Huflejt, M., Campbell, C. T., Gildersleeve, J. C., Gerlach, J. Q., Kilcoyne, M., Joshi, L., Serna, S., Reichardt, N. C., Pera, N. P., Pieters, R. J., Eng, W., & Mahal, L. K.** (2014). Cross-platform comparison of glycan microarray formats. *Glycobiology*, *24*(6), 507–517.

**Wang, X., Preston III, J. F., & Romeo, T.** (2004). The *pgaABCD* Locus of *Escherichia coli* Promotes the Synthesis of a Polysaccharide Adhesin Required for Biofilm Formation. *Journal of Bacteriology*, *186*(9), 2724–2734.

**Weis, W. I., Drickamer, K., & Hendrickson, W. A.** (1992). Structure of a C-type mannose-binding protein complexed with an oligosaccharide. *Nature*, *360*(6400), 127–134.

**Whitfield, G. B., Marmont, L. S., & Howell, P. L.** (2015). Enzymatic modifications of exopolysaccharides enhance bacterial persistence. *Frontiers in Microbiology*, *6*, 471.

**WHO**. (2011). *Report on the burden of endemic health care-associated infection worldwide*.

**Wild, J., Robinson, D., & Winchester, B.** (1983). Isolation of mannose-binding proteins from human and rat liver. *Biochemical Journal*, *210*(1), 167–174.

**Wingren, C., & Borrebaeck, C. A. K.** (2006). Antibody microarrays: Current status and key technological advances. *OMICS A Journal of Integrative Biology*, *10*(3), 411–427.

**Winstel, V., Kühner, P., Salomon, F., Larsen, J., Skov, R., Hoffmann, W., Peschel, A., & Weidenmaier, C.** (2015). Wall teichoic acid glycosylation governs *Staphylococcus aureus* nasal colonization. *MBio*, *6*(4).

**Woehl, J. L., Stapels, D. A. C., Garcia, B. L., Ramyar, K. X., Keightley, A., Ruyken, M., Syriga, M., Sfyroera, G., Weber, A. B., Zolkiewski, M., Ricklin, D., Lambris, J. D., Rooijakkers, S. H. M., & Geisbrecht, B. V**. (2014). The extracellular adherence protein from *Staphylococcus aureus* inhibits the classical and lectin pathways of complement by blocking formation of the C3 proconvertase. *Journal of Immunology*, *193*(12), 6161–6171.

**Yan, X., Sivignon, A., Yamakawa, N., Crepet, A., Travelet, C., Borsali, R., Dumych, T., Li, Z., Bilyy, R., Deniaud, D., Fleury, E., Barnich, N., Darfeuille-Michaud, A., Gouin, S. G., Bouckaert, J., & Bernard, J.** (2015). Glycopolymers as antiadhesives of *E. coli* strains inducing inflammatory bowel diseases. *Biomacromolecules*, *16*(6), 1827–1836.

**Yang, Y.-H., Jiang, Y.-L., Zhang, J., Wang, L., Bai, X.-H., Zhang, S.-J., Ren, Y.-M., Li, N., Zhang, Y.-H., Zhang, Z., Gong, Q., Mei, Y., Xue, T., Zhang, J.-R., Chen, Y., & Zhou, C.-Z.** (2014). Structural Insights into SraP-Mediated *Staphylococcus aureus* Adhesion to Host Cells. *PLoS Pathogens*, *10*(6).

**Yasuda, E., Tateno, H., Hirabayashi, J., Iino, T., & Sako, T.** (2011). Lectin microarray reveals binding profiles of *Lactobacillus casei* strains in a comprehensive analysis of bacterial cell wall polysaccharides. *Applied and Environmental Microbiology*, *77*(16), 5834.

**Yokota, Y., Arai, T., & Kawasaki, T.** (1995). Oligomeric structures required for complement activation of serum mannan- binding proteins. *Journal of Biochemistry*, *117*(2), 414–419.

**Yokoyama, R., Itoh, S., Kamoshida, G., Takii, T., Fujii, S., Tsuji, T., & Onozaki, K.** (2012). Staphylococcal superantigen-like protein 3 binds to the toll-like receptor 2 extracellular domain and inhibits cytokine production induced by *Staphylococcus aureus*, cell wall component, or lipopeptides in murine macrophages. *Infection and Immunity*, *80*(8), 2816–2825.

**York, M. R., Nagai, T., Mangini, A. J., Lemaire, R., Van Seventer, J. M., & Lafyatis, R.** (2007). A macrophage marker, siglec-1, is increased on circulating

monocytes in patients with systemic sclerosis and induced by type I interferons and toll-like receptor agonists. *Arthritis and Rheumatism*, *56*(3), 1010–1020.

**Zanoni, I., & Granucci, F.** (2013). Role of CD14 in host protection against infections and in metabolism regulation. *Frontiers in Cellular and Infection Microbiology*, *3*, 32.

**Zapotoczna, M., O'Neill, E., & O'Gara, J. P.** (2016). Untangling the Diverse and Redundant Mechanisms of *Staphylococcus aureus* Biofilm Formation. *PLoS Pathogens*, *12*(7).

**Zhang, F., Ren, S., & Zuo, Y.** (2014). DC-SIGN, DC-SIGNR and LSECtin: C-type lectins for infection. *International Reviews of Immunology*, *33*(1), 54–66.

**Zhang, Q., Collins, J., Anastasaki, A., Wallis, R., Mitchell, D. A., Becer, C. R., & Haddleton, D. M.** (2013). Sequence-controlled multi-block glycopolymers to inhibit DC-SIGN-gp120 binding. *Angewandte Chemie - International Edition*, *52*(16), 4435–4439.

**Zhao, D., Han, X., Zheng, X., Wang, H., Yang, Z., Liu, D., Han, K., Liu, J., Wang, X., Yang, W., Dong, Q., Yang, S., Xia, X., Tang, L., & He, F.** (2016). The Myeloid LSECtin Is a DAP12-Coupled Receptor That Is Crucial for Inflammatory Response Induced by Ebola Virus Glycoprotein. *PLoS Pathogens*, *12*(3).

**Zivkovic, A., Sharif, O., Stich, K., Doninger, B., Biaggio, M., Colinge, J., Bilban, M., Mesteri, I., Hazemi, P., Lemmens-Gruber, R., & Knapp, S.** (2011). TLR 2 and CD14 mediate innate immunity and lung inflammation to staphylococcal panton-valentine leukocidin in vivo. *Journal of Immunology*, *186*(3), 1608–1617.

# Chapter 2

# Profiling *S. aureus* and *A. baumannii* wildtype and PNAG-deficient mutants for lectin and carbohydrate interactions

## 2. Profiling *S. aureus* and *A. baumannii* wildtype and PNAG-deficient mutants for lectin and carbohydrate interactions

### 2.1. Introduction

Bacterial pathogens have evolved complex mechanisms to adapt to different environmental conditions. For example, bacteria can survive on metals and plastics associated with medical devices, thrive on the skin where temperature, pH changes and the salt from sweat becomes more prominent, to internally in the body where carbon and mineral sources have to be scavenged and used wisely to survive within the host (Chowdhury *et al.*, 1996). Biofilms are used strategically by bacteria to adapt to these environmental changes and protect bacteria from the host immune system. The expression of poly-*N*-acetylglucosamine (PNAG), a major component of *Staphylococcus. aureus* and *Acinetobacter baumannii* biofilms, can be influenced by a range of environmental factors including the availability of glucose, glucosamine (GlcN), urea, iron and ethanol, and environmental factors such as osmolarity and pH changes (Cerca & Jefferson, 2008; Conlon *et al*., 2002; Götz, 2002).

Although PNAG plays a fundamental role in the adhesion of *S. aureus* and *A. baumannii* within a biofilm matrix, there are contradictory pieces of evidence to suggest whether PNAG has an effect on the virulence of bacteria within a host. In a murine model of bacteraemia, renal infection and sepsis, *S. aureus ica* gene mutants displayed decreased virulence compared to the wildtype (WT) strain (Kropec *et al.*, 2005). Similarly, in a rat endocarditis model, mutation of the *ica* operon resulted in no death, while infection with the wildtype strain caused 10 out of 24 deaths (Maira-Litran *et al.*, 2004). On the other hand, the *ica* operon was not implicated as a virulence factor in a murine model of pneumonia or foreign body infections carried out on animals (Wardenburg *et al.*, 2007). However, PNAG isoforms of high molecular weight purified from *S. aureus* were shown to be highly immunogenic by eliciting high antibody titres in mice and rabbit models (Maira-Litrán *et al*., 2002). It appears that PNAG is important for bacterial pathogenesis but the exact mechanisms of interaction and recognition by the host's immune system and the consequential effect on the immune system is still uncertain (Lin *et al.*, 2015; Vuong *et al.*, 2004). In particular, the accessibility or presentation of PNAG on the bacterial cell surface

and whether PNAG directly contributes to or modulates the bacterial interactions with the host cell receptors is unknown.

Interestingly, there was no difference in clinical characteristics or outcomes between patients with pneumonia caused by *A. baumannii* biofilm-forming or non-biofilm-forming isolates (Wang *et al.*, 2018). Although it has been shown that *A. baumannii* clinical isolates express PNAG (Choi *et al.*, 2009), there has been no correlation between PNAG production in *A. baumannii* and virulence to date. Interestingly, correlations have been made with *S. aureus* antibiotic susceptibility and PNAG production, and antibiotic susceptibility and biofilm formation in *A. baumannii* (O'Neill *et al.*, 2007; Pozzi *et al.*, 2012; Wang *et al.*, 2018).

Glucose added to growth media of methicillin sensitive *S. aureus* (MSSA) strains promoted PNAG-mediated biofilm formation. It was shown that the *gbaAB* operon was involved in glucose-induced biofilm formation for *S. aureus* 8325-4 in a PNAG-dependent manner (You *et al*., 2014). Addition of glucose into the growth media also decreased the pH of the local cellular environment for *S. aureus* and resulted in reduced *agr* expression (Regassa *et al.*, 1992). Moreover, glucose increased the number of *S. aureus* cells within a biofilm matrix (Reśliński & Dabrowiecki, 2013). Glucose also promoted biofilm formation for 42 out of 47 *S. aureus* strains tested and DNA played a role in biofilm formation formed for all 47 *S. aureus* isolates (Sugimoto *et al.*, 2018). Glucose and NaCl promoted PNAG-mediated biofilm formation for MSSA strain 8325-4 (Lim *et al.*, 2004; Pozzi *et al.*, 2012). However, addition of glucose to methicillin resistant *S. aureus* (MRSA) clinical isolates promoted biofilm formation via an *ica*-independent mechanism that involved extracellular surface proteins such as FnBPAB and extracellular DNA (eDNA) (Fitzpatrick *et al.*, 2005; O'Neill *et al.*, 2008, 2007). In many *S. aureus* strains, particularly MSSA, NaCl promotes biofilm formation which is regulated by the alternative transcription factor, sigma B (O'Neill *et al*., 2007; Rachid *et al*., 2000; Sugimoto *et al*., 2018). It was also shown that addition of NaCl into the growth media for *S. aureus* alters the abundance of many surface proteins, including IsaA, a putative lytic transglycosylase, and was hypothesised that NaCl altered the biofilm architecture for *S. aureus* (Islam *et al.*, 2015). Furthermore, NaCl decreased the amount of proteins and eDNA in the extracellular matrix of *S. aureus*, which may contribute to any unknown differences in biofilm architecture (Sugimoto *et al*.,

2018). However, addition of NaCl to the culture medium of MRSA promoted *icaA* transcription but no biofilm was formed and PNAG was not detected, which indicated little correlation between *ica* transcription and biofilm formation in MRSA isolates (O'Neill *et al.*, 2007). Furthermore, increased *ica* transcription does not necessarily lead to an increase in PNAG production (Jaione *et al.*, 2003). Therefore, research has shown that MSSA primarily produces PNAG-mediated biofilm following growth in both glucose and NaCl, while glucose promotes PNAG-independent biofilm formation for MRSA isolates and NaCl results in no biofilm formation. In biofilm formation, it has been postulated that electrostatic interactions play a crucial role. For biofilms that are dependent on extracellular surface proteins, such as those formed by MRSA, it has been proposed that eDNA acts as an electrostatic net that connects positively charged surface proteins in low pH environments within a biofilm matrix (Dengler *et al.*, 2015). There are also many negatively charged molecules on the surface of bacteria, thus it is hypothesised that the positively charged amine groups on PNAG act as an electrostatic glue that interacts with these negative charges and helps hold a biofilm matrix together (Otto, 2008). It has been proposed that different growth media help *S. aureus* to alter the pH of the growth media which can greatly impact biofilm biomass (Sugimoto *et al*., 2018). Although we know for some *S. aureus* strains that glucose and NaCl promotes PNAG production, it remains unknown how glucose and NaCl affect PNAG conformation and biofilm architecture.

In addition to PNAG, there are many bacterial surface-bound proteins with adhesin and lectin function involved in biofilm formation and organisation including fibronectin binding proteins (FnBPs), Protein A, Bap and SasG in *S. aureus*. Whether some of these proteins are secreted in to the biofilm matrix to contribute to biofilm formation is currently unknown. Protein A contains a carbohydrate binding module named LysM that binds to GlcNAc-containing polymers such as chitin and peptidoglycan (Buist *et al.*, 2008). Mutation of *lysM* in *A. baumannii* reduces biofilm formation (Cabral *et al.*, 2011), suggesting a role for this GlcNAc-binding module for *A. baumannii* biofilm formation. Bap expression on *S. aureus* is associated with strong biofilm formation and Bap homologous proteins are found in many phylogenetically unrelated bacteria such as *E. coli* and *A. baumannii* (Lasa & Penadés, 2006). In *A. baumannii*, an outer membrane protein, OmpA, is required for

adherence to human alveolar cells and biofilm formation on plastic (Gaddy *et al.*, 2009). Lectins on the surface of bacteria could account for the binding of PNAG to the bacterial cell surface as well as to specific host carbohydrate ligands. Although some lectins such as SasG have been identified in *S. aureus*, none have been found to directly associate with PNAG to promote biofilm formation. However, SasG and its homologue Aap in *S. epidermidis*, were postulated to bind to *N*-acetylglucosamine via their G5 lectin domains and both proteins were found to be involved in biofilm formation, zinc-dependent cell-cell adhesion and are able to bind to human epithelial cells via their lectin domain (Bateman *et al.*, 2005; Conrady *et al.*, 2013; Formosa-Dague *et al.*, 2016; Roche *et al.*, 2003).

To date, only limited carbohydrate specificities have been characterised for *S. aureus* or *A. baumannii*, and, to the best of our knowledge, there has been no investigation as to whether carbohydrate-binding function has been associated with antibiotic resistance or environmental conditions. Understanding the composition of the bacterial glycome and their interactions with host receptors and ligands can provide fundamental insights in to the possible roles and biological consequences of these interactions.

Lectin microarrays have been used for profiling bacterial surface glycosylation (Hsu *et al.*, 2006; Kilcoyne *et al.*, 2014; Yasuda *et al.*, 2011) while carbohydrate microarrays have been used to characterise the structural specificity of bacterial interactions (Flannery *et al.*, 2015). In this study, the wildtype (WT) and *ica* mutant (Δ*ica*) of three Gram-positive *S. aureus* strains, two MSSA and one MRSA, as well as the PNAG-producing Gram-negative bacterium, *A. baumannii*, WT and Δ*pga*, were grown in different media to promote PNAG production. These strains were then profiled on lectin and carbohydrate microarrays to characterise how the presence and absence of PNAG affects bacterial surface glycosylation and lectin expression.

## 2.2. Materials and methods

### 2.2.1. Materials and strains used

Agar, Alexa Fluor® 555 (AF555) carboxylic acid succinimidyl ester fluorescent label, Pierce™ enhance chemiluminescence (ECL) Western blotting substrate, Nunc™ MicroWell™ 96-well microtitre plates and SYTO™ 82 nucleic acid stain was purchased from Thermo-Fisher Scientific (Waltham, MA, U.S.A.). Brain Heart Infusion (BHI) agar and crystal violet were obtained from Sigma-Aldrich Co. (Dublin, Ireland). Proteinase K was from QIAGEN (Venlo, the Netherlands). Casein was purchased from BDH (Merck, Darmstadt, Germany). Nexterion® Slide H microarray slides were supplied by Schott AG (Mainz, Germany). The 8-well gasket slide and incubation cassette system and DAKO rabbit anti-human IgG antibody conjugated to horse radish peroxidase (HRP) were from Agilent Technologies Ireland, Ltd., (Cork, Ireland). Immoblion-P 0.45 µm polyvinylidene difluoride (PVDF) membrane was from Merck Millipore (Cork, Ireland). Pure, unlabelled lectins were purchased from EY Labs (San Mateo, CA, USA) or Vector Laboratories Inc. (Burlingame, CA, U.S.A.). Neoglycoconjugates (NGCs) were purchased from Dextra Laboratories Ltd. (Reading, U.K.), IsoSep AB (Tullinge, Sweden) or made in house (Kilcoyne, Gerlach, Kane, *et al*., 2012). Anti-PNAG monoclonal antibody (mAb) (F598) was a kind gift from Prof. Gerald Pier, Harvard University, Boston, MA, U.S.A. (Kelly-Quintos, *et al*, 2006). All other reagents were purchased from Sigma-Aldrich unless otherwise stated and were of the highest grade available.

A number of *S. aureus* and *A. baumannii* strains were used in this study (Table 2.1) which were kind gifts from Prof. J. P. O'Gara, NUI Galway, Galway, Ireland and from Prof. G. Pier, Harvard University, MA, USA (*S. aureus* Mn8m and Mn8 Δ*ica*, and *A. baumannii* S1 WT and Δ*pga*). As *A. baumannii* S1 is the only *A. baumannii* strain used in this study, it will be named *A. baumannii* hereafter.

### 2.2.2. Bacterial growth conditions

Bacteria were grown on Brain Heart Infusion (BHI) (Sigma-Aldrich) agar. Agar was supplemented with tetracycline (5 µg/mL) for all *S. aureus* Δ*ica* strains. Bacteria were grown overnight in 5 mL cultures at 37 °C with shaking at 180 rpm in BHI, BHI supplemented with 1% (w/v) glucose (BHI glucose) or BHI supplemented with

4% (w/v) NaCl (BHI NaCl) where indicated. Overnight cultures are 17 h incubations.

**Table 2.1. Bacteria used in this study.**

| Bacteria strains used | Details | Reference |
|---|---|---|
| *S. aureus* 8325-4 WT | 8325 derivative cured of prophages. 11-bp deletion in *rsbU* | (Horsburgh *et al.*, 2002) |
| *S. aureus* 8325-4 Δ*ica* | *icaADBC*::Tr$^r$ isogenic mutant of 8325-4 | (Fitzpatrick *et al.*, 2005) |
| *S. aureus* Mn8m WT | Chemostat derived mutant of Mn8 (toxic shock syndrome isolate). Biofilm positive. Overproducer of PNAG. | (McKenney *et al.*, 1999) |
| *S. aureus* Mn8 Δ*ica* | *icaADBC*::Tr$^r$ isogenic mutant of Mn8 | (Jefferson *et al.*, 2003) |
| *S. aureus* BH1CC WT | MRSA clinical isolate. Biofilm positive. SCCmec type, MLST type 8, clonal complex 8. Isolate from Beaumont Hospital, Dublin. | (O'Neill *et al.*, 2007) |
| *S. aureus* BH1CC Δ*ica* | *icaADBC*::Tr$^r$ isogenic mutant of BH1CC | (Fitzpatrick *et al.*, 2005) |
| *A. baumannii* S1 WT | Clinical isolate. Mucoid phenotype. Biofilm positive. | (Choi *et al.*, 2009) |
| *A. baumannii* S1 Δ*pga* | S1 derivative with in-frame deletion of *pgaABC* | (Choi *et al.*, 2009) |

### 2.2.3. Assays for presence of PNAG

Cultures were grown overnight in BHI NaCl, washed three times in Tris-buffered saline supplemented with $Ca^{2+}$ and $Mg^{2+}$ ions (TBS; 20 mM Tris-HCl, 100 mM NaCl, 1 mM $CaCl_2$, 1 mM $MgCl_2$, pH 7.2) and cells were adjusted to an absorbance of approximately 1.0 at 595 nm. Bacteria cultures were placed in to tubes in 1 mL aliquots to act as a positive control and were set aside. Next, separate 1 mL cultures were washed one to five times by resuspending in TBS, centrifuging the bacteria in to a pellet at 5,000 x g and removing the supernatant each time. After the final wash, bacterial pellets were resuspended in 1 mL TBS or TBS with 0.05%, 0.02% or 0.01% (v/v) Tween® 20. Washed and unwashed 1 mL bacterial suspensions were

collected by centrifugation (5,000 × g for 5 min), resuspended in 250 µL of 0.5 M ethylenediaminetetraacetic acid (EDTA) and boiled for 5 min. Samples were centrifuged and 40 µL aliquots of the supernatant were treated with 10 µL of 20 µg/mL proteinase K at 65 $^{o}$C for 1 h to digest any proteins. Samples were then boiled again for 5 min to inactivate the proteinase K.

PVDF membrane (0.45 µm) was pre-treated for 15 s in methanol before being soaked in TBS for 5 min. The membrane was allowed to partially dry before pipetting 2 µL of the proteinase K-treated samples on to the membrane in triplicate. The membrane was allowed to dry for 5 min and then washed twice in deionised water. Membranes were incubated for 1 h in 5% (w/v) skimmed milk in TBS at room temperature. Blocking solution was removed from the membrane and anti-PNAG IgG1 mAb (800 µg/mL TBS with 0.0001% Tween® 20 and 1% skimmed milk) was added to the membrane and incubated at room temperature for 1 h. The primary antibody solution was then drawn off and the membrane washed three times for 5 min each in TBS with 0.0001% Tween® 20 and once in TBS for 5 min. HRP conjugated rabbit anti-human IgG antibody (200 µg/mL TBS with 0.0001% Tween® 20 and 1% skimmed milk) was applied to the membrane and incubated at room temperature for 1 h. The membrane was washed as described above and Pierce™ ECL Western blotting substrate was added to the membrane for 1 min before HRP activity on the membrane was imaged (FluorChem® FC2, Alpha Innotech, Kasendorf, Germany). Digital images (.jpg) were saved and used to relatively quantify the amounts of PNAG present on the membrane compared to the control (PNAG without three washes) using ImageJ software (National Institutes of Health, Bethesda, MD, U.S.A.). Measurements using the same size frame were taken for each dot, the frames were analysed and the resulting data was exported into Excel v.2010 (Microsoft, CA, U.S.A.). The mean of technical triplicates was taken for each condition and expressed as a percentage of intensity of unwashed cells.

### 2.2.4. Biofilm assays

Overnight cultures grown in BHI media were adjusted with BHI media to an absorbance at 595 nm of 1.0 and diluted at 1:200 with the required media (BHI, BHI glucose or BHI NaCl). Samples were mixed and 100 µL was placed in each well of Nunclon (Δ surface) tissue culture treated 96-well microtitre plates in triplicate per

sample. Plates were then incubated at 37 °C for 24 h, washed three times in a basin of deionised water and dried at 80 °C for up to 2 h. Crystal violet solution (0.4% (w/v) in distilled water, 100 µL) was added to each well and incubated for 5 min at room temperature. The wells were then washed three times with sterile water and 100 µL of 5% (v/v) acetic acid was added to the wells. Absorbance was measured at 490 nm on a SpectraMax M5e microplate reader (Molecular Devices, Inc., Berkshire, UK). Experiments were carried out in triplicate and the average absorbance and standard error was calculated using Excel.

To assess biofilm formation by *A. baumannii*, bacteria were grown overnight in BHI media at 37 °C with shaking at 180 rpm. Overnight cultures were diluted 1:200 in BHI glucose in 10 mL borosilicate glass culture tubes in a total volume of 2 mL. Cultures were incubated at 37 °C for 5 h with shaking at 270 rpm. Cultures were removed from the tubes and the tubes were washed three times with PBS and dried at 80 °C for 3 h. Crystal violet (0.4%) was added to the tubes (3 mL) for 10 min, then washed three times in water, dried at 80 °C for 3 h and the stained tubes imaged using a digital camera. Digital images were stored as .tif files.

### 2.2.5. Lectin and carbohydrate microarray construction

Lectin and carbohydrate microarrays were prepared essentially as previously described (Kilcoyne *et al.*, 2014; Naughton *et al.*, 2013) with minor modifications. In brief, a panel of lectins of known specificities were printed at 0.5 mg/mL in phosphate buffered saline (PBS), pH 7.4, supplemented with 1 mM of their respective haptentic monosaccharides (Table 2.2). For carbohydrate microarrays, NGCs and glycoproteins were printed at 1 mg/mL in PBS across two paired microarrays, A and B, with 15 of the same probes in the same print position to facilitate later data normalisation across the paired microarrays (Table 2.3). Probes (lectins, NGCs and glycoproteins) were printed on Nexterion ® slide H microarray slides (Schott, Mainz, Germany) using a SciFlexArrayer S3 (Scienion,Berlin, Germany) under constant 60% (+/- 2%) humidity at 18 °C (+/- 2 °C). For each slide, features of approximately 1 nL were printed in replicates of 6 per probe per subarray and eight replicate subarrays per microarray slide. Following printing, slides were placed in a humidity chamber overnight at room temperature. Slides were then blocked with 100 mM ethanolamine in 50 mM sodium borate, pH 8.0, for 1 h at

room temperature. Slides were washed three times with PBS with 0.05% Tween® 20 (PBS-T), and once with PBS. Slides were dried by centrifugation (1,500 x g, 5 min) and stored at 4 °C sealed with desiccant until use.

Validation of lectin printing and retained function on the microarray surface was carried out by incubating one microarray from each batch with a panel of AF555 labelled glycoproteins (fetuin, asialofetuin, invertase, RNase B and alpha-1-acid glycoprotein) and the NGC GlcNAc-BSA (each incubated at 1 µg/mL in TBS-T). Validation of neoglycoconjugate and glycoprotein printing and accessibility of the presented carbohydrates on the microarray surface was done by incubating one microarray from each batch with a panel of TRITC labelled lectins (WGA, MAA, AIA, Con A, PHA-E, GS-II and SBA, each incubated at 5 µg/mL).

### 2.2.6. Fluorescent labelling of bacteria

Bacterial labelling was carried out in the dark as previously described (Kilcoyne *et al,* 2014) with some minor alterations. Bacteria were grown overnight in 5 mL BHI broth at 37 °C for 24 h in an orbital shaker (180 rpm). Bacteria were harvested, pelleted by centrifugation (5,000 × g, 5 min), washed three times in TBS and resuspended in 5 mL TBS. Bacteria were diluted with TBS to an absorbance at 595 nm of approximately 1.0. To determine the optimum dye concentration, each bacterial strain was incubated with a range of 5 to 50 µM SYTO® 82 nucleic acid (λex 541 nm, λem 560 nm) at 37 °C for 1 h with 180 rpm rotation. Following incubation, the fluorescently labelled cells were washed three times in TBS by resuspending bacteria in 1 mL TBS, centrifuging to pellet at 5,000 x g for 5 min, removing the supernatant and repeating to remove excess dye. Bacterial cells were finally resuspended in 0.5 mL of TBS-T (Tween-20 0.025%) and 100 uL of each concentration was placed in each well of a 96 black microtitre plate. Fluorescence was measured at 541 nm excitation and 560 nm emission using a SpectraMax M5e microplate reader (Molecular Devices, Inc., Berkshire, UK). The optimum dye concentration was determined based on maximum fluorescence intensity obtained for the strain or, in the case of *S. aureus* BH1CC, optimum signal to noise ratio achieved on the lectin microarray.

For microarray experiments, *S. aureus* strains were grown overnight in BHI, BHI 1% glucose or BHI 4% NaCl. Bacteria were washed three times with TBS and adjusted to an

**Table 2.2. Lectins printed, their binding specificities, their simple print sugars (1 mM) and the supplying company.**

| Abbreviation | Source | Species | Common name | General binding specificity* | Print sugar | Supplier |
|---|---|---|---|---|---|---|
| AIA, Jacalin | Plant | *Artocarpus integrifolia* | Jack fruit lectin | Gal, Gal-β-(1,3)-GalNAc (sialylation independent) | Gal | EY Labs |
| RPbAI | Plant | *Robinia pseudoacacia* | Black locust lectin | Gal | Gal | EY Labs |
| SNA-II | Plant | *Sambucus nigra* | Sambucus lectin-II | Gal/GalNAc | Gal | EY Labs |
| SJA | Plant | *Sophora japonica* | Pagoda tree lectin | β-GalNAc | Gal | EY Labs |
| DBA | Plant | *Dolichos biflorus* | Horse gram lectin | GalNAc | Gal | EY Labs |
| GHA | Plant | *Glechoma hederacea* | Ground ivy lectin | GalNAc | Gal | EY Labs |
| SBA | Plant | *Glycine max* | Soy bean lectin | GalNAc | Gal | EY Labs |
| VVA | Plant | *Vicia villosa* | Hairy vetch lectin | GalNAc | Gal | EY Labs |
| BPA | Plant | *Bauhinia purpurea* | Camels foot tree lectin | GalNAc/Gal | Gal | EY Labs |
| WFA | Plant | *Wisteria floribunda* | Japanese wisteria lectin | GalNAc/sulfated GalNAc | Gal | EY Labs |
| HPA | Animal | *Helix pomatia* | Edible snail lectin | α-GalNAc | Gal | EY Labs |
| GSL-I-A4 | Plant | *Griffonia simplicifolia* | Griffonia isolectin I A4 | GalNAc | Gal | EY Labs |
| ACA | Plant | *Amaranthus caudatus* | Amaranthin | Sialylated/Gal-β-(1,3)-GalNAc | Lac | Vector Labs |
| ABL | Fungus | *Agaricus bisporus* | Edible mushroom lectin | Gal-β(1,3)-GalNAc, GlcNAc | Lac | EY Labs |
| PNA | Plant | *Arachis hypogaea* | Peanut lectin | Gal-β-(1,3)-GalNAc | Lac | EY Labs |
| GSL-II | Plant | *Griffonia simplicifolia* | Griffonia lectin-II | GlcNAc | GlcNAc | EY Labs |
| sWGA | Plant | *Triticum vulgaris* | Succinyl WGA | GlcNAc | GlcNAc | EY Labs |
| DSA | Plant | *Datura stramonium* | Jimson weed lectin | GlcNAc | GlcNAc | EY Labs |
| STA | Plant | *Solanum tuberosum* | Potato lectin | GlcNAc oligomers | GlcNAc | EY Labs |
| LEL | Plant | *Lycopersicum eculentum* | Tomato lectin | GlcNAc-β-(1,4)-GlcNAc | GlcNAc | EY Labs |
| NPA | Plant | *Narcissus pseudonarcissus* | Daffodil lectin | α-(1,6)-Man | Man | EY Labs |
| GNA | Plant | *Galanthus nivalis* | Snowdrop lectin | Man-α-(1,3)- | Man | EY Labs |
| HHA | Plant | *Hippeastrum hybrid* | Amaryllis agglutinin | Man-α-(1,3)-Man-α-(1,6)- | Man | EY Labs |
| ConA | Plant | *Canavalia ensiformis* | Jack bean lectin | Man, Glc, GlcNAc | Man | EY Labs |
| Lch-B | Plant | *Lens culinaris* | Lentil isolectin B | Man, core fucosylated, agalactosylated biantennary *N*-glycans | Man | EY Labs |

| | | | | | | |
|---|---|---|---|---|---|---|
| Lch-A | Plant | *Lens culinaris* | Lentil isolectin A | Man/Glc | Man | EY Labs |
| PSA | Plant | *Pisum sativum* | Pea lectin | Man, core fucosylated trimannosyl *N*-glycans | Man | EY Labs |
| TJA-I | Plant | *Trichosanthes japonica* | Trichosanthes japonica Agglutinin I | NeuAc-α-(2,6)-Gal-β-(1,4)-GIcNAc | Lac | Medicago |
| WGA | Plant | *Triticum vulgaris* | Wheat germ agglutinin | NeuAc/GlcNAc | GlcNAc | EY Labs |
| MAA | Plant | *Maackia amurensis* | Maackia agglutinin | Sialic acid-α-(2,3)-linked | Lac | EY Labs |
| SNA-I | Plant | *Sambucus nigra* | Sambucus lectin-I | Sialic acid-α-(2,6)-linked | Lac | EY Labs |
| PHA-L | Plant | *Phaseolus vulgaris* | Kidney bean leukoagglutinin | Tri- and tetraantennary β-Gal/Gal-β-(1,4)-GlcNAc | Lac | EY Labs |
| PHA-E | Plant | *Phaseolus vulgaris* | Kidney bean erythroagglutinin | Biantennary with bisecting GlcNAc,β-Gal/Gal-β-(1,4)-GlcNAc | Lac | EY Labs |
| RCA-I/120 | Plant | *Ricinus communis* | Castor bean lectin I | Gal-β-(1,4)-GlcNAc | Gal | Vector Labs |
| AMA | Plant | *Arum maculatum* | Lords and ladies lectin | Gal-β-(1,4)-GlcNAc | Lac | EY Labs |
| CPA | Plant | *Cicer arietinum* | Chickpea lectin | Complex oligosaccharides | Lac | EY Labs |
| CAA | Plant | *Caragana arborescens* | Pea tree lectin | Gal-β-(1,4)-GlcNAc | Lac | EY Labs |
| ECA | Plant | *Erythrina cristagalli* | Cocks comb/coral tree lectin | Gal-β-(1,4)-GlcNAc oligomers | Lac | EY Labs |
| TJA-II | Plant | *Trichosanthes japonica* | Trichosanthes japonica Agglutinin II | Fuc-α-(1,2)-Gal-β-(1,4)-GlcNAc | Lac | Medicago |
| AAL | Fungi | *Aleuria aurantia* | Orange peel fungus lectin | Fuc-α-(1,6)-linked, Fuc-α-(1,3)-linked | Fuc | Vector Labs |
| LTA | Plant | *Lotus tetragonolobus* | Lotus lectin | Fuc-α-(1,3)-linked | Fuc | EY Labs |
| UEA-I | Plant | *Ulex europaeus* | Gorse lectin-I | Fuc-α-(1,2)-Gal | Fuc | EY Labs |
| PA-I | Bacteria | *Pseudomonas aeruginosa* | Pseudomonas lectin | Terminal α-linked Gal, Gal derivatives | Gal | EY Labs |
| EEA | Plant | *Euonymous europaeus* | Spindle tree lectin | Terminal α-linked Gal | Gal | EY Labs |
| MPA | Plant | *Maclura pomifera* | Osage orange lectin | Terminal α-linked Gal | Gal | EY Labs |
| VRA | Plant | *Vigna radiata* | Mung bean lectin | Terminal α-linked Gal | Gal | EY Labs |
| MOA | Fungus | *Marasmius oreades* | Fairy ring mushroom lectin | Terminal α-linked Gal | Gal | EY Labs |

* Reported recognition based on literature consensus or experimental evidence generated within our laboratory.

**Table 2.3. NGC and glycoprotein microarray A and B print list, concentration printed source and structure.** Linkers 4AP and ITC depicted between NGC and glycoprotein A and B printlist.

| **NCG and glyocoprotein A** | | | | |
|---|---|---|---|---|
| **Abbreviation** | **Neoglycoconjugate** | **Concentration** | **Source** | **Structure** |
| Fetuin | Fetuin | 1 mg/mL | Sigma | |
| ASF | Asialofetuin | 1 mg/mL | Sigma | |
| Fibronectin | Fibronectin | 1 mg/mL | Collaborative Research Inc. | |
| Ov | Ovalbumin | 1 mg/mL | Sigma | |
| RB | RNAse B | 1 mg/mL | Sigma | |
| Xferrin | Transferrin | 1 mg/mL | Sigma | |
| 4APHSA | 4AP-HAS | 1 mg/mL | Lab Stock | *See structure below* |
| α-C | α -Crystallin from bovine lens | 1 mg/mL | Sigma | |
| M3BSA | Man α1,3(Man α1,6)Man-BSA | 1 mg/mL | Dextra | Mana1,3(Mana1,6)Man-BSA |
| GlcNAcBSA | GlcNAc-BSA | 1 mg/mL | Dextra | GlcNAc-Sp14-NH2(Lys)-BSA |
| LacNAcBSA | LacNAc-BSA | 1 mg/mL | Dextra | Galb1-4GlcNAc-Sp3-BSA |
| 3SLNBSA | 3'SialylLacNAc-BSA | 1 mg/mL | Dextra | |
| 3SLacHSA | 3´-Sialyllactose-APD-HSA, | 1 mg/mL | IsoSep | Neu5Aca2-3Galb1-4(Glc)-APD-HSA |
| 6SLacHSA | 6´-Sialyllactose-APD-HSA, | 1 mg/mL | IsoSep | Neu5Aca2-6Galb1-4(Glc)-APD-HSA |
| 2FLBSA | 2'Fucosyllactose-BSA | 1 mg/mL | Dextra | Fuca1-2Galb1-4Glc-Sp3-BSA |
| 3SFLBSA | 3'Sialyl-3-fucosyllactose-BSA | 1 mg/mL | Dextra | Neu5Aca2-3Galb1-4(Fuca1-3)Glc-Sp3-BSA |
| H2BSA | H Type II-APE-BSA | 1 mg/mL | IsoSep | Fuca1-2Galb1-4GlcNAcb1-APE-BSA |
| BGABSA | Blood Group A-BSA | 1 mg/mL | Dextra | GalNAca(1-3)[Fuca(1-2)]Gal-BSA |
| BGBHSA | Blood Group B-HSA | 1 mg/mL | Dextra | Gala(1-3)[Fuca(1-2)]Gal-BSA |
| Ga3GBSA | Galα1,3Gal-BSA | 1 mg/mL | Dextra | Gala1-3Gal-Sp3-BSA |
| Gb4GBSA | Galb1,4GalBSA | 1 mg/mL | Dextra | Galb1-4Gal-Sp3-BSA |

| | | | | |
|---|---|---|---|---|
| Ga2GBSA | Gala1,2GalBSA | 1 mg/mL | Dextra | Gala1-2Gal-Sp3-BSA |
| LNFPIBSA | Lacto-*N*-fucopentaose I-BSA | 1 mg/mL | Dextra | Fuc-a-1,2-Gal-b-1,3-GlcNAc-b-1,3-Gal-b-1,4-Glc-BSA |
| LNFPIIBSA | Lacto-*N*-fucopentaose II-BSA | 1 mg/mL | Dextra | Fuc-a-1,3-Gal-b-1,3-GlcNAc-b-1,3-Gal-b-1,4-Glc-BSA |
| LNFPIIIBSA | Lacto-*N*-fucopentaose III-BSA | 1 mg/mL | Dextra | Gal-b-1,4-(Fuc-a-1,3)-GlcNAc-b-1,3-D-Gal-b-1,4-Glc-BSA |
| LNDHIBSA | Lacto-*N*-difucohexaose I-BSA | 1 mg/mL | Dextra | Fuca1-2Galb1-3(Fuca1-4)GlcNAcb1-3Galb1-4(Glc)-Sp3-BSA |
| LebBSA | LNDI-BSA/ Lewis b-BSA | 1 mg/mL | IsoSep | Fuca1-2Galb1-3(Fuca1-4)GlcNAcb1-3Galb1-4(Glc)-APD-BSA |
| LexBSA | Lewis x-BSA | 1 mg/mL | Dextra | Gal1-b-4[Fuc1-α-3]GlcNAc-BSA |
| DiLexBSA | Di-Lex-APE-BSA | 1 mg/mL | IsoSep | Galb1-(Fuca1-3)4GlcNAcb1-3Galb1-(Fuca1-3)4GlcNAcb1-O-APE-BSA |
| DiLexHSA | Di-Lewisx-APE-HSA | 1 mg/mL | IsoSep | Galb1-(Fuca1-3)4GlcNAcb1-3Galb1-(Fuca1-3)4GlcNAcb1-O-APE-HSA |
| 3LexHSA | Tri-Lex-APE-HSA | 1 mg/mL | IsoSep | Galb1-(Fuca1-3)4GlcNAcb1-3Galb1-(Fuca1-3)4GlcNAcb1-3Galb1-(Fuca1-3)4GlcNAcb1-O-APE-HSA |
| 3SLexBSA3 | 3'Sialyl Lewis x-BSA | 1 mg/mL | Dextra | Neu5Aca2-3Galb1-4(Fuca1-3)GlcNAc-Sp3-BSA |
| SLexBSA14 | 3'Sialyl Lewis x-BSA | 1 mg/mL | Dextra | Neu5Aca2-3Galb1-4(Fuca1-3)GlcNAc-Sp14 |
| 6SuLexBSA | 6-Sulfo Lewis x-BSA | 1 mg/mL | Dextra | (SO4)6Galb1-4(Fuca1-3)GlcNAc-Sp3-BSA |
| 6SuLeaBSA | 6-Sulfo Lewis a-BSA | 1 mg/mL | Dextra | (SO4)6Galb1-3(Fuca1-4)GlcNAc-SP3-BSA |
| 3SuLeaBSA | 3-Sulfo Lewis a-BSA | 1 mg/mL | Dextra | (SO4)3Galb1-3(Fuca1-4)GlcNAc |
| PBS | PBS | | | |
| DFPLNHHSA | Difucosyl-para-lacto-N-hexaose-APD-HSA, (Lea/Lex) | 1 mg/mL | IsoSep | Galb1-(Fuca1-4)3GlcNAcb1-3Galb1-(Fuca1-3)4GlcNAcb1-3Galb1-4(Glc)-APD-HSA |
| LeaBSA | Lewis a-BSA | 1 mg/mL | Dextra | Galb(1-3)[Fuca(1-4)]GlcNAc-Sp3-BSA |
| LeyHSA | Lewis y-tetrasaccharide-APE-HSA | 1 mg/mL | IsoSep | Fuca1-2Galb1-(Fuca1-3)4GlcNAcb1-O-APE-HSA |
| 3FLeyHSA | Tri-fucosyl-Ley-heptasaccharide-APE-HSA | 1 mg/mL | IsoSep | Fuca1-2Galb1-(Fuca1-3)4GlcNAcb1-3Galb1-4(Fuca1-3)GlcNAcb1-O-APE-HSA |
| LNnTHSA | Lacto-N-neotetraose-APD-HSA | 1 mg/mL | IsoSep | Galb1-4GlcNAcb1-3Galb1-4(Glc)-APD-HSA |
| LNTHSA | Lacto-N-tetraose-APD-HSA | 1 mg/mL | IsoSep | Galb1-3GlcNAcb1-3Galb1-4(Glc)-APD-HSA |
| MMLNnHHSA | Monofucosyl, monosialyllacto-N-neohexaose-APD-HSA | 1 mg/mL | IsoSep | Neu5Aca2-3Galb1-4GlcNAcb1-3[Galb1-4(Fuca1-3)GlcNAcb1-6]Galb1-4(Glc)-APD-HSA |
| SLNnTHSA | Sialyl-LNnT-penta-APD-HSA | 1 mg/mL | IsoSep | Neu5Aca2-3Galb1-4GlcNAcb1-3Galb1-4(Glc)-APD-HSA |

| | | | | |
|---|---|---|---|---|
| aGM1HSA | Asialo-GM1-tetrasaccharide-APD-HSA | 1 mg/mL | IsoSep | Galb1-3GalNAcb1-4Galb1-4(Glc)-APD-HSA |
| GlobNTHSA | Globo-N-tetraose-APD-HSA | 1 mg/mL | IsoSep | GalNAcb1-3Gala1-4Galb1-4(Glc)-APD-HSA |
| GlobTHSA | Globotriose-APD-HSA | 1 mg/mL | IsoSep | Gala1-4Galb1-4Glcb1-APE-HSA |

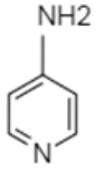


**4-aminophenyl-β-D-glucopyranoside (4AP)**

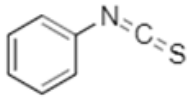


**β-D-glucopyranosyl phenylisothiocyanate (ITC)**

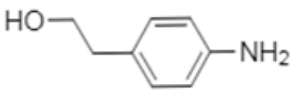


***p*-aminophenylethyl (APE)**

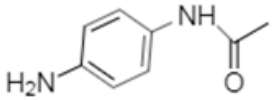


**Acetyl-phenylenediamine (APD)**

| NCG and glyocoprotein B | | | | |
|---|---|---|---|---|
| **Abbreviation** | **Neoglycoconjugate** | **Concentration** | **Source** | **Structure** |
| Fetuin | Fetuin | 1 mg/mL | Sigma | |
| Inv | Invertase | 1 mg/mL | Sigma | |
| Fibrin | Fibrinogen | 0.5 mg/mL | Sigma | |
| Ov | Ovalbumin | 1 mg/mL | Sigma | |
| PBS | PBS | | | |
| A1AT | alpha-1-antitrypsin | 1 mg/mL | Sigma | |
| 4APHSA | 4AP-HSA | 1 mg/mL | Lab Stock | |
| α -C | α-Crystallin from bovine lens | 1 mg/mL | Sigma | |
| M3BSA | Manα1,3(Manα1,6)Man-BSA | 1 mg/mL | Dextra | Mana1,3(Mana1,6)Man-BSA |
| GlcNAcBSA | GlcNAc-BSA | 1 mg/mL | Dextra | GlcNAc-Sp14-NH2(Lys)-BSA |
| Cerulo | Ceruloplasmin | 1 mg/mL | Sigma | |
| AGP | alpha-1-acid glycoprotein | 1 mg/mL | Sigma | |
| 3SLacHSA | 3´-Sialyllactose-APD-HSA | 1 mg/mL | IsoSep | Neu5Aca2-3Galb1-4(Glc)-APD-HSA |
| 6SLacHSA | 6´-Sialyllactose-APD-HSA | 1 mg/mL | IsoSep | Neu5Aca2-6Galb1-4(Glc)-APD-HSA |
| LacNAcaBSA | LacNAc-α-4AP-BSA | 1 mg/mL | Lab stock | |
| LacNAcb4APBSA | LacNAc-β-4AP-BSA | 1 mg/mL | Lab stock | |
| H2BSA | H Type II-APE-BSA | 1 mg/mL | IsoSep | Fuca1-2Gab1-4GlcNAcb1-APE-BSA |
| PBS | PBS | | | |
| Ovomuc | Ovomucoid | 0.5 mg/mL | Dextra | |
| Ga3GBSA | Galα1,3Gal-BSA | 1 mg/mL | Dextra | Gala1-3Gal-Sp3-BSA |
| RhaBSA | L-Rhamnose-Sp14-BSA | 1 mg/mL | Dextra | |
| PBS | PBS | 1 mg/mL | | |
| LNFPIBSA | Lacto-*N*-fucopentaose I-BSA | 1 mg/mL | Dextra | Fuc-a-1,2-Gal-b-1,3-GlcNAc-b-1,3-Gal-b-1,4-Glc-BSA |
| XManaBSA | Man-α-ITC-BSA | 1 mg/mL | Dextra | |

| | | | | |
|---|---|---|---|---|
| PBS | PBS | | Dextra | |
| XManbBSA | Man-β-4AP-BSA | 1 mg/mL | Lab stock | |
| LebBSA | LNDI-BSA/ Lewis b-BSA | 1 mg/mL | IsoSep | Fuca1-2Galb1-3(Fuca1-4)GlcNAcb1-3Galb1-4(Glc)-APD-BSA |
| LexBSA | Lewis x-BSA | 1 mg/mL | Dextra | Gal1-b-4[Fuc1-α-3]GlcNAc-BSA |
| XGalbBSA | Gal-β-ITC-BSA | 1 mg/mL | Lab stock | |
| XylbBSA | Xyl-β-4AP-BSA | 1 mg/mL | Lab stock | |
| 3LexHSA | Tri-Lex-APE-HSA | 0.5 mg/mL | IsoSep | Galb1-(Fuca1-3)4GlcNAcb1-3Galb1-(Fuca1-3)4GlcNAcb1-3Galb1-(Fuca1-3)4GlcNAcb1-O-APE-HSA |
| XylaBSA | Xyl-α-4AP-BSA | 1 mg/mL | Lab stock | |
| XGlcbBSA | Glc-β-4AP-BSA | 1 mg/mL | Lab stock | |
| FucaBSA | Fuc-α-4AP-BSA | 1 mg/mL | Lab stock | |
| 6SuLeaBSA | 6-Sulfo Lewis a-BSA | 1 mg/mL | Dextra | (SO4)6Galb1-3(Fuca1-4)GlcNAc-SP3-BSA |
| FucbBSA | Fuc-β-4AP-BSA | 1 mg/mL | Lab stock | |
| GlcbITCBSA | Glc-β-ITC-BSA | 1 mg/mL | Lab stock | |
| Galb4APBSA | Gal-β-4AP-BSA | 1 mg/mL | Lab stock | |
| Neu5GcBSA | Neu5Gc-BSA | 1 mg/mL | Lab stock | |
| LeyHSA | Lewis y-tetrasaccharide-APE-HSA | 1 mg/mL | IsoSep | Fuca1-2Galb1-(Fuca1-3)4GlcNAcb1-O-APE-HSA |
| PBS | | | | |
| PBS | | | | |
| LNTHSA | Lacto-N-tetraose-APD-HSA | 1 mg/mL | IsoSep | Galb1-3GlcNAcb1-3Galb1-4(Glc)-APD-HSA |
| PBS | | | IsoSep | |
| PBS | | | IsoSep | |
| D-GlobTHSA | Globotriose-HSA | 1 mg/mL | Dextra | Gala1-4Galb1-4Glc-Sp3-BSA |
| GlobNTHSA | Globo-N-tetraose-APD-HSA | 1 mg/mL | IsoSep | GalNAcb1-3Gala1-4Galb1-4(Glc)-APD-HSA |
| GlobTHSA | Globotriose-APE-HSA | 1 mg/mL | IsoSep | Gala1-4Galb1-4Glcb1-APE-HSA |

absorbance at 595 nm of 1.0. *S. aureus* Mn8 WT and Δ*ica* mutant and *A. baumannii* WT and Δ*pga* mutant were stained with 5 μM SYTO® 82, *S. aureus* 8325-4 WT and Δ*ica* mutant with 10 μM and *S. aureus* BH1CC WT and Δ*ica* mutant with 15 μM for 1 h at 37 °C at 180 rpm in the dark. Excess dye was removed by washing three times in TBS, and bacterial pellets were resuspended in 500 μL TBS supplemented with 0.025% Tween® 20 (v/v) for an approximate absorbance at 595 nm of 2.0 for each strain.

### 2.2.7. Microarray incubation and scanning

All microarray incubations were carried out in the dark. Labelled bacteria or labelled lectins or glycoproteins diluted in TBS-T were incubated on lectin or NGC microarrays using an 8 well gasket at 70 μL per well and incubated with gentle rotation (4 rpm) at 37 °C for 1 h. Incubation chambers were disassembled under TBS-T, washed twice in TBS-T for 2 min each wash in a Coplin jar and once with TBS. Microarray slides were dried by centrifugation (1,500 x g, 5 min) and imaged immediately by scanning in an Agilent G2505B microarray scanner equipped with a 532 nm laser (90% PMT, 5 μm resolution). Images were stored as .tif files for later extraction and processing. Experiments were carried out in technical triplicate with sample incubation on one slide considered one experimental replicate.

Bacteria were initially titrated on each microarray platform by incubating dilutions of stained bacteria at absorbance at 595 nm of 2.0 with TBS-T. Based on optimal signal to background, bacterial incubations were carried out in triplicate using a dilution of 50 μL of stained bacteria in a final volume of 70 μL with TBS-T.

### 2.2.8. Data extraction and analysis

Data extraction was performed essentially as previously described (Kilcoyne *et al.*, 2014). In brief, image files (.tif) of lectin and carbohydrate microarrays from the microarray scanner were used to extract raw intensity values using GenePix Pro v6.1.0.4 software (Molecular Devices, Berkshire, U.K.) and a proprietary .gal file that held the address and identity of each feature using adaptive diameter (70-160%) circular alignment based on 230 mm features and were exported as text to Excel (Version 2007, Microsoft, Dublin, Ireland). Local background subtracted median

feature intensity data (F543median-B543) was analysed. The median of six replicate spots per subarray was handled as a single data point for graphical and statistical analysis. For lectin microarray analysis, data were normalized to the per subarray mean total intensity value of three replicate microarray slides and binding data was presented as a bar chart of average intensity of three experimental replicates with error bars of +/- one standard deviation (SD) of the mean. For carbohydrate microarray analysis, the same process was carried out as for lectin microarray analysis, except that total per subarray intensity was normalised to the common 15 probes across the paired A and B microarrays (Utratna *et al.*, 2017).

Unsupervised hierarchical clustering of bacteria-lectin and bacteria-NGC binding data was carried out using Hierarchial Clustering Explorer v3.0 (http://www.cs.umd.edu/hcil/hce/hce3.html; National Institutes of Health, Bethesda, MD, U.S.A.). Normalised microarray data was scaled to the maximum signal intensity per sample and the binding patterns were clustered using the following parameters: no pre-filtering, complete linkage and Euclidean distance.

## 2.3. Results

Bacterial surface glycosylation and ability to bind to carbohydrates play imperative roles in infections and host immune evasion (Gerlach *et al*., 2018; Hajishengallis *et al*., 2011). To determine the role of PNAG in surface glycosylation and carbohydrate interactions, we chose a range of PNAG-producing and non-producing bacteria and incubated them on lectin and NGC microarrays. MSSA strains 8325-4 and Mn8m and *A. baumannii* S1 were chosen for this study for their ability to produce PNAG-mediated biofilms while MRSA strain BH1CC was selected as a non-PNAG producing strain. The WT and corresponding PNAG-deficient mutants, Δ*ica* or Δ*pga*, were grown under various environmental conditions to promote biofilm formation (Table 2.4). The WT and Δ*ica* or Δ*pga* strains were optimised for fluorescent staining under biofilm-promoting conditions and were profiled for differences in surface glycosylation and binding to carbohydrate ligands.

### 2.3.1. Confirmation of biofilm production of bacteria cultured in BHI supplemented with glucose or NaCl

To verify that the *ica* or *pga* mutants did not form biofilm or had reduced biofilm formation, biofilm assays were performed on all strains in the presence of either 4% NaCl and/or 1% glucose supplemented in to the growth media (Fig. 2.1). For biofilm assays, all bacterial strains were grown in the presence of glucose (Table 2.4). NaCl was added to the growth media of MRSA BH1CC as it has been shown to promote *icaA* transcription, but not form biofilm (O'Neill *et al.*, 2007). As a comparative, the MSSA strain 8325-4 was also grown in the presence of NaCl which is also known to increase PNAG-mediated biofilm formation in this strain (Kennedy, *et al*, 2004).

Addition of glucose to BHI increased biofilm formation by *S. aureus* 8325-4 WT by approximately 165% in comparison to *S. aureus* 8325-4 grown in BHI media (Fig. 2.1 (A)). Biofilm formation was further increased to approximately 311% with the addition of NaCl to BHI, compared to *S. aureus* 8325-4 WT grown in BHI alone. *S. aureus* 8325-4 Δ*ica* decreased biofilm formation to approximately 73%, 66% and 96% compared to the WT grown in the same media, respectively BHI media, BHI glucose or BHI NaCl (Fig. 2.1 (A)). Biofilm formation by *S. aureus* Mn8m WT was increased slightly (approximately 5%) by the addition of glucose in comparison to

no supplementation (Fig. 2.1 (B)). *S. aureus* Mn8 Δ*ica* biofilm formation was decreased to approximately 92% in BHI and 86% in BHI glucose of the biofilm formed by the WT strain under the same conditions (Fig. 2.1 (B)). Overall, these data confirmed that *S. aureus* strains 8325-4 and Mn8m WT had increased biofilm formation in the presence of glucose and/or NaCl. The Δ*ica* mutation greatly decreased biofilm formation under all conditions.

BHI glucose promoted biofilm formation for *S. aureus* BH1CC by approximately 62% compared to growth in BHI alone (Fig. 2.1 (C)). Addition of NaCl to the growth media decreased the formation of biofilm by 90% in comparison to BHI media alone (Fig. 2.1 (C)). *S. aureus* BH1CC Δ*ica* decreased biofilm formation slightly approximately 16% and 13% to that of the WT grown in the same media, respectively BHI media or BHI NaCl, and increased biofilm formation by approximately 2% after growth in BHI glucose (Fig. 2.1 (C)). Overall, these data confirmed that *S. aureus* BH1CC WT had increased biofilm formation in the presence of glucose and decreased or abolished biofilm formation in the presence of NaCl. The Δ*ica* mutation had little to no effect on biofilm formation under all conditions.

**Table 2.4. Summary of known effects of glucose and NaCl on biofilm formation by bacterial strains used in this study.** All reports for *S. aureus* are based on biofilm assays carried out on hydrophilic 96-well plates. Reports for *A. baumannii* are based on biofilm formation on borosilicate glass tubes. N/D – not determined in reports to date. N/A – not applicable.

| Strain | Sensitivity | Additive | Transcription | Effect on biofilm formation | Mediated by | Biofilm type | | | References |
|---|---|---|---|---|---|---|---|---|---|
| | | | | | | Protein | DNA | PNAG | |
| *S. aureus* 8325-4 | MSSA | Glc | N/D | Increase | Ica proteins | | | ✓ | (Lim *et al.*, 2004; Pozzi *et al.*, 2012) |
| | | NaCl | N/D | Increase | Ica proteins | | | ✓ | (Kennedy & O'Gara, 2004) |
| *S. aureus* Mn8m | MSSA | Glc | ↓ *icaR* | Increase | Ica proteins | | | ✓ | (Jefferson *et al.*, 2003, 2004) |
| | | NaCl | N/D | N/D | N/D | N/D | N/D | N/D | N/A |
| *S. aureus* BH1CC | MRSA | Glc | ↑ *fnbAB* | Increase | FnbAB, eDNA | ✓ | ✓ | | (Houston *et al.*, 2011) |
| | | NaCl | ↑*icaA* | Decrease | N/A | N/D | N/D | N/D | (Fitzpatrick *et al.*, 2005) |
| *A. baumannii* S1 | N/D | Glc | N/D | N/D | Pga proteins | | | ✓ | (Choi *et al.*, 2009) |
| | | NaCl | N/D | N/D | N/D | N/D | N/D | N/D | N/A |

As *A. baumannii* preferentially forms biofilm on glass, *A. baumannii* S1 WT and Δ*pga* were grown in the presence of BHI glucose in a borosilicate glass culture tube with vigorous shaking. Crystal violet stained clumps of *A. baumannii* were visualised on the glass culture tube that contained *A. baumannii* S1 WT and were more intense on the tube that contained *A. baumannii* S1 WT compared to the Δ*pga* mutant. Thus, the *pga* operon and PNAG on *A. baumannii* S1 contributes to clumping and attachment on to glass surfaces (Fig 2.1 (D)).

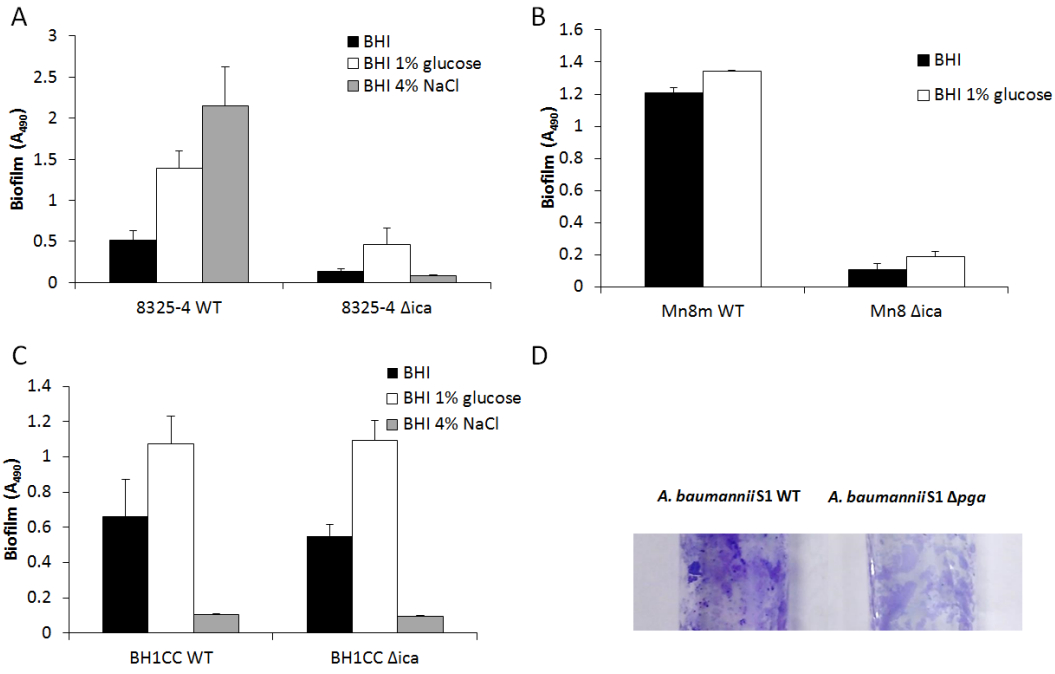


**Fig. 2.1. Biofilm assays for (A) *S. aureus* 8325-4 WT and Δ*ica*, (B) *S. aureus* Mn8m WT and Δ*ica*, (C) *S. aureus* BH1CC WT and Δ*ica*, and (D) *A. baumannii* S1 WT and Δ*pga*.** (A), (B) and (C) Bacteria were grown BHI, BHI glucose or BHI NaCl in a hydrophilic 96-well tissue culture treated plate for 18 hours. Biofilm was quantified by adding Crystal Violet and reading absorbance at 490 nm. Experiments were carried out in technical triplicates and data is depicted as the mean of the three technical replicates of three experiments with error bars of +/- one SD of the mean. (D) Bacteria were grown for 18 hours in borosilicate glass tubes. Tubes were washed and stained with Crystal Violet, washed with water, dried and imaged using a camera.

### 2.3.2. Optimisation of fluorescent dye concentration for bacterial strains

To elucidate the interactions between bacteria and probes on the microarray platform, bacteria must be fluorescently labelled to allow for detection of bacterial binding. To determine the optimal concentration of SYTO®82 to use for each bacterial strain, titrations using different dye concentrations (5-50 μM) were carried out for each strain (Fig. 2.2).

*S. aureus* 8325-4 WT and Δ*ica* had maximum fluorescence at 10 μM (Fig. 2.2 (A)), with greater dye concentrations decreasing the bacterial fluorescence. Similarly *S. aureus* Mn8m WT and Δ*ica* at the lowest concentration tested of 5 μM (Fig. 2.2 (B)) and fluorescence intensity decreased with higher concentrations tested. Therefore, the SYTO®82 concentrations of maximum fluorescence were chosen for these *S. aureus* strains. In contrast, the fluorescence of *S. aureus* BH1CC WT and Δ*ica* increased with increasing dye concentration, and bacterial fluorescence plateaued slightly at 15 μM and again at 40 μM (Fig. 2.2 (C)).

To determine the optimal concentration for use with the lectin and carbohydrate microarray platforms, *S. aureus* BH1CC was stained with 15 and 40 μM SYTO®82 and incubated on a lectin microarray to screen for optimal intense signal and low background intensity. There was high background fluorescence (> 1,000 RFU) on the lectin microarray when *S. aureus* BH1CC was stained with 40 mM SYTO®82, while background fluorescence was consistently close to or below 500 RFU when *S. aureus* BH1CC was stained with 15 mM SYTO®82, except for one lectin, *Datura stramonium* agglutinin (DSA) (Fig. 2.2 (E)). As the criterion for background fluorescence is 500 RFU or less for these platforms (Wang *et al.*, 2014) (Fig. 2.2 (E)), the first maximum of 15 μM was chosen for *S. aureus* BH1CC WT and also selected for *S. aureus* BH1CC Δ*ica* for consistency.

*A. baumannii* WT had maximum fluorescence intensity at 5 μM, followed by a decrease to approximately 70% of the maximum intensity at 10 μM and a maintained plateau at this intensity for higher concentrations. The maximum intensity for *A. baumannii* Δ*pga* was obtained at 40 μM but all dye concentrations tested maintained approximately 70-90% of maximum fluorescence (Fig. 2.2 (D)). Therefore, 5 μM was selected for *A. baumannii* WT and also the Δ*pga* strain to maintain consistency with *A. baumannii* WT.

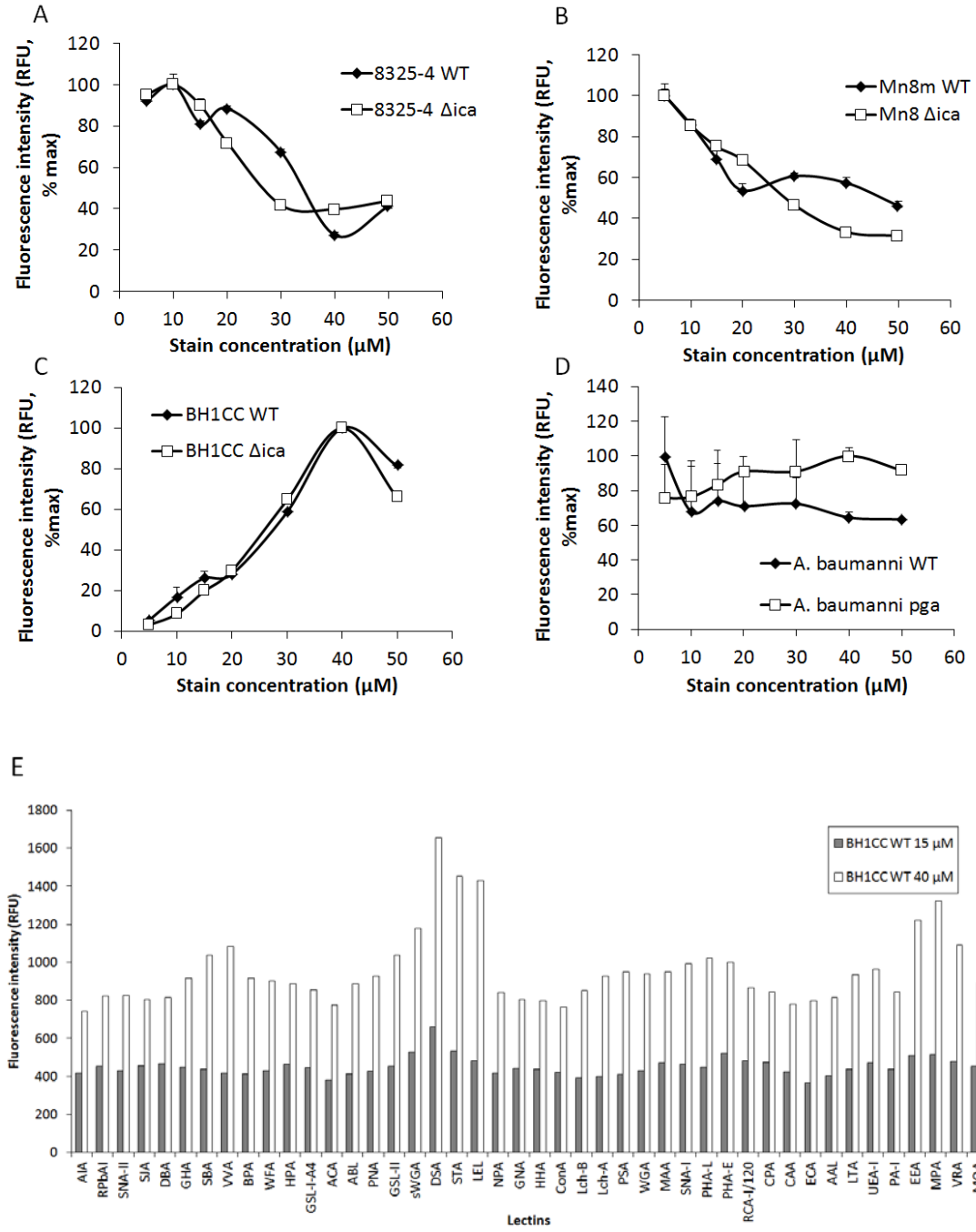


**Figure 2.2. SYTO®82 concentration titration for fluorescence of (A) *S. aureus* 8325-4 WT and Δ*ica*, (B) *S. aureus* Mn8m WT and Δ*ica*, (C) *S. aureus* BH1CC WT and Δ*ica* and (D) *A. baumannii* S1 WT and Δ*pga* and (E) background fluorescence of BH1CC WT stained with 15 and 40 μM SYTO®82 on the lectin microarray.** (B), (C) and (D) Bacteria were grown overnight in BHI glucose, except (A) *S. aureus* 8325-4 which was grown in BHI NaCl, and incubated with 5-50 μM SYTO®82. Fluorescence of the stained bacteria was measured at λex 541 nm and λem 560 nm and plotted as a percentage of maximum fluorescence obtained for each strain. Error bars represent SD of the mean of

three technical replicates. (E) BH1CC WT stained with 15 and 40 μM SYTO®82 incubated on the lectin microarray and the local average background around each lectin is represented as a bar chart. Titration of detergent concentration for optimal PNAG retention after staining and washing.

To facilitate bacterial incubations on glycomics microarrays, a study was carried out to identify the effect detergent concentration and washing after SYTO®82 staining of bacteria had on the retention of PNAG on the bacterial surface. The positive reference of maximal (100%) PNAG retention was for *S. aureus* 8325-4 WT grown overnight in BHI NaCl, washed initially three times in TBS from culture, then stained with SYTO®82 and not washed after staining. The presence of PNAG was tested by detection of retained PNAG with an anti-PNAG antibody under conditions of washing the stained cells three times and resuspending in TBS with varying concentrations of Tween-20 (0.01-0.05%). Cells washed in TBS had an approximate 40% reduction in PNAG retained on the cell surface while the inclusion of varying concentrations of Tween-20 reduced the PNAG present on the bacteria cell surface by approximately 50%, (Fig. 2.3), with no significant difference between Tween-20 concentrations but a slightly greater retention of PNAG at 0.025% Tween-20.

Not washing cells after staining is not desirable for use with microarrays as the remaining unincorporated charged dye results in high background fluorescence and may interfere in interactions. Furthermore, a lack of inclusion of detergent in microarray incubations results in bacterial clumping. Therefore, washing the stained bacteria three times and resuspension in TBS supplemented with 0.025% Tween-20 was selected for all microarray experiments. Thus, approximately 50% of PNAG was removed prior to all microarray incubations and this may vary from experiment to experiment (Fig. 2.3).

### 2.3.3. *S. aureus* BH1CC WT titration on the lectin microarray platform

As *S. aureus* BH1CC had the lowest fluorescence following SYTO®82 staining compared to the other *S. aureus* strains and *A. baumannii*, titrations were carried out with BH1CC to obtain optimal cell concentration for a good signal to background noise ratio.

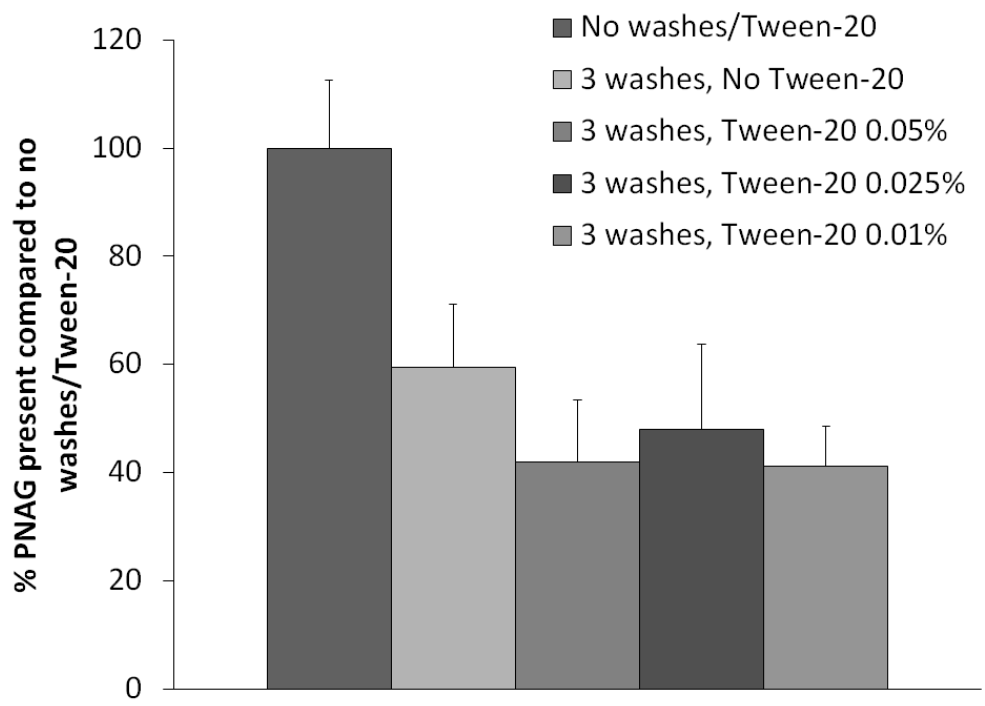


**Fig. 2.3. Detection of PNAG on *S. aureus* 8325-4 WT surface with no washes and after three washes with no and varying Tween-20 concentrations.** *S. aureus* 8325-4 WT was grown overnight in BHI NaCl. Bacteria were washed initially 3 times followed by resuspension in TBS-T (no washes/Tween-20), washed 3 times and resuspended in TBS (3 washes, no Tween-20), washed 3 times and resuspended in TBS-T 0.05% (3 washes, Tween-20 0.05%), washed 3 times and resuspended in TBS-T 0.025% (3 washes, Tween-20 0.025%), and washed 3 times and resuspended in TBS-T 0.01% (3 washes, Tween-20 0.01%). After washes, bacterial suspensions were spotted on to PVDF membrane and PNAG was detected using an anti-PNAG antibody. Quantification of PNAG present after washing in no or different concentrations of Tween-20 was carried out by densitometry of the spots and the presence of PNAG was plotted as a relative percentage of no washing after staining (100%).

Following *S. aureus* BH1CC WT titrations on the lectin microarray, binding patterns were the same for all bacterial concentrations and binding intensities were concentration dependent for the majority of lectins (Fig. 2.4). Although the undiluted sample of *S. aureus* BH1CC WT resulted in the highest fluorescence intensity binding with all lectins, the background fluorescence was approximately 800 RFU which exceeded the background threshold imposed for these microarrays (Wang *et al*, 2014). The 50 µL dilution had high binding fluorescence intensities and a lower

background fluorescence of approximately 500 RFU (Fig. 2.4). Therefore, *S. aureus* BH1CC diluted 50 μL to a final volume of 70 μL was chosen as the optimal concentration of bacteria for use on the microarray platform. To maintain consistency for comparisons across different bacterial strains, the same dilution was also used for other bacteria in this study.

### 2.3.4. Lectin microarray profiles of MSSA strains 8325-4 and Mn8m WT and Δ*ica* in different growth media

*S. aureus* strains 8325-4 and Mn8m WT and Δ*ica* were grown in BHI, BHI glucose, BHI NaCl or BHI and BHI glucose, respectively, and profiled on the lectin microarray. The GlcNAc-specific lectins *Griffonia simplicifolia* lectin-II (GSL-II), succinylated *Triticum vulgaris* agglutinin (sWGA) and *Triticum vulgaris* agglutinin (WGA) had the greatest binding to *S. aureus* 8325-4 WT after growth in BHI, BHI glucose or BHI NaCl (Fig. 2.5 (A)) (Table 2.2). GSL-II and WGA bound the greatest number of *S. aureus* 8325-4 WT cells grown in BHI media, compared to other lectins. sWGA also bound *S. aureus* 8325-4 WT grown in BHI, but to a lower degree compared to GSL-II and WGA (Fig. 2.5 (A)). WGA bound to the highest number of *S. aureus* 8325-4 WT cell grown in BHI glucose compared to sWGA and GSL-II, while GSL-II displayed a moderate binding intensity, and sWGA and WGA displayed weak binding intensities to *S. aureus* 8325-4 grown in BHI NaCl (Fig. 2.5 (A)).

As PNAG is a primary component of *S. aureus* 8325-4 biofilm, it is likely that PNAG contributed to the binding of GSL-II, sWGA and WGA to this strain. The varying ratios between the three lectins for binding intensities to bacteria grown under different conditions indicated glucose and/or NaCl-induced differences in the expression, structure and/or presentation of GlcNAc-containing cell surface molecules to make them more or less recognisable to GSL-II, sWGA and WGA.

The pattern and overall relative intensity of lectin interactions with *S. aureus* 8325-4 Δ*ica* compared to 8325-4 WT was similar under the same conditions (Fig. 2.5 (B) and (C)), except GSL-II which bound less to *S. aureus* 8325-4 Δ*ica* cells compared to *S. aureus* 8325-4 WT cells after growth in BHI NaCl (Fig. 2.5 (C)). This suggsted that PNAG produced by *S. aureus* 8325-4 following growth in NaCl may serve as one of many cell surface ligands for GSL-II.

Except in the presence of NaCl, the mutation of the *ica* operon did not reduce the binding of GSL-II, sWGA or WGA to *S. aureus* 8325-4. Therefore, PNAG may not be the most prominent molecule contributing to binding of these lectins or more likely, removal of PNAG from the cell surface uncovered or exposed other abundant and prominent GlcNAc-containing structures, such as peptidoglycan, which then became the main contributors to the binding to the GlcNAc-specific lectins.

GSL-II, sWGA and WGA also bound to *S. aureus* Mn8m WT, suggesting that the main contributor(s) to lectin binding were GlcNAc-containing molecule(s) including PNAG. Binding of GSL-II and WGA to *S. aureus* Mn8m grown in BHI glucose was reduced by approximately half compared to *S. aureus* Mn8m grown in BHI. This indicated that glucose consumption promoted some cell surface glycosylation changes involving GlcNAc-containing molecules. These changes could include changes in expression or alterations in the structure or conformation of PNAG (Fig. 2.5 (D)).

The lectins sWGA and WGA bound *S. aureus* Mn8m WT to a greater intensity compared to *S. aureus* Mn8 Δ*ica*, but no great differences in binding intensities were observed for GSL-II (Fig. 2.5 (E)). This result suggests that PNAG associated with *S. aureus* Mn8m, grown in the presence or absence of glucose, was a ligand for sWGA and may have been one of many ligands for WGA.

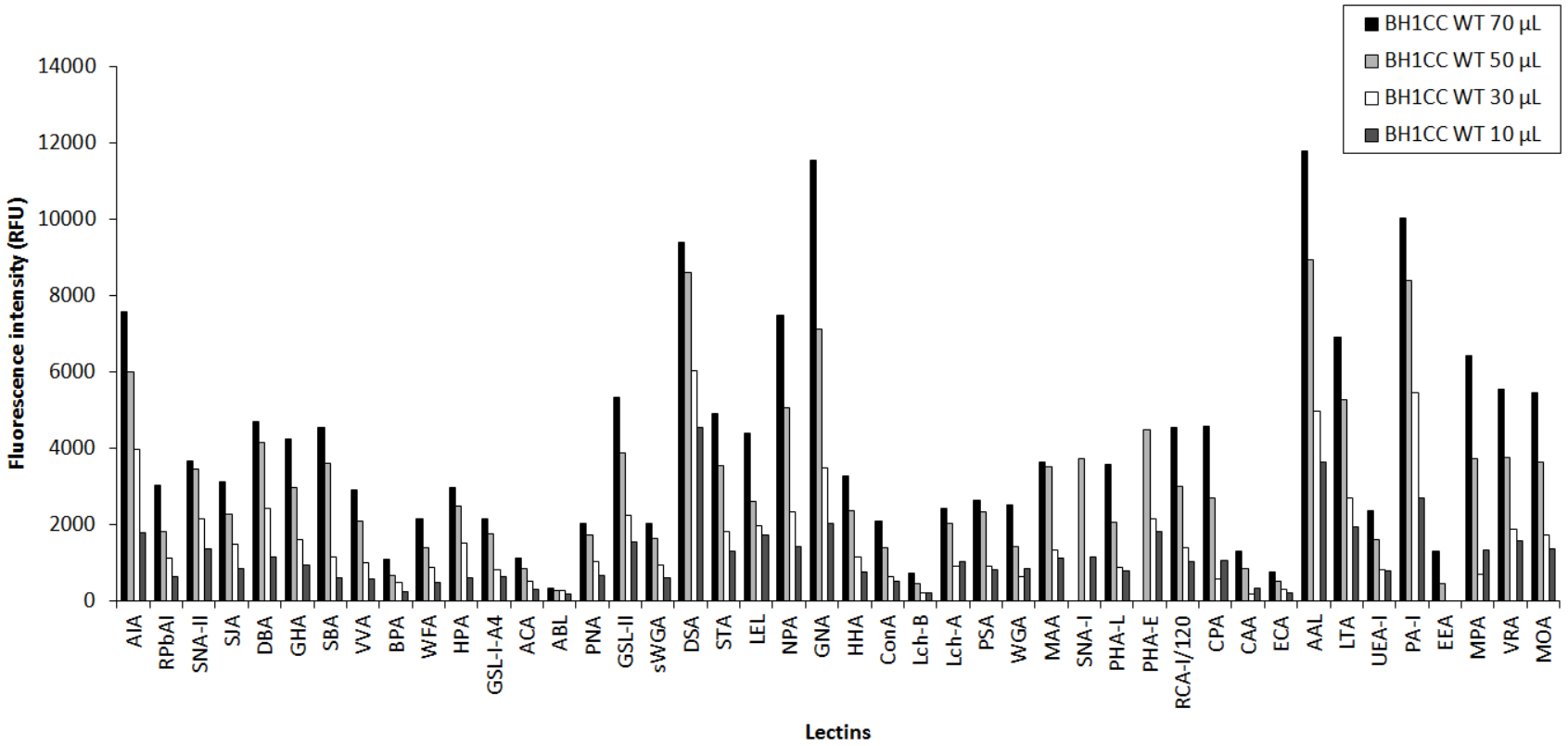


**Fig. 2.4. *S. aureus* BH1CC WT titration on the lectin microarray.** *S. aureus* BH1CC was either not diluted (BH1CC WT 70 µL), 50 µL of the stained bacteria were diluted with TBS-T to a final volume of 70 µL (BH1CC WT 50 µL), 30 µL diluted to a final volume of 70 µL (BH1CC WT 30 µL) or 10 µL diluted to a final volume of 70 µL (BH1CC WT 10 µL) and incubated on the lectin microarray. Bars represent *S. aureus* BH1CC WT titrations on the lectin microarray platform. Bars represent the binding intensity from one experiment and the median data from six technical replicates.

A

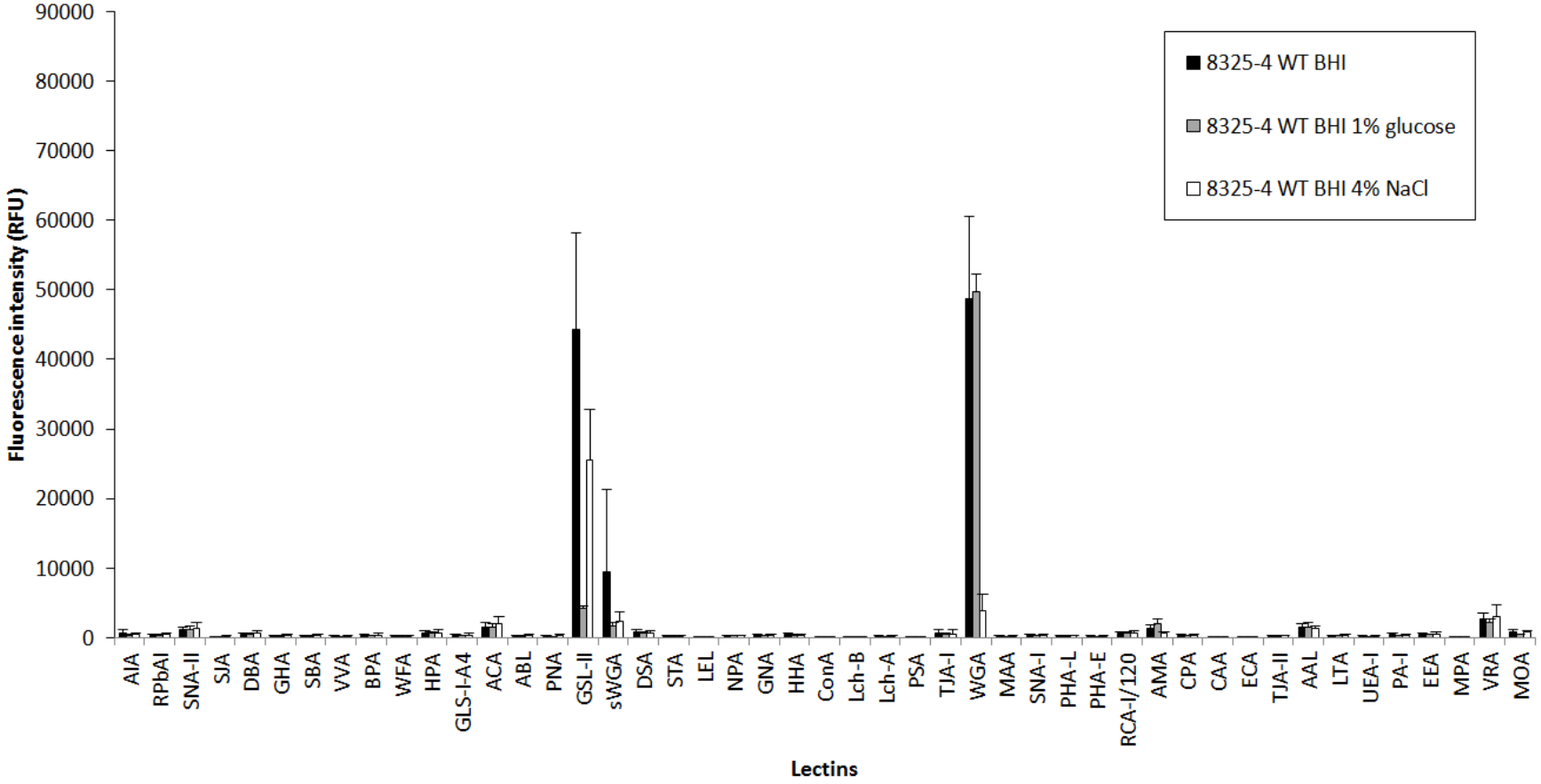
90000
80000
70000
60000
50000
40000
30000
20000
10000
0
Fluorescence intensity (RFU)
8325-4 WT BHI
8325-4 WT BHI 1% glucose
8325-4 WT BHI 4% NaCl
AIA
RPbAI
SNA-II
SJA
DBA
GHA
SBA
VVA
BPA
WFA
HPA
GLS-I-A4
ACA
ABL
PNA
GSL-II
sWGA
DSA
STA
LEL
NPA
GNA
HHA
ConA
Lch-B
Lch-A
PSA
TJA-I
WGA
MAA
SNA-I
PHA-L
PHA-E
RCA-I/120
AMA
CPA
CAA
ECA
TJA-II
AAL
LTA
UEA-I
PA-I
EEA
MPA
VRA
MOA
Lectins

B

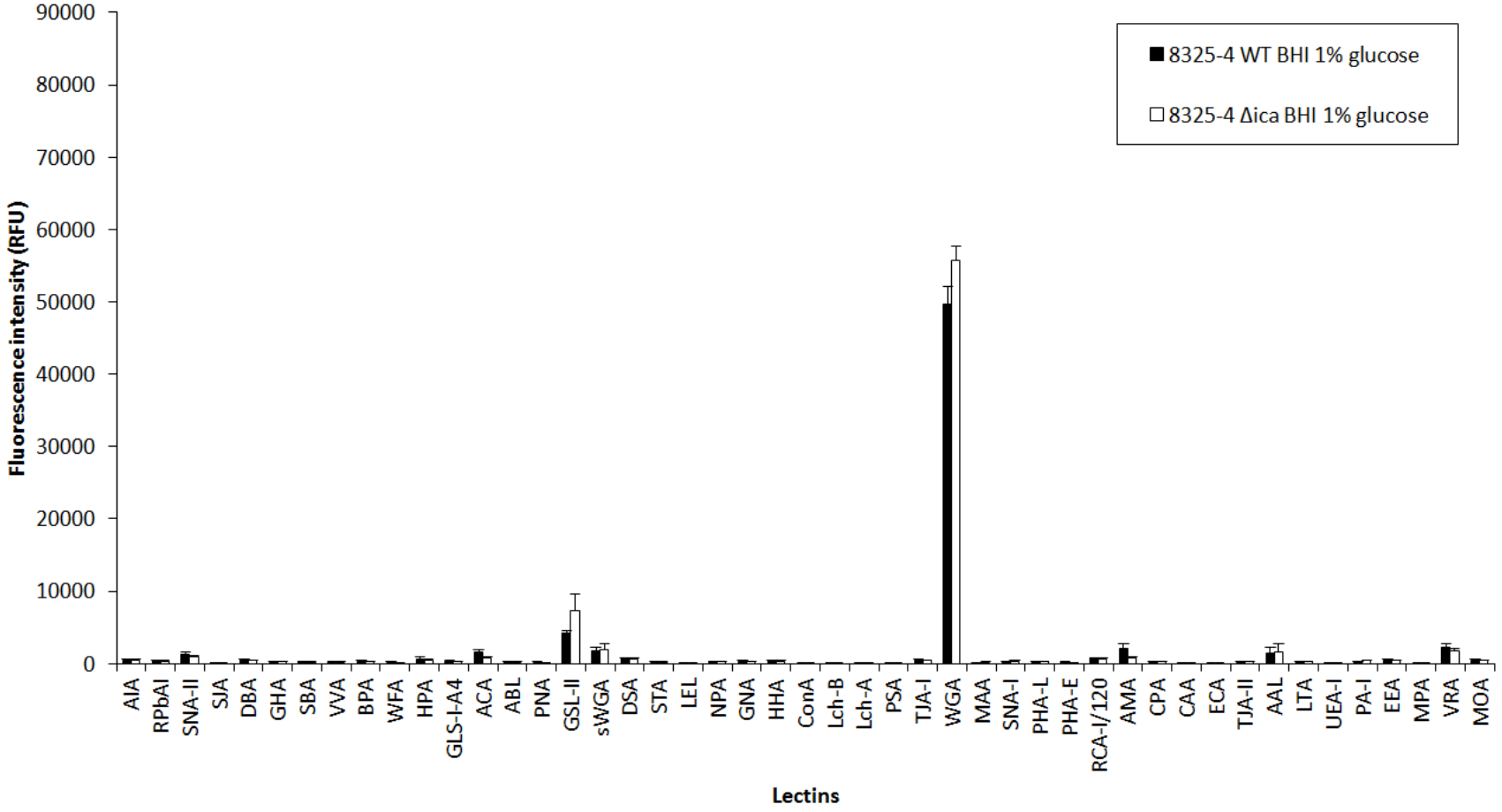
8325-4 WT BHI 1% glucose
8325-4 Δica BHI 1% glucose
Fluorescence intensity (RFU)
90000
80000
70000
60000
50000
40000
30000
20000
10000
0
AIA
RPbAI
SNA-II
SJA
DBA
GHA
SBA
VVA
BPA
WFA
HPA
GLS-I-A4
ACA
ABL
PNA
GSL-II
sWGA
DSA
STA
LEL
NPA
GNA
HHA
ConA
Lch-B
Lch-A
PSA
TJA-I
WGA
MAA
SNA-I
PHA-L
PHA-E
RCA-I/120
AMA
CPA
CAA
ECA
TJA-II
AAL
LTA
UEA-I
PA-I
EEA
MPA
VRA
MOA
Lectins

C

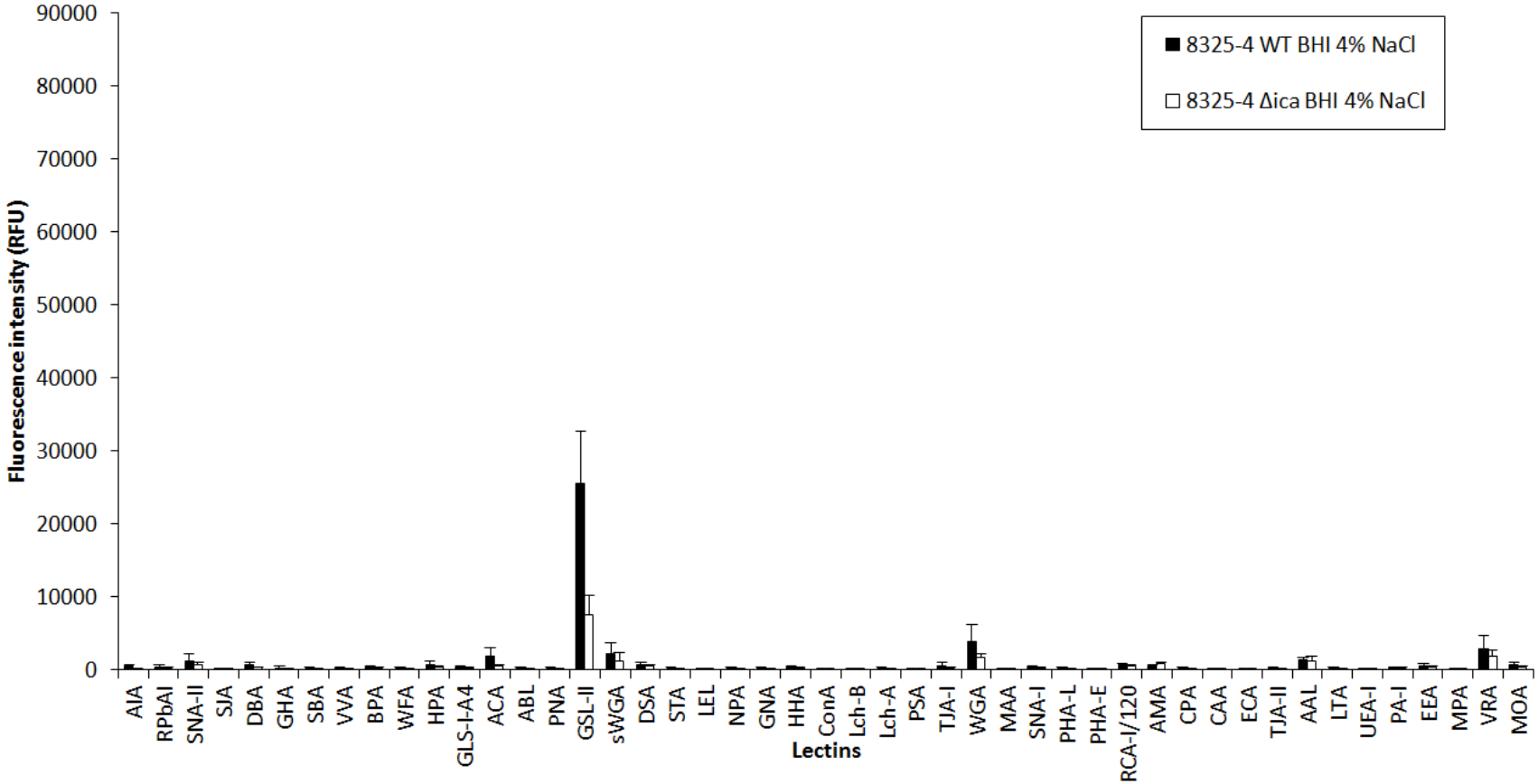
90000
80000
70000
60000
50000
40000
30000
20000
10000
0
Fluorescence intensity (RFU)
8325-4 WT BHI 4% NaCl
8325-4 Δica BHI 4% NaCl
AIA
RPbAI
SNA-II
SJA
DBA
GHA
SBA
VVA
BPA
WFA
HPA
GLS-I-A4
ACA
ABL
PNA
GSL-II
sWGA
DSA
STA
LEL
NPA
GNA
HHA
ConA
Lch-B
Lch-A
PSA
TJA-I
WGA
MAA
SNA-I
PHA-L
PHA-E
RCA-I/120
AMA
CPA
CAA
ECA
TJA-II
AAL
LTA
UEA-I
PA-I
EEA
MPA
VRA
MOA
Lectins

D

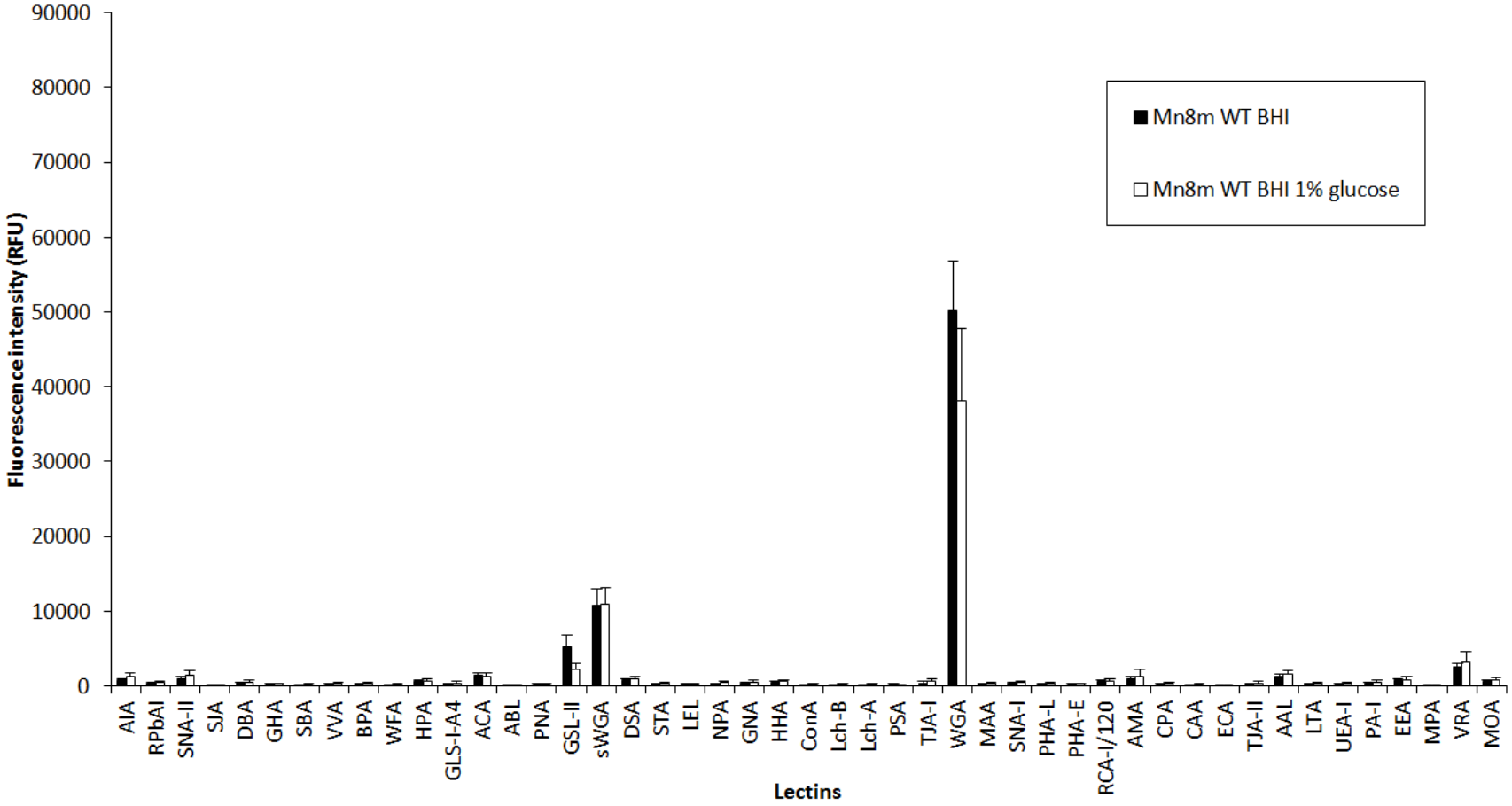
90000
80000
70000
60000
50000
40000
30000
20000
10000
0
Fluorescence intensity (RFU)
Mn8m WT BHI
Mn8m WT BHI 1% glucose
AIA
RPbAI
SNA-II
SJA
DBA
GHA
SBA
VVA
BPA
WFA
HPA
GLS-I-A4
ACA
ABL
PNA
GSL-II
sWGA
DSA
STA
LEL
NPA
GNA
HHA
ConA
Lch-B
Lch-A
PSA
TJA-I
WGA
MAA
SNA-I
PHA-L
PHA-E
RCA-I/120
AMA
CPA
CAA
ECA
TJA-II
AAL
LTA
UEA-I
PA-I
EEA
MPA
VRA
MOA
Lectins

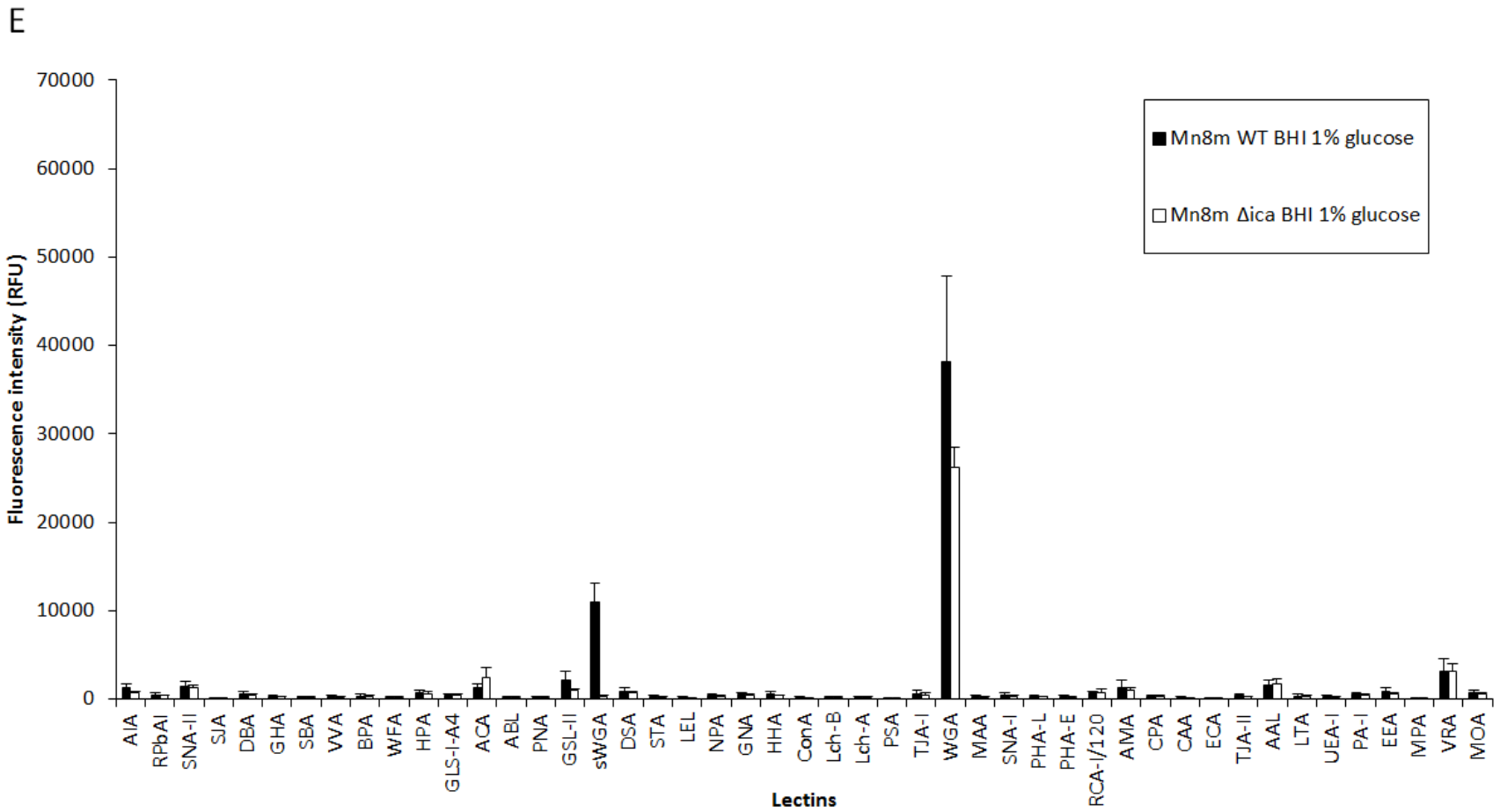


**Fig. 2.5. Lectin microarray profile of *S. aureus* 8325-4 and Mn8m WT and Δ*ica* grown in media with and without glucose or NaCl.** Bar charts represent binding intensities of *S. aureus* 8325-4 WT to lectins printed on the lectin microarray platform after growth in (A) BHI, BHI glucose BHI NaCl, (B) *S. aureus* 8325-4 WT and Δ*ica* to lectins after growth in BHI glucose and (C) BHI NaCl and binding intensities of *S. aureus* Mn8m WT on the lectin microarray platform after growth in (D) BHI and BHI glucose, and (E) *S. aureus* Mn8m WT and Δica on lectin microarrays after growth in BHI glucose. Histograms represent the mean of three experiments with error bars of +/- one standard deviation of the mean.

### 2.3.5. Lectin microarray profile of MRSA strain BH1CC WT and Δ*ica* grown in BHI and BHI glucose

MRSA strain BH1CC WT and Δ*ica* were cultured in BHI and BHI glucose and profiled on the lectin microarray (Fig. 2.6). As overall binding intensities were very low (<1,500 RFU) by comparison to the MSSA strains, a threshold of fluorescence intensity values greater than 500 RFU (background fluorescence) was applied to indicate binding. *S. aureus* BH1CC WT grown in BHI bound with greatest intensity to *Helix pomatia* agglutinin (HPA) which has specificity for α-linked GalNAc residues, GSL-II, *Datura stramonium* agglutinin (DSA), which has specificity for GlcNAc residues, and *Aleuria aurantia* lectin (AAL), which has specificity for α-(1,6)- and α-(1,3)-linked Fuc residues (Fig. 2.6 (A)) (Table 2.2). Moderate binding intensity was observed with the terminal α-linked Gal residues specific lectins *Pseudomonas aeruginosa* lectin (PA-I), *Euonymous europaeus* agglutinin (EEA), *Maclura pomifera* agglutinin (MPA) and *Vigna radiata* agglutinin (VRA). Binding was also evident by *Sophora japonica* agglutinin (SJA) which has specificity towards β-GalNAc and *Sambucus nigra* agglutinin-II (SNA)-II which has specificity for Gal and/or GalNAc. Moderate binding intensities were also observed for the sialic acid specific lectins *Sambucus nigra*-I (SNA-I) and *Amaranthus caudatus* agglutinin (ACA) which have specificity for sialic sacid-α-(2,6)-linked and sialylated/Gal-β-(1,3)-GalNAc carbohydrates, respectively. WGA, which has specificity towards NeuAc and GlcNAc, and sWGA, which has specificity towards GlcNAc, also bound to *S. aureus* BH1CC WT (Fig. 2.6 (A)). These data indicated that GlcNAc-containing molecules were not the main contributor(s) to *S. aureus* BH1CC WT cell surface or biofilm glycosylation. This indicated the likely absence or lack of availability of PNAG on the MRSA cell surface, or the interaction of the lectins only with the large cell surface-bound proteins under both conditions profiled and lack of accessibility for the lectins to the bacterial cell surface.

Growth in BHI glucose slightly increased HPA, sWGA and GSL-II binding to *S. aureus* BH1CC WT, had little effect on DSA, EEA, MPA or VRA binding and slightly reduced AAL and PA-I binding (Fig. 2.6 (A)). These data indicated that there were only minor changes in cell surface glycosylation of *S. aureus* BH1CC cultured in BHI or BHI glucose, but appeared that the addition of glucose promoted the expression of ligands for HPA, sWGA and GSL-II (Gal and GlcNAc) and

decreased the expression of ligands for AAL (Fuc). These minor changes could tend to support the proposal that the lectins could only interact with the large surface-bound glycoproteins rather than the bacterial cell surface itself.

Although PNAG is not expressed by BH1CC WT following growth in BHI glucose (O'Neill *et al.*, 2007), we wanted to elucidate whether the presence of the *ica* operon played a role in *S. aureus* BH1CC surface glycosylation with and without glucose in the growth environment. Generally, lectins such as GSL-II, DSA, AAL, PA-I, MPA and VRA bound greater to *S. aureus* BH1CC WT compared to *S. aureus* Δ*ica* after cells were grown in BHI without supplementation. However, HPA bound greater to BH1CC Δ*ica* compared to the parental strain (Fig. 2.6 (B)). Following growth of BH1CC WT and Δ*ica* in the presence of glucose, HPA and GSL-II were the two primary lectins that bound greater to the wildtype, compared to the *ica* mutant, BH1CC Δ*ica* (Fig. 2.6 (B)). Overall, these results suggested that the *ica* operon plays a role in the surface glycosylation of BH1CC. With the supplementation of glucose, the presence of the *ica* operon promoted attachment to HPA and GSL-II, therefore, the *ica* operon may play a role in the expression of terminal α-linked GalNAc and or GlcNAc on the surface of MRSA, which in turn provided ligands for these two lectins.

A

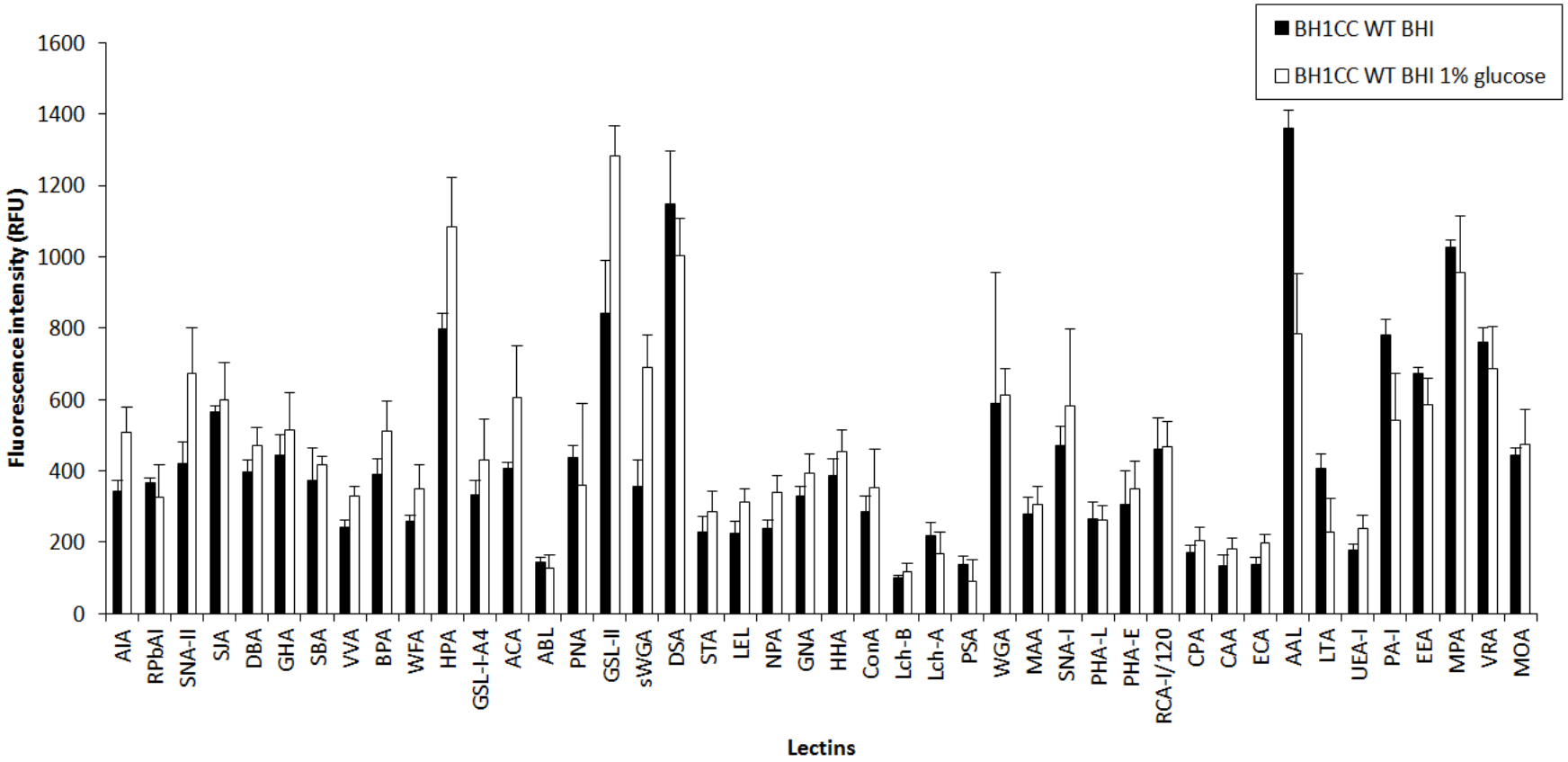
BH1CC WT BHI
BH1CC WT BHI 1% glucose
Fluorescence intensity (RFU)
0
200
400
600
800
1000
1200
1400
1600
AIA
RPbAI
SNA-II
SJA
DBA
GHA
SBA
VVA
BPA
WFA
HPA
GSL-I-A4
ACA
ABL
PNA
GSL-II
sWGA
DSA
STA
LEL
NPA
GNA
HHA
ConA
Lch-B
Lch-A
PSA
WGA
MAA
SNA-I
PHA-L
PHA-E
RCA-I/120
CPA
CAA
ECA
AAL
LTA
UEA-I
PA-I
EEA
MPA
VRA
MOA
Lectins

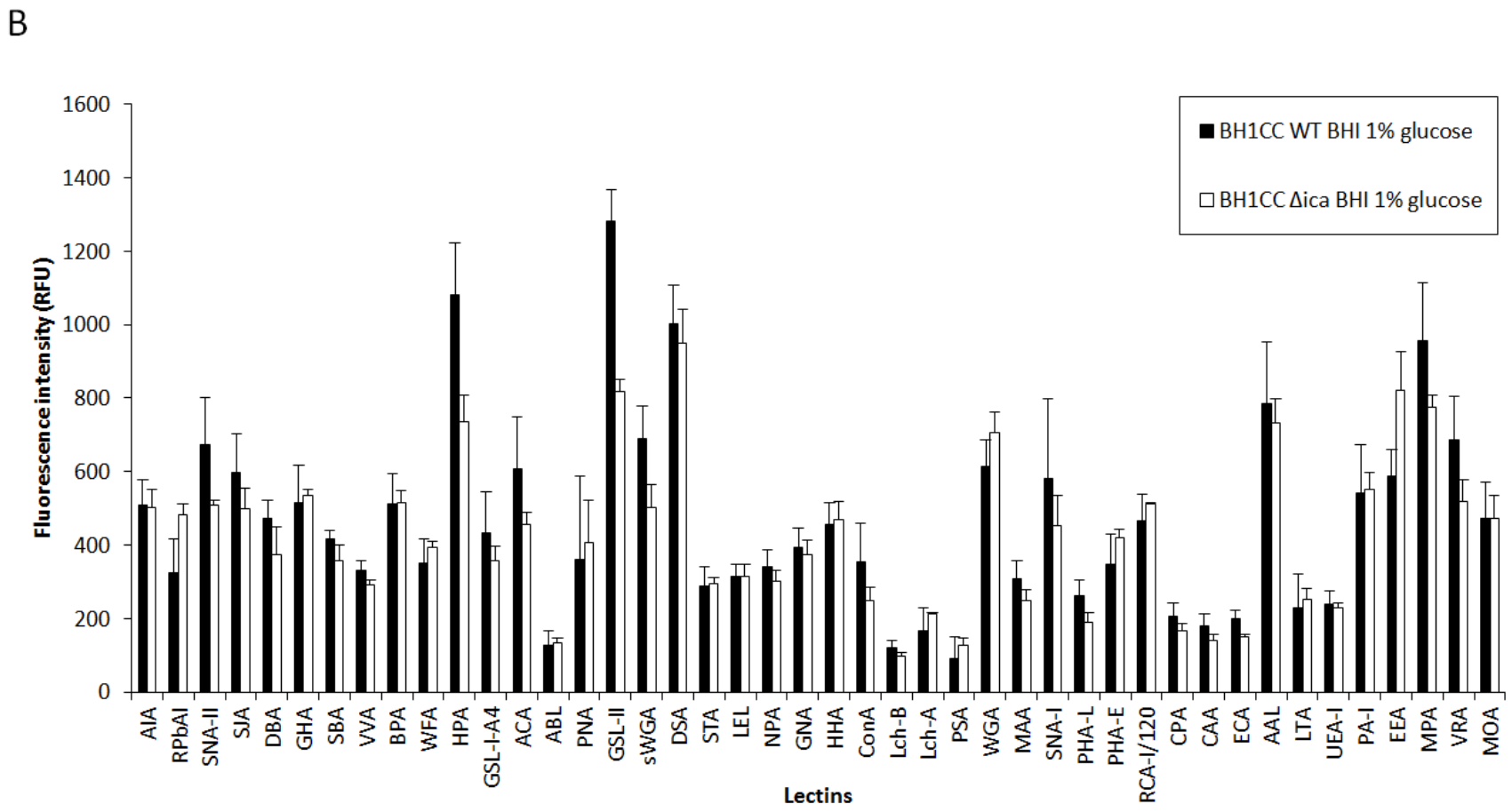


**Fig. 2.6. Bar chart depicting the binding intensities of *S. aureus* BH1CC WT and Δ*ica* to lectins printed on the lectin microarray platform after growth in BHI or BHI glucose.** (A) BH1CC WT and Δ*ica* grown in BHI and (B) BH1CC WT and Δ*ica* grown in BHI glucose and profiled on the lectin microarray. Histogram represents the mean of three experiments with error bars of +/- one standard deviation of the mean.

### 2.3.6. Lectin microarray profile of Gram-negative *A. baumannii* WT and Δ*pga* following growth in BHI and BHI glucose

The PNAG-producing, Gram-negative *A. baumannii* strain WT and Δ*pga* grown in BHI and BHI glucose were profiled on the lectin microarray platform. *A. baumannii* WT grown in BHI had the greatest binding to VRA, *Cicer arietinum* agglutinin (CPA), DBA, *Amaranthus caudatus* agglutinin (ACA), and *Arum maculatum* agglutinin (AMA) (Fig. 2.7). For mammalian glycosylation, DBA has specificity for GalNAc residues, ACA for sialylated Gal-β-(1,3)-GalNAc, AMA for Gal-β-(1,4)-GlcNAc, CPA for complex oligosaccharides and VRA for terminal α-linked Gal residues (Table 2.2). If lectin specificities are similar for bacterial glycosylation as they are for mammalian glycosylation, this could indicate that *A. baumannii* has a cell surface rich in Gal and GalNAc-containing structures.

Bacterial binding to these lectins increased when *A. baumannii* was grown in BHI glucose (Fig. 2.7). In addition, the low binding of WGA to *A. baumannii* grown in BHI alone almost tripled in intensity when cultured in BHI glucose, which indicated the increased expression or availability of cell surface GlcNAc-containing molecules such as PNAG, although this interaction was relatively moderate in binding intensity compared to binding to DBA, CPA and VVA. Interestingly, *A. baumannii* Δ*pga* demonstrated reduced attachment to DBA, ACA, CPA and VRA, but not WGA or any other GlcNAc-specific lectins in comparison to the WT (Fig. 2.7) (Table 2.2). As the *pga* locus is responsible for PNAG production, this result suggested that PNAG associated with *A. baumannii* promoted binding to DBA, ACA, CPA and VRA. Since these lectins mainly have specificity for Gal and GalNAc structures, this may suggest that differences in PNAG presentation or structural modifications alter the molecular conformation enough to facilitate interactions with these lectins. Further, it may potentially indicate the direct or indirect involvement of the *pga* operon in Gal and GalNAc glycosylation in *A. baumannii*.

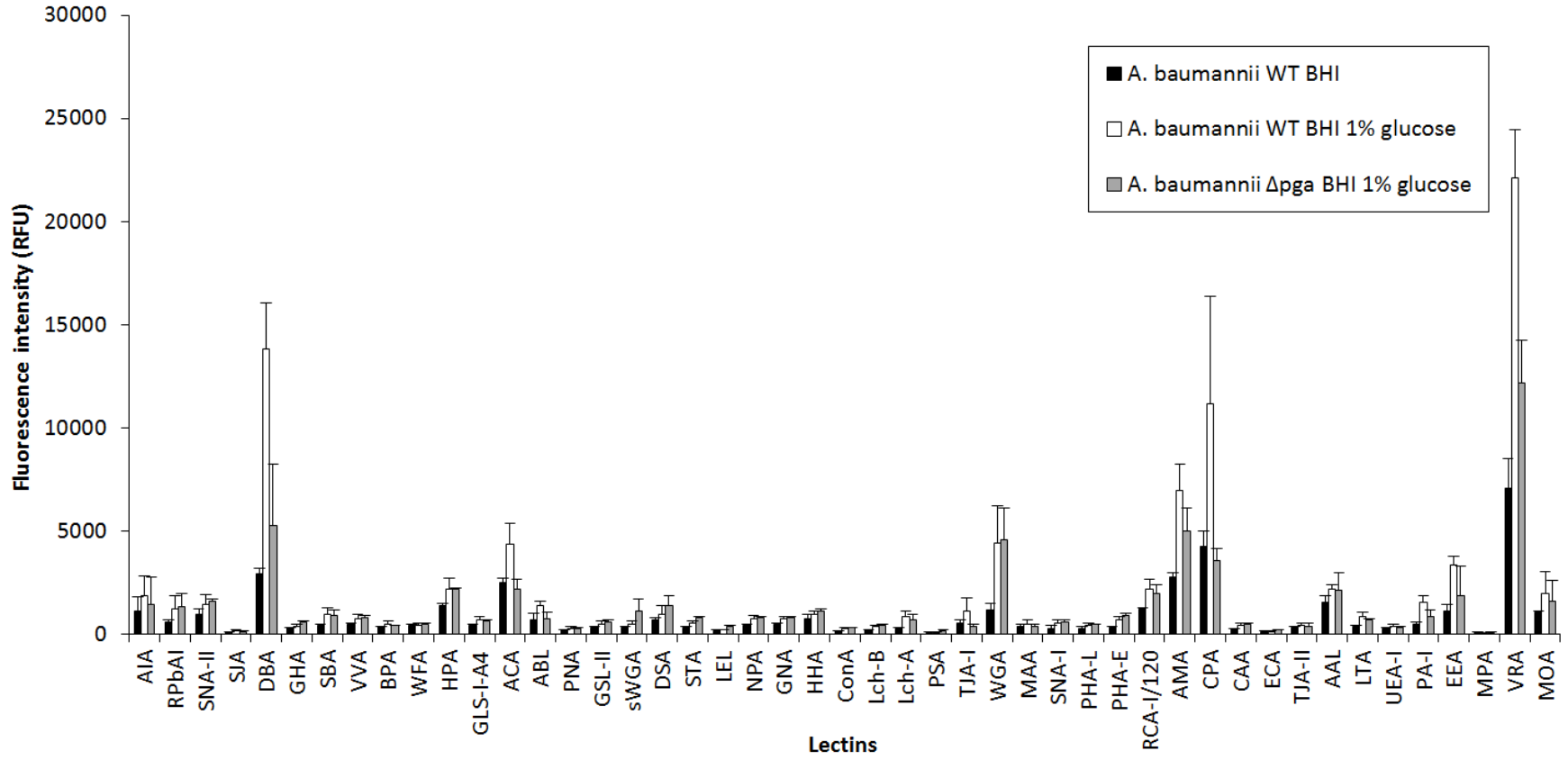


**Fig. 2.7. Lectin microarray profiles of *A. baumannii* WT and Δ*pga* grown in BHI and BHI glucose.** Bar chart represents the mean binding intensities lectins to *A. baumannii* WT and Δ*pga* after growth in BHI, BHI glucose and BHI NaCl. Histogram represents the mean of three experiments with error bars of +/- one standard deviation of the mean.

### 2.3.7. Comparison of MSSA, MRSA and *A. baumannii* lectin binding profiles

Hierarchical clustering of the lectin binding profiles of all bacteria cultured in BHI glucose using scaled normalised data showed that *S. aureus* 8325-4 and Mn8m were the most similar in lectin binding patterns with 84% similarity (Fig. 2.8). *A. baumannii* was distinctly different to *S. aureus* Mn8m and 8325-4 in lectin binding pattern but had 45% similarity to these two *S. aureus* strains. Unsurprisingly, *S. aureus* BH1CC was only 13% similar to the other two *S. aureus* strains and the Gram-negative *A. baumannii* in lectin binding pattern (Fig. 2.8). Overall, results suggest clear differences in surface glycosylation depending on PNAG production, with the two PNAG-producing MSSA strains most similar in cell surface glycosylation, followed by the PNAG-producing *A. baumannii*, and finally the MRSA strain which does not produce PNAG as the least similar to all other three bacteria (Fig. 2.8). However, the actual cell surface glycosylation profile of *S. aureus* 8325-4 and Mn8m may be similar to that of *S. aureus* BH1CC, except these cell surface carbohydrates are masked by extracellular PNAG for the MSSA strains and cell surface-bound proteins for the MRSA strain, and therefore, were not exposed and available for lectin interactions.

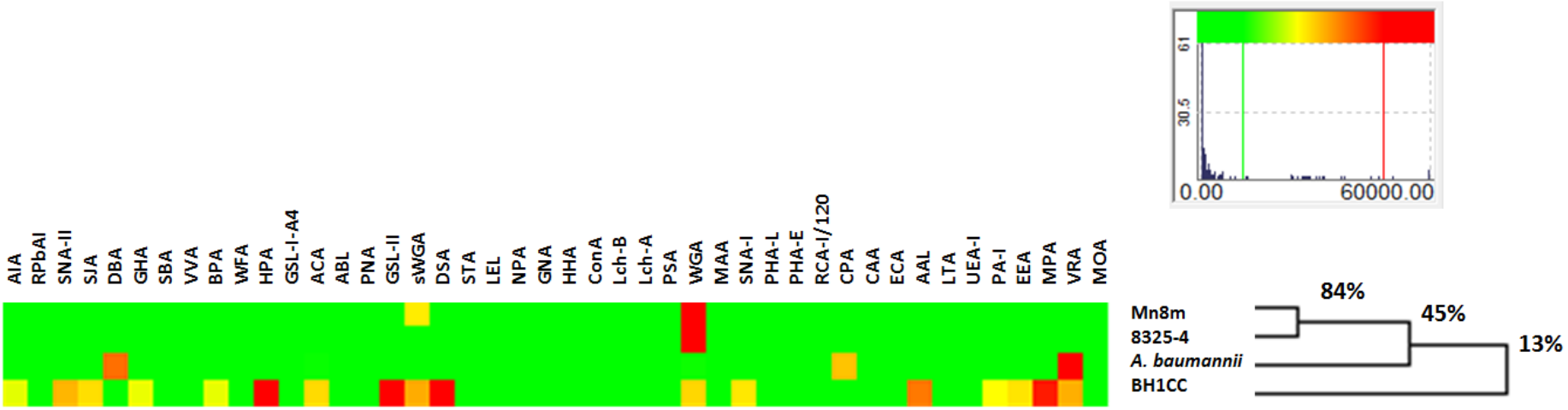


**Fig. 2.8. Unsupervised hierarchical clustering of lectin microarray profiles of *S. aureus* Mn8m WT, 8325-4 WT, BH1CC WT and *A. baumannii* WT grown in BHI supplemented with 1% glucose.** Normalised data was scaled to maximum intensity of 60,000 RFU per bacteria and clustering was carried out using the parameters of complete linkage and Euclidean distance.

### 2.3.8. Neoglycoconjugate microarray profiles of MSSA strains 8325-4 and Mn8m WT and Δ*ica* in different growth media

The MSSA strains 8325-4 and Mn8m WT and their isogenic Δ*ica* mutants were grown in BHI, BHI glucose and BHI NaCl to promote biofilm formation and incubated on the NGC microarray (Fig. 2.9). Overall, the most common NGCs bound by *S. aureus* 8325-4 WT, following growth in BHI, BHI glucose or BHI NaCl, were α-crystallin (α-C), 3'-sialyllactose-ADP-HSA (3SLacHSA), 6'-sialyllactose-ADP-HSA (6SLacHSA), H Type II-APE-BSA (H2BSA), Lacto-*N*-tetraose-APD-HAS (LNTHSA), Man-α-ITC-BSA (XManaBSA) and Glc-β-ITC-BSA (GlcbITCBSA) (Fig. 2.9 (A)) (Table. 2.3). Addition of glucose to the growth media caused the most noticeable effect on *S. aureus* 8325-4 WT-NGC binding, and resulted in increased adherence to α-C, 3SLacHSA, 6SLacHSA, H2BSA, LNTHSA, L-Rhammose (RhaBSA), XManaBSA and GlcbITCBSA. Addition of NaCl to the growth media did not greatly change *S. aureus* 8325-4 WT binding to NGCs compared to growth in BHI alone (Fig. 2.9 (A)). This result showed that *S. aureus* 8325-4 bound to GlcbITCBSA > XManaBSA > 3SLacHSA > 6SLacHSA > H2BSA > LNTHSA > α-C, and binding to these NGCs increased with the addition of glucose to the growth media, while the addition of NaCl did not cause noticeable changes in binding (Fig. 2.9).

8325-4 WT and Δ*ica* were growth in BHI glucose and profiled on the NGC microarray (Fig. 2.9 (B)). Microarray results showed that 8325-4 Δ*ica* did not bind several NGCs as well as the WT. These NGCs were α-C, 3SLacHSA, 6SLacHSA, H2BSA, $Le^b$-BSA (LebBSA), Di-$Le^x$-BSA (DiLexBSA), Di-$Le^x$HSA (DiLexHSA), Difucosyl-para-lacto-*N*-hexaose-ADP-HAS (DFPLNHHSA), RhaBSA, XManaBSA and GlcbITCBSA (Table 2.3). This result suggested that the presence of the *ica* operon and therefore PNAG, promoted binding to these NGCs following growth in the presence of media supplemented with glucose (Fig. 2.9 (B)). In comparison, microarray results showed that 8325-4 Δ*ica* bound several NGCs much better than the WT following growth in media supplemented with NaCl (Fig. 2.9 (C)). These NGCs included; RNaseB (RB) which has high mannose structures, H2BSA, LNTHSA, Fibrinogen (Fibrin), XManaBSA and GlcbITCBSA (Table 2.3). This result indicated that the presence of the *ica* operon, and PNAG, lowers binding to these NGCs, following growth in media supplemented with NaCl (Fig. 2.9 (C)).

*S. aureus* Mn8m WT bound to most NCGs on the microarray platform, but similarly to *S. aureus* 8325-4 WT, bound greatest to α-C, 3SLacHSA, 6SLacHSA, H2BSA, LebBSA, DiLexBSA, DiLexHSA, DFPLNHHSA, LNTHSA, RhaBSA, XManaBSA and GlcbITCBSA (Fig. 2.9 (D)). Addition of glucose to BHI media promoted binding to H2BSA, RhaBSA, XManaBSA and GlcbITCBSA, compared to MN8m WT growth in BHI alone (Fig 2.9 (D)). This result demonstrated that glucose may promote the overexpression of already-present surface receptors and/or expression of new surface receptors to promote binding to these NGCs.

Interestingly, *S. aureus* Mn8m Δ*ica* had different patterns of binding to NGCs compared to *S. aureus* Mn8m WT following growth in BHI glucose (Fig. 2.9 (E)). For example, a lower RFU signal was detected for Mn8m Δ*ica* bound to 3'SialylLacNAc-BSA (3SLNBSA), Blood Group A-BSA (BGABSA), Blood Group B-BSA (BGBBSA), Gala1,3Gal-BSA (Ga3GBSA), Galb1,4GalBSA (Gb4GBSA), Gala1,2GalBSA (Ga2GBSA), Lacto-*N*-fucopentaose I-BSA (LNFPIBSA) and Lacto-*N*-fucopentaose II-BSA (LNFPIIBSA), compared to Mn8m WT grown in BHI glucose (Fig. 2.9 (E)) (Table 2.3). In contrast, a higher amount of Mn8m Δ*ica* bound to GlcbITCBSA compared to *S. aureus* Mn8m WT. This result demonstrated that the presence of the *ica* operon, and PNAG on the cell surface, promoted binding to 3SLNBSA, BGABSA, BGBBSA, Ga3GBSA, Gb4GBSA, Ga2GBSA, LNFPIBSA and LNFPIIBSA, and reduced binding to GlcbITCBSA, following growth of *S. aureus* Mn8m WT and Δ*ica* in BHI glucose (Fig. 2.9 (E)).

Overall, this result showed that MSSA 8325-4 and Mn8m commonly bound with greatest intensity to GlcbITCBSA, XManaBSA, 3SLacHSA, 6SLacHSA, H2BSA, LNTHSA and α-C after growth in BHI, BHI glucose and BHI NaCl. Mutation of the *ica* operon increased or decreased binding to these NGCs depending on the presence of glucose of NaCl. Addition of glucose to BHI resulted in a general overall decrease in binding to NGCs for *S. aureus* 8325-4 and caused a general overall increase in binding to NGCs for *S. aureus* Mn8m. Therefore, this result demonstrated that GlcbITCBSA, XManaBSA, 3SLacHSA, 6SLacHSA, H2BSA, LNTHSA and α-C are common ligands for *S. aureus* 8325-4 and Mn8m, and PNAG played a role in these interactions which was influenced by the presence of glucose or NaCl to the growth media.

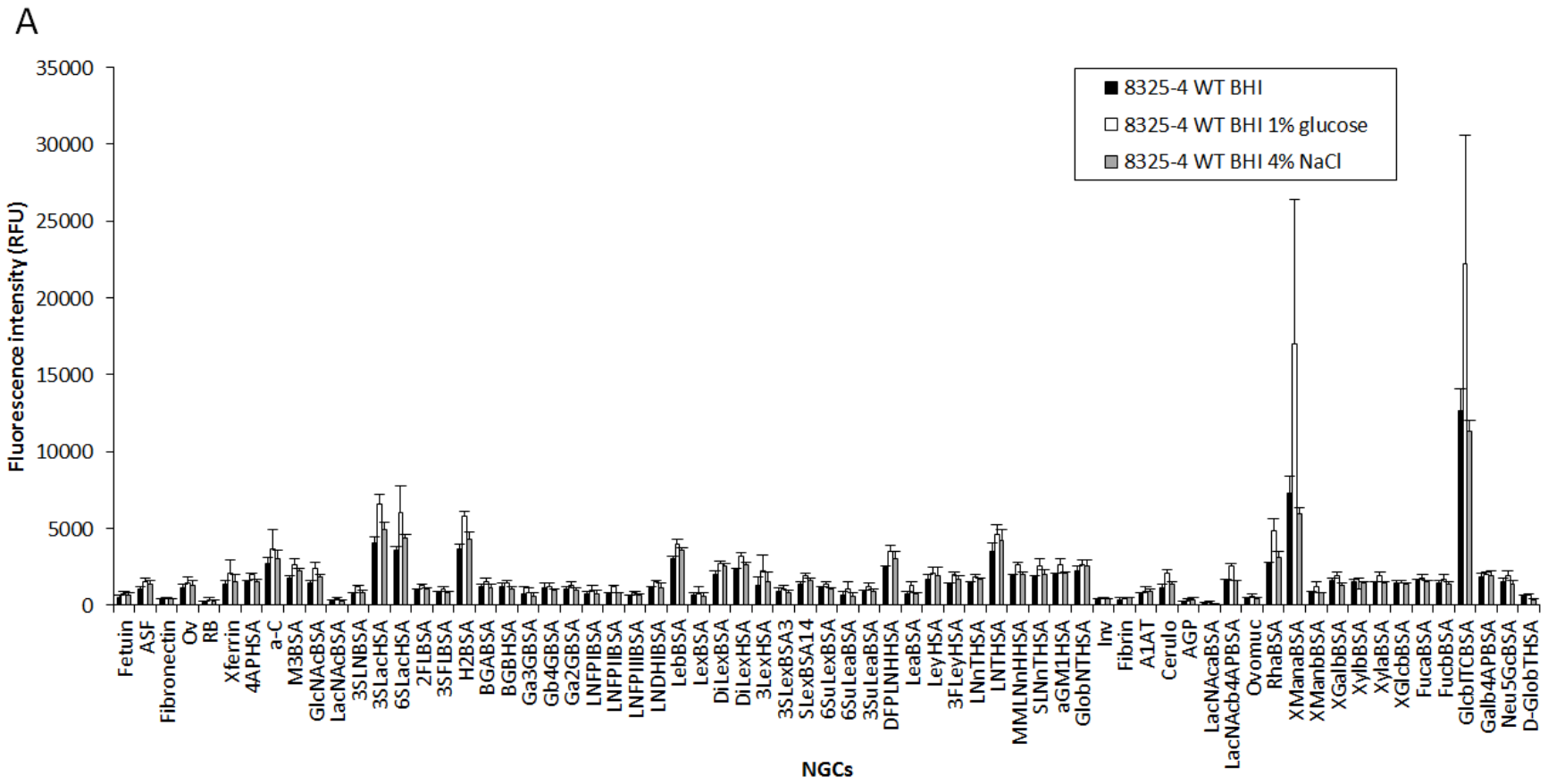
A
Fluorescence intensity (RFU)
35000
30000
25000
20000
15000
10000
5000
0
8325-4 WT BHI
8325-4 WT BHI 1% glucose
8325-4 WT BHI 4% NaCl
Fetuin
ASF
Fibronectin
Ov
RB
Xferrin
4APHSA
a-C
M3BSA
GlcNAcBSA
LacNAcBSA
3SLNBSA
3SLacHSA
6SLacHSA
2FLBSA
3SFLBSA
H2BSA
BGABSA
BGBHSA
Ga3GBSA
Gb4GBSA
Ga2GBSA
LNFPIBSA
LNFPIIBSA
LNFPIIIBSA
LNDHIBSA
LebBSA
LexBSA
DiLexBSA
DiLexHSA
3LexHSA
3SLexBSA3
SLexBSA14
6SuLexBSA
6SuLeaBSA
3SuLeaBSA
DFPLNHHSA
LeaBSA
LeyHSA
3FLeyHSA
LNnTHSA
LNTHSA
MMLNnHHSA
SLNnTHSA
aGM1HSA
GlobNTHSA
Inv
Fibrin
A1AT
Cerulo
AGP
LacNAcaBSA
LacNAcb4APBSA
Ovomuc
RhaBSA
XManaBSA
XManbBSA
XGalbBSA
XylbBSA
XylaBSA
XGlcbBSA
FucaBSA
FucbBSA
GlcbITCBSA
Galb4APBSA
Neu5GcBSA
D-GlobTHSA
NGCs

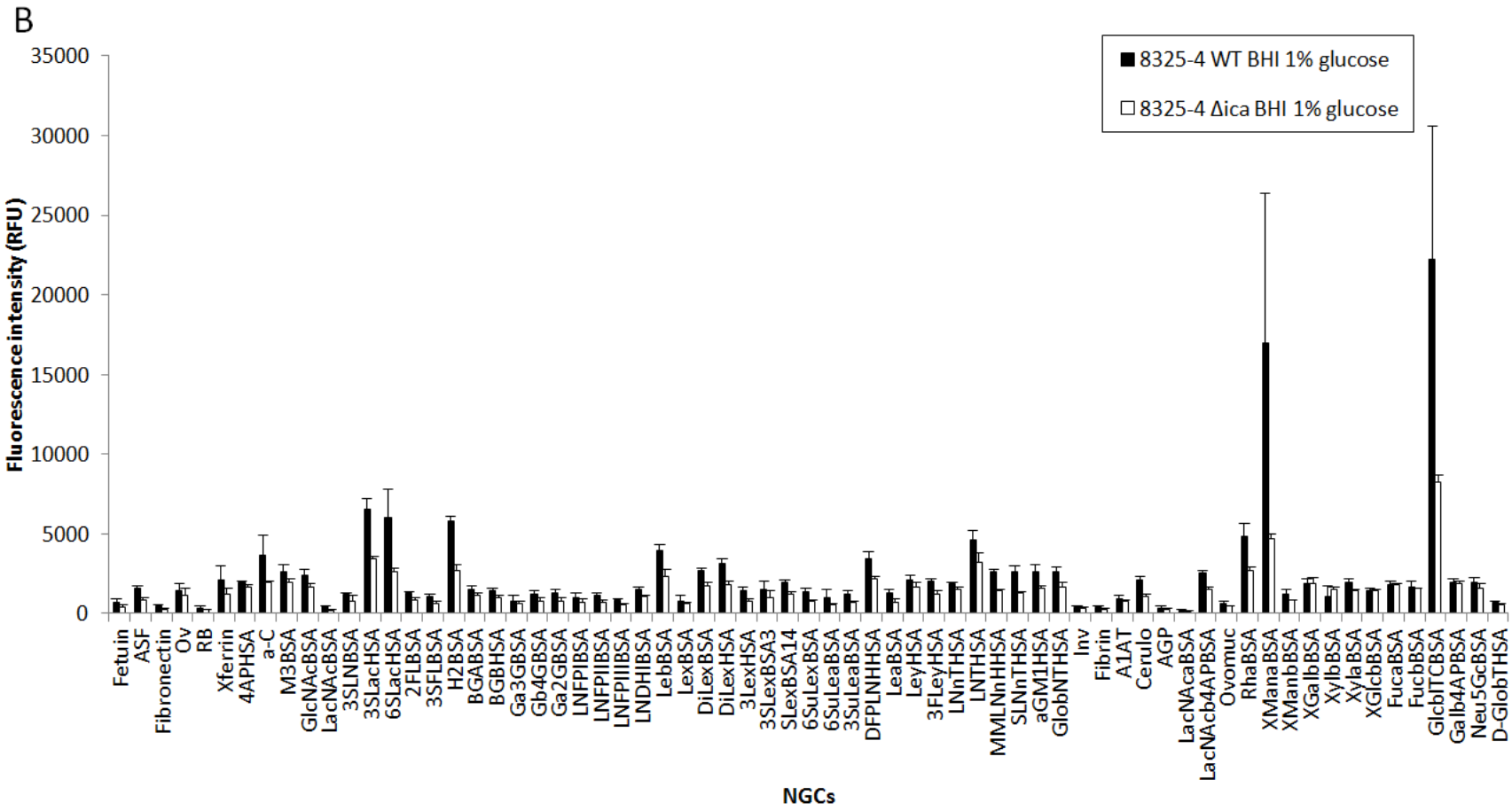
B
8325-4 WT BHI 1% glucose
8325-4 Δica BHI 1% glucose
Fluorescence intensity (RFU)
35000
30000
25000
20000
15000
10000
5000
0
Fetuin
ASF
Fibronectin
Ov
RB
Xferrin
4APHSA
a-C
M3BSA
GlcNAcBSA
LacNAcBSA
3SLNBSA
3SLacHSA
6SLacHSA
2FLBSA
3SFLBSA
H2BSA
BGABSA
BGBHSA
Ga3GBSA
Gb4GBSA
Ga2GBSA
LNFPIBSA
LNFPIIBSA
LNFPIIIBSA
LNDHIBSA
LebBSA
LexBSA
DiLexBSA
DiLexHSA
3LexHSA
3SLexBSA3
SLexBSA14
6SuLexBSA
6SuLeaBSA
3SuLeaBSA
DFPLNHHSA
LeaBSA
LeyHSA
3FLeyHSA
LNnTHSA
LNTHSA
MMLNnHHSA
SLNnTHSA
aGM1HSA
GlobNTHSA
Inv
Fibrin
A1AT
Cerulo
AGP
LacNAcaBSA
LacNAcb4APBSA
Ovomuc
RhaBSA
XManaBSA
XManbBSA
XGalbBSA
XylbBSA
XylaBSA
XGlcbBSA
FucaBSA
FucbBSA
GlcbITCBSA
Galb4APBSA
Neu5GcBSA
D-GlobTHSA
NGCs

C

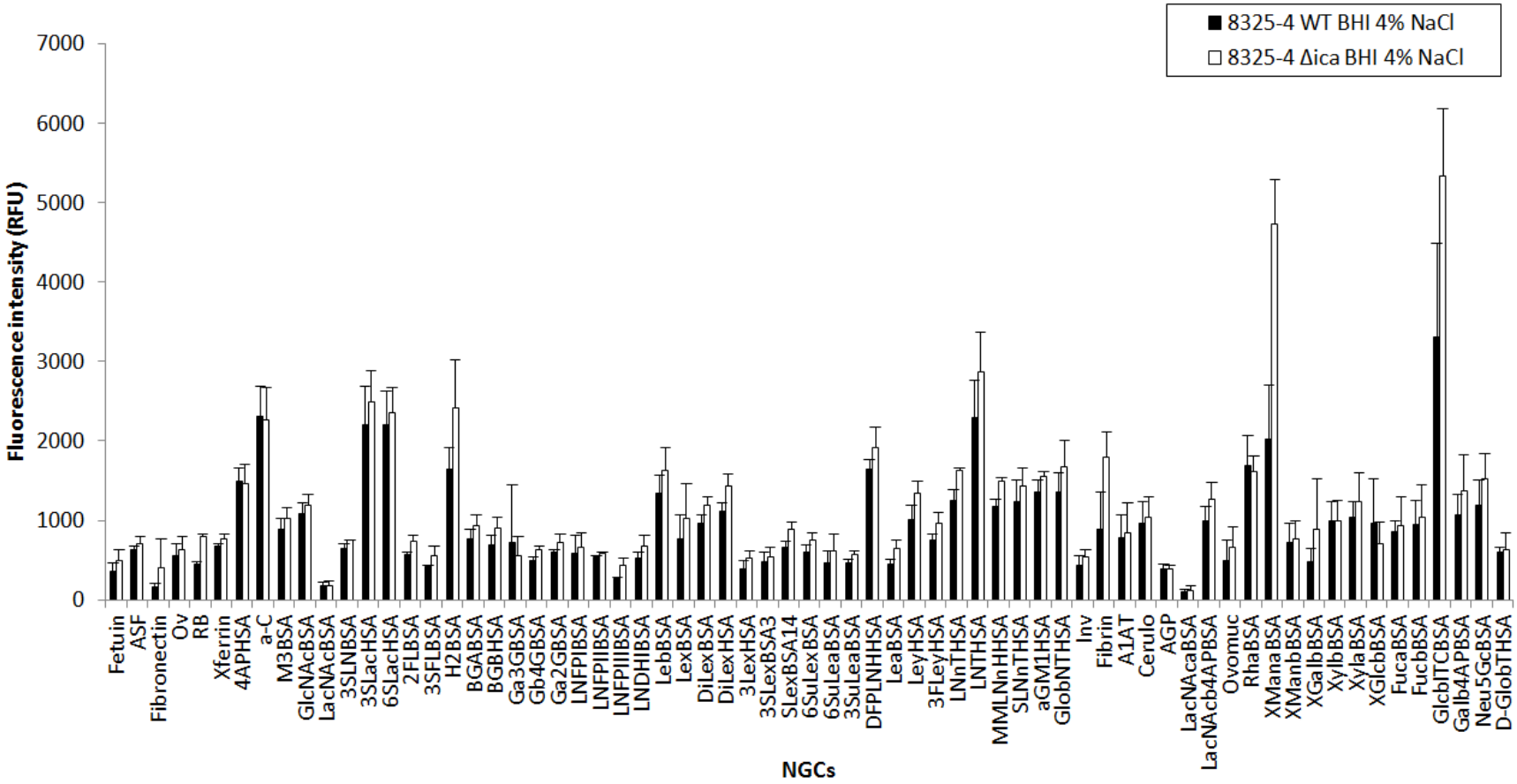
8325-4 WT BHI 4% NaCl
8325-4 Δica BHI 4% NaCl
Fluorescence intensity (RFU)
7000
6000
5000
4000
3000
2000
1000
0
Fetuin
ASF
Fibronectin
Ov
RB
Xferrin
4APHSA
a-C
M3BSA
GlcNAcBSA
LacNAcBSA
3SLNBSA
3SLacHSA
6SLacHSA
2FLBSA
3SFLBSA
H2BSA
BGABSA
BGBHSA
Ga3GBSA
Gb4GBSA
Ga2GBSA
LNFPIBSA
LNFPIIBSA
LNFPIIIBSA
LNDHIIBSA
LebBSA
LexBSA
DiLexBSA
DiLexHSA
3LexHSA
3SLexBSA3
SLexBSA14
6SuLexBSA
6SuLeaBSA
3SuLeaBSA
DFPLNHHSA
LeaBSA
LeyHSA
3FLeyHSA
LNnTHSA
LNTHSA
MMLNnHHSA
SLNnTHSA
aGM1HSA
GlobNTHSA
Inv
Fibrin
A1AT
Cerulo
AGP
LacNAcaBSA
LacNAcb4APBSA
Ovomuc
RhaBSA
XManaBSA
XManbBSA
XGalbBSA
XylbBSA
XylaBSA
XGlcbBSA
FucaBSA
FucbBSA
GlcbITCBSA
Galb4APBSA
Neu5GcBSA
D-GlobTHSA
NGCs

D

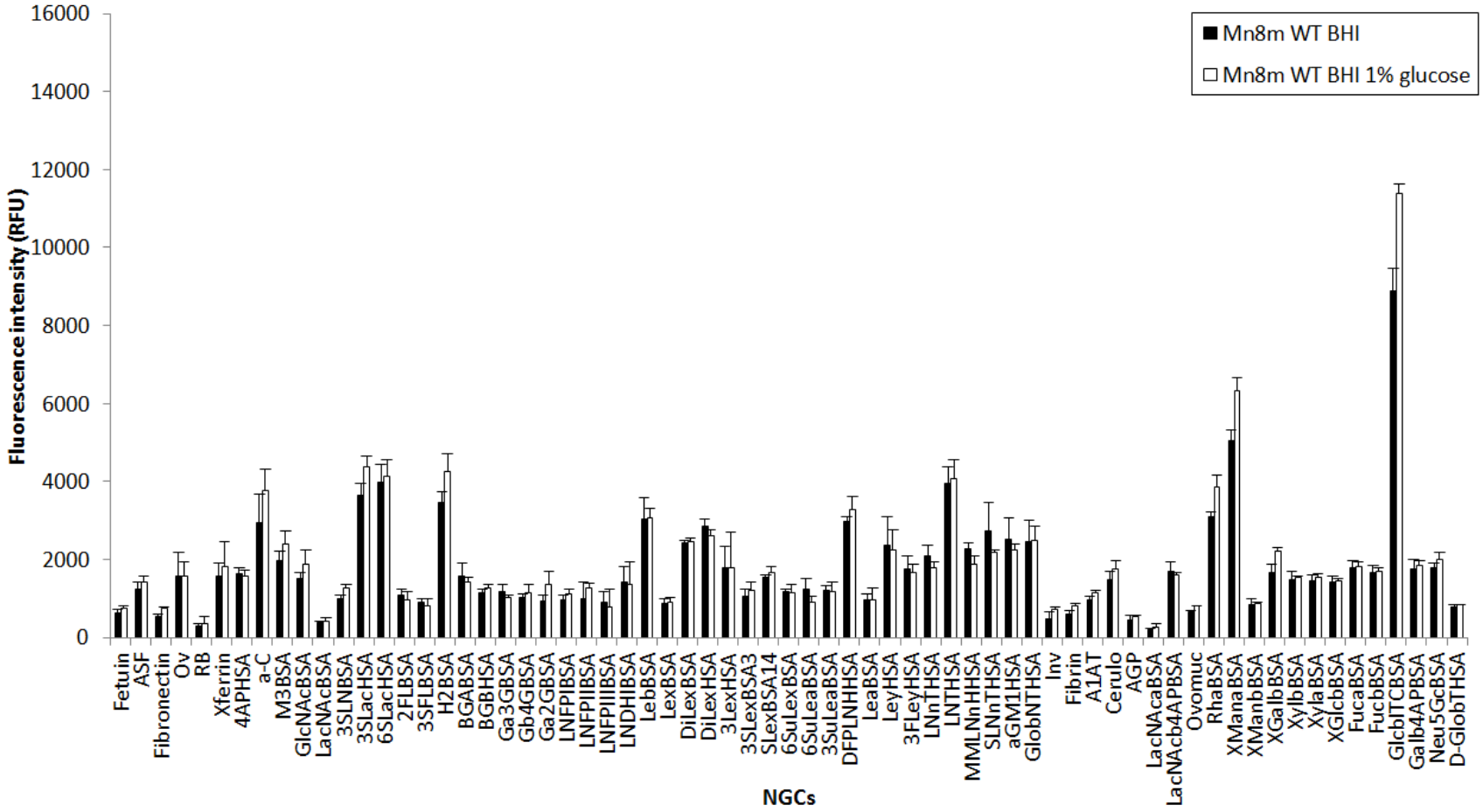
Mn8m WT BHI
Mn8m WT BHI 1% glucose
Fluorescence intensity (RFU)
16000
14000
12000
10000
8000
6000
4000
2000
0
Fetuin
ASF
Fibronectin
Ov
RB
Xferrin
4APHSA
a-C
M3BSA
GlcNAcBSA
LacNAcBSA
3SLNBSA
3SLacHSA
6SLacHSA
2FLBSA
3SFLBSA
H2BSA
BGABSA
BGBHSA
Ga3GBSA
Gb4GBSA
Ga2GBSA
LNFPIBSA
LNFPIIBSA
LNFPIIIBSA
LNDHIBSA
LebBSA
LexBSA
DiLexBSA
DiLexHSA
3LexHSA
3SLexBSA3
SLexBSA14
6SuLexBSA
6SuLeaBSA
3SuLeaBSA
DFPLNHHSA
LeaBSA
LeyHSA
3FLeyHSA
LNnTHSA
LNTHSA
MMLNnHHSA
SLNnTHSA
aGM1HSA
GlobNTHSA
Inv
Fibrin
A1AT
Cerulo
AGP
LacNAcaBSA
LacNAcb4APBSA
Ovomuc
RhaBSA
XManaBSA
XManbBSA
XGalbBSA
XylbBSA
XylaBSA
XGlcbBSA
FucaBSA
FucbBSA
GlcbITCBSA
Galb4APBSA
Neu5GcBSA
D-GlobTHSA
NGCs

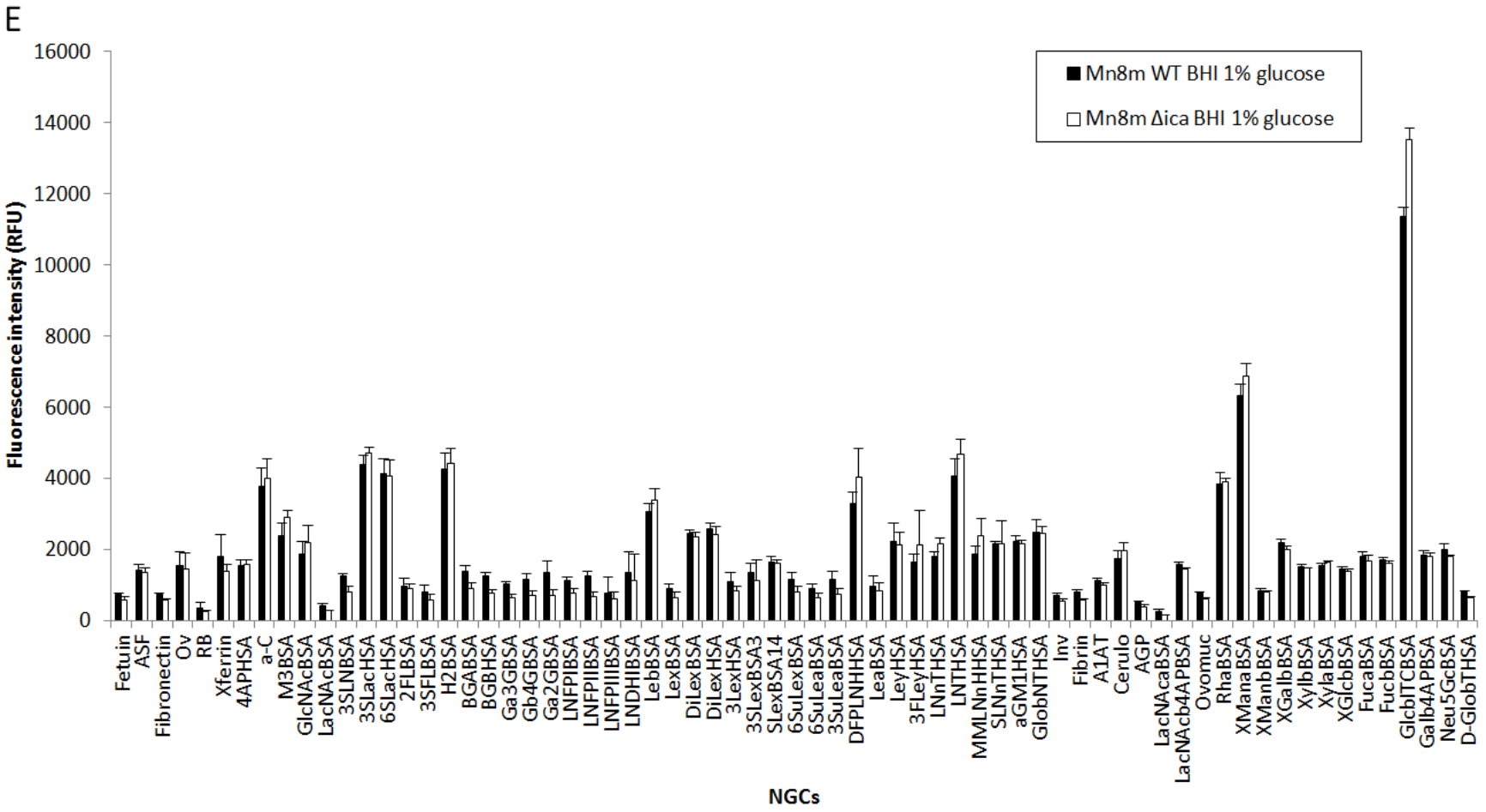


**Fig. 2.9. Neoglycoconjugate microarray profiles of MSSA 8325-4 and Mn8m WT and Δ*ica* grown in different growth media.** Bar charts represent NGC binding profiles of *S. aureus* (A) 8325-4 WT grown in BHI, BHI glucose and BHI NaCl (B) 8325-4 WT Δica grown in BHI glucose (C) and BHI NaCl, (D) Mn8m WT grown in BHI and BHI glucose and (E) Mn8m WT and Δ*ica* grown in BH1CC WT and Δ*ica* grown in BHI glucose. Histograms represent the mean of three experiments with error bars of +/- one standard deviation of the mean.

### 2.3.9. Neoglycoconjugate microarray profile of MRSA strain BH1CC WT and Δ*ica* grown in BHI, BHI glucose and BHI NaCl

For comparison, the MRSA strain, BH1CC WT and Δ*ica*, was incubated on the NGC microarray platform after growth in BHI, BHI glucose and BHI NaCl (Fig. 2.10). Similar to lectin microarray results, overall binding intensities were very low by comparison to the MSSA strains (<1,500 RFU), therefore, a threshold of fluorescence intensity values greater than 500 RFU (background fluorescence) was applied to indicate binding. *S. aureus* BH1CC WT grown in BHI bound to similar NGCs as *S. aureus* 8325-4 WT and Mn8m WT, namely; α-C, 3SLacHSA, 6SLacHSA, H2BSA, LebBSA, DiLexBSA, DiLexHSA, DFPLNHHSA, LNTHSA, RhaBSA, XManaBSA and GlcbITCBSA, but also bound ovalbumin (Ov), 4AP-HAS (4APHSA), Manα1,3(Manα1,6)Man-BSA (M3BSA), GlcNAc-BSA (GlcNAcBSA), 3SLNBSA, Di-Lex-APE-BSA (DiLexBSA), Di-Lewis x-APE-HAS (Di-Lewis x-APE-HAS), Lewis y-tetrasaccharide-APE-HAS (LeyHSA), Tri-fucosyl-Leyheptasaccharide-APE-HAS (3FLecyHSA), Lacto-*N*-neotetraose-APD-HAS (LNnTHSA), monofucosyl, monosialyllacto-*N*-neohexaose-APD-HAS (MMLNnHHSA), Sialyl-LNnT-penta-APD-HAS (SLNnTHSA), asialo-GM1-tetrasaccharide-APD-HAS (aGM1HSA), Globo-*N*-tetraose-APD-HAS (GlobNTHSA), LacNAc-b-4AP-BSA (LacNAcb4APBSA), ovomucoid (Ovomuc), RhaBSA, Man-b-4AP-BSA (XManbBSA), Xyl-b-4AP-BSA (XylbBSA), Xyl-a-4AP-BSA (XylaBSA), Glc-b-4AP-BSA (XGlcbBSA), Fuc-a-4AP-BSA (FucaBSA), Fuc-b-4AP-BSA (FucbBSA), Gal-b-4AP-BSA (Galb4APBSA), Neu5Gc-BSA (Neu5GcBSA) and Globotriose-HAS (D-GlobTHSA). Generally, addition of glucose in to the growth media increased binding of BH1CC WT to these NGCs compared to BH1CC WT grown in media that was not supplemented. Addition of NaCl to the growth media caused the greatest effect on BH1CC WT binding to NGCs, and increased binding to these NGCs compared to BH1CC WT grown in BHI or BHI glucose (Fig. 2.10 (A)).

To understand whether the presence of *ica* operon in *S. aureus* BH1CC altered bacterial binding to NGCs, *S. aureus* BH1CC WT and Δ*ica* were grown in BHI glucose and BHI NaCl and incubated on the NGC microarray (Fig. 2.10 (B), (C)). Following growth in BHI glucose, *S. aureus* BH1CC Δ*ica* demonstrated no change, or slightly increased binding, to almost all NGCs compared to BH1CC WT (Fig.

2.10 (B)). As these changes in NGC binding were minute, it was likely that the *ica* operon did not contribute to NGC binding following growth in BHI glucose (Fig. 2.10 (B)). In contrast, following growth in BHI NaCl, *S. aureus* BH1CC Δ*ica* demonstrated decreased binding to almost all NGCs compared to BH1CC WT (Fig. 2.10 (B)). In particular, there was a big reduction in binding to α-C, M3BSA, 3SLacHSA, 6SLacHSA, H2BSA, LebBSA, DiLexBSA, DiLexHSA, 3'Sialyl Lewis x-BSA (SLexBSA14), DFPLNHHSA, LeyHSA, LNTHSA, SLNnTHSA, aGM1HSA , GlobNTHSA, Fibrinogen (Fibrin), ceruloplasmin (Cerulo), RhaBSA, XManaBSA, XylbBSA, GlcbITCBSA and Neu5GcBSA, compared to *S. aureus* BH1CC WT (Fig. 2.10 (C)). This broad reduced binding to NGCs due to mutation of the *ica* operon in *S. aureus* BH1CC, may suggest a direct or indirect role for the *ica* operon, following growth in the presence of NaCl, in helping *S. aureus* BH1CC bind to these carbohydrates.

### 2.3.10. Neoglycoconjugate microarray profile of Gram-negative *A. baumannii* S1 WT and Δ*pga* following growth in BHI and BHI glucose

Next, we screened for carbohydrate ligands for *A. baumannii* WT grown in BHI glucose (Fig. 2.11). Similar to *S. aureus* 8325-4, Mn8m and BH1CC, *A. baumannii* WT bound to 3SLacBSA, 6SLacBSA, H2BSA, DFPLNHHSA, LNTHSA, XManaBSA and GlcbITCBSA. Furthermore, *A. baumannii* WT bound to DiLexBSA, DiLexHSA, LeyHSA, XylaBSA and XGalbBSA (Fig. 2.11). Mutation of the *pga* operon caused increased binding to GlcNAc-BSA, BGABSA and Ovomuc, and decreased binding to XManaBSA, XylaBSA, XGalbBSA and GlcbITCBSA compared to the WT strain, *A. baumannii* WT. Overall, addition of glucose in to the growth media increased *A. baumannii* binding to Ov, transferrin (Xferrin), α-C, 3SLacBSA, 6SLacBSA, 2'Fucosyllactose-BSA (2FLBSA), 3'Sialyl-3-fucosyllactose-BSA (3SFLBSA), H2BSA, BGABSA, BGBHSA, Ga3GBSA, Gb4GBSA, Ga2GBSA, LNFPIBSA, LNFPIIBSA, DiLexBSA, DiLexHSA, 3'Sialyl Lewis x-BSA (3SLexBSA3), SLexBSA14, 6-Sulfo Lewis x-BSA (6SuLexBSA), LeyHSA, LNnTHSA, LNTHSA, MMLNnHHSA, SLNnTHSA, aGM1HSA, GlobNTHSA, α-1 Antitrypsin (A1AT), Cerulo, Ovomuc, XManaBSA, XGalbBSA, XylaBSA, GlcbITCBSA and Neu5GcBSA (Fig. 2.11). *A. baumannii* Δ*pga* grown in BHI glucose increased binding to GlcNAc-BSA, BGABSA and Ovomuc, and decreased binding to XManaBSA, XGalbBSA and GlcbITCBSA compared to *A.*

*baumannii* WT grown in BHI glucose. This result showed that addition of glucose in to the growth media promoted *A. baumannii* binding to various NGCs, and the *pga* operon, and therefore PNAG, was involved in reducing binding to GlcNAc-BSA, BGABSA and Ovomuc, and increasing binding to XManaBSA, XGalbBSA and GlcbITCBSA. Overall, this result suggested a role for PNAG in masking *A. baumannii* binding to GlcNAc-BSA, BGABSA and Ovomuc and promoting binding to XManaBSA, XGalbBSA and GlcbITCBSA (Fig. 2.11).

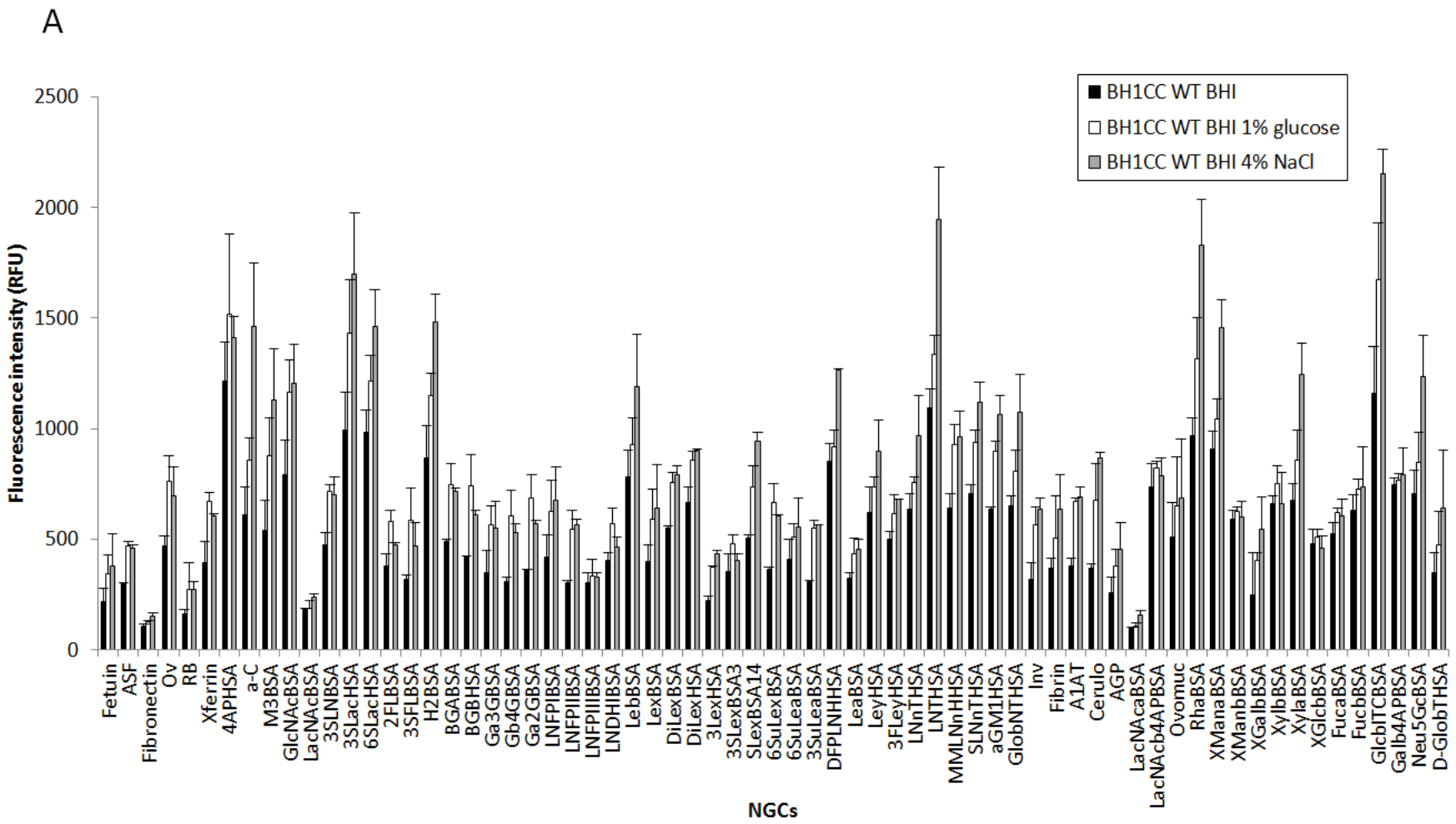
A
BH1CC WT BHI
BH1CC WT BHI 1% glucose
BH1CC WT BHI 4% NaCl
Fluorescence intensity (RFU)
2500
2000
1500
1000
500
0
Fetuin
ASF
Fibronectin
Ov
RB
Xferrin
4APHSA
a-C
M3BSA
GlcNAcBSA
LacNAcBSA
3SLNBSA
3SLacHSA
6SLacHSA
2FLBSA
3SFLBSA
H2BSA
BGABSA
BGBHSA
Ga3GBSA
Gb4GBSA
Ga2GBSA
LNFPIBSA
LNFPIIBSA
LNFPIIIBSA
LNDHIBSA
LebBSA
LexBSA
DiLexBSA
DiLexHSA
3LexHSA
3SLexBSA3
SLexBSA14
6SuLexBSA
6SuLeaBSA
3SuLeaBSA
DFPLNHHSA
LeaBSA
LeyHSA
3FLeyHSA
LNnTHSA
LNTHSA
MMLNnHHSA
SLNnTHSA
aGM1HSA
GlobNTHSA
Inv
Fibrin
A1AT
Cerulo
AGP
LacNAcaBSA
LacNAcb4APBSA
Ovomuc
RhaBSA
XManaBSA
XManbBSA
XGalbBSA
XylbBSA
XylaBSA
XGlcbBSA
FucaBSA
FucbBSA
GlcbITCBSA
Galb4APBSA
Neu5GcBSA
D-GlobTHSA
NGCs

B

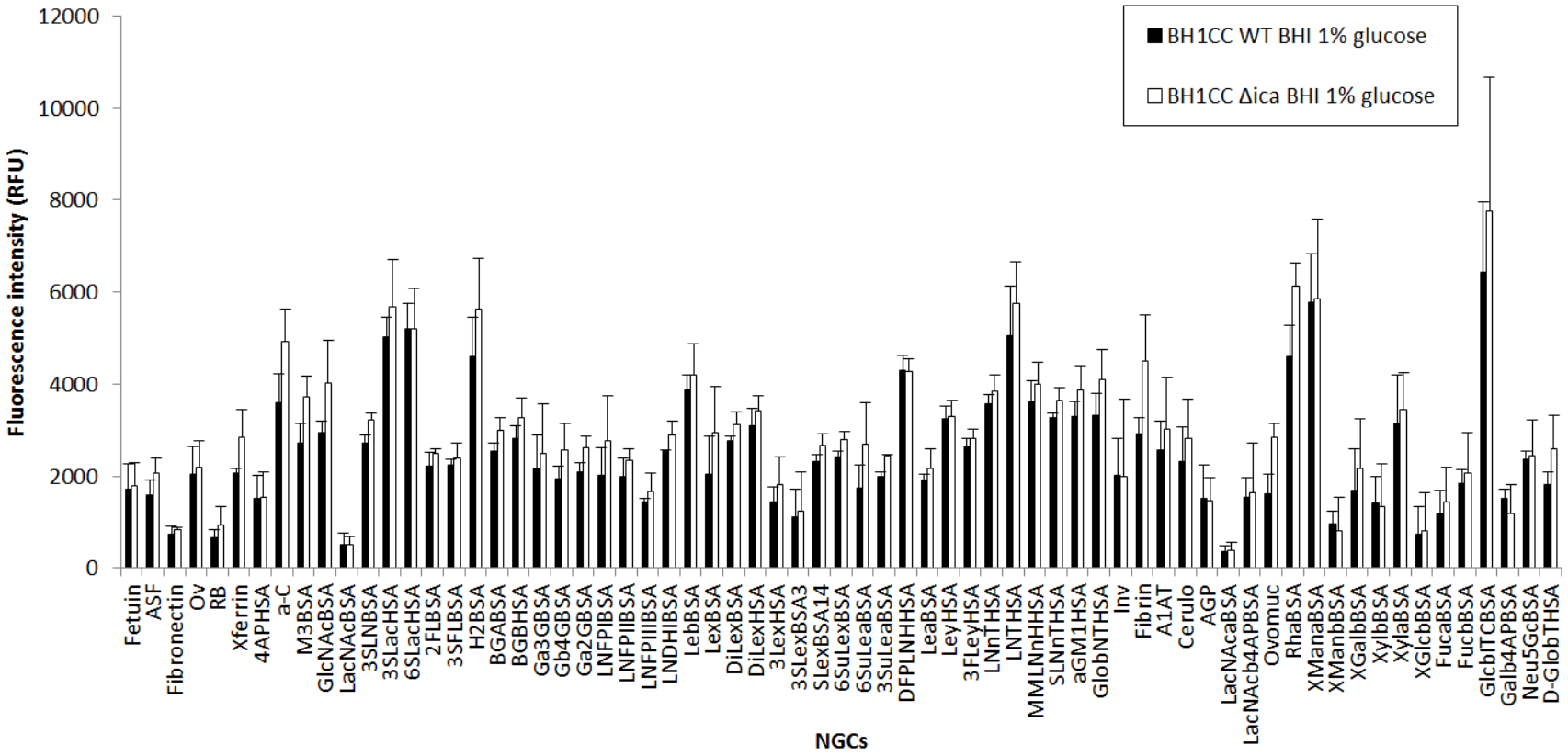
BH1CC WT BHI 1% glucose
BH1CC Δica BHI 1% glucose
Fluorescence intensity (RFU)
12000
10000
8000
6000
4000
2000
0
NGCs
Fetuin
ASF
Fibronectin
Ov
RB
Xferrin
4APHSA
a-C
M3BSA
GlcNAcBSA
LacNAcBSA
3SLNBSA
3SLacHSA
6SLacHSA
2FLBSA
3SFLBSA
H2BSA
BGABSA
BGBHSA
Ga3GBSA
Gb4GBSA
Ga2GBSA
LNFPIBSA
LNFPIIBSA
LNFPIIIBSA
LNDHIBSA
LebBSA
LexBSA
DiLexBSA
DiLexHSA
3LexHSA
3SLexBSA3
SLexBSA14
6SuLexBSA
6SuLeaBSA
3SuLeaBSA
DFPLNHHSA
LeaBSA
LeyHSA
3FLeyHSA
LNnTHSA
LNTHSA
MMLNnHHSA
SLNnTHSA
aGM1HSA
GlobNTHSA
Inv
Fibrin
A1AT
Cerulo
AGP
LacNAcaBSA
LacNAcb4APBSA
Ovomuc
RhaBSA
XManaBSA
XManbBSA
XGalbBSA
XylbBSA
XylaBSA
XGlcbBSA
FucaBSA
FucbBSA
GlcbITCBSA
Galb4APBSA
Neu5GcBSA
D-GlobTHSA

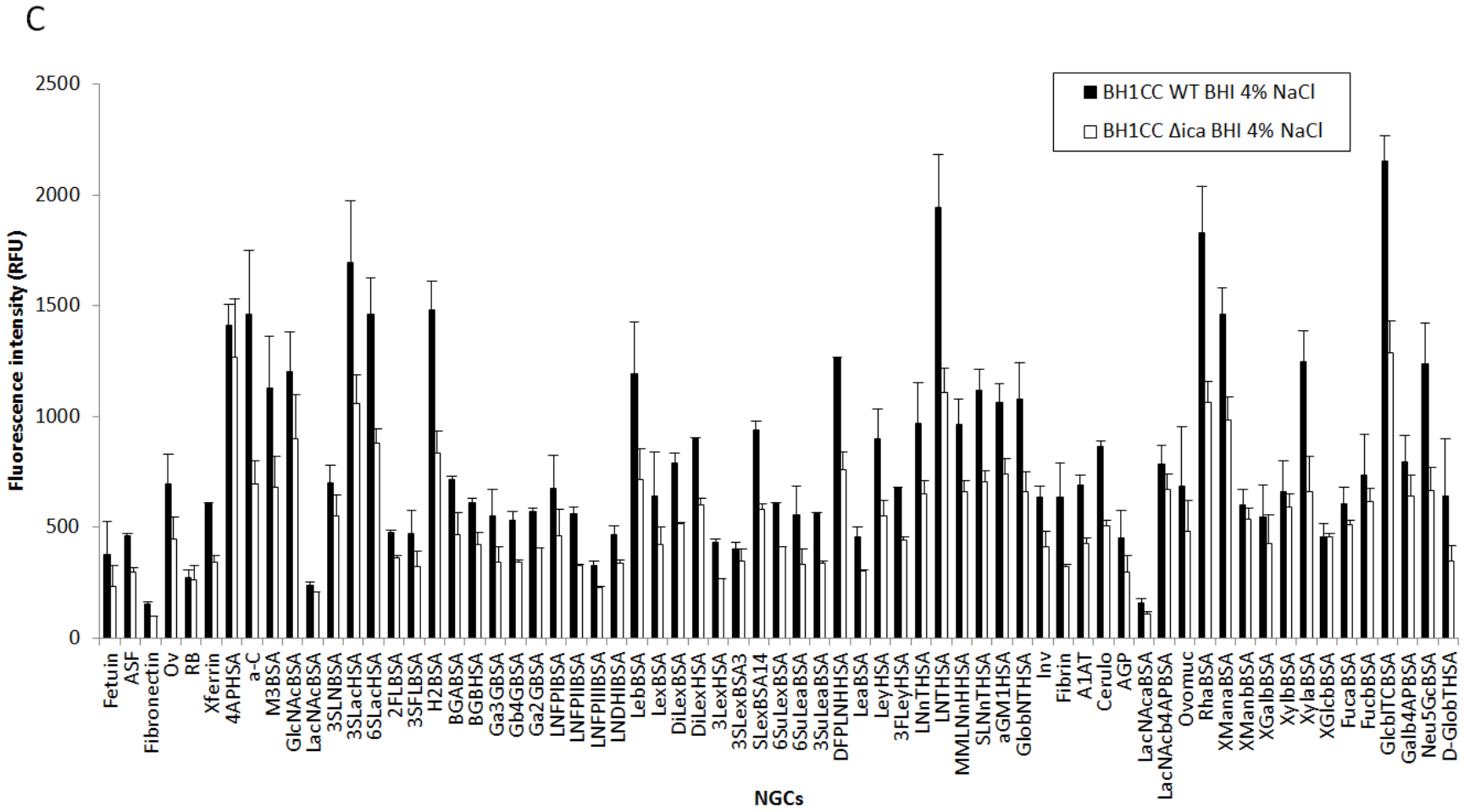


**Fig. 2.10. Neoglycoconjugate microarray profiles of MRSA BH1CC WT and Δ*ica* grown in different growth media.** Bar charts represent NGC binding profiles of *S. aureus* (A) BH1CC grown in BHI, BHI glucose and BHI NaCl (B) BH1CC WT Δ*ica* grown in BHI glucose (C) and BHI NaCl. Bar chart represents three experiments with error bars of +/- one standard deviation of the mean of the three experiments.

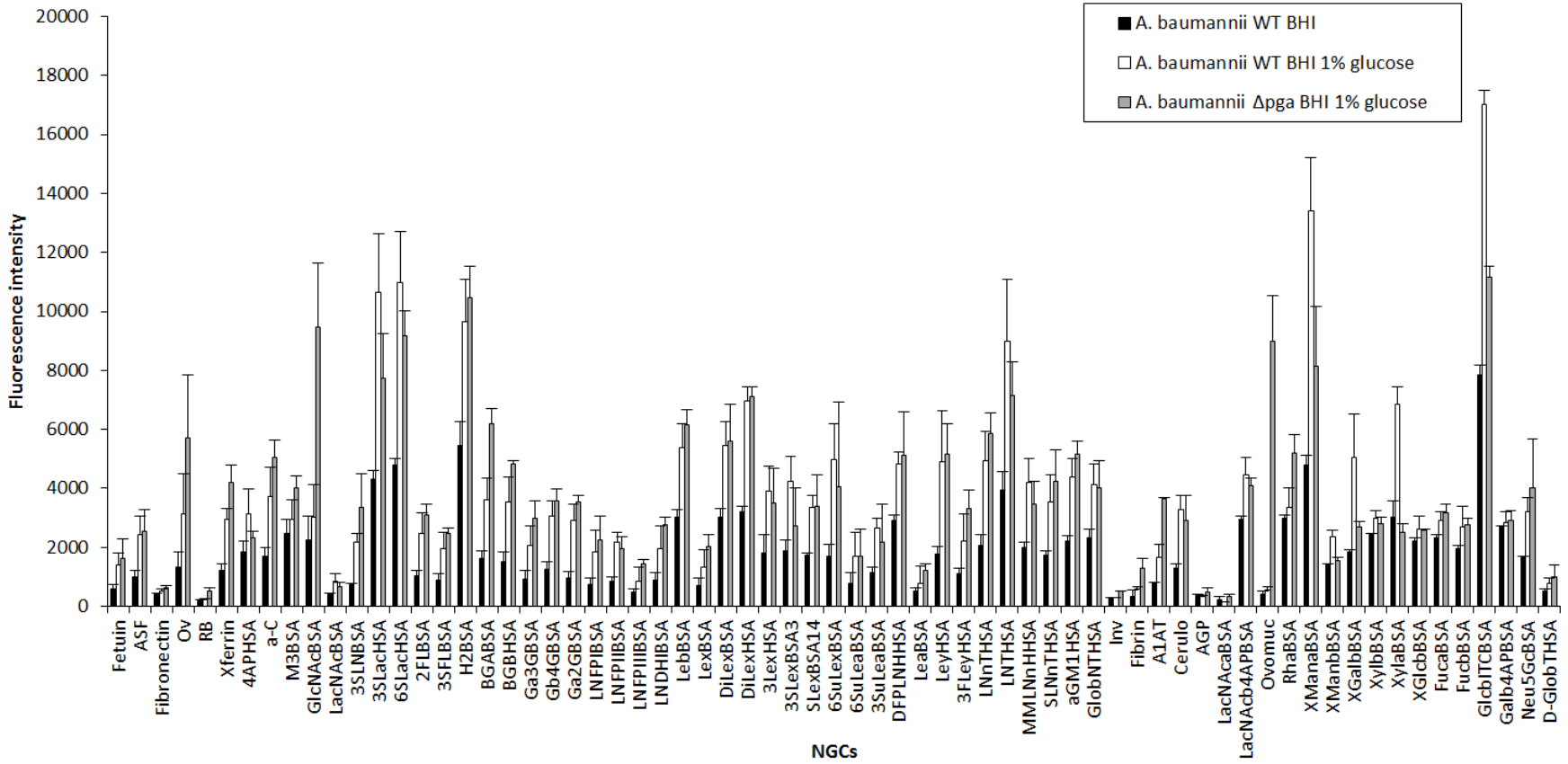


**Fig. 2.11. Neoglycoconjugate microarray profiles of *A. baumannii* WT and Δ*pga* grown in BHI glucose.** Bar chart represents NGC binding profile of *A. baumannii* WT grown in BHI and *A. baumannii* WT and Δ*pga* grown in BHI glucose. Histogram represents the mean of three experiments with error bars of +/- one standard deviation of the mean.

### 2.3.11. Comparison of carbohydrate binding profiles for *S. aureus* Mn8m, 8325-4, BH1CC WT and *A. baumannii* WT grown under different growth conditions

Carbohydrate binding profiles of WT bacteria cultured in BHI glucose or BHI NaCl were subjected to hierarchical clustering using scaled normalised binding intensity data was performed to determine similarities and differences within the different bacterial genera, strains and glucose/NaCl promoted interactions with NGCs (Fig. 2.12).

Two major groups were created from clustering NGC binding profiles of bacteria grown in BHI glucose or NaCl: the first group was *S. aureus* Mn8m WT, *S. aureus* 8325-4 and *A. baumannii* WT grown in BHI glucose. The second, which displayed 13% similarity to the first group, was: *S. aureus* 8325-4 and BH1CC WT grown in BHI NaCl and BH1CC WT grown in BHI glucose. Unsupervised hierarchical clustering of all bacteria grown in BHI glucose or NaCl showed that PNAG-expressing bacteria (*S. aureus* 8325-4, Mn8m and *A. baumannii*) cluster together. The Gram-negative PNAG-producing *A. baumannii* strain, S1, grown in BHI glucose shared 56% NGC binding similarity to *S. aureus* 8325-4 and Mn8m WT grown in BHI glucose. Addition of NaCl into BHI media resulted in *S. aureus* 8325-4 and BH1CC clustering together, even though an antibody specific against PNAG previously showed that PNAG was not produced by *S. aureus* BH1CC using a dot blot method (Table 2.4). Unexpectedly, *S. aureus* 8325-4 WT grown in BHI glucose did not cluster together with *S. aureus* 8325-4 WT grown in BHI NaCl, and only shared 13% similarity in NGC binding. This suggested that addition of glucose or NaCl in to the growth media can have a great effect on bacteria-carbohydrate interactions. On the other hand, *S. aureus* BH1CC grown in BHI glucose and BHI NaCl clustered together, although *S. aureus* BH1CC grown in BHI glucose was only 56% similar in NGC binding patterns compared to *S. aureus* BH1CC and 8325-4 WT grown in BHI NaCl and only 13% similar in NCG binding patterns compared to *S. aureus* 8325-4, Mn8m and *A. baumannii* grown in BHI glucose. Finally, *S. aureus* BH1CC grown in BHI glucose, consequently not producing detectable PNAG (Table 2.4), shared only 13% similarity in NGC binding to the other bacteria. This suggested that glucose promoted different bacterial lectins or carbohydrate-binding molecules for MRSA, compared to MSSA and *A. baumannii*, or, *S. aureus* 8325-4,

*S. aureus* Mn8m and *A. baumannii* expressed a certain carbohydrate-binding molecule that masked other smaller carbohydrate binding molecules, also present on *S. aureus* BH1CC (Fig. 2.12).

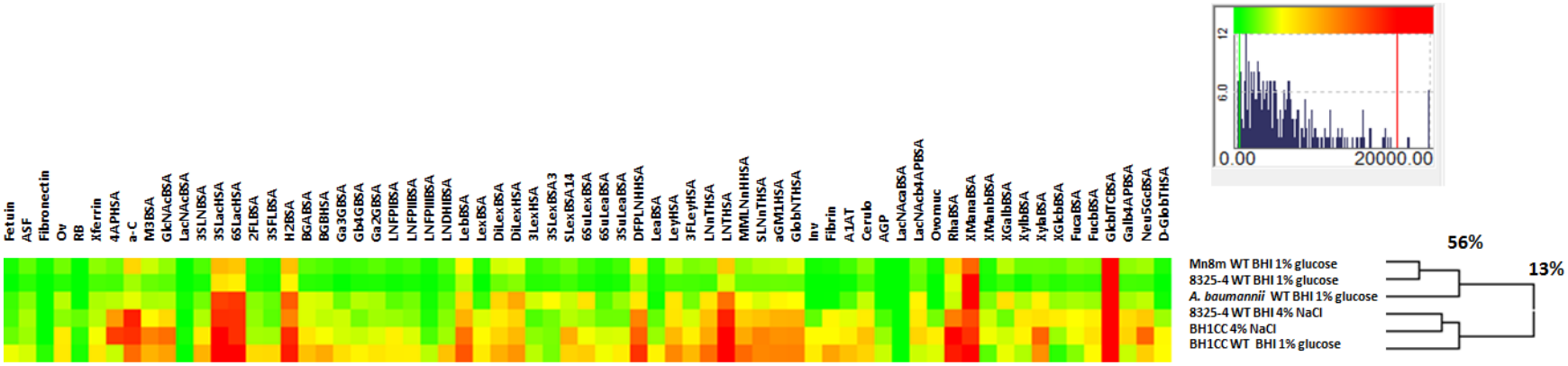


**Fig. 2.12. Unsupervised hierarchical clustering of NGC binding profiles for *S. aureus* Mn8m, 8325-4, BH1CC and *A. baumannii* WT grown in BHI glucose or BHI NaCl.** Normalised data was scaled to maximum intensity of 20,000 RFU per bacteria and clustering was carried out using the parameters of complete linkage and Euclidean distance.

## 2.4. Discussion

The ability of bacteria to alter surface glycosylation and to bind glycosylated surfaces has been shown to be associated with persistent infections, immune evasion and the manipulation of host cell signalling (Gerlach *et al.*, 2018; Hajishengallis *et al.*, 2011; Maldonado *et al.*, 2016). This study used stained bacteria, incubated them on lectin and NGC microarrays and established general patterns of bacterial surface glycosylation and carbohydrate ligands. Furthermore, we uncovered PNAG-specific lectins and described the possible differences in *ica* and *pga* function, PNAG presentation, conformation and function associated with *S. aureus* and *A. baumannii*.

Similar titration curves for dye fluorescence were obtained for the two MSSA *S. aureus* strains (8325-4 and Mn8m), but the concentration of the nucleic acid binding dye SYTO®82 for maximal fluorescence was significantly greater for the MRSA strain, BH1CC. This may be due to the increased cell wall thickness and altered peptidoglycan cross-linking associated with MRSA bacteria compared to MSSA strains (Bæk *et al.*, 2014; Kawai *et al.*, 2009), which may have prevented easy penetration of the SYTO®82 dye across the cell wall. For example, intermediate resistance to vancomycin in *S. aureus* was shown to be mediated by increased cell wall thickness and architecture. Therefore, vancomycin has to travel a longer distance to reach the lipid II target and large glycopeptides on the outer cell wall act to clog the diffusion of drugs (Foster, 2017). In turn, the lower concentration of dye used that was necessary for acceptable microarray background signal for *S. aureus* BH1CC staining may explain the lower overall fluorescence intensities for *S. aureus* BH1CC binding to the probes on the microarrays compared to *S. aureus* 8325-4 or Mn8m. Bacterial fluorescence was saturated in the lower concentration ranges tested for *A. baumannii,* which may be due to the thinner cell wall of Gram-negative bacteria being more easily penetrable for SYTO®82 (Silhavy *et al.*, 2010).

Washing steps following SYTO®82 staining removed approximately 40% of PNAG on the cell surface. Although this did not impact the binding signal intensities of the PNAG producing *S. aureus* and *A. baumannii* strains, it is unknown whether removal of this amount of PNAG impacted on the cell's ability to bind to different probes on the microarray platform. Other methods to fluorescently label bacteria that do not require wash steps, such as integration of a fluorescent protein gene into the bacterial

chromosome, could be employed in future to answer this question, although gene insertion may alter expression of cell surface molecules itself.

The GlcNAc-binding lectin WGA has been used as a 'Gold Standard' to detect and indicate the presence of PNAG within a biofilm matrix and has been used to confirm the presence of PNAG within a purified EPS sample (Begun *et al.*, 2007; Doroshenko *et al.*, 2014; Sanford *et al.*, 1995; Satorius *et al.*, 2013). In literature, WGA was proven to bind to PNAG, as fluorescently labelled WGA did not bind to a PNAG mutant, but bound to the WT strain, and, fluorescently labelled WGA did not bind to a proteinaceous biofilm formed by *S. aureus* (Formosa-Dague *et al.*, 2016). However, WGA has been shown to bind to bacteria that do not produce PNAG, indicating that WGA binds other bacterial cell surface molecules besides PNAG. For example, it was shown that WGA bound to cells within a biofilm matrix of *P. aeruginosa* (Strathmann *et al.*, 2002), even though *P. aeruginosa* does not express PNAG (Cywes-Bentley *et al*., 2013). Furthermore, research showed that fluorescently labelled WGA bound to a greater surface area of a *S. epidermidis* biofilm matrix compared to a fluorescently labelled antibody specific for PNAG, suggesting that WGA binds to other cell surface molecules apart from PNAG (Cerca *et al*., 2006).

In this study, the reduction in WGA binding to *S. aureus* 8325-4 and Mn8m Δ*ica* grown in BHI glucose, compared to the WT strains suggested that WGA has some specificity towards PNAG. However, there were little differences in WGA binding to *S. aureus* 8325-4 Δ*ica* grown in BHI NaCl compared to the WT strain and no differences in binding to *A. baumannii* Δ*pga* compared to the WT strain. These data supported findings by Ramos *et al* (2019), that WGA binds to other molecules on the surface of bacteria apart from PNAG (Ramos *et al.*, 2019). However, this does not mean that WGA does not have specificity for PNAG, but it is likely that the absence of PNAG on the cell surface allows other bacterial cell surface structures to be uncovered and exposed and made available for WGA interaction. These uncovered structures include GlcNAc-containing molecules such as peptidoglycans, glycoproteins, capsules, WTAs, LTA and LPS (Davis & Weiser, 2011; Richie *et al.*, 2016; Scott *et al.*, 2014; Xia *et al.*, 2010). To the best of our knowledge, WGA has not been shown to bind LTA or LPS, however, WGA has been used to detect GlcNAc on *S. aureus* WTA, in peptidoglycan and glycans on OmpA-like

glycoproteins from *Porphyromonas gingivalis* (Monteiro *et al.*, 2015; Murakami *et al.*, 2014; G Xia *et al.*, 2010). Furthermore, WGA also binds to NeuAc, and GalNAc, although the affinity for GalNAc is five times lower than for GlcNAc. Therefore, the multiple specificities of WGA may have contributed to WGA binding to PNAG mutants in this study (Goldstein & Poretz, 1986).

However, sWGA displayed reduced binding to *S. aureus* Mn8m Δ*ica* compared to the WT strain, even though this was not comparable for WGA. This might suggest that sWGA had greater specificity for PNAG produced by *S. aureus* Mn8m WT after growth in BHI glucose compared to WGA. GSL-II has specificity for terminal GlcNAc residues and an increase in GSL-II interactions were observed for *S. aureus* 8325-4 Δ*ica* grown in BHI glucose compared to the WT strain. This suggested that there were higher proportions of terminal GlcNAc residues in the absence of PNAG. Since the opposite occurred for *S. aureus* 8325-4 grown in BHI NaCl, we speculate that the addition of NaCl contributes to PNAG with more terminal, unmodified GlcNAc structures, although research would be required to prove this hypothesis. Moreover, bacteria grown in different environments, such as glucose-rich and NaCl-rich environments, may change the structure or conformation of polysaccharides, which in turn leaves terminal GlcNAc residues more or less exposed for binding to GSL-II. Understanding why growing *S. aureus* 8325-4 in the presence of NaCl would promote GSL-II binding to PNAG and why growing *S. aureus* 8325-4 in the presence of glucose would promote sWGA binding to PNAG is still unknown, but there are several speculations that might explain these data. Modifications of PNAG such as deacetylation and *O*-succinylation vary depending on the bacterial genus and strain (Whitfield *et al.*, 2015). For example, PNAG isolated from *S. epidermidis* is between 15-20% deacetylated and 6% *O*-succinylated (Mack *et al.*, 1996; Sadovskaya *et al.*, 2005), PNAG isolated from *S. aureus* Mn8m is approximately 5% deacetylated and not *O*-succinylated, although 10% succyinlated was reported on PNAG isolated from this strain previously but now verified as an experimental artefact (Maira-Litrán *et al*., 2002; McKenney *et al*., 1999), PNAG isolated from *E. coli* is deacetylated approximately 3-5% and not *O*-succinylated (Wang *et al.*, 2004) and PNAG isolated from *A. baumannii* S1 is approximately 40% deacetylated and not *O*-succinylated (Choi *et al.*, 2009). It has been shown that growth in NaCl reduces the yield of PNAG for purification (Ganesan *et al.*, 2013). To our

knowledge, no research has been carried out to identify whether the supplementation of glucose or NaCl to growth media causes structural changes to PNAG, but it is possible that addition of glucose or NaCl to the growth media could influence the degrees of deacetylation and/or *O*-succinylation of PNAG, thus changing the overall charge and the structural conformation of the molecule, making it more or less likely to adhere to certain GlcNAc-specific lectins such as GSL-II or sWGA.

Alternatively, addition of glucose in to BHI media and allowing cells to grow, results in an accumulation of acidic by-products, such as acetic acid, and reduces the pH of the media to 6 (O'Neill *et al.,* 2008). Chitosan (~75% deacetylated poly-*N*-acetylglucosamine) is structurally similar to PNAG, except that it is β-(1,4)-linked while PNAG is β-(1,6)-linked and chitosan has a higher degree of deacetylation compared to PNAG. Chitosan has a high charge density at pH below 6.5 and behaves in a stable manner. On the other hand, PNAG has a much lower degree of deacetylation causing it to be unstable at low pH. Therefore, addition of glucose to the growth medium may promote acidic conditions that contribute to changes in biofilm architecture, PNAG structural conformation, topography, mobility of the bacteria and the ability of bacteria to bind to protein ligands (Stewart *et al.*, 2015).

The absence of PNAG in BH1CC WT biofilm formation was supported by lectin microarray profiling, which further demonstrated a lack of prominent binding by GlcNAc-containing molecules. This indicated the likely absence of PNAG on the MRSA cell surface for the interaction of the lectins, with only large molecules, such as proteins, on bacterial cell surface. *S. aureus* BH1CC WT appeared to change surface glycosylation, primarily fucosylated following growth in BHI and primarily GlcNAcylated grown in BHI glucose. It is unclear as to whether these glycosylation changes have an impact on MRSA biofilm formation or not, although it has been reported that glycosylation of a *S. aureus* surface protein with *N*-acetylhexosaminyl residues enhanced biofilm formation (Bleiziffer *et al.*, 2017).

Unexpectedly, lectin microarray analysis suggested that PNAG on *A. baumannii* was a ligand of DBA, CPA and VRA. The structural conformation of PNAG on or associated with *A. baumannii* could be very different to PNAG from *S. aureus* due to the higher degree of deacetylation (50% and 5% deacetylated respectively) (Choi *et al.*, 2009; Maira-Litrán *et al.*, 2002), creating different architectures – some more

likely to promote interactions with DBA, CPA and VRA than others. Alternatively, highly deacetylated PNAG may support tight adherence to the cell surface and promote other interactions with lectins. For example, CPS isolated from *A. baumannii* NIPH146 was primarily composed of D-Glc, D-Gal and D-GalNac and contained a α-D-Galp-(1→6)-β-D-Glcp-(1→3)-D-GalpNAc-(1→ trisaccharide fragment common among many *A. baumannii* strains (Arbatsky *et al*., 2015), the O-antigen isolated from *A. baumannii* strain 9 and ATCC 17961 had structures consisting primarily of α-D-Glcp, D-GalpNAc (MacLean *et al.*, 2009), and unnamed glycoproteins isolated from *A. baumannii* were determined have a β-GlcNAc3NAcA4OAc-4-(β-GlcNAc-6-)-α-Gal-6-β-Glc-3-β-GalNAc-S/T structure (Iwashkiw *et al.*, 2012). Thus, PNAG may have a role in the recognition of *A. baumannii* CPS or O-antigen by lectins. On the other hand, PNAG on *A. baumannii* may be cleaved from the cell surface at a high rate. Supporting this statement is the fact that PgaB on *E. coli* and *Bordetella bronchiseptica* are deacetylated PNAG hydrolases (Little *et al*, 2018). Similarly, PgaB on *A. baumannii* may be a hydrolase for deacetylated PNAG and as PNAG associated with *A. baumannii* S1 is approximately 40% deacetylated, may be cleaved at a higher rate, compared to *S. aureus*, generally creating differences in conformation, coil and helic formation, stiffness and PNAG rigidity. Thus, the conformation of PNAG on *A. baumannii* may be very different to that on *S. aureus* and support a conformation more preferable to DBA, CPA or VRA compared to WGA. However, lectin specificities for bacterial carbohydrates have not yet been fully characterised, leaving some ambiguity in the interpretation of these results. Although DBA, CPA and VRA have specificities for Gal and GalNAc structures based on mammalian glycosylation, these lectins may also have specificity for deacetylated PNAG when it is located on the *A. baumannii* cell surface, with other structures, such as LPS and CPS.

Taking the above observations in to account, and supporting findings by Ramos *et al* (2019) regarding the lack of specificity of WGA binding to PNAG, it is thus not advisable to use fluorescently labelled WGA as a method for specifically identifying PNAG in biofilm matrices or for PNAG isolation. Instead, we suggest that specific PNAG detection or isolation be carried out using a recognition molecule that is specific for the PNAG structure itself rather than the more general GlcNAc constituent, such as a labelled antibody against PNAG.

Overall, these data suggest that PNAG presentation, conformation, accessibility and/or composition are not the same depending on the bacterial genus, species and strain, and may also vary depending on the environmental growth conditions. These results highlight the importance of growing a range of PNAG-producing bacteria in biologically relevant media to help elucidate the role, structure and composition of PNAG, more similar to PNAG in *in vivo* settings.

In this work, specific carbohydrate ligands for *S. aureus* 8325-4, Mn8m, BH1CC and *A. baumannii* S1 were demonstrated for the first time. MSSA, MRSA and *A. baumannii* WT strains showed similar patterns in NGC binding, regardless of being grown in the presence of glucose or NaCl. Across the different bacteria, α-C and the NGCs 3SLacHSA, 6SLacHSA, H2BSA, LebBSA, lacto-*N*-tetrose, α-linked Man (mannose) and GlcbITCBSA and XManaBSA were the most common carbohydrate ligands. Binding to GlcbITCBSA was consistent for all bacteria, however, bacteria did not bind to β-linked glucose when on a different linker (4AP-BSA linker for XGlcbBSA). It is known that this particular linker interacts with a variety of lectins when unconjugated to a carbohydrate, but loses a high proportion of these non-specific interactions when a carbohydrate is further conjugated to the linker (Kilcoyne *et al.*, 2012). Given that all bacterial strains bound to XManaBSA and GlcbITCBSA, and that binding intensities and patterns to M3BSA and XGlcbBSA were not similar to XManaBSA and GlcbITCBSA, respectively, we hypothesize these interactions were mediated via the ITC linker, and not the carbohydrate.

Interestingly, bacteria showed preferential binding to certain NGCs depending on anomeric configurations, linkages and slight differences in structure. For example, bacteria showed preferential binding towards 3'-Sialylactose-APD-HAS compared to 3'SialyLAcNAc-BSA and Lewis b-BSA compared to Lewis a-BSA. Furthermore, bacteria bound with greater intensity to the blood group antigen acceptor substrate lacto-*N*-tetraose (Lacto-*N*-tetraose-APD-HAS) compared to lacto-*N*-neotetraose (Lacto-*N*-neotetraose-APD-HAS). Given the greater binding of these bacteria to H type 2 antigen (H Type II-APE-BSA), and $Le^b$ (Lewis b-BSA ) compared to blood group A (Blood Group A-BSA) and blood group B (Blood Group B-BSA) might suggest preferential binding to structures which incorporate terminal α-(1,2)-Fuc rather than terminal Gal structures. Thus, these bacteria may have preferential binding to secretor hosts that have a functional FUT2 gene which makes the enzyme

α-1,2-fucosyltransferase rather than non-secretors who have a non-functional *FUT2* gene. This would be similar to bifidobacteria where host expression of the *FUT2* gene, which defines secretor status and the expression of blood group A, B and H and Lewis antigens (α-(1,2)-linked fucose), is a genotypic factor that contributes to microbial diversity, particularly bifidobacteria diversity, in the intestinal microbiota (Wacklin *et al.*, 2011). Nonetheless, it has been shown in literature that some *S. aureus* strains have an affinity towards $Le^a$ (Saadi *et al.*, 1994). Fucosylation plays an important role for host-microbe interactions. For example, *H. pylori* recognises and attaches to $Le^b$ and H antigens on glycosphingolipids via a 78 kDa glycosylated protein named BabA and has preferential binding to $Le^b$>type 1 H antigen>$ALe^b$ and $BLe^b$ and does not bind to $Le^a$, $Le^x$ or $Le^y$. BabA along with sialic acid binding protein (SabA) and the lipoprotein binding proteins AlpA/AlpB promote adhesion and virulence contributing to chronic infection and inflammation (Aspholm-Hurtig *et al.*, 2004; Cooling, 2015; Ilver *et al.*, 1998). It would be interesting to decipher whether a ligand for fucosylated structures on the surface of *S. aureus* and *A. baumannii* could have a similar part to play in infection and inflammation.

SraP is a 225 kDa protein on *S. aureus* that recognises type two sialylated structures with high affinity towards NeuAc-α-(2,3)-Gal-β-(1,4)-GlcNAc and promotes adhesion and invasion to lung epithelial cells (Yang *et al.*, 2014). SraP did not have high specificity for NeuAc-α-(2,3)-Gal-β-(1,4)-GlcNAc but moderate affinity towards NeuAc-α-(2,6)-Gal-β-(1,4)-GlcNAc (Kukita *et al* 2013), suggesting that this protein may contribute to *S. aureus* binding to 6SLacHSA (NeuAc-α-(2,6)-Gal-β-(1,4)-GlcNAc-ADP-HAS) in this work.

The *ica* and *pga* mutants bound to the NGCs described above, namely: 3SLacHSA, 6SLacHSA, H2BSA, LebBSA, LNTHSA, XManaBSA and GlcbITCBSA depending on the presence of glucose or NaCl. In some *S. aureus* strains, including the 8325-4 and Mn8m strains in this work, glucose or NaCl promote biofilm formation via PNAG production (O'Neill *et al.*, 2007), but whether additional modifications to PNAG are carried out because of the growth media in additional to expression of PNAG remains unknown. Our data suggested that the absence of PNAG on the surface of *A. baumannii* increased attachment to certain NGCs. We are unsure why the absence of PNAG promoted binding to different NGCs, but we hypothesise that the absence of PNAG allowed other cell surface structures such as lectins, LPS,

LOS, glycoproteins, and/or CPS available to interact with NGCs. For example, it was shown that 20 out of 47 *A. baumannii*, biofilm forming, urinary tract and urinary catheter infection isolates displayed lectin activity (Pour *et al.*, 2011). PNAG and pilins, CsuA and CsuB, FimA/F17-A and A1S_1507 were found in the biofilm matrix of *A. baumannii* pellicles. FimA/F17-A was 46% identical to the F17A pilin expressed by *E. coli*, which is a subunit of the F17A-G pili system expressed by *E. coli*. F17A-G fimbrial adhesin has a lectin domain with an affinity to GlcNAc (Nait Chabane *et al.*, 2014). It may be possible that *A. baumannii* WT also used F17-like pili to bind to GlcNAc to promote biofilm formation. Therefore, rendering the bacterial cell without PNAG may have uncovered these lectins and/or left these lectins without a ligand, allowing them to bind GlcNAc containing NGCs, such as GlcNAc-BSA and ovalbumin (Harvey *et al.*, 2000), on the NGC microarray platform. On the other hand, bacterial carbohydrates contribute to the structure of LOS and LPS. LOS and LPS were shown to be involved in carbohydrate-carbohydrate interactions with terminal carbohydrate structures associated with blood group A, B and O, Lewis antigens, sialic acids and glycosaminoglycans (Day *et al.*, 2015). Thus, the absence of PNAG may have encouraged LOS and LPS attachment to NGCs. As pili, LOS and LPS are common antigens used for host detection of an invading pathogen, it would make sense for PNAG to shield these antigens to evade the host's immune system. Finally, mutation of PgaA, PgaB and PgaC, may have consequentially altered the cell surface topography, contributing to differences in NGC interactions. Indeed, binding to XManaBSA, XGalbBSA and GlcbITCBSA decreased for *A. baumannii* Δ*pga* compared to *A. baumannii* WT, however, we hypothesize that PNAG was binding to the ITC linker rather than the carbohydrate. If PNAG on *A. baumannii* bound to XManaBSA and GlcbITCBSA, we would expect similar interactions with M3BSA and XGlcbBSA. Therefore, we propose that ITC linkers are unsuitable for assessing bacterial interactions with carbohydrates.

Compared to *S. aureus*, PNAG on the surface of *A. baumannii* appears to play a role in biofilm integrity under shear force, whereas PNAG on MSSA plays a vital role in biofilm formation under static conditions (Choi *et al.*, 2009). The MRSA isolate BH1CC does not produce PNAG on the cell surface when glucose is added to growth media, however, promoting *icaA* transcription through the addition of NaCl

in to the growth media clearly altered NGC binding in this study (O'Neill *et al.*, 2007). Interestingly, it was shown that *icaA* transcription does not correspond to PNAG production, as PNAG was not detected in BH1CC cell culture supernatants of *S. aureus* BH1CC via a PNAG specific antibody (O'Neill *et al.*, 2007). Therefore, it could be hypothesised that *icaA* transcription, and potentially *icaDBC*, have alternative roles to play, besides PNAG production. In this study, the general decrease of *S. aureus* BH1CC Δ*ica* binding to NGCs compared to *S. aureus* BH1CC WT grown in BHI NaCl suggested that mutation of the *ica* operon reduced the ability of *S. aureus* BH1CC to bind to many NGCs. Why mutation of the *ica* decreased binding to NGCs if PNAG is not detectable on the cell wall of *S. aureus* BH1CC WT is unknown. If mutation of IcaB caused this overall decrease in binding to NGCs, we would predict there would be a similar result for the MSSA strain, 8325-4. As this was not the case, we can assume that mutating the only surface-exposed protein, IcaB, did not contribute to this reduction in binding to NGCs. Therefore, the presence of the *ica* operon caused cell surface changes to *S. aureus* BH1CC WT grown in BHI NaCl, which likely did not involve the expression of PNAG. Further research is required to identify the reasons why and how the *ica* operon promoted binding to certain NGCs. Indeed, it was shown that the presence of *icaADB* contributed to bacterial survival, even in the absence of PNAG, and suggested that the IcaADB proteins could have alternative functions within the cell (Brooks & Jefferson, 2014). Further research is required to elucidate whether NaCl-induced expression of IcaADBC plays alternative roles for *S. aureus* BH1CC WT, such as aiding bacterial attachment to carbohydrates. Overall these results suggested a role for the *ica*/*pga* operon in NGC interactions and not just PNAG production.

Overall, this chapter demonstrated the different effects glucose and NaCl can have on bacterial glycosylation and carbohydrate recognition. Our results also showed the striking differences between the *ica* and *pga* operon in both bacterial glycosylation and NGC recognition, with the *pga* operon playing a more profound and unexpected role compared to the *ica* operon. Our results suggested that PNAG on Gram negative bacteria may have a different role, conformation, relative quantity or presentation compared to PNAG on *S. aureus,* but further research to elucidate the conformation and presentation of cell-associated PNAG from different PNAG-producing bacteria would be required to prove this hypothesis. Nonetheless, this study is the first to

report carbohydrate ligands for *S. aureus* and *A. baumannii*. Our research may be used to help delve deeper in to the role of the *ica* and *pga* operon, and in *S. aureus*, *A. baumannii* and other bacteria, one that spans not just surface glycosylation, but also carbohydrate mediated interactions. Novel carbohydrate targets for *S. aureus* and *A. baumannii* found in this study have the potential to impact our understanding of pathogen-carbohydrate mediated interactions in multiple biological systems and in biofilm assembly.

## 2.5. References


**Arbatsky, N. P., Shneider, M. M., Kenyon, J. J., Shashkov, A. S., Popova, A. V, Miroshnikov, K. A., Volozhantsev, N. V, & Knirel, Y. A.** (2015). Structure of the neutral capsular polysaccharide of *Acinetobacter baumannii* NIPH146 that carries the KL37 capsule gene cluster. *Carbohydrate Research*, *413*, 12–15.

**Aspholm-Hurtig, M., Dailide, G., Lahmann, M., Kalia, A., Ilver, D., Roche, N., Vikström, S., Sjöström, R., Lindén, S., Bäckström, A., Lundberg, C., Arnqvist, A., Mahdavi, J., Nilsson, U. J., Velapatño, B., Gilman, R. H., Gerhard, M., Alarcon, T., López-Brea, M., Nakazawa, T., Fox, J. G., Correa, P., Dominguez-Bello, M. G., Perez-Perez, G. I., Blaser, M. J., Normark, S., Carlstedt, I., Oscarson, S., Teneberg, S., Berg, D. E., & Borén, T.** (2004). Functional adaptation of BabA the *H. pylori* ABO blood group antigen binding adhesin. *Science*, *305*(5683), 519–522.

**Bæk, K. T., Gründling, A., Mogensen, R. G., Thøgersen, L., Petersen, A., Paulander, W., & Frees, D.** (2014). β-lactam resistance in methicillin-resistant *Staphylococcus aureus* USA300 is increased by inactivation of the ClpXP protease. *Antimicrobial Agents and Chemotherapy*, *58*(8), 4593–4603.

**Bateman, A., Holden, M. T. G., & Yeats, C.** (2005). The G5 domain: A potential *N*-acetylglucosamine recognition domain involved in biofilm formation. *Bioinformatics*, *21*(8), 1301–1303.

**Begun, J., Gaiani, J. M., Rohde, H., Mack, D., Calderwood, S. B., Ausubel, F. M., & Sifri, C. D.** (2007). Staphylococcal biofilm exopolysaccharide protects against Caenorhabditis elegans immune defenses. *PLoS Pathogens*, *3*(4), 526–540.

**Bleiziffer, I., Eikmeier, J., Pohlentz, G., McAulay, K., Xia, G., Hussain, M., Peschel, A., Foster, S., Peters, G., & Heilmann, C.** (2017). The Plasmin-Sensitive Protein Pls in Methicillin-Resistant *Staphylococcus aureus* (MRSA) Is a Glycoprotein. *PLoS Pathogens*, *13*(1).

**Brooks, J. L., & Jefferson, K. K.** (2014). Phase Variation of Poly-*N*-Acetylglucosamine Expression in *Staphylococcus aureus*. *PLoS Pathogens*, *10*(7).

**Buist, G., Steen, A., Kok, J., & Kuipers, O. P.** (2008). LysM, a widely distributed protein motif for binding to (peptido)glycans. *Molecular Microbiology*, *68*(4), 838–847.

**Cabral, M. P., Soares, N. C., Aranda, J., Parreira, J. R., Rumbo, C., Poza, M., Valle, J., Calamia, V., Lasa, I., & Bou, G.** (2011). Proteomic and functional analyses reveal a unique lifestyle for *Acinetobacter baumannii* biofilms and a key role for histidine metabolism. *Journal of Proteome Research*, *10*(8), 3399–3417.

**Cerca, N., & Jefferson, K. K.** (2008). Effect of growth conditions on poly-*N*-acetylglucosamine expression and biofilm formation in *Escherichia coli*. *FEMS Microbiology Letters*, *283*(1), 36–41.

**Cerca, N., Jefferson, K. K., Oliveira, R., Pier, G. B., & Azeredo, J.** (2006). Comparative antibody-mediated phagocytosis of *Staphylococcus epidermidis* cells grown in a biofilm or in the planktonic state. *Infection and Immunity*, *74*(8), 4849–4855.

**Choi, A. H. K., Slamti, L., Avci, F. Y., Pier, G. B., & Maira-Litrán, T.** (2009). The pgaABCD locus of *Acinetobacter baumannii* encodes the production of poly-β-1-6-*N*-acetylglucosamine, which is critical for biofilm formation. *Journal of Bacteriology*, *191*(19), 5953–5963.

**Chowdhury, R., Sahu, G. K., & Das, J.** (1996). Stress response in pathogenic bacteria. *Journal of Biosciences*, *21*(2), 149–160.

**Conlon, K. M., Humphreys, H., & O'Gara, J. P.** (2002). icaR encodes a transcriptional repressor involved in environmental regulation of ica operon expression and biofilm formation in *Staphylococcus epidermidis*. *Journal of Bacteriology*, *184*(16), 4400–4408.

**Conrady, D. G., Wilson, J. J., & Herr, A. B.** (2013). Structural basis for $Zn^{2+}$-dependent intercellular adhesion in staphylococcal biofilms. *Proceedings of the National Academy of Sciences*, *110*(3), E202 LP-E211.

**Cooling, L.** (2015). Blood Groups in Infection and Host Susceptibility. *Clinical Microbiology Reviews*, *28*(3), 801–870.

**Cywes-Bentley, C., Skurnik, D., Zaidi, T., Roux, D., DeOliveira, R. B., Garrett, W. S., Lu, X., O'Malley, J., Kinzel, K., Zaidi, T., Rey, A., Perrin, C., Fichorova, R. N., Kayatani, A. K. K., Maira-Litràn, T., Gening, M. L., Tsvetkov, Y. E., Nifantiev, N. E., Bakaletz, L. O., Pelton, S. I., Golenbock, D. T., & Pier, G. B.** (2013). Antibody to a conserved antigenic target is protective against diverse prokaryotic and eukaryotic pathogens. *Proceedings of the National Academy of Sciences of the United States of America*, *110*(24), E2209–E2218.

**Davis, K. M., & Weiser, J. N.** (2011). Modifications to the Peptidoglycan Backbone Help Bacteria To Establish Infection. *Infection and Immunity*, *79*(2), 562-570.

**Day, C. J., Tran, E. N., Semchenko, E. A., Tram, G., Hartley-Tassell, L. E., Ng, P. S. K., King, R. M., Ulanovsky, R., McAtamney, S., Apicella, M. A., Tiralongo, J., Morona, R., Korolik, V., & Jennings, M. P.** (2015). Glycan:glycan interactions: High affinity biomolecular interactions that can mediate binding of pathogenic bacteria to host cells. *Proceedings of the National Academy of Sciences of the United States of America*, *112*(52), E7266–E7275.

**Dengler, V., Foulston, L., DeFrancesco, A. S., & Losick, R.** (2015). An electrostatic net model for the role of extracellular DNA in biofilm formation by *Staphylococcus aureus*. *Journal of Bacteriology*, *197*(24), 3779–3787.

**Doroshenko, N., Tseng, B. S., Howlin, R. P., Deacon, J., Wharton, J. A., Thurner, P. J., Gilmore, B. F., Parsek, M. R., & Stoodley, P.** (2014). Extracellular DNA impedes the transport of vancomycin in *Staphylococcus*

*epidermidis* biofilms preexposed to subinhibitory concentrations of vancomycin. *Antimicrobial Agents and Chemotherapy*, *58*(12), 7273–7282.

**Fitzpatrick, F., Humphreys, H., & O'Gara, J. P.** (2005). Evidence for icaADBC-independent biofilm development mechanism in methicillin-resistant *Staphylococcus aureus* clinical isolates. *Journal of Clinical Microbiology*, *43*(4), 1973–1976.

**Flannery, A., Gerlach, Q. J., Joshi, L., & Kilcoyne, M.** (2015). Assessing Bacterial Interactions Using Carbohydrate-Based Microarrays. *Microarrays 4*(4), 690-713.

**Formosa-Dague, C., Feuillie, C., Beaussart, A., Derclaye, S., Kucharíková, S., Lasa, I., Van Dijck, P., & Dufreîne, Y. F.** (2016). Sticky Matrix: Adhesion Mechanism of the Staphylococcal Polysaccharide Intercellular Adhesin. *ACS Nano*, *10*(3), 3443–3452.

**Formosa-Dague, C., Speziale, P., Foster, T. J., Geoghegan, J. A., & Dufrêne, Y. F.** (2016). Zinc-dependent mechanical properties of *Staphylococcus aureus* biofilm-forming surface protein SasG. *Proceedings of the National Academy of Sciences*, *113*(2), 410-415.

**Foster, T. J.** (2017). Antibiotic resistance in *Staphylococcus aureus*. Current status and future prospects. *FEMS Microbiology Reviews*, *41*(3), 430–449.

**Gaddy, J. A., Tomaras, A. P., & Actis, L. A.** (2009). The *Acinetobacter baumannii* 19606 OmpA protein plays a role in biofilm formation on abiotic surfaces and in the interaction of this pathogen with eukaryotic cells. *Infection and Immunity*, *77*(8), 3150–3160.

**Ganesan, M., Stewart, E. J., Szafranski, J., Satorius, A. E., Younger, J. G., & Solomon, M. J.** (2013). Molar Mass, Entanglement, and Associations of the Biofilm Polysaccharide of *Staphylococcus epidermidis*. *Biomacromolecules*, *14*(5), 1474–1481.

**Gerlach, D., Guo, Y., De Castro, C., Kim, S.-H., Schlatterer, K., Xu, F.-F., Pereira, C., Seeberger, P. H., Ali, S., Codée, J., Sirisarn, W., Schulte, B., Wolz, C., Larsen, J., Molinaro, A., Lee, B. L., Xia, G., Stehle, T., & Peschel, A.** (2018). Methicillin-resistant *Staphylococcus aureus* alters cell wall glycosylation to evade immunity. *Nature*, *563*(7733), 705–709.

**Goldstein, I. J., & Poretz, R. D.** (1986). *The Lectins: Properties, Functions, and Applications in Biology and Medicine*. Academic Press Inc., 35-244

**Götz, F.** (2002). Staphylococcus and biofilms. *Molecular Microbiology*, *43*(6), 1367–1378.

**Hajishengallis, G., & Lambris, J. D.** (2011). Microbial manipulation of receptor crosstalk in innate immunity. *Nature Reviews Immunology*, *11*(3), 187–200.

**Harvey, D. J., Wing, D. R., Küster, B., & Wilson, I. B. H.** (2000). Composition of N-linked carbohydrates from ovalbumin and co-purified glycoproteins. *Journal of the American Society for Mass Spectrometry*, *11*(6), 564–571.

**Horsburgh, M. J., Aish, J. L., White, I. J., Shaw, L., Lithgow, J. K., & Foster, S. J.** (2002). δB modulates virulence determinant expression and stress resistance: Characterization of a functional rsbU strain derived from *Staphylococcus aureus* 8325-4. *Journal of Bacteriology*, *184*(19), 5457–5467.

**Houston, P., Rowe, S. E., Pozzi, C., Waters, E. M., & O'Gara, J. P.** (2011). Essential role for the major autolysin in the fibronectin-binding protein-mediated *Staphylococcus aureus* biofilm phenotype. *Infection and Immunity*, *79*(3), 1153–1165.

**Hsu, K.-L., Pilobello, K. T., & Mahal, L. K.** (2006). Analyzing the dynamic bacterial glycome with a lectin microarray approach. *Nature Chemical Biology*, *2*(3), 153–157.

**Ilver, D., Arnqvist, A., Ögren, J., Frick, I.-M., Kersulyte, D., Incecik, E. T., Berg, D. E., Covacci, A., Engstrand, L., & Borén, T.** (1998). *Helicobacter pylori* adhesin binding fucosylated histo-blood group antigens revealed by retagging. *Science*, *279*(5349), 373–377.

**Iwashkiw, J. A., Seper, A., Weber, B. S., Scott, N. E., Vinogradov, E., Stratilo, C., Reiz, B., Cordwell, S. J., Whittal, R., Schild, S., & Feldman, M. F.** (2012). Identification of a General O-linked Protein Glycosylation System in *Acinetobacter baumannii* and Its Role in Virulence and Biofilm Formation. *PLOS Pathogens*, *8*(6), e1002758.

**Jaione, V., Alejandro, T.-A., Carmen, B., Jean-Marc, G., Beatriz, A., R., P. J., & Iñigo, L.** (2003). SarA and not σB is essential for biofilm development by *Staphylococcus aureus*. *Molecular Microbiology*, *48*(4), 1075–1087.

**Jefferson, K. K., Cramton, S. E., Götz, F., & Pier, G. B.** (2003). Identification of a 5-nucleotide sequence that controls expression of the ica locus in *Staphylococcus aureus* and characterization of the DNA-binding properties of IcaR. *Molecular Microbiology*, *48*(4), 889–899.

**Jefferson, K. K., Pier, D. B., Goldmann, D. A., & Pier, G. B.** (2004). The Teicoplanin-Associated Locus Regulator (TcaR) and the Intercellular Adhesin Locus Regulator (IcaR) Are Transcriptional Inhibitors of the ica Locus in *Staphylococcus aureus*. *Journal of Bacteriology*, *186*(8), 2449–2456.

**Islam, N., Ross, J. M., & Marten, M. R.** (2015). Proteome Analyses of *Staphylococcus aureus* Biofilm at Elevated Levels of NaCl. Clinical Microbiology, *4*(5), 219.

**Kawai, M., Yamada, S., Ishidoshiro, A., Oyamada, Y., Ito, H., & Yamagishi, J.-I.** (2009). Cell-wall thickness: Possible mechanism of acriflavine resistance in meticillin-resistant *Staphylococcus aureus*. *Journal of Medical Microbiology*, *58*(3), 331–336.

**Kelly-Quintos, C., Cavacini, L. A., Posner, M. R., Goldmann, D., & Pier, G. B.** (2006). Characterization of the opsonic and protective activity against *Staphylococcus aureus* of fully human monoclonal antibodies specific for the bacterial surface polysaccharide poly-*N*-acetylglucosamine. Infection and Immunity, 74(5), 2742–2750.

**Kennedy, C. A., & O'Gara, J. P.** (2004). Contribution of culture media and chemical properties of polystyrene tissue culture plates to biofilm development by *Staphylococcus aureus*. *Journal of Medical Microbiology*, *53*(11), 1171–1173.

**Kilcoyne, M., Gerlach, J. Q., Kane, M., & Joshi, L.** (2012). Surface chemistry and linker effects on lectin-carbohydrate recognition for glycan microarrays. *Analytical Methods*, *4*(9), 2721–2728.

**Kilcoyne, M., Twomey, M. E., Gerlach, J. Q., Kane, M., Moran, A. P., & Joshi, L.** (2014). *Campylobacter jejuni* strain discrimination and temperature-dependent glycome expression profiling by lectin microarray. *Carbohydrate Research*, *389*(1), 123–133.

**Kropec, A., Maira-Litran, T., Jefferson, K. K., Grout, M., Cramton, S. E., Götz, F., Goldmann, D. A., & Pier, G. B.** (2005). Poly-*N*-acetylglucosamine production in *Staphylococcus aureus* is essential for virulence in murine models of systemic infection. *Infection and Immunity*, *73*(10), 6868–6876.

**Kukita, K., Kawada-Matsuo, M., Oho, T., Nagatomo, M., Oogai, Y., Hashimoto, M., Suda, Y., Tanaka, T., & Komatsuzawa, H.** (2013). *Staphylococcus aureus* SasA is responsible for binding to the salivary agglutinin gp340, derived from human saliva. *Infection and Immunity*, *81*(6), 1870–1879.

**Lasa, I., & Penadés, J. R.** (2006). Bap: A family of surface proteins involved in biofilm formation. *Research in Microbiology*, *157*(2), 99–107.

**Lim, Y., Jana, M., Luong, T. T., & Lee, C. Y.** (2004). Control of Glucose- and NaCl-Induced Biofilm Formation by rbf in *Staphylococcus aureus*. *Journal of Bacteriology*, *186*(3), 722–729.

**Lin, M. H., Shu, J. C., Lin, L. P., Chong, K. Y., Cheng, Y. W., Du, J. F., & Liu, S.-T.** (2015). Elucidating the crucial role of poly N-acetylglucosamine from *Staphylococcus aureus* in cellular adhesion and pathogenesis. *PLoS ONE*, *10*(4).

**Little, D. J., Pfoh, R., Le Mauff, F., Bamford, N. C., Notte, C., Baker, P., Guragain, M., Robinson, H., Pier, G. B., Nitz, M., Deora, R., Sheppard, D. C., & Howell, P. L.** (2018). PgaB orthologues contain a glycoside hydrolase domain that cleaves deacetylated poly-β(1,6)-*N*-acetylglucosamine and can disrupt bacterial biofilms. PLoS Pathogens, 14(4).

**Mack, D., Fischer, W., Krokotsch, A., Leopold, K., Hartmann, R., Egge, H., & Laufs, R.** (1996). The intercellular adhesin involved in biofilm accumulation of *Staphylococcus epidermidis* is a linear β-1,6-linked glucosaminoglycan: Purification and structural analysis. *Journal of Bacteriology*, *178*(1), 175–183.

**MacLean, L. L., Perry, M. B., Chen, W., & Vinogradov, E.** (2009). The structure of the polysaccharide O-chain of the LPS from *Acinetobacter baumannii* strain ATCC 17961. *Carbohydrate Research*, *344*(4), 474–478.

**Maira-Litrán, T., Kropec, A., Abeygunawardana, C., Joyce, J., Mark III, G., Goldmann, D. A., & Pier, G. B.** (2002). Immunochemical properties of the

Staphylococcal poly-*N*-acetylglucosamine surface polysaccharide. *Infection and Immunity*, *70*(8), 4433–4440.

**Maira-Litran, T., Kropec, A., Goldmann, D., & Pier, G. B.** (2004). Biologic properties and vaccine potential of the staphylococcal poly-*N*-acetyl glucosamine surface polysaccharide. *Vaccine*, *22*(7), 872–879.

**Maldonado, R. F., Sá-Correia, I., & Valvano, M. A.** (2016). Lipopolysaccharide modification in Gram-negative bacteria during chronic infection. *FEMS Microbiology Reviews*, *40*(4), 480–493.

**McKenney, D., Pouliot, K. L., Wang, Y., Murthy, V., Ulrich, M., Döring, G., Lee, J. C., Goldmann, D. A., & Pier, G. B.** (1999). Broadly protective vaccine for *Staphylococcus aureus* based on an in vivo-expressed antigen. *Science*, *284*(5419), 1523–1527.

**Monteiro, J. M., Fernandes, P. B., Vaz, F., Pereira, A. R., Tavares, A. C., Ferreira, M. T., Pereira, P. M., Veiga, H., Kuru, E., VanNieuwenhze, M. S., Brun, Y. V, Filipe, S. R., & Pinho, M. G.** (2015). Cell shape dynamics during the staphylococcal cell cycle. *Nature Communications*, *6*, 8055.

**Murakami, Y., Hasegawa, Y., Nagano, K., & Yoshimura, F.** (2014). Characterization of wheat germ agglutinin lectin-reactive glycosylated OmpA-like proteins derived from Porphyromonas gingivalis. *Infection and Immunity*, *82*(11), 4563–4571.

**Nait Chabane, Y., Marti, S., Rihouey, C., Alexandre, S., Hardouin, J., Lesouhaitier, O., Vila, J., Kaplan, J. B., Jouenne, T., & Dé, E.** (2014). Characterisation of Pellicles Formed by *Acinetobacter baumannii* at the Air-Liquid Interface. *PLOS ONE*, *9*(10), e111660.

**Naughton, J. A., Mariño, K., Dolan, B., Reid, C., Gough, R., Gallagher, M. E., Kilcoyne, M., Gerlach, J. Q., Joshi, L., Rudd, P., Carrington, S., Bourke, B., & Clyne, M.** (2013). Divergent mechanisms of interaction of *Helicobacter pylori* and *Campylobacter jejun*i with mucus and mucins. *Infection and Immunity*, *81*(8), 2838–2850.

**O'Neill, E., Pozzi, C., Houston, P., Humphreys, H., Robinson, D. A., Loughman, A., Foster, T. J., & O'Gara, J. P.** (2008). A novel *Staphylococcus aureus* biofilm phenotype mediated by the fibronectin-binding proteins, FnBPA and FnBPB. *Journal of Bacteriology*, *190*(11), 3835–3850.

**O'Neill, E., Pozzi, C., Houston, P., Smyth, D., Humphreys, H., Robinson, D. A., & O'Gara, J. P.** (2007). Association between methicillin susceptibility and biofilm regulation in *Staphylococcus aureus* isolates from device-related infections. *Journal of Clinical Microbiology*, *45*(5), 1379–1388.

**Otto, M.** (2008). Staphylococcal biofilms. *Current Topics in Microbiology and Immunology* 332, 207-228.

**Pour, N. K., Zamin, F. R., Chopade, B. A., Dusane, D. H., Zinjarde, S. S., & Dhakephalkar, P. K.** (2011). Biofilm formation by *Acinetobacter baumannii* strains isolated from urinary tract infection and urinary catheters. *FEMS*

*Immunology & Medical Microbiology*, *62*(3), 328–338.

**Pozzi, C., Waters, E. M., Rudkin, J. K., Schaeffer, C. R., Lohan, A. J., Tong, P., Loftus, B. J., Pier, G. B., Fey, P. D., Massey, R. C., & O'Gara, J. P.** (2012). Methicillin resistance alters the biofilm phenotype and attenuates virulence in *Staphylococcus aureus* device-associated infections. *PLoS Pathogens*, *8*(4).

**Rachid, S., Ohlsen, K., Wallner, U., Hacker, J., Hecker, M., & Ziebuhr, W.** (2000). Alternative transcription factor σB is involved in regulation of biofilm expression in a *Staphylococcus aureus* mucosal isolate. *Journal of Bacteriology*, *182*(23), 6824–6826.

**Ramos, Y., Rocha, J., Hael, A. L., van Gestel, J., Vlamakis, H., Cywes-Bentley, C., Cubillos-Ruiz, J. R., Pier, G. B., Gilmore, M. S., Kolter, R., & Morales, D. K.** (2019). PolyGlcNAc-containing exopolymers enable surface penetration by non-motile *Enterococcus faecalis*. *PLOS Pathogens*, *15*(2), e1007571.

**Regassa, L. B., Novick, R. P., & Betley, M. J**. (1992). Glucose and nonmaintained pH decrease expression of the accessory gene regulator (agr) in *Staphylococcus aureus*. Infection and Immunity, *60*(8), 3381 LP-3388.

**Reśliński, A., & Dabrowiecki, S. (2013).** Evaluation of the effect of glucose on Staphylococcus aureus and Escherichia coli biofilm formation on the surface of polypropylene mesh. Medycyna Doświadczalna i Mikrobiologia, *65*(1), 19-26.

**Richie, D. L., Takeoka, K. T., Bojkovic, J., Metzger IV, L. E., Rath, C. M., Sawyer, W. S., Wei, J.-R., & Dean, C. R.** (2016). Toxic Accumulation of LPS Pathway Intermediates Underlies the Requirement of LpxH for Growth of *Acinetobacter baumannii* ATCC 19606. *PLOS ONE*, *11*(8), e0160918.

**Roche, F. R., Meehan, M., & Foster, T. J.** (2003). The *Staphylococcus aureus* surface protein SasG and its homologues promote bacterial adherence to human desquamated nasal epithelial cells. *Microbiology*, *149*(10), 2759–2767.

**Saadi, A. T., Weir, D. M., Poxton, I. R., Stewart, J., Essery, S. D., Caroline Blackwell, C., Raza, M. W., & Busuttil, A.** (1994). Isolation of an adhesin from *Staphylococcus aureus* that binds Lewis blood group antigen and its relevance to sudden infant death syndrome. *FEMS Immunology and Medical Microbiology*, *8*(4), 315–320.

**Sadovskaya, I., Vinogradov, E., Flahaut, S., Kogan, G., & Jabbouri, S.** (2005). Extracellular Carbohydrate-Containing Polymers of a Model Biofilm-Producing Strain, *Staphylococcus epidermidis* RP62A. *Infection and Immunity*, *73*(5), 3007 LP-3017.

**Sanford, B. A., Thomas, V. L., Mattingly, S. J., Ramsay, M. A., & Miller, M. M.** (1995). Lectin-biotin assay for slime present in in situ biofilm produced by *Staphylococcus epidermidis* using transmission electron microscopy (TEM). *Journal of Industrial Microbiology*, *15*(3), 156–161.

**Satorius, A. E., Szafranski, J., Pyne, D., Ganesan, M., Solomon, M. J., Newton, D. W., Bortz, D. M., & Younger, J. G.** (2013). Complement C5a generation by staphylococcal biofilms. *Shock*, *39*(4), 336–342.

**Scott, N. E., Kinsella, R. L., Edwards, A. V. G., Larsen, M. R., Dutta, S., Saba, J., Foster, L. J., & Feldman, M. F.** (2014). Diversity within the O-linked protein glycosylation systems of *Acinetobacter* species. *Molecular & Cellular Proteomics : MCP*, *13*(9), 2354–2370.

**Silhavy, T. J., Kahne, D., & Walker, S.** (2010). The bacterial cell envelope. *Cold Spring Harbor Perspectives in Biology*, *2*(5).

**Strathmann, M., Wingender, J., & Flemming, H.-C.** (2002). Application of fluorescently labelled lectins for the visualization and biochemical characterization of polysaccharides in biofilms of *Pseudomonas aeruginosa*. *Journal of Microbiological Methods*, *50*(3), 237–248.

**Sugimoto, S., Sato, F., Miyakawa, R., Chiba, A., Onodera, S., Hori, S., & Mizunoe, Y.** (2018). Broad impact of extracellular DNA on biofilm formation by clinically isolated Methicillin-resistant and -sensitive strains of *Staphylococcus aureus*. *Scientific Reports*, *8*(1).

**Utratna, M., Annuk, H., Gerlach, J. Q., Lee, Y. C., Kane, M., Kilcoyne, M., & Joshi, L.** (2017). Rapid screening for specific glycosylation and pathogen interactions on a 78 species avian egg white glycoprotein microarray. *Scientific Reports*, *7*(1), 6477.

**Vuong, C., Voyich, J. M., Fischer, E. R., Braughton, K. R., Whitney, A. R., DeLeo, F. R., & Otto, M.** (2004). Polysaccharide intercellular adhesin (PIA) protects *Staphylococcus epidermidis* against major components of the human innate immune system. *Cellular Microbiology*, *6*(3), 269–275.

**Wacklin, P., Mäkivuokko, H., Alakulppi, N., Nikkilä, J., Tenkanen, H., Räbinä, J., Partanen, J., Aranko, K., & Mättö, J.** (2011). Secretor genotype (FUT2 gene) is strongly associated with the composition of bifidobacteria in the human intestine. *PLoS ONE*, *6*(5).

**Wang, L., Cummings, R. D., Smith, D. F., Huflejt, M., Campbell, C. T., Gildersleeve, J. C., Gerlach, J. Q., Kilcoyne, M., Joshi, L., Serna, S., Reichardt, N. C., Pera, N. P., Pieters, R. J., Eng, W., & Mahal, L. K.** (2014). Cross-platform comparison of glycan microarray formats. *Glycobiology*, *24*(6), 507–517.

**Wang, X., Preston III, J. F., & Romeo, T.** (2004). The pgaABCD Locus of Escherichia coli Promotes the Synthesis of a Polysaccharide Adhesin Required for Biofilm Formation. *Journal of Bacteriology*, *186*(9), 2724–2734.

**Wang, Y.-C., Huang, T.-W., Yang, Y.-S., Kuo, S.-C., Chen, C.-T., Liu, C.-P., Liu, Y.-M., Chen, T.-L., Chang, F.-Y., Wu, S.-H., How, C.-K., & Lee, Y.-T.** (2018). Biofilm formation is not associated with worse outcome in *Acinetobacter baumannii* bacteraemic pneumonia. *Scientific Reports*, *8*(1).

**Wardenburg, J. B., Patel, R. J., & Schneewind, O.** (2007). Surface proteins and exotoxins are required for the pathogenesis of *Staphylococcus aureus* pneumonia. *Infection and Immunity*, *75*(2), 1040–1044.

**Whitfield, G. B., Marmont, L. S., & Howell, P. L.** (2015). Enzymatic

modifications of exopolysaccharides enhance bacterial persistence. *Frontiers in Microbiology*, *6*, 471.

**Xia, G., Kohler, T., & Peschel, A.** (2010). The wall teichoic acid and lipoteichoic acid polymers of *Staphylococcus aureus*. *International Journal of Medical Microbiology*, *300*(2), 148–154.

**Xia, G., Maier, L., Sanchez-Carballo, P., Li, M., Otto, M., Holst, O., & Peschel, A.** (2010). Glycosylation of wall teichoic acid in *Staphylococcus aureus* by TarM. *Journal of Biological Chemistry*, *285*(18), 13405–13415.

**Yang, Y.-H., Jiang, Y.-L., Zhang, J., Wang, L., Bai, X.-H., Zhang, S.-J., Ren, Y.-M., Li, N., Zhang, Y.-H., Zhang, Z., Gong, Q., Mei, Y., Xue, T., Zhang, J.-R., Chen, Y., & Zhou, C.-Z.** (2014). Structural Insights into SraP-Mediated *Staphylococcus aureus* Adhesion to Host Cells. *PLoS Pathogens*, *10*(6).

**Yasuda, E., Tateno, H., Hirabayashi, J., Iino, T., & Sako, T.** (2011). Lectin microarray reveals binding profiles of *Lactobacillus casei* strains in a comprehensive analysis of bacterial cell wall polysaccharides. *Applied and Environmental Microbiology*, *77*(16), 5834.

**You, Y., Xue, T., Cao, L., Zhao, L., Sun, H., & Sun, B.** (2014). Staphylococcus aureus glucose-induced biofilm accessory proteins, GbaAB, influence biofilm formation in a PIA-dependent manner. International Journal of Medical Microbiology, 304(5), 603–612.

# Chapter 3

# Modulating targeted bacterial interactions using glycoclusters on a microarray platform

# 3. Modulating targeted bacterial interactions using glycoclusters on a microarray platform

## 3.1. Introduction

Bacterial pathogens have many carbohydrate-containing surface molecules such as peptidoglycan, lipopolysaccharide (LPS) and lipoteichoic acid (LTA) (Tra & Dube, 2014; Weidenmaier & Peschel, 2008) which are recognised by host pathogen recognition receptors (PRRs). These recognition events initiate an immune response to eliminate the pathogen or, by the manipulation of the bacterial molecules, help the bacteria to evade the host's immune system (Casas-Solvas & Vargas-Berenguel, 2015). Indeed, the initial attachment of bacteria to host cell surfaces and extracellular matrix (ECM) molecules is the first step in infection or colonisation and is frequently carbohydrate-mediated. Therefore preventing adhesion of the pathogen to the relevant host cell has long been proposed as a crucial intervention point for infection prevention. However, elucidating individual molecular interactions between the cells or assessing the efficacy or efficiency of targeting specific interactions is often difficult due to the multiplicity of parallel biological interactions and complexity of both pathogen and host surface molecules presented.

Targeting specific carbohydrate-mediated pathogen-host interactions for anti-infective or therapeutic strategies is a major goal of glycocluster synthesis (Casas-Solvas *et al.*, 2015). Calix[4]arene-based glycoclusters functionalized with galactosides or fucosides were shown to be effective in the reduction of the surface adhesins LecB- and LecA–dependent *Pseudomonas aeruginosa* aggregation, biofilm formation, cell adhesion and lung infection in a mouse model (Boukerb *et al.*, 2014). Recently, a panel of glycoclusters with *N*-acetylglucosamine (GlcNAc) as the bioactive headgroups were synthesized to inhibit carbohydrate-lectin interactions (André *et al.*, 2015). These compounds varied in valency from bi- to tetra-valent, in scaffold length and orientation, and anomeric linkages. GlcNAc-mediated binding inhibition of fetuin, asialofetuin (ASF), agalactoASF, the GlcNAc-BSA neoglycoconjugate and the wildtype and the glycosylation mutants Lec2 and Lec8 Chinese hamster ovary (CHO) cells was assessed using wheat germ agglutinin (WGA) and *Griffonia simplicifolia* lectin-II (GSL-II) and these glycoclusters in 96 well microtitre plate-based assays. The 96 well microtitre plate format assays are

typically used to assess inhibition and half inhibitory concentration ($IC_{50}$) values for synthetic glycoclusters (André *et al.*, 2015; Buffet *et al.*, 2016; Maierhofer *et al.*, 2007; Swanson *et al.*, 2015), but this format requires larger quantities of glycoclusters and biologically derived molecules which may have only limited availability.

Lectin microarrays were developed to sensitively and rapidly profile glycosylation associated with different molecules and the surfaces of organisms and to elucidate carbohydrate-lectin interactions (Hu *et al*., 2009). Lectin microarrays have been used for a variety of applications and samples including glycoprotein, bacteria, eukaryotic cell, virus and virus-related particle profiling, but have not been frequently used for quantitative measurements (Hsu et al., 2006; Kilcoyne et al., 2014; Krishnamoorthy et al., 2009; Rosenfeld et al., 2007; Tao et al., 2008). Previously, lectin microarray platforms have been used for quantifying the lowest limit of detection of lectins for various carbohydrate structures (Uchiyama *et al.*, 2008) and $IC_{50}$ and apparent dissociation constants (Liang *et al*., 2007; Wang *et al*., 2013). Thus, lectin microarray technology may provide a more sensitive platform for routine generation of $IC_{50}$ measurements with low sample and reagent consumption.

Poly-*N*-acetylglucosamine (PNAG) is a common cell surface bacterial antigen found on a wide range of pathogenic bacteria such as *Staphylococcus*, *Enterococcus* species, *Candida*, *Escherichia*, *Klebsiella*, *Enterobacter* species and *Acinetobacter*. PNAG is often involved in bacterial biofilm formation, is a major component of certain biofilms, and has also been used as a vaccine candidate against many pathogenic bacteria such as methicillin resistant *Staphylococcus aureus* (MRSA) (Skurnik *et al.*, 2016). This β-(1→6)-linked GlcNAc polysaccharide is partially deacetylated to varying degrees, depending on the bacterial genus and species (Mack *et al*., 1996; Maira-Litrán *et al*., 2002; Wang *et al*., 2004). *S. aureus* PNAG was associated with an increase in abscess lesions and bacterial burden in a mouse model, promotion of bacterial adherence to human nasal epithelial cells (Lin *et al.*, 2015), found to be essential for virulence in murine models of systemic infection (Kropec *et al.*, 2005) and found to be an important component involved in biofilm formation that contribute to medical device associated infections (O'Neill *et al.*, 2007). PNAG is also the primary virulence factor for *S. epidermidis* (O'Gara, 2007). *S. aureus* is classified as a priority level 2 by the World Health Organisation for the development

of novel antimicrobial agents against this pathogen (Tacconelli *et al.*, 2018). Furthermore, *S. aureus* is commonly associated with medical device infections, which can be promoted by PNAG (Archer *et al.*, 2011).

In addition, *S. aureus* is one of the most frequently found pathogens in lung infections in cystic fibrosis (CF) patients (Kiedrowski *et al.*, 2018) and is known to preferentially bind to respiratory mucus from both CF and normal lungs (Ulrich *et al.*, 1998). Although PNAG is known to promote binding of *S. aureus* to human nasal epithelial cells (Lin *et al.*, 2015), it's role in *S. aureus* binding to lung mucin in CF patients is unknown. While progress has been made in the development of glycoclusters that inhibit biofilm formation of *P. aeruginosa* (Ligeour *et al.*, 2015; Smadhi *et al.*, 2014), a common lung pathogen in CF patients, to the best of our knowledge, glycoclusters have not been used to modulate *Staphylococcus*-lectin mediated interactions. Thus, targeting PNAG interactions of *S. aureus* with lectins or mucins or targeting *S. aureus* biofilm formation using tailored glycoclusters may provide therapeutic benefit.

WGA has binding specificity for GlcNAc and sialic acid residues (Monsigny *et al.*, 1980) and labelled WGA is routinely used to detect PNAG in biofilms (Arciola *et al.*, 2015; Begun *et al.*, 2007; Singh *et al.*, 2010), although the particular WGA-PNAG interactions have not been studied to date. In this study, lectin microarrays were assessed for sensitivity and suitability for measuring $IC_{50}$ values of a panel of six divalent GlcNAc glycoclusters by inhibiting ovalbumin and the neoglycoconjugate GlcNAc-BSA binding to WGA. Partially purified *S. aureus* PNAG was fluorescently labelled by direct conjugation and by covalently attaching the polysaccharide to a fluorescent bead of 1 μm in diameter, which is similar to the diameter of a bacterial cell. These two novel labelling techniques for PNAG provide methods of directly detecting PNAG in two presentations that would be physiologically similar to that in a biofilm matrix, PNAG as an extracellular polymeric substance within the biofilm matrix and adhered to a bacterium. In a novel application of the lectin microarray platform, the glycoclusters were used to inhibit binding of PNAG and whole *S. aureus* to WGA. In addition, the glycoclusters were assessed for their ability to inhibit biofilm formation of *S. aureus*. One glycocluster was also tested for inhibition of binding of whole *S. aureus* and PNAG to lung mucin from a CF patient. Overall, this research contributes to the development of a

novel, high throughput (HTP) method of measuring glycocluster $IC_{50}$ inhibition values with low reagent consumption. Moreover, physiologically relevant methods of labelling PNAG provided in this study will facilitate the identification of PNAG associated host-microbe interactions using methods that require fluorescent labelling for analysis.

## 3.2. Materials and methods

### 3.2.1. Materials and bacterial strains

Alexa Fluor® 555 (AF555) carboxylic acid succinimydyl ester, FluoSpheres™ (FS) carboxylate-modified microspheres (1.0 μm orange fluorescent (540/560), 2% (w/v)), mouse anti-LTA IgG monoclonal antibody, mouse anti-peptidoglycan monoclonal IgG1 antibody (3F6B3 (10H6)), Pierce™ Enhanced Chemiluminescence (ECL) Western Blotting Substrate, and Nunclon™ (Δ surface) 96-well microtitre plates were purchased from Thermo-Fisher Scientific (Dublin, Ireland). The Δ certification is a proprietary cell culture surface treatment that offers maximum adhesion for a broad range of cell types and is used for biofilm assays. Amicon® Ultra 3 kDa molecular weight cut off (MWCO) centrifugal filters and Immobilon-P 0.45 μm polyvinylidene difluoride (PVDF) membrane were from Merck-Millipore (Cork, Ireland). Pure, unlabelled lectins were from EY Labs (CA, USA) or Vector Labs (Peterborough, United Kingdom) (Table 3.1). Hydrophobic 96-well microtitre plates were obtained from Starstedt Ltd. (Wexford, Ireland). Corning® Costar® 96-Well Cell Culture Plates, and ovalbumin were purchased from Sigma-Aldrich (Wicklow, Ireland). Rabbit anti-human IgG antibody conjugated to horse radish peroxidase (HRP) and goat anti-mouse Ig-HRP were purchased from DAKO (CA, USA). GlcNAc-BSA was purchased from Dextra Labs (Reading, UK). Partially purified PNAG from *S. aureus* Mn8m and mAb anti-PNAG F598 were kind gifts from Prof. G. Pier, Harvard University, MA, USA (Kelly-Quintos *et al.,* 2006). Glycoclusters were a kind gift from Prof. Paul Murphy, NUI Galway, Ireland (André *et al.*, 2015). Siliconized microcentrifuge tubes, water for cell biology (free of endotoxins, ultrafiltered and autoclaved), polypropylene 1-ethyl-3-(3-dimethylaminopropyl)carbodiimide (EDC), 2-(*N*-morpholino)ethanesulfonic acid hydrate (MES), *N*-hydroxysulfosuccinimide sodium salt (sulfo-NHS), ethalonamine and other regents were purchased from Sigma-Aldrich (Wicklow, Ireland) unless otherwise stated and were of the highest grade available. All other materials used were as per section 2.2.1.

*S. aureus* strains 8325-4, 8325-4 Δ*ica*, Mn8m, Mn8 Δ*ica*, BH1CC and BH1CC Δ*ica* (Table 2.1) were used in this study.

### 3.2.2. Bacterial growth conditions

Bacteria were grown on Brain Heart Infusion (BHI) agar. Agar was supplemented with tetracycline (5 μg/mL) for all *S. aureus* Δ*ica* strains. Bacteria were grown in overnight in 5 mL cultures at 37 °C shaking at 180 rpm in BHI, BHI supplemented with 1% (w/v) glucose (BHI glucose) or BHI supplemented with 4% (w/v) NaCl (BHI NaCl) where indicated. Overnight cultures were approximately 17 h incubations.

### 3.2.3. Direct fluorescent labelling of proteins and PNAG

Ovalbumin (1 mg), GlcNAc-BSA (1 mg) and invertase (1 mg) were labelled with AF555 carboxylic acid succinimidyl ester according to the manufacturer's instructions. Briefly, 500 μL of a 2 mg/mL solution of the individual protein in 100 mM sodium bicarbonate, pH 8, was placed in an amber tube and 0.1 mg of Alexa Fluor® 555 solubilised in 10 μL dimethylsulfoxide (DMSO) was added. The mixture was incubated at 25 °C for 2 h in the dark and protected from light throughout the procedure. The conjugated proteins were then purified using a 3 kDa MWCO centrifugal filter with phosphate buffered saline (PBS), pH 7.4, according to manufacturer's instructions. PBS (300 μL) was added three times to ensure complete buffer exchange and then 200 μL of PBS was added to the filter retentate and recovered. AF555 labelled GlcNAc-BSA (GlcNAc-BSA-AF555) and ovalbumin (ovalbumin-AF555) were quantified for protein concentration and label substitution according to manufacturer's instructions using the extinction coefficients and molecular masses of 29,300 $M^{-1}$ $cm^{-1}$ (Batra *et al.*, 1990) and 42,700 Da (Nisbet *et al.*, 1981), respectively, for ovalbumin, 43,824 $M^{-1}$ $cm^{-1}$ and 66,430 Da for GlcNAc-BSA (the extinction coefficient at 280 nm and molecular mass of BSA, respectively) (Wang *et al*., 2011) and 621,000 $M^{-1}$ $cm^{-1}$ and 270,000 Da for invertase (Andjelković *et al.*, 2010).

For labelling, PNAG was initially solubilised at 4 mg/mL in 5 M HCl and pH was immediately adjusted to 7 with 5 M NaOH. The solubilised PNAG was then diluted to 2 mg/mL in 0.1 M sodium borate (final concentration) and 0.1 mg of AF555 carboxylic acid succinimidyl ester in 10 μL DMSO was added. The mixture was incubated and purified as detailed above. AF555 labelled PNAG (PNAG-AF555)

(approximately 5 mg/mL) was not directly quantified after labelling but was titrated for optimal incubation concentration on lectin microarrays as detailed below.

### 3.2.4. Bacterial fluorescent labelling

Bacterial labelling was carried out as previously described (Kilcoyne *et al.*, 2014; Section 2.2.6) with some minor alterations. *S. aureus* Mn8m wildtype (WT) and Mn8 Δ*ica* were grown overnight in 5 mL BHI glucose at 37 °C for 24 h at 180 rpm. Bacteria were harvested, pelleted by centrifugation (5,000 × g, 5 min), washed three times in Tris(hydroxymethyl)aminomethane (Tris) buffered saline supplemented with 1 mM each of $Ca^{2+}$ and $Mg^{2+}$ ions (TBS; 20 mM Tris-HCl, 100 mM NaCl, 1 mM $CaCl_2$, 1 mM $MgCl_2$, pH 7.2), and resuspended in TBS to an absorbance at 595 nm of approximately 1.0. Bacteria (1 mL) were stained by adding 5 μM SYTO® 82 and incubated at 37 °C for 1 h at 180 rpm. The fluorescently labelled cells were then washed three times in TBS by resuspending bacteria in 1 mL TBS, centrifuging at 5,000 x g for 5 min and removing the supernatant. Bacterial cells were finally resuspended in 0.5 mL of TBS supplemented with 0.025% Tween-20 (TBS-T).

### 3.2.5. Conjugation of protein and PNAG to FluoSpheres®

For activation, 100 μL of the carboxylate-modified FS was added to 1 mL 50 mM 2-(N-morpholino)ethanesulfonic acid (MES), pH 6 (activation buffer), in a 1.5 mL siliconised microcentrifugal tube. The FluoSpheres® were mixed thoroughly before centrifugation at 6,000 x g for 20 min. The supernatant was discarded and this washing step with activation buffer was repeated two more times. The FS were then resuspended in 1 mL activation buffer, and dispersed by vortexing. Immediately after preparation, EDC was solubilised in 18.2 MΩ water and added to the 1 mL FS solution to a final concentration of 3.8 mM and sulfo-NHS was solubilised in activation buffer and added to the 1 mL FS solution to a final concentration of 38 mM. The samples were mixed for 30 min at 10 rpm at room temperature. The FS were washed three times with activation buffer and finally resuspended in 700 μL of activation buffer.

Sixty uL of 2 mg/mL protein or polysaccharide in activation buffer was added to 140 μL of the activated FS solution and mixed for 2.5 h at 10 rpm at room temperature. The mixture was made to 1 mL with activation buffer, ethanolamine was added to a

final concentration of 500 mM and then mixed for 30 min at 10 rpm at room temperature. The conjugated FS were then centrifuged as above, the supernatant was removed and the pellet was resuspended in 1 mL of 50 mM Tris supplemented with 0.5% casein (w/v), pH 8 (blocking buffer). The samples were mixed thoroughly and incubated overnight at 4 °C at 10 rpm. Then the conjugated FS were washed twice in blocking buffer by centrifugation, resuspended in 500 µL TBS (approximately 1 x $10^5$ conjugated FS), stored at 4 °C and used within 2 d. For FS conjugated samples, the designation –FS is used from hereon (e.g. PNAG-FS).

### 3.2.6. Dot blot assays to verify the presence of PNAG

PVDF membrane (0.45 µm) was pre-treated for 15 s in methanol and then soaked in TBS, pH 7.2, for 5 min. Samples (2 µL each of 1 mg/mL partially purified PNAG, stock PNAG-AF555 or stock PNAG-FS) were applied by pipette to the wet membrane, allowed to dry for 5 min and then washed twice in distilled water. Membranes were then incubated for 1 h in 5% (w/v) skimmed milk in TBS (blocking solution) at room temperature. After removal of blocking solution, the membrane was incubated with human anti-PNAG IgG1 monoclonal antibody (F598) (800 µg/mL in TBS supplemented with 0.0001% Tween 20 and 1% skimmed milk (incubation solution)) and incubated at room temperature for 1 h. The primary antibody solution was removed and the membrane was washed three times for 5 min each in TBS supplemented with 0.0001% Tween-20 and once in TBS for 5 min. The membrane was then incubated in HRP-conjugated rabbit anti-human IgG antibody (200 µg/mL in incubation solution) for 1 h at room temperature. The membrane was washed again as described above and incubated with 1 mL ECL substrate for 1 min. HRP activity was visualised immediately using a chemiluminescent camera (FluorChem FC2 Imaging System, Alpha Innotech, Kasendorf, Germany) and digital images were stored as .tif files.

For the detection of peptidoglycan, the same procedure was carried out as described above, except 2 µL of heat killed *S. aureus* Mn8m (8 x $10^8$ cells/mL) was spotted on the membrane as a positive control. A mouse anti-peptidoglycan IgG1 monoclonal antibody was used as the primary antibody (1:50 dilution in incubation solution) and a goat anti-mouse-HRP antibody (200 µg/mL in incubation solution) was used as the secondary antibody.

For detection of LTA, 2 µL of 1 mg/mL partially purified PNAG or dilutions of SA-LTA (25, 6.25 and 1.56 µg/mL) in endotoxin-free, sterilised water for a standard curve was applied to the membrane and incubated as described above. The primary antibody was a mouse anti-LTA IgG monoclonal antibody (1 in 50 dilution in incubation solution) and detection was done using a goat anti-mouse-HRP antibody (200 µg/mL in incubation solution). Digital images were converted to .jpg and used to relatively quantify the LTA. Intensities for LTA standard concentrations were quantified in duplicates using ImageJ software (NIH, available via https://imagej.nih.gov/ij/) using the same size frame for each sample. The average of the intensities for each LTA standard concentration was graphed as a line and the approximate concentration of LTA in the partially purified PNAG was quantified.

### 3.2.7. Lectin microarray construction

Lectin microarrays were prepared essentially as previously described (Kilcoyne *et al.*, 2014) and Section 2.2.5. In brief, a panel of 48 lectins of known specificities (Table 3.1) were printed at 0.5 mg/mL in PBS, pH 7.4 supplemented with 1 mM of their respective haptenic simple sugars (Table 3.1) on Nexterion ® slide H microarray slides using a SciFlexArrayer S3 (Scienion, Berlin, Germany) equipped with a 90 um diameter uncoated glass nozzle under constant humidity (62 +/- 2%) at 18 °C (+/- 2 °C). Lectins were printed as features of approximately 1 nL and each lectin was printed in 6 replicates per subarray, with 8 replicate subarrays per microarray slide. Printed slides were placed in a humidity chamber overnight and then blocked with 100 mM ethanolamine in 50 mM sodium borate, pH 8, for 1 h at room temperature. Slides were washed three times with PBS with 0.05% Tween-20 (PBS-T), and once with PBS for 2 min per wash. Slides were dried by centrifugation (1,500 x g, 5 min) and stored at 4°C with desiccant until use. Quality control of lectin printing and function was carried out by incubation of each subarray individually with a panel of AF555 labelled glycoproteins (1 µg/mL in TBS-T each of bovine fetuin, asialofetuin, yeast invertase, hen egg ovalbumin, RNase B, alpha-1 acid glycoprotein and GlcNAc-BSA).

**Table 3.1. Lectins printed, their binding specificities, their print sugars (1 mM) and the supplying company.**

| Abbreviation | Source | Species | Common name | General binding specificity* | Print sugar | Supplier |
|---|---|---|---|---|---|---|
| AIA, Jacalin | Plant | *Artocarpus integrifolia* | Jack fruit lectin | Gal, Gal-β-(1,3)-GalNAc (sialylation independent) | Gal | EY Labs |
| RPbAI | Plant | *Robinia pseudoacacia* | Black locust lectin | Gal | Gal | EY Labs |
| SNA-II | Plant | *Sambucus nigra* | Sambucus lectin-II | Gal/GalNAc | Gal | EY Labs |
| SJA | Plant | *Sophora japonica* | Pagoda tree lectin | β-GalNAc | Gal | EY Labs |
| DBA | Plant | *Dolichos biflorus* | Horse gram lectin | GalNAc | Gal | EY Labs |
| GHA | Plant | *Glechoma hederacea* | Ground ivy lectin | GalNAc | Gal | EY Labs |
| SBA | Plant | *Glycine max* | Soy bean lectin | GalNAc | Gal | EY Labs |
| VVA | Plant | *Vicia villosa* | Hairy vetch lectin | GalNAc | Gal | EY Labs |
| BPA | Plant | *Bauhinia purpurea* | Camels foot tree lectin | GalNAc/Gal | Gal | EY Labs |
| WFA | Plant | *Wisteria floribunda* | Japanese wisteria lectin | GalNAc/sulfated GalNAc | Gal | EY Labs |
| HPA | Animal | *Helix pomatia* | Edible snail lectin | α-GalNAc | Gal | EY Labs |
| GSL-I-A4 | Plant | *Griffonia simplicifolia* | Griffonia isolectin I A4 | GalNac | Gal | EY Labs |
| ACA | Plant | *Amaranthus caudatus* | Amaranthin | Sialylated/Gal-β-(1,3)-GalNAc | Lac | Vector Labs |
| ABL | Fungus | *Agaricus bisporus* | Edible mushroom lectin | Gal-β(1,3)-GalNAc, GlcNAc | Lac | EY Labs |
| PNA | Plant | *Arachis hypogaea* | Peanut lectin | Gal-β-(1,3)-GalNAc | Lac | EY Labs |
| GSL-II | Plant | *Griffonia simplicifolia* | Griffonia lectin-II | GlcNAc | GlcNAc | EY Labs |
| sWGA | Plant | *Triticum vulgaris* | Succinyl WGA | GlcNAc | GlcNAc | EY Labs |
| DSA | Plant | *Datura stramonium* | Jimson weed lectin | GlcNAc | GlcNAc | EY Labs |
| STA | Plant | *Solanum tuberosum* | Potato lectin | GlcNAc oligomers | GlcNAc | EY Labs |
| LEL | Plant | *Lycopersicum eculentum* | Tomato lectin | GlcNAc-β-(1,4)-GlcNAc | GlcNAc | EY Labs |
| Calsepa | Plant | *Calystegia sepium* | Bindweed lectin | Man/Maltose | Man | EY Labs |
| NPA | Plant | *Narcissus pseudonarcissus* | Daffodil lectin | α-(1,6)-Man | Man | EY Labs |
| GNA | Plant | *Galanthus nivalis* | Snowdrop lectin | Man-α-(1,3)- | Man | EY Labs |
| HHA | Plant | *Hippeastrum hybrid* | Amaryllis agglutinin | Man-α-(1,3)-Man-α-(1,6)- | Man | EY Labs |
| ConA | Plant | *Canavalia ensiformis* | Jack bean lectin | Man, Glc, GlcNAc | Man | EY Labs |
| Lch-B | Plant | *Lens culinaris* | Lentil isolectin B | Man, core fucosylated, agalactosylated biantennary *N*-glycans | Man | EY Labs |
| Lch-A | Plant | *Lens culinaris* | Lentil isolectin A | Man/Glc | Man | EY Labs |
| PSA | Plant | *Pisum sativum* | Pea lectin | Man, core fucosylated | Man | EY Labs |

| | | | | | | |
|---|---|---|---|---|---|---|
| | | | | trimannosyl *N*-glycans | | |
| TJA-I | Plant | *Trichosanthes japonica* | Trichosanthes japonica Agglutinin I | NeuAc-α-(2,6)-Gal-β-(1,4)-GIcNAc | Lac | Medicago |
| WGA | Plant | *Triticum vulgaris* | Wheat germ agglutinin | NeuAc/GlcNAc | GlcNAc | EY Labs |
| MAA | Plant | *Maackia amurensis* | Maackia agglutinin | Sialic acid-α-(2,3)-linked | Lac | EY Labs |
| SNA-I | Plant | *Sambucus nigra* | Sambucus lectin-I | Sialic acid-α-(2,6)-linked | Lac | EY Labs |
| CCA | Animal | *Cancer antennarius* | California crab lectin | *O*-acetyl sialic acids | Lac | EY Labs |
| PHA-L | Plant | *Phaseolus vulgaris* | Kidney bean leukoagglutinin | Tri- and tetraantennary β-Gal/Gal-β-(1,4)-GlcNAc | Lac | EY Labs |
| PHA-E | Plant | *Phaseolus vulgaris* | Kidney bean erythroagglutinin | Biantennary with bisecting GlcNAc,β-Gal/Gal-β-(1,4)-GlcNAc | Lac | EY Labs |
| AMA | Plant | *Arum maculatum* | Lords and ladies lectin | Gal-β-(1,4)-GlcNAc | Lac | EY Labs |
| CPA | Plant | *Cicer arietinum* | Chickpea lectin | Complex oligosaccharides | Lac | EY Labs |
| CAA | Plant | *Caragana arborescens* | Pea tree lectin | Gal-β-(1,4)-GlcNAc | Lac | EY Labs |
| ECA | Plant | *Erythrina cristagalli* | Cocks comb/coral tree lectin | Gal-β-(1,4)-GlcNAc oligomers | Lac | EY Labs |
| TJA-II | Plant | *Trichosanthes japonica* | Trichosanthes japonica Agglutinin II | Fuc-α-(1,2)-Gal-β-(1,4)-GlcNAc | Lac | Medicago |
| AAL | Fungi | *Aleuria aurantia* | Orange peel fungus lectin | Fuc-α-(1,6), -α-(1,3) | Fuc | Vector Labs |
| LTA | Plant | *Lotus tetragonolobus* | Lotus lectin | Fuc-α-(1,3) | Fuc | EY Labs |
| UEA-I | Plant | *Ulex europaeus* | Gorse lectin-I | Fuc-α-(1,2) | Fuc | EY Labs |
| PA-I | Bacteria | *Pseudomonas aeruginosa* | Pseudomonas lectin | α-Gal, Gal derivatives | Gal | EY Labs |
| MPA | Plant | *Maclura pomifera* | Osage orange lectin | α-Gal | Gal | EY Labs |
| VRA | Plant | *Vigna radiata* | Mung bean lectin | α-Gal | Gal | EY Labs |
| MOA | Fungus | *Marasmius oreades* | Fairy ring mushroom lectin | α-Gal | Gal | EY Labs |

* Reported recognition based on literature consensus or experimental evidence generated within our laboratory.

### 3.2.8. Lectin microarray incubations

All microarray incubations were carried out in the dark. In general, 70 uL of sample in TBS-T per subarray were incubated on each subarray of the lectin microarrays using an 8 well gasket (Agilent Technologies, Cork, Ireland) and incubated with gentle rotation (4 rpm) at 37 °C for 1 h. Microarray and gasket slides were disassembled under TBS-T, washed three times in TBS-T for 3 min each and once with TBS. Microarray slides were dried by centrifugation (1,500 x g, 5 min) and imaged immediately by scanning in a microarray scanner (G2505B microarray scanner, Agilent, CA,USA) equipped with a 532 nm laser (90% PMT, 5 µm resolution). Images were stored digitally as .tif files.

For incubations, labelled bacteria, PNAG-AF555, PNAG-FS, ovalbumin-AF555 and GlcNAc-BSA-AF555 were initially titrated by dilution in TBS-T to determine optimal signal to noise ratio and dilutions of 20 uL labelled bacteria: 50 µL TBS-T, 0.2 µL stock PNAG-AF555 per mL of TBS-T, 50 uL stock PNAG-FS: 20 µL TBS-T, 1 µg/mL of ovalbumin-AF555 and 0.1 µg/mL GlcNAc-BSA-AF555 in TBS-T were used. Glycoclusters were initially solubilised in 100 – 150 µL of DMSO, diluted to 10 mM in 18.2 MΩ water and stored at -20 °C until use. For glycocluster modulation studies, varying concentrations of glycoclusters (ranging from 0.01 fM to 1 mM) were pre-incubated with bacteria, PNAG-AF555, PNAG-FS, ovalubumins-AF555 or GlcNAc-BSA-AF555 for 15 min at room temperature prior to incubation on the microarray. The same concentration of DMSO present in the highest concentration of glycoclusters was also used as a control to monitor any potential effect on binding interactions.

### 3.2.9. Lectin microarray data extraction and analysis

Data extraction was performed essentially as previously described (Kilcoyne *et al.,* 2014; Section 2.2.8). In brief, raw intensity values were extracted from microarray image files (.tif) using GenePix Pro v6.1.0.4 software (Molecular Devices, Berkshire, U.K.) and a proprietary .gal file that held the address and identity of each feature using adaptive diameter (70-160%) circular alignment based on 230 mm features and were exported as text to Excel (Version 2007, Microsoft, Dublin, Ireland). Local background subtracted median feature intensity data (F543median-

B543) was analysed. The median of six replicate spots per subarray was handled as a single data point for graphical and statistical analysis. Data were normalized to the per subarray mean total intensity value of three replicate microarray slides and binding data was presented as a bar chart of average intensity of three experimental replicates with error bars of one standard deviation (SD) of the mean.

$IC_{50}$ curves were generated using GraphPad Prism 7 (GraphPad Software Inc., La Jolla, CA). Lectin microarray data were fitted to a four parameter Log (inhibitor) vs. response curve using a robust fit and an least squares fit to generate potency (IC $EC_{50}$) and best fit ($R^2$) values. Three replicate microarray slides were used to generate standard curves.

### 3.2.10. Biofilm inhibition assays

Each well of a Nunclon™ (Δ surface) 96-well microtitre plate was coated with 0.5 mM or 1 mM of each glycocluster in BHI glucose or BHI NaCl in triplicate for 30 min at room temperature. Overnight cultures grown in BHI media were adjusted to an absorbance at 595 nm of 1.0 in BHI glucose or BHI NaCl as appropriate. Cultures (100 µL) were added to each pre-incubated well (final cell dilution of 1:200). Plates were then incubated at 37 °C for 24 h, washed three times in a basin of distilled water and dried at 80 °C for up to 2 h. Crystal violet solution (0.4% (w/v) in deionised water, 100 µL) was added to each well and incubated for 5 min at room temperature. The wells were then washed three times with sterile water and 100 µL of 5% (v/v) acetic acid was added to each well. Staining was quantified by measuring absorbance at 490 nm on a SpectraMax M5e microplate reader (Molecular Devices, Inc., Berkshire, UK). Experiments were carried out in triplicate and the average absorbance of three experimental replicates was plotted as a bar chart with error bars of one SD of the mean. Significant differences were calculated by unpaired student's t-test using Excel v.10 (Microsoft, Washington, USA).

### 3.2.11. Bacterial tolerance assessment

*S. aureus* 8325-4 was grown overnight in BHI media, diluted to an absorbance of 0.06 at 595 nm in BHI media and 100 uL was placed in each well of a 96 well hydrophobic microtitre plate. Each glycocluster was added to bacteria in triplicate to a final concentration of 1 mM per well in triplicate for each glycocluster. Plates were

sealed with a breathable film and incubated at 37 °C for 24 h and absorbance at 595 nm was read every 30 min for 24 h with mixing for 1 min before measuring absorbance on a Tecan Sunrise Microplate Reader (Tecan UK Ltd., Reading, UK) with Megellan data analysis software.

### 3.2.12. Purification of human CF lung mucin

Lung mucus from anonymised CF patients was obtained from Dr. Michael O'Mahony from the University College Hospital Galway (UCHG) and mucin was purified by Dr. Marie Le Berre (NUI Galway, Ireland). Approval to retrieve CF mucin for research was granted by NUI Galway and University College Hospital Galway ethical committees. Mucin purification was carried out as described by Kilcoyne *et al.* (2012). In brief, sputum was collected from CF patients *via* non-invasive expectoration during an exacerbation episode. Mucins were purified from samples as follows: sputum was solubilised with 8 M guanidine hydrochloride (GndHCl) to a final concentration of 4 M and fully dissolved over 3 days while gently rotating. Samples were reduced with 10 mM dithiothreitol and alkylated with 25 mM iodoacetamide. Cesium chloride (CsCl) in 4 M GndHCl was added to the sample at a starting density of 1.42 g/mL. A isopycnic density gradient centrifugation was performed for 18 h at 65,000 rpm and 10 °C using an Optima LE-80K ultracentrifuge (Beckman-Coulter, California, USA) with a 70 Ti rotor. Following centrifugation, the gradient was unpacked and 1 mL fractions collected. Mucin-rich fractions were identified by dot blots using periodic acid – Schiff's (PAS) reagent. The PAS-positive (i.e. mucin-rich) fractions were pooled. The high molecular weight components of the samples were collected by Sepharose™ Cl 4B (GE Healthcare, Illinois, USA) chromatography eluted with PBS with fractions containing mucins identified via dot blots with PAS reagent. The pooled samples were then desalted and buffer exchanged with water using Bio-Gel P-6 (BIO-RAD, California, USA) (10 x 1 cm) at a flow rate of 1 mL/min and 0.5 mL fractions were collected. PAS-positive fractions were lyophilised to dryness and weighed and dry purified mucins were stored at - 20 °C until use.

### 3.2.13. Competitive binding assay of PNAG and *S. aureus* binding to human CF lung mucin

Wells of a 96 well Costar® cell culture microtitre plate were coated with 100 µL of 100 µg/mL CF lung mucin in PBS, pH 7.4, for 2 h at room temperature. Wells were washed gently with PBS three times and 100 µL SYTO® 82 labelled *S. aureus* Mn8m diluted in TBS with 1 mM of sos2211 (final concentration) or the equivalent volume of sterile water (approximately 1 x $10^6$ cells/mL) was added to each well. Similarly, 100 µL of PNAG-AF555 diluted 1 in 100 in TBS from stock with 1 mM final concentration of sos2211 or the equivalent volume of sterile water was added to each well. This experiment was carried out once using one well per sample due to limited human CF lung mucin availability. Plates were then incubated for 1 h at 37°C, washed gently three times with PBS, pH 7.4, and imaged using an Operetta® High Content Imaging System (PerkinElmer, London, U.K.). The number of *S. aureus* cells per wells were counted and the mean fluorescence intensity from PNAG-AF555 or labelled bacteria per well was calculated using Harmony 3.1.1 software (PerkinElmer).

### 3.3. Results

To establish whether the lectin microarray platform would be suitable for sensitively and reproducibly quantifying the inhibition of lectin binding using glycoclusters, six glycoclusters were chosen to inhibit WGA binding to GlcNAc-BSA and ovalbumin, and $IC_{50}$ values were calculated. Similarly, the ability of glycoclusters to inhibit lectin binding to *S. aureus* and PNAG on the lectin microarray platform was then assessed. To elucidate the potential therapeutic role of these glycoclusters, two additional glycoclusters were added to the glycocluster panel for biofilm inhibition studies with two *S. aureus* PNAG-producing strains. Finally, two glycoclusters were used for inhibition studies of *S. aureus* and PNAG binding to mucins purified from the lungs of CF patients.

#### 3.3.1. Structures of glycoclusters used in this study

A panel of six divalent glycoclusters bearing GlcNAc as the bioactive head group was used in this study. Differences between the glycoclusters included variations in anomeric configuration, valency and the use of O- or S- glycosidic linkages (Fig. 3.1). Distances between the GlcNAc headgroups were estimated to be approximately 16 Å (André *et al*., 2015).

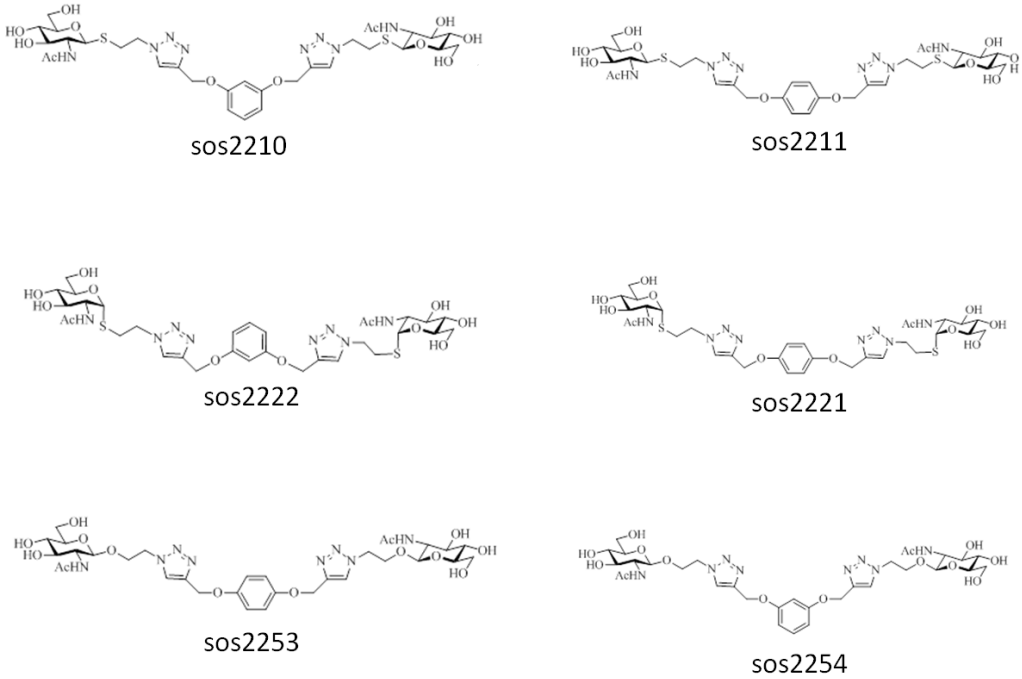


**Fig. 3.1. Structures of glycoclusters used in this study and their individual codes.**

### 3.3.2. Suitability of lectin microarray platform for quantifying inhibition of lectin binding using glycoclusters

Before using ovalbumin-AF555 and GlcNAc-BSA-AF555 as GlcNAc-containing molecules on the lectin microarray platform, we profiled them on the lectin microarrays to decipher lectins that had specificity towards them. Several lectins bound to ovalbumin-AF555 including *Calystegia sepium* agglutinin (Calsepa) and *Hippeastrum hybrid* agglutinin (HHA), which have binding specificity for mannose residues (Table 3.1) and *Griffonia simplicifolia* lectin II (GSL-II) and WGA that have specificity for GlcNAc residues. Other lectins which bound to ovalbumin-AF555 included *Sambucus nigra* agglutinin II (SNA-II) that has specificity for Gal/GalNAc residues, *Galanthus nivalis* agglutinin (GNA) that has specificity for mannose structures, *Erythrina cristagalli* agglutinin (ECA) and *Caragana arborescens* agglutinin (CAA) that have affinity for Gal-β-(1,4)-GlcNAc (*N*-acetyllactosamine (LacNAc)) oligomers and *Trichosanthes japonica* agglutinin II (TJA-II) that has specificity towards Fuc-α-(1,2)-Gal-β-(1,4)-GlcNAc (H-2 antigen) (Fig. 3.2 (A), (B) and (C)).

Ovalbumin contains high-mannose structures, hybrid and complex structures with some terminal and bisecting GlcNAc residues, and a low proportion of hybrid and complex structures with terminal α-Gal residues (Harvey *et al.,* 2000). These lectin microarray interactions mainly agree with the presence of the known ovalbumin structures, except for the interaction with TJA-II as the presence of the H-2 antigen has not been previously shown in ovalbumin *N*-linked structures (Fig. 3.2). On the other hand, the lack of interaction of ovalbumin-AF555 with UEA-I indicated that an α-(1,2)-linked fucose (Fuc) residue was not present. However, TJA-II has also been shown to interact with terminal α-linked Gal residues which are linked to GlcNAc residues (Yamashita *et al.*, 1992), therefore it is likely the presence of the low proportion of terminal α-Gal residues present on ovalbumin glycans which caused this binding interaction. Lectin specificity towards GlcNAc residues on ovalbumin-AF555 was confirmed with 100 mM GlcNAc abolishing WGA interactions with ovalbumin-AF555 (Fig. 3.2 (A)) while 100 mM Man did not change WGA binding ovalbumin-AF555. Furthermore, 100 mM Man reduced Calsepa and HHA binding to ovalbumin-AF555, supporting the presence of high-mannose structures (Fig. 3.2

(B). Calsepa binding to ovalbumin-AF555 was not completely abolished by 100 mM Man or GlcNAc, supporting findings that Calsepa preferentially binds N-linked glycans with high-mannose structures containing bisecting core GlcNAc structures (Nagae *et al.*, 2017). These data showed WGA binding to ovalbumin was due to the presence of GlcNAc-containing glycans on ovalbumin.

Similarly, GlcNAc-BSA was profiled on the lectin microarray and was primarily bound by WGA, followed by sWGA (Fig. 3.2 (D), (E) and (F)). WGA binding to GlcNAc-BSA was GlcNAc-mediated as 100 mM GlcNAc abolished this interaction (Fig 3.2 (D)) while 100 mM Man had no effect on WGA binding (Fig 3.2 (E)). To exemplify the specificity of the glycoclusters towards GlcNAc-specific lectins, sos2252 and sos2222 were used to modulate lectin-GlcNAc interactions. One mM of glycocluster sos2254 completely inhibited GSL-II and WGA binding to ovalbumin-AF555, but did not affect the binding of non-GlcNAc-specific lectins Calsepa, GNA, HHA, CAA or ECA to ovalbumin-AF555 (Fig. 3.2 (C)). The binding of GlcNAc- and LacNAc-specific lectin *Datura stramonium* agglutinin (DSA) (Kuno *et al.*, 2005) was slightly increased. In the presence of the glycocluster, either the lectin or the ovalbumin structures may have assumed a slightly different conformation which favoured the binding of DSA to LacNAc or LacNAc oligomers, which are also present on ovalbumin N-linked structures (Harvey *et al.*, 2000). Interestingly, sos2254 also inhibited binding to LacNAc-binding TJA-II (Yamashita *et al.*, 1992) (Fig. 3.2 (C)). This indicated that the GlcNAc residue of LacNAc also plays a role in TJA-II binding in addition to the Gal residue. Similarly, 1 mM of sos2222 completely abolished sWGA and WGA binding to GlcNAc-BSA-AF555 on the lectin microarray (Fig. 3.2 (F)).

These data showed that the GlcNAc-containing glycoclusters exhibited targeted binding to lectins that have specificity for GlcNAc on the lectin microarray. Furthermore, WGA bound to ovalbumin-AF555 (Fig. 3.2 (A)) and GlcNAc-BSA-AF555 (Fig. 3.2 (B)) in a GlcNAc-mediated manner (Fig. 3.2 (A) and (D)), which made ovalbumin-AF555 and GlcNAc-BSA-AF555 suitable to use for glycocluster inhibition studies with WGA.

A

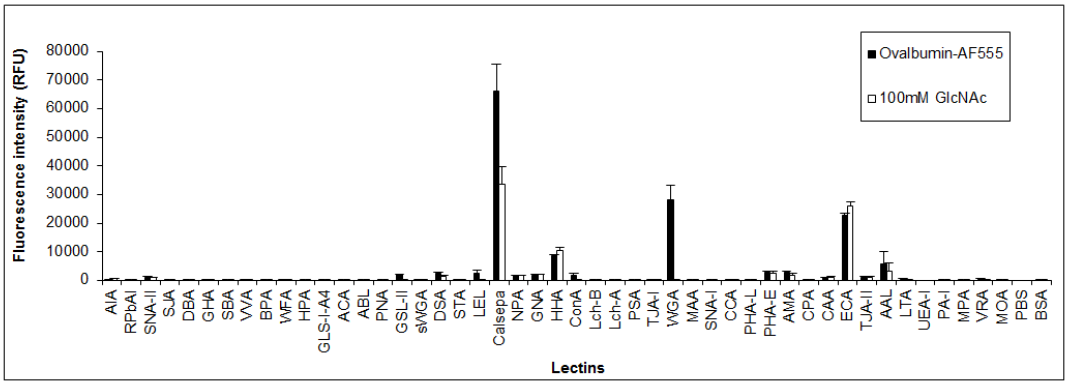
Ovalbumin-AF555
100mM GlcNAc
Fluorescence intensity (RFU)
80000
70000
60000
50000
40000
30000
20000
10000
0
AIA RPbAI SNA-II SJA DBA GHA SBA VVA BPA WFA HPA GLS-I-A4 ACA ABL PNA GSL-II sWGA DSA STA LEL Calsepa NPA GNA HHA ConA Lch-B Lch-A PSA TJA-I WGA MAA SNA-I CCA PHA-L PHA-E AMA CPA CAA ECA TJA-II AAL LTA UEA-I PA-I MPA VRA MOA PBS BSA
Lectins

B

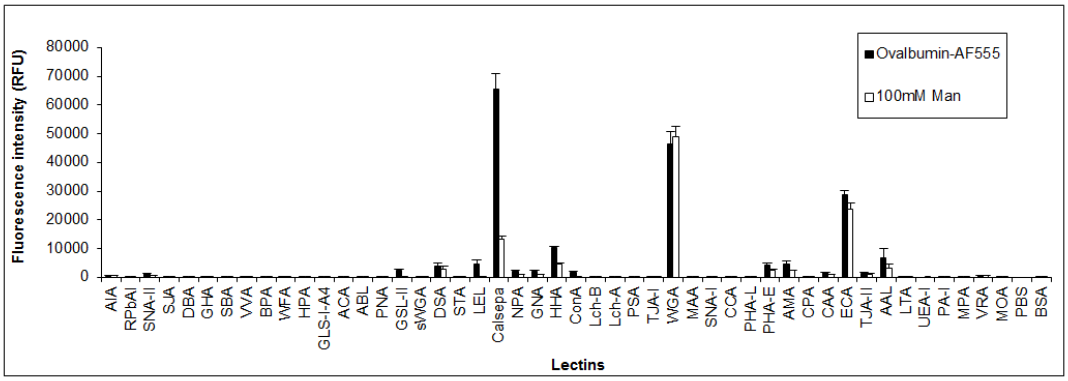
Ovalbumin-AF555
100mM Man
Fluorescence intensity (RFU)
80000
70000
60000
50000
40000
30000
20000
10000
0
AIA RPbAI SNA-II SJA DBA GHA SBA VVA BPA WFA HPA GLS-I-A4 ACA ABL PNA GSL-II sWGA DSA STA LEL Calsepa NPA GNA HHA ConA Lch-B Lch-A PSA TJA-I WGA MAA SNA-I CCA PHA-L PHA-E AMA CPA CAA ECA TJA-II AAL LTA UEA-I PA-I MPA VRA MOA PBS BSA
Lectins

C

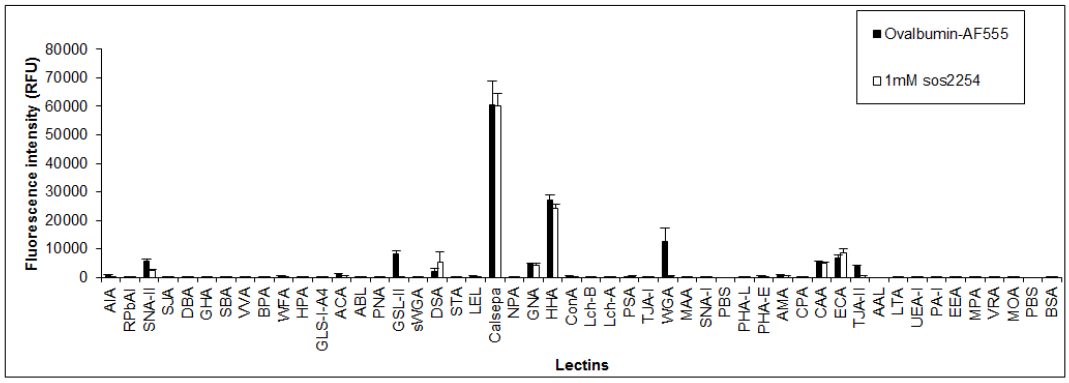
Ovalbumin-AF555
1mM sos2254
Fluorescence intensity (RFU)
80000
70000
60000
50000
40000
30000
20000
10000
0
AIA RPbAI SNA-II SJA DBA GHA SBA VVA BPA WFA HPA GLS-I-A4 ACA ABL PNA GSL-II sWGA DSA STA LEL Calsepa NPA GNA HHA ConA Lch-B Lch-A PSA TJA-I WGA MAA SNA-I PBS PHA-L PHA-E AMA CPA CAA ECA TJA-II AAL LTA UEA-I PA-I EEA MPA VRA MOA PBS BSA
Lectins

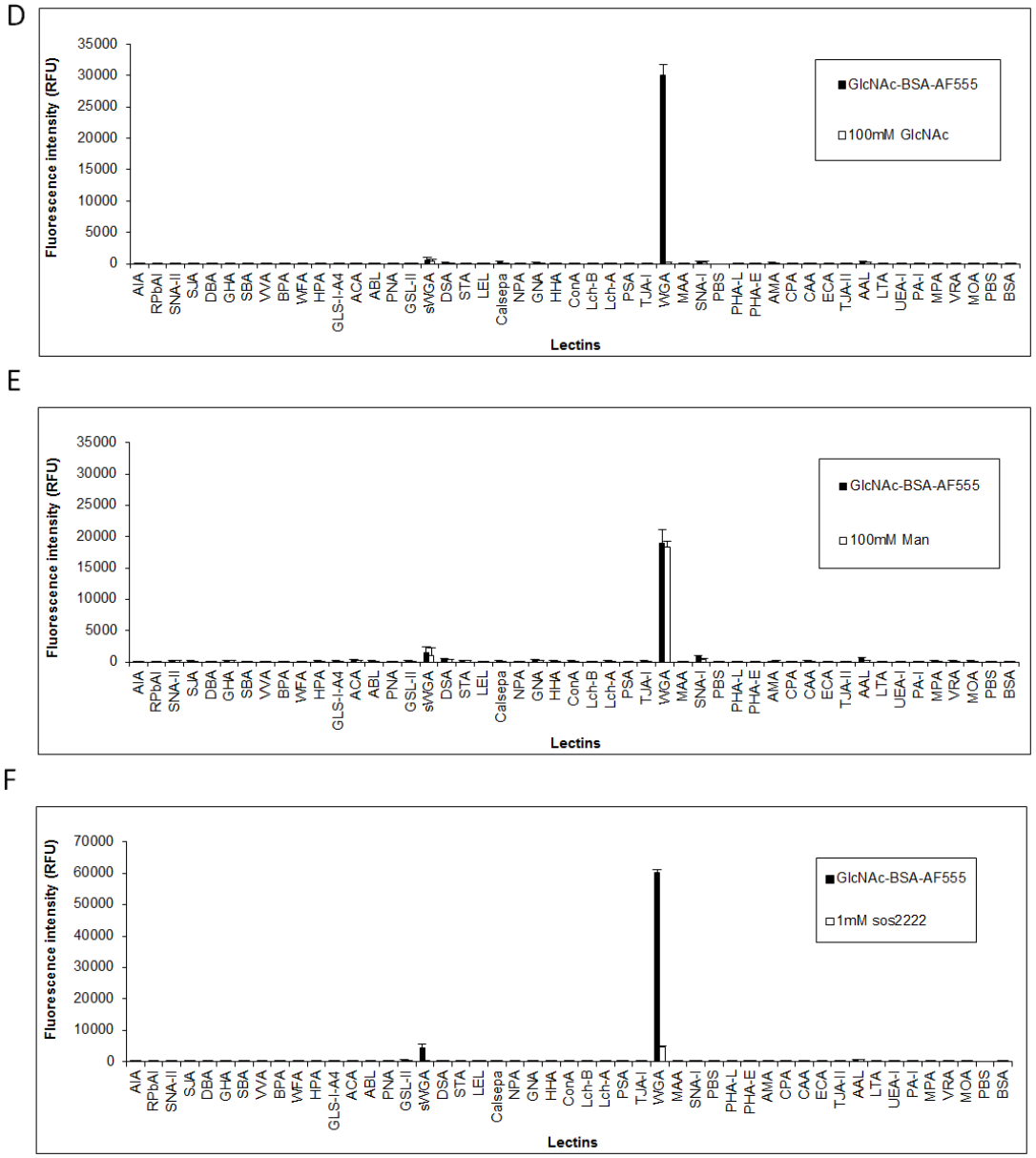


**Fig. 3.2. GlcNAc, Man and glycocluster inhibition of lectin binding ovalbumin-AF555 and GlcNAc-BSA-AF555.** Bar chart represents (A) 100 mM GlcNAc incubated with ovalbumin-AF555 and (D) GlcNAc-BSA-AF555, (B) 100 mM Man incubated with ovalbumin-AF555 and (E) GlcNAc-BSA-AF555, (C) 1 mM of sos2254 incubated with ovalbumin-AF555 and (F) 1 mM sos2222 incubated with GlcNAc-BSA-AF555 on lectin microarrays. Experiments were carried out on three different microarray slides and error bars represent +/- one SD of the mean.

To obtain $IC_{50}$ values for each glycocluster for WGA binding inhibition on the lectin microarray platform, GlcNAc-BSA-AF555 was co-incubated with a range of 0.01 fM – 1 mM for each glycocluster (Fig. 3.4) and a range of 0.25 µM – 1 mM was used for ovalbumin-AF555 (Fig. 3.3), and $IC_{50}$ values were calculated for each glycocluster inhibition of WGA binding to ovalbumin-AF555 and GlcNAc-BSA-AF555 (Table 3.3).

Using all glycoclusters to inhibit WGA binding ovalbumin-AF555 produced relatively concentration-dependent inhibition curves (Fig. 3.3 (A) to (E) (ii)). Glycoclusters sos2222 and sos2221 provided the lowest $IC_{50}$ inhibition values for WGA binding to ovalbumin-AF555 of 0.6554 and 0.7957 µM, respectively (Table 3.3). However, 1 mM of these glycoclusters did not completely abolish binding of WGA to ovalbumin-AF555 and only reduced binding to approximately 20% of uninhibited binding (Fig. 3.3 (C) and (D) (i)). Glycoclusters sos2210 and sos2211 gave $IC_{50}$ values of 1.515 and 1.707 µM, respectively (Table 3.3) and concentrations greater than 0.25 mM completely abolished binding of WGA to ovalbumin-AF555 for these two glycoclusters (Fig. 3.3 (C) and (D) (i) and (ii)). Glycoclusters sos2253 and sos2254 gave the highest $IC_{50}$ values for WGA binding inhibition to ovalbumin-AF555 of 4.36 and 16.64 µM, respectively (Table 3.3). Glycocluster sos2253 provided concentration-dependent inhibition curves (Fig. 3.3 (E) (i) and (ii)), however, high concentrations relative to other glycoclusters were required to obtain inhibitions of greater than 50%, resulting in high $IC_{50}$ values. Interestingly, concentrations between 0.25 – 1 µM of sos2254 increased WGA binding to ovalbumin-AF555 and sos2254 concentrations of greater than 1 µM were required to inhibit WGA binding to ovalbumin-AF555 (Fig. 3.3 (F) (i) and (ii)), which also resulted in higher $IC_{50}$ values compared to the other glycoclusters (Table 3.3).

The panel of glycoclusters did not provide relatively smooth concentration-dependent inhibition curves for WGA binding inhibition to GlcNAc-BSA-AF555 for the concentration range of glycoclusters tested. Low concentrations of glycocluster sos2221 (between 0.01 fM and 10 pM) promoted WGA binding to GlcNAc-BSA-AF555 (Fig. 3.4 (D) (i) and (ii)) demonstrating the low-dose hook effect (D. Wild & Kodak, 2013), but had the third lowest $IC_{50}$ value of 0.03007 nM after sos2210 which had the highest $IC_{50}$ value of 5.32 aM, followed by sos2253 which had

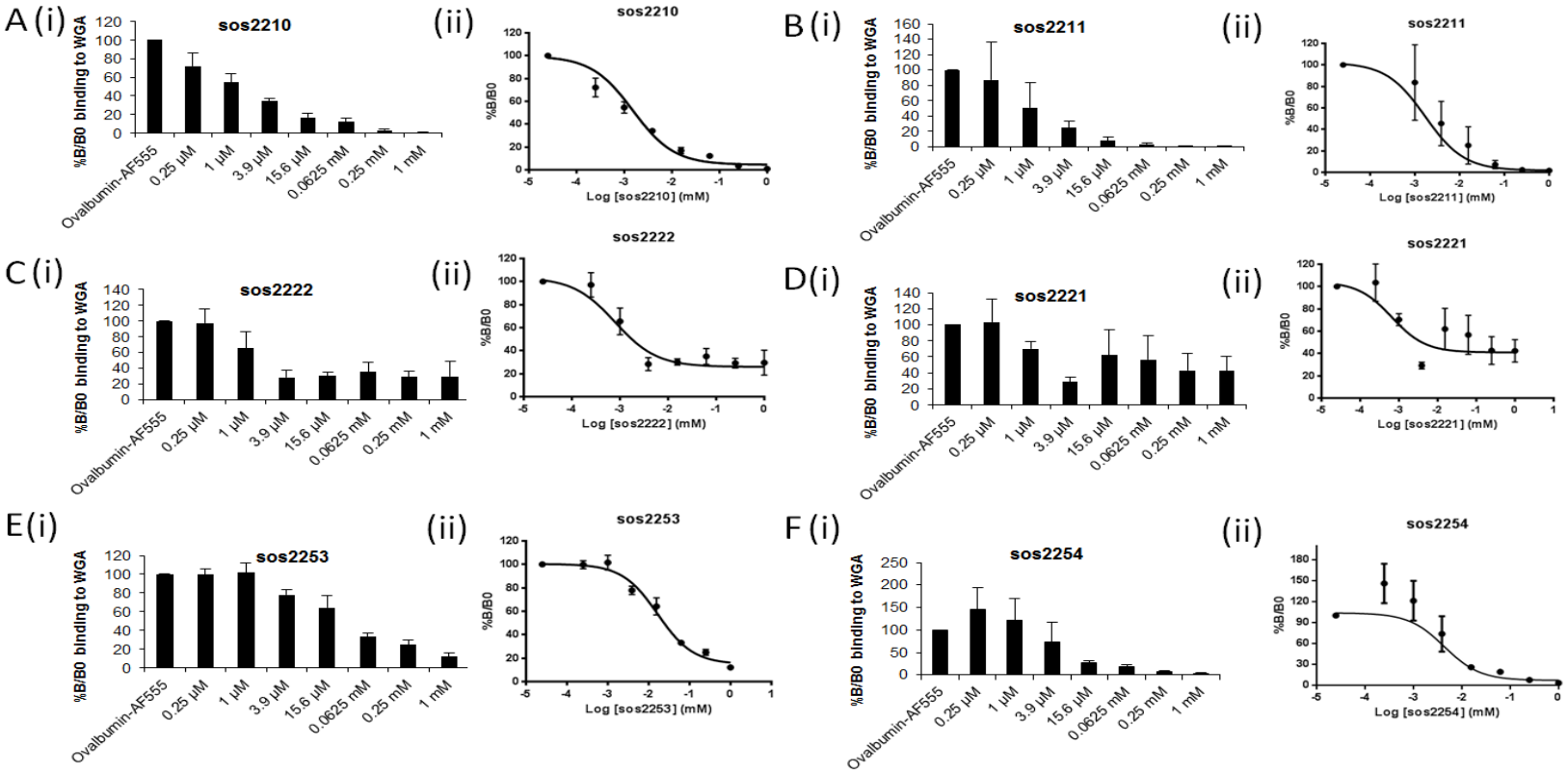


**Fig. 3.3. Glycocluster inhibition of WGA binding to ovalbumin-AF555 binding on the microarray platform represented as %B/B0 as (i) bar charts and (ii) inhibition curves**. Glycoclusters (A) sos2210, (B) sos2211, (C) sos2222, (D) sos2221 (E) sos2253 and (F) sos2254 inhibition of WGA binding to ovalbumin-AF555. (i) B0 represents 100% of binding of ovalbumin-AF555 to WGA while %B represents the percentage of ovalbumin-AF555 binding to WGA remaining in the presence of the glycocluster. (ii) All inhibition curves are shown as the log of the concentration of glycocluster used for inhibition studies on the x-axis. Experiments were carried out on three different microarray slides and error bars represent +/- one SD of the mean.

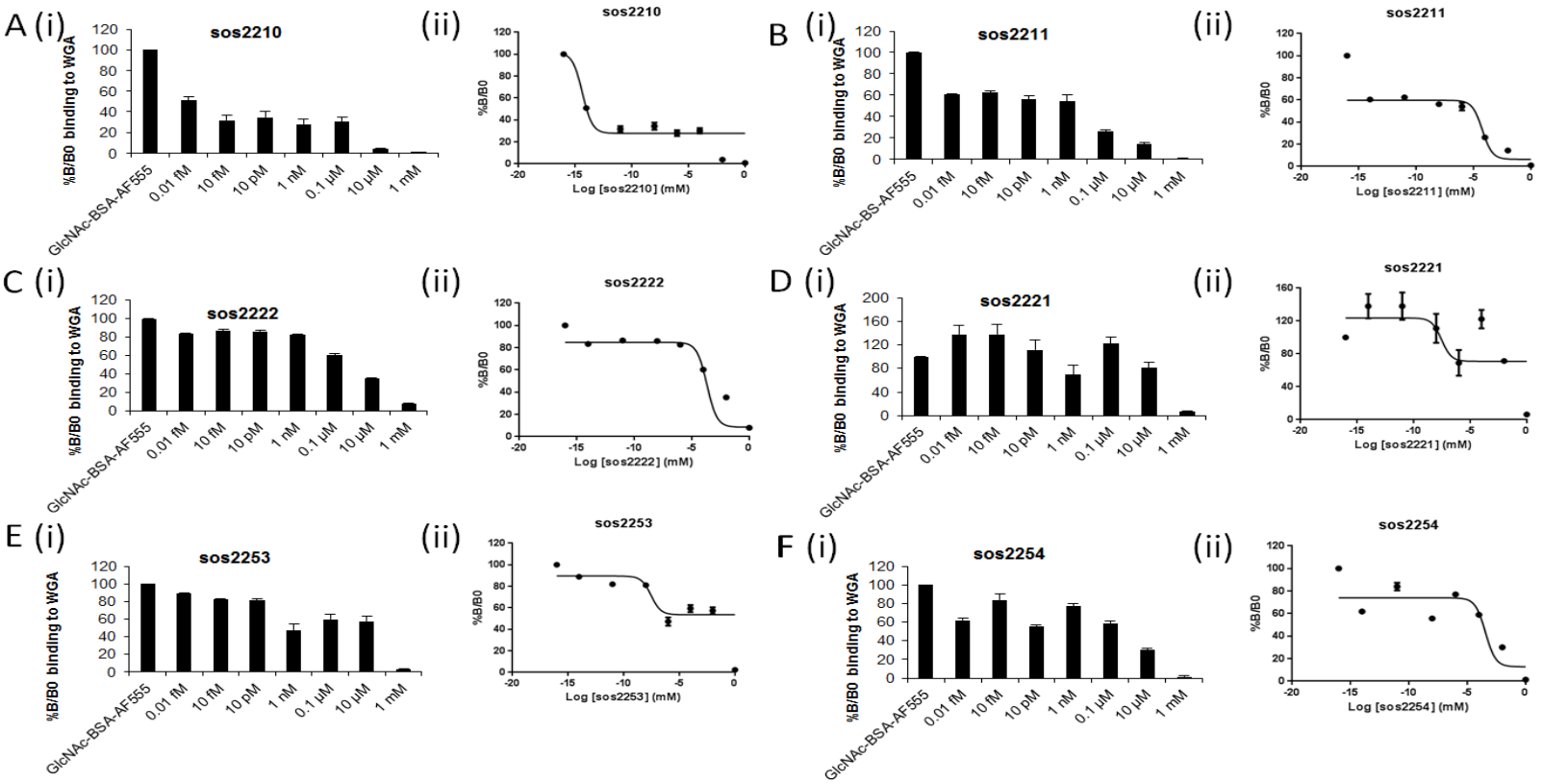


**Fig. 3.4. Glycocluster inhibition of WGA binding to GlcNAc-BSA-AF555 binding on the microarray platform represented as %B/B0 as (i) bar charts and (ii) inhibition curves**. Glycoclusters (A) sos2210, (B) sos2211, (C) sos2222, (D) sos2221 (E) sos2253 and (F) sos2254 inhibition of WGA binding to ovalbumin-AF555. (i) B0 represents 100% of binding of ovalbumin-AF555 to WGA while %B represents the percentage of ovalbumin-AF555 binding to WGA remaining in the presence of the glycocluster. (ii) All inhibition curves are shown as the log of the concentration of glycocluster used for inhibition studies on the x-axis. Experiments were carried out on three different microarray slides and error bars represent +/- one SD of the mean.

0.02969 nM (Table 3.3). Glycoclusters sos2210 and sos2211 inhibited WGA binding to GlcNAc-BSA-AF555 by approximately 40% with concentrations as low as 0.01 fM, but concentrations between 0.1 μM and 1 mM were required to completely inhibit WGA binding to GlcNAc-BSA-AF555 (Fig. 3.4 (A) and (B) (i) and (ii)). $IC_{50}$ values of 5.32 aM and 0.005913 μM were obtained for sos2210 and sos2211, respectively (Table 3.3). Overall glycocluster sos2254 decreased WGA binding to GlcNAc-BSA-AF555 in a concentration dependent manner from 1 nM and upwards. However, the pattern of binding inhibition was cyclical below 1 nM, with 10 pM of sos2254 having lower binding than 1 nM (approximately 60% of binding), 10 fM having greater binding than 10 pM (approximately 80%) and 0.01 fM decreasing WGA binding to GlcNAc-BSA-AF555 to 60%, similar to 10 pM (Fig. 3.4 (F) (i) and (ii)). This pattern of cyclically decreased binding was also seen with sos2221 and sos2253 (Fig. 3.4 (D) and (E) (i) and (ii)).

Glycocluster sos2221 generated the lowest $IC_{50}$ value for inhibiting WGA binding to ovalbumin-AF555 with 0.6554 μM, followed by sos2222, sos2210, sos2211, sos2254 and sos2253. Glycocluster sos2253 was the most potent in inhibiting WGA binding to GlcNAc-BSA-AF555 with an $IC_{50}$ value of 2.969 pM, followed by sos2221, sos2211, sos2222, sos2254 and sos2210 (Table 3.3). Moreover, the lectin microarray platform gave reproducible results as shown by low %CV values, particularly for WGA. (Table 3.2) Nonetheless, standard deviation of results between microarray slides for sos2211, sos2221 and sos2254 inhibition of WGA binding to ovalbumin-AF555 (Fig. 3.3 (B), (D), (E)) and sos2221 WGA binding inhibition to GlcNAc-BSA555 (Fig 3.4 (D)) were higher at low glycoclusters resulting in a high %CV.

Using a least squares fit rather than an robust fit to create inhibition curve and limiting our data points and calculate $IC_{50}$ values resulted in different $IC_{50}$ values, but sos2210 still maintained a position of being the best glycocluster to inhibit WGA binding GlcNAc-BSA on the lectin microarray platform and produced the second best $R^2$ value compared to the other glycoclusters. Overall, these data demonstrate that the microarray platform is a suitable, reproducible and sensitive platform for measuring glycocluster inhibition of lectin binding with a panel of glycoclusters.

**Table 3.2. Comparison of the average percentage coefficient of variance (%CV) across slides for lectins incubated with dilutions of (A) glycoclusters and ovalbumin-AF555 and dilutions of (B) glycoclusters and GlcNAc-BSA-AF555.**

A

| | Ovalbumin-AF555 | 0.25 µM | 1 µM | 3.9 µM | 15.6 µM | 0.0625 µM | 0.25 µM | 1 mM |
|---|---|---|---|---|---|---|---|---|
| AIA | 53.9 | 51.5 | 25.5 | 45.1 | 45.1 | 23.2 | 17.6 | 30.1 |
| RPbAI | 28.1 | 20.0 | 16.7 | 18.2 | 18.2 | 18.6 | 21.7 | 42.9 |
| SNA-II | 39.8 | 17.0 | 10.4 | 21.0 | 21.0 | 25.1 | 13.2 | 35.4 |
| SJA | 44.9 | 7.9 | 6.7 | 15.3 | 15.3 | 8.1 | 8.0 | 30.2 |
| DBA | 40.7 | 12.2 | 12.3 | 26.3 | 26.3 | 19.9 | 12.6 | 28.3 |
| GHA | 34.1 | 12.9 | 10.8 | 31.0 | 31.0 | 20.3 | 19.7 | 21.4 |
| SBA | 25.4 | 19.0 | 17.8 | 19.2 | 19.2 | 19.2 | 13.6 | 25.3 |
| VVA | 29.8 | 14.2 | 13.4 | 23.5 | 23.5 | 10.6 | 11.9 | 13.2 |
| BPA | 39.6 | 6.6 | 12.5 | 22.2 | 22.2 | 8.3 | 6.5 | 9.8 |
| WFA | 47.6 | 14.7 | 14.3 | 37.8 | 37.8 | 23.9 | 24.0 | 38.1 |
| HPA | 45.6 | 9.4 | 8.2 | 13.5 | 13.5 | 9.8 | 8.2 | 11.1 |
| GLS-I-A4 | 42.3 | 15.9 | 14.6 | 15.4 | 15.4 | 16.4 | 10.3 | 22.7 |
| ACA | 37.0 | 20.8 | 22.0 | 16.1 | 16.1 | 19.4 | 16.2 | 23.8 |
| ABL | 33.1 | 27.4 | 27.4 | 43.3 | 43.3 | 30.4 | 18.7 | 39.7 |
| PNA | 39.3 | 20.6 | 13.7 | 20.2 | 20.2 | 19.3 | 16.4 | 38.8 |
| GSL-II | 14.3 | 4.8 | 5.6 | 8.9 | 8.9 | 7.9 | 10.2 | 15.7 |
| sWGA | 45.8 | 17.4 | 15.4 | 16.9 | 16.9 | 10.5 | 9.8 | 15.3 |
| DSA | 58.7 | 29.5 | 30.0 | 49.2 | 49.2 | 25.4 | 26.8 | 51.1 |
| STA | 21.5 | 63.7 | 38.7 | 22.4 | 22.4 | 29.6 | 9.5 | 17.7 |
| LEL | 36.9 | 44.9 | 27.5 | 28.4 | 28.4 | 34.6 | 28.5 | 28.0 |
| Calsepa | 30.4 | 142.2 | 46.4 | 23.1 | 23.1 | 36.2 | 21.4 | 26.2 |
| NPA | 47.5 | 15.3 | 14.2 | 16.0 | 16.0 | 24.2 | 22.2 | 30.9 |
| GNA | 14.0 | 5.4 | 5.2 | 9.4 | 9.4 | 6.1 | 8.8 | 13.8 |
| HHA | 22.0 | 8.8 | 13.3 | 17.0 | 17.0 | 11.9 | 9.2 | 13.3 |
| ConA | 44.6 | 13.8 | 6.7 | 12.3 | 12.3 | 12.7 | 8.9 | 18.8 |
| Lch-B | 42.8 | 37.2 | 45.5 | 19.1 | 19.1 | 45.5 | 34.7 | 22.7 |
| Lch-A | 31.7 | 29.6 | 42.3 | 60.4 | 60.4 | 36.9 | 42.7 | 44.1 |
| PSA | 24.1 | 19.9 | 18.2 | 20.1 | 20.1 | 16.8 | 10.3 | 18.4 |
| TJA-I | 22.0 | 14.7 | 22.0 | 22.2 | 22.2 | 19.6 | 15.6 | 11.8 |
| WGA | 33.9 | 22.6 | 16.5 | 32.1 | 32.1 | 18.6 | 19.9 | 20.2 |
| MAA | 14.4 | 9.3 | 9.1 | 24.0 | 24.0 | 17.7 | 12.5 | 21.7 |
| SNA-I | 8.7 | 8.3 | 8.5 | 10.3 | 10.3 | 11.3 | 6.1 | 17.7 |
| PHA-L | 44.1 | 10.8 | 11.5 | 10.1 | 10.1 | 11.5 | 15.0 | 26.1 |
| PHA-E | 50.0 | 35.3 | 30.4 | 32.2 | 32.2 | 30.5 | 32.5 | 46.8 |
| AMA | 38.3 | 9.7 | 12.9 | 20.1 | 20.1 | 17.1 | 19.4 | 22.6 |
| CPA | 50.6 | 15.1 | 13.8 | 10.0 | 10.0 | 7.0 | 9.3 | 24.5 |
| CAA | 30.1 | 16.8 | 15.7 | 12.4 | 12.4 | 11.3 | 10.0 | 10.7 |
| ECA | 31.5 | 13.0 | 13.3 | 23.3 | 23.3 | 15.7 | 9.9 | 15.4 |
| TJA-II | 53.5 | 7.5 | 6.5 | 16.5 | 16.5 | 12.9 | 14.2 | 28.1 |
| AAL | 3.6 | 6.2 | 11.2 | 8.7 | 8.7 | 24.4 | 23.1 | 77.6 |
| LTA | 19.3 | 5.9 | 8.3 | 22.3 | 22.3 | 11.6 | 14.3 | 22.2 |
| UEA-I | 23.9 | 11.5 | 8.9 | 13.2 | 13.2 | 15.8 | 15.0 | 31.6 |
| PA-I | 34.9 | 16.4 | 11.8 | 20.4 | 20.4 | 13.4 | 13.6 | 7.6 |
| MPA | 20.1 | 12.9 | 13.1 | 12.9 | 12.9 | 14.1 | 8.5 | 22.8 |
| VRA | 70.9 | 9.8 | 4.6 | 17.6 | 17.6 | 4.4 | 4.2 | 10.0 |
| MOA | 51.4 | 47.1 | 35.7 | 24.3 | 24.3 | 27.4 | 34.2 | 36.6 |

B

| GlcNAc-BSA-AF555 | 0.001 fM | 1 fM | 1 pM | 100 pM | 0.01 µM | 1 µM | 1 mM |
|---|---|---|---|---|---|---|---|
| 37.9 | 17.7 | 15.4 | 25.3 | 55.1 | 47.5 | 37.7 | 17.0 |
| 10.3 | 12.5 | 11.5 | 21.6 | 30.9 | 32.1 | 32.8 | 12.1 |
| 14.6 | 12.5 | 9.9 | 20.0 | 33.9 | 37.7 | 38.7 | 10.7 |
| 11.2 | 15.1 | 11.9 | 19.2 | 23.4 | 37.7 | 34.9 | 11.6 |
| 9.8 | 14.2 | 9.9 | 19.8 | 30.6 | 35.9 | 32.4 | 8.4 |
| 33.7 | 14.1 | 10.1 | 17.0 | 31.0 | 40.5 | 37.7 | 8.0 |
| 22.4 | 14.6 | 14.0 | 22.0 | 31.4 | 40.0 | 36.1 | 12.9 |
| 13.6 | 15.8 | 11.6 | 21.6 | 27.0 | 41.7 | 35.2 | 11.3 |
| 9.3 | 14.6 | 12.0 | 17.6 | 37.1 | 40.4 | 35.1 | 11.2 |
| 34.6 | 8.0 | 23.5 | 17.1 | 42.4 | 42.5 | 33.8 | 14.8 |
| 9.4 | 18.7 | 18.0 | 17.9 | 28.2 | 41.1 | 33.1 | 13.8 |
| 14.2 | 16.2 | 17.1 | 17.4 | 30.8 | 42.3 | 34.3 | 15.4 |
| 10.3 | 15.7 | 16.8 | 16.4 | 32.0 | 39.5 | 33.2 | 14.5 |
| 13.5 | 14.2 | 11.7 | 17.3 | 28.8 | 34.0 | 33.7 | 11.4 |
| 32.1 | 27.8 | 16.8 | 38.4 | 66.5 | 60.8 | 58.8 | 39.3 |
| 23.3 | 19.4 | 14.4 | 27.0 | 35.9 | 29.9 | 34.7 | 10.0 |
| 25.7 | 16.2 | 24.4 | 30.7 | 26.2 | 17.1 | 32.6 | 10.4 |
| 8.1 | 9.8 | 14.8 | 21.3 | 31.7 | 34.7 | 28.3 | 9.3 |
| 13.4 | 12.9 | 18.7 | 20.5 | 29.4 | 31.1 | 40.3 | 12.0 |
| 23.2 | 19.9 | 20.2 | 20.2 | 57.7 | 50.8 | 47.3 | 38.2 |
| 14.0 | 9.7 | 13.3 | 17.3 | 39.1 | 33.5 | 31.2 | 7.4 |
| 14.6 | 17.6 | 16.0 | 21.6 | 29.7 | 29.7 | 38.2 | 8.2 |
| 7.9 | 17.2 | 12.6 | 17.5 | 25.3 | 33.4 | 34.2 | 12.4 |
| 20.9 | 21.1 | 18.8 | 28.5 | 25.3 | 27.5 | 32.9 | 7.8 |
| 31.7 | 21.4 | 22.5 | 29.7 | 46.2 | 29.4 | 34.1 | 19.9 |
| 52.1 | 17.8 | 17.4 | 21.0 | 48.4 | 47.5 | 35.0 | 16.4 |
| 10.8 | 33.4 | 21.8 | 21.9 | 26.2 | 26.3 | 37.6 | 13.4 |
| 43.5 | 20.6 | 32.8 | 36.4 | 79.1 | 56.1 | 40.1 | 25.8 |
| 53.2 | 41.1 | 30.4 | 46.1 | 72.8 | 68.3 | 39.5 | 28.0 |
| 2.6 | 1.3 | 2.0 | 2.1 | 6.7 | 4.6 | 6.4 | 16.6 |
| 12.6 | 13.2 | 11.8 | 18.5 | 26.4 | 33.2 | 35.8 | 11.3 |
| 8.6 | 8.9 | 10.6 | 16.7 | 31.7 | 29.8 | 30.0 | 5.0 |
| 10.5 | 16.0 | 12.3 | 18.3 | 34.0 | 35.5 | 35.0 | 16.2 |
| 14.5 | 15.2 | 24.5 | 19.8 | 47.7 | 40.6 | 42.8 | 19.9 |
| 12.6 | 18.7 | 19.5 | 22.9 | 45.6 | 34.0 | 35.5 | 16.2 |
| 18.3 | 13.2 | 12.0 | 15.8 | 30.8 | 42.1 | 28.1 | 13.2 |
| 22.4 | 33.0 | 35.3 | 37.1 | 51.0 | 36.2 | 40.1 | 15.2 |
| 15.1 | 15.4 | 11.9 | 20.3 | 29.6 | 38.1 | 35.1 | 9.1 |
| 27.6 | 11.5 | 13.4 | 21.3 | 31.3 | 33.9 | 37.1 | 12.5 |
| 22.2 | 20.6 | 24.6 | 25.4 | 45.6 | 61.5 | 45.0 | 16.6 |
| 24.4 | 11.1 | 22.0 | 26.3 | 29.3 | 31.5 | 39.5 | 15.5 |
| 8.0 | 13.6 | 17.0 | 18.9 | 28.3 | 29.5 | 33.2 | 11.7 |
| 17.9 | 18.7 | 17.1 | 21.3 | 35.8 | 33.8 | 38.4 | 10.5 |
| 17.2 | 13.6 | 12.4 | 23.7 | 32.2 | 36.9 | 34.8 | 12.3 |
| 22.7 | 16.1 | 15.8 | 18.3 | 38.5 | 44.9 | 30.1 | 10.8 |
| 13.6 | 16.7 | 13.1 | 18.7 | 27.9 | 36.0 | 30.1 | 13.5 |

**Table 3.3. $IC_{50}$ values (μM) for glycocluster and monosaccharide inhibitions of surface conjugated WGA (0.5 mg/mL) binding to ovalbumin-AF555 (1 μg/mL) and GlcNAc-BSA-AF555 (0.1 μg/mL).** $IC_{50}$ values were generated from three experimental replicates using a robust fit and seven concentrations of glycoclusters (A) and least squares fit removing the two lowest concentrations of glycoclusters – 0.01 fM and 10 fM (B). $R^2$ values for least squares fit appear in brackets.

| Glycocluster/ monosaccharide | Ovalbumin-AF555 (A) | GlcNAc-BSA-AF555 (A) | GlcNAc-BSA-AF555 (B) |
|---|---|---|---|
| sos2210 | 1.5 | $5.3 \times 10^{-12}$ | $2.9 \times 10^{-6}$ (0.88) |
| sos2211 | 1.7 | $5.9 \times 10^{-2}$ | $1.7 \times 10^{-3}$ (0.80) |
| sos2222 | 0.8 | $2.1 \times 10^{-1}$ | $1.4 \times 10^{-1}$(0.92) |
| sos2221 | 0.7 | $3.0 \times 10^{-5}$ | $8.3 \times 10^{-4}$ (0.62) |
| sos2253 | 16.6 | $3.0 \times 10^{-5}$ | $2.3 \times 10^{-1}$(0.47) |
| sos2254 | 4.4 | $3.7 \times 10^{-1}$ | 6.3 (0.80) |
| GlcNAc | 781 | 37.3 | 11.1 (0.77) |
| Man | Not inhibitory | Not inhibitory | Not inhibitory |

*$IC_{50}$ values are estimates based on different mathematical models

### 3.3.3. Contribution of PNAG on the surface of *S. aureus* Mn8m to lectin binding

PNAG production relies on a four-gene locus that is named differently depending on the bacteria, usually intercellular adhesion (*ica*) in Gram-positive bacteria, or the polyglucosamine (*pga*) operon in Gram-negative bacteria (Skurnik *et al.*, 2016). To determine whether glycoclusters could modulate bacterial carbohydrate-mediated lectin interactions, *S. aureus* Mn8m was chosen due to a 5-nucleotide deletion within the promoter region of the *ica* locus in the parental strain, Mn8, resulting in the over-expression of PNAG. *S. aureus* Mn8m WT and Mn8 Δ*ica*, which cannot express PNAG, were incubated on the lectin microarray platform to identify lectins that bound intensely to *S. aureus* Mn8m and PNAG on the bacterial cell surface.

Several lectins bound to *S. aureus* Mn8m, but the lectins that bound with the greatest intensely were the GlcNAc-specific lectins GSL-II, sWGA and WGA (Fig. 3.5 (A), Table 3.1). Other lectins also bound to *S. aureus* Mn8m but at very low intensities

(<2,000 RFU) including SNA-II, which has binding specificity for β-linked Gal residues and *N*-acetylgalactosamine (GalNAc) residues, *Aleuria aurantia* lectin (AAL) that has binding specificity for α-(1,6)- and α-(1,3)-linked Fuc residues, and *Vigna radiata* agglutinin (VRA) that has binding specificity for terminal α-linked Gal residues (Table 3.1). WGA, GSL-II and sWGA had reduced binding to *S. aureus* Mn8 Δ*ica* compared to the WT strain (Fig 3.5 (A)), with sWGA binding almost completely abolished (97% reduction), GSL-II binding decreased by approximately 57% and WGA by approximately 18%. Overall, these results indicate that sWGA, GSL-II and WGA bound to *S. aureus* Mn8m, the presence of PNAG increased the binding of the bacterium to these three lectins and sWGA binding in particular was almost completely dependent on the presence of PNAG presented on the surface of the cell.

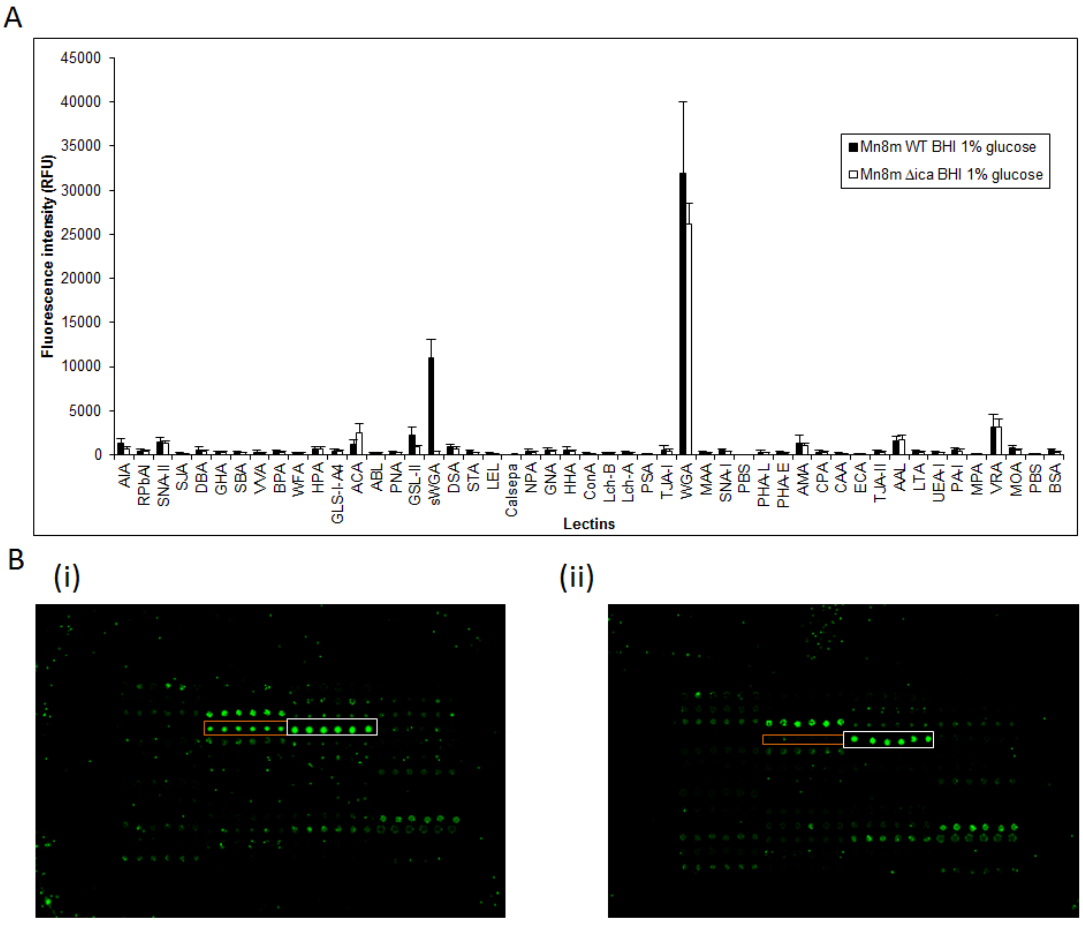


**Fig. 3.5. Binding profiles of *S. aureus* Mn8m WT and Δ*ica* on the lectin microarray platform.** (A) Bar chart representing the binding intensity of lectins binding *S. aureus* Mn8m WT and Mn8 Δ*ica* grown in BHI glucose on the lectin microarray. Bars are the average of intensities from three replicate experiments and error bars depict +/- one SD of

the mean. (B) Images of scanned lectin microarray subarrays of (i) *S. aureus* Mn8m WT and (ii) Mn8 Δ*ica* mutant attachment to lectins on the same microarray slide. Orange squares depict where sWGA was printed on the subarray and white squares where WGA was printed on the subarray.

### 3.3.4. Specificity of lectin binding to PNAG and assessment of lectin recognition of PNAG following conjugation to FluoSpheres® and Alexa Fluor® 555

To deduce which subset of lectins interacted with PNAG only and examine the effect of different presentations of PNAG on lectin recognition, PNAG partially purified from *S. aureus* Mn8m WT was fluorescently labelled in two formats and incubated on the lectin microarray. The first format was direct labelling of PNAG using a fluorophore conjugated to the free amine groups on PNAG (PNAG-AF555). The second format covalently attached PNAG via free amine groups to fluorescent beads of 1 µm diameter (PNAG-FS), which is the same approximate size as a bacterium.

To assess how sample conjugation to FS affected recognition by lectins, several glycoproteins and GlcNAc-BSA were conjugated to FS and AF555, incubated on the lectin microarray and binding profiles were compared. Ovalbumin-AF555 and ovalbumin conjugated to FS (ovalbumin-FS) bound to the same lectins although the relative binding intensities of the lectins, or the binding pattern, did vary depending on the labelling technique (Fig. 3.6 (A)), which reflected the differential presentation and accessibility of the carbohydrates but the same identity. Similarly, invertase-AF555 and invertase-FS also bound to the same lectins but the relative intensities of binding remained similar for both labelling methods (Fig. 3.6 (B)). GlcNAc-BSA-AF555 and GlcNAc-FS also interacted with the same lectins, although it was difficult to compare relative binding intensities as the intensity of GlcNAc-BSA-AF555 binding was very low due to inadvertent underloading (Fig. 3.6 (C)). Overall, these data indicated that different presentation of molecules affected the relative biological pattern recognition by receptors as the accessibility of the carbohydrates was altered, although it did not change the identity of the receptors that were engaged as this binding was based on structural components.

PNAG-AF555 and PNAG-FS bound to the same lectins, sWGA and WGA, and had the same relative binding intensities on the lectin microarray (Fig. 3.6 (D)). This

result demonstrated that the altered presentation of PNAG-FS, compared to PNAG-AF555, did not change the identity of the lectins which recognised the polysaccharide and still allowed for recognition by lectins. To verify that the fluorescent beads alone did not contribute to lectin binding, casein blocked FS (casein-FS) were incubated on lectin microarrays at similar loading concentrations to the FS-labelled glycoproteins and polysaccharide. There was no notable binding to lectins, confirming the lack of contribution of beads and blocking with casein to lectin binding (Fig. 3.6 (E)).

A

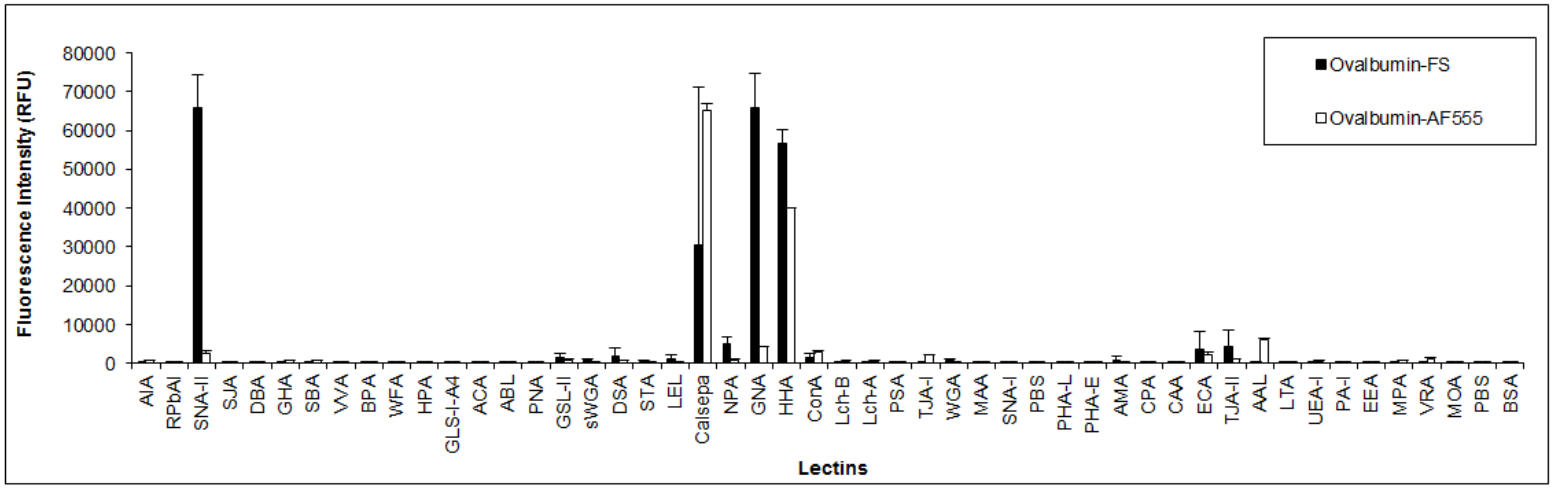
Fluorescence Intensity (RFU)
80000
70000
60000
50000
40000
30000
20000
10000
0
Ovalbumin-FS
Ovalbumin-AF555
AIA RPbAI SNA-II SJA DBA GHA SBA VVA BPA WFA HPA GLS-I-A4 ACA ABL PNA GSL-II sWGA DSA STA LEL Calsepa NPA GNA HHA ConA Lch-B Lch-A PSA TJA-I WGA MAA SNA-I PBS PHA-L PHA-E AMA CPA CAA ECA TJA-II AAL LTA UEA-I PA-I EEA MPA VRA MOA PBS BSA
Lectins

B

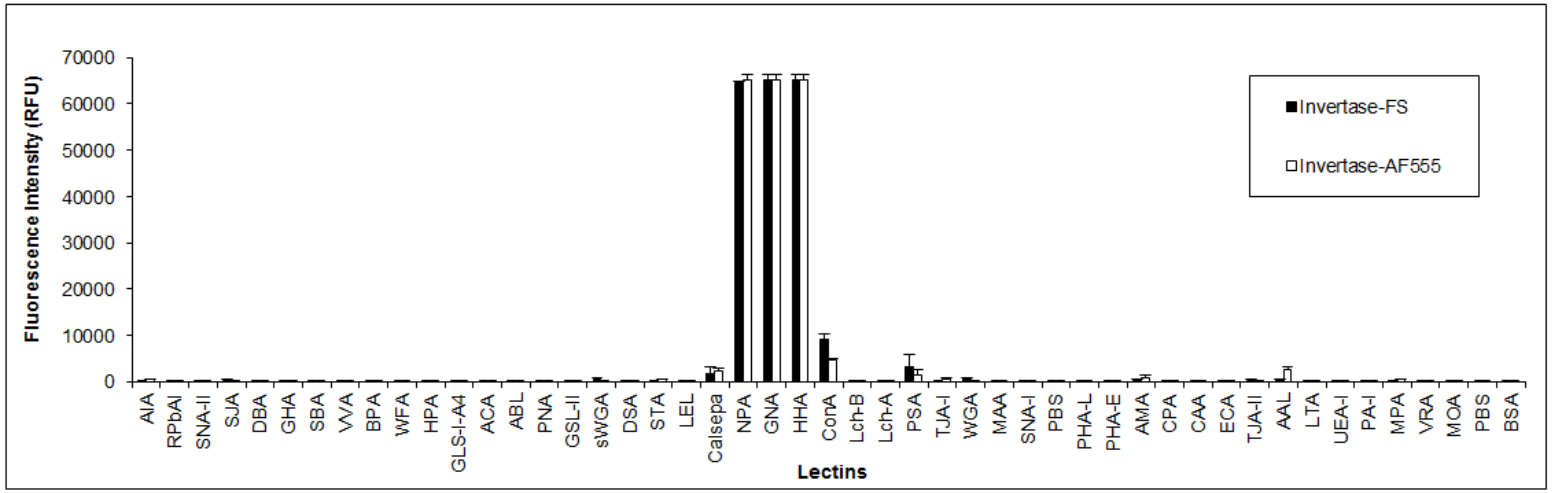
Fluorescence Intensity (RFU)
70000
60000
50000
40000
30000
20000
10000
0
Invertase-FS
Invertase-AF555
AIA RPbAI SNA-II SJA DBA GHA SBA VVA BPA WFA HPA GLS-I-A4 ACA ABL PNA GSL-II sWGA DSA STA LEL Calsepa NPA GNA HHA ConA Lch-B Lch-A PSA TJA-I WGA MAA SNA-I PBS PHA-L PHA-E AMA CPA CAA ECA TJA-II AAL LTA UEA-I PA-I MPA VRA MOA PBS BSA
Lectins

C

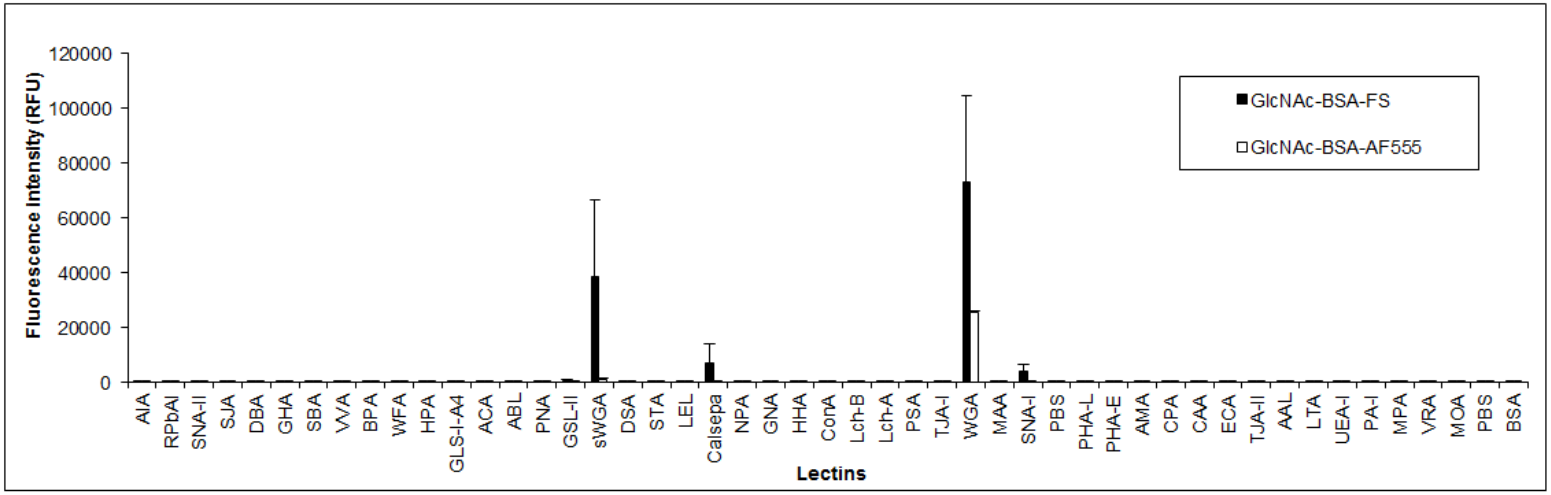
Fluorescence Intensity (RFU)
120000
100000
80000
60000
40000
20000
0
GlcNAc-BSA-FS
GlcNAc-BSA-AF555
AIA RPbAI SNA-II SJA DBA GHA SBA VVA BPA WFA HPA GLS-I-A4 ACA ABL PNA GSL-II sWGA DSA STA LEL Calsepa NPA GNA HHA ConA Lch-B Lch-A PSA TJA-I WGA MAA SNA-I PBS PHA-L PHA-E AMA CPA CAA ECA TJA-II AAL LTA UEA-I PA-I MPA VRA MOA PBS BSA
Lectins

D

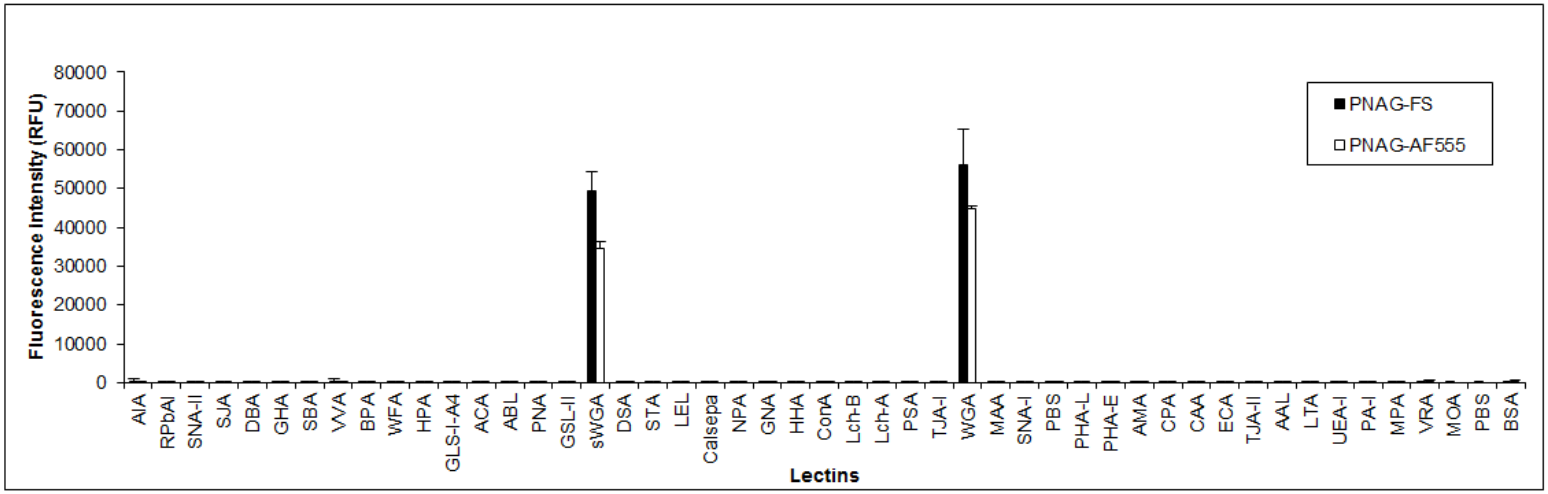
Fluorescence Intensity (RFU)
80000
70000
60000
50000
40000
30000
20000
10000
0
PNAG-FS
PNAG-AF555
AIA RPbAI SNA-II SJA DBA GHA SBA VVA BPA WFA HPA GLS-I-A4 ACA ABL PNA GSL-II sWGA DSA STA LEL Calsepa NPA GNA HHA ConA Lch-B Lch-A PSA TJA-I WGA MAA SNA-I PBS PHA-L PHA-E AMA CPA CAA ECA TJA-II AAL LTA UEA-I PA-I MPA VRA MOA PBS BSA
Lectins

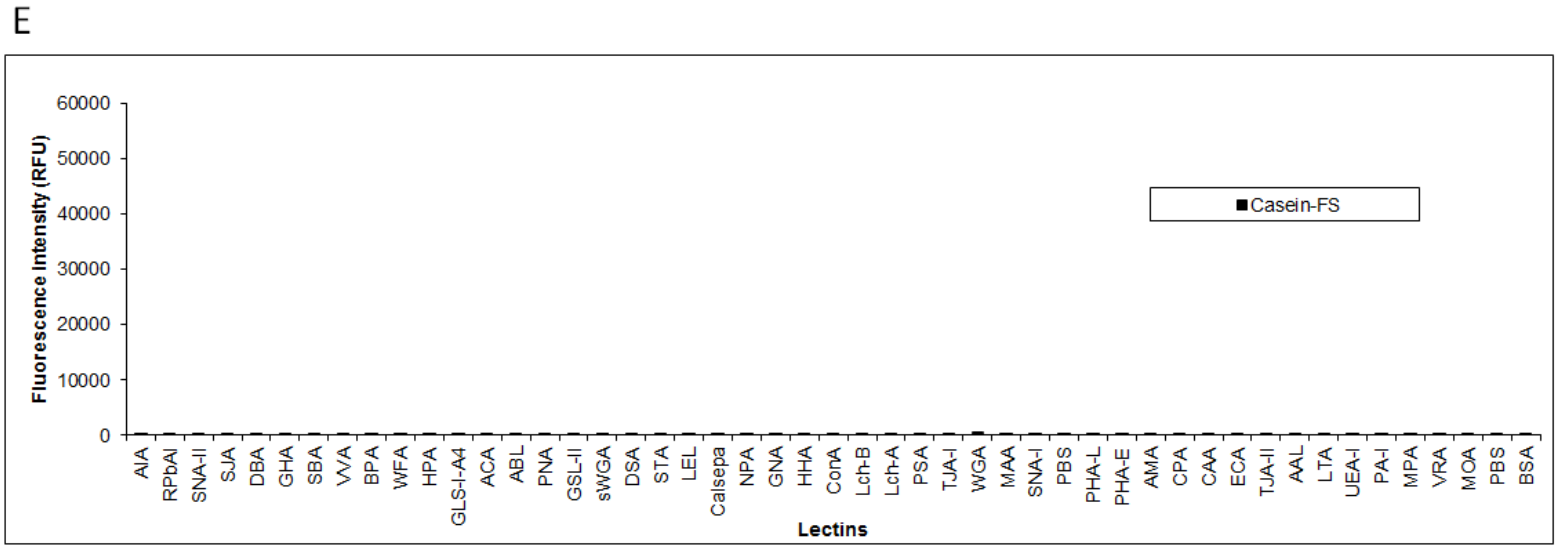


**Fig 3.6. Bar charts comparing lectin binding profiles of glycoproteins or carbohydrates conjugated to FluoSpheres® or Alexa Fluor® 555**. Lectin microarray binding profiles of (A) ovalbumin-AF555 and ovalbumin-FS, (B) invertase-AF555 and invertase-FS, (C) GlcNAc-BSA-AF555 and GlcNAc-BSA-FS, (D) PNAG-AF555 and PNAG-FS and (E) blocking agent casein-FS. All experiments were carried out on three separate slides. Error bars represent +/- one SD of the mean.

### 3.3.5. Assessment of antibody recognition of PNAG following conjugation to FluoSpheres® and Alexa Fluor® 555

To elucidate whether PNAG conjugation to FS or AF555 caused conformational changes to the polysaccharide, we used an antibody specific for PNAG to see if it recognised PNAG-AF555 and PNAG-FS. An anti-PNAG monoclonal antibody (mAb) bound to unlabelled, partially purified PNAG, PNAG-AF555 and PNAG-FS (Fig. 3.7 (A)) in a dot blot but not ovalbumin-FS or ovalbumin-AF555 (Fig. 3.7 (B)). These data indicated that the labelling techniques did not alter the antibody recognition of PNAG, implying that the presentation of the structure remained similar to the unlabelled PNAG and recognisable despite the different labelling formats. In addition, these data confirmed that the anti-PNAG antibody was specific for PNAG (Fig. 3.7 (A)) and did not bind to the AF555 or FS labels, or ovalbumin (Fig. 3.7 (B)). Thus, these observations supported that the structure of PNAG covalently attached to FS or AF555 was still identifiable by a PNAG specific antibody and the antibody recognised PNAG alone, and not FS or the AF555 fluorophore.

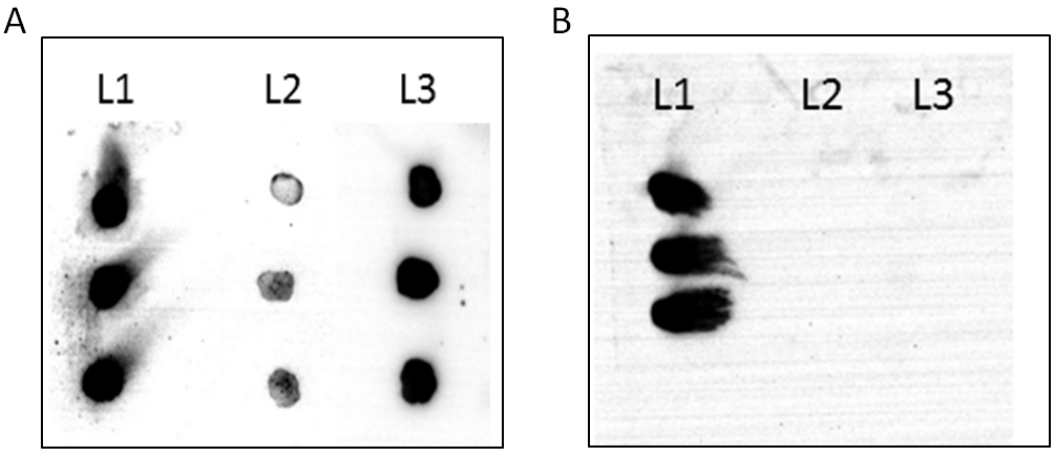


**Fig. 3.7. Dot blot assays using anti-PNAG monoclonal antibody to identify PNAG attached to FluoSpheres® and Alexa Fluor® 555.** (A) Dot blot of (L1) unlabelled partially purified PNAG, (L2) PNAG-FS and (L3) PNAG-AF555 using anti-PNAG mAb (F598) and detected with HRP-labelled rabbit anti-human antibody. (B) Dot blot of (L1) unlabelled partially purified PNAG, (L2) ovalbumin-FS and (L3) ovalbumin-AF555 probed and detected as in (A). All samples were spotted in triplicate.

### 3.3.6. Assessment of partially purified PNAG contaminants

Dot blots were carried out to determine whether there was any contaminating lipoteichoic acid (LTA) or peptidoglycan in the partially purified PNAG preparation. To test for the presence of LTA contamination, purified *S. aureus* LTA was used as a positive control and to generate densitometry units and a standard curve (Fig. 3.8 (A) and (B)). The presence of LTA was detected in the PNAG preparation and was quantified as 3.5 µg of LTA per mg of PNAG (0.35% (w/w)). Thus LTA could be contributing to PNAG binding, although the effects are most likely only minor considering the trace quantity present. Partially purified PNAG was spotted at 1 mg/mL and probed with anti-peptidoglycan antibody at using whole bacteria as a positive control. However the antibody did not bind at any dilution tested to any concentration of PNAG (Fig. 3.8 (C)) which confirmed the absence of peptidoglycan contamination in the PNAG preparation. Overall, these results show that minor quantities of LTA were present in the partially purified PNAG but peptidoglycan was not detected as a contaminant.

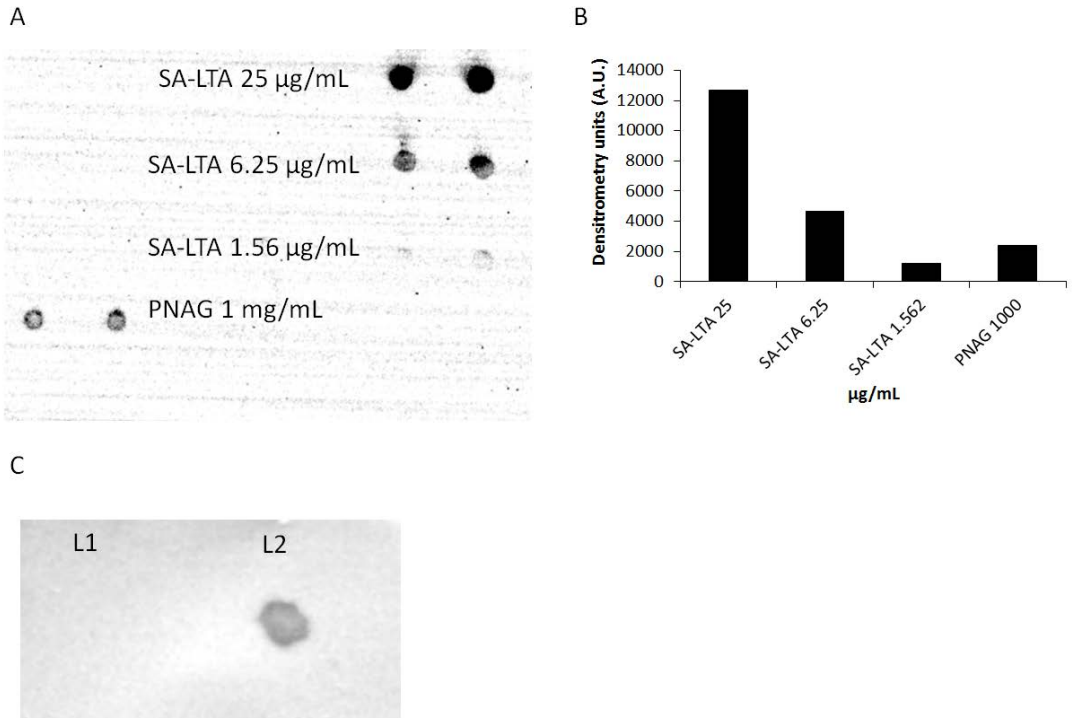


**Fig. 3.8. Dot blot assay for the detection of LTA and peptidoglycan.** (A) Dot blot assay of a standard curve of *S. aureus* LTA (SA-LTA) at 25, 6.25 and 1.56 µg/mL and partially purified PNAG (1 mg/mL). Black colour intensity represents anti-LTA antibody binding. Spotting was carried out in duplicates. (B) Densitometry analysis of image (A) using ImageJ

software. (C) Dot blot assay for the detection of peptidoglycan using a monoclonal antibody against peptidoglycan. L1 represents partially purified PNAG and L1 represents 8 x $10^8$ cells/mL of heat killed *S. aureus.*

### 3.3.7. Glycoclusters at a concentration of 1 mM do not kill *S. aureus* 8325-4

To assess whether the glycoclusters or DMSO had any effect on *S. aureus* growth, a 24 h growth curve was carried out with *S. aureus* 8325-4 in the presence of media supplemented with 1 mM of each glycocluster or DMSO. Addition of DMSO alone in to the growth media reduced log phase growth compared to the control (*S. aureus* 8325-4 in growth media only) (Fig. 3.9). Glycoclusters did not significantly promote or reduce growth of *S. aureus* 8325-4 WT compared to the control. A small reduction in growth appeared to be caused by DMSO, and not the glycoclusters.

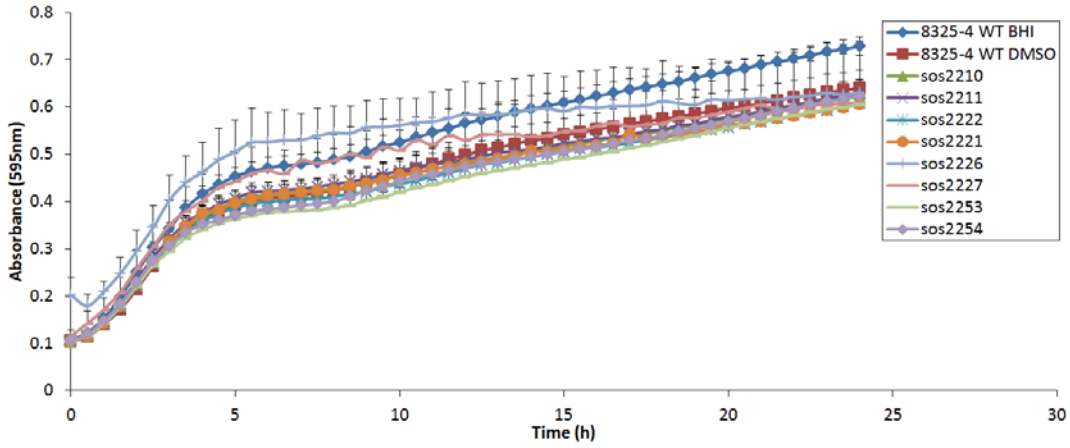


**Fig. 3.9. Growth curve of *S. aureus* in the presence of glycoclusters and DMSO.** Growth assay of *S. aureus* 8325-4 with and without DMSO or glycoclusters (1 mM). Assays were carried out in a hydrophobic 96-well plate for 24 h at 37°C in BHI media supplemented or unsupplemented with the test compounds. Absorbance at 595 nm every 30 min was plotted to indicate bacterial growth. This assay was carried out once and three replicate wells were used to calculate the mean and +/- one SD of the mean, represented as error bars.

Glycoclusters sos2226 and sos2227 (Fig. 3.13) were used only for section 3.3.10 of the results (biofilm inhibition study) but were added to this tolerance assay to verify that these glycoclusters were not killing *S. aureus*. Glycoclusters sos2226 and sos2227 induced small changes in absorbance readings, which suggested that small

aggregates may have been formed in the presence of sos2226 and sos2227, which prevented typical incremental increases usually seen in bacterial growth assays (Fig. 3.9). Overall, this result indicated that the glycoclusters did not kill *S. aureus*, but the presence of DMSO slightly, but not significantly, reduced the growth rate of *S. aureus*.

### 3.3.8. Glycocluster-mediated modulation of lectin binding to PNAG

Due to the lack of availability of certain compounds and the potency of compound sos2211 in inhibiting WGA binding to GlcNAc-BSA-AF555, sos2211 was assessed for its ability to modulate WGA binding to PNAG labelled in the two different formats and *in situ* on the surface *S. aureus*. Glycocluster concentrations of 0.001 mM and 1 mM were used to modulate PNAG-AF555, PNAG-FS, and SYTO® 82 stained *S. aureus* Mn8m interactions with WGA (Fig. 3.10). Compound sos2211 at 10 µM significantly reduced WGA binding to PNAG-AF555 by 80%, increased the binding of WGA to PNAG-FS by 20% and decreased the binding of WGA to *S. aureus* Mn8m by approximately 40%, although the latter two modulations of binding were not significant. Using 1 mM of sos2211 abolished the binding of WGA to PNAG-AF555 and PNAG-FS. Furthermore, 1 mM of sos2211 reduced WGA binding to *S. aureus* Mn8m by approximately 90% (Fig. 3.10 (C)).

To screen for a potent potential inhibitor, all six glycoclusters (Fig. 3.1) were co-incubated with PNAG-AF555 to assess the modulation of lectin binding to PNAG-AF555 (Fig. 3.10 (A) and 3.11). A dilution range of 0.01 fM - 1 mM of sos2211 modulated WGA binding to PNAG-AF555. A reciprocal correlation of decreased binding corresponding to increased glycocluster concentration was not observed until sos2211 concentrations of greater than 0.1 µM were used. Very low concentrations of sos2211 (10 fM) significantly reduced the binding of WGA to PNAG-AF555, however, higher concentrations in the pM range and above promoted binding of WGA again compared to 10 fM (Fig. 3.10 (B)).

The sometimes increased binding to WGA at lower concentrations observed for sos2211 occurred frequently with other glycoclusters, shown with glycocluster sos2211, sos2221 and sos2253 (but at different concentrations), which may indicate aggregation of the glycoclusters at different concentrations. Furthermore,

glycoclusters sos2211, sos2222 and sos2221 also promoted WGA binding to PNAG-AF555 at 0.01 fM (Fig. 3.11 (B), (C) and (D)). At 1 mM concentrations, glycoclusters sos2210, sos2211 and sos2253 reduced WGA binding to PNAG-AF555 by at least 20% (Fig. 3.11 (A), (B) and (E)). These glycoclusters maintained specificity towards GlcNAc-specific lectins and did not promote the binding of any other lectins, besides sWGA and WGA, to PNAG-AF555 (Fig. 3.10 (A)).

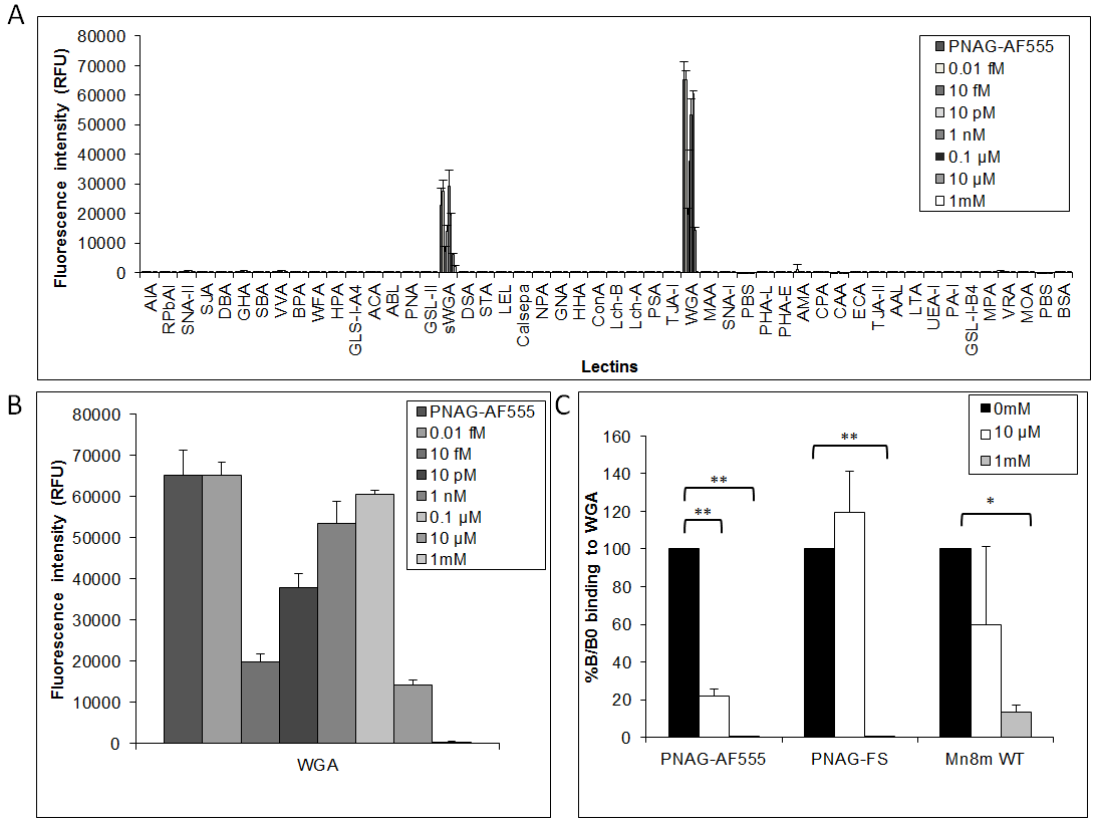


**Fig. 3.10. Glycocluster sos2211 inhibition of WGA binding to PNAG.** (A) Bar chart represents lectin binding inhibition to PNAG-AF555 with sos2211. (B) Bar chart of glycocluster sos2211 modulation of WGA binding to PNAG-AF555from image (A). (C) Inhibition of WGA binding to PNAG-AF555, PNAG-FS and *S. aureus* Mn8m without and with 0.01 and 1 mM of glycocluster sos2211. *S. aureus* Mn8m was initially grown in BHI glucose. B0 represents 100% of binding of PNAG-AF555, PNAG FS or *S. aureus* Mn8m to WGA while %B represents the percentage of PNAG-AF555, PNAG FS or *S. aureus* Mn8m binding to WGA remaining in the presence of the glycocluster. Experiments were carried out on three microarray slides and error bars represent +/- one SD of the mean. Statistical analyses were carried out using normalised lectin microarray data with student's t-test * $P \leq 0.05$, ** $P \leq 0.01$, *** $P \leq 0.001$.

Overall these data show that sos2211 was capable of reducing WGA binding PNAG-AF, PNAG-FS and whole *S. aureus* Mn8m at 1 mM concentrations, but, depending

on the glycocluster, may promote WGA binding to PNAG-AF555 depending on the concentration used.

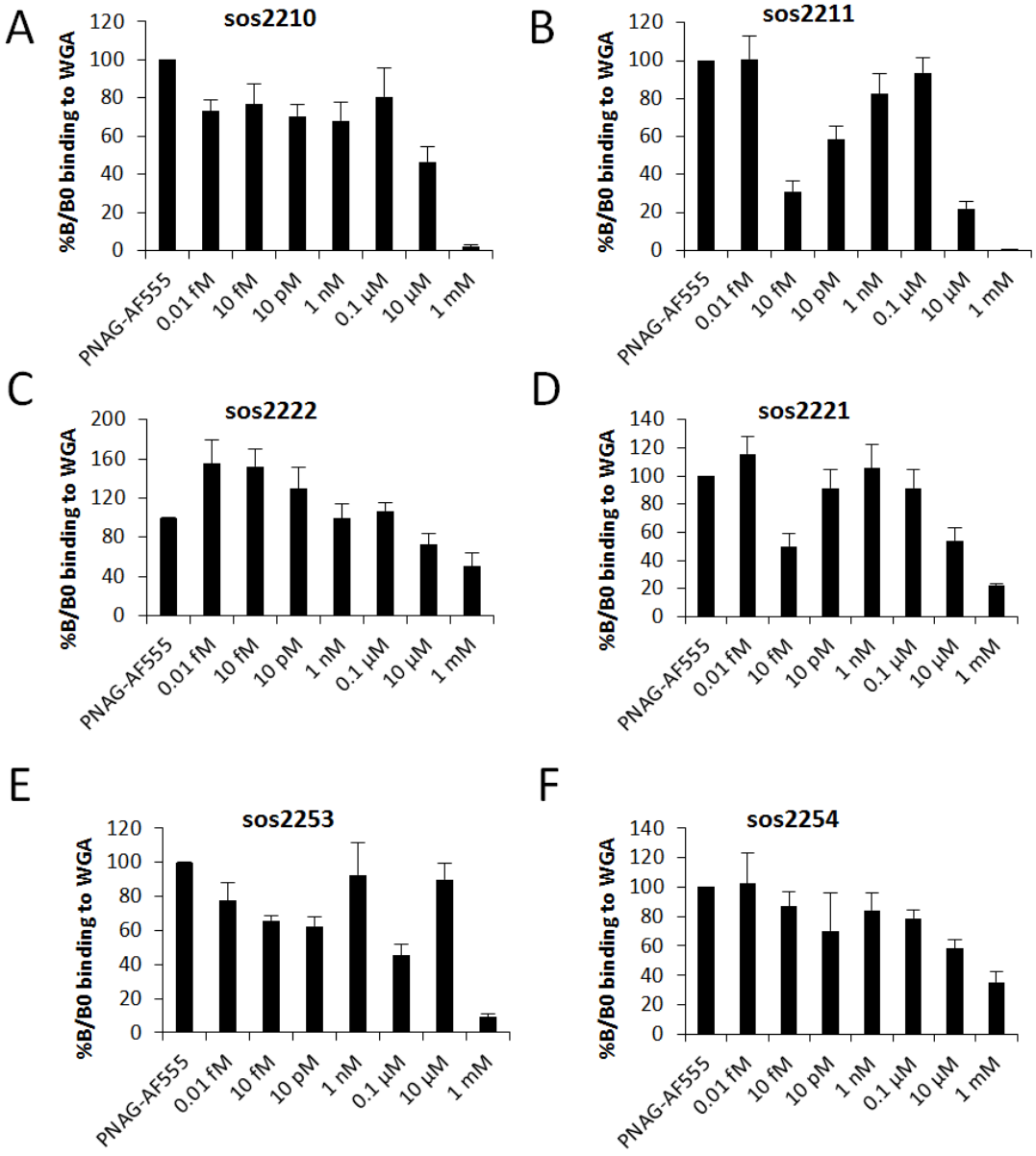


**Fig. 3.11. Glycocluster modulation of WGA binding to PNAG-AF555.** Glycoclusters (A) sos2210, (B) sos2211, (C) sos2222, (D) sos2221 (E) sos2253 and (F) sos2254 inhibition of WGA binding to PNAG-AF555. B0 represents 100% of binding of PNAG-AF555 to WGA while %B represents the percentage of PNAG-AF555 binding to WGA remaining in the presence of the glycocluster. Experiments were carried out on three different microarray slides and error bars represent +/- one SD of the mean.

### 3.3.9. GlcNAc targeted modulation of PNAG and whole *S. aureus* Mn8m binding to CF human lung mucin

As glycoclusters modulated binding of both free PNAG and PNAG *in situ* on whole bacteria to WGA, the potential modulation of whole *S. aureus* and partially purified labelled PNAG interactions with lung mucin purified from patients suffering from CF was assessed using glycoclusters. Purified lung mucin from two different CF patients were coated in a well of a 96-well plate and incubated with PNAG-AF555 or fluorescently stained *S. aureus* Mn8m with and without sos2211 (Fig. 3.12). Interestingly, addition of sos2211 with PNAG-AF555 or *S. aureus* Mn8m slightly increased binding to purified CF mucin from patient 1 (CF1) (Fig. 3.12 (A) and (B). On the other hand, sos2211 reduced binding of PNAG-AF555 to CF lung mucin from patient 2 (CF2) by approximately 20%. However, addition of sos2211 promoted binding of *S. aureus* Mn8m to CF2 by approximately 100% (Fig. 3.12 (A) and (B). These data suggested that although this compound may have positive modulatory effects on PNAG, this does not necessarily mean that it will be the same for whole bacteria. In addition, if anti-adhesive compounds were to be deployed clinically, they should be screened for individual patients as the effects were different depending on the patient.

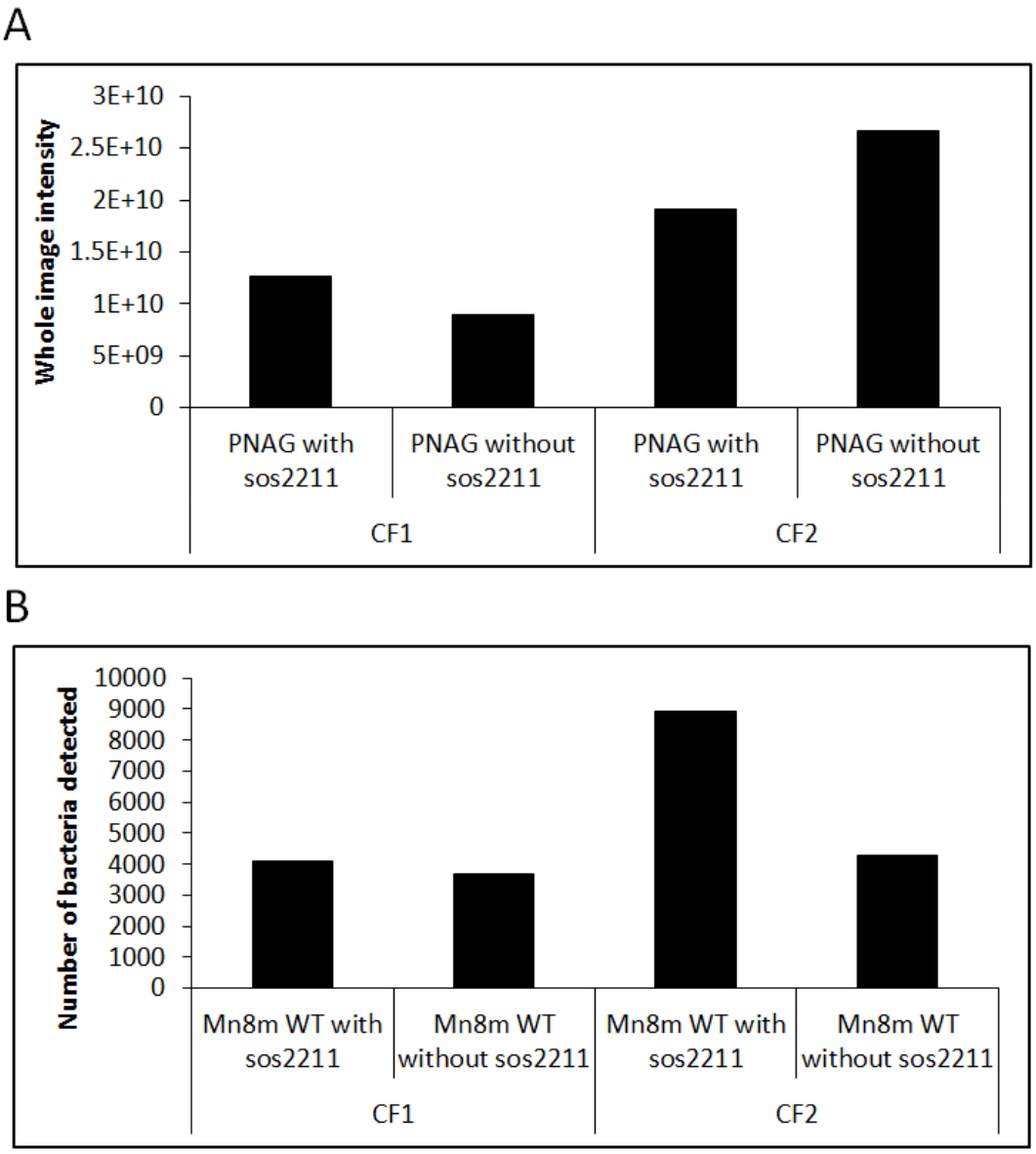


**Fig. 3.12. Glycocluster sos2211 modulation of PNAG-AF555 and *S. aureus* binding to CF human lung mucin.** (A) Bar chart represents whole image intensity of PNAG-AF555 binding to CF lung mucin from patient 1 (CF1) and patient 2 (CF2), with and without 1 mM of sos2211. (B) Histogram represents the number of fluorescent *S. aureus* Mn8m cells bound to CF1 and CF2 following incubation with and without 1 mM of sos2211. This experiment was carried out once, using one well per sample.

### 3.3.10. A trivalent and tetravalent glycocluster were added for biofilm inhibition studies

A trivalent (sos2227) and tetravalent (sos2226) glycocluster with GlcNAc as the bioactive head group (Fig. 3.13) were added to the panel of six glycoclusters (Fig. 3.1) for biofilm inhibition studies. Sos2226 was estimated to have distances of 14 Å/27 Å/30 Å (latter across the diagonal) between GlcNAc head groups which were α-linked *via* sulfur. Sos2227 was estimated to have a distance of 16 Å between each GlcNAc head group also α-linked *via* sulfur (Fig. 3.13). These two glycoclusters were not assessed in the assays detailed earlier due to very limited quantity availability.

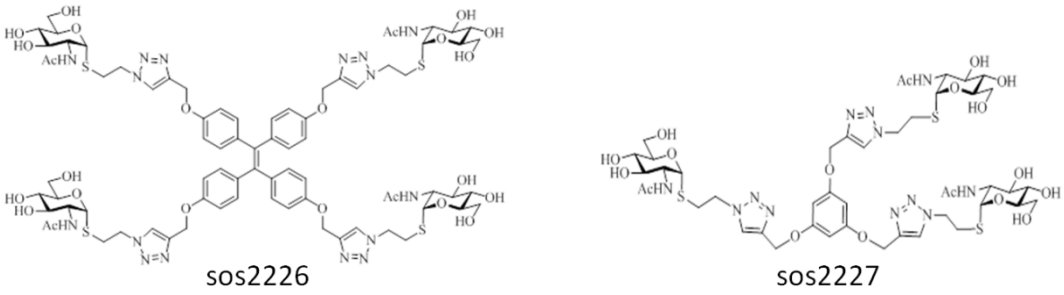


**Fig. 3.13. Structures of additional glycoclusters used for biofilm inhibition studies.**

### 3.3.11. Impact of glycoclusters on PNAG-dependent biofilm formation

To elucidate whether the expanded panel of 8 glycoclusters had any inhibitory effect on PNAG-mediated biofilm formation, delta surface treated microtitre plates were coated with 0.5 mM or 1 mM of each glycocluster in BHI NaCl or BHI glucose followed by addition of *S. aureus* Mn8m WT and Δ*ica* or *S. aureus* 8325-4 WT and Δ*ica*. NaCl was used for culturing *S. aureus* 8325-4 and glucose for *S. aureus* Mn8m to promote biofilm formation for each *S. aureus* strain. Both strains required the *ica* operon for biofilm formation, which indicated a dependence on PNAG for biofilm formation (Fig. 3.14 (A) and (B)). Addition of DMSO to the culture medium did not affect biofilm formation of *S. aureus* 8325-4 (Fig. 3.14 (A)) or *S. aureus* Mn8m (Fig. 3.14 (B)).

The addition of 1 mM of sos2222 and sos2221 significantly reduced *S. aureus* 8325-4 biofilm formation, by 16% and 19%, respectively ($P \leq 0.05$) (Fig 3.14 (A)).

Glycocluster sos2226 at 1 mM and sos2227 at 0.5 mM and 1 mM significantly reduced biofilm formation of *S. aureus* 8325-4 ($P \leq 0.01$), by 87%, 68% and 90%, respectively (Fig. 3.14 (A)). Glycoclusters sos2211 and sos2222 at 1 mM significantly reduced biofilm formation by *S. aureus* Mn8m ($P \leq 0.05$), by 12% and 29%, respectively (Fig. 3.14 (B)). Similar to *S. aureus* 8325-4, glycocluster sos2226 at 1 mM and sos2227 at 0.5 mM and 1 mM significantly reduced biofilm formation for *S. aureus* Mn8m ($P \leq 0.01$), by 46%, 36% and 75%, respectively (Fig. 3.14 (B)). Overall, these data show that sos2211 at 1 mM, sos2222 at 1 mM, sos2226 at 1 mM and sos2227 at 0.5 and 1 mM significantly reduced biofilm formation for two different PNAG-producing *S. aureus* strains.

### 3.3.12. Compound sos2226 reduced PNAG-independent, protein-dependent biofilm formation by MRSA strain BH1CC

To establish whether biofilm inhibition by glycoclusters was dependent on PNAG-mediated biofilms, a proteinaceous biofilm producer, *S. aureus* BH1CC, was assessed for glycocluster biofilm inhibition. Stocks of the most potent biofilm inhibitor sos2227 were exhausted in previous biofilm inhibition assays, therefore, the second best biofilm inhibitor, sos2226 (Fig. 3.14), was used for the *S. aureus* BH1CC biofilm inhibition assay. Biofilm formation was significantly reduced following incubation with 0.5 mM and 1 mM of sos2226, by 51% ($P \leq 0.05$) and 76% ($P \leq 0.01$), respectively (Fig. 3.15). This result showed that sos2226 inhibited protein-dependent biofilm formation by *S. aureus* BH1CC. Therefore inhibition of biofilm formation by sos2226 was not wholey PNAG-mediated.

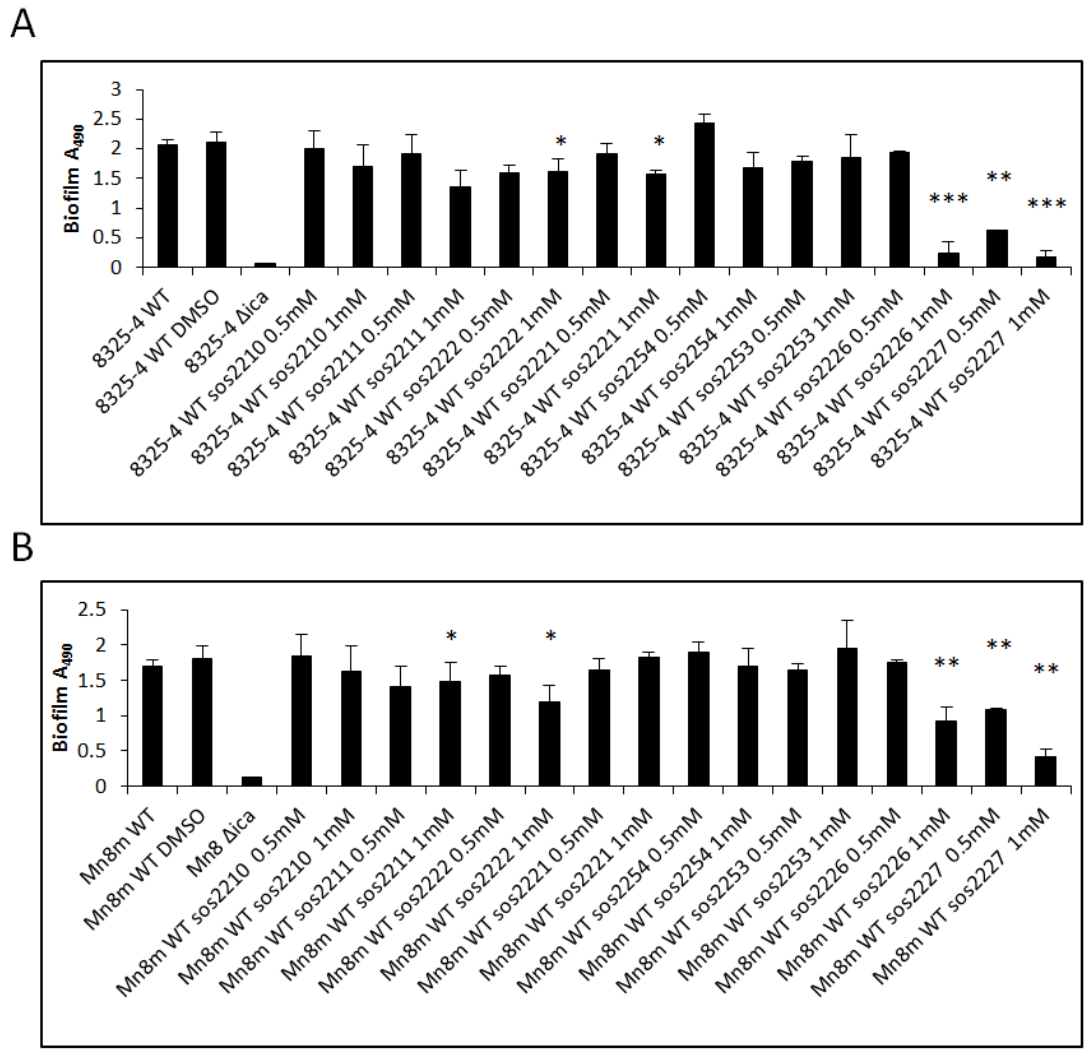


**Fig. 3.14. Biofilm inhibition assay with *S. aureus* 8325-4 and Mn8m with 0.5 or 1 mM of glycocluster.** Nunc (Δ) surface treated plates were pre-incubated with (A) BHI NaCl (*S. aureus* 8325-4 WT and Δ*ica*) or (B) BHI glucose (Mn8m WT and Mn8 Δ*ica*) with various glycoclusters at 0.5 mM or 1 mM. Bacteria were added to wells and plates were incubated for 24 h at 37°C under static conditions. Bars represent the absorbance at 495 nm of crystal violet stained biofilm and one biological experiment in technical triplicate per sample. Average taken from readings of the 3 wells and error bars represent +/- one SD of the mean. Statistical analysis was carried out with student's t-test * $P \leq 0.05$, ** $P \leq 0.01$, *** $P \leq 0.001$.

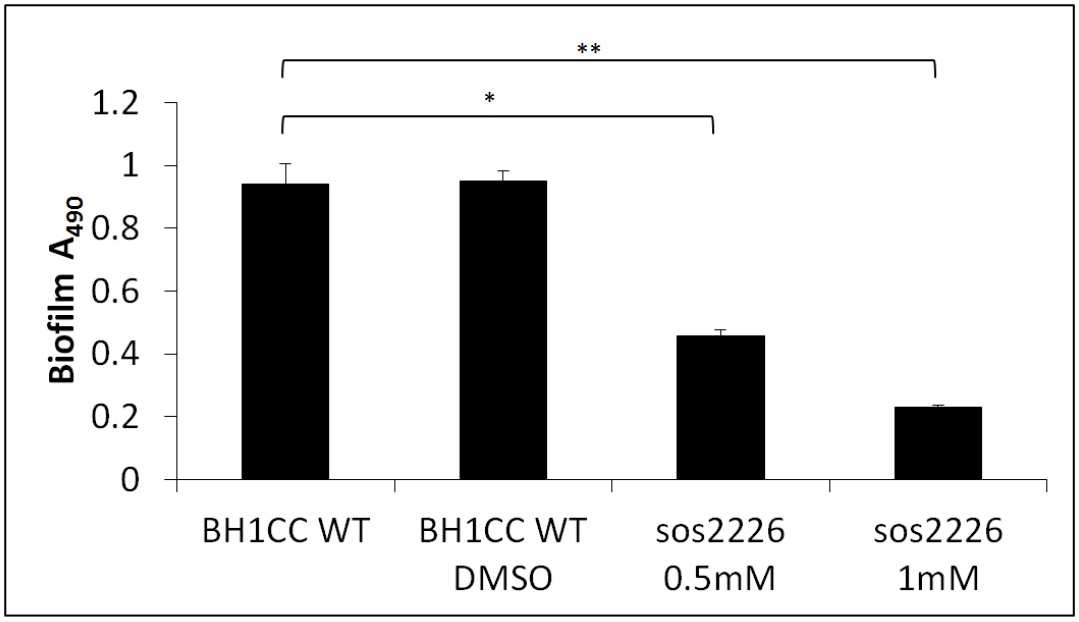


**Fig. 3.15. Biofilm inhibition assay for *S. aureus* BH1CC with 0.5 or 1 mM of sos2226.** Nunc (Δ) surface treated plates were pre-incubated with BHI glucose with 0.5 mM or 1 mM sos2226. *S. aureus* BH1CC were added to wells and plates were incubated for 24 h at 37°C under static conditions. Bars represent the absorbance at 495 nm of crystal violet stained biofilm and one biological experiment in technical triplicate per sample. Average taken from readings of the 3 wells and error bars represent +/- one SD of the mean. Statistical analysis was carried out with student's t-test * $P \leq 0.05$, ** $P \leq 0.01$, *** $P \leq 0.001$.

### 3.3.13. Elucidation of the mechanism of sos2226-mediated biofilm inhibition

To elucidate the mechanism of how glycocluster sos2226 inhibited biofilm formation, sos2226 was used to inhibit *S. aureus* strains 8325-4 and BH1CC again, and wells were visualised for biofilm morphology. Normal biofilm was smooth on the bottom of the well for *S. aureus* strains 8325-4 and BH1CC. However, addition of 0.5 mM or 1 mM of sos2226 caused clear aggregation of cells and a clear reduction in biofilm coating on the bottom of the 96-well plate (Fig. 3.16).

In addition, following this result, it was noted that compounds sos2226 and sos2227 were increasingly insoluble after several freeze-thaw cycles and began to precipitate out of solution and crystallised in growth media. Therefore, these data suggested that precipitated sos2226 inhibited biofilm formation of *S. aureus* strains BH1CC, 8325-

4 and Mn8m by clumping bacterial cells together, forming aggregates in wells of 96-well plates, and therefore preventing biofilm formation.

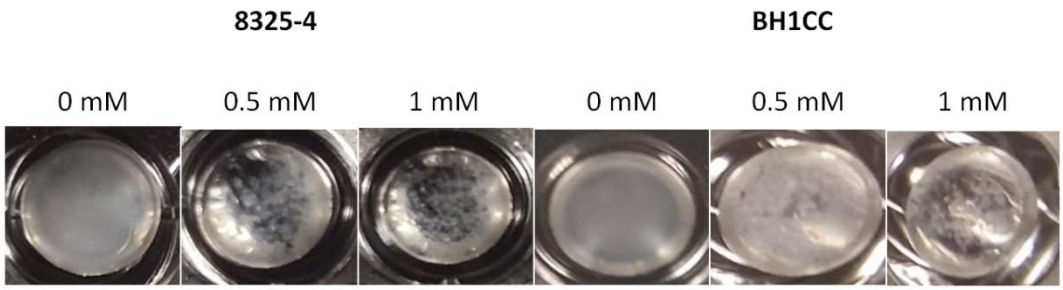


**Fig. 3.16. Images of *S. aureus* strains 8325-4 and BH1CC biofilm in wells from a 96-well plate following pre-incubation with sos2226.** Images represent biofilms formed by *S. aureus* 8325-4 or BH1CC on Δ surface treated 96-well plates following 24 h incubation, with or without sos2226.

### 3.4. Discussion

HTP methods of identifying potent inhibitors of *S. aureus*- and PNAG-mediated interactions will be of great importance in the rapid development of novel therapeutics to combat *S. aureus* and biofilm associated infections. In this study, lectin microarrays were established as a suitable and reproducible platform for determining $IC_{50}$ values. HTP lectin microarrays were then used to demonstrate the suitability of glycoclusters to inhibit targeted lectin binding to PNAG and *S. aureus*. Finally, while one glycocluster inhibited PNAG binding to lung mucin from a CF patient, it also promoted the binding of the whole bacteria. Certain glycoclusters reduced biofilm formation by MSSA and MRSA, hypothesised to be a result of glycocluster micelle formation and bacterial aggregation resulting in no bacterial adherence to the 96-well plate.

Previously, a panel of glycoclusters, which included the subset of glycoclusters assessed in this work, was shown to inhibit WGA binding to GlcNAc-containing molecules using a microtiter plate assay (André *et al.*, 2015). The GlcNAc-containing molecules included an agalacto version of asialofetuin (ASF) and GlcNAc-BSA, which were absorbed on to the surface of microtitre plate wells. Following blocking, biotinylated WGA and GSL-II were incubated in each well with or without the various glycoclusters. Using a streptavidin-peroxidase and an enzymatic substrate mixture, absorbance was read which corresponded to bound biotinylated lectin. Compounds and glycocluster stocks are often limited, and plate assays can be time consuming with overnight coating and 1 hour incubation steps. On the other hand, lectin microarrays take approximately 3 hours to complete, use very low volumes and can be highly multiplexed, meaning lower quantities of valuable compounds or glycoclusters are required. Furthermore, individual lectins do not have to be assessed separately, but multiple glycocluster targets can be screened at once. To compare assay platforms, we used a smaller number of glycoclusters to compare the values of WGA binding inhibition to GlcNAc-BSA. Although not directly comparable to agalactoASF, the natural glycoprotein ovalbumin, which has terminal GlcNAc and mannose structures (Harvey *et al.*, 2000), was also assessed on the lectin microarray platform.

The GlcNAc glycoclusters were successful in inhibiting targeted GlcNAc-mediated WGA binding to GlcNAc-BSA and ovalbumin binding on the lectin microarray platform. In the microtitre plate assay, the glycocluster sos2211 was the most potent inhibitor of WGA binding to GlcNAc-BSA, next was sos2210, followed by sos2253 and sos2221 followed by the least potent, sos2254 and sos2222 (André *et al.*, 2015). In comparison, the lectin microarray demonstrated that the glycoclusters sos2210, sos2221 and sos2253 were the most potent at inhibiting WGA binding to GlcNAc-BSA, while sos2254 and sos2222 were the least potent using a robust fit for inhibition curves (Table 3.4). It is evident from these results that the lectin microarray platform was a more sensitive platform for calculating $IC_{50}$ values compared to the 96-well plate platform. Furthermore, lectin microarray data showed clear reproducibility of data between different microarray slides represented by low %CV values glycocluster inhibition of WGA binding to ovalbumin-AF555 (16.5 – 33.9) and GlcNAc-BSA-AF555 (1.3 – 16.6). A possible explanation why the lectin microarray was a more sensitive platform may be due to the conjugation of WGA to the microarray slide, preventing free movement as was the case for the 96-well plate assay. Perhaps, WGA conjugated to a microarray slide gave glycoclusters better access to WGA binding sites compared to freely suspended biotinylated WGA. Another possible explanation of the difference in order of potency and $IC_{50}$ values could be due to different presentations of GlcNAc-BSA depending on whether it is coated on to a microtitre plate or fluorescently tagged with a fluorophore.

Higher concentrations of glycoclusters were required to inhibit WGA binding to ovalbumin-AF555 compared to GlcNAc-BSA. The most potent glycocluster inhibitors were sos2222 and sos2221, both consisting of GlcNAc head groups attached via sulfur in an α-linkage. Interestingly, the least potent glycocluster inhibitor for WGA binding to ovalbumin was sos2253, which was one of the most potent inhibitors of GlcNAc-BSA binding to WGA. This suggested that WGA bound preferentially to the biantennary GlcNAc present on ovalbumin, rather than the GlcNAc presented on sos2253, and a higher concentration of sos2253 was required to compete with this interaction. WGA is a stable homodimer with axial twofold symmetry. Distances between WGA adjacent binding sites can be as small as 13 - 14 Å, or as large as 29 Å or 37 Å for linear binding sites (Wittmann & Pieters, 2013). The spacing between GlcNAc bioactive headgroups on the panel of glycoclusters

was approximately 16 Å apart, and probably suiting to binding WGA adjacent binding sites close to each other. In contrast, ovalbumin has complex GlcNAc-containing glycans and can have up to five antenne (Harvey *et al.*, 2000). Therefore, GlcNAc found on ovalbumin may be more suitable to bind binding sites that are close to one another as well as further away. Consequently, higher concentrations of glycoclusters were required to compete or displace WGA-ovalbumin interactions. Likewise, glycoclusters that can bind two WGA binding sites at once at fixed distances that are presented on a rigid scaffold would be more potent than GlcNAc residues presented singly at random distances and that are presented on a mobile scaffold (GlcNAc-BSA) and may have accounted for the lower $IC_{50}$ inhibition values compared to ovalbumin.

Interestingly, by using a least squares fit to generate $IC_{50}$ values for glycoclusters inhibiting WGA binding to GlcNAc-BSA, there was a change in the order of the potency for some of the glycoclusters (Table 3.4). Nonetheless, sos2210 still remained the most potent glycocluster. In the future, it would be crucial to ensure an adequate supply of glycoclusters to carry out multiple replicates to determine glycocluster-specific concentration ranges, and, to produce composite curves in order to include errors for the $IC_{50}$ and confidence in the reproducibility of the values produced for the standard curves. Overall, this proof of concept work demonstrates the microarray platform could be viable platform for screening or ranking glycoclusters to go to the next stage of the the glycocluster screening and development pipeline.

**Table 3.4. $IC_{50}$ values (µM) for glycocluster and monosaccharide inhibitions of WGA binding to GlcNAc-BSA on the lectin microarray or using a 96-well plate format.** GlcNAc-BSA-AF555 (0.1 µg/mL) and surface conjugated WGA (0.5 mg/mL) was used on for lectin microarrays in this study and IC50 values were calculated using a robust fit and 7 glycocluster concentrations or a least squares fit and five glycocluster concentrations. WGA (0.02 µg/mL) and surface conjugated GlcNAc-BSA (0.02 µg) was used on for the 96-well plate format (André *et al.*, 2015).

| Glycocluster/ monosaccharide | GlcNAc-BSA Lectin microarray *Robust fit* | GlcNAc-BSA Lectin microarray *Least Squares fit* | GlcNAc-BSA 96-well plate |
|---|---|---|---|
| sos2210 | $5.3 \times 10^{-12}$ | $2.9 \times 10^{-6}$ | 11 |
| sos2211 | $5.9 \times 10^{-2}$ | $1.7 \times 10^{-3}$ | 8.5 |
| sos2222 | $2.1 \times 10^{-1}$ | $1.4 \times 10^{-1}$ | 26 |
| sos2221 | $3.0 \times 10^{-5}$ | $8.3 \times 10^{-4}$ | 15 |
| sos2253 | $3.0 \times 10^{-5}$ | $2.3 \times 10^{-1}$ | 15 |
| sos2254 | $3.7 \times 10^{-1}$ | 6.3 | 19 |
| GlcNAc | 37.3 | 11.1 | 25,000 |
| Man | Not Inhibitory | Not Inhibitory | Not Determined |

WGA is widely used to demonstrate the presence of PNAG, both on bacterial surfaces and in biofilm matrices (Arciola *et al.*, 2015; Begun *et al.*, 2007; Singh *et al.*, 2010). However from these data it was clear that WGA binding was not specific for just PNAG on the bacterial cell surface, but also other cell surface structures that contain GlcNAc. Indeed, WGA has been previously shown to bind to the wall teichoic acids, peptidoglycan and capsular polysaccharide on the cell surface of *S. aureus* (Hancock & Cox, 1991; Kiriyama *et al.*, 2014; Lotan *et al.*, 1975; Xia *et al.*, 2010). Moreover, it has been shown that WGA interacts specifically with *N*-acetylated sugar residues in highly de-*N*-acetylated chitosan, and this interaction was not inhibited by fully de-*N*-acetylated chitosan, suggesting that WGA has preferential binding to *N*-acetylated GlcNAc rather than de-*N*-acetylated GlcNAc

(Kristiarisen *et al.,* 1999). Therefore we propose that WGA should no longer be used as a diagnostic for the presence of PNAG. On the other hand, our data showed sWGA preferentially bound to PNAG. Succinylation of WGA changes the protein isoelectric pH (p*I*) from 8.5 to an acidic p*I* of 4 (Monsigny *et al.,* 1979) and in a pH of 7.2 gives the protein a negative charge (Moullier *et al.,* 1986). In addition, it abolishes the additional binding that WGA has for the charged residue sialic acid and renders the binding of sWGA for exclusively GlcNAc residues. In future, the use of sWGA should be promoted as a more specific diagnostic for the presence of PNAG rather than WGA.

Specific binding of sWGA and WGA to PNAG was also seen with PNAG-AF555 and PNAG-FS confirming that sWGA and WGA interacts with PNAG on the lectin microarray platform. Notably, a minor quantity of contaminating LTA was found in the PNAG preparation which may have contributed to lectin binding. Although it has been shown that *S. aureus* LTA can be glycosylated with GlcNAc, LTA from *S. aureus* Mn8m was reported to not contain GlcNAc from purified LTA extracts (Kho & Meredith, 2018; Morath *et al.,* 2001; Vinogradov *et al.,* 2006). Combined with the minor quantity (0.35% (w/w)), it is therefore unlikely that LTA contributed significantly to PNAG binding to the lectins.

To the best of our knowledge, this is the first study to report direct conjugation of a fluorescent probe on to the PNAG molecule, and conjugation of PNAG on to FluoSpheres® to model 'free floating' PNAG and PNAG attached to a bacterial cell surface, respectively. Despite the labelling orientation influencing the pattern of recognition for ovalbumin and GlcNAc-BSA, it did not alter the identity of the lectins that bound to these glycoproteins. On the other hand, neither the pattern of recognition nor the identity of the lectins were influenced by the labelling strategy for PNAG binding, which is possibly due to the greater flexibility of PNAG compared to ovalbumin and GlcNAc-BSA. This multiple format labelling strategy to model biologically relevant presentations can provide valuable insight in to potentially altered biological responses that may be dependent on molecular presentation for future studies.

The panel of glycoclusters was also used to inhibit WGA binding to PNAG-AF555, however, concentration-dependent inhibition of WGA binding to PNAG-AF555 was

not obtained with the concentration ranges of glycoclusters used in this study. High concentrations of each glycocluster were needed to significantly reduce WGA binding to PNAG-AF555. The sensitivity of the lectin microarray platform allowed us to observe fluctuating increases and decreases in WGA binding to PNAG-AF555 with glycocluster concentrations lower than 10 µM, in particular for sos2211, sos2221 and sos2253. Why sos2211, sos2221 and sos2253 promoted WGA binding to PNAG-AF555 at certain concentrations is unknown, but we speculate the low-dose hook effect has some part to play. The low dose hook effect typically occurs during competitive assays and causes an increase in analyte binding to the ligand at low concentrations (Bindslev, 2008). Therefore, at concentrations close to the dissociation constant for the displacer ligand (glycocluster), an increase or fluctuations in WGA binding PNAG-AF555 was observed before decreased binding was observed with higher concentrations, of displacer ligand (glycocluster). The only similarity between these three glycoclusters is that the flexibility of the linker would be similar for all three glycoclusters. Based on a similar panel of glycoclusters with GalNAc as the bioactive headgroups, glycoclusters sos2211, sos2221 and sos2253 have approximately 1 Å increase in distance between the anomeric carbons of GlcNAc compared to sos2210 and sos2254 (André *et al.*, 2015), which did not increase WGA binding to PNAG at any concentration. Interestingly, fluctuating increases and decreases in WGA binding to GlcNAc-BSA was also seen with sos2221 sos2253 and sos2254.

Sos2210 and sos2254 had the same valency and anomeric configuration, but differed in linkages – sos2210 had S-linkages while sos2254 had O-linkage to connect GlcNAc headgroups to the linker arms. Since WGA has four binding sites, presentation of GlcNAc headgroups on scaffolds, and relative spacing of GlcNAc molecules to one another is very important (Schwefel *et al.*, 2010). These data suggested that PNAG associated and disassociated with WGA at different concentrations of glycoclusters. Molecules can assume several conformations in solution, and depending on the concentration of a molecule present, there can be different distributions of the different molecular conformations (Lerbret *et al.*, 2005). It may be possible that particular binding sites on WGA could be preferentially occupied by particular conformations of glycocluster, depending on the concentration of each glycocluster present. This work also draws attention to the fact

that mammalian type structure, such as ovalbumin and fetuin, or monosaccharides that are commonly used in inhibition studies, are not representative of the interactions of bacterial structures. Studies that involved *in silico* modelling of these different carbohydrate molecules would help elucidate this hypothesis. This research highlights the need for interaction studies using bacterial derived molecules and whole bacteria to truly help understand lectin-bacteria mediated interactions, which will in turn aid the development of glycoclusters and compounds to modulate these interactions.

A multitude of compounds have been used previously to inhibit *S. aureus* biofilm formation, but, to our knowledge, none of these compounds included glycoclusters (Chung & Toh, 2014; Sabatini *et al*., 2017; Shrestha *et al*., 2016). In terms of biofilm inhibition, strategies employing synthetic glycoclusters have focused on inhibition of *P. aeruginosa* biofilm formation. This is likely due to the fact that *P. aeruginosa* relies on surface lectins for the formation of biofilms and this provides target lectins for the glycocluster research and development. *P. aeruginosa* biofilm formation is partially mediated by PA-IL, also known as LecA and which has specificity for D-Gal residues, and PA-IIL, also known as LecB and which has specificity for L-Fuc residues. However, no lectin targets are known for *S. aureus* biofilms. Greater concentrations of the divalent glycoclusters tested in this study were required for *S. aureus* biofilm inhibition compared to the tetravalent mannose-centered galactosclusters that were shown to have reduced *P. aeruginosa* biofilm formation. For example, Ligeour *et al.* (2015) inhibited *P. aeruginosa* biofilm by 40% with 10 μM of galactocluster (Ligeour *et al.*, 2015), whereas 500 μM of sos2227 was required to inhibit *S. aureus* Mn8m biofilm by 36% in this study. In comparison, glycoclusters used for this research were not as potent, but this work may suggest that there are GlcNAc-binding adhesins on *S. aureus* that are involved in biofilm formation that would result in some divalent glycoclusters capable of reducing biofilm formation for *S. aureus* and so may be a promising anti-biofilm or anti-adhesion target for future developments in *S. aureus*-targeted therapeutics. Sos2222 was the common glycocluster that significantly reduced biofilm formation for *S. aureus* 8325-4 and Mn8m, the glycocluster with the greatest distance between the α-linked GlcNAc headgroups, and this may provide insight of the spacing and configuration of GlcNAc ligands that are involved in *S. aureus* biofilm formation.

Both tri- and tetra-valent glycoclusters, sos2226 and sos2227, caused significant reductions in biofilm formation for two PNAG-producing MSSA strains and the MRSA strain and the mechanism was indicated to be independent of PNAG. Thus, we hypothesise biofilm inhibition was caused by possible glycocluster micelle formation and bacterial agglutination. Nonetheless, sos2226 and sos2227 did not kill *S. aureus*, thus understanding how these changes to sos2226 and sos2227 prevented biofilm formation may provide supportive information for the development of glycocluster-containing coatings to prevent biofilm formation on surfaces such as medical devices.

Sos2211 had diverse effects on the ability of *S. aureus* Mn8m to bind to CF mucins. Glycocluster sos2211 had little effect on *S. aureus* Mn8m binding to CF1 but increased binding of *S. aureus* Mn8m to CF2 by approximately 2-fold compared to CF1. Contrastingly, sos2211 decreased PNAG-AF555 binding to CF2. This result highlights the importance of assessing glycoclusters or compounds using biological samples from multiple individuals and whole bacteria as well as bacterial molecules, as with the multiplicity of potential interactions, outcomes can be more complex than anticipated with single interaction studies. PNAG may facilitate bacteria binding to mucin, but evidently targeting PNAG-mediated interactions is not sufficient for inhibiting whole *S. aureus* interactions with mucins. It may be that glycoclusters prevent lectin-bacteria interactions, but promote interactions elsewhere in the body such as to mucin in mucous membranes, which could have significant negative knock-on effects for patients. For patient CF1 and CF2, addition of sos2211 increased the binding of whole *S. aureus* Mn8m. Although this may not be the case for the other glycoclusters, we suggest that glycoclusters should be assessed on a patient by patient basis, where a personalised or precision medicine approach may be more suitable. It remains to be elucidated what modulatory effect these glycoclusters have on whole *S. aureus* binding to healthy mucin samples, but will be an interesting avenue for further research in the future.

Most research carried out on CF has been on *P. aeruginosa* and its association with CF mucin (Devaraj *et al.,* 1994; Flynn *et al.,* 2016; Li *et al.,* 1997; Robinson *et al.,* 2012; Scharfman *et al.,* 1999). *S. aureus* is one of the most prevalent organisms in CF patients, especially in young children with CF (Stone & Saiman, 2007), yet specific interactions between *S. aureus* and CF mucins have not been identified.

Interestingly, *S. aureus* Mn8m bound to mucin purified from CF2 to a greater degree compared to binding to mucin purified from CF1. This suggested that the glycosylation of the mucin profile from CF2 provided more favourable ligands for whole *S. aureus* Mn8m. Beyond the increased binding effect that sos2211 had on *S. aureus* interactions with mucins purified from CF patients, our study highlights the importance of mucin composition in *S. aureus*-mediated interactions in CF and demonstrates for the first time that *S. aureus* can bind to the mucin itself. Moreover, the particular strain of *S. aureus* is likely to also play a major role in binding to mucins, as the binding of *S. aureus* to nasal mucin was previously shown to be strain dependent (Shuter *et al.*, 1996). This research provides preliminary data that showed preferential binding of *S. aureus* to CF mucin depending on the patient origin and/or composition of the purified CF mucin.

In conclusion, this study presents the lectin microarray platform as a sensitive, HTP platform that can assess suitable glycoclusters for inhibition studies and is suitable, sensitive and reproducible for calculating $IC_{50}$ values. On the same slide, the suitability of glycoclusters in lectin binding inhibition can be assessed for glycoproteins, neoglycoconjugates, polysaccharides and whole bacteria. Thus, HTP profiling and glycocluster section can be assessed within one day and with less reagents consumed compared to typical 96-well based assays. Specific PNAG interactions were visualised using two novel methods of labelling the polysaccharide, *via* conjugation to Alexa Fluor® 555 and FluoSpheres®. Finally, we present preliminary data to suggest that glycoclusters could reduce *S. aureus* biofilm formation, but the structure or solubility of the glycoclusters may have to be altered for increased potency. Nonetheless, caution must be exercised when assessing the potency of compounds or glycoclusters and their ability to modulate bacterial binding as one glycocluster tested in this study, sos2211, reduced *S. aureus* lectin interactions and biofilm formation, but increased *S. aureus* binding to lung mucin purified from a CF patient.

### 3.5. References


**Andjelković, U., Pićurić, S., & Vujčić, Z.** (2010). Purification and characterisation of Saccharomyces cerevisiae external invertase isoforms. *Food Chemistry*, *120*(3), 799–804.

**André, S., O'Sullivan, S., Gabius, H.-J., & Murphy, P. V**. (2015). Glycoclusters as lectin inhibitors: Comparative analysis on two plant agglutinins with different folding as a step towards rules for selectivity. *Tetrahedron*, *71*(38), 6867–6880.

**André, S., O'Sullivan, S., Koller, C., Murphy, P. V, & Gabius, H.-J.** (2015). Bi- to tetravalent glycoclusters presenting GlcNAc/GalNAc as inhibitors: From plant agglutinins to human macrophage galactose-type lectin (CD301) and galectins. *Organic and Biomolecular Chemistry*, *13*(14), 4190–4203.

**Archer, N. K., Mazaitis, M. J., Costerton, J. W., Leid, J. G., Powers, M. E., & Shirtliff, M. E.** (2011). *Staphylococcus aureus* biofilms: Properties, regulation and roles in human disease. *Virulence*, *2*(5), 445–459.

**Arciola, C. R., Campoccia, D., Ravaioli, S., & Montanaro, L.** (2015). Polysaccharide intercellular adhesin in biofilm: Structural and regulatory aspects. *Frontiers in Cellular and Infection Microbiology*, *5*, *7*.

**Batra, P. P., Roebuck, M. A., & Uetrecht, D.** (1990). Effect of lysine modification on the secondary structure of ovalbumin. *Journal of Protein Chemistry*, *9*(1), 37–44.

**Begun, J., Gaiani, J. M., Rohde, H., Mack, D., Calderwood, S. B., Ausubel, F. M., & Sifri, C. D.** (2007). Staphylococcal biofilm exopolysaccharide protects against Caenorhabditis elegans immune defenses. *PLoS Pathogens*, *3*(4), 526–540.

**Bindslev, N.** (2008). *Drug-Acceptor Interactions: Modeling Theoretical Tools to Test and Evaluate Experimental Equilibrium Effects*. Co-Action Publishing, 70-71.

**Boukerb, A. M., Rousset, A., Galanos, N., Méar, J.-B., Thépaut, M., Grandjean, T., Gillon, E., Cecioni, S., Abderrahmen, C., Faure, K., Redelberger, D., Kipnis, E., Dessein, R., Havet, S., Darblade, B., Matthews, S. E., De Bentzmann, S., Guéry, B., Cournoyer, B., Imberty, A., & Vidal, S.** (2014). Antiadhesive properties of glycoclusters against Pseudomonas aeruginosa lung infection. *Journal of Medicinal Chemistry*, *57*(24), 10275–10289.

**Buffet, K., Nierengarten, I., Galanos, N., Gillon, E., Holler, M., Imberty, A., Matthews, S. E., Vidal, S., Vincent, S. P., & Nierengarten, J.-F.** (2016). Pillar[5]arene-Based Glycoclusters: Synthesis and Multivalent Binding to Pathogenic Bacterial Lectins. *Chemistry - A European Journal*, *22*(9), 2955–2963.

**Casas-Solvas, J. M., & Vargas-Berenguel, A.** (2015). Glycoclusters and their Applications as Anti-Infective Agents, Vaccines, and Targeted Drug Delivery Systems. In *Carbohydrate Nanotechnology* (pp. 175–210).

**Chung, P. Y., & Toh, Y. S.** (2014). Anti-biofilm agents: Recent breakthrough against multi-drug resistant *Staphylococcus aureus*. *Pathogens and Disease*, *70*(3), 231–239.

**Devaraj, N., Sheykhnazari, M., Bhavanandan, V. P., Warren, W. S., & Devaraj, N.** (1994). Differential binding of *Pseudomonas aeruginosa* to normal and cystic fibrosis tracheobronchial mucins. *Glycobiology*, *4*(3), 307–316.

**Flynn, J. M., Niccum, D., Dunitz, J. M., & Hunter, R. C.** (2016). Evidence and Role for Bacterial Mucin Degradation in Cystic Fibrosis Airway Disease. *PLoS Pathogens*, *12*(8).

**Hancock, I. C., & Cox, C. M.** (1991). Turnover of cell surface-bound capsular polysaccharide in *Staphylococcus aureus*. *FEMS Microbiology Letters*, *77*(1), 25–30.

**Harvey, D. J., Wing, D. R., Küster, B., & Wilson, I. B. H.** (2000). Composition of N-linked carbohydrates from ovalbumin and co-purified glycoproteins. *Journal of the American Society for Mass Spectrometry*, *11*(6), 564–571.

**Hsu, K.-L., Pilobello, K. T., & Mahal, L. K.** (2006). Analyzing the dynamic bacterial glycome with a lectin microarray approach. *Nature Chemical Biology*, *2*(3), 153–157.

**Hu, S., & Wong, D. T.** (2009). Lectin microarray. *Proteomics. Clinical Applications*, *3*(2), 148–154.

**Kelly-Quintos, C., Cavacini, L. A., Posner, M. R., Goldmann, D., & Pier, G. B.** (2006). Characterization of the opsonic and protective activity against *Staphylococcus aureus* of fully human monoclonal antibodies specific for the bacterial surface polysaccharide poly-*N*-acetylglucosamine. *Infection and Immunity*, *74*(5), 2742–2750.

**Kho, K., & Meredith, T. C.** (2018). Saltinduced stress stimulates a lipoteichoic acidspecific three-component glycosylation system in *Staphylococcus aureus*. *Journal of Bacteriology*, *200*(12).

**Kiedrowski, M. R., Gaston, J. R., Kocak, B. R., Coburn, S. L., Lee, S., Pilewski, J. M., Myerburg, M. M., & Bomberger, J. M.** (2018). *Staphylococcus aureus* Biofilm Growth on Cystic Fibrosis Airway Epithelial Cells Is Enhanced during Respiratory Syncytial Virus Coinfection. *MSphere*, *3*(4).

**Kilcoyne, M., Gerlach, J. Q., Gough, R., Gallagher, M. E., Kane, M., Carrington, S. D., & Joshi, L.** (2012). Construction of a natural mucin microarray and interrogation for biologically relevant glyco-epitopes. Analytical Chemistry, 84(7), 3330–3338.

**Kilcoyne, M., Twomey, M. E., Gerlach, J. Q., Kane, M., Moran, A. P., & Joshi, L.** (2014). *Campylobacter jejuni* strain discrimination and temperature-dependent glycome expression profiling by lectin microarray. *Carbohydrate Research*, *389*(1), 123–133.

**Kiriyama, Y., Yazawa, K., Tanaka, T., Yoshikawa, R., Yamane, H., Hashimoto,**

**M., Sekiguchi, J., & Yamamoto, H.** (2014). Localization and expression of the Bacillus subtilis DL-endopeptidase LytF are influenced by mutations in LTA synthases and glycolipid anchor synthetic enzymes. *Microbiology (United Kingdom)*, *160*, 2639–2649.

**Krishnamoorthy, L., Bess Jr., J. W., Preston, A. B., Nagashima, K., & Mahal, L. K.** (2009). HIV-1 and microvesicles from T cells share a common glycome, arguing for a common origin. *Nature Chemical Biology*, *5*(4), 244–250.

**Kristiarisen, A., Nysaæer, Å., Grasdalen, H., & Vårum, K. M.** (1999). Quantitative studies of the binding of wheat germ agglutinin (WGA) to chitin-oligosaccharides and partially *N*-acetylated chitosans suggest inequivalence of binding sites. *Carbohydrate Polymers*, *38*(1), 23–32.

**Kropec, A., Maira-Litran, T., Jefferson, K. K., Grout, M., Cramton, S. E., Götz, F., Goldmann, D. A., & Pier, G. B.** (2005). Poly-*N*-acetylglucosamine production in *Staphylococcus aureus* is essential for virulence in murine models of systemic infection. *Infection and Immunity*, *73*(10), 6868–6876.

**Kuno, A., Uchiyama, N., Koseki-Kuno, S., Ebe, Y., Takashima, S., Yamada, M., & Hirabayashi, J.** (2005). Evanescent-field fluorescence-assisted lectin microarray: a new strategy for glycan profiling. *Nature Methods*, *2*, 851.

**Lerbret, A., Bordat, P., Affouard, F., Descamps, M., & Migliardo, F.** (2005). How homogeneous are the trehalose, maltose, and sucrose water solutions? An insight from molecular dynamics simulations. *Journal of Physical Chemistry B*, *109*(21), 11046–11057.

**Li, J.-D., Dohrman, A. F., Gallup, M., Miyata, S., Gum, J. R., Kim, Y. S., Nadel, J. A., Prince, A., & Basbaum, C. B.** (1997). Transcriptional activation of mucin by *Pseudomonas aeruginosa* lipopolysaccharide in the pathogenesis of cystic fibrosis lung disease. *Proceedings of the National Academy of Sciences of the United States of America*, *94*(3), 967–972.

**Liang, P.-H., Wang, S.-K., & Wong, C.-H.** (2007). Quantitative Analysis of Carbohydrate−Protein Interactions Using Glycan Microarrays: Determination of Surface and Solution Dissociation Constants. *Journal of the American Chemical Society*, *129*(36), 11177–11184.

**Ligeour, C., Vidal, O., Dupin, L., Casoni, F., Gillon, E., Meyer, A., Vidal, S., Vergoten, G., Lacroix, J.-M., Souteyrand, E., Imberty, A., Vasseur, J.-J., Chevolot, Y., & Morvan, F.** (2015). Mannose-centered aromatic galactoclusters inhibit the biofilm formation of *Pseudomonas aeruginosa*. *Organic and Biomolecular Chemistry*, *13*(31), 8433–8444.

**Lin, M. H., Shu, J. C., Lin, L. P., Chong, K. Y., Cheng, Y. W., Du, J. F., & Liu, S.-T.** (2015). Elucidating the crucial role of poly *N*-acetylglucosamine from *Staphylococcus aureus* in cellular adhesion and pathogenesis. *PLoS ONE*, *10*(4).

**Lotan, R., Sharon, N., & Mirelman, D.** (1975). Interaction of Wheat-Germ Agglutinin with Bacterial Cells and Cell-Wall Polymers. *European Journal of Biochemistry*, *55*(1), 257–262.

**Mack, D., Fischer, W., Krokotsch, A., Leopold, K., Hartmann, R., Egge, H., & Laufs, R.** (1996). The intercellular adhesin involved in biofilm accumulation of *Staphylococcus epidermidis* is a linear β-1,6-linked glucosaminoglycan: Purification and structural analysis. *Journal of Bacteriology*, *178*(1), 175–183.

**Maierhofer, C., Rohmer, K., & Wittmann, V.** (2007). Probing multivalent carbohydrate-lectin interactions by an enzyme-linked lectin assay employing covalently immobilized carbohydrates. *Bioorganic and Medicinal Chemistry*, *15*(24), 7661–7676.

**Maira-Litrán, T., Kropec, A., Abeygunawardana, C., Joyce, J., Mark III, G., Goldmann, D. A., & Pier, G. B.** (2002). Immunochemical properties of the Staphylococcal poly-N-acetylglucosamine surface polysaccharide. *Infection and Immunity*, *70*(8), 4433–4440.

**Monsigny, M., Roche, A. -C., Sene, C., Maget-DANA, R., & Delmotte, F.** (1980). Sugar-Lectin Interactions: How Does Wheat-Germ Agglutinin Bind Sialoglycoconjugates? *European Journal of Biochemistry*, *104*(1), 147–153.

**Monsigny, M., Sene, C., Obrenovitch, A., Roche, A.-C., Delmotte, F., & Boschetti, E.** (1979). Properties of Succinylated Wheat-Germ Agglutinin. *European Journal of Biochemistry*, *98*(1), 39–45.

**Morath, S., Geyer, A., & Hartung, T.** (2001). Structure-function relationship of cytokine induction by lipoteichoic acid from *Staphylococcus aureus*. *Journal of Experimental Medicine*, *193*(3), 393–397.

**Moullier, P., Daveloose, D., Leterrier, F., & Hoebeke, J.** (1986). Comparative binding of wheat germ agglutinin and its succinylated form on lymphocytes. *European Journal of Biochemistry*, *161*(1), 197–204.

**Nagae, M., Mishra, S. K., Yamaguchi, Y., Hanashima, S., & Tateno, H.** (2017). Distinct roles for each N-glycan branch interacting with mannose-binding type Jacalin-related lectins Orysata and Calsepa. *Glycobiology*, *27*(12), 1120–1133.

**Nisbet, A. D., Saundry, R. H., Moir, A. J. G., Fothergill, L. A., & Fothergill, J. E.** (1981). The Complete Amino-Acid Sequence of Hen Ovalbumin. *European Journal of Biochemistry*, *115*(2), 335–345.

**O'Gara, J. P.** (2007). ica and beyond: Biofilm mechanisms and regulation in *Staphylococcus epidermidis* and *Staphylococcus aureus*. *FEMS Microbiology Letters*, *270*(2), 179–188.

**O'Neill, E., Pozzi, C., Houston, P., Smyth, D., Humphreys, H., Robinson, D. A., & O'Gara, J. P.** (2007). Association between methicillin susceptibility and biofilm regulation in *Staphylococcus aureus* isolates from device-related infections. *Journal of Clinical Microbiology*, *45*(5), 1379–1388.

**Robinson, C. V, Elkins, M. R., Bialkowski, K. M., Thornton, D. J., & Kertesz, M. A.** (2012). Desulfurization of mucin by *Pseudomonas aeruginosa*: Influence of sulfate in the lungs of cystic fibrosis patients. *Journal of Medical Microbiology*, *61*(PART12), 1644–1653.

**Rosenfeld, R., Bangio, H., Gerwig, G. J., Rosenberg, R., Aloni, R., Cohen, Y., Amor, Y., Plaschkes, I., Kamerling, J. P., & Maya, R. B.-Y.** (2007). A lectin array-based methodology for the analysis of protein glycosylation. *Journal of Biochemical and Biophysical Methods*, *70*(3), 415–426.

**Sabatini, S., Piccioni, M., Felicetti, T., De Marco, S., Manfroni, G., Pagiotti, R., Nocchetti, M., Cecchetti, V., & Pietrella, D.** (2017). Investigation on the effect of known potent: *S. aureus* NorA efflux pump inhibitors on the staphylococcal biofilm formation. *RSC Advances*, *7*(59), 37007–37014.

**Scharfman, A., Degroote, S., Beau, J., Lamblin, G., Roussel, P., & Mazurier, J.** (1999). *Pseudomonas aeruginosa* binds to neoglycoconjugates bearing mucin carbohydrate determinants and predominantly to sialyl-Lewis x conjugates. *Glycobiology*, *9*(8), 757–764.

**Schwefel, D., Maierhofer, C., Beck, J. G., Seeberger, S., Diederichs, K., Möller, H. M., Welte, W., & Wittmann, V.** (2010). Structural basis of multivalent binding to wheat germ agglutinin. *Journal of the American Chemical Society*, *132*(25), 8704–8719.

**Shrestha, L., Kayama, S., Sasaki, M., Kato, F., Hisatsune, J., Tsuruda, K., Koizumi, K., Tatsukawa, N., Yu, L., Takeda, K., & Sugai, M.** (2016). Inhibitory effects of antibiofilm compound 1 against *Staphylococcus aureus* biofilms. *Microbiology and Immunology*, *60*(3), 148–159.

**Shuter, J., Hatcher, V. B., & Lowy, F. D.** (1996). *Staphylococcus aureus* binding to human nasal mucin. *Infection and Immunity*, *64*(1), 310–318.

**Singh, R., Ray, P., Das, A., & Sharma, M.** (2010). Enhanced production of exopolysaccharide matrix and biofilm by a menadione-auxotrophic *Staphylococcus aureus* small-colony variant. *Journal of Medical Microbiology*, *59*(5), 521–527.

**Skurnik, D., Cywes-Bentley, C., & Pier, G. B.** (2016). The exceptionally broad-based potential of active and passive vaccination targeting the conserved microbial surface polysaccharide PNAG. *Expert Review of Vaccines*, *15*(8), 1041–1053.

**Smadhi, M., De Bentzmann, S., Imberty, A., Gingras, M., Abderrahim, R., & Goekjian, P. G.** (2014). Expeditive synthesis of trithiotriazine-cored glycoclusters and inhibition of *Pseudomonas aeruginosa* biofilm formation. *Beilstein Journal of Organic Chemistry*, *10*, 1981–1990.

**Stone, A., & Saiman, L.** (2007). Update on the epidemiology and management of *Staphylococcus aureus*, including methicillin-resistant *Staphylococcus aureus*, in patients with cystic fibrosis. *Current Opinion in Pulmonary Medicine*, *13*(6), 515–521.

**Swanson, M. D., Boudreaux, D. M., Salmon, L., Chugh, J., Winter, H. C., Meagher, J. L., André, S., Murphy, P. V, Oscarson, S., Roy, R., King, S., Kaplan, M. H., Goldstein, I. J., Tarbet, E. B., Hurst, B. L., Smee, D. F., De La Fuente, C., Hoffmann, H.-H., Xue, Y., Rice, C. M., Schols, D., Garcia, J. V, Stuckey, J. A., Gabius, H.-J., Al-Hashimi, H. M., & Markovitz, D. M.**

(2015). Engineering a Therapeutic Lectin by Uncoupling Mitogenicity from Antiviral Activity. *Cell*, *163*(3), 746–758.

**Tacconelli, E., Carrara, E., Savoldi, A., Harbarth, S., Mendelson, M., Monnet, D. L., Pulcini, C., Kahlmeter, G., Kluytmans, J., Carmeli, Y., Ouellette, M., Outterson, K., Patel, J., Cavaleri, M., Cox, E. M., Houchens, C. R., Grayson, M. L., Hansen, P., Singh, N., Theuretzbacher, U., Magrini, N., Aboderin, A. O., Al-Abri, S. S., Awang Jalil, N., Benzonana, N., Bhattacharya, S., Brink, A. J., Burkert, F. R., Cars, O., Cornaglia, G., Dyar, O. J., Friedrich, A. W., Gales, A. C., Gandra, S., Giske, C. G., Goff, D. A., Goossens, H., Gottlieb, T., Guzman Blanco, M., Hryniewicz, W., Kattula, D., Jinks, T., Kanj, S. S., Kerr, L., Kieny, M.-P., Kim, Y. S., Kozlov, R. S., Labarca, J., Laxminarayan, R., Leder, K., Leibovici, L., Levy-Hara, G., Littman, J., Malhotra-Kumar, S., Manchanda, V., Moja, L., Ndoye, B., Pan, A., Paterson, D. L., Paul, M., Qiu, H., Ramon-Pardo, P., Rodríguez-Baño, J., Sanguinetti, M., Sengupta, S., Sharland, M., Si-Mehand, M., Silver, L. L., Song, W., Steinbakk, M., Thomsen, J., Thwaites, G. E., van der Meer, J. W., Van Kinh, N., Vega, S., Villegas, M. V, Wechsler-Fördös, A., Wertheim, H. F. L., Wesangula, E., Woodford, N., Yilmaz, F. O., & Zorzet, A.** (2018). Discovery, research, and development of new antibiotics: the WHO priority list of antibiotic-resistant bacteria and tuberculosis. *The Lancet Infectious Diseases*, *18*(3), 318–327.

**Tao, S.-C., Li, Y., Zhou, J., Qian, J., Schnaar, R. L., Zhang, Y., Goldstein, I. J., Zhu, H., & Schneck, J. P.** (2008). Lectin microarrays identify cell-specific and functionally significant cell surface glycan markers. *Glycobiology*, *18*(10), 761–769.

**Tra, V. N., & Dube, D. H.** (2014). Glycans in pathogenic bacteria-potential for targeted covalent therapeutics and imaging agents. *Chemical Communications*, *50*(36), 4659–4673.

**Uchiyama, N., Kuno, A., Tateno, H., Kubo, Y., Mizuno, M., Noguchi, M., & Hirabayashi, J.** (2008). Optimization of evanescent-field fluorescence-assisted lectin microarray for high-sensitivity detection of monovalent oligosaccharides and glycoproteins. *Proteomics*, *8*(15), 3042–3050.

**Ulrich, M., Herbert, S., Berger, J., Bellon, G., Louis, B., Miinker, G., & Doring, G.** (1998). Localization of *Staphylococcus aureus* in infected airways of patients with cystic fibrosis and in a cell culture model of *S. aureus* adherence. *Pneumologie*, *52*(12), 729.

**Vinogradov, E., Sadovskaya, I., Li, J., & Jabbouri, S.** (2006). Structural elucidation of the extracellular and cell-wall teichoic acids of *Staphylococcus aureus* MN8m, a biofilm forming strain. *Carbohydrate Research*, *341*(6), 738–743.

**Wang, X., Matei, E., Deng, L., Koharudin, L., Gronenborn, A. M., Ramström, O., & Yan, M.** (2013). Sensing lectin-glycan interactions using lectin super-microarrays and glycans labeled with dye-doped silica nanoparticles. *Biosensors and Bioelectronics*, *47*, 258–264.

**Wang, X., Preston III, J. F., & Romeo, T.** (2004). The pgaABCD Locus of *Escherichia coli* Promotes the Synthesis of a Polysaccharide Adhesin Required for Biofilm Formation. *Journal of Bacteriology*, *186*(9), 2724–2734.

**Wang, X., Wu, L., Ren, J., Miyoshi, D., Sugimoto, N., & Qu, X.** (2011). Label-free colorimetric and quantitative detection of cancer marker protein using noncrosslinking aggregation of Au/Ag nanoparticles induced by target-specific peptide probe. *Biosensors and Bioelectronics*, *26*(12), 4804–4809.

**Weidenmaier, C., & Peschel, A.** (2008). Teichoic acids and related cell-wall glycopolymers in Gram-positive physiology and host interactions. *Nature Reviews Microbiology*, *6*(4), 276–287.

**Wild, D., & Kodak, E.** (2013). *The Immunoassay Handbook* (3rd ed.). 111-112.

**Wittmann, V., & Pieters, R. J.** (2013). Bridging lectin binding sites by multivalent carbohydrates. *Chemical Society Reviews*, *42*(10), 4492–4503.

**Xia, G., Maier, L., Sanchez-Carballo, P., Li, M., Otto, M., Holst, O., & Peschel, A.** (2010). Glycosylation of wall teichoic acid in *Staphylococcus aureus* by TarM. *Journal of Biological Chemistry*, *285*(18), 13405–13415.

**Yamashita, K., Ohkura, T., Umetsu, K., & Suzuki, T.** (1992). Purification and characterization of a Fucα1→2Galβ1→ and GalNAcβ1→-specific lectin in root tubers of Trichosanthes japonica. *Journal of Biological Chemistry*, *267*(35), 25414–25422.

# Chapter 4

# Elucidation of PNAG interactions with innate immune receptors and consequential signalling responses

# 4. Elucidation of PNAG interactions with innate immune receptors and consequential signalling responses

## 4.1. Introduction

Cells of the innate immune system, such as neutrophils, monocytes, macrophages and dendritic cells, are often the first line of defence against invading pathogens (Mogensen, 2009). These cells detect microorganisms *via* soluble and membrane bound pathogen recognition receptors (PRRs). Once a pathogen is detected, PRRs trigger a signalling cascade via specific pathway(s), such as complement or Toll-like receptor (TLR) pathways, to activate phagocytosis, the production of cytokines and chemokines, and the adaptive immune system to eradicate the invading pathogens (Mogensen, 2009; Mukhopadhyay *et al.*, 2004).

PRRs recognise a wide variety of microbial components, referred to as pathogen-associated molecular patterns (PAMPs), to activate an innate and adaptive immune response. Often PAMPs are lipid-based structures such as lipopolysaccharide (LPS), lipooligosaccharide (LOS), lipopeptides and lipoteichoic acid (LTA), or carbohydrate-based structures such as LPS, LOS, LTA, glycoproteins, peptidoglycan and capsular polysaccharides (CPS). Because these PAMPs are broadly found on Gram-positive or Gram-negative bacteria, PRRs play a pivotal role in the detection of and response to foreign invaders (Kumar *et al.*, 2009; Mogensen, 2009).

However, bacteria have developed mechanisms of modifying PAMPs to promote bacterial colonisation and evade recognition by PRRs. These modifications can include acetylation, deacetylation, epimerization and succinylation (Whitfield *et al.*, 2015). Thus, once a PRR binds to a PAMP on invading pathogens, some bacteria can manipulate receptor cross-talk and subsequent cell signalling cascades that would normally function to eliminate the infection (Hajishengallis *et al*., 2011).

*Enterococcus faecium, S. aureus, Klebsiella pneumoniae, Acinetobacter baumannii*, *Pseudomonas aeruginosa*, and *Enterobacter* spp. are known as the ESKAPE pathogens which are associated with antimicrobial resistance and cause a large majority of hospital-related infections in the United States (Rice, 2008). Poly-*N*-acetylglucosamine (PNAG, also known as polysaccharide intercellular adhesin (PIA)) is a surface located polysaccharide and major biofilm component found on *S.*

*aureus*, *K. pneumoniae*, *A. baumannii* and *Enterobacter* species (Skurnik *et al.*, 2016). PNAG production is generally mediated by the *icaADBC* operon in Gram-positive bacteria and the *pgaABCD* operon in Gram-negative bacteria. PNAG is a potential PAMP and in *S. epidermidis* PNAG activates the complement cascade, protects against phagocytic killing, reduces macrophage uptake and macrophage NF-κB mediated inflammatory responses (Aarag Fredheim *et al.*, 2011; Cerca *et al.*, 2006; Schommer *et al.*, 2011). Furthermore, it was shown that *S. epidermidis* PNAG binds to TLR2 to promote IL-8 signalling in astrocytes (Stevens *et al.*, 2009). For *S. aureus*, PNAG was found to be essential for evasion of opsonic killing (Kropec *et al.*, 2005). However, PRRs which bind to PNAG from *S. aureus* and other PNAG-expressing ESKAPE pathogens have yet to be identified. Identification of PRR ligands for PNAG would help elucidate the precise mechanisms of PNAG-mediated immune evasion or PNAG detection by the innate immune system and could help to lead to new strategies for elimination of persistent PNAG-producing pathogens.

In this study, a PRR microarray was constructed to evaluate the interactions of *S. aureus* and *A. baumannii* wild type and PNAG-deficient mutants along with a PNAG fraction isolated from *S. aureus* with 23 different PRRs. Signalling responses were then evaluated using a reporter THP-1 monocytic cell line that stably expresses a number of TLRs and CD14 and a combination of antibodies to block binding to individual PRRs. Finally, cytokine and chemokine expression in THP-1 cells in response to the bacteria and PNAG was quantified using multiplexed Luminex assay and ELISA.

## 4.2. Materials and methods

### 4.2.1. Materials and bacterial strains

Recombinantly expressed PRRs, anti-human CD14, anti-human TLR2 and anti-peptidoglycan monoclonal antibodies, IgG1 and IgG2B isotype antibodies, DuoSet ELISA kits for IL-8, IL-1β and RANTES, and the Luminex multiplex assay (cat. no. LXSAHM) were purchased from R & D Systems (Abingdon, U.K.). RPMI-1640 medium, LB broth, fetuin, invertase, and lysozyme were from Sigma-Aldrich Co. (Dublin, Ireland). The Pierce enhanced chemiluminescence (ECL) Western blotting substrate, Alexa Fluor® 555 (AF555) carboxylic acid NHS ester (succinimidyl ester) and Alexa Fluor® 647 (AF647) carboxylic acid succinimidyl ester fluorescent labels, 3.5 kDa MWCO cellulose membrane dialysis cassettes and anti-lipoteichoic acid monoclonal antibody (55) were obtained from Thermo-Fisher Scientific (Waltham, MA, U.S.A.). 3SLacHSA, 3SuleaBSA and GlcNAC-BSA were purchased from Dextra Laboratories Ltd. (Reading, UK). Hydrogen peroxide solution (6%) was from Ovelle Pharmaceuticals (Dundalk, Ireland). The human IL-8/CXCL8, human IL-1/IL-1F2 and human CCL5/RANTES DuoSet ELISA kits were from Bio-techne (Minneapolis, MN, U.S.A.). The synthetic diacetylated lipoprotein, FSL-1, *S. aureus* lipoteichoic acid (SA-LTA), *E. coli* K12 lipopolysaccharide (LPS), heat killed *Listeria monocytogenes* (HKLM), synthetic triacetylated lipoprotein (Pam3CSK4), the transformed cell line THP1-XBlue™-CD14, endotoxin-free $H_2O$, normocin, zeocin, and G418 (geneticin) antibiotics, and anti-human TLR1 (hTLR1) immunoglobulin G (IgG), anti-hTLR4-IgG and anti-hTLR6-IgG1 antibodies were purchased from InvivoGen (Toulouse, France). Immobilon-P 0.45 µm polyvinylidene difluoride (PVDF) membrane was from Merck Millipore (Dublin, Ireland). All other materials used were as per section 2.2.1 and 3.2.1.

In addition to the bacterial strains in Table 2.1, *S. epidermidis* RP62A and *E. coli* 1532 were used in this study (Table 4.1) which were kind gifts from Prof. James O'Gara, NUI Galway, Galway, Ireland. PNAG purified from A. baumannii S1 was a kind gift from Prof. Gerald Pier, Harvard University, Boston, MA, U.S.A.

**Table 4.1. Additional bacterial strains used in this study.**

| Bacteria strains used | Relevant details | Reference |
|---|---|---|
| *S. epidermidis* RP62A wildtype (WT) | Biofilm positive. Blood culture isolate. | (Conlon *et al.*, 2002) |
| *E. coli* 1532 | Originated from canine. ATCC® 35218 | *Escherichia coli* (ATCC® 35218™). www.attc.org |

### 4.2.2. Fluorescent labelling of NGCs, proteins and PNAG

Neoglycoconjugates (NGCs, 3SLacHSA, 3SuleaBSA and GlcNAC-BSA), glycoproteins (fetuin and invertase) and PNAG were fluorescently labelled with AF555 as described in Chapter 3, section 3.2.3). AF555 labelled GlcNAc-BSA (GlcNAc-BSA-AF555), and 3SuLeaBSA (3SuLeaBSA-AF555) were quantified for protein concentration and label substitution according to manufacturer's instructions using the extinction coefficients and molecular masses of 43,824 $M^{-1}$ $cm^{-1}$ and 66,430 Da (the extinction coefficient at 280 nm and molecular mass of BSA, respectively) (Wang *et al*., 2011). Similarly, the concentration of fluorescently labelled invertase (invertase-AF555) (621,000 $M^{-1}$ $cm^{-1}$ and 270,000 Da) (Lampen, 1971), fetuin (fetuin-AF555) (19,844 $M^{-1}$ $cm^{-1}$ and 48,400 Da) (Spiro, 1960) and 3SLacHSA (3SLacHSA-AF555) (35,495 M-1 cm-1 and 66,470 Da) (Pace *et al.*, 1995) were calculated. Fluorescently labelled PNAG (PNAG-AF555) was considered to be approximately 90% of the concentration used initially for labelling.

### 4.2.3. Preparation of FluoSpheres

Protein and PNAG coating on to FluoSpheres® was carried out as described in Chapter 3, section 3.2.5.

### 4.2.4. Fluorescent labelling of bacteria

Fluorescent labelling of bacteria was carried out as described in Chapter 2, section 2.2.6 and Chapter 3, section 3.2.4).

### 4.2.5. PRR microarray construction

All PRRs were solubilised in PBS, pH 7.4, 0.05% HAS and printed at a concentration of 0.5 mg/ mL (single PRR printed) or 0.25 mg/mL (each, for combinations of two PRR printed together) in 1 mM sucrose (Table 4.2) on Nexterion ® slide H (Schott, Mainz, Germany) using a SciFlexArrayer S3 (Scienion, Berlin, Germany) under constant 60% (+/- 2%) humidity at 18 °C (+/- 2°C). For each slide, features of approximately 1 nL were printed in replicates of 6 per probe per subarray and eight replicate subarrays per microarray slide. Following printing, slides were placed in a humidity chamber overnight. Slides were then blocked with 100 mM ethanolamine in 50 mM boric acid, pH 8 for 1 h at room temperature. Slides were washed three times with PBS with 0.05% Tween-20 (PBS-T), and once with PBS. Slides were dried by centrifugation (1,500 x g, 5 min). Slides were stored at 4 °C sealed with desiccant and used within 48 h of printing. Validation of maintained binding function of the printed PRRs was carried out using fluorescently labelled protein and NGC standards, as well as SYTO®82 labelled *E. coli* for bacteria-specific PRRs (section 4.2.5 for SYTO®82 labelling).

**Table 4.2. PRRs used in this study, printed concentration and source.**

| Abbreviation | Name | Print buffer | Concentration (µg/µL) | Supplier | Broad specificity | References |
|---|---|---|---|---|---|---|
| hESel_T | Human E-Selectin | 1 mM Suc | 0.5 | R&D Systems | $SLe^x$ antigen | (Varki, 1992) |
| hLSel_T | Human L-Selectin | 1 mM Suc | 0.5 | R&D Systems | $SLe^x$ antigen, heparin/ heparin sulfate | (Varki, 1992) |
| hPSel_T | Human P-Selectin | 1 mM Suc | 0.5 | R&D Systems | PSGL1, $SLe^x$ antigen, heparin/ heparin sulfate | (Varki, 1992) |
| hSig-1 | Human Siglec-1 | 1 mM Suc | 0.5 | R&D Systems | Sialylated structures | (MacAuley *et al.*, 2014) |
| hSig-2 | Human Siglec-2 | 1 mM Suc | 0.5 | R&D Systems | Sialylated structures | (MacAuley *et al.*, 2014) |
| rMAG | Rat myelin-associated glycoprotein (Siglec-4) | 1 mM Suc | 0.5 | R&D Systems | Sialylated structures | (MacAuley *et al.*, 2014) |
| hSig-10 | Human Siglec-10 | 1 mM Suc | 0.5 | R&D Systems | Sialylated structures | (MacAuley *et al.*, 2014) |
| DCSIGN | DC-SIGN | 1 mM Suc | 0.5 | R&D Systems | Mannosylated and fucosylated structures | (van Liempt *et al.*, 2006) |
| DCSIGNR | DC-SIGNR | 1 mM Suc | 0.5 | R&D Systems | Mannosylated structures | (Feinberg *et al.*, 2001) |
| DCSIGN/DCSIGNR | | 1 mM Suc | 0.25/0.25 | R&D Systems | | |
| Dec_1 | Dectin-1 | 1 mM Suc | 0.5 | R&D Systems | β-glucan | (Brown *et al.*, 2003) |
| Dec_2 | Dectin-2 | 1 mM Suc | 0.5 | R&D Systems | α-mannan | (McGreal *et al.*, 2006) |
| Lsec | LSECtin | 1 mM Suc | 0.5 | R&D Systems | Terminal GlcNAc structures | (Echeverria *et al.*, 2018) |
| MMR | Macrophage mannose receptor | 1 mM Suc | 0.5 | R&D Systems | Mannan | (Gow *et al.*, 2011) |
| Fic-1_S | Human ficolin-1 (M) | 1 mM Suc | 0.5 | R&D Systems | Acetylated carbohydrates (GlcNAc and GalNAc)/non carbohydrates, sialic acid | (Frederiksen *et al.*, 2005; Kjaer *et al.*, 2011; Teh *et al.*, 2000) |
| Fic-2_S | Human ficolin-2 (L) | 1 mM Suc | 0.5 | R&D Systems | Acetylated carbohydrates (GlcNAc, heparin, sialic acid)/non carbohydrates | (Aoyagi *et al.*, 2008; Gout *et al.*, 2010; Krarup *et al.*, |

| | | | | | | |
|---|---|---|---|---|---|---|
| | | | | | | 2004) |
| Fic-3_S | Human ficolin-3 (H) | 1 mM Suc | 0.5 | R&D Systems | GlcNAc, GalNAc, D-fucose | (Matsushita *et al.*, 1996; Sugimoto *et al*., 1998) |
| rh-CHIT | Human Chitotriosidase | 1 mM Suc | 0.1 | R&D Systems | β-(1,4)-linked GlcNAc | (Kanneganti *et al.*, 2012) |
| MBL | Mannose binding lectin | 1 mM Suc | 0.5 | R&D Systems | Mannose, GlcNAc, ManNAc, fucose, glucose | (Turner, 2003) |
| TLR-2 | Toll like receptor 2 | 1 mM Suc | 0.5 | R&D Systems | Lipoproteins, peptidoglycan, LTA, lipoarabinomannan, PSM, glycolipids | (Akira *et al*., 2004) |
| TLR-4 | Toll like receptor 4 | 1 mM Suc | 0.5 | R&D Systems | LPS | (Akira *et al.*, 2004) |
| TLR-6 | Toll like receptor 6 | 1 mM Suc | 0.5 | R&D Systems | Diacyl lipopeptides (with TLR1) | (Akira *et al.*, 2004) |
| CD14 | Cluster of differentiation 14 | 1 mM Suc | 0.5 | R&D Systems | LPS, polyuronic acid, LTA, peptidoglycan, rhamnose, lipoarabinomannan | (Landmann *et al.*, 2000) |
| TLR-2/4_0.25 | | 1 mM Suc | 0.25/0.25 | R&D Systems | | |
| TLR-2/6_0.25 | | 1 mM Suc | 0.25/0.25 | R&D Systems | | |
| TLR-2/CD14_0.25 | | 1 mM Suc | 0.25/0.25 | R&D Systems | | |
| TLR-4/CD14_0.25 | | 1 mM Suc | 0.25/0.25 | R&D Systems | | |
| TLR-4/6_0.25 | | 1 mM Suc | 0.25/0.25 | R&D Systems | | |
| TLR-6/CD14_0.25 | | 1 mM Suc | 0.25/0.25 | R&D Systems | | |
| MBL/DCSIGN_0.25 | | 1 mM Suc | 0.25/0.25 | R&D Systems | | |
| MBL_CLEC10A_0.25 | | 1 mM Suc | 0.25/0.25 | R&D Systems | | |
| CLEC10A | CLEC10A/ CD301/ MGL | 1 mM Suc | 0.5 | R&D Systems | Terminal GalNAc structures | (Zizzari *et al*., 2015) |
| WGA | Wheat germ agglutinin | 1 mM GlcNAc | 0.5 | EY Labs | GlcNAc, sialic acid | (Monsigny *et al*., 1979) |
| sWGA | succinylated wheat germ agglutinin | 1 mM GlcNAc | 0.5 | Vector Labs | GlcNAc | (Monsigny *et al*., 1979) |
| PBS | PBS | | | | | |

### 4.2.6. PRR microarray incubations

Fluorescently labelled bacteria in TBS-T were not diluted or diluted 50 µL, 40 µL, 30 µL and 20 µL to give a final volume of 70 µL in TBS-T and incubated on the PRR microarray platform for selection of the optimal bacterial number for further experiments based on non-saturated binding within the dynamic range of the microarray scanner and low background fluorescence. For bacterial incubations on PRR microarrays, the SYTO®82 stained bacterial cultures were diluted in TBS-T as follows: *E. coli* and *S. epidermidis* RP62A were diluted 50 µL to a final volume of 70 µL, and *S. aureus* Mn8m WT and Mn8 Δ*ica*, 8325-4 WT/Δ*ica*, BH1CC WT/Δ*ica* and *A. baumannii* S1 WT/Δ*pga* were diluted 20 µL to a final volume of 70 µL. Bacteria were incubated on the PRR microarray using an 8 well gasket (Agilent Technologies, Cork, Ireland) at 70 µL per well and incubated with gentle rotation (4 rpm) at 37 °C for 1 h. Microarray and gasket slides were disassembled under TBS-T, washed three times in TBS-T for 3 min each and once with TBS. Microarray slides were dried by centrifugation (1,500 x g, 5 min) and imaged immediately by scanning in a microarray scanner (G2505B microarray scanner, Agilent, CA,USA) equipped with a 532 nm laser (90% PMT, 5 µm resolution). Images were stored digitally as .tif files. All experiments were carried out in technical triplicates and error bars represent +/- one standard deviation (SD) of the mean.

### 4.2.7. Data extraction

Data extraction was performed essentially as previously described (Kilcoyne *et al.*, 2014; Chapter 2, section 2.2.8; Chapter 3.2.9). In brief, image files (.tif) of lectin and NGC microarrays from the microarray scanner were used to extract raw intensity values using GenePix Pro v6.1.0.4 software (Molecular Devices, Berkshire, U.K.) and a proprietary .gal file that held the address and identity of each feature using adaptive diameter (70-160%) circular alignment based on 230 mm features and were exported as text to Excel (Version 2007, Microsoft, Dublin, Ireland). Local background subtracted median feature intensity data (F543 median-B543) was analysed. The median of six replicate spots per subarray was handled as a single data point for graphical and statistical analysis. Data were normalized to the per subarray mean total intensity value of three replicate microarray slides and binding data was

presented as a bar chart of average intensity of three experimental replicates +/- SD of the mean.

### 4.2.8. Heat-killing bacteria

Bacteria were grown overnight on BHI agar, inoculated in 5 mL of BHI glucose (*S. aureus* Mn8m and *A. baumannii*) or BHI NaCl (*S. aureus* 8325-4 and BH1CC) and grown overnight at 37 °C. Bacterial cells were washed by centrifugation at 5,000 x g for 5 min, discarding the supernatant and resuspending the pellet with sterile TBS. Finally, bacterial cells were standardised to an absorbance at 595 nm of approximately 1.0 (approximately 8 x $10^8$ cells/mL) in endotoxin-free water. Cells were killed by heating to 95 °C for 40 min. Heat-killed bacteria were then streaked on BHI agar plates and incubated overnight at 37 °C to confirm cell death by lack of growth.

### 4.2.9. THP1-XBlue™-CD14 cell reporter assay

THP1-XBlue™-CD14 cells (THP1 cells) were grown in RPMI 1640 supplemented with 2 mM L-glutamine, 10% heat inactivated fetal bovine serum, 100 μg/mL Normocin™, Penicillin-Streptomycin (Pen-Strep) 100 U/mL-100 μg/mL) (denoted as growth media from hereon). Cells were passaged every 2 - 3 days, grown at 37 °C at 5% $CO_2$ and cell concentration was not allowed to exceed 2 x $10^6$ cells/mL. Every second passage 200 μg/mL of Zeocin and 250 μg/mL of G418 were added to the growth media.

The reporter assay demonstrating TLR stimulation *via* the activation of transcription factors and subsequently the secretion of SEAP which is easily detectable with the addition of QUANTI-Blue™, a medium that turns purple/blue in the presence of SEAP, was carried out as per the manufacturer's instructions with some minor alterations. In brief, after at least three passages, THP1 cells were centrifuged at 200 x g for 2 min and resuspended in pre-warmed growth media. Cells in growth media were added to wells of a 96 well plate (100,000 cells/well). To assess TLR activation, LPS (TLR4 agonist), FSL-1 (TLR2/6 agonist), SA-LTA (TLR2 agonist) and Pan3CSK4 (TLR1/2 agonist) were added to each well and final concentrations of these agonists varied depending on the experiment (see figure results for details). Heat-killed *Listeria monocytogenes* (HKLM) (TLR2 agonist), heat-killed *S. aureus*

Mn8m WT and Δ*ica*, heat-killed *S. aureus* 8325-4 WT and Δ*ica* and heat-killed *A. baumannii* WT and Δ*pga* were also incubated with THP1 cells at various concentrations depending on the experiment (see figure results for details). Plates were incubated at 37 °C at 5% $CO_2$ for 20 h. The activity of secreted embryonic alkaline phosphatase (SEAP) was detected by removing 20 µL of THP1 cell culture supernatant and adding to 180 µL of QUANTI-Blue™ Solution in a new 96 well plate. Plates were incubated at 37 °C at 5% $CO_2$ for 4 h for heat-killed bacterial assays and 16 h for non-bacterial assays and absorbance was measured at 650 nm using a SpectraMax M5e microplate reader (Molecular Devices, Inc., Berkshire, UK).

To determine which PRR was responsible for the signalling response, anti-PRR antibodies at a final concentration of 10 µg/mL per well were added to the cells in 20 µL quantities and the plate was pre-incubated for 30 min at 37 °C at 5% $CO_2$. Endotoxin-free water was added to the cells instead of antibodies as a control. Following pre-incubation, the assay was continued with the addition of the ligands or heat killed bacteria as above. At least 3 wells were used per experiment and all experiments were carried out at least 3 times.

### 4.2.10. Dot blot assay

Dot blot assays were carried out as described in Chapter 3, section 3.2.6, with minor alterations. PVDF (0.45 µm) membrane was treated for 15 s in methanol and then soaked in TBS for 5 min. The membrane was allowed to partially dry so that the membrane was still wet, but TBS droplets were not visible on the membrane, before pipetting 2 µL of PNAG preparation and 2 µL of heat killed bacteria ($OD_{595\ nm}$ of 1.0; approximately 8 x $10^8$ cells/mL) to the activated membrane and allowed to dry. Membranes were then incubated for 1 h in 5% (w/v) skimmed milk in TBS (blocking solution) at room temperature. Blocking solution was removed from the membrane and the primary antibody (human IgG1 anti-PNAG mAb (F598), 800 µg/mL or mouse IgG1 anti-peptidoglycan mAb 1:100 dilution) diluted in TBS 0.0001% Tween 20, 1% skimmed milk was added to the membrane and incubated at room temperature for 1 h. The primary antibody solution was drawn off and the membrane was washed three times for 5 min in TBS 0.0001% Tween and once in TBS for 5 min. Horseradish peroxidase (HRP) conjugated secondary antibody was

diluted (rabbit anti-human IgG antibody (200 µg/mL) for anti-PNAG primary and goat anti-mouse immunoglobulins (200 µg/mL) for anti-peptidoglycan primary) in TBS with 0.0001% Tween and 1% skimmed milk), applied to the membrane and incubated at room temperature for 1 h. The membrane was washed as described above and a chemiluminescent substrate for the detection of HRP activity was added to the membrane for 1 min before visualisation using a chemiluminescent camera (Alpha Innotech FluorChem FC2 Imaging System). Images were stored digitally as .tif files.

For the detection of LTA, a dot blot was carried out as above except 2 µL of 1 mg/mL PNAG preparation (from *S. aureus* Mn8m) and 2 µL dilutions of LTA derived from *S. aureus* (SA-LTA) were spotted on to the activated PVDF membrane. The membrane was blocked as described above, incubated with anti-LTA mAb (1:50 dilution in TBS-T 0.001%, 1% skimmed-milk) for 1 h at room temperature followed by incubation with HRP-labelled goat anti-mouse IgG antibody (200 µg/mL in TBS-T 0.001%, 1% skimmed-milk). The membrane was washed three times in TBS-T and finally in TBS for 5 min. HRP activity was detected as described above and image was recorded.

### 4.2.11. Lysozyme treatment of PNAG

Solubilised PNAG (described in Chapter 3, section 3.2.3) was added to lysozyme (1 mg/mL in 100 mM Tris, pH 7.4), and further diluted in endotoxin-free water to give a final concentration of 100 µg/mL PNAG and 10 µg/mL lysozyme. As controls for cell activation assays, lysozyme solution was diluted with endotoxin-free water to a final concentration of 10 µg/mL and solubilised PNAG was diluted with endotoxin-free water to a final concentration of 100 µg/mL. Samples were incubated at 37 °C for 4 h and then heated to 80 °C for 30 min to deactivate the lysozyme. Samples were stored at 4 °C until use in the cell-based assays within 3 days.

### 4.2.12. Sodium metaperiodate treatment of PNAG

Solubilised PNAG (described in Chapter 3, section 3.2.3) was added to 800 mM sodium metaperiodate and further diluted in endotoxin-free water to give a final concentration of 100 µg/mL PNAG in 400 mM sodium metaperiodate. As controls for cell activation assays, sodium metaperiodate was diluted with endotoxin-free

water to give a final concentration of 400 mM, and solubilised PNAG was diluted with endotoxin-free water to give a final concentration of 100 μg/mL. All samples were incubated at room temperature for 4 h in the dark and then dialysed against distilled water overnight in 3.5 kDa MWCO cellulose membrane dialysis cassettes. Recovered samples were adjusted to the same original incubation volumes by adding endotoxin-free water or evaporation in a centrifugal evaporator. Samples were stored at 4 °C until use in the cell-based assays within 3 days.

### 4.2.13. Hydrogen peroxide treatment of PNAG

Solubilised PNAG (described in Chapter 3, section 3.2.3) was added to a $H_2O_2$ solution (aqueous) to give a final concentration of 100 μg/mL PNAG and 0.9% $H_2O_2$ in a glass V-vial and sealed with a PVDF lined screw top lid. As controls for cell activation assays, $H_2O_2$ was diluted with endotoxin-free water to give a final concentration of 0.9% and the same volume as the experimental sample, and solubilised PNAG was diluted with endotoxin-free water to a final concentration of 100 μg/mL. Samples were incubated at 37 °C for 4 h and then dialysed against water overnight in 3.5 kDa MWCO cellulose membrane dialysis cassettes. Recovered samples were adjusted to the same original incubation volumes by adding endotoxin-free $H_2O$ or evaporation in a centrifugal evaporator. Samples were stored at 4 °C until use in the cell-based assays within 3 days.

### 4.2.14. NaOH treatment of PNAG

Solubilised PNAG (described in Chapter 3, section 3.2.3) was added to NaOH to give a final concentration of 100 μg/mL and 200 mM, respectively. As controls for cell activation assays, the same volume of endotoxin-free water was added to 5 M NaOH, and PNAG was diluted in endotoxin-free water to a final concentration of 100 μg/mL. Samples were incubated at 37 °C for 18 h and then dialysed against water overnight in 3.5 kDa MWCO cellulose membrane dialysis cassettes. Recovered samples were adjusted to the same original incubation volumes by adding endotoxin-free water or evaporation in a centrifugal evaporator. Samples were stored at 4 °C until use in the cell-based assays within 3 days.

### 4.2.15. *N*-acetylation of PNAG

*N*-acetylation of PNAG was carried out as described by Kurita, Chikaoka, Kamiya, & Koyama (1988) with minor modifications. Briefly, 20 μL of 1 mg/mL PNAG was diluted in a 90 μL 1:1 methanol:10% acetic acid solution and added to a 90 μL 1:1 solution of pyridine:acetic anhydride to give a final PNAG concentration of 100 μg/mL. As controls for cell activation assays, water replaced PNAG in the *N*-acetylation reaction, and PNAG was diluted to 100 μg/mL with endotoxin-free water (no *N*-acetylation). Samples were incubated at room temperature for 5 h and then dialysed against water overnight in 3.5 kDa MWCO cellulose membrane dialysis cassettes.. Recovered samples were adjusted to the same original incubation volumes by adding endotoxin-free water or evaporation in a centrifugal evaporator. Samples were stored at 4 °C until use in the cell-based assays within 3 days.

### 4.2.16. Imaging flow cytometry

THP1 cells (100,000 cells/well) were incubated with endotoxin-free water or anti-CD14 antibody at a final concentration of 10 μg/mL per well of a 96-well plate for 30 min at 37 °C, 5% $CO_2$ as described in section 4.2.9. AF555-labelled PNAG from *S. aureus* and *A. baumannii* (SA-PNAG-AF555 and AB-PNAG-AF555, respectively) was added to each well to a final concentration of 10 μg/mL and incubated for 20 h at 37 °C and 5% $CO_2$. All cells were washed and resuspended in FACs buffer (2% FBS in PBS (without $Ca^{2+}$/$Mg^{2+}$)) and incubated for 30 min at 4 °C before staining. Half of the samples with THP1 cells/endotoxin-free water/SA-PNAG-AF555 or AB-PNAG-AF555 were incubated first with FACs buffer at 4 °C for 30 min. Next THP1 cells diluted in FACs buffer were incubated with anti-CD14-AF647 to a final concentration of 6 μg/mL for 30 min at 4 °C. The other half of the samples and THP1 cell/anti-CD14/PNAG-AF555 samples were incubated with the same volume FACs buffer for 30 min at 4 °C. Anti-CD14-AF647 was carried out as described previously (Chapter 3, section 3.2.4). All samples were centrifuged at 200 x g for 3 min, washed with FACs buffer, filtered through a 40 μm mesh and resuspended in 30 μL FACs buffer at a cell concentration of 2 x $10^7$ cells/mL. Samples were analysed using the ImageStream®X Mark II system (Merck Millipore, MA, USA) with the 488 nm laser and channel 03 to detect SA-PNAG-AF555 and AB-PNAG-AF555, and the 647 nm laser and channel 11 used to detect anti-CD14-

AF647. Full stain control was THP1 cells with AB-PNAG-AF555 and anti-CD14-AF647. Data from the imaging flow cytometer was analysed using IDEAS® (Merck Millipore, MA, USA).

### 4.2.17. Profiling inflammatory response of THP1 cells

THP1 cells (100,000 cells/well) were incubated for 20 h at 37 °C, 5% $CO_2$ with antagonist antibodies against CD14, TLR1, 2, 4 and 6, separately or in combinations, to give a final antibody concentration of 10 μg/mL, as carried out for the THP1-XBlue™-CD14 Cell reporter assay (described above – section 4.2.10) with modifications to the end of the experiment. Instead of incubating 20 μL of cell culture supernatant with QUANTI-Blue™, the total volume from each well was centrifuged at 12,000 x g for 10 min and the supernatant was collected and frozen until use.

A Luminex human magnetic assay with 10 analytes (MCP-1, CCL5/RANTES, IL-8, IFN-gamma, IL-1beta, IL-10, IL-12, IL-2, IL-6 and TNF-alpha) was carried out on the stimulated cell supernatants as per the manufacturer's instructions. Briefly, reagents and standards were prepared on the same day as the assay was carried out. Standards were placed in 50 μL aliquots per well in duplicate. Samples were diluted 1:2 in calibrator diluent RD6-52 and each sample on the plate was analysed in duplicate. Diluted human magnetic premixed microparticle cocktail (provided by the supplier containing concentrated analyte-specific antibodies that are pre-coated onto magnetic microparticles with preservative) at 50 μL was added to each well and incubated for 2 h at room temperature with gentle shaking (800 rpm). Using a handheld magnetic washer (Bio-Rad, CA, USA) to recover the microparticles, wells were washed 3 times with 100 μL of wash buffer. Human pre-mixed biotin-labelled antibody cocktail (provided by the supplier containing concentrated biotinylated antibody cocktail specific to the analytes of interest, with preservatives) at 50 μL was added to each well and incubated for 1 h at room temperature on a shaker at 800 rpm. The wells were washed 3 times as previously described with wash buffer, 50 μL of diluted Streptavidin-PE was added to each well and the plate was incubated for 30 min at room temperature. Wells were washed 3 times in wash buffer as described previously and 100 μL of wash buffer was added to each well, incubated for 2 min at room temperature on a shaker at 800 rpm. Immediately after, quantification of

analytes present in the samples was carried out using the Bio-Plex® 200 Immunoassay System (Bio-Rad, CA, USA) and results were exported to Excel (Microsoft, WA, USA) for analysis.

### 4.2.18. Quantification of PNAG-induced cytokine and chemokine production by THP1 cells

Incubations of PNAG and bacteria with THP1 cells were carried out as described in section 4.2.17. IL-8, IL-1β and RANTES were quantified in the cell supernatant using separate enzyme-linked immunosorbent assays (ELISAs) as instructed by the manufacturer. Briefly, the capture antibody was diluted to a working concentration in PBS and coated on to 96-well plate plates in 100 µL aliquots. Plates were sealed and incubated overnight at room temperature. Liquid was aspirated from each well and washed with wash buffer 3 times. The plates were blocked with blocking buffer and incubated at room temperature for 2 h. Plates were again washed 3 times in wash buffer. Samples and standards were diluted in reagent diluent and growth media in a 1:1 ratio and 100 µL of each sample or standard was added per well and incubated for 2 h at room temperature. Wells were washed 3 times in wash buffer and 100 µL of detection antibody diluted in Reagent Diluent was added to each well and incubated for 2 h at room temperature in the dark. Wells were washed again 3 times and 100 µL of Steptavidin-HRP was added to each well. Plates were covered and incubated in the dark for 20 min at room temperature. Wells were washed 3 times and 50 µL of 2 M $H_2SO_4$ was added to each well and mixed thoroughly. Absorbance was measured at 450 and 540 nm and the 540 nm absorbances were subtracted from the 450 nm readings to correct for optical imperfections in the plate. Samples and standards were analysed in technical duplicates and assays were carried out in biological triplicate. The blank well readings were subtracted from the average well readings and concentrations of IL-8, IL-1β and RANTES were calculated from the standard curves and plotted as a bar chart. Error bars represent +/- one SD of the mean.

## 4.3. Results

PRR microarrays were printed and functional analysis of the slides was carried out. Following verification that PRRs were functional, *S. aureus* and *A. baumannii* were incubated on the PRR microarray platform to screen for PRRs that target and bind to *S. aureus* and *A. baumannii*. Next, *S. aureus* and *A. baumannii* WT and Δ*ica*/*pga* and *S. aureus* Mn8m PNAG preparation (labelled by two different strategies) were incubated on the PRR microarray to elucidate potential PRRs that recognise and bind to PNAG by itself and on the bacterial cell surface to provide target PRRs for further cell signalling studies. One potential PRR-PNAG interaction was brought forward for cell signalling studies using the PNAG preparation (unlabelled and unmodified) and PNAG-deficient mutants.

### 4.3.1. Functional analysis of PRRs on microarray surface

All PRRs were printed in isolation at 0.5 μg/mL, or printed in combination with another PRR, each PRR at 0.25 μg/mL. Some PRRs, such as TLR2 and TLR6 form a heterodimers on the cell surface to recognise a molecule, activating a signalling response (Oliveira-Nascimento *et al.*, 2012). Although there was no transmembrane region of the recombinant TLRs printed and they do not have any mobility after conjugation to the microarray surface, TLRs were printed in isolation and in combination to elucidate whether heterodimers could form on the microarray platform and could detect molecules differentially than when printed in isolation. TLR2, TLR4, TLR6 and CD14, selected due to their known carbohydrate-based binding, were co-printed in various combinations (Table 4.2). Other TLRs were not printed due to cost and their association primarily with nucleic acids, not carbohydrates. Finally, WGA and sWGA were printed as a control for the detection of GlcNAc structures.

Following printing, functional analysis of the PRRs was carried out. A range of AF555 labelled glycoproteins, NGCs and SYTO® 82 stained bacteria were incubated on the PRR microarray platform. Most PRRs bound to *E. coli* to some degree (Fig. 4.1). E-selectin, L-selectin and P-selectin bound to *E. coli* and 3SuLeaBSA as expected (Galustian *et al.*, 1999). P-selectin also bound to GlcNAc-BSA suggesting affinity to GlcNAc which was not shown with the other selectins (Descheny *et al.*, 2006). Siglecs, and to some degree 3SuleaBSA, also bound *E. coli*

while MAG (Siglec-4) bound to 3SLacHSA confirming its preferential binding to α-(2,3)-linked sialic acid compared to the other siglecs printed on the microarray (Kelm *et al.*, 1994). DC-SIGN and DC-SIGNR bound to all functional control samples to some degree while LSECtin bound with greatest intensity to *E. coli*, *S. epidermidis* and GlcNAc-BSA. Dectin-1 bound with greatest intensity to *E. coli* while dectin-2 bound preferentially to invertase as expected as invertase is a yeast glycoprotein with oligomannose structures (Trimble *et al.*, 1983). Ficolin-3 showed specificity towards 3SLacHSA, 3SuleaBSA and GlcNAc-BSA and had a much greater binding intensity for all binding samples compared to ficolin-1 and ficolin-2. The immobilised chitotriosidase did not bind to any specific ligands but bound to *E. coli* and 3SuLeaBSA to some degree. TLRs printed separately and in combinations all bound to *E. coli* to some degree but, as expected, binding was greatest when TLR4 and CD14 were involved. Moreover, TLR4 also had specificity for 3SuLeaBSA (Ståhl *et al.*, 2006; Tükel *et al.*, 2010). CD14, MBL/DC-SIGN and MBL/CLEC10A bound to all samples but with greatest intensity to *E. coli*, 3SuLeaBSA and invertase. As expected, WGA bound to sialylated and GlcNAc containing structures, while sWGA bound only GlcNAc-containing structures (Monsigny *et al*., 1979).

Overall, these data showed that the PRRs were functional in terms of their binding on the microarray platform.

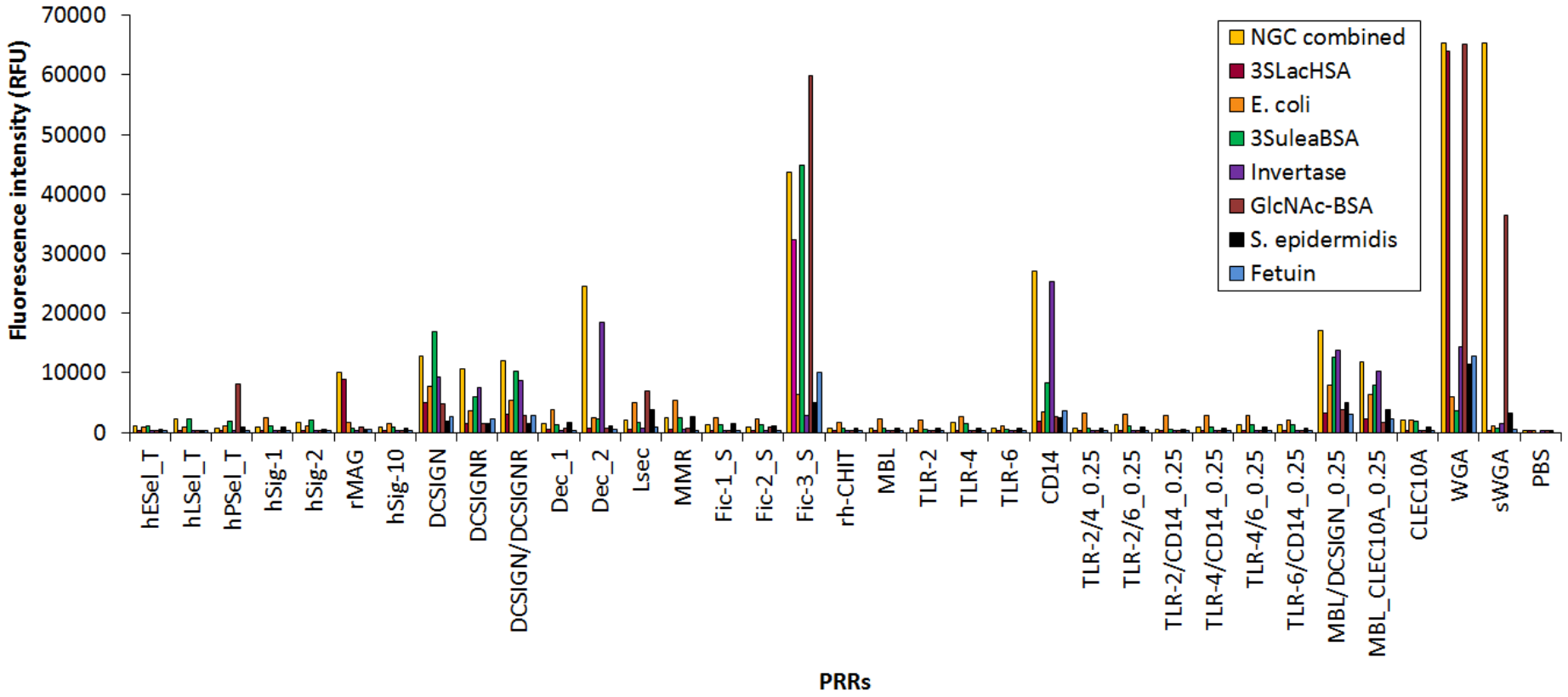


**Fig. 4.1. Quality control analysis of PRR microarray using fluorescently labelled NGCs, proteins and bacteria.** Bars represent binding of AF555 labelled 3SLacHSA, 3SuleaBSA, invertase, GlcNAc-BSA and fetuin. *E. coli* and SYTO® 82 stained *S. epidermidis* to PRRs printed on the microarray surface. Each bar represents the average binding intensity from one experiment.

### 4.3.2. Bacteria titrations on the PRR microarray platform

To establish a cell concentration which produced a good signal to noise ratio on the PRR microarray, SYTO® 82 stained cells were titrated in TBS-T and incubated on the PRR microarray platform (Fig. 4.2). To achieve a binding signal detectable by our scanner and low background, 20 µL of *S. aureus* Mn8m and BH1CC, and *A. baumannii* diluted in 50 µL TBS-T was chosen for the dilution factor for PRR microarray triplicate experiments (Fig. 4.2 (B), (C) and (D)). *S. aureus* 8325-4 diluted 30 µL with 40 µL TBS-T was also chosen for future experiments (Fig. 4.2 (B). Overall, PRRs bound to *S. aureus* Mn8m, 8325-5 and BH1CC WT and Mn8 Δ*ica* and *A. baumannii* WT and Δ*pga* in a concentration manner except for MBL/DCSIGN and MBL/CLEC10A where binding was not concentration dependent (Fig. 4.2).

### 4.3.3. Screening for PRR-*S. aureus* 8325 and Mn8m interactions

To screen for potential PRRs that bound to MSSA and to help elucidate specific interactions attributed to the presence of PNAG, *S. aureus* 8325-4 WT and Δ*ica* and Mn8m WT and Mn8 Δ*ica* were incubated on the PRR microarray and assessed for interactions with PRRs (Fig. 4.3 (A) and (B)). WGA, sWGA, DC-SIGN, DC-SIGNR, DC-SIGN/DC-SIGNR, LSECtin, MMR, ficolin-3, CD14, MBL/DC-SIGN and MBL/CLEC10A all bound to *S. aureus* Mn8m and 8325-4 WT. The Δ*ica* mutants displayed reduced binding to CD14, MBL/DC-SIGN, MBL/CLEC10A, WGA and sWGA for both *S. aureus* 8325-4 Δ*ica* and Mn8 Δ*ica* compared to *S. aureus* 8325-4 WT and Mn8m WT, respectively. However, this reduction in binding was not statistically significant. WGA did not bind to *S. aureus* Mn8m to a similar fluorescence intensity as seen in previous experiments (Chapter 2 and Chapter 3), which suggested that there was a lower amount of GlcNAc containing polysaccharides (such as PNAG) on the cell surface in this preparation compared to previous experiments and signals seen for the WT may have been lower than expected (Fig. 4.3). In terms of selecting a PRR to further investigate for potential PNAG modulation of binding and potential impact on immune signalling for the bacteria, MBL/DC-SIGN and MBL/CLEC10A were not considered due to their non-concentration dependent binding (Fig. 4.2) while CD14, which did show

concentration dependent binding and a decrease in binding intensity in the absence of PNAG, was selected as the PRR candidate for further investigation.

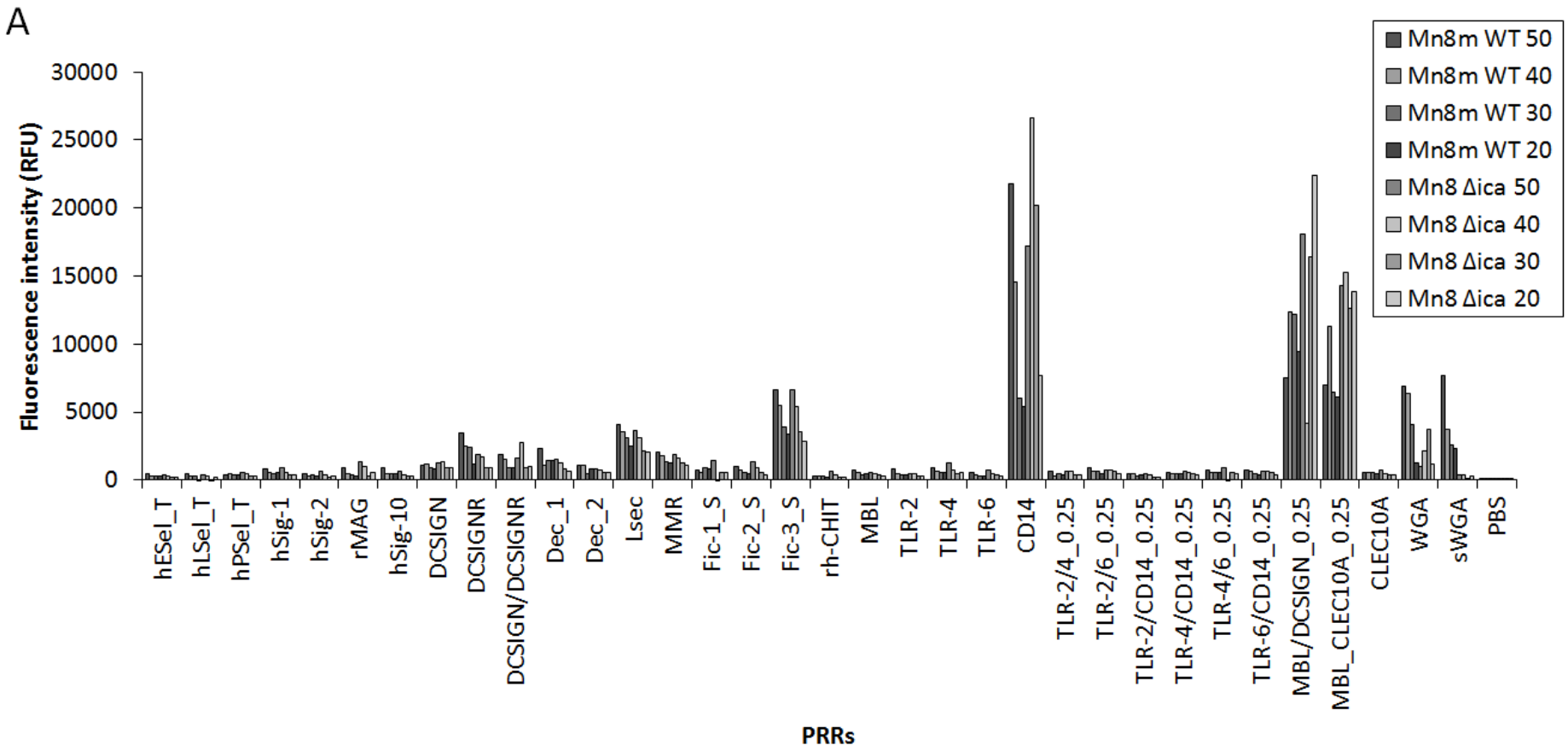
A
Fluorescence intensity (RFU)
30000
25000
20000
15000
10000
5000
0
Mn8m WT 50
Mn8m WT 40
Mn8m WT 30
Mn8m WT 20
Mn8 Δica 50
Mn8 Δica 40
Mn8 Δica 30
Mn8 Δica 20
hESel_T
hLSel_T
hPSel_T
hSig-1
hSig-2
rMAG
hSig-10
DCSIGN
DCSIGNR
DCSIGN/DCSIGNR
Dec_1
Dec_2
Lsec
MMR
Fic-1_S
Fic-2_S
Fic-3_S
rh-CHIT
MBL
TLR-2
TLR-4
TLR-6
CD14
TLR-2/4_0.25
TLR-2/6_0.25
TLR-2/CD14_0.25
TLR-4/CD14_0.25
TLR-4/6_0.25
TLR-6/CD14_0.25
MBL/DCSIGN_0.25
MBL_CLEC10A_0.25
CLEC10A
WGA
sWGA
PBS
PRRs

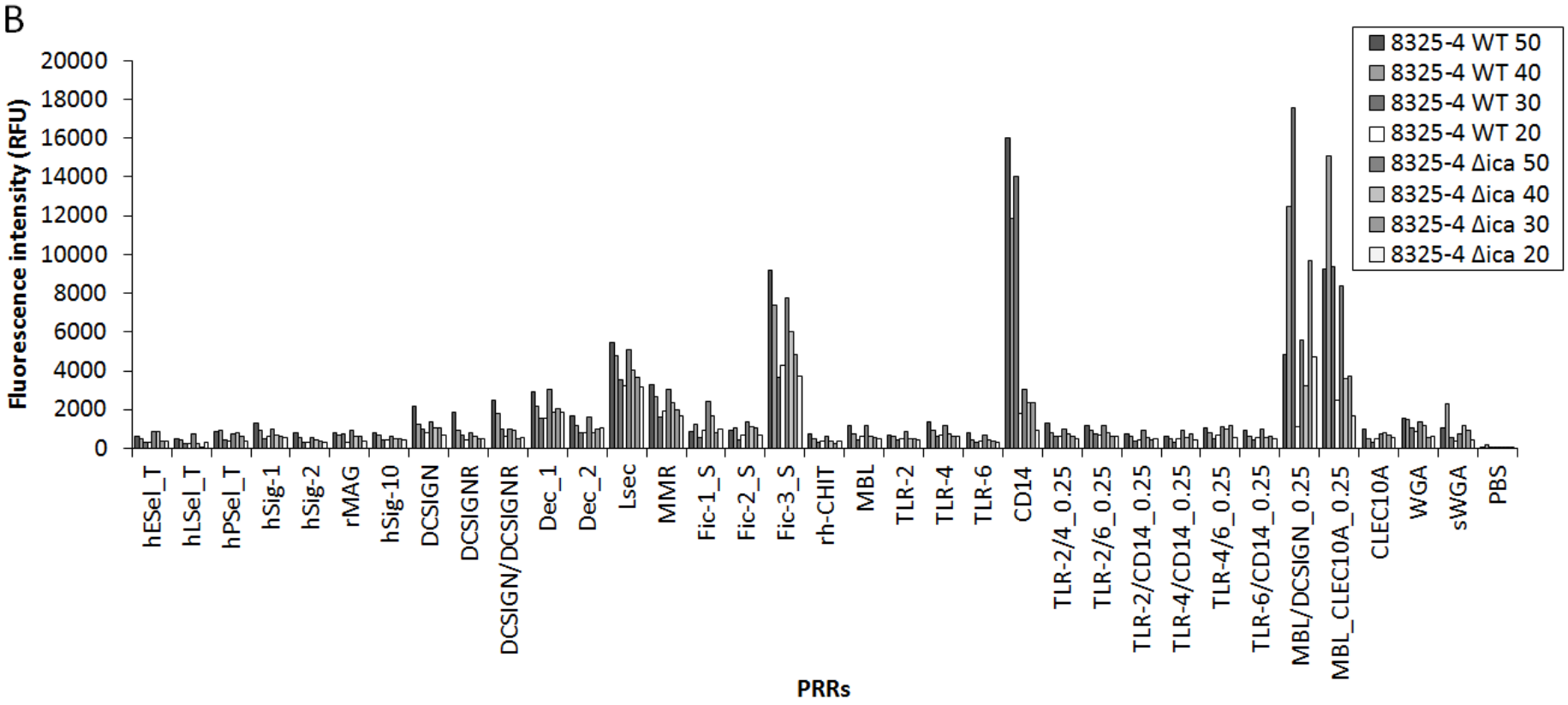
B
Fluorescence intensity (RFU)
20000
18000
16000
14000
12000
10000
8000
6000
4000
2000
0
8325-4 WT 50
8325-4 WT 40
8325-4 WT 30
8325-4 WT 20
8325-4 Δica 50
8325-4 Δica 40
8325-4 Δica 30
8325-4 Δica 20
hESel_T
hLSel_T
hPSel_T
hSig-1
hSig-2
rMAG
hSig-10
DCSIGN
DCSIGNR
DCSIGN/DCSIGNR
Dec_1
Dec_2
Lsec
MMR
Fic-1_S
Fic-2_S
Fic-3_S
rh-CHIT
MBL
TLR-2
TLR-4
TLR-6
CD14
TLR-2/4_0.25
TLR-2/6_0.25
TLR-2/CD14_0.25
TLR-4/CD14_0.25
TLR-4/6_0.25
TLR-6/CD14_0.25
MBL/DCSIGN_0.25
MBL_CLEC10A_0.25
CLEC10A
WGA
sWGA
PBS
PRRs

C

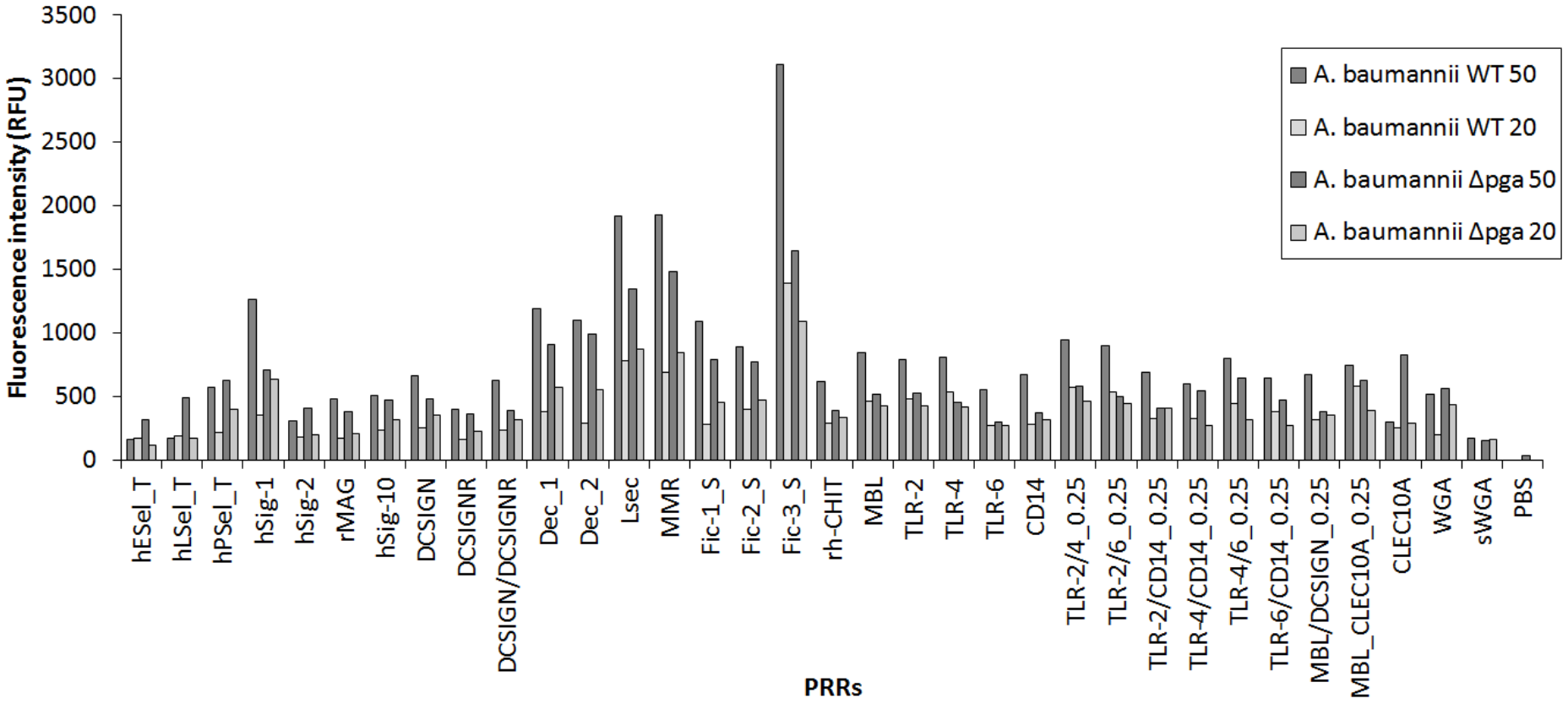
Fluorescence intensity (RFU)
3500
3000
2500
2000
1500
1000
500
0
A. baumannii WT 50
A. baumannii WT 20
A. baumannii Δpga 50
A. baumannii Δpga 20
hESel_T
hLSel_T
hPSel_T
hSig-1
hSig-2
rMAG
hSig-10
DCSIGN
DCSIGNR
DCSIGN/DCSIGNR
Dec_1
Dec_2
Lsec
MMR
Fic-1_S
Fic-2_S
Fic-3_S
rh-CHIT
MBL
TLR-2
TLR-4
TLR-6
CD14
TLR-2/4_0.25
TLR-2/6_0.25
TLR-2/CD14_0.25
TLR-4/CD14_0.25
TLR-4/6_0.25
TLR-6/CD14_0.25
MBL/DCSIGN_0.25
MBL_CLEC10A_0.25
CLEC10A
WGA
sWGA
PBS
PRRs

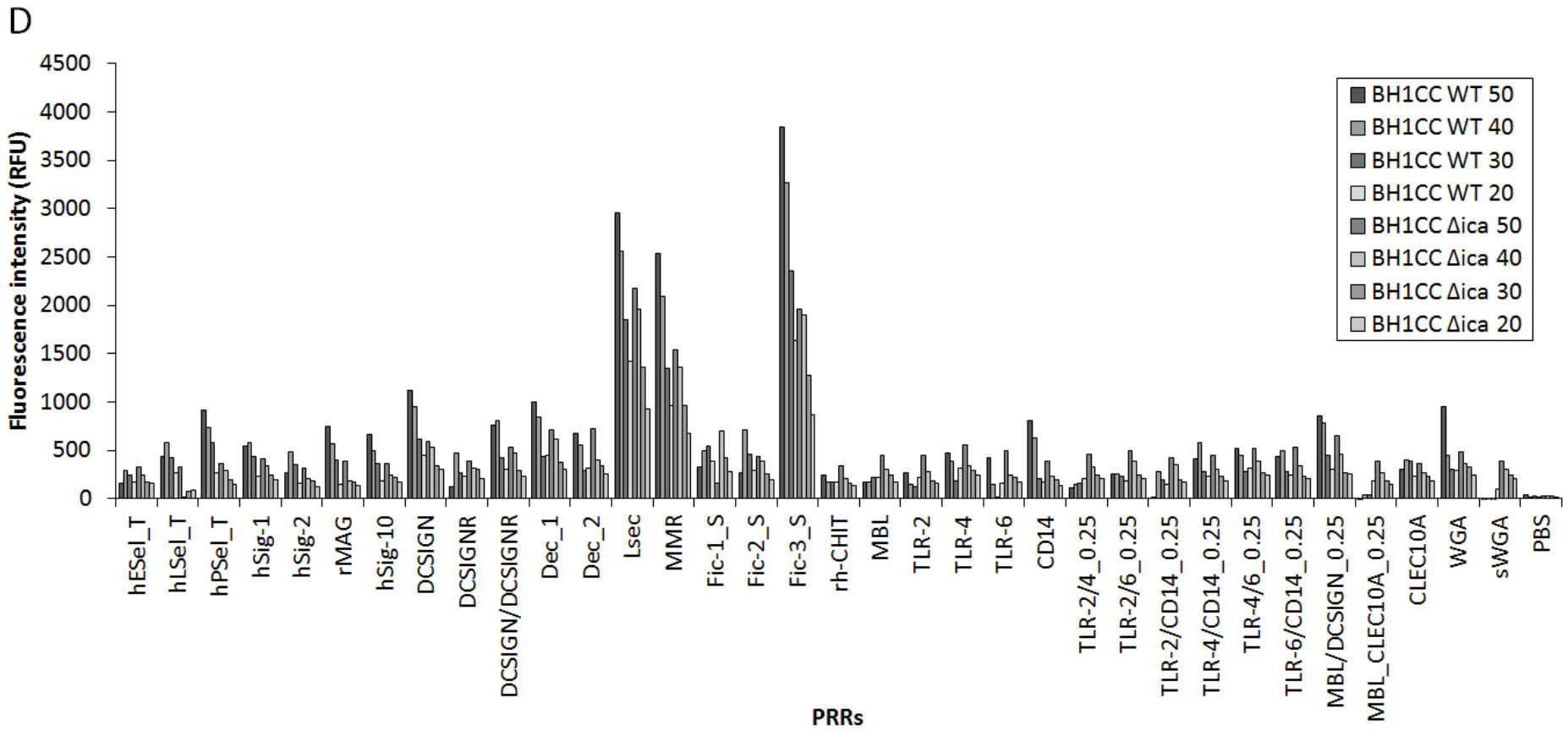


**Fig. 4.2. *S. aureus* Mn8m WT and Δ*ica* titration on the PRR microarray.** Bar chart represents (A) *S. aureus* Mn8m WT and Δ*ica*, (B) *S. aureus* 8325-4 WT and Δ*ica*, and (D) *S. aureus* WT titrated 50, 40, 30 and 20 µL to give a final volume of 70 µL and (C) *A. baumannii* WT and Δ*pga* WT titrated 50 and 20 µL to give a final volume of 70 µL on the PRR microarray platform. Bar chart represents one experiment, and data per PRR from one experiment represents the median of six data points.

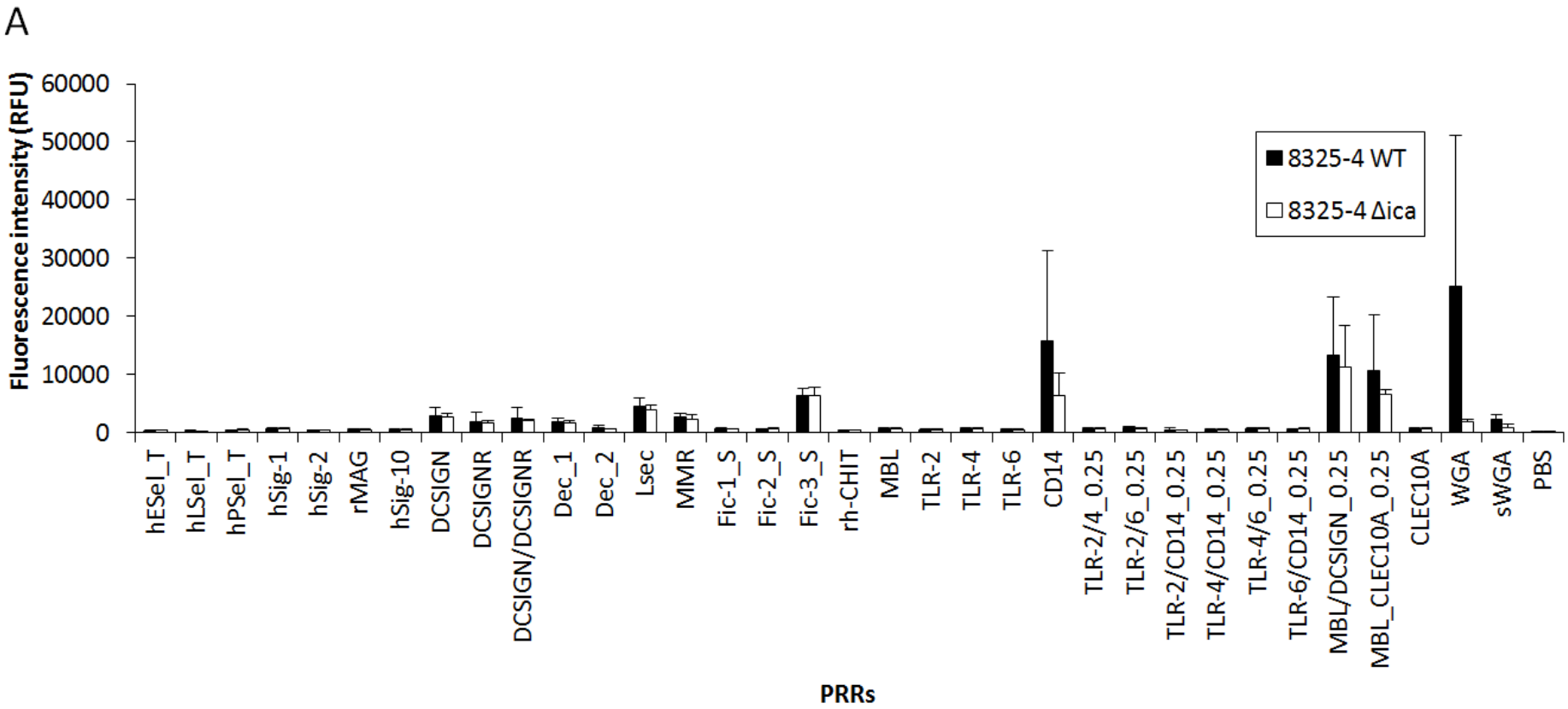
A
Fluorescence intensity (RFU)
60000
50000
40000
30000
20000
10000
0
8325-4 WT
8325-4 Δica
hESel_T
hLSel_T
hPSel_T
hSig-1
hSig-2
rMAG
hSig-10
DCSIGN
DCSIGNR
DCSIGN/DCSIGNR
Dec_1
Dec_2
Lsec
MMR
Fic-1_S
Fic-2_S
Fic-3_S
rh-CHIT
MBL
TLR-2
TLR-4
TLR-6
CD14
TLR-2/4_0.25
TLR-2/6_0.25
TLR-2/CD14_0.25
TLR-4/CD14_0.25
TLR-4/6_0.25
TLR-6/CD14_0.25
MBL/DCSIGN_0.25
MBL_CLEC10A_0.25
CLEC10A
WGA
sWGA
PBS
PRRs

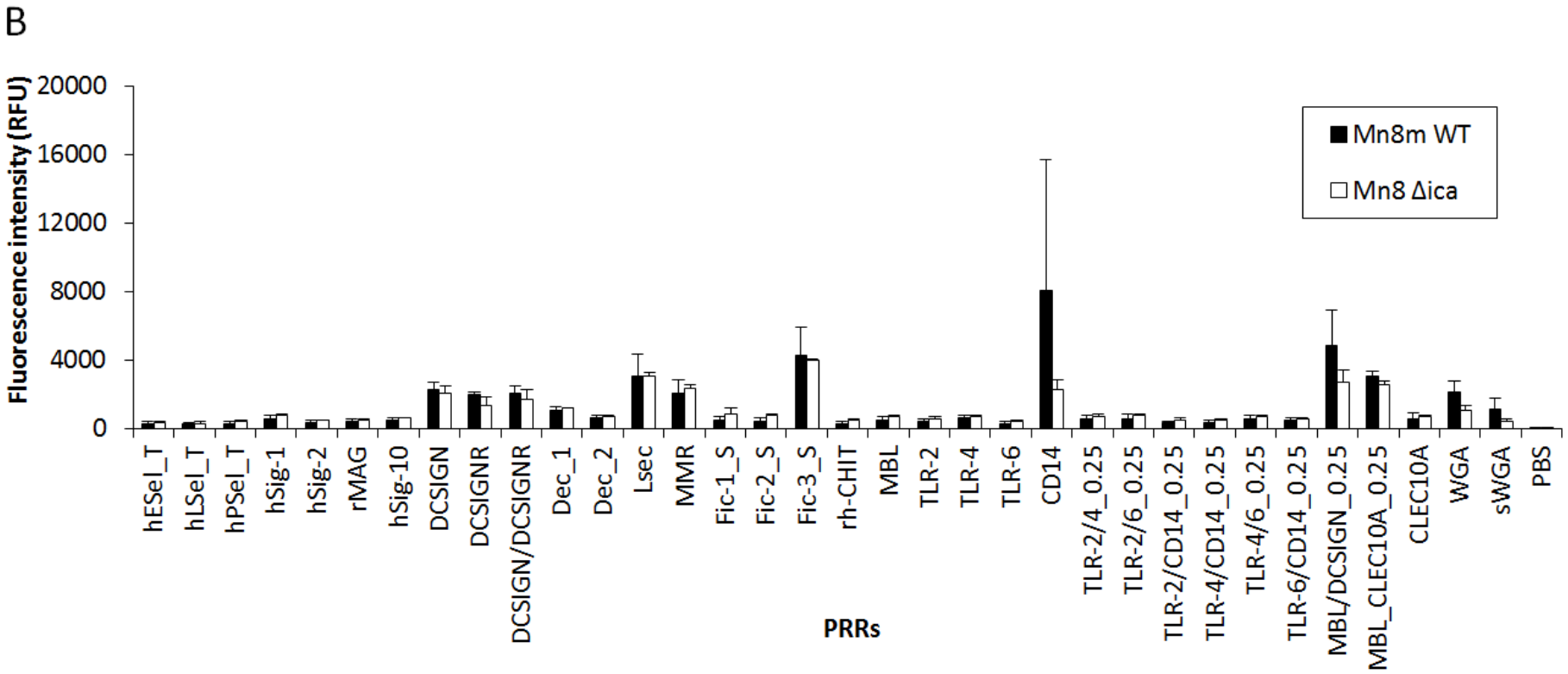


**Fig. 4.3. PRR microarray profile of *S. aureus* 8325-4 and Mn8m WT and Δ*ica*.** Bar charts represent binding intensities of *S. aureus* 8325-4 WT to PRRs printed on the PRR microarray platform after (A) 8325-4 WT and Δica grown in BHI NaCl and (B) *S. aureus* Mn8m WT and Mn8 Δ*ica* grown in BHI glucose. Bar charts represent the mean of three technical experiments with error bars of +/- one SD of the mean.

### 4.3.4. Assessment of glycoclusters sos2210 and sos2254 for modulating *S. aureus*–PRR interactions

In Chapter 3, a variety of glycoclusters were used to modulate WGA binding to whole bacteria demonstrating that the microarray platform was suitable for measuring glycocluster inhibition of lectin interactions. To advance this study, two glycoclusters were assessed to elucidate their potential in modulating human lectin-(PRR-)bacteria interactions.

Glycoclusters sos2210 and sos2254 were incubated with *S. aureus* Mn8m and then on to the PRR microarray platform (Fig 4.4 (A) and (B)). As a control, the glycocluster solvent, DMSO, was added to *S. aureus* Mn8m without any glycoclusters in the same concentration used to solubilise the glycoclusters. Addition of DMSO or compounds at 0.1 mM did not significantly impact any PRR binding to *S. aureus* Mn8m (Fig 4.4 (A)). Similarly, 0.1 mM of sos2210 or sos2254 did not alter PRR binding to *S. aureus* 8325-4, except 0.1 mM of sos2254 did reduce binding of CD14 to *S. aureus* 8325-4 WT, although this inhibition was not significant. However, addition of DMSO and both compounds did reduce *S. aureus* WGA binding to *S. aureus* 8325-4 (Fig. 4.4 (B)). This impact on WGA binding in the presence of DMSO was not observed before in Chapter 3. Therefore, these results show that glycoclusters sos2210 and sos2254 at 0.1 mM concentrations do not modulate PRR binding to *S. aureus* Mn8m but may modulate binding of *S. aureus* 8325-4 to CD14. However, this latter effect may have been influenced by the presence of DMSO rather than the glycocluster itself. Based on the data from Chapter 3, it is likely that higher concentrations (1 mM) would be required to inhibit GlcNAc mediated interactions with PRRs but due to lack of glycocluster availability, only 0.1 mM was assessed.

A

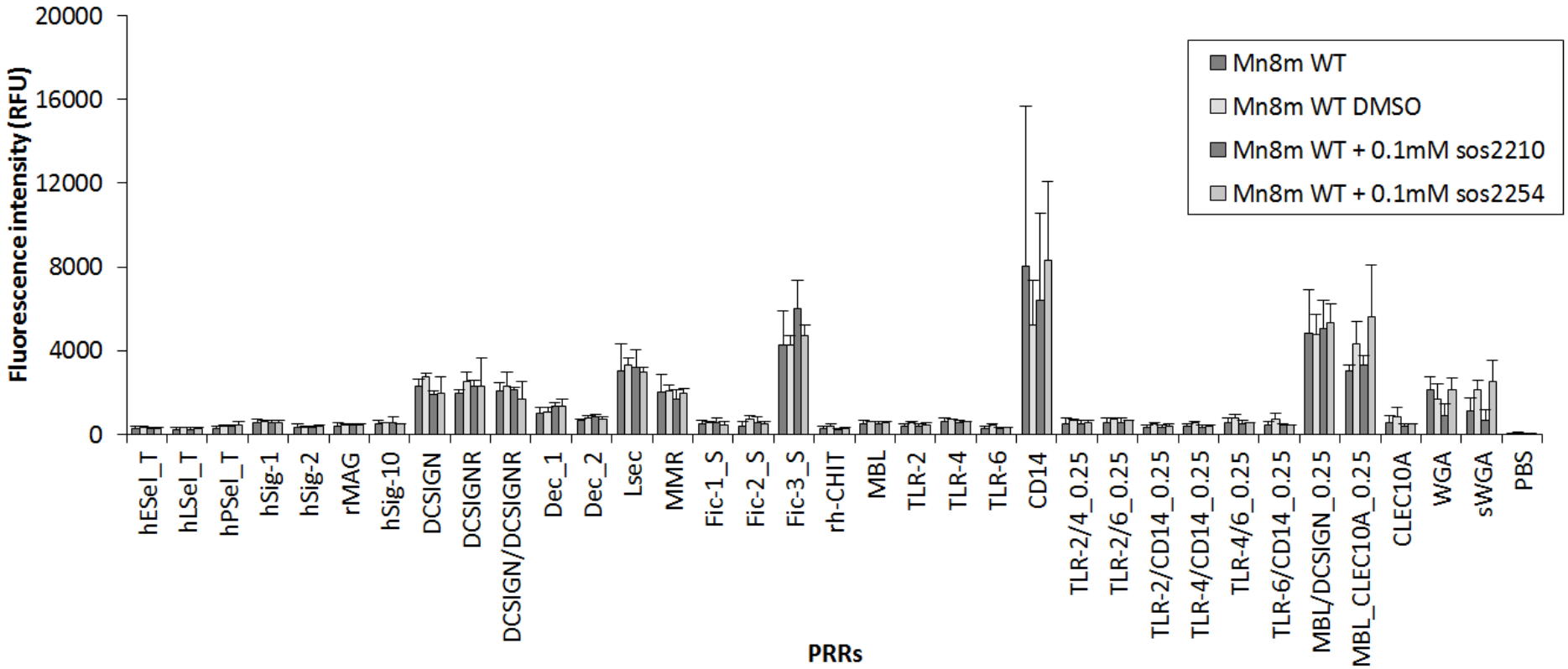
Fluorescence intensity (RFU)
20000
16000
12000
8000
4000
0
Mn8m WT
Mn8m WT DMSO
Mn8m WT + 0.1mM sos2210
Mn8m WT + 0.1mM sos2254
hESel_T
hLSel_T
hPSel_T
hSig-1
hSig-2
rMAG
hSig-10
DCSIGN
DCSIGNR
DCSIGN/DCSIGNR
Dec_1
Dec_2
Lsec
MMR
Fic-1_S
Fic-2_S
Fic-3_S
rh-CHIT
MBL
TLR-2
TLR-4
TLR-6
CD14
TLR-2/4_0.25
TLR-2/6_0.25
TLR-2/CD14_0.25
TLR-4/CD14_0.25
TLR-4/6_0.25
TLR-6/CD14_0.25
MBL/DCSIGN_0.25
MBL_CLEC10A_0.25
CLEC10A
WGA
sWGA
PBS
PRRs

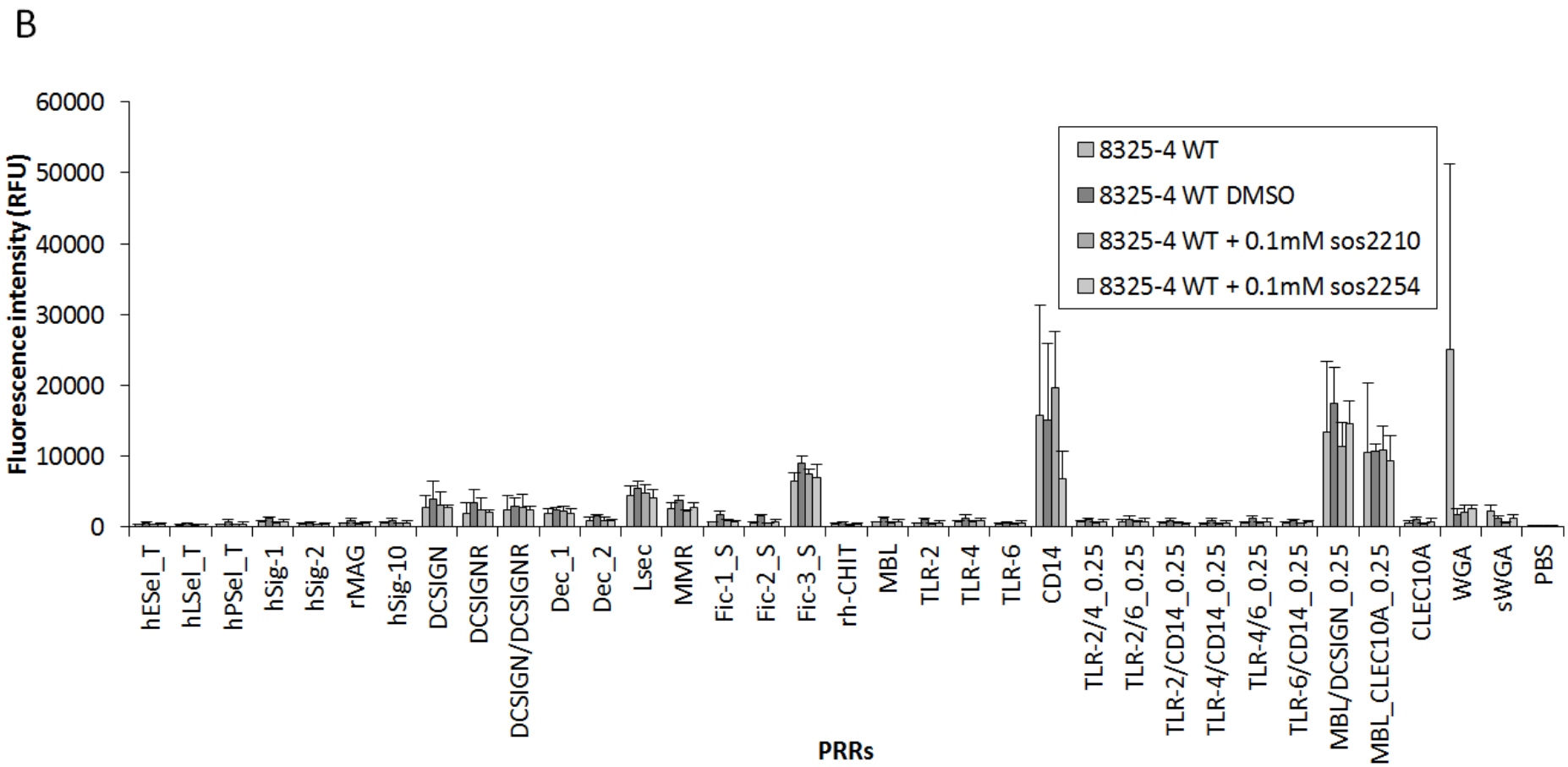


**Fig. 4.4. PRR microarray profile of *S. aureus* 8325-4 and Mn8m WT and Δ*ica* with 0.1 mM sos2210 and sos2254.** Bar charts represent binding intensities of (A) *S. aureus* 8325-4 WT and (B) *S. aureus* Mn8m to PRRs with and without the addition of 0.1 mM sos2210, sos2254 and DMSO (control). Bar charts represent the mean of three technical experiments with error bars of +/- one SD of the mean.

### 4.3.5. Effect of PNAG presentation on PRR recognition

As the absence of PNAG on the cell surface exposes other carbohydrate structures on the bacterial cell surface that also bind to PRRs, a difference in PRR binding between the WT and Δ*ica* mutants may not reveal all PRR interactions in which PNAG has a role. Therefore, a PNAG preparation purified from *S. aureus* Mn8m (gifted by Prof. G. Pier, Harvard) was screened for PRR interactions. It is important to note that this PNAG preparation contained approximately 0.35% LTA (Chapter 3 section 3.3.6). As the primary component of this cell surface preparation was PNAG, from here onwards this preparation is denoted as PNAG.

PNAG can be found bound to the bacterial surface or secreted in to the surrounding environment. To mimic PNAG in these two different structural conformations that would be physiologically similar to PNAG in a biofilm matrix, two labelling strategies were adopted; direct labelling of PNAG with AF555 *via* the free amine groups on PNAG (secreted PNAG) and immobilising PNAG (surface-bound) on a 1 μm fluorescent bead (FluoSphere).

PNAG-AF555 was titrated on the PRR microarray to establish high fluorescent binding signals and low background fluorescence and as 4:20,000 dilution gave the highest signal and minimal background fluorescence, this dilution was chosen for further experiments (Fig. 4.5 (A)). The maximum fluorescence detected by the microarray scanner was 65,000 RFU. PNAG-FS at 50, 40 and 30 μL emitted too high of a fluorescence when bound to P-selectin, DC-SIGNR, LSECtin, ficolin-3, CD14, MBL/DC-SIGN, WGA and sWGA. Therefore, PNAG-FS were standardised to an absorbance at 595 nm of approximately 1.0, resuspended in 500 μL TBS-T and diluted 20 μL to a final volume of 70 μL TBS-T to be detected on the PRR microarray and give bead numbers similar to cell numbers of *S. aureus* Mn8m incubated on the PRR microarray (Fig 4.5 (B)).

DC-SIGNR, CD14, MBL/DC-SIGN and MBL/CLEC10A bound to PNAG-AF555 and PNAG-FS (Fig. 4.5 (C)). LSECtin bound preferentially to PNAG-FS compared to PNAG-AF555 suggesting that LSECtin preferentially recognised PNAG on spherical surfaces, such as on bacteria, rather than in suspension. Interestingly, sWGA had greater specificity towards PNAG-AF555 and PNAG-FS compared to

WGA. Overall, these results suggest that several PRRs bind selectively to PNAG itself and the presentation of the PNAG polysaccharide may promote or reduce these interactions, possibly by altering the polysaccharide conformation to increase or decrease accessibility to particular ligands or sections. However, it must be noted that the trace LTA present in the PNAG preparation may have contributed to one or more of these interactions.

Attachment of PNAG on to FluoSpheres required a large quantity of PNAG and quantities available were quite limited in this study. Therefore, subsequent cell-based studies were carried out with PNAG-AF555 or unlabelled PNAG preparation only by necessity.

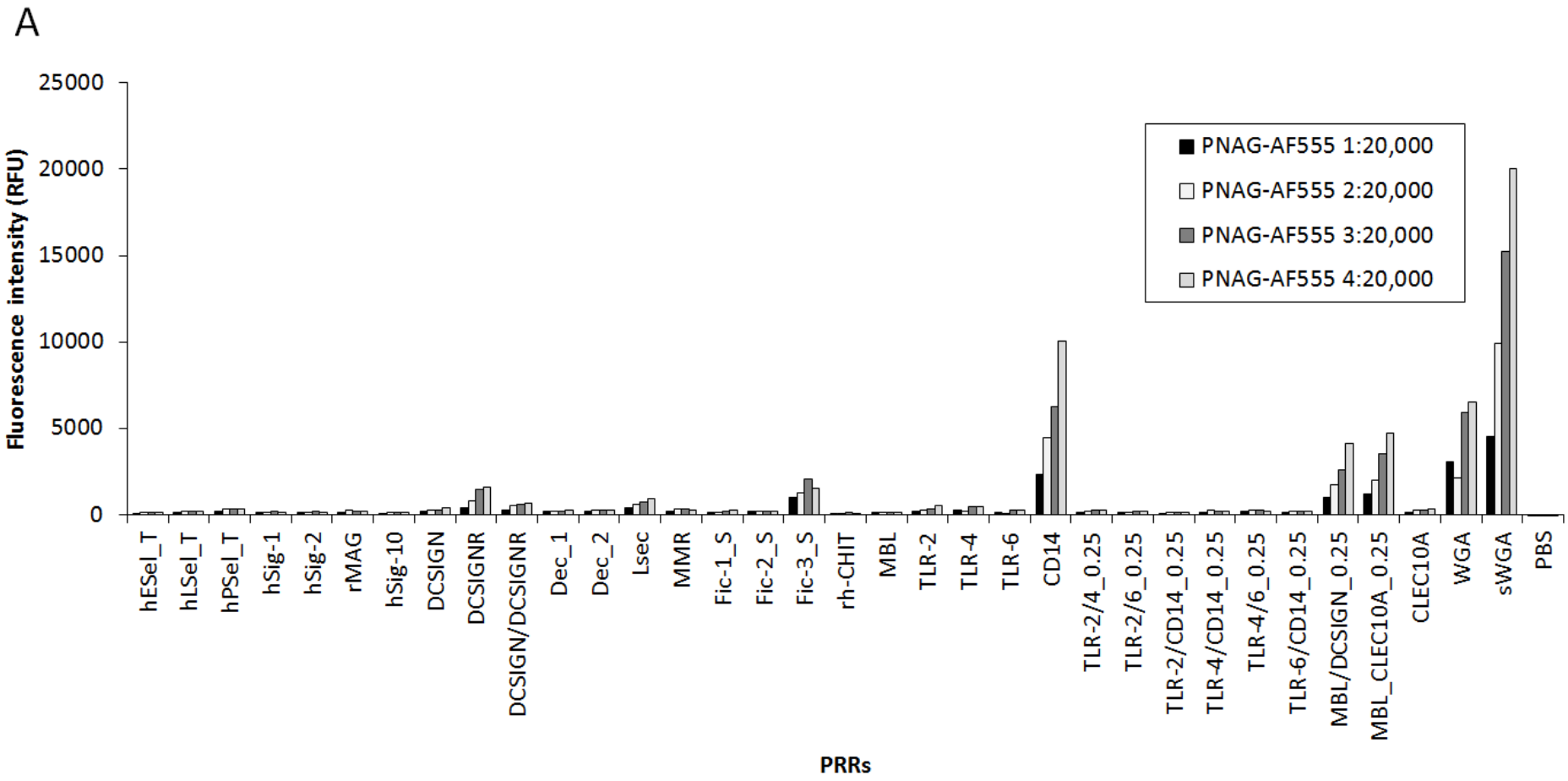
A
Fluorescence intensity (RFU)
25000
20000
15000
10000
5000
0
PNAG-AF555 1:20,000
PNAG-AF555 2:20,000
PNAG-AF555 3:20,000
PNAG-AF555 4:20,000
hESel_T
hLSel_T
hPSel_T
hSig-1
hSig-2
rMAG
hSig-10
DCSIGN
DCSIGNR
DCSIGN/DCSIGNR
Dec_1
Dec_2
Lsec
MMR
Fic-1_S
Fic-2_S
Fic-3_S
rh-CHIT
MBL
TLR-2
TLR-4
TLR-6
CD14
TLR-2/4_0.25
TLR-2/6_0.25
TLR-2/CD14_0.25
TLR-4/CD14_0.25
TLR-4/6_0.25
TLR-6/CD14_0.25
MBL/DCSIGN_0.25
MBL_CLEC10A_0.25
CLEC10A
WGA
sWGA
PBS
PRRs

B

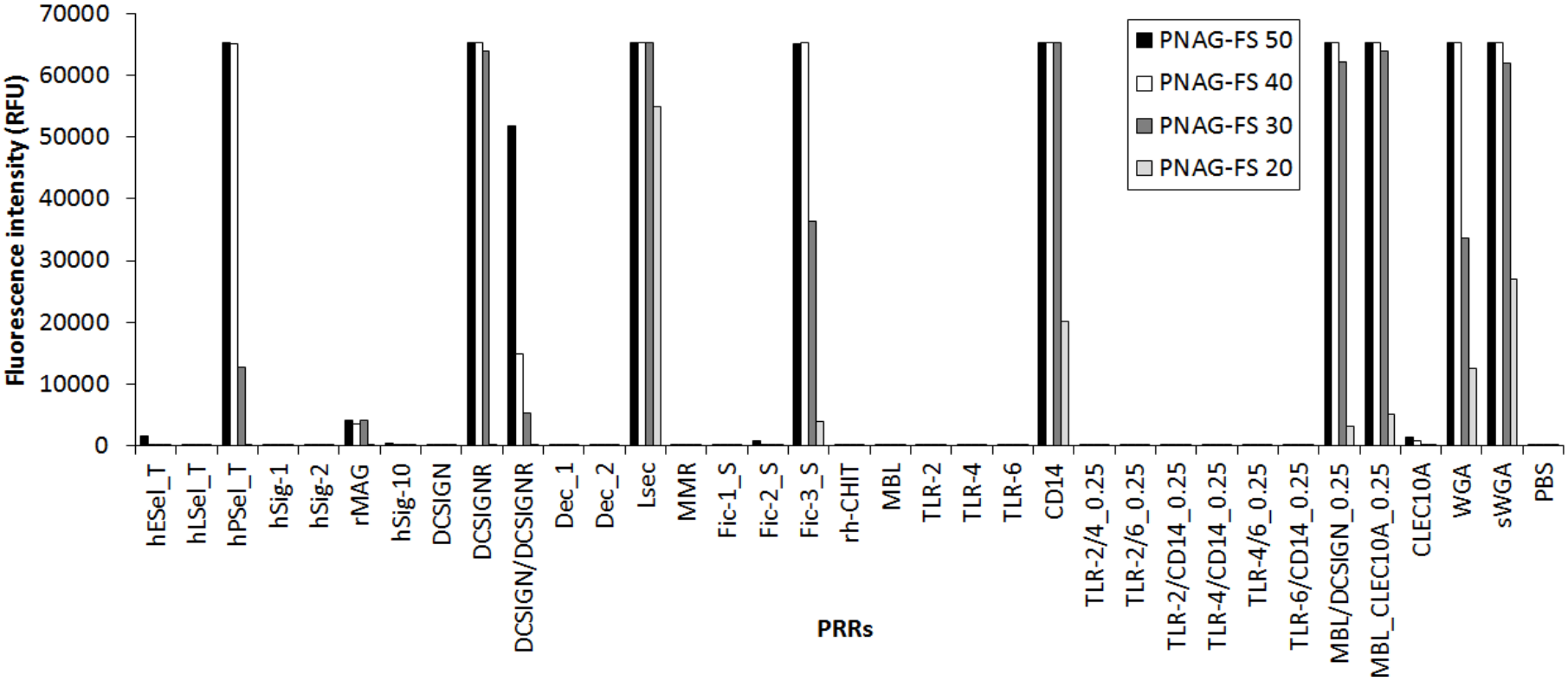
Fluorescence intensity (RFU)
70000
60000
50000
40000
30000
20000
10000
0
PNAG-FS 50
PNAG-FS 40
PNAG-FS 30
PNAG-FS 20
hESel_T
hLSel_T
hPSel_T
hSig-1
hSig-2
rMAG
hSig-10
DCSIGN
DCSIGNR
DCSIGN/DCSIGNR
Dec_1
Dec_2
Lsec
MMR
Fic-1_S
Fic-2_S
Fic-3_S
rh-CHIT
MBL
TLR-2
TLR-4
TLR-6
CD14
TLR-2/4_0.25
TLR-2/6_0.25
TLR-2/CD14_0.25
TLR-4/CD14_0.25
TLR-4/6_0.25
TLR-6/CD14_0.25
MBL/DCSIGN_0.25
MBL_CLEC10A_0.25
CLEC10A
WGA
sWGA
PBS
PRRs

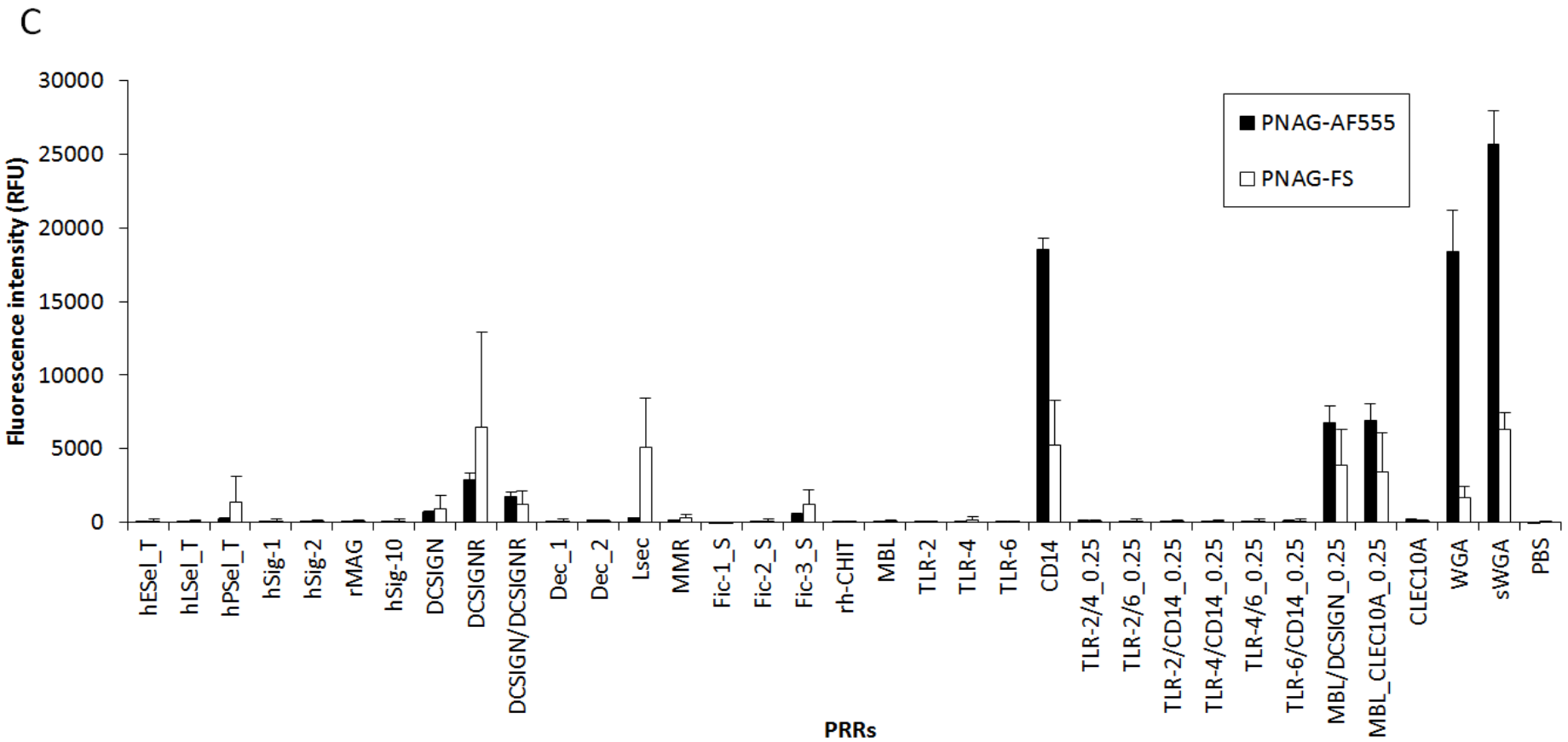


**Fig. 4.5. PRR microarray profile of PNAG-AF555 and PNAG-FS**. Bar charts represent (A) PNAG-AF555 diluted 1-4:20,000 dilution, (B) PNAG-FS titrated 50, 40, 30 and 20 µL to give a final volume of 70 µL and (C) PNAG-AF555 diluted 4:20,000 and PNAG-FS diluted 20 µL to give a final volume of 70 µL on the PRR microarray platform. Titrations (A) and (B) were 1 experiment, and data per PRR from one experiment represents the median of six data points. Bar chart in figure (C) represents the mean of three technical experiments with error bars of +/- one SD of the mean.

### 4.3.6. Assessment of glycoclusters sos2210 and sos2254 for modulating PNAG–PRR interactions

Glycoclusters sos2210 and sos2254 significantly ($P \leq 0.01$) promoted CD14 binding to PNAG-AF555 by 81% and 73%, respectively, compared to PNAG-AF-555 in DMSO. Furthermore, glycoclusters sos2210 significantly increased MBL/CLEC10A binding to PNAG-AF555, compared to PNAG-AF555 in DMSO. Glycocluster sos2254 also increased binding MBL/CLEC10A binding to PNAG-AF555, but this increase was not significant. (Fig. 4.6). Sos2210 and sos2254 increased binding to DC-SIGN, DC-SIGN/DC-SIGNR and, however the increased binding for DC-SIGN and DC-SIGN/DC-SIGNR was due to the presence of DMSO and not the glycoclusters. At 0.1 mM, glycocluster sos2210 reduced WGA and sWGA binding to PNAG by 78% and 61% respectively, but glycocluster sos2254 had little impact on binding. These results suggest that although glycoclusters, such as sos2210, may decrease plant lectin binding to PNAG, it does not necessarily mean it will inhibit human lectin (PRR) interactions. The increase in binding in the presence of the GlcNAc glycoclusters may signify a change in the conformation of the PRRs, which subsequently increased PRR binding to PNAG, or the creation of a 'binding bridge' between the PRR and the PNAG. In the latter case, both PRR and PNAG would bind to the glycoclusters, probably at different sites on the glycoclusters, which would facilitate and increased number of PNAG molecules binding to the PRRs.

### 4.3.7. Screening for PRR-*A. baumannii* S1 interactions

*A. baumannii* WT and Δ*pga* were incubated on the PRR microarray platform and assessed for interactions (Fig. 4.7). We chose a fluorescent intensity cut-off of 600 RFU (approximately three times the average background fluorescent intensity) to focus on high binders. Siglec-1, DC-SIGN, DC-SIGNR, DC-SIGN/DC-SIGNR, dectin-1, dectin-2, LSECtin, MMR, ficolin-1,-2, and -3, MBL, TLR2, TLR4, CD14, TLR2/4, TLR2/6, TLR2/CD14, TLR4/6, TLR6/CD14, MBL/DCSIGN and MBL/CLEC10A all bound to *A. baumannii* WT. *A. baumannii* Δ*pga* displayed reduced binding to the PRRs siglec-1, DC-SIGN, dectin-1, dectin-2, LSECtin, TLR2/4, TLR2/6 and TLR2/CD14 compared to the WT strain. This result suggested that PNAG, may be involved in these interactions. Interestingly, TLR2 printed in

combination with other TLRs, but not printed in isolation, promoted the recognition of *A. baumannii* WT compared to the Δ*pga* mutant strain. Thus, this indicated that TLR2 in combination with another TLR may be important for the recognition of PNAG. Surprisingly, WGA and sWGA bound to *A. baumannii* WT and Δ*pga* equally, in agreement with the observations in Chapter 2. Similarly, *A. baumannii* WT and Δ*pga* did not bind differentially to CD14 (Fig. 4.7), unlike *S. aureus* Mn8m and 8325-4 (Fig. 4.3). These data further supported the previous suggestion in Chapter 2 of different presentation or accessibility of PNAG on the cell surface of the Gram-negative *A. baumannii* compared to the Gram-positive *S. aureus* which impacts on biological recognition as demonstrated here and may further subsequently impact on the ensuing biological function

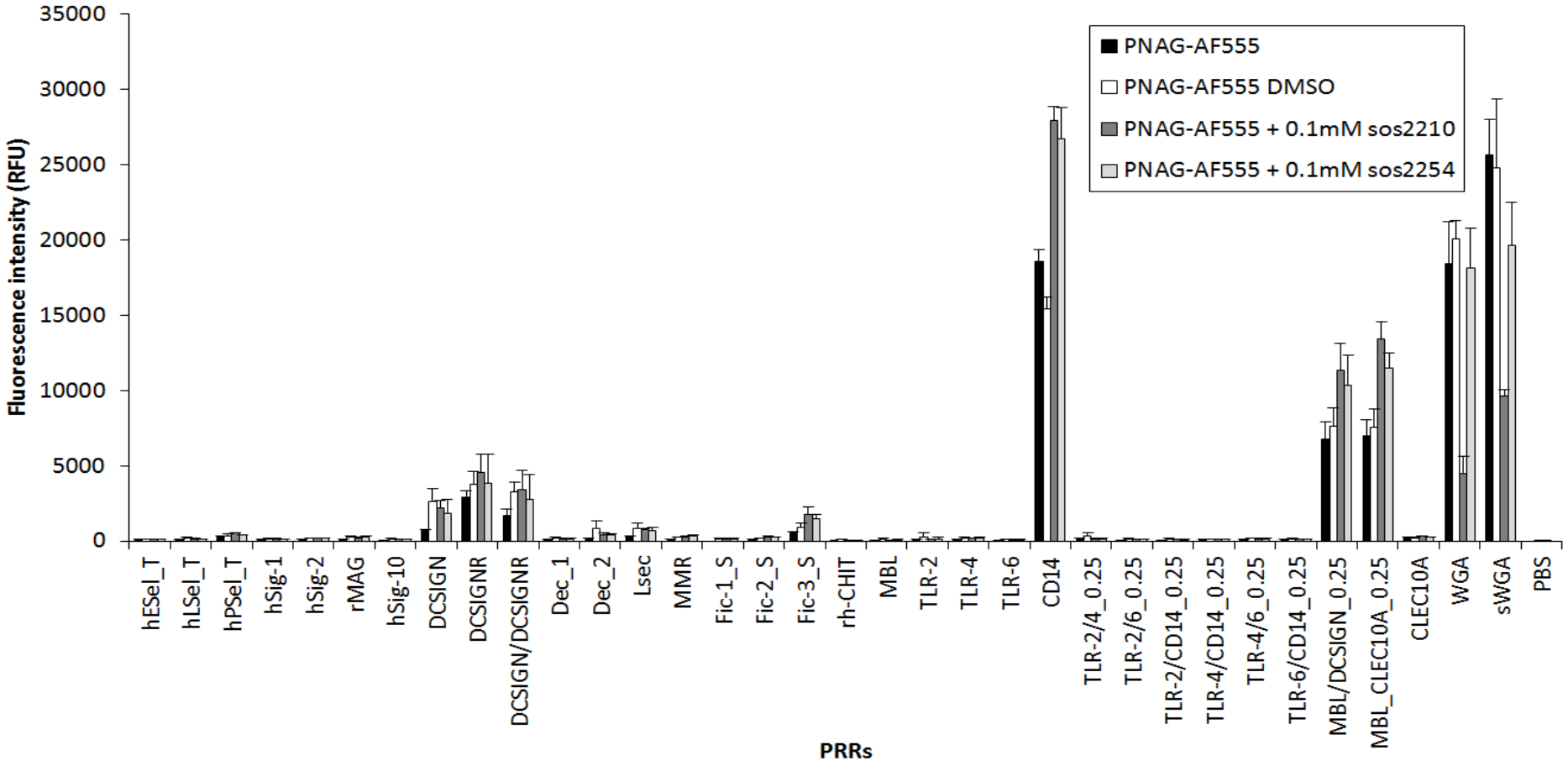


**Fig. 4.6. PRR microarray profile of PNAG-AF555 with 0.1 mM sos2210 and sos2254.** Bar charts represent binding intensities of PNAG-AF555 to PRRs with and without the addition of 0.1 mM sos2210, sos2254 and DMSO (control). Bar charts represent the mean of three technical experiments with error bars of +/- one SD of the mean.

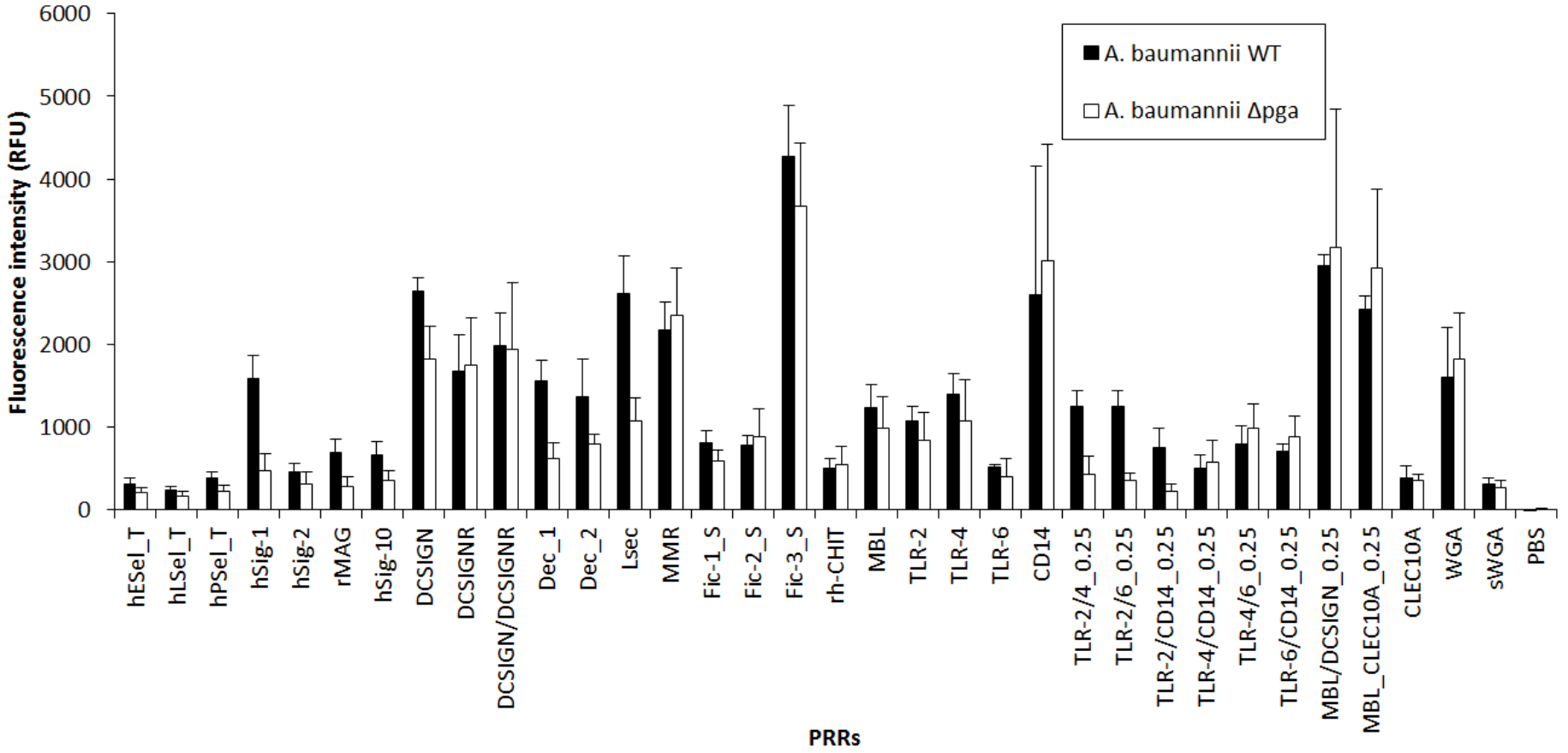


**Fig. 4.7. PRR microarray profile of *A. baumannii* WT and Δ*pga*.** Bar charts represent binding intensities of *A. baumannii* WT and Δ*pga* to PRRs printed on the PRR microarray platform after growth in BHI glucose. Bar charts represent the mean of three technical experiments with error bars of +/- one SD of the mean.

### 4.3.8. Screening for MRSA BH1CC WT and Δ*ica* binding to PRRs

Before incubation on the PRR microarray, *S. aureus* BH1CC was grown in BHI NaCl to promote *ica* transcription. Even though there is no evidence to suggest that this translated into PNAG production (O'Neill *et al.*, 2007; Chapter 2, section 2.3.1), we wanted to elucidate whether *ica* transcription would influence PRR binding to this MRSA strain. DC-SIGN, DC-SIGNR, DC-SIGN/DC-SIGNR, dectin-1, dectin-2, LSECtin, MMR, ficolin 3, CD14, MBL/DC-SIGN and MBL/CLEC10A bound to *S. aureus* BH1CC WT and Δ*ica* (Fig. 4.8) which suggested that these PRRs recognised surface structures on this MRSA bacterium. While there was very little difference in binding intensity of the WT and Δ*ica* mutant to the PRRs, interestingly LSECtin bound significantly ($P \leq 0.01$) fewer *S. aureus* Δ*ica* mutant cells compared to the WT. Mutation of the *ica* operon in *S. aureus* BH1CC resulting in a 32% decrease in LSECtin binding to this *S. aureus* strain. This altered LSECtin binding indicated that *ica* transcription may alter the expression or production of a cell surface ligand(s) that is not PNAG.

### 4.3.9. Selection of PRR for investigation of PNAG modulation

CD14 bound to MSSA strains in concentration-dependent manner, differentially bound to Δ*ica* mutant MSSA strains compared to MSSA WT strains and consistently bound to PNAG presented in two formats. Therefore, CD14-PNAG binding was chosen to further investigate the signalling consequences of this interaction.

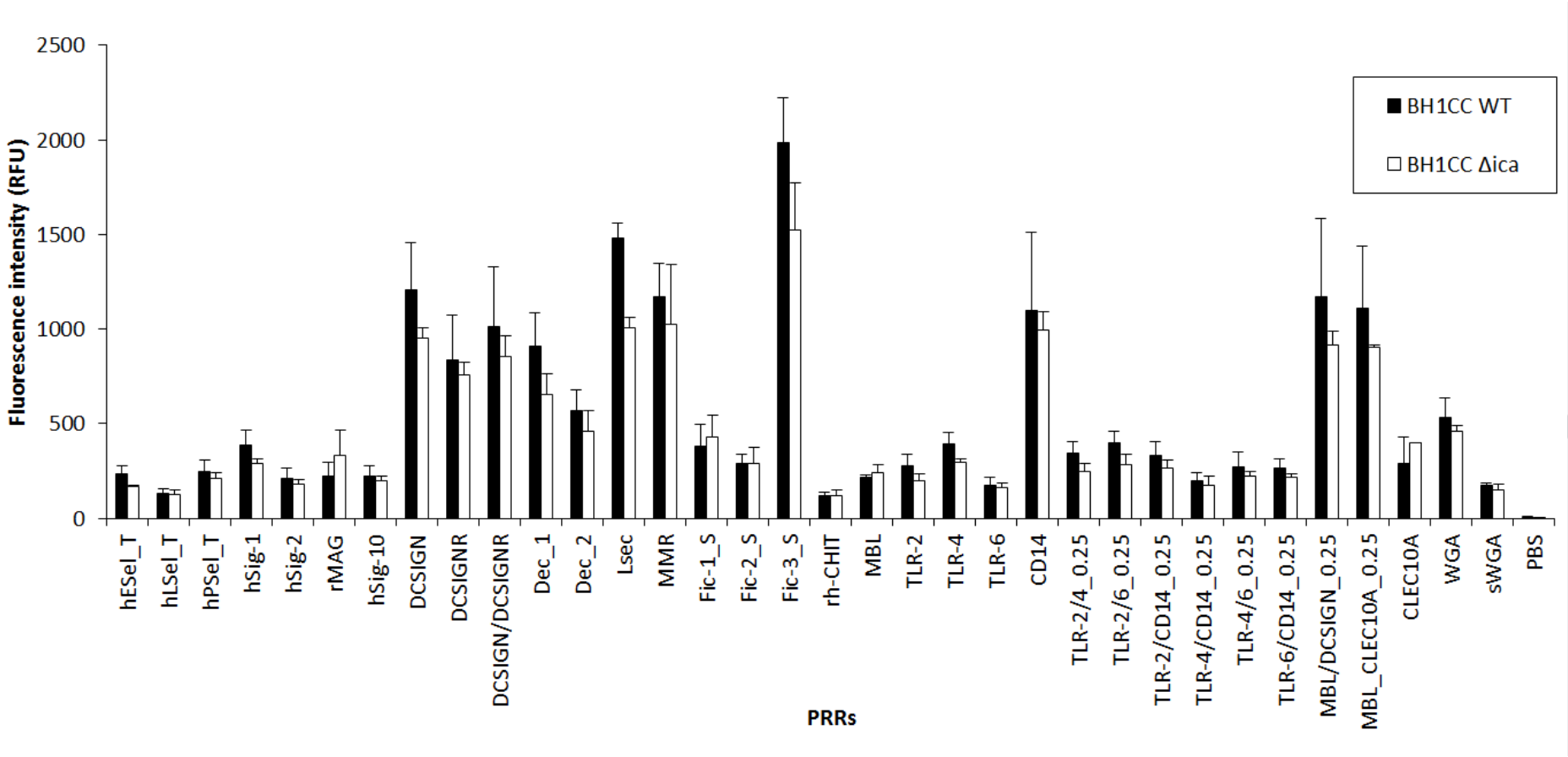


**Fig. 4.8. *S. aureus* PRR microarray profile of *S. aureus* BH1CC WT and Δ*ica*.** Bar chart represents binding intensities of *S. aureus* WT and Δ*ica* to PRRs printed on the PRR microarray platform after growth in BHI NaCl. Bar chart represents the mean of three technical experiments with error bars of +/- one SD of the mean.

### 4.3.10. Validation of PRR-dependent signalling response of THP1-Blue-CD14 cells

THP1-Blue-CD14 cells (THP1 cells) are derived from the THP1-Blue cell line, which are derived from the human monocytic THP-1 cell line. THP1 cells stably overexpress CD14 and express all TLRs, but respond only to ligands for TLR2, TLR1/2, TLR2/6, TLR4, TLR5 and TLR8, according to the manufacturer's specifications. Furthermore, THP1 cells express an NF-κB- and AP-1-inducible secreted embryonic alkaline phosphatase (SEAP) reporter gene. As TLR activation is often aided by CD14 and results in NF-κB/AP-1 activation and the production of SEAP, the SEAP concentration produced by this cell line the culture supernatant is quantified using a colourimetric assay to determine SEAP activity and indicative of TLR activity (Fig. 4.9 (A)).

To establish that the THP1 cell line was functionally responding to TLR stimuli, FSL-1 (TLR2/6 agonist), SA-LTA (TLR2 agonist), LPS (TLR4 agonist) and HKLM (TLR2 agonist) were incubated with the cell line for 20 hours (Fig. 4.9 (B)). NF-κB/AP-1 activation was concentration-dependent for each agonist and unlabelled PNAG also promoted NF-κB/AP-1 activation in a concentration-dependent manner.

To confirm that anti-PRR antibodies were neutralising specific PRR-mediated signalling response, several anti-PRR antibodies were tested to block NF-κB/AP-1 activation caused by an agonist specific for each TLR (Fig. 4.10). Anti-TLR1 and anti-TLR2 antibodies separately alone reduced NF-κB/AP-1 activation caused by Pam3CSK4 (TLR1/2 agonist) by 76% and 91%, respectively. Anti-TLR4 and anti-CD14 antibodies separately alone reduced NF-κB/AP-1 activation caused by LPS by 75% and 87%, respectively. Anti-TLR6 antibody reduced NF-κB/AP-1 activation caused by FSL-1 by 27%. Incubation of THP1-Blue-CD14 cells with IgG1 and IgG2B isotype controls did not promote NF-κB/AP-1 activation. Thus specific anti-PRR antibodies were functional in blocking NF-κB/AP-1 activation mediated by their respective PRR.

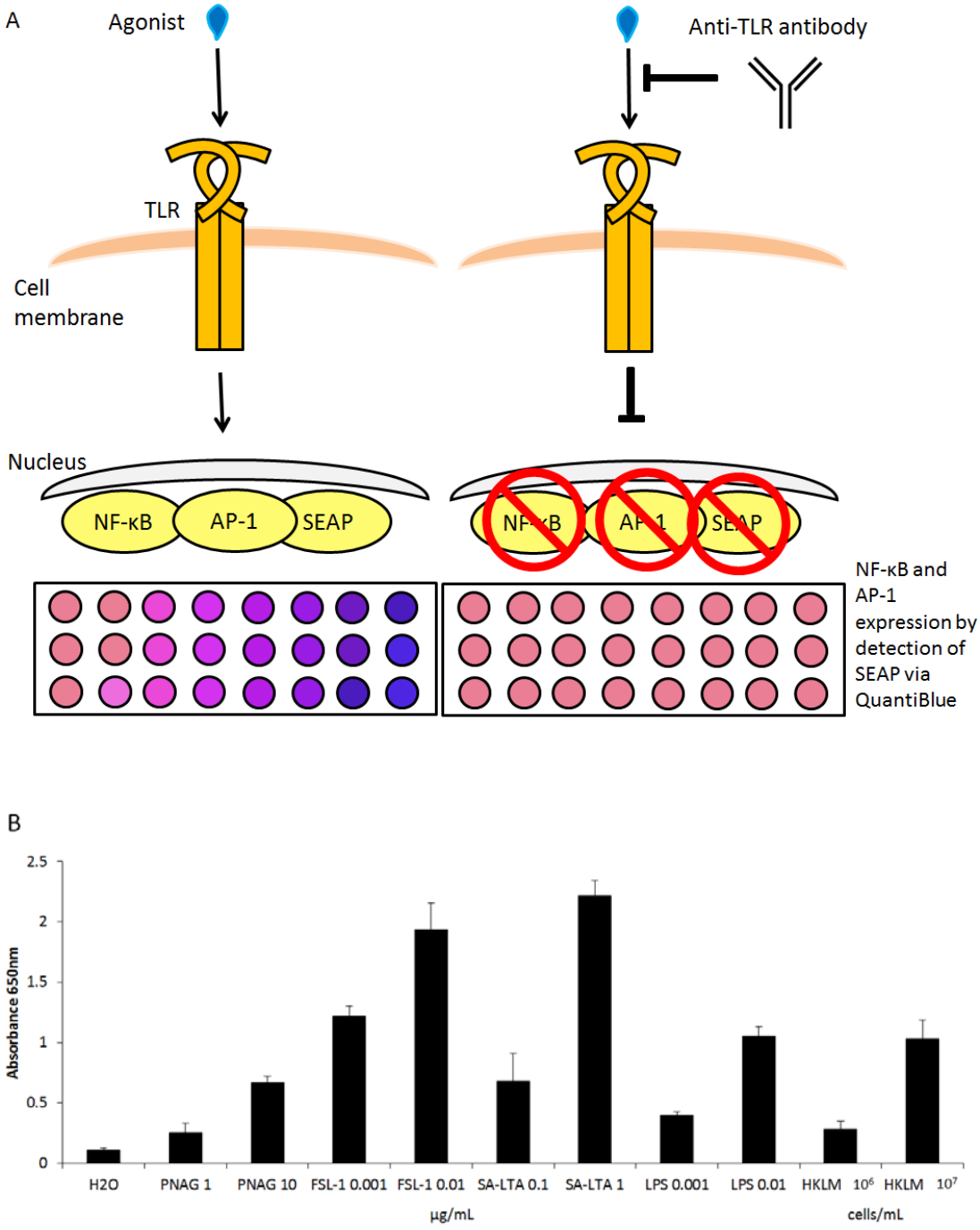


**Fig. 4.9. THP1-Blue-CD14 cell assay depiction and assay to confirm functionality.** (A) TLR agonists incubated with THP1 cells activate NF-κB/AP-1 resulting in the secretion of SEAP. The quantity of SEAP is directly proportional to NF-κB/AP-1 activation. SEAP is detected in the assay via QUANTI-Blue™ – a colourmetric enzyme assay used to determine alkaline phosphatase in an assay. Colour change to purple/blue can be quantitatively determined with a spectrophotometer. Addition of a neutralising antibody against CD14 and/or TLRs reduces NF-κB/AP-1 and thus SEAP in the assay. (B) THP1 cells were incubated with PNAG preparation at 1 and 10 μg/mL, FSL-1 (TLR2/6 agonist) at 0.001 and 0.01 μg/mL, SA-LTA (TLR2 agonist) at 0.1 and 1 μg/mL, LPS (TLR4 agonist) at 0.001 and

0.01 µg/mL and HKLM (TLR2 agonist) at 1 x $10^6$ cells/mL and 1 x $10^7$ cells/mL for 20 h. Cell culture supernatant was added to QUANTI-Blue™ reagent to quantify SEAP and AP activity (absorbance at 650 nm). Bar charts represent the absorbance of each sample at 659 nm in three biological replicates with error bars representing +/- one SD of the mean of the three biological replicates.

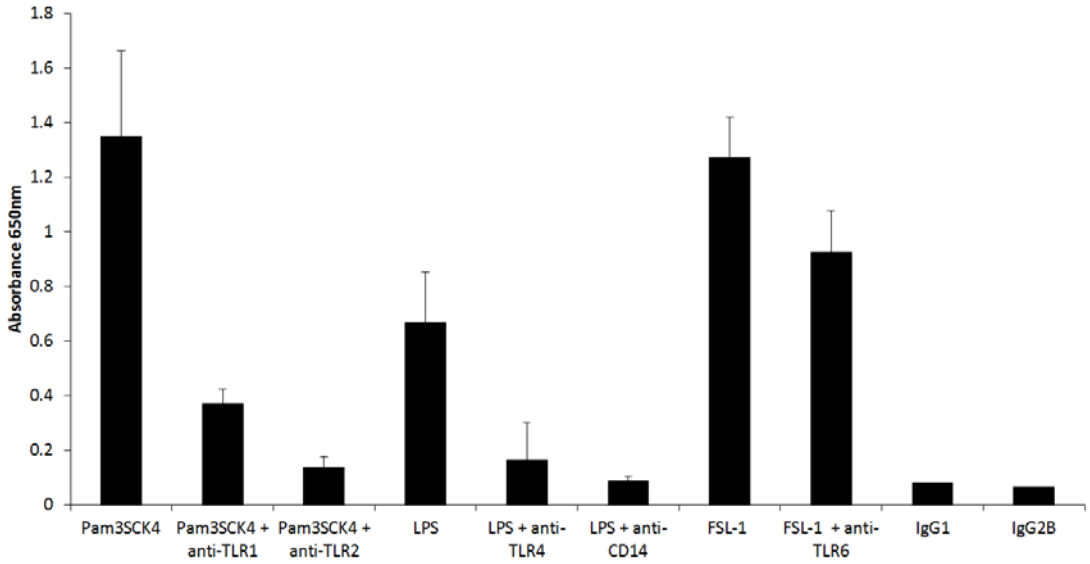


**Fig. 4.10. Elucidation of the functionality of anti-TLR and anti-CD14 antibodies.** THP1 cells were incubated with antibodies against TLR1, TLR2, TLR4, TLR6 and CD14 to give a final concentration of 10 µg/mL per well. Following a 20 h incubation, cell culture supernatants were added to QUANTI-Blue™ and absorbance was read at 650 nm. Isotype control antibodies IgG1 and IgG2B were added to cells to give a final concentration of 10 µg/mL per well to verify no agonistic effect. Error bars represent +/- one SD of the mean of three biological replicates.

### 4.3.11. Assessment of PNAG-mediated signalling response on *A. baumannii* and *S. aureus* whole cells

To make sure that bacteria would not kill the cell line due to virulence factors such as toxins, bacteria were heat-killed prior to incubation with THP1 cells. Heat-killed cells were spotted on to PVDF membrane to confirm the presence or absence of PNAG with an anti-PNAG antibody (Fig. 4.11 (A)). PNAG was present on *S. aureus* Mn8m and 8325-4 and *A. baumannii* WT strains and no PNAG was detected on *S. aureus* Mn8m Δ*ica* and 8325-4 Δ*ica* and *A. baumannii* Δ*pga* cells.

*S. aureus* 8325-4 and Mn8m WT and Δ*ica* were incubated with THP1 cells at 1, 2.5 and 5 x $10^6$ cells/mL, while *A. baumannii* WT and Δ*pga* were incubated with THP1-cells at 1, 2.5 and 5 x $10^4$ cells/mL to achieve comparable results after 20 h incubation periods (Fig. 4.11 (B)). The *S. aureus* Δ*ica* mutants significantly reduced NF-κB/AP-1 activation compared to the WT strain for Mn8m at 5 x $10^6$ cells/mL by 65%, and 8325-4 at 2.5 and 5 x$10^6$ cells/mL by 49% and 54% respectively. On the other hand, NF-κB/AP-1 activation by the *A. baumannii* Δ*pga* mutant was not significantly different compared to the WT strain at 1, 2.5 and 5 x $10^4$ cells/mL (Fig. 4.11 (B)). Therefore, these data showed that at higher cell concentrations, PNAG on *S. aureus* 8325-4 and Mn8m promoted NF-κB/AP-1 activation while PNAG on *A. baumannii* did not influence NF-κB/AP-1 activation at the cell concentrations tested in this assay (Fig. 4.11 (B)).

Overall, as PNAG was confirmed to be present in both *S. aureus* and *A. baumannii* WT strains (Fig. 4.11 (A)) but only altered cell activation in the case of *S. aureus* strains (Fig. 4.11 (B)), these data support the previous suggestions (sections 2.3.7 and 4.3.7) differences in PNAG presentation or structural modifications on Gram-positive *versus* Gram-negative cell surfaces with subsequent different effects on biological signalling response.

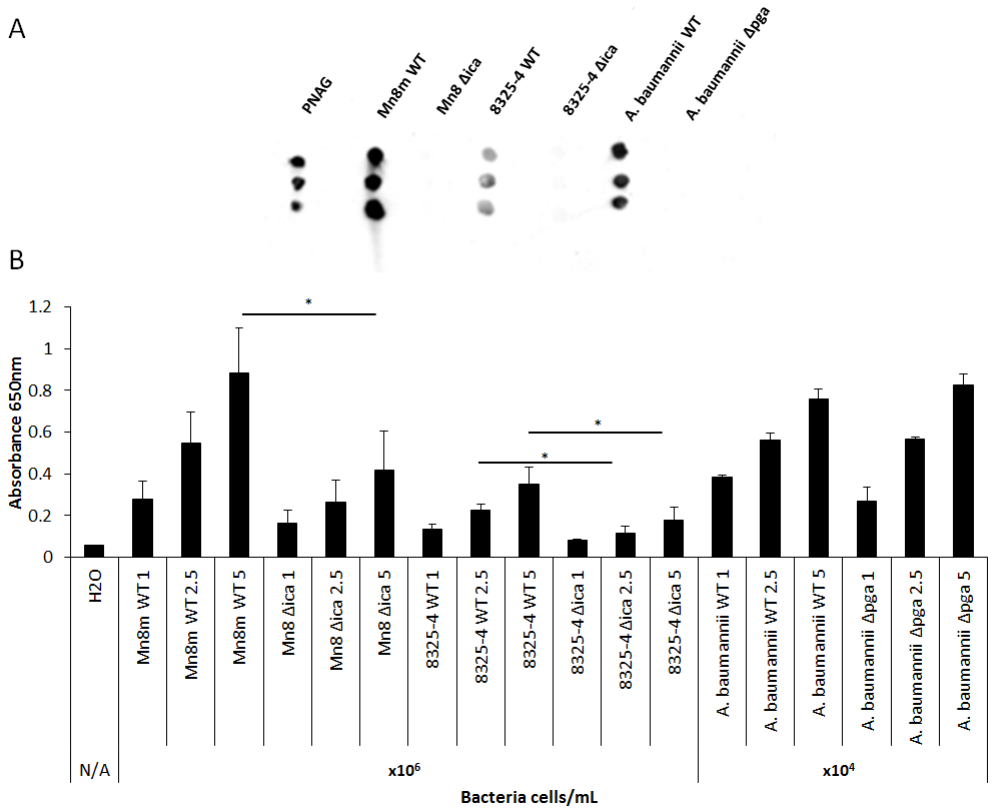


**Fig. 4.11. THP1-Blue-CD14 cell assay with heat-killed bacteria, with and without PNAG on the cell surface. (A)** Dot blot of heat killed *S. aureus* Mn8m WT/Δ*ica* and *A. baumannii* WT/Δ*pga* grown in BHI glucose and *S. aureus* 8325-4 WT/Δ*ica* grown in BHI NaCl. The presence of PNAG on WT bacteria and the absence on Δ*ica* /*pga* mutants was then confirmed with and anti-PNAG primary antibody (F598) and rabbit anti-human-HRP labelled secondary antibody. Samples were spotted in triplicates. **(B)** Heat killed *S. aureus* WT/Δ*ica* were added to THP1 cells in *S. aureus* final concentrations of 1, 2.5 and 5 x $10^6$ cells/mL, and *A. baumannii* added at concentrations of 1, 2.5 and 5 x $10^4$ cells/mL for 20 h incubations. Cell culture supernatants were added to QUANTI-Blue™ and NF-κB/AP-1 activation was quantified after 4 h incubation by reading absorbance at 650 nm. Error bars represent +/- one SD of the mean of three biological replicates. * $p \leq 0.05$, Student *t* test.

### 4.3.12. Assessment of THP1-Blue-CD14 NF-κB/AP-1 activation by PNAG preparation from *S. aureus* Mn8m and *A. baumannii*

Next we wanted to elucidate whether PNAG without the bacterial cells would have any effect on NF-κB/AP-1 activation. THP1 cells were incubated with antibodies against different TLRs for 30 minutes prior to incubation with 10 µg/mL of the PNAG preparation from *S. aureus* Mn8m (SA-PNAG). Antibodies against TLR2

and CD14 had the most substantial impact in reducing NF-κB/AP-1 activation followed by antibodies against TLR6 and TLR1. Thus, CD14 and TLR2 were likely the main ligands involved in binding to the SA-PNAG preparation and caused NF-κB/AP-1 activation. TLR1 and TLR6 were also involved but to a lesser degree compared to CD14 and TLR2 (Fig 4.12).

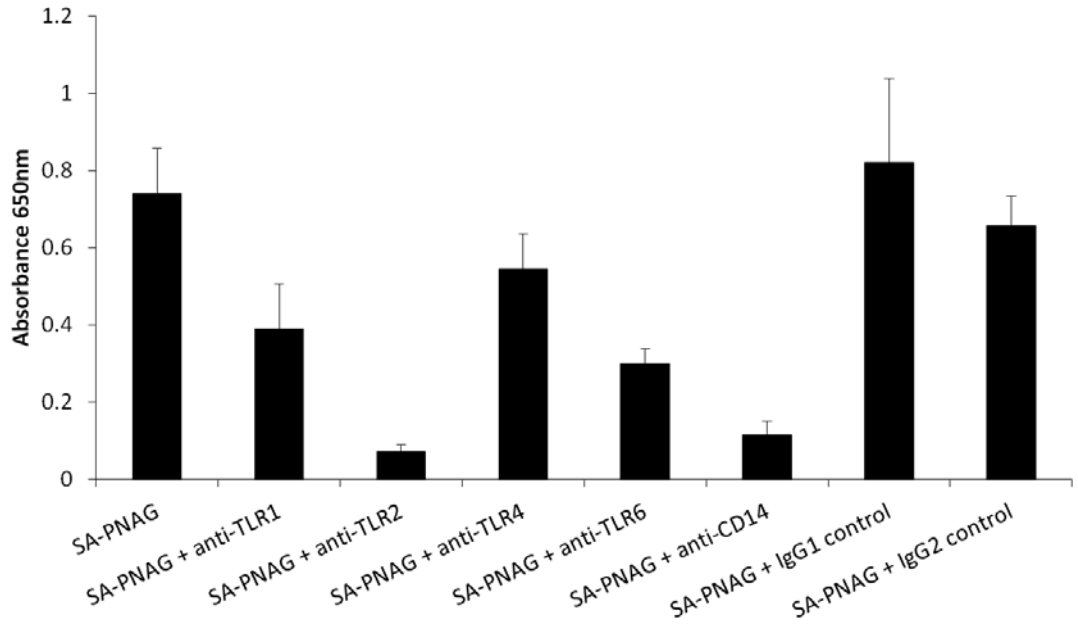


**Fig. 4.12. Assessment of TLR-mediated THP1 cell NF-κB/AP-1 activation by SA-PNAG preparation.** THP1 cells were incubated with antibodies against TLR1, TLR2, TLR4, TLR6 and CD14 to give a final concentration of 10 μg/mL per well and incubated with cells for 30 min at 37 °C with 5% $CO_2$. PNAG was added to each well to give a final concentration of 10 μg/mL. Following a 20 h incubation at 37°C with 5% $CO_2$, cell culture supernatants were added to QUANTI-Blue™ reagent to quantify SEAP and AP activity (absorbance at 650 nm). Graph represents three biological experiments and error bars represent SD of the mean.

However, as there was trace LTA quantities (0.35%) in the SA-PNAG preparation (section 3.3.6), different treatments were carried out on the polysaccharide to discriminate the source of the NF-κB/AP-1 signalling response (Fig. 4.13 (A)). SA-PNAG was treated with lysozyme to degrade any contaminating peptidoglycan and GlcNAc-β-(1,4)-GlcNAc linkages (Pangburn *et al.*, 1982). However, it should be noted that *S. aureus* peptidoglycan is highly resistant to lysozyme digestion due to *O*-acetylation of C-6 of *N*-acetylmuramic acid in peptidoglycan (Szweda *et al.*, 2012). SA-PNAG was also treated with hydrogen peroxide to break down lipids (Seo

& Nahm, 2009), sodium metaperiodate to break down carbohydrates (Kristiansen *et al.*, 2010) and NaOH was used to deacetylate SA-PNAG (Maira-Litrán *et al.*, 2005), however, NaOH would have also broken down any lipid content in the SA-PNAG preparation *via* saponification (Ryu *et al.*, 2009). Because PNAG from *A. baumannii* (AB-PNAG) is highly deacetylated (50% compared to 5% for *S. aureus* Mn8m), AB-PNAG was also treated to acetylate the PNAG.

SA-PNAG promoted NF-κB/AP-1 activation, however, enzymatic treatment of SA-PNAG with lysozyme reduced NF-κB/AP-1 activation by half (Fig. 4.13 (A)). Dot blot analysis of SA-PNAG and AB-PNAG confirmed the absence of peptidoglycan in the preparations, therefore, lysozyme treatment may have enzymatically cleaved β-(1,4) GlcNAc linkages that were not associated with peptidoglycan, present in the SA-PNAG preparation that contributed to NF-κB/AP-1 activation (Fig. 4.13 (B)). Hydrogen peroxide treatment of PNAG completely abolished NF-κB/AP-1 activation (Fig. 4.13 (A)), which demonstrated that lipids were responsible for the cell activation. Sodium metaperiodate treatment of SA-PNAG had no effect on NF-κB/AP-1 activation, which confirmed that the activation was not due to the polysaccharide. Furthermore, NaOH treatment of SA-PNAG abolished any NF-κB/AP-1 signalling (Fig. 4.13 (A)). Since highly deacetylated PNAG from AB-PNAG did not cause NF-κB/AP-1 activation, we hypothesized that NaOH treatment of the SA-PNAG preparation caused saponification of the lipid content in preparation, which resulted in no NF-κB/AP-1 activation.

AB-PNAG did not activate THP1 cells (Fig. 4.13 (A)). As the only difference in structures between AB-PNAG and SA-PNAG was in the degree of deacetylation, with SA-PNAG having approximately 95% acetylation (Maira-Litrán *et al.*, 2002) and AB-PNAG 60% acetylation (Choi *et al.*, 2009), AB-PNAG was acetylated and incubated with THP1 cells. Chemically acetylated AB-PNAG did not promote NF-κB/AP-1 signalling (Fig. 4.13 (A)). Therefore, differences in the degree of PNAG acetylation did not contribute to NF-κB/AP-1 signalling and also eliminated the possibility of a lower degree of acetylation, and high degree of deacetylation, shielding PNAG from detection by CD14 and/or TLRs to reduce NFκB/AP-1 activation and signalling.

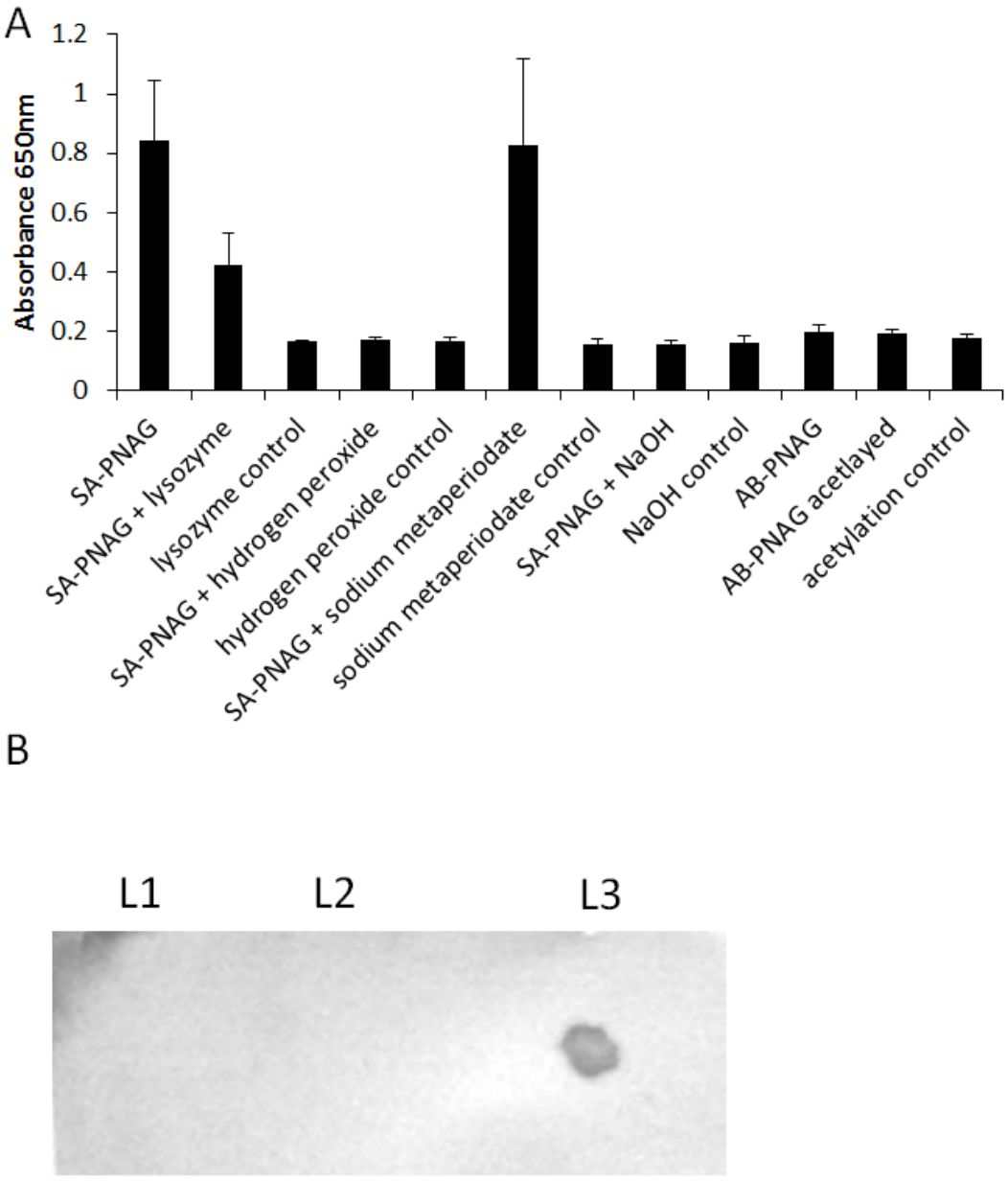


**Fig. 4.13. THP1-Blue-CD14 cell assay with chemically treated SA- and AB-PNAG. (A)** PNAG from *S. aureus* Mn8m at 100 µg/mL was treated with hydrogen peroxide, lysozyme PNAG and NaOH. PNAG from *A. baumannii* was treated with 1:1 methanol: 10% acetic acid and added to a 1:1 solution of pyridine:acetic for acetylation. Digested, undigested and control samples were dialysed against $H_2O$ and incubated with THP1 cells for 20 h. Graph represents biological triplicates and error bars represent SD of the mean. **(B)** Dot blot for peptidoglycan using 2 µL spots of 100 µg/mL PNAG from *A. baumannii* (L1), 100 µg/mL SA-PNAG (L2) and 8 x $10^8$ cells/mL heat killed *S. aureus* Mn8m WT (L3). Mouse anti-peptidoglycan, followed by HRP-labelled was used to detect peptidoglycan following addition of ECL to the membrane and chemiluminescence imaging.

Overall, this result suggested that neither SA-PNAG nor AB-PNAG promoted CD14 and/or TLR mediated NFκB/AP-1 in THP1-XBlue-CD14 cells. Thus, differences in activation of *S. aureus* and *A. baumannii* in the presence of PNAG are not due the slightly different structures of SA-PNAG and AB-PNAG (in terms of their degrees of acetylation), but rather are likely to be in the different presentation and subsequent biological recognition of the PNAG on the respective cell surfaces.

### 4.3.13. The effect of the *ica* operon on surface lipid composition of *S. aureus*

The data suggested that the *ica* operon, and therefore PNAG expression, on the surface of *S. aureus* promoted NF-κB/AP-1 activation but not in the case of *A. baumannii* (Fig. 4.11). We also showed that SA-PNAG bound to PRRs but SA-PNAG and AB-PNAG was not directly responsible for NF-κB/AP-1 activation. This implied that the cell surface PNAG is presented in such a manner on *A. baumannii* surface as to not activate or modulate NF-κB/AP-1 signalling responses, i.e. AB-PNAG does not take part in facilitating PRR dimerisation or forming complexes of the PRRs on host cell surfaces that initiate the cell signalling responses. In contrast, PNAG on the cell surface of *S. aureus* may be presented in a manner to facilitate modulation of PRR complex formation on host cell surfaces that increased signalling response.

On the other hand, *S. aureus* BH1CC, which does not express PNAG, demonstrated slightly different PRR interactions for the Δ*ica* mutant compared to the WT (section 4.3.8) which implied that the *ica* operon may impact on the expression of other surface structures. Since SA-PNAG and AB-PNAG by themselves did not promote NF-κB/AP-1 activation, we investigated further to establish whether lipids such as LTA on the surface of *S. aureus* were affected by mutating the *ica* operon. Dot blot analysis of heat-killed *S. aureus* 8325-4 and Mn8m using a mouse anti-LTA antibody demonstrated a reduction of approximately 50% in LTA expression from *ica* mutants compared to the WT strains (Fig. 4.14 (A) and (B)). Although these data are only preliminary results and would require multiple biological repeats to confirm, this results provides preliminary data to suggest that the *ica* operon may have a role in influencing the regulation of LTA expression in *S. aureus* strains. Alternatively, the surface area occupied by the Ica protein machinery may affect the surface

composition when it is absent in the Δ*ica* mutant, even if the *ica* operon itself does not regulate the expression of other surface structures.

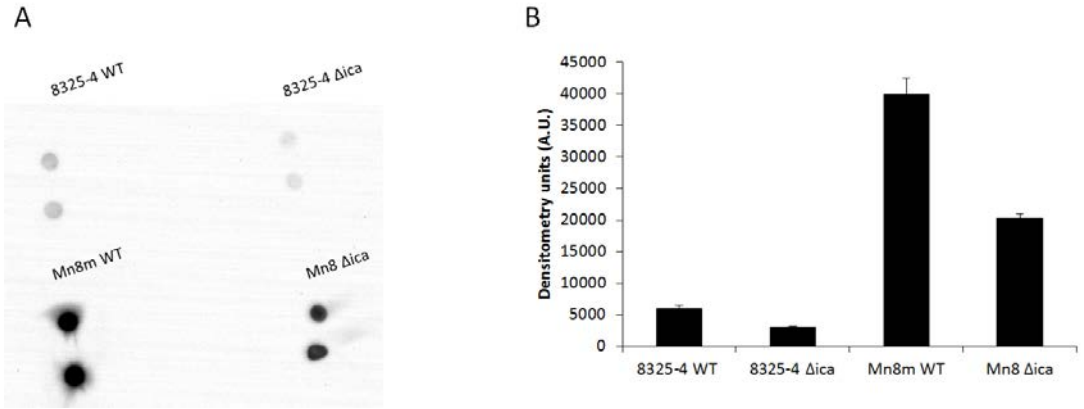


**Fig. 4.14. Dot blot assay to detect LTA present on heat-killed *S. aureus* Mn8m and 8325-4 WT and Δ*ica*.** (A) LTA present on *S. aureus* Mn8m and 8325-4 WT and Δ*ica* was detected using dot blot method with a mouse anti-LTA primary antibody and HRP-labelled goat anti-mouse secondary antibody. ECL reagent was added to the membrane and chemiluminescence was imaged. Samples were spotted in duplicates. (B) Densitometry of each spot was carried out using ImageJ software and the SD of the mean of the two spots was calculated to give error bars.

### 4.3.14. Assessment of THP1-Blue-CD14 NF-κB/AP-1 activation by *A. baumannii* whole cells

Results from PRR microarrays (Fig. 4.7) suggested that TLR2 in combination with other TLRs and/or CD14 bound to *A. baumannii*, and TLR2 in combination with other TLRs and/or CD14 had lower binding to the *pga* mutant compared to the WT strain, suggesting that PNAG may have been involved in these interactions. To elucidate further, antibodies against TLR2 with and without other anti-TLR and anti-CD14 antibodies were used to neutralise *A. baumannii*-mediated NFκB/AP-1 activation to elucidate the TLR combinations involved in this signalling response (Fig. 4.14). Blocking TLR2 completely abolished NF-κB/AP-1 activation implying that TLR2 was an important receptor involved in NF-κB/AP-1 for *A. baumannii* and this was independent of the presence of PNAG. Therefore, PNAG most likely did not contribute to TLR2 mediated NF-κB/AP-1 activation or, if it did, NF-κB/AP-1 may be activated by other cell surface molecules exposed in the absence of PNAG, as TLR2 recognises a wide range of Gram-negative bacterial cell wall components including peptidoglycan, lipoproteins, etc. Based on PRR microarray data (Fig. 4.7),

PNAG promoted binding to TLR2/4 and TLR2/6, however, Fig. 4.15 indicated that other cell surface components on *A. baumannii* are more potent NF-κB/AP-1 activators via TLR2. Furthermore, PNAG binding to TLR2/4 and TLR2/6 does not necessarily mean TLR activation and consequent NF-κB/AP-1 activation. It may even be inhibitory in some contexts.

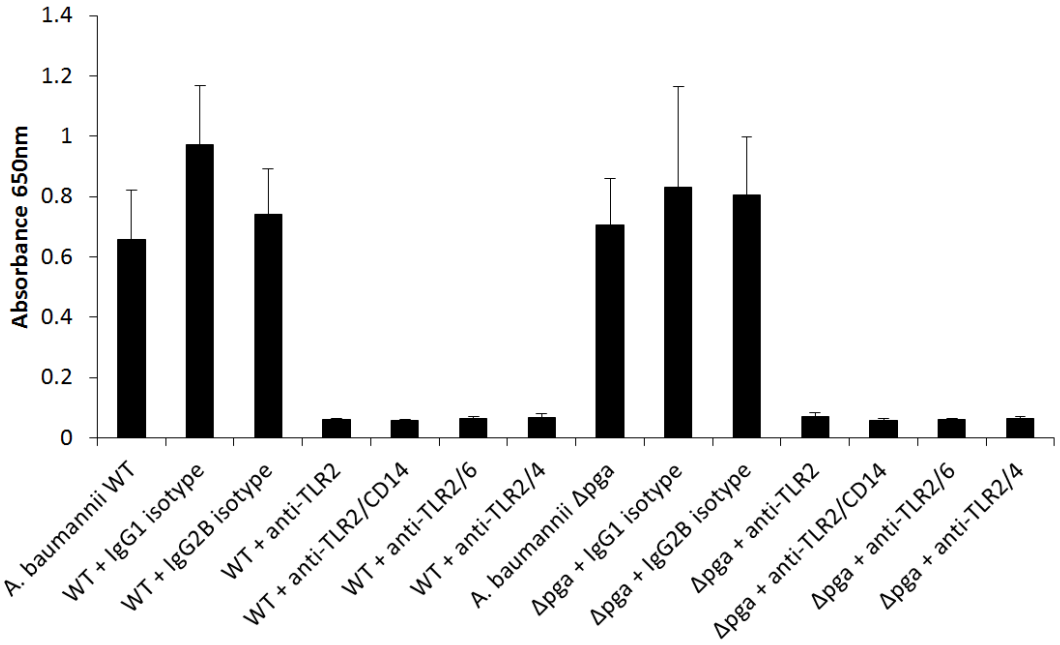


**Fig. 4.15. Assessment of TLR-mediated THP1 cell NF-κB/AP-1 activation by *A. baumannii* WT and Δ*pga*.** THP1 cells were incubated with antibodies against TLR1, TLR2, TLR4, TLR6 and CD14 to give a final concentration of 10 μg/mL per well and incubated for 30 min at 37 °C with 5% $CO_2$. PNAG was added to each well to give a final concentration of 10 μg/mL. Following a 20 h incubation at 37°C with 5% $CO_2$, cell culture supernatants were added to QUANTI-Blue™ reagent to quantify SEAP and AP activity (absorbance at 650 nm). Graph represents three biological experiments and error bars represent SD of the mean.

### 4.3.15. Localisation of PNAG from *S. aureus* Mn8m and *A. baumannii* on THP1 cells

CD14 bound to PNAG producing *S. aureus* and fluorescently labelled PNAG, therefore, we used an imaging flow cytometer to determine whether CD14 co-localised with SA-PNAG-AF555 and AB-PNAG-AF555. Pre-blocking CD14 using anti-CD14 antibody was also assessed to determine any reduction in potential PNAG binding to THP1 cells. The same concentration of PNAG from *S. aureus* Mn8m and

*A. baumannii* was incubated with cells, but images showed greater overall fluorescence intensity for AB-PNAG compared to SA-PNAG (Fig. 4.16 (A, iii) and (B, iii)). This is likely due to the higher degree of deacetylation on AB-PNAG compared to SA-PNAG, which left a higher number of free amines for labelling, thus producing higher fluorescence compared to SA-PNAG.

Upon co-incubation of SA-PNAG and AB-PNAG with THP1 cells and subsequent labelling with anti-CD14, it was clear that the receptor and polysaccharide did not co-localise (Fig 4.16 (A (iii) and (iv) and B (iii) and (iv)). Further, it was clear that the PNAG preparations from both *S. aureus* and *A. baumannii* had been internalised by the cells while all CD14 was located on the cell surface only. Addition of a CD14 neutralising antibody prior to incubation with SA-PNAG or AB-PNAG did not reduce binding of either PNAG preparations to THP1 cells (Fig. 4.16 (A (i) and (ii) and B (i) and (ii)).

Overall these results suggest that both SA-PNAG-AF555 and AB-PNAG-AF555 were internalised by THP1 cells cell, possibly by phagocytosis or PNAG-mediated penetration. The mechanism may not involve CD14 as pre-blocking CD14 with an antibody did not alter PNAG internalisation. To the best of our knowledge, this is the first report of PNAG internalisation by a monocyte in the absence of the whole bacteria.

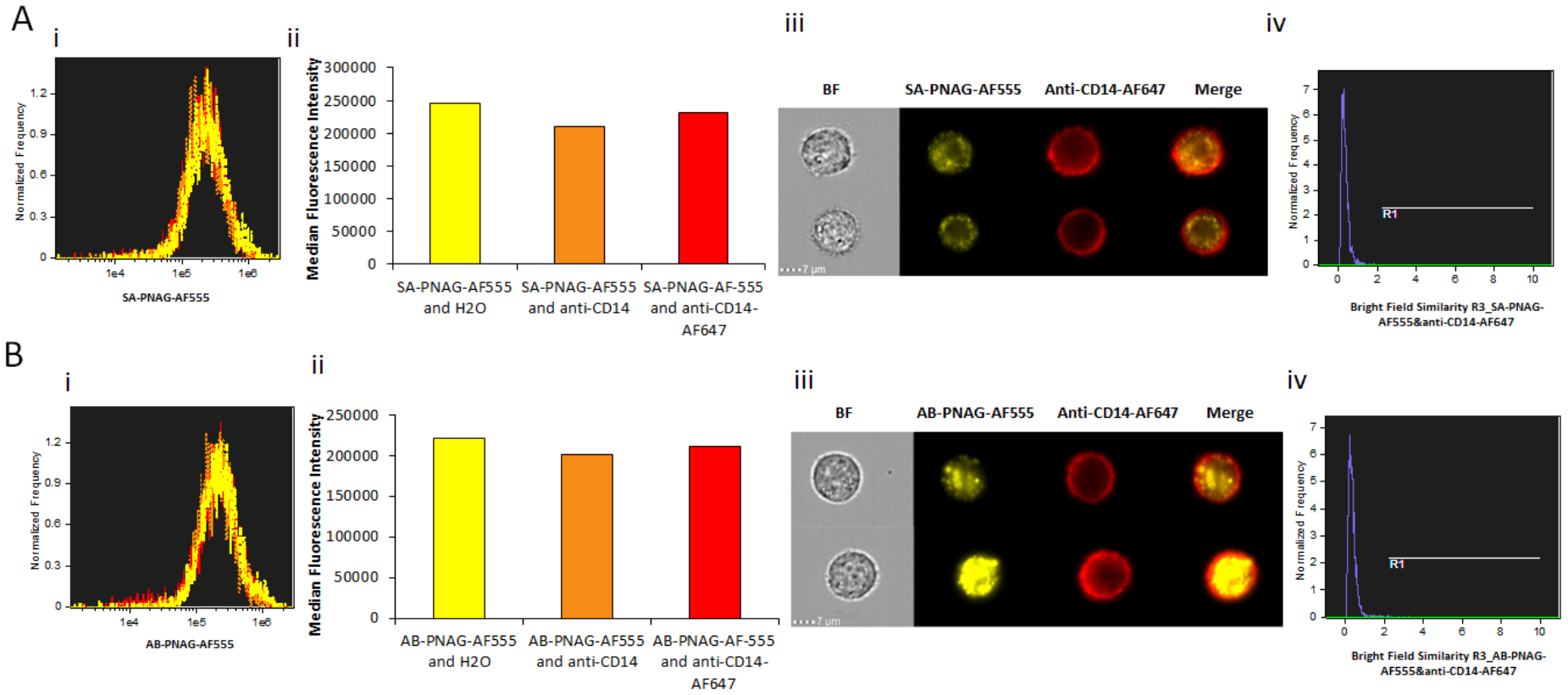


**Fig. 4.16. Localisation of SA- and AB-PANG on THP1 cells using imaging flow cytometry.** (A) Flow cytometry analysis of SA-PNAG on THP1 cells. (i) Flow cytometry analysis of THP-1 cells with SA-PNAG-AF555 incubated with $H_2O$ (yellow), THP1 cells incubated with SA-PNAG-AF555 pre-incubated with anti-CD14 (orange) and THP1 cells incubated with SA-PNAG-AF555 and anti-CD14-AF647 (red). (iii) Bar charts depicting median fluorescence intensities of SA-PNAG-AF555 on THP1 cells from flow cytometry analysis depicted in (i). (iii) Flow cytometry microscope images of THP1 cells incubated

with SA-PNAG-AF555 and anti-CD14-AF647. (iv) Bright detail similarity R3 feature that compared the small bright image detail of images of THP1 cells incubated with SA-PNAG-AF555 and anti-CD14-AF647. Similarity Bright Detail values of 1 have no significance and values of 3 or more indicate a high degree of correlation. Brightfield (BF). B (i), (ii) and (iii) depict the same images and samples as described above, but AB-PNAG-AF555 was used instead of SA-PNAG-AF555.

### 4.3.16. Assessing the effect of PNAG located on *S. aureus* and *A. baumannii* on cytokine and chemokine production by THP1 cells

To elucidate whether the decrease in NF-κB/AP-1 activation seen for *S. aureus* Δ*ica* mutant strains (Fig. 4.11) resulted in a change in signalling response, the supernatants from THP1 cells incubated with heat-killed bacteria were analysed for cytokine and chemokine expression, initially by multiplexed ELISA screening and based on the multiplex ELISA, quantitative ELISAs for two selected chemokines (RANTES and IL-8) and one cytokine (IL-1β) was carried out. As SA-PNAG and AB-PNAG did not promote NF-κB/AP-1 activation in THP1 cells (Fig. 4.13), these preparations were not included in multiplexed screening or ELISA quantification assays.

To identify cytokines and chemokines expressed by THP1 cells in the presence of whole *S. aureus* WT and Δ*ica* mutant cells, THP1 cell supernatants were screened for the expression of ten cytokines and chemokines using a multiplexed bead-based ELISA assay (Luminex) (Fig. 4.17 (A)). *S. aureus* was used initially for screening because differences in NF-κB/AP-1 activation were seen for *ica* mutants compared to the WT strains, which was not the case for an *A. baumannii* Δ*pga* mutant and WT strain. Overall, *S. aureus* 8325-4 and Mn8m WT significantly increased THP1 cell expression of CCL2/MCP-1, CXCL8/IL-8, IL-1β, IL-12 p70, IL-6, CCL5/RANTES, IFN-γ and TNF- α compared to the control (THP1 cells with endotoxin free $H_2O$). PNAG expressed by *S. aureus* 8325-4 and Mn8m WT significantly increased CCL2/MCP-1, CXCL8/IL-8, IL-1β, IL-12 p70, IL-6, CCL5/RANTES, IFN-γ and TNF- α production by THP1 cells compared to *S. aureus* 8325-4 and Mn8 Δ*ica* cells not expressing PNAG. This suggested that the *ica* operon and PNAG expressed on the surface of *S. aureus* 8325-4 and Mn8m contributed to THP1 cell expression of CCL2/MCP-1, CXCL8/IL-8, IL-1β, IL-12 p70, IL-6, CCL5/RANTES, IFN-γ and TNF- α (Fig. 4.17 (A)). The three most significant results and the results which gave us the highest detectable concentrations of cytokines and chemokines were for CXCL8/IL-8, IL-1β and RANTES, therefore, quantitative ELISAs for the detection of CXCL8/IL-8, IL-1β and RANTES was carried out (Fig. 4.17 (B)). Addition of heat killed *S. aureus* 8325-4 and 8325-4 (most noticeably at cell concentrations of 5 x $10^6$ cells/mL) promoted CXCL8/IL-8, IL-1β and RANTES expression by THP1

cells compared to cells incubated with endotoxin free $H_2O$. Furthermore, increased CXCL8/IL-8, IL-1β and RANTES expression was directly proportional to the concentration of *S. aureus* 8325-4 or Mn8m WT incubated with THP1 cells. The presence of the PNAG had the most profound effect for *S. aureus* Mn8m, followed by 8325-4 and little effect for *A. baumannii*. For example, when 5 x $10^6$ *S. aureus* Mn8m WT cells were incubated with THP1 cells, this increased the production of IL-8, IL-1β and RANTES by 87%, 98.5% and 56%, respectively, compared to 5 x $10^6$ *S. aureus* Mn8m Δ*ica* cells. Similarly, 5 x $10^6$ *S. aureus* 8325-4 WT cells increased THP1 cell production of IL-8, IL-1β and RANTES by 88%, 108% and 40% respectively, compared to compared to 5 x $10^6$ *S. aureus* 8325-4 Δ*ica* cells while *A. baumannii* WT at 5 x $10^4$ cells/mL increased THP1 cell production of IL-8, IL-1β and RANTES by 39%, 14% and 23% compared to 5 x $10^4$ *A. baumannii* Δ*pga* cells. Overall, these data show that PNAG on *S. aureus* promoted the production of cytokines and chemokines, while PNAG on *A. baumannii* had a less profound effect.

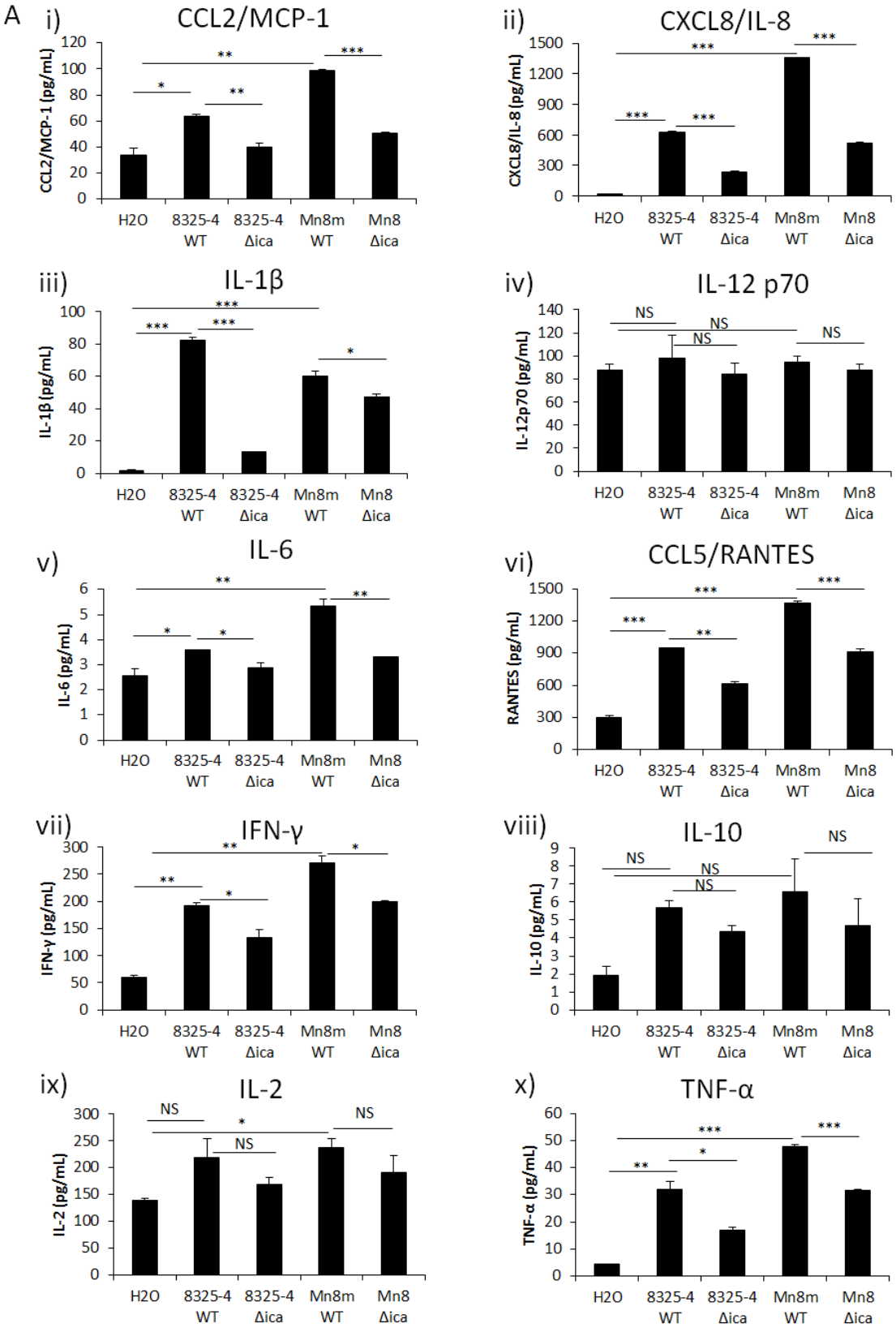
A
i)
CCL2/MCP-1
CCL2/MCP-1 (pg/mL)
ii)
CXCL8/IL-8
CXCL8/IL-8 (pg/mL)
iii)
IL-1β
IL-1β (pg/mL)
iv)
IL-12 p70
IL-12p70 (pg/mL)
v)
IL-6
IL-6 (pg/mL)
vi)
CCL5/RANTES
RANTES (pg/mL)
vii)
IFN-γ
IFN-γ (pg/mL)
viii)
IL-10
IL-10 (pg/mL)
ix)
IL-2
IL-2 (pg/mL)
x)
TNF-α
TNF-α (pg/mL)
H2O
8325-4 WT
8325-4 Δica
Mn8m WT
Mn8 Δica
NS

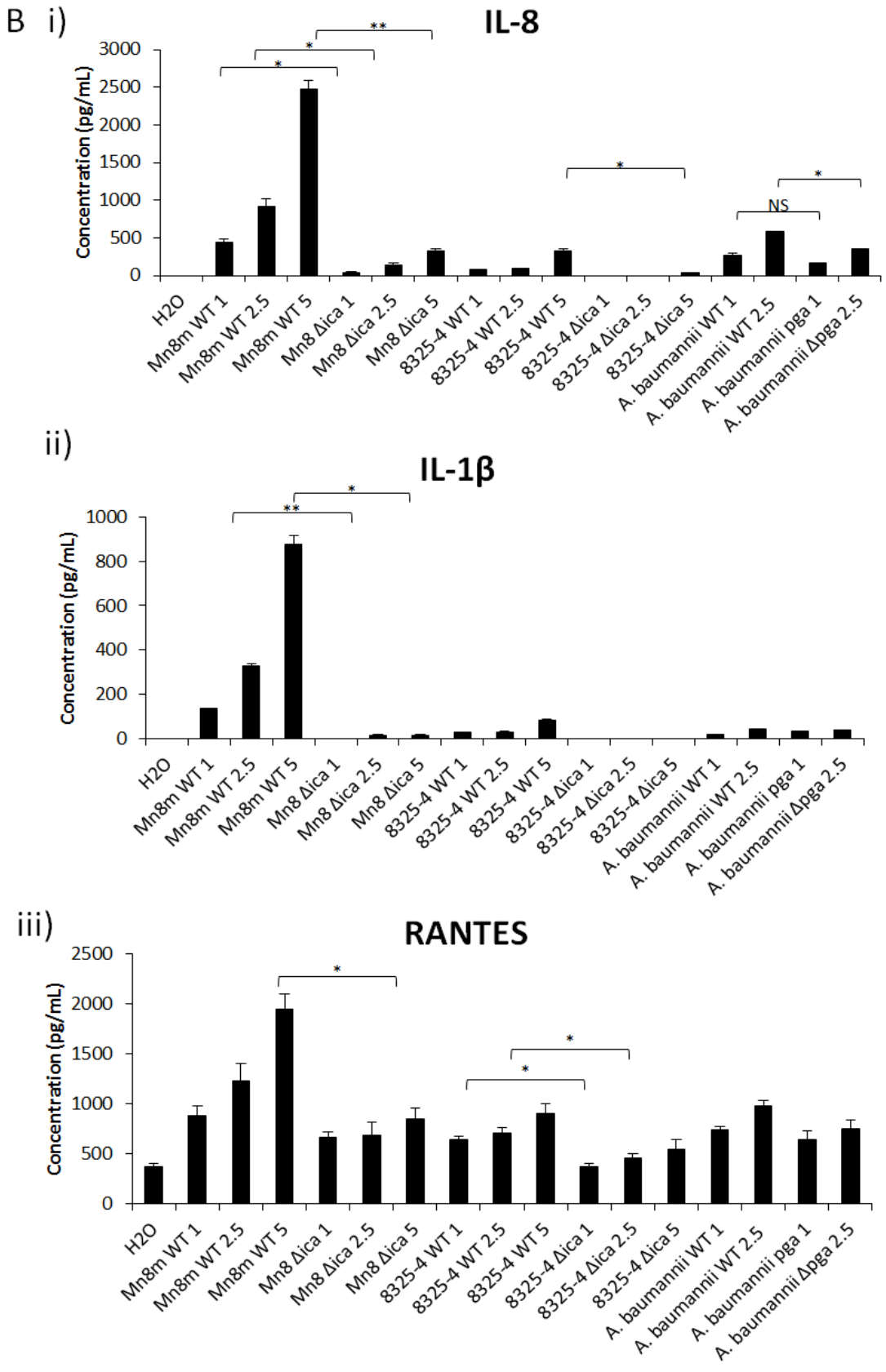


**Fig. 4.17. Cytokine and chemokine response by THP1 cells in response to stimulation with *ica* positive and negative *S. aureus* strains 8325-4 and Mn8m.** (A) Luminex multiplex ELISA carried out with ten different analytes. Bars represent the mean of one

biological assay in technical duplicate with error bars depicting +/- one standard deviation of the mean. (B) Quantification of expression of IL-8, IL-1β and RANTES produced by THP1-Blue-CD14 cells in response to stimulation with different cell numbers of *ica* positive and negative *S. aureus* strains 8325-4 and Mn8m and *pga* positive and negative *A. baumannii*. Numbers following strain name on the x axis indicate the number x $10^6$ cells for *S. aureus* strains and x $10^4$ cells for *A. baumannii*. Bars represent the mean of one biological experiment in technical triplication with error bars of +/- one standard deviation of the mean. * $p \leq 0.05$, ** $p \leq 0.01$, *** $p \leq 0.001$, Student *t* test.

## 4.4. Discussion

Although certain PRR-bacteria interactions have been elucidated, this is the first study to elucidate PRR-microbial interactions on a PRR microarray. This PRR microarray provided high-throughput screenings for PRR interactions with two MSSA, one MRSA and an *A. baumannii* strain. Furthermore, using isogenic *ica* mutants and fluorescently labelled PNAG, we were provided with target PRR-PNAG interactions to focus further experiments. This research provided an insight in to potential PRR-mediated interactions with whole *S. aureus* and *A. baumannii* cells, not just PNAG.

Certain PRRs can recognise specific carbohydrate structures associated with microbes to activate the innate immune system. Similarities in PRR interactions were seen among the three *S. aureus* strains used in this study. For example, DC-SIGN, DC-SIGNR, LSECtin, ficolin-3 and CD14 bound to *S. aureus*, These PRRs also bound to *A. baumannii*, as well as siglec-1, dectin-1 and dectin-2, MMR, MBL, TLR2 and TLR4. PRRs can be soluble, such as ficolins and mannose binding lectin (MBL), or membrane bound, such as selectin, DC-SIGN, DC-SIGNR, dectin, LSECtin, macrophage mannose receptor (MMR) and macrophage galactose-type lectin (MGL, also known as CLEC10A) (Sancho & Reis e Sousa, 2012; Takeuchi *et al*., 2010; Vasta, 2009). In our PRR microarray, all PRRs were covalently bound to the glass surface, thus, PRRs cannot form multimers, homo- or hetero-dimers on the microarray surface as some PRRs would often do *in vivo*. Therefore, the PRR microarray platform allowed us to screen for broad interactions and provided us with a suitable target PRR (CD14) to investigate subsequent signalling interactions with CD14-expressing monocytes.

Our PRR microarray platform also provided us with a tool to screen two glycoclusters for their ability to inhibit PRR-PNAG and PRR-bacterial interactions. Interestingly, neither sos2210 nor sos2254 at 0.1 mM reduced PRR interactions with SA-PNAG or *S. aureus*. Surprisingly, 0.1 mM of sos2210 increased CD14 binding to PNAG-AF555, but significantly reduced WGA and sWGA binding to PNAG-AF555, whereas sos2254 did not cause significant changes in PRR interactions. In contrast, 0.1 mM of sos2254 reduced CD14 binding to *S. aureus* 8325-4 but not *S. aureus* Mn8m, while sos2210 had no impact on PRR-mediated interactions. Therefore, we conclude that plant lectins should only be used in preliminary

polysaccharide-lectin interactions and purified PRRs are required to get a true understanding of glycogluster potency in inhibiting or modulating polysaccharide-host interactions. As seen in this study, glycoclusters may increase PRR-bacteria binding as well as decrease or inhibit binding. How glycoclusters increase PRR-PNAG interactions and the consequence this would have on the host's immune response remains to be determined.

DC-SIGN, DC-SIGNR and LSECtin are involved in cell adhesion, antigen capture and recognition on dendritic, liver, lymph node and sinusoidal endothelial cells (Zhang *et al.*, 2014). Overall *S. aureus* and *A. baumannii* bound to DC-SIGN, DC-SIGNR and DC-SIGN/DC-SIGNR co-printed together. Although little research has been carried out in this field, Appelmelk *et al.* (2003) found that a clinical *S. aureus* strain did not bind to DC-SIGN in a soluble DC-SIGN-Fc adhesion assay. However, only the extracellular portion of DC-SIGN was used and only one strain of *S. aureus* was analysed in this study. Similarly, a DC-SIGN homologue, SIGN-R1, did not capture *S. aureus* in a mouse model (Takahara *et al.*, 2004). In this study, three different *S. aureus* strains and one *A. baumannii* strain bound to DC-SIGN and DC-SIGNR on the PRR microarray platform, which suggests that DC-SIGN and DC-SIGNR have specificity towards *S. aureus* and *A. baumannii*. Our platform may prove to be favourable in binding assays as we measure direct binding of PRRs to whole *S. aureus* as other assays that require antibodies may be more likely to obtain false negative results due to the fact that *S. aureus* has protein A (SpA) which can bind to the Fc region of antibodies (Boyle & Reis, 1987). Nevertheless, cell-based confirmation studies of DC-SIGN and DC-SIGNR interactions with *S. aureus* are required. DC-SIGN is known to have specificity towards fucose and mannose structures (Zhang *et al.*, 2014), although it was shown that DC-SIGN and DC-SIGNR bind to oligosaccharides containing Man and GlcNAc and/or Fuc and GlcNAc and thus proposed that DC-SIGN and DC-SIGNR have the highest specificity towards GlcNAc residues (Zhang *et al.*, 2006). Therefore, carbohydrate, or carbohydrate-containing, structures on the surface of *S. aureus* such as capsular polysaccharides or glycoproteins, could be potential ligands for DC-SIGN on dendritic cells. Similarly, GlcNAc in LPS was established as a ligand for DC-SIGN and may have been the primary ligand of DC-SIGN for *A. baumannii* in our PRR microarray (Zhang *et al.*, 2006). A reduction in binding to DC-SIGN was seen for *A.*

*baumannii* Δ*pga* compared to the WT, which suggested that PNAG may have been one of many DC-SIGN ligands on *A. baumannii*.

*S. aureus* also bound to the DC-SIGN homologue, DC-SIGNR. DC-SIGN is often associated with dendritic cells and macrophages, while DC-SIGNR is linked to endothelial placenta, liver and lymph node cells (Pöhlmann *et al.*, 2001) and appears to act only as an adhesion receptor, unlike DC-DIGN which acts as an adhesion and signalling receptor (Guo *et al.*, 2004). Although DC-SIGN and DC-SIGNR were co-printed on the PRR microarray platform, it is unknown whether these PRRs are located near one another *in vivo* or if they form dimers. Binding seen on the PRR microarray may be due to the binding of either DC-SIGN or DC-SIGNR, and not due to heterodimer type recognition of PAMPs on the bacteria. Interestingly, MBL and CLEC10A co-printed together bound to PNAG on the PRR microarray and although this binding was not verified using *ica* mutants, it is an interesting observation that much lower binding occurred when MBL and CLEC10A were printed separately. To date, binding to DC-SIGNR has been primarily associated with viral infections and thus, this is the first piece of evidence to suggest *S. aureus* as a potential ligand for this PRR.

Finally, LSECtin, which is another member of the DC-SIGN family, bound to *S. aureus* and *A. baumannii*. LSECtin is found on liver sinusoidal endothelial cells and plays a crucial role in hepatic T-cell immune suppression (Tang *et al.*, 2009). It would be interesting to elucidate whether *S. aureus* or *A. baumannii* uses LSECtin to supress the adaptive immune response to persist in the liver. Interestingly, research carried out in our lab showed that DC-SIGN, DC-SIGNR and LSECtin bound to six other *S. aureus* strains on the PRR microarray platform (data not shown), providing an interesting avenue for future research.

Other PRRs had specificity towards *S. aureus* and *A. baumannii*, such as MMR and ficolin-3. MMR is found on a variety of cells including tissue macrophages and epithelial cells and is involved in endocytosis, phagocytosis, activation of macrophages and antigen presentation (Linehan *et al.*, 2000). *S. aureus* and *A. baumannii* were ligands for MMR, and binding to MMR may be a potential mechanism for humans to detect these bacteria for phagocytosis and endocytosis. Ficolins recognise acetyl groups and therefore bind carbohydrates such as GlcNAc,

GalNAc and ManNAc. Ficolins and MBL, which binds to mannose structures, play a role in the innate immune system by binding to microorganisms and activating the complement system and can also act as an opsonin to promote phagocytosis (Ren *et al.*, 2014). Interestingly, ficolin-3 bound to *A. baumannii* and, to the best of our knowledge, is the first report to suggest *A. baumannii* as a target ligand for ficolin-3. Ficolin-3 bound to *S. aureus* on the PRR platform which adds to the collection of contradictory results to date. Liu *et al.* (2005) showed that ficolin-1 bound to *S. aureus via* flow cytometry. However, by quantifying the amount of recombinant ficolin that bound to *S. aureus*, based on a sandwich-type time-resolved immunofluorometric assay (TRIFMA), Kjaer *et al.* (2011) could not identify binding of ficolin-1, -2 or -3 to *S. aureus*, albeit using different strains to those used by Liu, *et al.* (2005). Research to date suggests that *S. aureus* is a ligand for ficolin-1 and ficolin-2, and not a ligand for ficolin-3 (Krarup *et al*., 2005; Liu *et al*., 2005). Discrepancies in results could be due to different *S. aureus* strains being used, different methods of detection and differential expression of surface PAMP due to differences in growth media.

Considerable differences were seen for PRR interactions with *S. aureus* and *A. baumannii* based on the mutation of the *ica* and *pga* operon, respectively. Mutation of the *ica* operon in *S. aureus* reduced interactions with only one PRR, CD14. On the other hand, mutation of the *pga* operon in *A. baumannii* reduced interactions with several PRRs. Siglecs are sialic acid binding immunoglobulin-like lectins that recognise a diverse range of carbohydrate structures, and are thought to regulate immune responses via intercellular signalling (Von Gunten *et al*., 2008). Siglec-1 bound to *A. baumannii* WT to a greater degree compared to the *pga* mutant strain, suggesting that siglec-1 binds to PNAG on *A. baumannii*. Siglec-1 binds GlcNAc-containing structures as it bound GlcNAc-BSA on the microarray surface. It has been shown that siglecs have a direct and indirect impact on TLR-mediated immune responses by downregulating NF-κB activation, reducing the production of pro-inflammatory cytokines or promoting the production of anti-inflammatory cytokines to encourage immune tolerance and immune evasion by invading pathogens (Ando *et al.*, 2008; Boyd *et al.*, 2009; Calderwood & Murshid, 2015; Wu *et al.*, 2016). It has been shown that siglec-1 promotes LPS tolerance and supresses the innate immune system by up-regulating TGF-β1 production, which in turn down-regulates

NF-κB activation (Wu *et al.*, 2016). It may be possible that siglec-1 interacts with PNAG on *A. baumannii* and also contributes to down regulation of NF-κB/AP-1 activation, promoting immune tolerance. Therefore, PNAG purified from, and on, *A. baumannii* may have the potential to activate NF-κB/AP-1 signalling in our experiments, but PNAG-expressing *A. baumannii* also bound to PRRs associated with NF-κB/AP-1 down regulation (siglec-1), which could have down-regulated NF-κB/AP-1 expression, leaving the overall NF-κB/AP-1 production non-detectable in our THP1 cell assays. It would be interesting to see if other PRRs on our microarray platform that bound to PNAG had any role to play in the potential down-regulation of NF-κB/AP-1 to *A. baumannii* PNAG and lead us to conclude PNAG on whole *A. baumannii* and AB-PNAG did not activate NF-κB/AP-1 signalling.

Dectin-1 and -2 are primarily expressed in dendritic cells and macrophages and recognise β-glucans and α-mannans (often associated with fungi), respectively (Saijo & Iwakura, 2011) (Saijo *et al.*, 2011). Mutation of the *pga* operon also reduced interactions with dectin-1 and dectin-2, which suggests interaction of these PRRs with PNAG and an expanded role of interaction with bacteria, and not just fungi, in the innate immune response.

TLRs are involved in innate immunity by forming heterodimers or homodimers to detect a variety of different PAMPs associated with bacteria, fungi, protozoa and viruses from the body and can be found in the plasma membrane or expressed in endosomes and lysosomes. To date, it has been found that TLR1, TLR2, TLR4 and TLR6 recognise lipids and carbohydrates associated with pathogenic microorganisms, while TLR3, TLR7, TLR8 and TLR9 detect nucleic acids. TLR5 has shown specificity for flagella, while no specific ligand has yet been discovered for TLR10 (Hayashi *et al.*, 2001; Parkunan *et al.*, 2014; Takeda *et al.*, 2005). Mutation of the *pga* operon reduced *A. baumannii* binding to TLR2/4 and TLR2/6 but did not affect the binding of TLR2, TLR4 or TLR6 to *A. baumannii* when printed in isolation. Cell-based studies with whole, heat-killed *A. baumannii* suggested that TLR2 was a major signalling ligand involved in NF-κB/AP-1, however, based on our observations with a Δ*pga* mutant, this signalling response was not due to the *pga* operon and PNAG on the surface of *A. baumannii*. It is probable that other TLRs are involved in NF-κB/AP-1 activation following interactions with *A. baumannii*, but only TLR2 was tested for this cell based assay. Previously, it was shown that LPS-

deficient *A. baumannii* stimulated NF-κB activation via a TLR2-dependent mechanism (Moffatt *et al.*, 2013). Interestingly, *A. baumannii* can stop LPS and LOS synthesis, resulting in resistance to host antimicrobial treatment. The down-regulation of LPS and LOS resulted in increased expression of lipoproteins, phospholipids and PNAG (Boll *et al.*, 2016). Although researchers are unaware of how LPS- and LOS-deficient *A. baumannii* escape the immune system to persist within the host, this work may provide novel PRR targets to help answer these questions. Indeed, it is possible that other cell surface molecules are much more potent stimuli of TLR activation compared to PNAG.

Furthermore, the *pga* operon may be involved in the production of ligands for TLR2/4 or TLR2/6, but this does not necessarily mean that a signalling cascade is activated, thus helping *A. baumannii* evade the immune system. Finally, signals may be damped by more potent TLR stimuli found on the surface of *A. baumannii*. PNAG from *S. aureus* and *A. baumannii* are reported to be the same molecule, except for variations in the degree of acetylation. As mentioned, this could certainly contribute to discrepancies seen between PRR interactions with *A. baumannii* and *S. aureus*. Other reasons might include that mutation of the *ica* and *pga* operon in *S. aureus* and *A. baumannii* may significantly alter the cell surface composition of the bacteria, especially since PgaB in *A. baumannii* is a lipoprotein found in the periplasm (similarly to the Gram-negative bacteria *E. coli*) and the IcaB is a protein located on the cell surface of *S. aureus* (Pokrovskaya *et al.*, 2013; Wang *et al.*, 2004). Lipoproteins are known stimuli of PRRs, and could explain some differences seen in PRR interactions (Ernst & Chandler, 2017; Nguyen & Götz, 2016). As PNAG purified from *A. baumannii* was not profiled on the PRR microarray, we cannot confirm that any of these PRR interactions were primarily due to PNAG based on differences seen with Δ*pga* mutants compared to the WT strain, especially if *pgaB* encodes for a lipoprotein that is a ligand for any of these PRRs printed on the microarray.

Although CD14 has no signalling domain, this protein forms a multi-receptor complex with PAMPs and different TLRs (namely TLR4, TLR1/2, TLR3, TLR6, TLR7 and TLR9) to activate the TLR signalling pathway and consequently the production of cytokines, chemokines and type I IFNs (Zanoni *et al.*, 2013). SA-PNAG preparations incubated on our PRR microarray suggested that CD14 bound to

SA-PNAG which was supported by PNAG-expressing *S. aureus* promoting a greater NF-κB/AP-1 response compared to *S. aureus* not expressing PNAG. However, NF-κB/AP-1 activation caused by PNAG isolated from *S. aureus* Mn8m was due to contaminating lipid structures, not PNAG, as hydrogen peroxide treatment of the preparation eliminated NF-κB/AP-1 activation. These lipid structures promoted NF-κB/AP-1 activation via TLR1, TLR2, TLR6 and CD14. It has been reported that LTA binds to CD14 and TLR2, and lipopeptides bind to TLR1/2 or TLR2/6 depending on whether the lipopeptide is a tri- or di-acetylglycerol lipid respectively (Ho *et al.*, 2008; Jin *et al.*, 2007).

To the best of our knowledge, the consequential effect of mutating the *ica* operon on other genes has not yet been investigated. Preliminary data suggested that LTA expression on our *S. aureus ica* mutants was decreased compared to wildtype strains. Based on the IcaB protein entry in the Swiss Institute of Bioinformatics (SIB) database for identifying protein-protein interactions (https://string-db.org/), IcaB has many other predicted functional partners apart from IcaA. These include the glycosyltransferase CrtQ which has a role in cell wall biosynthesis, TagX in teichoic acid biosynthesis, TarS in β-O-GlcNAcylation of teichoic acids and glycosyl transferase SACOL0764 which is also involved in cell wall modification and synthesis (Szklarczyk *et al.*, 2015). It is plausible that removal of *icaB* could have a consequential impact on these glycosyltransferases which in turn may alter cell surface glycosylation beyond simply removal of PNAG and thus contribute to altered recognition of *ica* negative *S. aureus* strains by PRRs compared to WT. In addition, IcaB has an electropositive patch that was suggested to be a suitable interaction point between phosphate groups on LTA (Little *et al.*, 2014). As LTA plays an important role in cell surface homeostatisis and biofilm formation, it could be hypothesised that mutation of the *ica* operon, and positively charged PNAG, might result in a decrease in negatively charged LTA to maintain equilibrium on the outside of the cell. LTA from *Lactobacillus plantarum* reduces biofilm formed by *S. aureus* by reducing *icaB* and *icaC* transcription via the release of the quorum sensing molecule, AI-2 (Ahn *et al.*, 2018). Interestingly, wall teichoic acids were shown to have a regulatory effect on the *ica* operon as mutation of *tagO*, which encodes for a protein that is involved in the first steps of WTA synthesis, reduced *ica* transcription (Holland *et al.*, 2011). Therefore, it could be possible that mutation of the *ica* operon

has effects on teichoic acids and mutation of the *ica* operon has an impact on many other surface molecules apart from PNAG, causing *ica* mutant strains to have lower interactions with PRRs compared to *ica* positive *S. aureus*.

Another possibility is that PNAG is recognised only when it is on the cell, thus purified PNAG would give false negative results in biological assays. Physiologically, this would be relevant, as it would be important for the host to distinguish between unbound PNAG and PNAG that is located on the bacterial cell wall to eliminate the cell itself and not just spent PNAG polysaccharide. Indeed, it was shown by Cerca *et al.* (2007) that *S. aureus* expressing surface-bound PNAG had increased human IgG1 monoclonal antibody killing but had increased survival rates in a murine bacteraemia model compared to *S. aureus* expressing non-surface-bound PNAG, further highlighting the importance of PNAG presentation and cellular association in receptor recognition and immune evasion (Cerca *et al.*, 2007).

Stevens *et al.* (2009) showed that PIA (PNAG) from *S. epidermidis* promoted IL-8 expression via a mechanism involving TLR2 in astrocytes. However, several discrepancies are noted between that work and this study. Firstly, the plant lectin *Lycopersicon esculentum* (LEL) was used to help identify the purity of the PNAG preparation, however our research showed that PNAG on, or isolated from, *S. aureus* does not bind to this lectin (section 2.3.5). Stevens *et al.* (2009) showed that treatment of the PNAG preparation with hydrogen peroxide did not affect IL-8 signalling in astrocytes, but our research showed that hydrogen peroxide treatment of the PNAG preparation abolished any NF-κB/AP-1 signalling in monocytes. Similarly to our research, mutation of the *ica* operon in *S. epidermidis* did reduce the production of IL-8 compared to the parental strain. Stevens *et al.* (2009) also reported that IL-8 production caused by PNAG was due to the deacetylation of the polysaccharide. In this study, deacetylation of PNAG from *S. aureus* (5% deacetylated) with NaOH did abolish NF-κB/AP-1. However, addition of NaOH would also hydrolyse LTA, making the contaminating LTA present in the PNAG preparation inactive. Confirmation that lipid structures were causing NF-κB/AP-1 activation was verified by treating the sample with sodium-metaperiodate which had no effect on NF-κB/AP-1 activation. Since acetylation of the highly deacetylated PNAG preparation from *A. baumannii* (50% deacetylated) did not promote NF-κB/AP-1 activation, we can hypothesise that PNAG purified from *S. aureus* and *A.*

*baumannii*, whether highly acetylated or deacetylated, does not promote NF-κB/AP-1 activation in this THP-1 derived monocytic cell line.

Nonetheless, it is evident that the *ica* operon has some role to play in NF-κB/AP-1 activation and cytokine production for *S. aureus*. It was reported that depletion of PNAG on the surface of *S. aureus*, using an *ica* mutant and wildtype strain, promoted IL-12 production in murine dendritic cells (Lisbeth *et al.*, 2016). TNF-α production was increased in dendritic cells stimulated with the *ica* mutant strain compared to the wildtype. Interestingly, these authors reported that only intact whole *S. aureus* could induce IL-12 and IL-10 production compared to fragmented bacteria. This supports our hypothesis that the arrangement of molecules on the surface of the bacteria is important in cell recognition and cytokine production. Thus, PNAG may have to be on intact cells for PRR recognition and NF-κB/AP-1 activation, and may be an occurrence with Gram-positive bacteria, such as *S. aureus*, and not Gram-negative bacteria, such as *A. baumannii*, due to the distinct differences in cell topography.

It has been shown that *S. aureus* and *A. baumannii* are internalised, or phagocytosed, by monocytes (García-Patiño *et al.*, 2017; Kamoshida *et al.*, 2016; Newman & Tucci, 1990). *S. aureus* LTA was shown to be rapidly internalised by monocytes which was dependent on CD14 (Nilsen *et al.*, 2008) and lipoproteins also promoted phagocytosis of *S. aureus* by human monocytes (Kang *et al*., 2011). Cell recognition of *A. baumannii* was proven to be *via* TLR2 and TLR4, although other PRRs may also be involved. It is hypothesised that LPS on *A. baumannii* is the main TLR4 ligand for *A. baumannii*, while the only TLR2 PAMP associated with *A. baumannii* to-date is outer membrane protein A (OmpA). Our preliminary results demonstrated that PNAG preparations from *S. aureus* and *A. baumannii* were internalised by THP1 cells. We questioned whether SA-PNAG internalisation could have been due to contaminating LTA, but as PNAG from *S. aureus* and *A. baumannii* were both internalised by monocytes, this lead us to conclude that this internalisation was mediated by the common macromolecule in both PNAG preparations, PNAG. Recently it was determined that PNAG on non-motile *Enterococcus faecalis* was responsible for penetrating semisolid surfaces and translocating across human epithelial cell monolayers (Ramos *et al.*, 2019). Interestingly, *S. aureus* Mn8 was also used in this study as a positive control and it was shown that an antibody against

PNAG reduced semisolid penetration of this bacteria. Furthermore, purified PNAG from *S. aureus* Mn8m was able to restore the penetration abilities of an *epaX E. faecalis* mutant unable to penetrate surfaces. Our results support finding by Ramos *et al.* (2019) that PNAG can penetrate surfaces which is not reliant on being bound to the cell surface. Another recent study showed that antibodies against PNAG provided protection against intracellular pathogens (Cywes-Bentley *et al*., 2018). Although there no correlation was made between PNAG and it being the causative agent for internalisation, it does prove that PNAG is a prime target for preventing internalising pathogens. More research is required to understand the molecular mechanisms involved in PNAG-mediated surface penetration, whether it is a key mediator in *S. aureus* and *A. baumannii* cellular internalisation and whether it is beneficial for the bacteria or the host. If PNAG was a primary factor involved in *S. aureus* and *A. baumannii* host immune evasion by hiding intracellularly, compounds could be developed to degrade or mask PNAG to inhibit PNAG-mediated cellular internalisation.

In summary, we hypothesise that the *ica* operon and potentially PNAG helps to promote NF-κB/AP-1 activation and the production of cytokines and chemokines when associated with *S. aureus* cell wall. The *ica* operon may play a role in the expression or composition of other cell surface molecules that contribute to these interactions, or PNAG may be recognised by PRRs, but only when it is associated to the cell wall does it cause NF-κB/AP-1 activation and consequently, cytokine and chemokine production. Contrastingly, we predict that the Pga proteins and PNAG associated to *A. baumannii* does not increase NF-κB/AP-1 activation, regardless of PNAG being attached to *A. baumannii* cell wall or not. However, Pga proteins and/or PNAG associated to *A. baumannii* does result in increased binding to many PRRs, such as siglec-1, dectin-1, dectin-2 and LSECtin. Therefore, PNAG associated with *A. baumannii* could have other cell signalling effects or even play a role in the dampening of cell signalling. Nonetheless, this study highlights the different roles for the *ica* and *pga* operon in PRR mediated interactions and innate immune system activation, and highlights the importance of the surface expression and presentation of PAMPs for eliciting signalling responses.

## 4.5. References


**Aarag Fredheim, E. G., Granslo, H. N., Flægstad, T., Figenschau, Y., Rohde, H., Sadovskaya, I., Mollnes, T. E., & Klingenberg, C.** (2011). *Staphylococcus epidermidis* polysaccharide intercellular adhesin activates complement. *FEMS Immunology and Medical Microbiology*, *63*(2), 269–280.

**Ahn, K. B., Baik, J. E., Yun, C.-H., & Han, S. H.** (2018). Lipoteichoic Acid Inhibits *Staphylococcus aureus* Biofilm Formation. *Frontiers in Microbiology*, *9*, 327.

**Akira, S., & Takeda, K.** (2004). Toll-like receptor signalling. *Nature Reviews Immunology*, *4*(7), 499–511.

**Ando, M., Tu, W., Nishijima, K. -i., & Iijima, S.** (2008). Siglec-9 enhances IL-10 production in macrophages via tyrosine-based motifs. *Biochemical and Biophysical Research Communications*, *369*(3), 878–883.

**Aoyagi, Y., Adderson, E. E., Rubens, C. E., Bohnsack, J. F., Min, J. G., Matsushita, M., Fujita, T., Okuwaki, Y., & Takahashi, S.** (2008). L-ficolin/mannose-binding lectin-associated serine protease complexes bind to group B streptococci primarily through *N*-acetylneuraminic acid of capsular polysaccharide and activate the complement pathway. *Infection and Immunity*, *76*(1), 179–188.

**Appelmelk, B. J., van Die, I., van Vliet, S. J., Vandenbroucke-Grauls, C. M. J. E., Geijtenbeek, T. B. H., & van Kooyk, Y.** (2003). Cutting Edge: Carbohydrate Profiling Identifies New Pathogens That Interact with Dendritic Cell-Specific ICAM-3-Grabbing Nonintegrin on Dendritic Cells. *The Journal of Immunology*, *170*(4), 1635 LP-1639.

**Boll, J. M., Crofts, A. A., Peters, K., Cattoir, V., Vollmer, W., Davies, B. W., & Trent, M. S.** (2016). A penicillin-binding protein inhibits selection of colistin-resistant, lipooligosaccharide-deficient *Acinetobacter baumannii*. *Proceedings of the National Academy of Sciences of the United States of America*, *113*(41), E6228–E6237.

**Boyd, C. R., Orr, S. J., Spence, S., Burrows, J. F., Elliott, J., Carroll, H. P., Brennan, K., Gabhann, J. N., Coulter, W. A., Johnston, J. A., & Jefferies, C. A.** (2009). Siglec-E is up-regulated and phosphorylated following lipopolysaccharide stimulation in order to limit TLR-driven cytokine production. *Journal of Immunology*, *183*(12), 7703–7709.

**Boyle, M. D. P., & Reis, K. J.** (1987). Bacterial Fc Receptors. *Bio/Technology*, *5*, 697.

**Brown, G. D., Herre, J., Williams, D. L., Willment, J. A., Marshall, A. S. J., & Gordon, S.** (2003). Dectin-1 mediates the biological effects of β-glucans. *Journal of Experimental Medicine*, *197*(9), 1119–1124.

**Calderwood, S. K., & Murshid, A.** (2015). Siglecs take a TOLL on inflammation: Deciphering the Hsp70 riddle. *EMBO Journal*, *34*(22), 2733–2734.

**Cerca, N., Jefferson, K. K., Maira-Litrán, T., Pier, D. B., Kelly-Quintos, C.,**

**Goldmann, D. A., Azeredo, J., & Pier, G. B.** (2007). Molecular Basis for Preferential Protective Efficacy of Antibodies Directed to the Poorly Acetylated Form of Staphylococcal Poly-N-Acetyl-β-(1-6)-Glucosamine. *Infection and Immunity*, *75*(7), 3406 LP-3413.

**Cerca, N., Jefferson, K. K., Oliveira, R., Pier, G. B., & Azeredo, J.** (2006). Comparative antibody-mediated phagocytosis of *Staphylococcus epidermidis* cells grown in a biofilm or in the planktonic state. *Infection and Immunity*, *74*(8), 4849–4855.

**Choi, A. H. K., Slamti, L., Avci, F. Y., Pier, G. B., & Maira-Litrán, T.** (2009). The pgaABCD locus of *Acinetobacter baumannii* encodes the production of poly-β-1-6-N-acetylglucosamine, which is critical for biofilm formation. *Journal of Bacteriology*, *191*(19), 5953–5963.

**Conlon, K. M., Humphreys, H., & O'Gara, J. P.** (2002). icaR encodes a transcriptional repressor involved in environmental regulation of ica operon expression and biofilm formation in *Staphylococcus epidermidis*. *Journal of Bacteriology*, *184*(16), 4400–4408.

**Cywes-Bentley, C., Rocha, J. N., Bordin, A. I., Vinacur, M., Rehman, S., Zaidi, T. S., Meyer, M., Anthony, S., Lambert, M., Vlock, D. R., Giguère, S., Cohen, N. D., & Pier, G. B.** (2018). Antibody to Poly-*N*-acetyl glucosamine provides protection against intracellular pathogens: Mechanism of action and validation in horse foals challenged with Rhodococcus equi. *PLOS Pathogens*, *14*(7), e1007160.

**Descheny, L., Gainers, M. E., Walcheck, B., & Dimitroff, C. J.** (2006). Ameliorating Skin-Homing Receptors on Malignant T Cells with a Fluorosugar Analog of N-acetylglucosamine: P-Selectin Ligand Is a More Sensitive Target than E-Selectin Ligand. *Journal of Investigative Dermatology*, *126*(9), 2065–2073.

**Echeverria, B., Serna, S., Achilli, S., Vivès, C., Pham, J., Thépaut, M., Hokke, C. H., Fieschi, F., & Reichardt, N.-C.** (2018). Chemoenzymatic Synthesis of N-glycan Positional Isomers and Evidence for Branch Selective Binding by Monoclonal Antibodies and Human C-type Lectin Receptors. *ACS Chemical Biology*, *13*(8), 2269–2279.

**Ernst, R. K., & Chandler, C. E.** (2017). Bacterial lipids: Powerful modifiers of the innate immune response. *F1000Research*, *6*.

**Feinberg, H., Mitchell, D. A., Drickamer, K., & Weis, W. I.** (2001). Structural basis for selective recognition of oligosaccharides by DC-SIGN and DC-SIGNR. *Science*, *294*(5549), 2163–2166.

**Frederiksen, P. D., Thiel, S., Larsen, C. B., & Jensenius, J. C.** (2005). M-ficolin, an innate immune defence molecule, binds patterns of acetyl groups and activates complement. *Scandinavian Journal of Immunology*, *62*(5), 462–473.

**Galustian, C., Lubineau, A., Le Narvor, C., Kiso, M., Brown, G., & Feizi, T.** (1999). L-selectin interactions with novel mono- and multisulfated Lewis(x) sequences in comparison with the potent ligand 3'-sulfated Lewisa. *Journal of*

*Biological Chemistry*, *274*(26), 18213–18217.

**García-Patiño, M. G., García-Contreras, R., & Licona-Limón, P.** (2017). The Immune Response against *Acinetobacter baumannii*, an Emerging Pathogen in Nosocomial Infections. *Frontiers in Immunology*, *8*, 441.

**Gout, E., Garlatti, V., Smith, D. F., Lacroix, M., Dumestre-Pérard, C., Lunardi, T., Martin, L., Cesbron, J.-Y., Arlaud, G. J., Gaboriaud, C., & Thielens, N. M.** (2010). Carbohydrate recognition properties of human ficolins: Glycan array screening reveals the sialic acid binding specificity of M-ficolin. *Journal of Biological Chemistry*, *285*(9), 6612–6622.

**Gow, N. A. R., van de Veerdonk, F. L., Brown, A. J. P., & Netea, M. G.** (2011). Candida albicans morphogenesis and host defence: discriminating invasion from colonization. *Nature Reviews Microbiology*, *10*, 112.

**Guo, Y., Feinberg, H., Conroy, E., Mitchell, D. A., Alvarez, R., Blixt, O., Taylor, M. E., Weis, W. I., & Drickamer, K.** (2004). Structural basis for distinct ligand-binding and targeting properties of the receptors DC-SIGN and DC-SIGNR. *Nature Structural and Molecular Biology*, *11*(7), 591–598.

**Hajishengallis, G., & Lambris, J. D.** (2011). Microbial manipulation of receptor crosstalk in innate immunity. *Nature Reviews Immunology*, *11*(3), 187–200.

**Hayashi, F., Smith, K. D., Ozinsky, A., Hawn, T. R., Yi, E. C., Goodlett, D. R., Eng, J. K., Akira, S., Underhill, D. M., & Aderem, A.** (2001). The innate immune response to bacterial flagellin is mediated by Toll-like receptor 5. *Nature*, *410*(6832), 1099–1103.

**Ho, S. S., Michalek, S. M., & Nahm, M. H.** (2008). Lipoteichoic acid is important in innate immune responses to gram-positive bacteria. *Infection and Immunity*, *76*(1), 206–213.

**Holland, L. M., Conlon, B., & O'Gara, J. P.** (2011). Mutation of tagO reveals an essential role for wall teichoic acids in *Staphylococcus epidermidis* biofilm development. *Microbiology*, *157*(2), 408–418.

**Jin, M. S., Kim, S. E., Heo, J. Y., Lee, M. E., Kim, H. M., Paik, S.-G., Lee, H., & Lee, J.-O.** (2007). Crystal Structure of the TLR1-TLR2 Heterodimer Induced by Binding of a Tri-Acylated Lipopeptide. *Cell*, *130*(6), 1071–1082.

**Kamoshida, G., Tansho-Nagakawa, S., Kikuchi-Ueda, T., Nakano, R., Hikosaka, K., Nishida, S., Ubagai, T., Higashi, S., & Ono, Y.** (2016). A novel bacterial transport mechanism of *Acinetobacter baumannii* via activated human neutrophils through interleukin-8. *Journal of Leukocyte Biology*, *100*(6), 1405–1412.

**Kang, H. J., Ha, J., Kim, H. S., Lee, H., Kurokawa, K., & Lee, B. L.** (2011). The role of phagocytosis in IL-8 production by human monocytes in response to lipoproteins on *Staphylococcus aureus*. *Biochemical and Biophysical Research Communications*, *406*(3), 449–453.

**Kanneganti, M., Kamba, A., & Mizoguchi, E.** (2012). Role of chitotriosidase

(Chitinase 1) under normal and disease conditions. *Journal of Epithelial Biology and Pharmacology*, *5*, 1–9.

**Kelm, S., Pelz, A., Schauer, R., Filbin, M. T., Tang, S., Bellard, M.-E. d., Schnaar, R. L., Mahoney, J. A., Hartnell, A., Bradfield, P., & Crocker, P. R.** (1994). Sialoadhesin, myelin-associated glycoprotein and CD22 define a new family of sialic acid-dependent adhesion molecules of the immunoglobulin superfamily. *Current Biology*, *4*(11), 965–972.

**Kjaer, T. R., Hansen, A. G., Sørensen, U. B. S., Nielsen, O., Thiel, S., & Jensenius, J. C.** (2011). Investigations on the pattern recognition molecule M-ficolin: Quantitative aspects of bacterial binding and leukocyte association. *Journal of Leukocyte Biology*, *90*(3), 425–437.

**Krarup, A., Sørensen, U. B. S., Matsushita, M., Jensenius, J. C., & Thiel, S.** (2005). Effect of capsulation of opportunistic pathogenic bacteria on binding of the pattern recognition molecules Mannan-binding lectin, L-ficolin, and H-ficolin. *Infection and Immunity*, *73*(2), 1052–1060.

**Krarup, A., Thiel, S., Hansen, A., Fujita, T., & Jensenius, J. C.** (2004). L-ficolin is a pattern recognition molecule specific for acetyl groups. *Journal of Biological Chemistry*, *279*(46), 47513–47519.

**Kristiansen, K. A., Potthast, A., & Christensen, B. E.** (2010). Periodate oxidation of polysaccharides for modification of chemical and physical properties. *Carbohydrate Research*, *345*(10), 1264–1271.

**Kropec, A., Maira-Litran, T., Jefferson, K. K., Grout, M., Cramton, S. E., Götz, F., Goldmann, D. A., & Pier, G. B.** (2005). Poly-*N*-acetylglucosamine production in *Staphylococcus aureus* is essential for virulence in murine models of systemic infection. *Infection and Immunity*, *73*(10), 6868–6876.

**Kumar, H., Kawai, T., & Akira, S.** (2009). Pathogen recognition in the innate immune response. *Biochemical Journal*, *420*(1), 1–16.

**Kurita, K., Chikaoka, S., Kamiya, M., & Koyama, Y.** (1988). Studies on Chitin. 14. *N*-Acetylation Behavior of Chitosan with Acetyl Chloride and Acetic Anhydride in a Highly Swelled State. *Bulletin of the Chemical Society of Japan*, *61*(3), 927–930.

**Lampen, J. O.** (1971). The Enzymes. In P. D. B. T.-T. E. Boyer (Ed.) (Vol. 5, pp. 291–305). Academic Press.

**Landmann, R., Müller, B., & Zimmerli, W.** (2000). CD14, new aspects of ligand and signal diversity. *Microbes and Infection*, *2*(3), 295–304.

**Linehan, S. A., Martínez-Pomares, L., & Gordon, S.** (2000). Macrophage lectins in host defence. *Microbes and Infection*, *2*(3), 279–288.

**Lisbeth, L. D., Ingmer, H., & Frøkiær, H.** (2016). D-alanylation of teichoic acids and loss of poly-*N*-acetyl glucosamine in *Staphylococcus aureus* during exponential growth phase enhance IL-12 production in murine dendritic cells. *PLoS ONE*, *11*(2).

**Little, D. J., Bamford, N. C., Pokrovskaya, V., Robinson, H., Nitz, M., & Howell, P. L.** (2014). Structural basis for the De-*N*-acetylation of poly-β-1,6-*N*-acetyl-D-glucosamine in gram-positive bacteria. *Journal of Biological Chemistry*, *289*(52), 35907–35917.

**Liu, Y., Endo, Y., Iwaki, D., Nakata, M., Matsushita, M., Wada, I., Inoue, K., Munakata, M., & Fujita, T.** (2005). Human M-ficolin is a secretory protein that activates the lectin complement pathway. *Journal of Immunology*, *175*(5), 3150–3156.

**MacAuley, M. S., Crocker, P. R., & Paulson, J. C.** (2014). Siglec-mediated regulation of immune cell function in disease. *Nature Reviews Immunology*, *14*(10), 653–666.

**Maira-Litrán, T., Kropec, A., Abeygunawardana, C., Joyce, J., Mark III, G., Goldmann, D. A., & Pier, G. B.** (2002). Immunochemical properties of the Staphylococcal poly-*N*-acetylglucosamine surface polysaccharide. *Infection and Immunity*, *70*(8), 4433–4440.

**Maira-Litrán, T., Kropec, A., Goldmann, D. A., & Pier, G. B.** (2005). Comparative opsonic and protective activities of *Staphylococcus aureus* conjugate vaccines containing native or deacetylated Staphylococcal Poly-*N*-acetyl-beta-(1-6)-glucosamine. *Infection and Immunity*, *73*(10), 6752–6762.

**Matsushita, M., Endo, Y., Taira, S., Sato, Y., Fujita, T., Ichikawa, N., Nakata, M., & Mizuochi, T.** (1996). A novel human serum lectin with collagen- and fibrinogen-like domains that functions as an opsonin. *Journal of Biological Chemistry*, *271*(5), 2448–2454.

**McGreal, E. P., Rosas, M., Brown, G. D., Zamze, S., Wong, S. Y. C., Gordon, S., Martinez-Pomares, L., & Taylor, P. R.** (2006). The carbohydrate-recognition domain of Dectin-2 is a C-type lectin with specificity for high mannose. *Glycobiology*, *16*(5), 422–430.

**Moffatt, J. H., Harper, M., Mansell, A., Crane, B., Fitzsimons, T. C., Nation, R. L., Li, J., Adler, B., & Boyce, J. D.** (2013). Lipopolysaccharide-deficient *Acinetobacter baumannii* shows altered signaling through host toll-like receptors and increased susceptibility to the host antimicrobial peptide LL-37. *Infection and Immunity*, *81*(3), 684–689.

**Mogensen, T. H.** (2009). Pathogen Recognition and Inflammatory Signaling in Innate Immune Defenses. *Clinical Microbiology Reviews*, *22*(2), 240 LP-273.

**Monsigny, M., Sene, C., Obrenovitch, A., Roche, A.-C., Delmotte, F., & Boschetti, E.** (1979). Properties of Succinylated Wheat-Germ Agglutinin. *European Journal of Biochemistry*, *98*(1), 39–45.

**Mukhopadhyay, S., Herre, J., Brown, G. D., & Gordon, S.** (2004). The potential for Toll-like receptors to collaborate with other innate immune receptors. *Immunology*, *112*(4), 521–530.

**Newman, S. L., & Tucci, M. A.** (1990). Regulation of human monocyte/macrophage function by extracellular matrix. Adherence of

monocytes to collagen matrices enhances phagocytosis of opsonized bacteria by activation of complement receptors and enhancement of Fc receptor function. *The Journal of Clinical Investigation*, *86*(3), 703–714.

**Nguyen, M. T., & Götz, F.** (2016). Lipoproteins of gram-positive bacteria: Key players in the immune response and virulence. *Microbiology and Molecular Biology Reviews*, *80*(3), 891–903.

**Nilsen, N. J., Deininger, S., Nonstad, U., Skjeldal, F., Husebye, H., Rodionov, D., von Aulock, S., Hartung, T., Lien, E., Bakke, O., & Espevik, T.** (2008). Cellular trafficking of lipoteichoic acid and Toll-like receptor 2 in relation to signaling; role of CD14 and CD36. *Journal of Leukocyte Biology*, *84*(1), 280–291.

**O'Neill, E., Pozzi, C., Houston, P., Smyth, D., Humphreys, H., Robinson, D. A., & O'Gara, J. P.** (2007). Association between methicillin susceptibility and biofilm regulation in *Staphylococcus aureus* isolates from device-related infections. *Journal of Clinical Microbiology*, *45*(5), 1379–1388.

**Oliveira-Nascimento, L., Massari, P., & Wetzler, L. M.** (2012). The role of TLR2 ininfection and immunity. *Frontiers in Immunology*, *3*(APR).

**Pace, C. N., Vajdos, F., Fee, L., Grimsley, G., & Gray, T.** (1995). How to measure and predict the molar absorption coefficient of a protein. *Protein Science*, *4*(11), 2411–2423.

**Pangburn, S. H., Trescony, P. V, & Heller, J.** (1982). Lysozyme degradation of partially deacetylated chitin, its films and hydrogels. *Biomaterials*, *3*(2), 105–108.

**Parkunan, S. M., Astley, R., & Callegan, M. C.** (2014). Role of TLR5 and flagella in Bacillus intraocular infection. *PLoS ONE*, *9*(6).

**Pöhlmann, S., Soilleux, E. J., Baribaud, F., Leslie, G. J., Morris, L. S., Trowsdale, J., Lee, B., Coleman, N., & Doms, R. W.** (2001). DC-SIGNR, a DC-SIGN homologue expressed in endothelial cells, binds to human and simian immunodeficiency viruses and activates infection in trans. *Proceedings of the National Academy of Sciences of the United States of America*, *98*(5), 2670–2675.

**Pokrovskaya, V., Poloczek, J., Little, D. J., Griffiths, H., Howell, P. L., & Nitz, M.** (2013). Functional characterization of *Staphylococcus epidermidis* IcaB, a De-*N*-acetylase important for biofilm formation. *Biochemistry*, *52*(32), 5463–5471.

**Ramos, Y., Rocha, J., Hael, A. L., van Gestel, J., Vlamakis, H., Cywes-Bentley, C., Cubillos-Ruiz, J. R., Pier, G. B., Gilmore, M. S., Kolter, R., & Morales, D. K.** (2019). PolyGlcNAc-containing exopolymers enable surface penetration by non-motile Enterococcus faecalis. *PLOS Pathogens*, *15*(2), e1007571.

**Ren, Y., Ding, Q., & Zhang, X.** (2014). Ficolins and infectious diseases. *Virologica Sinica*, *29*(1), 25–32.

**Rice, L. B.** (2008). Federal funding for the study of antimicrobial resistance in nosocomial pathogens: No ESKAPE. *Journal of Infectious Diseases*, *197*(8), 1079–1081.

**Ryu, Y. H., Baik, J. E., Yang, J. S., Kang, S.-S., Im, J., Yun, C.-H., Kim, D. W., Lee, K., Chung, D. K., Ju, H. R., & Han, S. H.** (2009). Differential immunostimulatory effects of Gram-positive bacteria due to their lipoteichoic acids. *International Immunopharmacology*, *9*(1), 127–133.

**Saijo, S., & Iwakura, Y.** (2011). Dectin-1 and Dectin-2 in innate immunity against fungi. *International Immunology*, *23*(8), 467–472.

**Sancho, D., & Reis e Sousa, C.** (2012). Signaling by myeloid C-Type lectin receptors in immunity and homeostasis. *Annual Review of Immunology*.

**Schommer, N. N., Christner, M., Hentschke, M., Ruckdeschel, K., Aepfelbacher, M., & Rohde, H.** (2011). *Staphylococcus epidermidis* uses distinct mechanisms of biofilm formation to interfere with phagocytosis and activation of mouse macrophage-like cells 774A.1. *Infection and Immunity*, *79*(6), 2267–2276.

**Seo, H. S., & Nahm, M. H.** (2009). Lipoprotein Lipase and Hydrofluoric Acid Deactivate Both Bacterial Lipoproteins and Lipoteichoic Acids, but Platelet-Activating Factor-Acetylhydrolase Degrades Only Lipoteichoic Acids. *Clinical and Vaccine Immunology*, *16*(8), 1187 LP-1195.

**Skurnik, D., Cywes-Bentley, C., & Pier, G. B.** (2016). The exceptionally broad-based potential of active and passive vaccination targeting the conserved microbial surface polysaccharide PNAG. *Expert Review of Vaccines*, *15*(8), 1041–1053.

**Spiro, R. G.** (1960). Studies on fetuin, a glycoprotein of fetal serum. I. Isolation, chemical composition, and physiochemical properties. *The Journal of Biological Chemistry*, *235*(10), 2860–2869.

**Ståhl, A., Svensson, M., Mörgelin, M., Svanborg, C., Tarr, P. I., Mooney, J. C., Watkins, S. L., Johnson, R., & Karpman, D.** (2006). Lipopolysaccharide from enterohemorrhagic *Escherichia coli* binds to platelets through TLR4 and CD62 and is detected on circulating platelets in patients with hemolytic uremic syndrome. *Blood*, *108*(1), 167 LP-176.

**Stevens, N. T., Sadovskaya, I., Jabbouri, S., Sattar, T., O'gara, J. P., Humphreys, H., & Greene, C. M.** (2009). *Staphylococcus epidermidis* polysaccharide intercellular adhesin induces IL-8 expression in human astrocytes via a mechanism involving TLR2. *Cellular Microbiology*, *11*(3), 421–432.

**Sugimoto, R., Yae, Y., Akaiwa, M., Kitajima, S., Shibata, Y., Sato, H., Hirata, J., Okochi, K., Izuhara, K., & Hamasaki, N.** (1998). Cloning and characterization of the Hakata antigen, a member of the ficolin/opsonin p35 lectin family. *Journal of Biological Chemistry*, *273*(33), 20721–20727.

**Szklarczyk, D., Franceschini, A., Wyder, S., Forslund, K., Heller, D., Huerta-**

**Cepas, J., Simonovic, M., Roth, A., Santos, A., Tsafou, K. P., Kuhn, M., Bork, P., Jensen, L. J., & Von Mering, C.** (2015). STRING v10: Protein-protein interaction networks, integrated over the tree of life. *Nucleic Acids Research*, *43*(D1), D447–D452.

**Szweda, P., Schielmann, M., Kotlowski, R., Gorczyca, G., Zalewska, M., & Milewski, S.** (2012). Peptidoglycan hydrolases-potential weapons against *Staphylococcus aureus*. *Applied Microbiology and Biotechnology*, *96*(5), 1157–1174.

**Takahara, K., Yashima, Y., Omatsu, Y., Yoshida, H., Kimura, Y., Kang, Y., Steinman, R. M., Park, C. G., & Inaba, K.** (2004). Functional comparison of the mouse DC-SIGN, SIGNR1, SIGNR3 and Langerin, C-type lectins. *International Immunology*, *16*(6), 819–829.

**Takeda, K., & Akira, S.** (2005). Toll-like receptors in innate immunity. *International Immunology*, *17*(1), 1–14.

**Takeuchi, O., & Akira, S.** (2010). Pattern Recognition Receptors and Inflammation. *Cell*, *140*(6), 805–820.

**Tang, L., Yang, J., Liu, W., Tang, X., Chen, J., Zhao, D., Wang, M., Xu, F., Lu, Y., Liu, B., Sun, Q., Zhang, L., & He, F.** (2009). Liver Sinusoidal Endothelial Cell Lectin, LSECtin, Negatively Regulates Hepatic T-Cell Immune Response. *Gastroenterology*, *137*(4), 1498–1508.e5.

**Teh, C., Le, Y., Lee, S. H., & Lu, J.** (2000). M-ficolin is expressed on monocytes and is a lectin binding to *N*-acetyl-D-glucosamine and mediates monocyte adhesion and phagocytosis of *Escherichia coli*. *Immunology*, *101*(2), 225–232.

**Trimble, R. B., Maley, F., & Chu, F. K.** (1983). Glycoprotein biosynthesis in yeast. Protein conformation affects processing of high mannose oligosaccharides on carboxypeptidase Y and invertase. *Journal of Biological Chemistry*, *258*(4), 2562–2567.

**Tükel, C., Nishimori, J. H., Wilson, R. P., Winter, M. G., Keestra, A. M., van Putten, J. P. M., & Bäumler, A. J.** (2010). Toll-like receptors 1 and 2 cooperatively mediate immune responses to curli, a common amyloid from enterobacterial biofilms. *Cellular Microbiology*, *12*(10), 1495–1505.

**Turner, M. W.** (2003). The role of mannose-binding lectin in health and disease. *Molecular Immunology*, *40*(7), 423–429.

**van Liempt, E., Bank, C. M. C., Mehta, P., García-Vallejo, J. J., Kawar, Z. S., Geyer, R., Alvarez, R. A., Cummings, R. D., Kooyk, Y. v., & van Die, I.** (2006). Specificity of DC-SIGN for mannose- and fucose-containing glycans. *FEBS Letters*, *580*(26), 6123–6131.

**Varki, A.** (1992). Selectins and other mammalian sialic acid-binding lectins. *Current Opinion in Cell Biology*, *4*(2), 257–266.

**Vasta, G. R.** (2009). Roles of galectins in infection. *Nature Reviews Microbiology*, *7*(6), 424–438.

**Von Gunten, S., & Bochner, B. S.** (2008). Basic and clinical immunology of Siglecs. *Annals of the New York Academy of Sciences*, *1143*, 62-82.

**Wang, X., Preston III, J. F., & Romeo, T.** (2004). The pgaABCD Locus of Escherichia coli Promotes the Synthesis of a Polysaccharide Adhesin Required for Biofilm Formation. *Journal of Bacteriology*, *186*(9), 2724–2734.

**Wang, X., Wu, L., Ren, J., Miyoshi, D., Sugimoto, N., & Qu, X.** (2011). Label-free colorimetric and quantitative detection of cancer marker protein using noncrosslinking aggregation of Au/Ag nanoparticles induced by target-specific peptide probe. *Biosensors and Bioelectronics*, *26*(12), 4804–4809.

**Whitfield, G. B., Marmont, L. S., & Howell, P. L.** (2015). Enzymatic modifications of exopolysaccharides enhance bacterial persistence. *Frontiers in Microbiology*, *6*, 471.

**Wu, Y., Lan, C., Ren, D., & Chen, G.-Y.** (2016). Induction of siglec-1 by endotoxin tolerance suppresses the innate immune response by promoting TGF-β1 production. *Journal of Biological Chemistry*, *291*(23), 12370–12382.

**Wu, Y., Ren, D., & Chen, G.-Y.** (2016). Siglec-E negatively regulates the activation of tlr4 by controlling its endocytosis. *Journal of Immunology*, *197*(8), 3336–3347.

**Zanoni, I., & Granucci, F.** (2013). Role of CD14 in host protection against infections and in metabolism regulation. *Frontiers in Cellular and Infection Microbiology*, *3*, 32.

**Zhang, F., Ren, S., & Zuo, Y.** (2014). DC-SIGN, DC-SIGNR and LSECtin: C-type lectins for infection. *International Reviews of Immunology*, *33*(1), 54–66.

**Zhang, P., Snyder, S., Feng, P., Azadi, P., Zhang, S., Bulgheresi, S., Sanderson, K. E., He, J., Klena, J., & Chen, T.** (2006). Role of N-Acetylglucosamine within Core Lipopolysaccharide of Several Species of Gram-Negative Bacteria in Targeting the DC-SIGN (CD209). *The Journal of Immunology*, *177*(6), 4002 LP-4011.

**Zizzari, I. G., Napoletano, C., Battisti, F., Rahimi, H., Caponnetto, S., Pierelli, L., Nuti, M., & Rughetti, A.** (2015). MGL Receptor and Immunity: When the Ligand Can Make the Difference. *Journal of Immunology Research*, *2015*, 8.

# Chapter 5

# Overall discussion and future perspectives

## 5. Overall discussion and future perspectives

Approximately 65% - 80% of nosocomial infections are associated with biofilms according to the CDC and NIH, respectively (Joo *et al*., 2012; Potera, 1999). PNAG is a common determining factor for biofilm formation and is produced by a range of bacteria, including *Escherichia coli*, *Yersinia pestis*, *Enterococcus faecium*, *Shigella* species, *Bordetella* species, *Enterobacteria* species, and *Vibrio parahemolyticus*, and has been associated with biofilm formation by *Staphylococcus* species, *Kelbsiella pneumoniae* and *A. baumannii* (Chen *et al*., 2014; Choi *et al*., 2009; Cywes-Bentley *et al*., 2013; Maira-Litrán *et al*., 2002; Skurnik *et al*., 2016). PNAG is not only associated with biofilm formation but also evasion of antibody-mediated phagocytosis, lowered macrophage activation and decreased immune protein deposition. However, PNAG expressing bacteria were found to induce complement activation and elicit host immune responses compared to PNAG deficient strains (Aarag Fredheim *et al.*, 2011; Ferreirinha *et al.*, 2016; Kristian *et al.*, 2008; Schommer *et al.*, 2011). More recently, it was shown that non-motile *Enterococcus faecalis* use PNAG to penetrate surfaces, including human intestinal epithelial cell monolayers (Ramos *et al.*, 2019). As we are discovering the vast number of bacteria that express PNAG, we are slowly uncovering the different roles for this polysaccharide in cell homeostasis, biofilm formation, pathogenicity, and immune evasion. However, a greater understanding of how PNAG-expressing bacteria, and PNAG itself, interacts with host proteins and carbohydrates is desperately needed to accelerate the development of anti-biofilm and anti-microbial agents that will aid the prognosis of patients that suffer from infections caused by PNAG-producing opportunistic pathogens. For this, it is crucial that we identify PNAG-host interactions, understand the consequence of these interactions and establish methods of modifying these interactions for the benefit of the patient.

### 5.1. Identification of PNAG-mediated interactions

We proposed that PNAG interacts with a specific subset of receptors to contribute to or modulate the immune response in favour of persistent colonisation or immune evasion for the PNAG-expressing bacteria. We used high throughput (HTP) microarray platforms to screen for lectin and PRR receptors of, and carbohydrate-mediated interactions with, PNAG-expressing bacteria and PNAG preparations. By

exposing bacteria to different growth conditions and screening multiple interactions at one time, our results showed that PNAG-ligand interactions may have been dependent on PNAG presentation, and the presentation of PNAG may have differed depending on the bacteria on which it is located on, and the physicochemical external environmental present during the time of production and adherence to the cell wall.

It has been shown that growth conditions influence biofilm composition for *S. aureus* (O'Neill *et al.*, 2008). Furthermore, it was shown that pH contributes to phase instability of EPS from *S. epidermidis* RP62A, a PNAG-producing bacteria, driving biofilm formation for this *S. epidermidis* strain (Stewart *et al*., 2015), and is a primary factor attributing to biofilm polysaccharide interactions (Ganesan *et al.*, 2013). Therefore, depending on the pH of the external environment, these polymeric matrices can switch from a viscous to a viscoelastic state (Stewart *et al*., 2015). It has been shown that isolated PNAG does not retain the mechanical behaviour of a biofilm, indicating other factors are involved in biofilm viscoelasticity. However, PNAG was shown to self-associate and form PNAG-protein and PNAG-PNAG complexes between pH 3-5.5 (Ganesan *et al.*, 2013). Our results supported evidence to suggest that pH may have changed how and if PNAG interacts with proteins. Indeed, the majority of our microarray experiments were carried out at a pH of approximately 7.2, however, bacteria were always grown in the presence of BHI glucose, and in chapter 2, BHI NaCl. Previously, it was described that glucose metabolism by staphylococci reduces the pH of the culture media and affects PNAG production and biofilm physiology (Cerca *et al*., 2011). Therefore, at low pH environments, PNAG may have formed aggregates of different conformations depending on the degree of PNAG deacetylation. Moreover, PNAG may have also aggregated with other cell surface proteins at low pH (Ganesan *et al.*, 2013). Depending on the bacterial cell surface composition, and the pH of the external environment, PNAG may form interactions with different proteins, or form electrostatic interactions with other cell surface molecules contributing to some lectin and PRR interactions seen in this thesis. *A. baumannii* cell surface is considerably different to that of *S. aureus*, comprising primarily of surface proteins, LOS, CPS and LPS (Giguère, 2015; Malanovic & Lohner, 2016). In comparison, *S. aureus* surface is comprised primarily of teichoic acids (WTA and LTA), surface

proteins and depending on the environmental conditions, surface polysaccharides (Malanovic *et al*., 2016; O'Riordan *et al*., 2004). PNAG may interact with a variety of these surface molecules forming different conformations and shapes, some more preferential to lectin or PRR interactions than others. These data highlight the need to understand polysaccharide morphology and conformation on pathogenic bacteria in environments that are physiologically similar to *in vivo* settings. Visually, this could be carried out by growing PNAG-producing and non-producing bacteria in different growth media and examining PNAG morphology via transmission electron microscopy. We propose that PNAG interactions should be studied further at pH ranges from 4.2-5.6 to mimic the pH of normal healthy skin, pH from 5.6-10 to mimic pH ranges recorded for wound infections, and 7.4 to mimic serum and blood pH in addition to pH 7.2 that was used during this work (Blank, 1971; Schwalfenberg, 2012; Wilhelm & Maibach, 1990). This should elucidate interactions that may occur at the pH of the biological microenvironment that we may not have observed under our experimental conditions.

We used PNAG preparations from *S. aureus* (SA-PNAG) and *A. baumannii* (AB-PNAG) to identify lectin and PRR interactions that may be specific for the two different deacetylated forms of PNAG. It is also possible that the molecular weight of PNAG from *S. aureus* and *A. baumannii* were also very different. It was determined that PNAG isolated from *S. aureus* Mn8m has three different masses; 460 kDa, 100 kDa and 21 kDa, and only PNAG with a molecular mass of 460 kDa was capable of an immune response mediated by immunoglobulin G (IgG) (Maira-Litrán *et al*., 2002). Interestingly, a 780 kDa fraction of PNAG purified from the 460 kDa fraction elicited an even great IgG response compared to the 460 kDa fraction, indicating that higher molecular weight fractions of PNAG cause a greater immune response (Maira-Litrán *et al*., 2002). Literature has not been published that describes the molecular weight of PNAG from *A. baumannii*, but we hypothesize that the molecular weight is smaller than that of PNAG from *S. aureus*. If PgaB produced by *A. baumannii* hydrolyses PNAG based on the degree of deacetylation (Little *et al*., 2018), the high degree of deacetylation found on PNAG from *A. baumannii* would mean more frequently cleaved PNAG compared and a lower molecular weight compared to PNAG from *S. aureus*, which may aid evasion of host immune detection. Therefore, we propose that different molecular mass PNAG preparations

should be included in these studies to elucidate the biological effects associated with each molecular mass.

In addition, we found that CD14 bound to SA-PNAG and CD14 had reduced binding to *S. aureus* Δ*ica* mutants compared to the widetype. However, our results suggested that free SA-PNAG did not activate NF-kB/AP-1 signalling but, in agreement with literature, increased NF-kB/AP-1 signalling when on the surface of *S. aureus* (Stevens *et al.*, 2009). Furthermore, neither free AB-PNAG nor PNAG on the surface of *A. baumannii* affected signalling. These data highlight the importance of analysing polysaccharide-receptor interactions using methods that will preserve the polysaccharide conformation, and presentation similarly found on a bacterial cell surface and by using a more combinational approach. We coated SA-PNAG on to FluoSpheres® to help maintain PNAG conformation and presentation but we did not use this presentation to carry out cell-based assays due to a lack of PNAG material available and the prohibitive expense of the quantity of FluoSpheres® that would be needed. To more fully explore the effect of PNAG presentation, we propose that cell-based assays should be carried out with PNAG on FluoSpheres® as well as free PNAG to model bacterial cell surface presentation.

Whole cell extracts should also be carried out to digest the bacterial cells, leaving only polysaccharides and proteins and use a combination of proteins and polysaccharides to coat FluoSpheres®. Methods would have to be developed to covalently attach any teichoic acids or polysaccharides not containing amine groups. On the other hand, purified PNAG could be coated on a non-PNAG producing *S. aureus* strain, such as BH1CC. To detect the presence of these cell surface molecules, it would be necessary to include printed antibodies against these surface antigens on the microarray platform to truly verify the relative quantity of PNAG and other cell surface structures on the bacterial cell surface or FluoSpheres® at the time of microarray incubation. We could also use dispersin B to enzymatically cleave β-(1,6)-GlcNAc polysaccharides, such as PNAG (Chaignon *et al*., 2007), on the cell surface of bacteria, instead of relying on genetic mutations that may alter the expression of other cell surface macromolecules. This way, we may be able to cleave PNAG from the cell surface to determine interactions with PNAG, without altering the genetic make-up of the bacteria.

## 5.2. Cell surface composition and molecular presentation

It has been shown that acetyl group position along chitosan chains influences the stiffness of the polysaccharide (Brugnerotto *et al.*, 2001). Indeed, this may prove to be the same for PNAG and the varying degrees of PNAG deacetylation may alter the recognition of PNAG and most probably change the structure of PNAG on the bacterial cell surface as the amine groups present on PNAG would likely be associated to the cell wall (Whitfield *et al.*, 2015). Therefore, more amine groups may mean that PNAG on *A. baumannii* is more tightly adhered to the cell surface compared to PNAG on *S. aureus*. Moreover, PgaB may be a PNAG hydrolase on *A. baumannii*, resulting in shorter PNAG chains (Little *et al.*, 2018) which may have caused the differences we saw in PNAG-receptor interactions. SEM analysis of PNAG-producing bacteria would help elucidate the structural conformation of PNAG associated with different bacteria. However, methods would have to be employed to ensure the matrix structures in the SEM images were PNAG, and not other cell surface polysaccharides. Therefore, a colloidal gold particle attached to a PNAG-specific antibody, or combined SEM imaging and fluorescence microscopy should be used (Gong *et al.*, 2014; Gounon *et al.*, 2000; Knutton *et al.*, 1999).

The STRING v10 database (Szklarczyk *et al.*, 2015) that provides direct and indirect functional associations between proteins showed many predicted functional partners to the Pga proteins for *A. baumannii*. Besides other Pga proteins, PgaB has a predicted glycosyltransferase functional partner which is a putative LPS core biosynthesis glycosyltransferase named LpsC, PgaC has many predicted functional partners including a putative urate catabolism protein, a UDP-glucose pyrophosphorylase named GalU, and a UDP-glucose 4-epimerase named GalE or Gne1. GalE is responsible for the interconversion of UDP-Gal and UDP-Glc, and species such as *Yersinia* use UPD-Glc and UPD-GlcNAc for epimerization (Hu *et al.*, 2013). Interestingly, GalU and GalE contribute to the synthesis of the K2 capsule for *A. baumannii*, which is a polysaccharide composed of Glc, Gal and GalNAc, and depending on the strain, pseudaminic acid (Kenyon *et al.*, 2014). It was proposed that secreted PNAG from *E. coli* has a physical interaction with LPS, and the authors showed that K1 capsule synthesis was associated with secreted PNAG-mediated biofilm formation (Amini *et al.*, 2009). Mutation of the *pga* operon may have downregulated *galU* or *galE*, which in turn changed or reduced K2 capsule synthesis

or structure, resulting in decreased binding to Gal and GalNAc specific lectins on our lectin microarray platform (DBA, CPA and VRA), or sialic acid and Glc specific PRRs on the PRR microarray platform such as siglec-1, dectin-1 and dectin-2.

The hypothesis that *pga* operon is linked to the transcription of other cell surface gene products is supported by research carried out by Henry *et al.* (2012) where an LPS-deficient (*lpxA*) *A. baumannii* strain compensated for LPS loss by up-regulating genes involved in PNAG production, resulting in increased PNAG production. Specifically, the LPS-deficient mutant had a 48.5 fold increase in *pgaC* transcription, 26 fold increase in *pgaA* transcription and a 14.9 fold increase in *pgaD* transcription (Henry *et al.*, 2012). Reverse transcription polymerase chain reaction (RT-PCR) of *lpxA*, *galU* and *galE* and K2 and LPS structure elucidation and quantification on the *A. baumannii* WT and Δ*pga* mutant would be required to prove that mutation of the *pga* operon causes a downregulation in *lpxA*, *galU* and *galE* transcription and a change in capsule or LPS production.

Furthermore, based on the STRING v10 database, IcaA in *S. aureus* COL has a predicted functional partner with a lipase, Lip1/Geh, and IcaA in *S. aureus* 8325-4 has a predicted functional partner MraY, a phospho-*N*-acetylmuramoyl-pentapeptide-transferase involved in the lipid cycle of peptidoglycan synthesis. This may impact on the lipid-containing molecular composition of the cell surface.

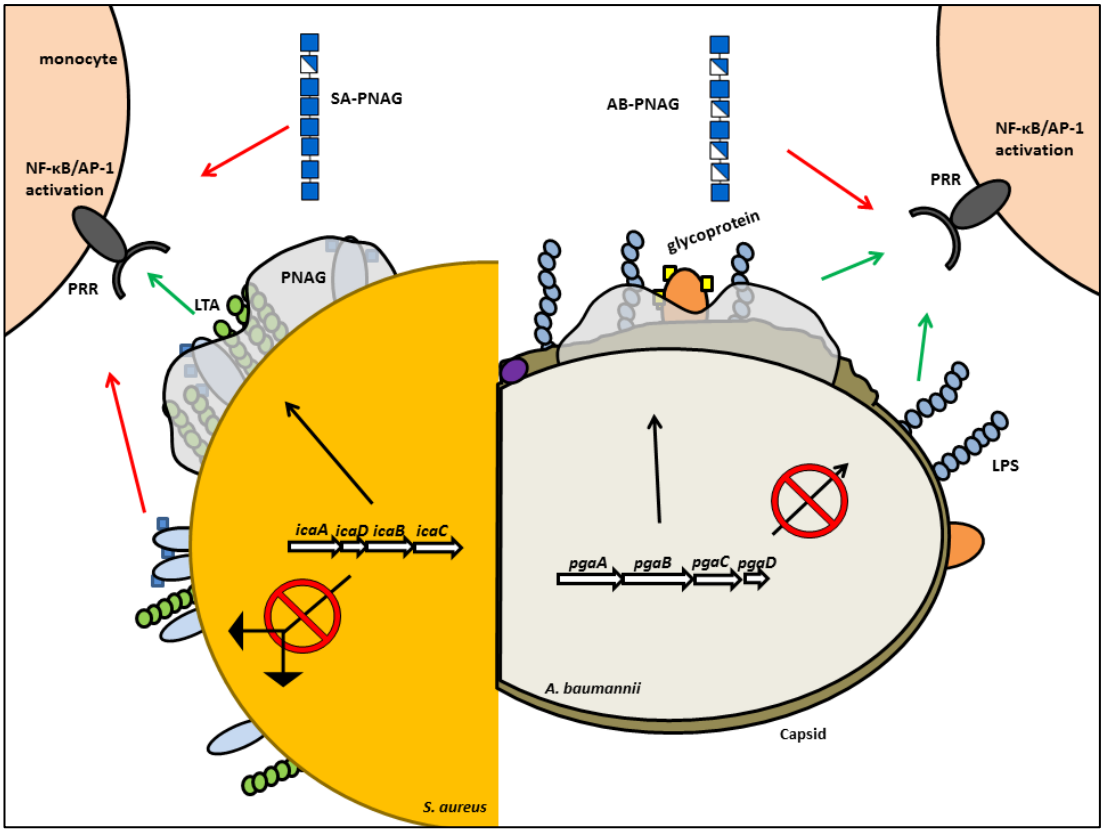


**Fig. 5.1. Potential roles of PNAG for *S. aureus* and *A. baumannii* in the host immune response.** The expression of *icaADBC* and *pgaABCD* leads to PNAG production. The expression of *ica* leads to *S. aureus*-mediated activation of NF-kB/AP-1, but *pga* expression and PNAG production does not cause significant differences in NF-kB/AP-1 activation compared to the Δ*pga* mutant strain. PNAG may only be detected by PRRs when it is on the surface of *S. aureus*, but *ica* expression may promote the transcription of genes that encode other TLR agonists. The structural conformation of PNAG may be different on the cell compared to secreted PNAG. Purified PNAG from *S. aureus* or *A. baumannii* did not promote NF-kB/AP-1 activation. Overall, the *ica* operon or PNAG conformation on *S. aureus* activates NF-kB/AP-1 in THP1 cells and PNAG on *A. baumannii*, whether on the cell or in a secreted form (purified) does not activate NF-kB/AP-1.

## 5.3. Elucidate the multiplicity of biological roles of PNAG *in vivo*

To the best of our knowledge, there has been no correlation of synthetic components, gene regulation or enzymes between LTA and Lip1 or MraY, but this prediction of functional partners does show that the Ica proteins may have functions beyond just PNAG synthesis. Therefore, to truly understand the biological roles of PNAG *in vivo*, the roles of the *pga* or *ica* operon have in the transcription of other genes apart from PNAG must be elucidated. If this is the case, we must not solely rely on

bacteria with genetic mutations to elucidate the function for that gene product. Instead, we must take a holistic approach to determine the true biological role of PNAG *in vivo*. If *ica* and *pga* operon mutations do prove to have roles in the transcription of other genes apart from PNAG, we must determine what other genes are affected and the impact this would have on publications that made claims based on bacterial mutations. Undoubtedly, this would mean that we could not solely rely on bacterial mutations to determine a singular cause and effect. It is, however, a good place to start for screening and once the gene product of the mutation is purified, the gene product, in a presentation that is similar to a presentation on the bacterial cell wall, can be used to verify specific interactions.

Our research would suggest that purified PNAG, whether isolated from *A. baumannii* or *S. aureus,* does not activate NF-κB/AP-1 signalling in monocytes (Fig. 5.1). Furthermore, preliminary data showed that PNAG can penetrate monocytes. These data suggest that PNAG, detached from the bacteria cell wall, may be able to penetrate and evade detection by monocytes. It has been shown that *S. aureus* can penetrate monocytes, reside intracellularly and eventually lyse the host cell from within (Horn *et al*., 2018) . Residing intracellularly means *S. aureus* can evade the immune system and travel around the host without being detected. Likewise, it has been shown that *A. baumannii* can reside intracellularly within host cells (Parra-Millán *et al*., 2018). More research would be required to determine whether PNAG on a bacterial cell promotes penetration through monocytes and if so, the mechanisms behind polysaccharide penetration. Interestingly, macrophages produce enzymes, such as chitinase, responsible for the degradation of β-(1,4)-GlcNAc polymers (Zhu *et al*., 2004). As GlcNAc is a common carbohydrate in N-linked glycans, and is found on THP-1 cell N-glycans, it may be possible that monocytes take extracellular GlcNAc, like PNAG, for GlcNAc recycling (Delannoy *et al*., 2017). To prove these hypotheses, SA-PNAG, AB-PNAG and dispersin B-treated and non-treated fluorescent *S. aureus* Mn8m and *A. baumannii* S1 should be incubated with monocytes and visualised via spinning disk confocal microscopy over a 2-48 hour time period. This would allow us to visualise whether PNAG and PNAG producing bacteria persist within monocytes or is degraded within the monocyte. Other cells types would also need to be tested to see if PNAG penetration was specific to monocytes, or common among multiple cell types. Nonetheless, this

finding provides interesting avenues for future research into bacterial immune evasion, or GlcNAc up-take and recycling by host cells.

### 5.4. Evaluation of targeted anti-*S. aureus* therapeutics

*S. aureus* has many surface proteins, yet little is known as to whether many lectins are on the surface of *S. aureus*. Protein A contains a carbohydrate binding module named LysM that binds to GlcNAc-containing polymers such as chitin, nodulation (Nod) factors (LPS consisting of 3-5 GlcNAc residues), and peptidoglycan (Buist *et al.*, 2008; Mesnage *et al.*, 2014). Furthermore, it was predicted that a homologue to SasG in *S. epidermidis*, Aap, binds GlcNAc the G5 lectin domain (Bateman *et al.*, 2005).

We successfully used HTP microarrays to screen for glycoclusters that modulated whole bacteria-protein and PNAG-protein interactions. However, depending on the concentration, glycocluster, and the protein target, some glycoclusters increased bacteria-protein interactions and preliminary data showed that increased bacteria-mucin interactions. Perhaps these lectins or other undiscovered *S. aureus* lectins had affinity for glycoclusters used in this study at certain concentrations and increased binding by using the glycoclusters as a 'carbohydrate bridge'. A goal of glycocluster synthesis is to reduce targeted interactions. Indeed the majority of our results showed this, but some interactions were also encouraged by glycocluster co-incubation. There may be lectins on the surface of *S. aureus* responsible for binding to GlcNAc and some of the glycoclusters used in this study. Further research using a *S. aureus* transposon mutant library and screening the wildtype and these mutants for their interaction with GlcNAc-BSA or glycoclusters would help test this hypothesis. Two glycoclusters, sos2226 and sos2227, were difficult to dissolve in water and often formed aggregates in solution. Although this would not be suitable to administer to a patient with the aims of clearing a bacterial infection, these insoluble compounds did prevent biofilm formation of two MSSA strains and an MRSA strain, BH1CC. Glycoclusters have been used to inhibit lectin mediated biofilm formation by *P. aeruginosa* (Boukerb *et al.*, 2014; Smadhi *et al.*, 2014). To the best of our knowledge, this is the first report of glycoclusters inhibiting both protein- and eDNA-mediated biofilm formation and PNAG-mediated biofilm formation. The insoluble glycocluster did not inhibit growth, therefore we are unsure of the

mechanism of biofilm inhibition. The high viscosity may make it more difficult for bacteria to connect to one another *via* polysaccharides, eDNA or proteins. Transmission electron microscopy of MSSA and MRSA with and without sos2226 and sos2227 would be required to test this hypothesis. This research provides preliminary data that could be used to develop a gel coating on medical devices that would be used locally to treat biofilm-mediated infections.

Nonetheless, there is a need to develop glycoclusters that are more water soluble to make them compatible with *in vivo* environments. We were unable to carry out PRR modulatory experiments with our full panel of glycoclusters used in chapter 3, but further screening should be carried out to determine whether the remaining five soluble glycoclusters have PRR-*S. aureus* and –*A. baumannii* modulatory characteristics.

Overall, this thesis provided lectin and PRR receptors specific for *S. aureus*, *A. baumannii* and PNAG associated with *S. aureus* and *A. baumannii*, providing a range of different lectins that could be used for *S. aureus* and *A. baumannii* detection and potential PRR receptors for future research. Our work highlighted the importance of investigating polysaccharide conformation and the possible effects of genetic mutations on cell surface composition. Also, we proved that HTP microarrays are a suitable platform to determine glycocluster $IC_{50}$ values. Finally, we determined that possible functions for glycoclusters in inhibiting lectin-bacteria, PRR-bacteria and biofilm formation, although more investigation is required to understand the overall impact of glycoclusters on bacteria-host interactions and human health.

## 5.5. References


**Aarag Fredheim, E. G., Granslo, H. N., Flægstad, T., Figenschau, Y., Rohde, H., Sadovskaya, I., Mollnes, T. E., & Klingenberg, C.** (2011). *Staphylococcus epidermidis* polysaccharide intercellular adhesin activates complement. *FEMS Immunology and Medical Microbiology*, *63*(2), 269–280.

**Amini, S., Goodarzi, H., & Tavazoie, S.** (2009). Genetic Dissection of an Exogenously Induced Biofilm in Laboratory and Clinical Isolates of E. coli. *PLOS Pathogens*, *5*(5), e1000432.

**Bateman, A., Holden, M. T. G., & Yeats, C.** (2005). The G5 domain: A potential N-acetylglucosamine recognition domain involved in biofilm formation. *Bioinformatics*, *21*(8), 1301–1303.

**Boukerb, A. M., Rousset, A., Galanos, N., Méar, J.-B., Thépaut, M., Grandjean, T., Gillon, E., Cecioni, S., Abderrahmen, C., Faure, K., Redelberger, D., Kipnis, E., Dessein, R., Havet, S., Darblade, B., Matthews, S. E., De Bentzmann, S., Guéry, B., Cournoyer, B., Imberty, A., & Vidal, S.** (2014). Antiadhesive properties of glycoclusters against Pseudomonas aeruginosa lung infection. *Journal of Medicinal Chemistry*, *57*(24), 10275–10289.

**Brugnerotto, J., Desbrières, J., Heux, L., Mazeau, K., & Rinaudo, M.** (2001). Overview on structural characterization of chitosan molecules in relation with their behavior in solution. *Macromolecular Symposia*, *168*(1), 1–20.

**Buist, G., Steen, A., Kok, J., & Kuipers, O. P.** (2008). LysM, a widely distributed protein motif for binding to (peptido)glycans. *Molecular Microbiology*, *68*(4), 838–847.

**Cerca, F., França, Â., Guimarães, R., Hinzmann, M., Cerca, N., Lobo da Cunha, A., Azeredo, J., & Vilanova, M.** (2011). Modulation of poly-*N*-acetylglucosamine accumulation within mature *Staphylococcus epidermidis* biofilms grown in excess glucose. *Microbiology and Immunology*, *55*(10), 673–682.

**Chaignon, P., Sadovskaya, I., Ragunah, C., Ramasubbu, N., Kaplan, J. B., & Jabbouri, S.** (2007). Susceptibility of staphylococcal biofilms to enzymatic treatments depends on their chemical composition. *Applied Microbiology and Biotechnology*, *75*(1), 125–132.

**Chen, K.-M., Chiang, M.-K., Wang, M., Ho, H.-C., Lu, M.-C., & Lai, Y.-C.** (2014). The role of pgaC in Klebsiella pneumoniae virulence and biofilm formation. *Microbial Pathogenesis*, *77*, 89–99.

**Choi, A. H. K., Slamti, L., Avci, F. Y., Pier, G. B., & Maira-Litrán, T.** (2009). The pgaABCD locus of *Acinetobacter baumannii* encodes the production of poly-β-1-6-N-acetylglucosamine, which is critical for biofilm formation. *Journal of Bacteriology*, *191*(19), 5953–5963.

**Cywes-Bentley, C., Skurnik, D., Zaidi, T., Roux, D., DeOliveira, R. B., Garrett, W. S., Lu, X., O'Malley, J., Kinzel, K., Zaidi, T., Rey, A., Perrin, C., Fichorova, R. N., Kayatani, A. K. K., Maira-Litràn, T., Gening, M. L.,**

**Tsvetkov, Y. E., Nifantiev, N. E., Bakaletz, L. O., Pelton, S. I., Golenbock, D. T., & Pier, G. B.** (2013). Antibody to a conserved antigenic target is protective against diverse prokaryotic and eukaryotic pathogens. *Proceedings of the National Academy of Sciences of the United States of America*, *110*(24), E2209–E2218.

**Delannoy, C. P., Rombouts, Y., Groux-Degroote, S., Holst, S., Coddeville, B., Harduin-Lepers, A., Wuhrer, M., Elass-Rochard, E., & Guérardel, Y.** (2017). Glycosylation Changes Triggered by the Differentiation of Monocytic THP-1 Cell Line into Macrophages. *Journal of Proteome Research*, *16*(1), 156–169.

**Ferreirinha, P., Pérez-Cabezas, B., Correia, A., Miyazawa, B., França, A., Carvalhais, V., Faustino, A., Cordeiro-da-Silva, A., Teixeira, L., Pier, G. B., Cerca, N., & Vilanova, M.** (2016). Poly-*N*-acetylglucosamine production by *Staphylococcus epidermidis* cells increases their in vivo proinflammatory effect. *Infection and Immunity*, *84*(10), 2933–2943.

**Ganesan, M., Stewart, E. J., Szafranski, J., Satorius, A. E., Younger, J. G., & Solomon, M. J.** (2013). Molar Mass, Entanglement, and Associations of the Biofilm Polysaccharide of *Staphylococcus epidermidis*. *Biomacromolecules*, *14*(5), 1474–1481.

**Giguère, D.** (2015). Surface polysaccharides from *Acinetobacter baumannii*: Structures and syntheses. *Carbohydrate Research*, *418*, 29–43.

**Gong, Z., Chen, B. K., Liu, J., Zhou, C., Anchel, D., Li, X., Ge, J., Bazett-Jones, D. P., & Sun, Y.** (2014). Fluorescence and SEM correlative microscopy for nanomanipulation of subcellular structures. *Light: Science &Amp; Applications*, *3*, e224.

**Gounon, P., Jouve, M., & Le Bouguénec, C.** (2000). Immunocytochemistry of the AfaE adhesin and AfaD invasin produced by pathogenic Escherichia coli strains during interaction of the bacteria with HeLa cells by high-resolution scanning electron microscopy. *Microbes and Infection*, *2*(4), 359–365.

**H. Blank, I.** (1971). *Patterns of Skin pH From Birth Through Adolescence: With a Synopsis on Skin Growth*. *Archives of Dermatology*, *104*, 224.

**Henry, R., Vithanage, N., Harrison, P., Seemann, T., Coutts, S., Moffatt, J. H., Nation, R. L., Li, J., Harper, M., Adler, B., & Boyce, J. D.** (2012). Colistin-resistant, lipopolysaccharide-deficient *Acinetobacter baumannii* responds to lipopolysaccharide loss through increased expression of genes involved in the synthesis and transport of lipoproteins, phospholipids, and poly-β-1,6-*N*-acetylglucosamine. *Antimicrobial Agents and Chemotherapy*, *56*(1), 59–69.

**Horn, J., Stelzner, K., Rudel, T., & Fraunholz, M.** (2018). Inside job: *Staphylococcus aureus* host-pathogen interactions. *International Journal of Medical Microbiology*, *308*(6), 607–624.

**Hu, D., Liu, B., Dijkshoorn, L., Wang, L., & Reeves, P. R.** (2013). Diversity in the Major Polysaccharide Antigen of *Acinetobacter baumannii* Assessed by DNA Sequencing, and Development of a Molecular Serotyping Scheme. *PLOS*

*ONE*, *8*(7), e70329.

**Joo, H.-S., & Otto, M.** (2012). Molecular basis of in vivo biofilm formation by bacterial pathogens. *Chemistry and Biology*, *19*(12), 1503–1513.

**Kenyon, J. J., Marzaioli, A. M., Hall, R. M., & De Castro, C.** (2014). Structure of the K2 capsule associated with the KL2 gene cluster of *Acinetobacter baumannii*. *Glycobiology*, *24*(6), 554–563.

**Knutton, S., Shaw, R. K., Anantha, R. P., Donnenberg, M. S., & Zorgani, A. A.** (1999). The type IV bundle-forming pilus of enteropathogenic Escherichia coli undergoes dramatic alterations in structure associated with bacterial adherence, aggregation and dispersal. *Molecular Microbiology*, *33*(3), 499–509.

**Kristian, S. A., Birkenstock, T. A., Sauder, U., Mack, D., Götz, F., & Landmann, R.** (2008). Biofilm formation induces C3a release and protects *Staphylococcus epidermidis* from IgG and complement deposition and from neutrophil-dependent killing. *Journal of Infectious Diseases*, *197*(7), 1028–1035.

**Little, D. J., Pfoh, R., Le Mauff, F., Bamford, N. C., Notte, C., Baker, P., Guragain, M., Robinson, H., Pier, G. B., Nitz, M., Deora, R., Sheppard, D. C., & Howell, P. L.** (2018). PgaB orthologues contain a glycoside hydrolase domain that cleaves deacetylated poly-β(1,6)-*N*-acetylglucosamine and can disrupt bacterial biofilms. *PLoS Pathogens*, *14*(4).

**Maira-Litrán, T., Kropec, A., Abeygunawardana, C., Joyce, J., Mark III, G., Goldmann, D. A., & Pier, G. B.** (2002). Immunochemical properties of the Staphylococcal poly-*N*-acetylglucosamine surface polysaccharide. *Infection and Immunity*, *70*(8), 4433–4440.

**Malanovic, N., & Lohner, K.** (2016). Gram-positive bacterial cell envelopes: The impact on the activity of antimicrobial peptides. *Biochimica et Biophysica Acta (BBA) - Biomembranes*, *1858*(5), 936–946.

**Mesnage, S., Dellarole, M., Baxter, N. J., Rouget, J.-B., Dimitrov, J. D., Wang, N., Fujimoto, Y., Hounslow, A. M., Lacroix-Desmazes, S., Fukase, K., Foster, S. J., & Williamson, M. P.** (2014). Molecular basis for bacterial peptidoglycan recognition by LysM domains. *Nature Communications*, *5*, 4269.

**O'Neill, E., Pozzi, C., Houston, P., Humphreys, H., Robinson, D. A., Loughman, A., Foster, T. J., & O'Gara, J. P.** (2008). A novel *Staphylococcus aureus* biofilm phenotype mediated by the fibronectin-binding proteins, FnBPA and FnBPB. *Journal of Bacteriology*, *190*(11), 3835–3850.

**O'Riordan, K., & Lee, J. C.** (2004). *Staphylococcus aureus* Capsular Polysaccharides. *Clinical Microbiology Reviews*, *17*(1), 218–234.

**Parra-Millán, R., Guerrero-Gómez, D., Ayerbe-Algaba, R., Pachón-Ibáñez, M. E., Miranda-Vizuete, A., Pachón, J., & Smani, Y.** (2018). Intracellular Trafficking and Persistence of *Acinetobacter baumannii* Requires Transcription Factor EB. *MSphere*, *3*(2), e00106-18.

**Potera, C.** (1999). Forging a link between biofilms and disease. *Science*, *283*(5409), 1837–1839.

**Ramos, Y., Rocha, J., Hael, A. L., van Gestel, J., Vlamakis, H., Cywes-Bentley, C., Cubillos-Ruiz, J. R., Pier, G. B., Gilmore, M. S., Kolter, R., & Morales, D. K.** (2019). PolyGlcNAc-containing exopolymers enable surface penetration by non-motile *Enterococcus faecalis*. *PLOS Pathogens*, *15*(2), e1007571.

**Schommer, N. N., Christner, M., Hentschke, M., Ruckdeschel, K., Aepfelbacher, M., & Rohde, H.** (2011). *Staphylococcus epidermidis* uses distinct mechanisms of biofilm formation to interfere with phagocytosis and activation of mouse macrophage-like cells 774A.1. *Infection and Immunity*, *79*(6), 2267–2276.

**Schwalfenberg, G. K.** (2012). The alkaline diet: Is there evidence that an alkaline pH diet benefits health? *Journal of Environmental and Public Health*, *2012*(727630), 7 pages.

**Skurnik, D., Cywes-Bentley, C., & Pier, G. B.** (2016). The exceptionally broad-based potential of active and passive vaccination targeting the conserved microbial surface polysaccharide PNAG. *Expert Review of Vaccines*, *15*(8), 1041–1053.

**Smadhi, M., De Bentzmann, S., Imberty, A., Gingras, M., Abderrahim, R., & Goekjian, P. G.** (2014). Expeditive synthesis of trithiotriazine-cored glycoclusters and inhibition of Pseudomonas aeruginosa biofilm formation. *Beilstein Journal of Organic Chemistry*, *10*, 1981–1990.

**Stevens, N. T., Sadovskaya, I., Jabbouri, S., Sattar, T., O'gara, J. P., Humphreys, H., & Greene, C. M.** (2009). *Staphylococcus epidermidis* polysaccharide intercellular adhesin induces IL-8 expression in human astrocytes via a mechanism involving TLR2. *Cellular Microbiology*, *11*(3), 421–432.

**Stewart, E. J., Ganesan, M., Younger, J. G., & Solomon, M. J.** (2015). Artificial biofilms establish the role of matrix interactions in staphylococcal biofilm assembly and disassembly. *Scientific Reports*, *5*.

**Szklarczyk, D., Franceschini, A., Wyder, S., Forslund, K., Heller, D., Huerta-Cepas, J., Simonovic, M., Roth, A., Santos, A., Tsafou, K. P., Kuhn, M., Bork, P., Jensen, L. J., & Von Mering, C.** (2015). STRING v10: Protein-protein interaction networks, integrated over the tree of life. *Nucleic Acids Research*, *43*(D1), D447–D452.

**Whitfield, G. B., Marmont, L. S., & Howell, P. L.** (2015). Enzymatic modifications of exopolysaccharides enhance bacterial persistence. *Frontiers in Microbiology*, *6*, 471.

**Wilhelm, K.-P., & Maibach, H. I.** (1990). Factors Predisposing to Cutaneous Irritation. *Dermatologic Clinics*, *8*(1), 17–22.

**Zhu, Z., Zheng, T., Homer, R. J., Kim, Y.-K., Chen, N. Y., Cohn, L., Hamid, Q., & Elias, J. A.** (2004). Acidic Mammalian Chitinase in Asthmatic Th2

Inflammation and IL-13 Pathway Activation. *Science*, *304*(5677), 1678 LP-1682.